Gels Horizons: From Science to Smart Materials

Anuj Kumar
Stefan Ioan Voicu
Vijay Kumar Thakur *Editors*

3D printable Gel-inks for Tissue Engineering

Chemistry, Processing, and Applications

Springer

Gels Horizons: From Science to Smart Materials

Series Editor

Vijay Kumar Thakur, School of Aerospace, Transport and Manufacturing, Cranfield University, Cranfield, Bedfordshire, UK

This series aims at providing a comprehensive collection of works on the recent advances and developments in the domain of *Gels*, particularly as applied to the various research fields of sciences and engineering disciplines. It covers a broad range of topics related to *Gels* ranging from *Polymer Gels, Protein Gels, Self-Healing Gels, Colloidal Gels, Composites/Nanocomposites Gels, Organogels, Aerogels, Metallogels* & *Hydrogels* to *Micro/Nano gels*. The series provides timely and detailed information on advanced synthesis methods, characterization and their application in a broad range of interrelated fields such as chemistry, physics, polymer science & engineering, biomedical & biochemical engineering, chemical engineering, molecular biology, mechanical engineering and materials science & engineering.

This Series accepts both edited and authored works, including textbooks, monographs, reference works, and professional books. The books in this series will provide a deep insight into the state-of-art of *Gels* and serve researchers and professionals, practitioners, and students alike.

More information about this series at http://www.springer.com/series/15205

Anuj Kumar · Stefan Ioan Voicu ·
Vijay Kumar Thakur
Editors

3D printable Gel-inks for Tissue Engineering

Chemistry, Processing, and Applications

Springer

Editors
Anuj Kumar
School of Chemical Engineering
Yeungnam University
Gyeongsan, Korea (Republic of)

Vijay Kumar Thakur
Biorefining and Advanced Materials
Scotland's Rural College
Dumfries, UK

Stefan Ioan Voicu
Faculty of Applied Chemistry
and Materials Science
Polytechnic University of Bucharest
Bucharest, Romania

ISSN 2367-0061 ISSN 2367-007X (electronic)
Gels Horizons: From Science to Smart Materials
ISBN 978-981-16-4666-9 ISBN 978-981-16-4667-6 (eBook)
https://doi.org/10.1007/978-981-16-4667-6

This Springer imprint is published by the registered company Springer Nature Singapore Pte Ltd.
The registered company address is: 152 Beach Road, #21-01/04 Gateway East, Singapore 189721, Singapore

Preface

Over the past decade, additive manufacturing technologies have emerged as one of the most wonderful fabrication methods in the field of tissue engineering and regenerative medicine due to their precise control and 3D printing of architectures as per tissue-specific or organ-specific demands using digital models based on medical imaging data. Among them, extrusion-based three-dimensional (3D) printing/bioprinting is a commonly used technique in tissue engineering areas. Various gel-inks or bio-inks have been developed and utilized for 3D printing by including natural and synthetic polymers, bioceramics, bioactive glasses, and glass-ceramics. Significant research has been performed in this area, but several challenges are remaining to be overcome in terms of data imaging, additive manufacturing technique, and design of biomaterial-inks (i.e. gel-inks or bio-inks) with their good printability and post-printing shape fidelity, 3D printing of curved and complex architectures, etc. Therefore, it is very important to understand the significance of 3D printing techniques, especially in tissue engineering applications, where healthcare issues are major concerns for human beings. A concise understanding and an overview of the chemistry and processing of biomaterials and 3D printing methods for various tissue engineering applications are provided in this book for the readers. Valuable knowledge is updated and organized according to various current studies worldwide in the field of tissue engineering.

This book provides an overview and discusses the chemistry, processing, and tissue engineering applications of the biomaterials that have been used for synthesizing 3D-printable gel-inks. This authoritative book provides the necessary fundamentals and background for researchers and research professionals who intend to work in the field of 3D bioprinting in tissue engineering. In 3D bioprinting, the design and development of the biomaterial-inks/bio-inks is a major challenge in providing a 3D microenvironment specifically to the anatomical and architectural demand of native tissues. Therefore, the main purpose of this book is to provide the basic chemistry of the biomaterials, their current processing developments and challenges, and recent advancements in tissue-specific 3D printing/bioprinting. The topics comprise mainly (1) biomaterial types, their synthesis and/or modifications, and processing for the particular 3D printing method, (2) characterization methods before printing and

post-printing as well as *in vitro* and *in vivo* analyses, and (3) their applications and uses in various tissue engineering applications. This book serves as a go-to reference on bioprinting and is ideal for students, researchers, and professionals, including those in academia, government, the medical industry, and health care.

Chapter 1 provides the introduction to 3D printing technology for biomedical applications, describing the progress and development of printing technology to create organs or tissues including limitations. Chapter 2 presents the characterization of bio-inks for 3D printing applications by explaining numerous characterization methods. Chapter 3 discusses the 3D printing of hydrogel constructs toward targeted development in tissue engineering. Chapter 4 presents and discusses 3D-printable self-healing scaffolds for tissue engineering applications. Chapter 5 focuses on gel-inks for 3D printing in corneal tissue engineering applications. Chapter 6 introduces the current state of 3D-printable gel-inks utilized for skin wound treatments, whereas Chap. 7 presents biofunctional inks for 3D printing in skin tissue engineering applications. Chapter 8 explores the possibilities of using starch gels combined with different bioceramics for additive manufacturing and alternative fabrication methods for developing biomimetic implants for filling large bone defects, while Chap. 9 focuses on additive manufacturing of bioceramic scaffolds for bone tissue engineering applications by emphasizing stereolithographic processing. Chapter 10 is concerned with 3D-printable gel-inks for microbes and microbial structures to study microbes and microbe-host interactions, biofilm formation, antibiotic resistance, and microbiome through 3D modeling of microbes and infections for understanding diseases in a broader sense. Chapter 11 describes the methods of polysaccharide crosslinking, specifically future crosslinking methods of alginate hydrogels for 3D printing for biomedical applications, including tissue engineering areas. Lastly, Chap. 12 discusses the future perspectives for gel-inks for 3D printing in tissue engineering by considering precursors and other specific challenges.

At last, but most importantly, we would like to thank and acknowledge the authors who contributed to this book. In addition, we thank all reviewers for giving their valuable time to provide their reviews timely to improve the quality of this book.

Gyeongsan, South Korea — Anuj Kumar
Bucharest, Romania — Stefan Ioan Voicu
Dumfries, UK — Vijay Kumar Thakur

About This Book

1. Provides the background for 3D printing and tissue engineering and their challenges.
2. Provides the chemistry, functionalization, and processing of biomaterials.
3. Describes the pre-printing and post-printing processes for biomaterials according to particular 3D printing methods.
4. Discusses the efficacy of gel-inks for various tissue engineering applications.
5. Discusses the futuristic perspective in terms of 3D, 4D, and 5D printing/bioprinting technology.

Contents

About the Editors

Dr. Anuj Kumar is an Assistant Professor at the School of Chemical Engineering, Yeungnam University, South Korea. He has completed one research project (3 years) as Principal Investigator (PI) awarded by the National Research Foundation of Korea (NRF) and recently received two more sponsored research projects for 3 years one as a PI awarded by NRF (Korea) and one Indo-Korea joint research project as a Co-PI awarded by Korea Research Foundation (KRF, Korea) and Department of Science and Technology (DST, India). He worked as a Postdoctoral Research Associate in the Department of Nano, Medical and Polymer Materials (School of Chemical Engineering) at Yeungnam University, South Korea and Assistant Professor in the Department of Chemistry at DIT University, India. He received his Ph.D. in Polymer Science and Engineering (Polymers & Biomaterials) in 2014 from Indian Institute of Technology (IIT) Roorkee, India. He received his M.Tech. (Fibre Science and Technology) in 2009 from IIT Delhi, India and M.Sc. (Organic Chemistry) in 2006 from Chaudhary Charan Singh University, Meerut, India, respectively. He has published more than 55 SCI articles and 7 book chapters. He has rich experiences in the field of polymer/fibre science, lignocellulosic biomass, synthesis and processing of bio-based polymers, nanocelluloses, carbon nanomaterials, surface modification of polymers, polymeric composites/nanocomposites, chemistry and design of nanocomposite biomaterials, bioceramics and bioactive glasses, hybrid scaffolds and hydrogels, additive manufacturing (e.g., 3D printing/bioprinting), hybrid materials for cancer therapy, etc. His current research is focused on developing 3D printable hydrogels for various tissue engineering applications.

Dr. Stefan Ioan Voicu Ph.D., (Habilitation) is a Professor at the Faculty of Applied Chemistry and Materials Science, Politehnica University of Bucharest and working in the Department of Analytical Chemistry and Environmental Engineering in the field of polymeric membrane materials and processes. He received his B.Sc. in Organic Chemistry, M.Sc. in Environmental Engineering, and Ph.D., in Polymeric Membranes, and since 2016 he also has Habilitation in Chemical Engineering, all at Politehnica University of Bucharest, Romania. In the fields of polymers, polymer

composites and polymeric membranes (for different applications—from water purification to sensors, fuel cells, and biomedical field), he has published over 50 SCI journal articles, 5 chapters, and 3 granted US patents.

Dr. Vijay Kumar Thakur is currently Professor in New Products from Biomass, Biorefining and Advanced Materials Research Centre, SRUC, UK. Prior to this, Dr. Thakur worked as a Staff Scientist in the School of Mechanical and Materials Engineering at Washington State University, USA. Some of his other prior significant appointments include being a Research Scientist in Temasek Laboratories at Nanyang Technological University, Singapore and a Visiting Research Fellow in the Department of Chemical and Materials Engineering at LHU–Taiwan. He did his post-doctoral study in Materials Science & Engineering at Iowa State University and received Ph.D., in Polymer Chemistry (2009). He received his B.Sc. (Chemistry, Physics and Mathematics), B.Ed. and M.Sc. degree in Organic Chemistry from Himachal Pradesh University, Shimla, India. Dr. Thakur is an editorial board member of several SCI peer reviewed international journals as well as member of scientific bodies around the globe.

Chapter 1
Introduction to 3D Printing Technology for Biomedical Applications

Satish Kumar, Ramaraju Bendi, and Vipin Kumar

Abstract The progress in tissue engineering and regenerative medicines has made organ replacement or regeneration easier, and its demand has increased rapidly in recent years. Bio-printing of human organs or tissues has become possible only because of the successful development of the bio-ink used in three-dimensional (3D) printing technology. Owing to the unique attributes of 3D printing, it can create an object of any complexity, including tissues with highly customized requirements for the subject (i.e., patient) specific applications. Development in smart materials, such as thermoplastics, powdered plastics, and photopolymers, enabled 3D printing to create objects with customized mechanical properties to mimic human organ models accurately. It brings new possibilities to create bionic tissues or organs, and it becomes even more desirable where the donor shortage is a severe problem. Despite cell printing, the effort remains to be made to accomplish the higher objectives of the in-vitro manufacturing of tissues or organs. This chapter sheds light on the progress and development of 3D printing technology to create organs or tissues. Also, the current state-of-the-art of the materials that can be processed, designed, is discussed comprehensively. The potential and major limitations of 3D printing technology in the field of bio-printing and related medical applications are discussed in brief.

S. Kumar
Department of Physics and Astrophysics, University of Delhi, New Delhi, Delhi 110007, India

R. Bendi
Department of Basic Science and Humanities (Chemistry), Aditya Institute of Technology and Management, Tekkali, Andhra Pradesh 532201, India

V. Kumar (✉)
Centre for Energy Studies, Indian Institute of Technology Delhi, Hauz Khas, New Delhi, Delhi 110016, India
e-mail: vkumar@ces.iitd.ac.in

A. Kumar et al. (eds.), *3D printable Gel-inks for Tissue Engineering*, Gels Horizons: From Science to Smart Materials, https://doi.org/10.1007/978-981-16-4667-6_1

1 Introduction

With the revolution in medical technology, healthcare facilities have been increased seamlessly in recent years [1]. However, transplantation of organs or tissues required for lesions and defects has remained a crucial problem and is the subject of further investigations [2]. The existing techniques, such as auto-transplantation, xeno-transplantation, and artificial mechanical organ implantation found ineffective in improving the quality of transplant and the patient's life [3, 4]. For example, auto-transplantation, which exhibits satisfactory outcomes, but at the cost of antilogous-health-organization. It may cause various difficulties and inevitable side-effects [5]. Xeno-transplantation or heterologous transplant allows living cells, organs, and tissues to be transplanted from one species to another is readily used for end-stage organ failure [6]. This approach invites various potential challenges such as immunological rejection and viral transmission [7]. The implantable artificial organ in medical treatments is a quite successful approach and has significantly improved patient life [8]. The most developed artificial organs include the heart and kidney, while the pacemakers and cochlear implants are the most developed medical components [9, 10]. The implantable organs become mandatory when an organ in a person's body is damaged due to injury or disease. The crucial requirement of implantable artificial organs or prosthetics is to imitate the function of the original organ. Precise control over the physical and mechanical properties is essential for artificial biological organs [11]. Three-dimensional (3D) printing (3D printing) technology, which is known for its extreme controllability, is primarily employed in medical applications [12]. Owing to the unique attributes of 3D-printing technologies, which include high precession and speed, it is expected to overcome the crucial challenges encountered while using congenital methods/tools.

In addition to industrial, commercial applications, 3D printing technology, also known as the additive-manufacturing (AM) technique, is widely adopted by the medical industry [13]. This technique's working principle is based on the layered construction of the materials that are overlapped layer-by-layer [13]. In constructing an object with any complexity, the process involves well-optimized virtual-design objects using computer-aided designs (CAD). The optimization of CAD, appropriate selection of 3D printers and materials, plays a crucial role in producing a 3D object. These files serve as the guiding principle for the subsequent printing steps. The typical process steps are schematically illustrated in Fig. 1, which include the following steps: (a) CAD-assisted design of the object that contains the entire geometric information about the 3D objects; (b) steps-wise construction of 3D object through slicing the information into different 2D subsets; (c) periodic drying or curing of 2D subsets, (d) controlled movement of the stage along the z-direction, (e) repeat the steps (b) and (c) as per the printing duration. The process steps show that 3D printing involves the continuous addition of the materials on top of a previously cured or dry 2D layer. 3D printing technology opens a broad spectrum of vital opportunities for medical applications to create more specific human organs or tissues [14].

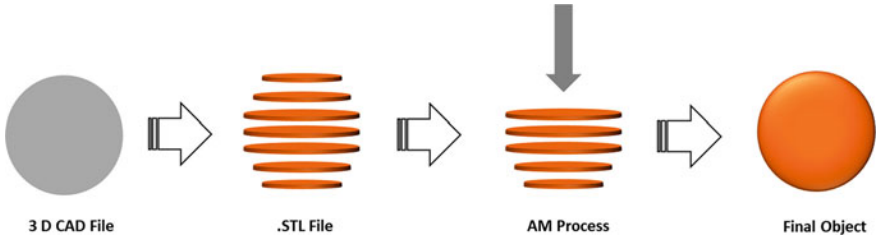

Fig. 1 Schematic illustration of the process steps involved during the development of a 3D printed object

Today, 3D printing technology has significantly developed the necessary research as well as skills for the new generation of surgeons [14]. Presently, the research on 3D printing technology for medical applications can be categorized into the following four primary areas of interest: (a) design and development of pathological organ models to help pre-operative planning and implant analysis [15], (b) personalized non-bioactive implants; (c) localized bio-active and bio-degradable supports or scaffolds, and (d) complete life-function of directly printed tissues or organs [16, 17]. Though the research focus remains far from the widespread medical applications due to various scientific and technical challenges, there are numerous printing techniques and materials available to give better results for tissue or organ designing. Nonetheless, some of the printing materials (i.e., printable biomaterials) are rigid and not suitable to meet the criteria of desirable flexibility and elasticity, progress in developing smart materials is made recently to fill the gap [18, 19].

2 Printing Mechanism: Classification of 3D Printing Techniques

Based on the printing mechanism, 3D printing can be classified into different categories. The commonly known printing mechanisms are given as follows; selective layer sintering (SLS), stereolithography (SLA), fused deposition modeling (FDM), and ink-jet printing. These mechanisms have their type of printable materials and advantages over others, see Table 1.

The strengths and limitations of each mechanism are described briefly in the following sections.

2.1 Selective Laser Sintering

This technique makes use of a high-power CO_2 laser, which is used to selectively fabricate the models in different steps. For example, 2D-slice data are generated

Table 1 Materials for different types of 3D printing techniques

Feature	SLS	SLA	FDM	Ink-jet
Materials	Metal (titanium, aluminide, stainless steel) and polymer powder	Polymer (light-sensitive) resin ceramic wax	Nylon, PLA, PVA, PC, wood-like, etc.,	Ceramic, plaster, plastic
Material's availability	Not-easily available	Easily available	Easily available	Easily available
Process	Chamber powder layer polymerization	Build plate basin exposure	Build plate extrusion layer bonding	Chamber powder layer bonding
Material cost	> $ 530/kg	> $ 700/kg	> $ 70/kg	> $ 350/kg

during the first step, which is put into the SLS machine that guides the laser's beam pathway. This laser beam scans the path on the powder surface, and this process heats it to sintering temperature, which makes it bond powder on the scanned path. After making the first fuse layer, the build layer descends, and the subsequent layer of powder can be put down and sintered. This procedure is repeated until the desired shape is accomplished. The un-fused powder on each layer serves as a supporting structure. During the sintering and cooling process, shrinkage and warpage become significant issues in the SLS method. These problems can be mitigated by using small-sized particle powder and airflow temperature within the sintering temperature window [20]. The advantage of this technique is that the product built by SLS can be reused even after being crushed into small pieces [21]. The schematics of SLS is shown in Fig. 2a.

2.2 Stereolithography

Stereolithography was originally known as the first 3D printing system and was invented in the 1980s. This technique's origin is based on photolithography, which is used to make a 2D pattern on the sample surface with high resolution. This technique is used to scan the UV light to cure the photo-resin with the desired pattern. After the UV exposure step, the resin tub moves up for a small distance in the z-direction to fill a new layer of resin on top or beneath the previous layer. The fill of the new layer by resin depends on the printer's configuration. Then, this newly filled resin layer will be again cured by UV light to make another pattern. This process repeats again and again until the complete 3D object is printed. The cost of this printer has reduced significantly because of the expiration of its significant patents in 2012. The high printing resolution in all x,y,z directions is the most remarkable advantage of the stereolithography technique. The shortcomings include lack of multi-material printing capability, small building dimensions, and it only works for photosensitive materials [22]. The schematics of the stereolithography is shown in Fig. 2b.

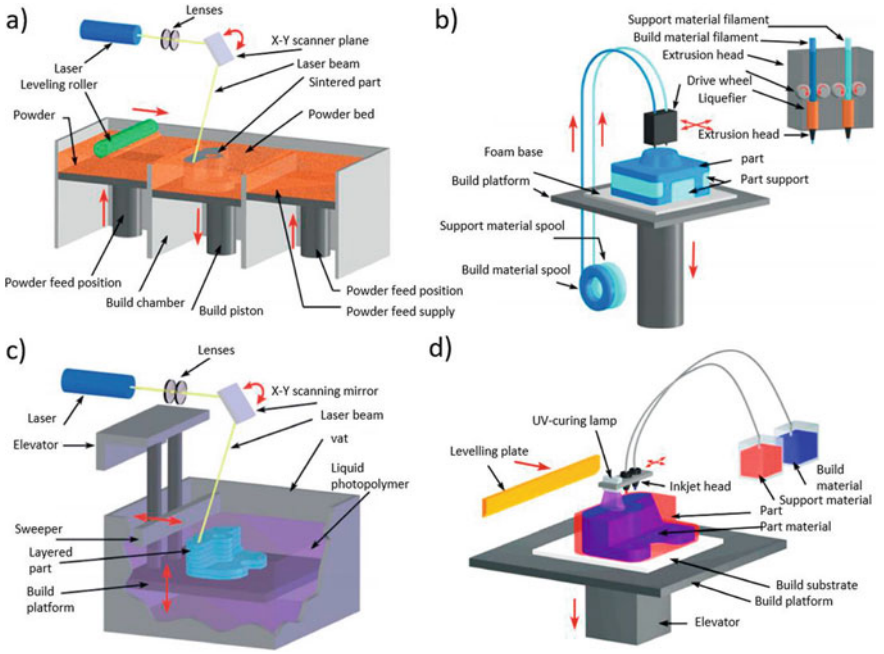

Fig. 2 Schematic illustration of the typical 3D printing mechanisms. **a** Selective layer sintering, **b** Stereolithography, **c** Fused deposition modeling (FDM), and **d** Ink-jet printing reproduced with permission [24]. Copyright @ 2018 Wiley–VCH Verlag GmbH & Co. KGaA, Weinheim

2.3 Fused Deposition Modeling

This method is another class of 3D printing mechanism in which the materials are extruded from the nozzle [23]. The jet is associated with a *x*–*y* driving system. The *x*–*y* motor system drives the nozzle to draw the pattern according to the layer information generated by the slicing software of the 3D printer. After finishing the pattern formation for one layer, the stage goes down to a certain distance, and the printer starts to follow the next layer's similar process. This is the most popular method for 3D printing. The expiration of patents made the printers affordable for the general public, and it is similar to stereolithography. This technique has better resolution (~300 μm) than that of the stereolithography, large building volume, low cost (less than 1 k USD), and multi-material printing capabilities that make it attractive for public and R & D activities. Nowadays, this method is widely used for bio-printing (3D printing biomaterial with or without cells). The schematics of the fused deposition machine is shown in Fig. 2c.

2.4 *Ink-Jet Printing*

The ink-jet 3D printing technique is similar to a desktop 2D ink-jet printer. Both methods have an array of the nozzle that is used to dispense tiny droplets of ink onto the substrate surface. In the next step, UV exposure is used to scan the entire layer to cure the droplets. After printing the first layer, a similar mechanism is used for another layer. The stage goes down to some distance, and the printing process repeats until finishing the whole object. This technique's resolution can be controlled by the droplet size, which is higher than that of the FDM printer; however, it is worse than the stereolithographic printer. The multi-material deposition is also feasible by dispensing different droplet types at the desired locations similar to that of the 2D color ink-jet printer. Typically, such printers are much more expensive (over 30 k USD) compared with the other contemporaries. The schematics of ink-jet printing machine is shown in Fig. 3d.

3 Evolution of 3D-Printed Medical Objects—Then and Now

Among 3D printing medical objects, bio-printing is the most recent and one of the attractive methods compared with many other technological developments. In the beginning, this research area was made extraordinary advances in some of the fields, and remained relatively stationary in others. There were limitations and technical

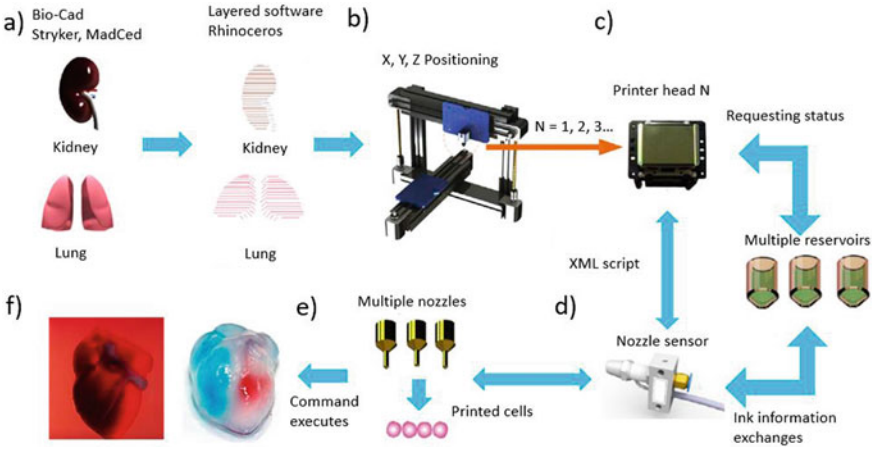

Fig. 3 Evolution and examples of bio-printing platforms. **a-e** Typical steps involved in the development of a human organ 3D-printed model, reproduced with permission [38]. Copyright @ 1969 Elsevier, **f** 3D-printed cardioid structure, reproduced with permission [37]. Copyright @ 2018 Wiley–VCH Verlag GmbH & Co. KGaA, Weinheim

challenges that are required to overcome before scaling-up this technique to the manufacturing level.

3D bio-printing moves up from the multidisciplinary combination of several other relatively cutting-edge technologies, for example, additive manufacturing, and cell patterning. Additive manufacturing technology is used for many other applications such as fabricating devices, components, and parts from materials such as metals and plastics. However, cell patterning and substrate patterning were related technologies used in R&D laboratories for probing cell–protein interactions. These techniques have been tried in combination to build a 3D living structure that could perhaps be used to replace the tissues and organs in a human patient [25–27]. The coined term was known as 'organ printing,' the precursor to 'bio-printing,' which we have accepted widely.

Bio-printing hardware consists of various parts and is shown in Fig. 3. Early bio-printers were based on custom-built, hacked, and ink-jet printers [29]. There are very few labs that are working in these areas to build their hardware. However, these custom devices were often incredibly difficult to operate because of full of software bugs and featured impossible user interfaces. Those lucky people who receive sufficient funding could utilize other 3D printing devices that were commercially available. Therefore, these devices were not engineered to print biological materials. The high cost for a single operational piece of hardware is around $ 100–200 k [30].

Meanwhile, the additive manufacturing technology continued to advance specifically in the open-source world, resulting in inexpensive but still buggy. Those printers were responsible for bio-printing only after substantial tinkering. Because of these limitations, bio-printing technology becomes more difficult but not impossible.

With time, the technology continued to evolve and bifurcate, as the terminology associated with other bio-printing facets. This progress was related to tissue liquidity and tissue fusion and developed a platform in which cell aggregates or tissue spheroids were deposited into a hydrogel biomaterial substrate. Both cell–cell and cell matrix-based interactions would fuse in a controllable manner and construct into a more extensive bioengineered tissue [29–38]. The aggregation of the cell was termed as bio-ink and bio-paper related to the hydrogel biomaterial component. However, bio-ink encompasses cells, biomaterials, and a combination thereof. More recently, a fully personalized, non-supplemented materials as bio-inks are demonstrated for printing of human organs (i.e., heart) [37]. The bio-inks consist of a fatty tissue, which is taken out from a patient and the bio-inks were processed from cellular and a-cellular materials. The potential of 3D-bio-printing technology to engineer vascularized cardiac patches is highlighted.

4 3D Printable Materials for Medical Applications

The specific materials that are used in 3D printing are allowed to transform to abide by the limitation of a specific model. The process can be executed in different steps; (i) materials' distortion by melting of a stiff filament; (ii) solidification of the melt

in the desired form or construction of the structure; and (iii) solidification of the power. To allow these processes to occur, a filler or supporting or additive material is required, which is often accommodated in the lattice forms to mitigate distortion of the model during the curing step. These supporting materials or fillers can easily be removed or disintegrate from the parent structure by simply using hands or with a specified cutting tool. However, risk of leaving an impression on the surface is always there, and therefore it requires an additional polishing step to get-rid-of the marks. Though polishing is essential to obtain a good quality printing, this step may increase the risk of deformation of the structure, may lose fine details, and breaking of the geometry [39].

The selection of the material depends upon printing technique, printer technical specifications, and requirements of the model. The mechanical/elastic properties of the materials are chosen based on the structure of interest, for example, the anatomical structures are highly sensitive toward the mechanical/elastic attributes of the printed materials [40]. The key distinction between different materials that characterize the human body includes a combination of rigid tissues and soft materials. For instance, bones and ligaments (i.e., articular cartilage) represent rigid tissues and soft materials, respectively. The bones are the easiest and simplest biological tissue that is ever been produced by 3D printing technique with the majority of rigid materials. There are examples in 3D printing to model bone construction, such as acrylonitrile butadiene styrene (ABS) [39], powder of plaster [41], and hydroquinone [40].

However, 3D printing of the soft tissues is in infancy, and further development is the need of the hour to harness the full potential of the techniques. There is a need to conduct a depth research to fill the vacuum among a 3D-printed anatomical model and a true structure of human organ or tissue. Most of the 3D printing materials severely lack realism to mimic or duplicate a soft biological tissue, and an additional step, i.e., post-processing is necessary to soften the printed structures. There are some examples of the reproduction of cartilaginous tissues [42], arteries of practicing valve replacement [43], hepatic segment [44], and hearts [45]. Besides that, there is an interesting example in the development of 3D-printed brain aneurysm using a flexible TangoPlus™ photopolymer, which is a useful tool for the treatment of congenital heart disease [46]. There are several 3D printing processes that work on different operating principles and significantly vary in terms of technologies and materials' selection and niche area of applications. Also, it is worth mentioning that 3D printing seamlessly allows the development of the reproduction of implantable custom devices. However, there is a long way to go to adopt 3D-printed critical organs (e.g., heart) for implantations, and more profound research is still needed to examine the difference between traditional and additive manufacturing in mechanical and structural properties [47].

5 Significance of 3D-Printed Objects in the Medical Field

In many areas of medical field, 3D printing technology is indispensable in modern medical technology. Every year, this technology offers many healthcare field applications that help to save and improve our lives. Indeed, 3D printing has a wide range of applications in the field of healthcare, for example, cardiology [43], cardiothoracic surgery [47], gastroenterology [48], neurosurgery [49], oral and maxillofacial surgery [50], ophthalmology [51], otolaryngology [52], plastic surgery [53], podiatry [54], pulmonology [55], radiation oncology [56], transplant surgery [57], urology [58], and vascular surgery [59]. 3D printing technology deserves to be recognized at large scale in the field of healthcare and medical due to its ease of availability and operation. The leading direct applications of 3D printing in the medical and clinical fields are discussed comprehensively in the following sections.

6 Applications of 3D Printing

3D printing has retained a great passion and invention to the modern medical science. It is now promising and virtually effortless to offer modified health care solutions to help to medicinal practitioners and patients alike. It is projected that 3D printing technology will be worth over $3.5bn by 2025 in the medical field, compared with $713.3 m in 2016. The industry's compound annual growth rate is supposed to reach around 17.7% between the years 2017 and 2025. As one might witness the journey of 3D printing technology has enabled customization in medicine, prototyping, manufacturing, and academic research activities. 3D printing has many functions in medical sciences, for instance, this technology could be successfully applied to transplantation of human organs, expediting surgical process, low-cost production of surgical tools for surgery process, and may significantly improve the lives of those reliant on prosthetic limbs. As one might expect, the area of applications is quite broad, which extends from surgical to dental to implant tissue regeneration. The following are the specific application areas;

- Printing of surgical preparation
- Custom-made prosthetics
- Dental
- 3D printing of tissues, organoids, and tissue regeneration
- Medication dosage and pharmacology
- Manufacturing of surgical tools and medical metal materials

6.1 3D Printing of Surgical Preparation

In the human body, the individual variances and complexities are significantly great and 3D-printed models could be ideal for surgical preparation, as the printed tools can be customized to a great extent. For controlled and precise model development, the imaging techniques are essential for 3D printing technology. Besides surgical, 3D printing is equally revolutionizing medicine. 3D printing is being used to mimic patient-specific organs that are used for practice purposes to fix well before the actual complicated operations take place. The application becomes much better and more accurate if examines the results with X-rays, CT scans, and MRIs. Ultimately, this technique of surgical preparation has proven to pick up speedy procedures and minimizes the possibility of patient injury. Dissections often compromised with the proper pathology, so they offer an additional lesson in anatomy than a surgical patient's representation. Across the globe, research organizations, healthcare professionals, and hospitals are using 3D-printed anatomical frameworks as reference tools for pre-operative planning, intraoperative visualization, and sizing or pre-fitting medical equipment for both highly complex and routine procedures.

By using 3D-printed technology, we can produce sterile surgical instruments such as forceps, hemostats, scalpel handles, and clamps. 3D printing techniques not only produce sterile tools but some are also can be made very small and precise origami with ancient Japanese technology for practice. These tools can be used to work on microscopic areas without causing extra harm to the patient. The key advantage of using 3D printing over the traditional manufacturing methods is the low cost and speedy nature of the process to produce surgical tools.

3D-printed models could be incredibly useful to neurosurgeons by idiomatic expressions of the complex structures of the organs in the human body (Fig. 4). The radiographic 2D images are sometimes difficult to concealed right connections among cranial nerves, cerebral structures, vessels, and skull construction. Even a small mistake in navigating this complex anatomy can have potentially devastating consequences to both patient and the operating personnel. A realistic 3D model of skull helps better to speculate or predict the relationship between a scratch and typical brain structures. It can also help determine the protected surgical corridor and could be equally important for the neurosurgeon to practice critical operations. For example, 3D-printed models have recently been used to study complicated spinal deformities.

3D-printed models have been utilized in numerous situations to gain a deeper understanding of patient's specific anatomy before conducting an actual operation. Biotexture Wet Model [60] was developed by a Japanese company Fasotec, bought by Stratasys, to realistically mimicking real organs, for instance lungs, which are used to practice by both the surgeons and students prior to perform the actual operation in the operation theater. Nowadays, 3D-printed models are widely helpful for planning complicated surgery procedures, and commercially available in the market and common places. It has assisted full face transplants [61], the first adult-to-child kidney transplant [62], removal of a kidney [63], or liver tumor [64] in hospital and acetabular reconstructive surgery [65].

Japan's Kobe University Hospital, pioneering surgeons planned to liver transplantations with 3D-printed models. They used 3D-printed models of a patient's organs to understand the best possible ways to carve a donor's liver with negligible tissue damage to fit perfectly to the receiver's abdominal crater. For such applications, 3D-printed models are required to be partially transparent and prepared with very low-cost materials, for example, acrylic-resin or polyvinyl-alcohol (PVA) with excess water content. The texture of these models mimics living tissues, which gives an advantage to the surgeons, and allowing them to experience a live penetration by the surgical knife edges [66].

3D-printed model does not cost more than a custom made models by other techniques, however, the processing time is way lesser than the previously reported techniques [67]. Recently, a 3D-printed polypeptide chain model was developed and allowed to wrinkle into subordinate structures until it reaches a limit of bond rotation barrier and degrees of freedom [23]. Such models could be useful to gain insight into the other similar types of biological or biochemical structures (see Fig. 5). Several studies have been conducted on such origami structures and identified that the students could conceptualize the molecular structures better when demonstrate with the help of such models.

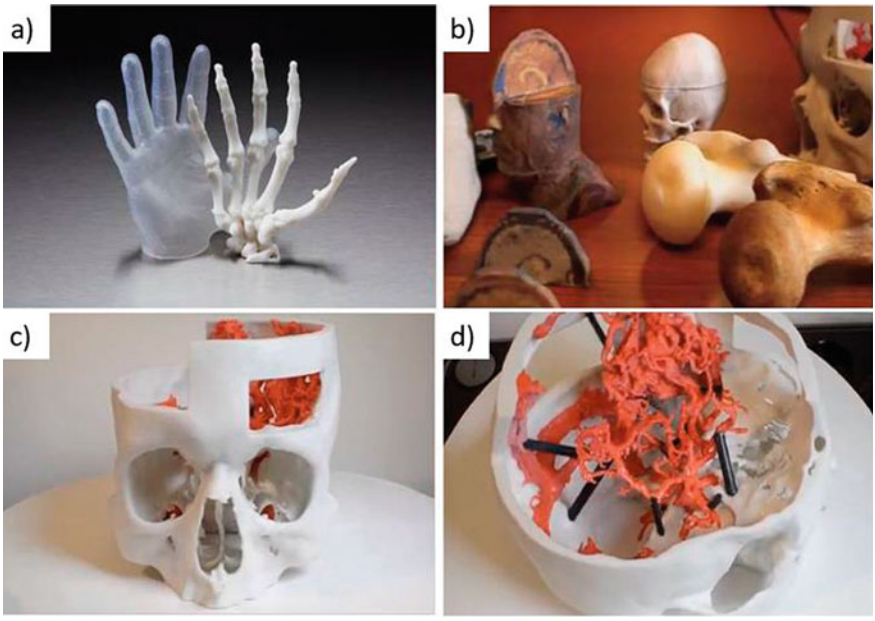

Fig. 4 **a.** Anatomical model of a hand, including the 'skin' made out of an elastic 3D printing material. **b.** Researchers at the National Library of Medicine generate digital files from clinical data, such as CT scans, that are used to make custom 3D-printed surgical and medical models. **c, d.** 3D model used for surgical planning by neurosurgeons at the Walter Reed National Military Medical Center. *Source* The Guardian (NIH 3D Printing Exchange)

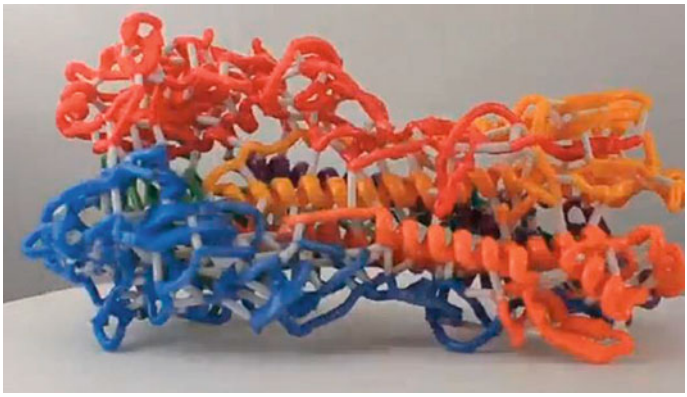

Fig. 5 An influenza hemagglutinin trimer 3D-printed model. *Source* The Guardian (NIH 3D Printing Exchange)

6.2 Custom-Made Prosthetics

3D printing has widely been used in the field of healthcare to model both normal and made-to-order prosthetic medical objects such as limbs and surgical implants [68–70]. This methodology has been used to construct dental, backbone, and hip transplants [68]. Earlier, surgeons had to execute bone-implant operations or use scalpels and drills to adjust implants by shaving pieces of metal and plastic to the anticipated shape/form, size, and fit, which is very time-consuming, and might not sound safe from patient's perspective. On the other hand, 3D printing has the ability to produce custom implants quickly. Prostheses solve an evident and persistent problem in orthopedics, where standard implants are often not sufficient/compatible with some patients, particularly in complex cases. A similar explanation is equally valid in neurosurgery. Due to irregular shapes and sizes of the skulls, it is very immensely challenging to regulate a cranial implant. The sufferers of skull wound, where the bone is discharged to give room to swell brain, the cranial plate that is later tailored must be unconditionally seamless. Although some of them are milled, more and more are developed using state-of-the art 3D printers, making it much stress-free to tailor, apt, and re-design, if required [70]. There have been many other viable and scientific accomplishments in the field of 3D printing of prostheses and transplants [23, 66, 68]. Researchers at BIOMED Research Institute in Belgium precisely implanted mandibular prosthesis of titanium (Ti) through 3D-printing technique [66]. The transplant was through a high-power laser to melt down thin layers of Ti-powder and developed the framework successively.

3D printing had a transformative effect on hearing aid production also. Today, 99% of hearing aids that suitably fit into the ear are custom-made by using any of 3D printing technologies. Each person's ear canal is shaped differently from others, and the use of 3D printing technology allows custom-shaped devices to be produced efficiently with low cost and no time [68]. 3D-printed modified hearing-aids to the

market were facilitated because Class I medical devices for external use are subject to fewer regulatory restrictions. Envisaging braces are another successful commercial use of 3D printing, with 50,000 printed every day [70]. These clear, removable, 3D-printed orthodontic braces are custom-made and unique to each user. This product provides an excellent example of how 3D printing can efficiently and profitably make single, customized, intricate items at a relatively low cost and less time [70].

3D printing technologies have made researchers and industries to make highly customized prosthetic design and produce limbs at incredibly more affordable price for those who are lacking money and direct reach to the big cities. At present in the market prosthetics cost you a huge chunk of money. In the US market, it may cost a family anywhere from 5000 to 50000 dollars, causing a significant financial burden. Moreover, prosthetics need to be custom fit to the individual requirements, which demands additional production time of a few weeks to a few months. The ease of availability and operation of 3D printers offers the ability to a person to design and print customized parts, all of which have made prosthetics radically more affordable and accessible to the required people around the globe. Manmade hands and arms are some of the most commonly accepted 3D-printed prosthetics. Ivan Owen was designed a bionic hand in 2011 and he shared his experience and made the files open for others to print and distribute the same. His efforts and experience led to creating the e-NABLE Community through volunteers from a global network of 3D printing to develop in printing and designing prosthetic hands. These hands tend to cost only $50 compared with thousands of dollars which these individuals would have to pay. More technically challenging, Limitless Solutions has begun clinical trials for their 3D-printed prosthetic arms. These arms use muscle-flexing in the remaining portion of the arm, detected by leads attached to the skin, to guide the prosthetic movement. These arms are cost around $1000, which is a tenth of the typical $10,000 price point [71] (see Fig. 6).

6.3 Dental

The first few engineering applications of 3D printing were in the arenas of quick-tooling and instant-prototyping (see Fig. 7). Thus, its use in dentistry, where particular, custom-made objects were mass-produced, was an obvious next step in the flight of 3D printing technology. 3D printing applications in dentistry have helped in various ways, from orthodontics to general dentistry. Various dental areas integrating 3D printing technology are producing customized and accurate braces, castable crowns, dental restorations, dental bridges, denture frameworks, and bases. 3D printing technologies in the field of medicine had helped the dental health field to offer convenient chair-side care with a cheaper controlled treatment plan. It also reduces the waiting time due to avoiding molding step and the feature with high resolution can be printed directly. Another important aspect of 3D printing in dentistry is its easy adoption into

Fig. 6 14-year-old Sudanese Daniel Omar is fitted with a 3D-printed prosthetic. *Source* The Guardian [71]

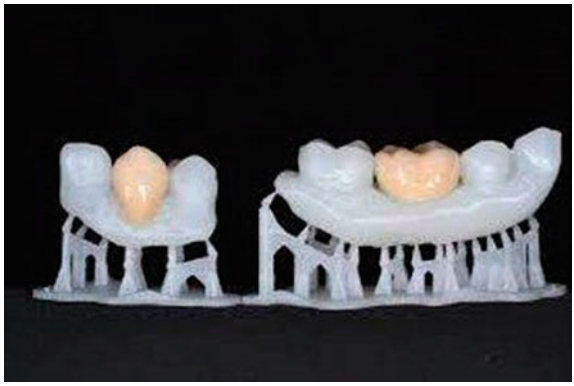

Fig. 7 3D-printed teeth in a reference model. (*Source* https://dental.formlabs.com)

a clinic, laboratory, or dental office. Speedy and accurately designed and developed solutions are critical to this application, and 3D printing in medicine does just what it requires.

Nowadays, by connecting oral-scanning, CAM/CAD design, and printing procedure, dental labs can rapidly and accurately yield various appliances, like pinnacles, connections, bandage/pebble models. In addition to that variety of orthodontic utilizations for instance, medical guides and aligners have been developed. In the place of painful imitations, a 3D scan is taken instead, later this 3D scan converted into a 3D prototypical and sent to a 3D printer to get the final print. 3D-printed prototypical can be used to generate a variety of orthodontic applications, distribution and positioning salvers, clear aligners, and retainers. Interestingly, the printed models can be conveniently stored digitally in the form of CAD (computer-assisted design) files.

This technique allows one to digitize the entire workflow, radically accelerating the construction time and considerably increasing the manufacturing capacity. Besides that, it allows one to eradicate the necessity of physical impressions and storing of replicas.

Today, there are various 3D printers are accessible in the market for both research and commercial purposes of dental and orthodontics. Besides 3D printing giant Stratasys (i.e., Stratasys for the 3D world [72]), there are various smaller companies or ventures available in the market such as Zenith 3D Printing Systems [73], Envision [74], AXSYS, Valplast, and many more. It is worth mentioning that the first FDA-certified 3D-printing material [75] and a new material (i.e., bio-ink) that kills bacteria [77] have been developed in recent years. 3D printed surgical-guides find their potential applications in dental practice, but remained unnoticed [79]. To highlight numerous low-cost printer for small, medium, and more extensive dental labs and clinics with unique accessible operation have been developed for both demonstration and serious medical facilities. The new materials that secure complete applications of 3D printing in dentistry need to be developed for constant growth of the field and applications. These 3D printers are in trend across the USA and will undoubtedly be followed by rest of the countries around the globe. Interestingly, the first, to the best of our knowledge, liability case concerning 3D printing (of dental aligners) has been submitted to a court in California [80].

6.4 3D Printing of Tissues, Organoids, and Tissue Regeneration

Manufacturing humanoid tissue by 3D printing is an exciting yet relatively untapped, flourishing area of potential applications [81–84]. 3D bio-printing envisages to reduce the shortage of supply of the critical organs in the donor market. This is incredibly applicable and exciting to the field of transplantation, as it solves any ethical and moral issues that may be tied to traditional transplant methods. It also increases acceptance as customized organ development utilizes the patient's cells. Skin tissue reconstruction and repair, kidney transplantation, heart transplantation, and limb replacement among others are being successfully attained through 3D printing technology in recent years. Bone and muscle repairs also have been possible with 3D printing in medicine with orthopedic implants. Being able to 3D print tissue cells and organs has promoted research work for diseases, like cancer to study how tumors grow and develop, with the intent to find a cure.

The critical application of lab-on-a-chip, i.e., exVive3D Liver, is a high-yield 3D-bioprinted tissue prototypical tool for scientific exploration, medicine finding, and toxicology [85], which has proposed in recent years. In recent times, the possibility of bio-printing using stem cells has unlocked new possibilities in this realm [84]. The very-first bio-ink [86] is offered by the Swedish startup company CELL-Ink [87]

and the American stem-cell company Rooster Bio [88]. Reasonable and consistent ingredients such as cell-friendly biomaterials are the fundamental requirements for a structure to be 3D printed. Uniform tissues, for instance, skin cells (printing skin cells on burn wounds), muffled and intricate solid organs, for example, a liver [90], have been printed through 3D printers using suitable bio-materials. Researchers from Chinese academy reported 3D bio-printing of the kidney (How do they 3D print kidney in China [91]), ears, and livers [92]. Although much progress is still required to make them implantation ready, preliminary studies on bio-printing of hard tissues such as bones (CT-Bone®: actual bone produced through 3D Printer [93]) and soft tissues such as cartilage and muscles [94] and other tissues have consistently been conducted to better understand their printing behaviors. Also, there is a novel thrilling substance, called self-healing bio-glass, that can be 3D printed and be used a cartilage replacement [95]. Recently, Atala and co-workers stated that the building of a combined tissue–organ printer (ITOP) can construct stable, human-scale tissue constructs of desired shape/size. The competencies of the ITOP are demonstrated by constructing jawbone and calvarial bone, cartilage, and skeletal muscle [96].

Plenty of 3D bio-printers introduced in the past decade, a low-cost bio-printer, by the Swedish startup CELL-Ink was displayed, which costs about 5000 $ for the less expensive model, and about 9000 $ for the more sophisticated version [97]. This printer allowed CELL-Ink to achieve remarkable outcomes, and it comprises of about 98% of alive cells when using their bio-ink in 3D printer. Not precisely a bio-printer but a tool called Bio-pen allowed surgeons to mending spoiled bone and cartilage by "sketch" new cells directly onto bone. This procedure could be conducted in the middle of a surgical process (see Fig. 8) (BioPen to redraft orthopedic implants surgery [98]). 3D-printed organs for replacements are still far away to grasp. Researchers from China, Xu Mingen, developer of the "Regenovo" bioprinter, projected that completely serviceable 3D-printed human organs are likely to develop in the time span of 20 years [99].

3D bio-printing has evolved as an effective tool to develop implants that accelerate bone regeneration under both *in-vitro* and *in-vivo* conditions [100–102]. The unmatchable attributes and technical capability of 3D printing create high resolution, repeat, and ordered porous scaffolds from a wide variety of materials (which include most of the metals, ceramics, and polymers). Studies have identified that a porous network could be an effective promoter of bone ingrowth. Through a traditional bone filling process, it is immensely difficult to manage critical-size bone defects, which, in most of the instances, leads to significant morbidity. A traditional bone filling method might not be effective to ensure a perfect bone integration, as a coherent blood supply to the graft is critical and essential, which is difficult to achieve through traditional filling methods. Though a coherent blood supply can be maintained under vascularization, this process requires a bone to be operated multiple times, which may lead to increase the possibility of morbidity.

Fig. 8 Carrying a special healing bio-ink, a Bio-pen being used on a bone model. (*Source* credit: University of Wollongong, Australia)

6.5 Medication Dosage and Pharmacology

3D printing in the field of drug delivery can possibly streamline pharmacology and drug administration. A modest explanation for patients with manifold disorders is made possible with a 3D-printed capsule that accommodates numerous drugs at once, each with a specific release time. An exemplary idea called 'Polypill' has been tested for diabetic patients. This application deals with the medication dosage and also solves issues of a diverse drug interaction. For the patient, it removes comprehensive 24-h care of medicine intake when their medications have different schedules. 3D-printed medicines in the Polypill concept can be very cost-effective. This makes the technology available to poor, developing countries and applicable to health programs at an affordable price.

Researchers at University College London have fabricated topical drug delivery systems using 3D bio-printing [103]. They investigated fused deposition modeling (FDM) and stereolithography (SLA) for the fabrication of devices to be worn on the nose and deliver salicylic acid for the treatment of acne. The salicylic acid is loaded into commercial polymer filaments using hot-melt extrusion. 3D printing lends itself to this process, as scanned images of the patient's anatomy can be used to create devices that fit precisely, maximizing contact and delivering an even dose of the drug. They found that while both methods created suitable devices, the SLA method was more convenient as a fabrication process. The dosage can also be varied when the filaments used for printing are prepared.

To demonstrate 3D printing capacity to produce drug tablets of sufficient quality for prescriptions, Khaled et al. at the University of Nottingham attempted to print Guaifenesin Bilayer tablets (Mucinex) using a desktop 3D printer bought for under $1,000 [107]. They compared the drug release profiles for their designs and found

Fig. 9 Cube, pyramid, cylinder, sphere, and torus paracetamol tablets. Reproduced with permission [108].

that one of them showed a cumulative drug release profile that remained within 10% of the release profile of the commercial drug over a 14-h dosage cycle. They also evaluated the weight variation, hardness, thickness, and friability of the tablets they had produced. Given the new design freedom that 3D printing in pharmaceuticals provides, Goyanes et al. investigated the effect of tablets' different shapes on drug-release profiles [108]. They investigated torus, pyramid, cube, sphere, and cylinder shapes using an FDM process to print paracetamol-loaded filaments of PVA. Their printed tablets are shown in Fig. 9. They first demonstrated that the stability of the drug was unaffected by the printing process. They then investigated the amount of the drug that was released in each tablet and showed, as expected, a clear dependence on the surface area to volume ratio. They state that these complex geometries would be impossible to fabricate using traditional powder compaction methods and better control drug-release profiles.

A precise control over the amount of drug release is important for transdermal applications, as a high dose might perforate the skin tissues or may lead to skin infection. The natural distribution network of skin serves as a medium for the sustained release of a multitude of transdermal drugs molecules [104]. Presently, transdermal drugs are delivered through patches, which cover a large area of skin to enhance the effectiveness of the drug. A continuous drug delivery through patches can be provided to the upper layer of epidermis. On the other hand, a micro-needle array penetrates the upper layer of skin without affecting its integrity is effective and promising approach. In the context of transdermal drug delivery, 3D printing can offer an advantage in developing simple and complex patches or micro-needle arrays structures. The complex structure of patches or arrays is designed to allow drug release at different rates [105]. 3D printing techniques, for instance, SLA, have previously been employed to print micro-needle arrays with a high degree of precision with a wide variety of materials [106].

6.6 Manufacturing of Surgical Tools and Medical Metal Materials

Biomedical materials, hard metals (e.g., Ti), various kinds of materials, such as thermoplastic, elastomeric polymers, for instance polystyrene, PLGA and PDMS, hydrogel, and oxide materials, have been largely employed to generate permanent transplants or accepted as matrix substrates in 3D-printing technologies [109]. Metal materials that are used in medical field are mostly used to develop fixed implants, for instance, orthopedic or dental implants that are made of several metal alloys. For example, stainless steel, cobalt–chromium alloy, titanium alloy, and tantalum alloy. These alloys in diverse chemical compositions exhibit good bio-compatibility and meet most of the medical standards.

Various surgical devices and medical tools can be created with 3D-printed technology, where mainly metal or metal alloys are employed as the base materials. 3D-printing tools include forceps, scalpel handles, sterile tools, clamps, hemostats, and many more. 3D-printed products are having high purity with low cost (almost 1/10 times) than that of stainless steel tool equivalents. This technology is explicitly fascinating to design specific tools in a unique size and shape as needed.

Biomedical metal materials that are produced using 3D-printed technology have many benefits over conventional implants. 3D-printed biomedical metal transplants are known to have enhanced mechanical attributes with small grains over other non-metallic materials. Moreover, an extremely organized printing environment ensures a good quality of the printed portions, thus preserving the required attributes of the printing materials. In addition to that, the design complication of 3D-printed custom-made products can be reduced, permitting customization of implants with mechanical performances that are akin to those of natural bone. Several surface treatments techniques, such as chemical alteration, electrochemical plating, and alkali-metal heat treatment, are generally carried out to augment the bio-activity of the metal implants. As a part of the biomedical metal 3D-printing value chain, the heat treatment can concomitantly tailor both biocompatibility and mechanical properties of the implant. A highly hydrophobic, rough surface is generally obtained through SLM (selective laser melting) and to acquire an extremely consistent surface heat-treatment process is much essential. Surface feature analysis unveiled that the hardness and Young's modulus are the prerequisite to resisting cracking and fatigue of the implant. Besides that, the biocompatibility of the implant improved significantly after heat treatment, as revealed by cell proliferation analysis, where an enhanced cell adhesion and even spreading was observed after heat treatment [110]. Thus, 3D-printed biomedical materials (i.e., metal implants) with successive thermal treatment is a useful process for attaining desirable physicochemical properties with low cost and improved cyto-compatibility. Countless biomaterials have been developed for medical applications because of the cytotoxic properties of aluminum or vanadium or a combination thereof (e.g., Ti_6Al_4V) in common porous scaffolds. For instance, the metal alloys (e.g., titanium-niobium metal alloy) are more valuable materials for

biomedical applications owing to their very low Young's modulus, exceptional biocompatibility, high-strength, and low-cytotoxic element content [111]. To further decrease the elastic modulus and to minimize stress shielding's adverse impact, tantalum can be added as a stabilizing element in the scaffold of titanium [112]. The composites of titanium–tantalum that is made via selective laser melt exhibit a higher strength and lower elastic modulus than that of titanium–aluminum alloys. Sing et al. developed a regression analysis method to prove the feasibility of titanium–tantalum cellular lattice structures in laser-manufactured porous scaffolds [113]. The process parameters are pivotal and can greatly affect the dimensional precision and mechanical properties of titanium–tantalum alloy lattice structures. Researchers also used the SLM technology to solve the problem of processing complicated constructions, while maintaining titanium–tantalum alloys' key properties, i.e., superelasticity and shape memory [114]. A special Ni–Ti unit cell shows compression properties within the range of cortical and trabecular bone and shows improved fatigue life. Owing to its relatively low corrosion potential, magnesium (Mg) metal has also been examined as an excellent option for implants. Owing to its ability to entirely degrade in the body and its Young's modulus, which is also similar to the natural bone Mg, it minimizes the stress-shielding effect [115]. Mg is one of the most vital components of the human body, it helps to enhance bone cells' proliferation and differentiation. Since copper has a well-known antimicrobial activity and promotes metabolism, other novel antibacterial alloys of copper (e.g., Co-Cr-W-Cu) with intriguing mechanical properties and biocompatibility have been further designed to solve bacterial infection or inflammations. Lu et al. [116] investigated the role of copper metal to influence the properties of cobalt–chromium-based alloys, which are extensively used in orthopedics and dentistry.

7 Potential and Major Limitations

3D printing for biomaterials and tissue engineering applications is a relatively new aspect and it has opened tremendous possibilities of biomimicry and tissue regeneration. Biomimicry plays a vital role in screening drugs, regenerative medicine, and understanding pathology [118]. 3D-printed biomimetic microfluidic chips have a great potential to conduct drug screening tests instead of conducting animal studies.

Each of the 3D printing techniques has a different requirement for the bio-ink and has their own limitations. For example, inkjet-printing technique offers high-resolution and accurate cell positioning. However, it compromises with the structural integrity due to the requirement of a relatively low concentration of bio-ink. Yet, inkjet printing has shown great success in developing skin and neural tissues [121].

Current research demonstrates that the combination of more than one technique could be a feasible and efficient solution to the complex manufacturing and printing processes [119]. For instance, a combination of ink-jet and laser-assisted 3D printing technique could provide the desirable combination for producing a scaffold, which consists of both physiologically relevant proportions as well as supports viable cells.

A new aspect of 3D printing for biomedical applications is its potential to prevascularization (which recently emerged as a promising concept in tissue engineering to perform microvasculature in tissue constructs prior to their implantation) [120]. Prevascularization is important to mitigate the possibilities of necrotic failure of the implants. 3D printing of bio-materials shows a great potential in constructing neural networks within large structures [121].

The apparent advantages of 3D printing technology enabled the researchers to improve the existing medical tools/techniques and allowed them to explore new material systems that are incompatible with traditional printing processes. This technology has already been reached a significant and exciting level; however, the revolutionary application, such as bio/organ printing [122], demands more time and extensive research and development to evolve. In the field of medical or bio-printing applications, 3D printing technology is severely challenged by a number of limitations, for example, high cost, incompatibility with most of the common materials, slow printing speed, not environmental benign, excessive dependence on the plastic materials. Another fundamental issue with 3D-printed bio-materials is the vasculature of the printed tissues. 3D-printed tissue requires a constantly supply of oxygen and nutrients to sustain. Diffusion of oxygen and nutrients by itself will only occur up to a thickness of 150 μm, above this thickness, the tissue will not develop uniformly.

References

1. Shohet IM, Lavy S (2004) Healthcare facilities management: state of the art review. Facilities 22:210–220
2. Krafts KP (2010) Tissue repair the hidden drama. Organogenesis 6:225–233
3. Boneva RS, Folks TM, Chapman IE (2001) Infectious disease issues in xeno-transplantation. Clin Microbiol Rev 14:1–14
4. Stevens S (2017) Synthetic biology in cell and organ transplantation, Cold Spring Harb Perspect Biol 9:a029561
5. Tang H, Shen Z, Hou M, Wu L (2017) Autotransplantation of mature and immature third molars in 23 Chinese patients: a clinical and radiological follow-up study. BMC Oral Health 17:163
6. Platt JL, Cascalho M, Piedrahita JA (2019) Xenotransplantation: progress along paths uncertain from models to application. ILAR J 59:286–308
7. Erlbaum C (2018) Xenotransplantation: the science, the advantages, the ethics. Sc J Lander Coll Arts Sci 12:53–58
8. Mao AS, Mooney DJ (2015) Regenerative medicine: current therapies and future directions. PNAS 112:47
9. Hueso M, Navarro E, Sandoval D, Cruzado JM (2019) Progress in the development and challenges for the use of artificial kidneys and wearable dialysis devices. Kidney Dis 5:3–10
10. Khan S, Jehangir W (2014) Evolution of artificial hearts: an overview and history. Cardiol Res 5:121–125
11. Moraes C, Mehta G, Lesher-perez SC, Takayama S (2012) Organs-on-a-chip: a focus on compartmentalized microdevices. Ann Biomed Eng 40:1211–1227
12. Ventola CL (2014) Medical applications for 3D printing: current and projected uses. P & T 39:704

13. Ngoa TD, Kashania A, Imbalzanoa G, Nguyena KTQ, Huib D (2018) Additive manufacturing (3D printing): a review of materials, methods, applications and challenges. Compos B 143:172–196
14. Ghilan A, Chiriac AP, Nita LE, Rusu AG, Neamtu I, Chiriac VM (2020) Trends in 3D printing processes for biomedical field: opportunities and challenges. J Polym Environ 28:1345–1367
15. Butscher A, BohnerM DoebelinN, Hofmann S, Müller R (2013) New depowdering-friendly designs for three-dimensional printing of calcium phosphate bone substitutes. Acta Biomater 9:9149–9158
16. Saunders RE, Gough JE, Derby B (2008) Delivery of human fibroblast cells by piezoelectric drop-on-demand inkjet printing. Biomaterials 29:193–203
17. Derby B (2012) Printing and prototyping of tissues and scaffolds. Science 338:921
18. Castro NJ, Meinert C, LevettP HDW (2017) Current developments in multifunctional smart materials for 3D/4D bioprinting. Curr Opin Biomed Eng 2:67–75
19. Montero FE, Rezende RA, Silva JVL, Sabino MA (2019) Development of a smart bioink for bioprinting applications. Front Mater Eng 5:56
20. Wohlers T, Gornet T (2014) History of additive manufacturing, Wohlers Report
21. Kruth JP, Wang X, Laoui T, Froyen L (2003) Lasers and materials in selective laser sintering 23:4
22. Hoy MB (2013) 3D printing: making things at the library. Med Ref Serv Q 32:1
23. Gross BC, Erkal JL, Lockwood SY (2014) Evaluation of 3D printing and its potential impact on biotechnology and the chemical sciences. Anal Chem 86:3240–3253
24. Anthony KA, Wilson H, Lisa FH, Albert F (2016) 3D-Printed microfluidics. Angew Chem 55:3862
25. Mironov V, Boland T, Trusk T, Forgacs G, Markwald RR (2003) Organ printing:computer-aided jet-based 3D tissue engineering. Trends Biotechnol 21:157–161
26. Boland T, Mironov V, Gutowska A, Roth EA, Markwald RR (2003) Cell and organprinting 2: fusion of cell aggregates in three-dimensional gels. Anat Rec A Discov Mol Cell Evol Biol 272:497–502
27. Mironov V (2003) Printing technology to produce living tissue. Expert Opinion Biol Therapy 3:701–704
28. Jakab K, Neagu a, Mironov V, Forgacs G, (2004) Organ printing: fiction or science. Biorheology 41:371–375
29. Jakab K, Neagu A, Mironov V, Markwald RR, Forgacs G (2004) Engineering biological structures of prescribed shape using self-assembling multicellular systems. Proc Natl Acad Sci USA 101:2864–2869
30. Ozbolat IT, Moncal KK, Gudapati H (2017) Evaluation of bioprinter technologies. Addit Manuf 13:179–200
31. Fleming PA (2010) Fusion of uniluminal vascular spheroids: A model for assembly of blood vessels. Develop Dyn 239:398–406
32. Jakab K, Damon B, Neagu A, Kachurin A, Forgacs G (2006) Three-dimensional tissue constructs built by bioprinting. Biorheology 43:509–513
33. Jakab K (2008) Tissue engineering by self-assembly of cells printed into topologically defined structures. Tissue Eng Part A 14:413–421
34. Mironov V (2009) Organ printing: tissue spheroids as building blocks. Biomaterials 30:2164–2174
35. Neagu A, Jakab K, Jamison R, Forgacs G (2005) Role of physical mechanisms in biological self-organization, Phys Rev Lett 95:178104
36. Norotte C, Marga FS, Niklason LE, Forgacs G (2009) Scaffold-free vascular tissue engineering using bioprinting. Biomaterials 30:5910–5917
37. Noor N, Shapira A, Edri R, Gal I, Wertheim L, Dvir T (2019) 3D printing of personalized thick and perfusable cardiac patches and hearts. Adv Sci 11:19003434
38. Munaz A, Vadivelu RK, John JS, Barton M, Kamble H, Nguyen NT (2016) Three dimensional printing of biological matters. J Sci: Adv Mater Devic 1:1–17

39. Helguero CG, Mustahsan VM, Parmar S (2017) Biomechanicalproperties of 3D-printed bone scaffolds are improvedby treatment by CRFP. J Orthop Surg Res 12:195
40. Garcia J, Yang Z, Mongrain R, Leask RL, Lachapelle K (2017) 3D printing materials and their use in medicaleducation: a review of current technology and trends for the future. BMJ Simul Technol Enhanc Learn 4:27–40
41. Asadi-Edyvand M, Solati-Hasjin M, Farzad A, Osman NAA (2015) Effect of technical parameters on porous structure and strength of 3D printed calcium sulfate prototypes. Robot Comput-Integr Manufact 37:57–67
42. Mannoor MS, Jiang Z, James T (2013) 3D printed bionic ears. Nano Lett 13:2634–2539
43. Vukievic M, Mosadesgh B, Little JK, Little SH (2017) Cardiac 3D printing and its future directions, JACC Cardiovasc Imaging 10:171–184
44. Soon DSC, Chae MP, Pilgrim CHC, Rozen WM, Spychal RT, Hunter-Smith DJ (2016) 3D haptic modeling for preoperative planning of hepatic resection: a systematic review. Ann Med Surg 10:1–7
45. Abudayyeh I, Gordon B, Ansari MM, Jutzy K, Stoletniy L, Hilliard A (2017) A practical guide to cardiovascular 3D printing in clinical practice: overview and examples. J Interv Cardiol 31:375–383
46. Cantinotti M, Valverde I, Kutty S, Eckert J (2016) Three dimensional printed models in congenital heart disease. Int J Cardiovascuol Imag 33:137–144
47. Kurenov SN, Ionita C, Sammons D, Demmy TL (2015) Free-dimensional printing to facilitate anatomic study, device development, simulation, and planning in thoracic surgery, J Thorac Cardiovasc Surg, 149:973–979
48. Jeon H, Kang K, Park SA (2017) Generation of multilayered 3D structures of HepG2 cells using a bio-printing technique. Gut and Liver 11:121–128
49. Randazzo M, Pisapia JM, Singh N, Awani JP (2016) 3D printing in neurosurgery: a systematic review. Surg Neurol Int 7:801–809
50. Lino H, Igawa K, Kanno Y (2009) Maxillofacial reconstruction using custom-made artificial bones fabricated byinkjet printing technology. J Artif Organ 12:200–205
51. Huang W, Zhang X (2014) 3D printing: print the future of ophthalmology. Invest Opthalmol Vis Sci 55:5380–5381
52. Crafts TD, Ellsperman SE, Wannemuehler TJ, Bellicchi TD, Shipchandler TZ, Mantravadi AV (2017) Thrree-dimensional printing and its applications in otorhinolaryngology-head and neck surgery. Otolaryngol-Head Neck Surg 156:999–1010
53. Chae MP, Rozen WM, McMenamin PG (2015) Emerging applications of bedside 3D printing in plastic surgery. Front Surg 16:25
54. Williams C, James A, Chae MP, Hunter-Smith DJ (2015) 3D printing in clinical podiatry: a pilot study and review. J Foot Ankle Res 8:41
55. Guilbert N, Mhanna L, Didier A (2018) Integration of 3D printing and additive manufacturing in the interventional pulmonologist's toolbox. Respir Med 134:139–142
56. Su S, Moran K, Robar JL (2014) Design and production of 3D printed bolus for electron radiation therapy. J Appl Clin Med Phys 15:194–211
57. Zein NN, Hanouneh IA, Bishop PD (2013) Three dimensional print of a liver for preoperative planning in living donor liver transplantation. Liver Transpl 19:1304–1310
58. Soliman Y, Feibus AH, Baum N (2017) 3D printing and its urologic applications. Urology 17:20–24
59. Hangge P, Pershad Y, Witting AA, Albadawi H, Oklu R (2018) Three-dimensional (3D) printing and its applications for aortic diseases. Cardiovascul Diagnos Therapy 8:19–25
60. Tanaka T, Shimada Y, Furumoto H, Makino Y, Kudo Y, Maehara S, Hagiwara M, Kakihana M, Kajiwara N, Ohira T, Ikeda N (2021) Comparative analysis of results of video assisted thoracic surgery lobectomy simulation using the three-dimensional-printed biotexure wet-lung model and surgen's experience, Interact Cariodvasc Thorac Surg 32(2):284
61. Ramly EP, Kantar RS, Diaz Siso JR, Alfonso AR, Rodriguez ED (2019) Computerized approach to facial transplantation: Evolution and application in 3 consecutive face transplants, Plastic and Reconstructive Surgery-Global Open 7:e2379

62. Healy PJ, McDonald R, Waldhausen JHT (2000) Transplantation of adult living donor kidneys into infants and small children. Arch Surg 135:1035–1041
63. Wood K, Keys T, Mufarriji P, Assimos DG (2011) Impact of Stone Removal on Renal Function: A Review. Review in Urology 13:73–89
64. Dodziuk H (2016) Applivations of 3D printing in healthcare, Cardiochir Torakochirurgia Pol. 13(3):283
65. Duncan JM, Nahas S, Akhtar K, Daurka J (2015) The use of a 3D printer in pre-operative planning for a patient requiring acetabular reconstructive surgery. Journal of Orthopedics Case Report 5:23–25
66. Klein GT, Lu Y, Wang MY (2013) 3D printing and neurosurgery-ready for prime time? World Neurosurgery 80:233–235
67. Hoy MB (2013) 3D printing: making things at the library. Medical Reference Service Quarterly 32:94–99
68. Banks J (2013) Adding value in additive manufacturing: Researchers in the United Kingdom and Europe look to 3D printing for customization. IEEE Pulse 4:22–26
69. Bartlett S (2013) Printing organs on demand, The Lancet. Respir Med 1:684
70. Lipson H (2013) New world of 3-D printing offers "completely new ways of thinking:" Q & A with author, engineer, and 3-D printing expert Hod Lipson. IEEE Pulse 4:12–14
71. Daniel, (2014) The Future of Prosthetics, Project Daniel at Not Impossible Lab (www.notimpossible.com)
72. Stratasys for 3D world, (2016) Object30 Ortho Desk (https://www.stratasys.com)
73. Zenith3d 2016 (www.zenith3d.co.kr/eng/)
74. EnvisionTEC Digital Dentistry, (2016) (envisiontec.com/3d-printing-industries/medical/dental/)
75. Lee J, (2015) FDA approves 3D printable denture base material
76. (https://www.dentalproductsreport.com/view/fda-approves-3d-printable-denture-base-material)
77. TothD, (2015) New 3D-printed teeth also kill bacteria
78. (https://www.dentalproductsreport.com/view/new-3d-printed-teeth-also-kill-bacteria)
79. Valluri A, (2019) 3D designs, 3D printing case studies, 3D software (https://www.think3d.in/3d-printed-surgical-guides/)
80. Kain C R M, Price J M, Reilly P H, (2015) Five of the top drug & device developments (http://www.faegrebd.com/five-of-the-top-drug-device-developments-in-2015)
81. Murphy SV, Atala A (2014) 3D bioprinting of tissues and organs. Nat Biotechnol 32:773–785
82. Atala A, Yoo J J, (2015) Essentials of 3D biofabrication and translation, Elsevier (eds), Amsterdam
83. Chua CK, Yeong WY (2015) Bioprinting: Principles and applications. World Scientific Publishing, Singapore
84. Hildreth C, (2015) How 3D printing with stem cells will alter the future of medicine (https://bioinformant.com/what-if-3d-printing-was-100x-or-1000x-faster/)
85. Speights K, (2016) Will 2016 Be Organovo Holdings, Inc.'s Best Year Yet? 3 reasons this 3D bioprinting company might be in for a happy new year (http://www.fool.com/investing/general/2016/01/13/will-2016-be-organovo-holdings-incs-best-year-yet.aspx)
86. Frederick M, (2015) RoosterBio Inc. Launches Industry's First Ready-to-Print Stem Cell Product, PRWebebook (http://www.prweb.com/releases/2015/10/prweb13027227.htm)
87. Cellink life sciences, (2016) Cellink featured in business insider: Sweden's hottest biotech startup is now 3D printing tumors to help cure cancer (https://www.cellink.com/cellink-featured-business-insider-swedens-hottest-biotech-startup-now-3d-printing-tumors-help-cure-cancer/)
88. RoosterBio 2016 (http://www.roosterbio.com/)
89. Printing skin cells on burn wounds, 2016 (https://school.wakehealth.edu/Research/Institutes-and-Centers/Wake-Forest-Institute-for-Regenerative-Medicine/Research/Military Applications/Printing-Skin-Cells-on-Burn-Wounds

90. Scott C, (2016) University of California San Diego's 3D Printed liver tissue may be the closest we've gotten to a real printed liver, (https://3dprint.com/118932/uc-san-diego-3d-printed-liver/)
91. How do they 3D print kidney in China 2015, (http://www.3ders.org/articles/20130815-how-do-they-3d-print-kidney-in-china.html)
92. Quigley J T, (2013) Chinese scientists are 3D printing ears and livers – With Living Tissue, (http://thediplomat.com/2013/08/chinese-scientists-are-3d-printing-ears-and-livers-with-living-tissue/, 2013)
93. CT-Bone®: real bone from the 3D Printer 2016, (www.xilloc.com/ct-bone/)
94. Herkewitz W, (2016) Incredible 3D printer can make bone, cartilage, and muscle. (http://www.popularmechanics.com/science/health/a19443/3d-printer-bone-cartilidge-andmuscle/)
95. Grunewald S J, (2016) New self-healing bio-glass may be used as 3D printed cartilage replacements, (https://3dprint.com/134070/3d-print-cartilage-replacement/)
96. Kang HW, Lee SJ, Ko IK, Kengla C, Yoo JJ, Atala A (2016) A 3D bioprinting system to produce human-scale tissue constructs with structural integrity. Nat Biotechnol 34:312–319
97. Sher D, Exclusive: (2015) CELLINK's $5,000 3D bioprinter is making the INKREDIBLE… Credible, (http://3dprintingindustry.com/news/cellink-new-3d-bioprint-er-is-making-the-inkredible-credible-56733/)
98. BioPen to rewrite orthopaedic implants surgery, (2016) (https://www.kurzweilai.net/biopen-to-rewrite-orthopaedic-implants-surgery)
99. Mingen Xu, (2013) Chinese scientists are 3D printing ears and livers – with living tissue, (http://thediplomat.com/2013/08/chinese-scientists-are-3d-printing-ears-and-livers-with-living-tissue)
100. Yang C, Wang X, Ma B, Zhu H, Huan Z, Ma N, Wu C, Chang J (2017) 3D-Printed Bioactive Ca3SiO5 Bone Cement Scaffolds with Nano Surface Structure for Bone Regeneration. ACS Applied Materials Interfaces 9:5757–5767
101. Shao H, Ke X, Liu A, Sun M, He Y, Yang X, Fu J, Liu Y, Zhang L, Yang G (2017) Bone regeneration in 3D printing bioactive ceramic scaffolds with improved tissue/material interface pore architecture in thin-wall bone defect, Biofabrication 9:025003
102. Zhang W, Feng C, Yang G, Li G, Ding X, Wang S, Dou Y, Zhang Z, Chang J, Wu C (2017) 3D-printed scaffolds with synergistic effect of hollow-pipe structure and bioactive ions for vascularized bone regeneration. Biomaterials 135:85–95
103. Goyanes A, Det-Amornrat U, Wang J, Basit AW, Gaisford S (2016) 3D scanning and 3D printing as innovative technologies for fabricating personalized topical drug delivery systems. J Control Release 28:41–48
104. Pastore MN, Kalia YN, Horstmann M, Roberts MS (2015) Transdermal patches: History, development and pharmacology. British Journal of Pharmalogy 172:2179–2209
105. Economidou SN, Lamprou DA, Douroumis D (2018) 3D printing applications for transdermal drug delivery. International Journal Pharmalogy 544:415–424
106. Pere CPP, Economidou SN, Lall G, Ziraud C, Boateng JS, Alexander BD, Lamprou DA, Douroumis D (2018) 3D printed microneedles for insulin skin delivery. International Journal Pharmalogy 544:425–432
107. Khaled SA, Burley JC, Alexander MR, Roberts CJ (2014) Desktop 3D printing of controlled release pharmaceutical bilayer tablets. Int J Pharm 461:105–111
108. Goyanes A, Martinez PR, Buanz A, Basit AW, Gaisford S (2015) Effect of geometry on drug release from 3D printed tablets. Int J Pharm 494:657–663
109. Yang Y, Wang K, Gu X, Leong KW (2017) Biophysical regulation of cell behavior-cross talk between substrate stiffness and nanotopography. Engineering 3:36–54
110. Wang M, Wu Y, Lu S, Chen T, Zhao Y (2016) Fabrication and characterization of selective laser melting printed Ti–6Al–4V alloys subjected to heat treatment for customized implants design. Progress in Natural Science: Materials International 26:671–677
111. Fischer M, Joguet D, Robin G, Peltier L, Laheurte P (2016) In situ elaboration of a binary Ti-26Nb alloy by selective laser melting of elemental titanium and niobium mixed powders. Materials Science and Engineering: C Materials for Biological Application 62:852–859

112. Sing SL, Yeong WY, Wiria FE (2016) Selective laser melting of titanium alloy with 50 wt% tantalum: microstructure and mechanical properties. Journal of Alloys and Compound 660:461–470
113. Sing SL, Wiria FE, Yeong WY (2018) Selective laser melting of lattice structures: a statistical approach to manufacturability and mechanical behavior. Robotics and Computer-Integrated Manufacturing 49:170–180
114. Speirs M, Hooreweder VB, Humbeeck VJ, Kruth JP (2017) Fatigue behaviour of NiTi shape memory alloy scaffolds produced by SLM, a unit cell design comparison. J Mech Behav Biomed Mater 70:53–59
115. Yang Y, Wu P, Lin X, Liu Y, Bian H (2016) System development, formability quality and microstructure evolution of selective laser-melted magnesium. Virtual and Physical Prototyping 11:173–181
116. Lu Y, Ren L, Wu S, Yang C, Lin W (2018) CoCrWCu alloy with antibacterial activity fabricated by selective laser melting: densification, mechanical properties and microstructural analysis. Powder Technol 325:289–300
117. Lu Y, Ren L, Xu X, Yang Y, Wu S, Luo J (2018) Effect of Cu on microstructure, mechanical properties, corrosion resistance and cytotoxicity of CoCrW alloy fabricated by selective laser melting. J Mech Behav Biomed Mater 81:130–141
118. Zhang G (2012) Biomimicry in biomedical research. Organogenesis 8:101–102
119. Kim BS, Lee JS, Gao G, Cho DW (2017) Direct 3D cell-printing of human skin with functional transwell system. Biofabrication 9:025034
120. Matthias WL, Michael DM (2016) Prevascularization in tissue engineering: Current concepts and future directions. Biotechnol Adv 34:112–121
121. Tse C, Whiteley R, Yu T, Stringer J, MacNeil S, Haycock J W, Smith PJ (2016) Inkjet printing Schwann cells and neuronal analogue NG108–15 cells, Biofabrication 8:015017
122. Ventola CL (2014) Medical applications for 3D printing: current and projected uses. Pharmacy and Therapeutics 39:704–711

Chapter 2
Characterization of Bioinks for 3D Bioprinting

Sayandeep Saha and Pallab Datta

Abstract 3D bioprinting is progressing at a rapid pace in the discipline of biomedical engineering due mainly to its ability to simultaneously process cells and biomaterials as per a pre-designed arrangement for the generation of 3D tissue constructs. Biomaterials and cells comprise the bioinks, which may contain other biologics. Ideally, a bioink should possess functionality resembling the natural tissues. Presently, there is an imperative need for high-quality bioinks, which are biocompatible and bioprintable while concurrently providing bioactives to ensure that the cells differentiate and grow uniformly. Essentially, the retention of the structural design by the 3D-printed constructs is governed by the nature and constituents of the bioink. Achieving high fidelity in the process of conversion from design to final construct depends primarily upon the thorough understanding of the rheological characteristics and biofunctionality of the bioinks. Further optimization and characterization of the bioinks for specialized tissues depend on multiple assays and image-based assessments. While the biomaterials utilized in the present era may be broadly classified into synthetic and natural, there are many other aspects to be considered before selecting compatible materials for a bioink. Here, in this chapter, we have considered the numerous existing methods of characterization of bioinks along with a brief discussion on a persistent scope for optimization.

1 Bioink Definition, Related Terms

In the modern era of tissue engineering, 3D bioprinting continues to leap towards becoming increasingly relevant. The primary reason being its virtue of ex-vivo production of definite biomimetic tissue constructs resembling the complex multicellular arrangement of specific organs, and more so because it offers a renewed

S. Saha
Centre for Healthcare Science and Technology, Indian Institute of Engineering Science and Technology (IIEST), Shibpur, Howrah, West Bengal 711103, India

P. Datta (✉)
Department of Pharmaceutics, National Institute of Pharmaceutical Education and Research (NIPER), Kolkata, West Bengal 700054, India

A. Kumar et al. (eds.), *3D printable Gel-inks for Tissue Engineering*, Gels Horizons: From Science to Smart Materials, https://doi.org/10.1007/978-981-16-4667-6_2

opportunity for producing patient-specific tissues and organs without having the requirement of external donors. Though originally intended for tissue fabrication, the tool of bioprinting finds its application in the understanding of disease biology or screening of drugs against many diseases, viz., tumour and congenital diseases [1, 2]. With its increasing global market value, more and more sophisticated approaches are being consistently taken towards shaping this technology into achieving higher translational value. A key differentiator in the outcome of a bioprinting technology is the selection of materials for forming compositions, which act as biological 'inks', or simply 'bioinks' to print constructs, which require meeting the tissue-specific characteristics.

Initially introduced alongside 'biopaper', a term used to refer bioprinted hydrogels, the concept of bioink has evolved through time. Earlier, the living cells and the cellular aggregates had to be separately added to a printed biopaper, and therefore, the definition of a bioink was only restricted to being the supplementary cellular components in a three-dimensional bioprinted hydrogel. However, with an increasing number of superior 3D bioprinting techniques, bioprinting has enabled simultaneous printing of biomaterial-based scaffolds and cells, thereby allowing complete control over several aspects of the tissue constructs such as cell distribution, resolution and scalability. Currently, bioink can be rightly defined as a formulation of cells mixed with biomaterials, typically with a biopolymer-based hydrogel, tailored precisely to provide an ideal microenvironment for cell growth, with or without the incorporation of other biologics, processed altogether under an automated biofabrication system [3]. In the majority of studies, hydrogel precursors have been used for the bioink formulation, which are either semi-cross-linked prior to the fabrication process or are ultimately cross-linked to form hydrogels in the post-fabrication process [4]. The cellular constituents may include single cells, cellular rods, aggregated cells that form spheroids, cells arranged to form minute tissues along organoids, which are material-coated cells. Depending on the application of the bioprinted constructs, additional components like nucleic acids, cytokines, growth factors, growth media or serum may be included [3].

The components of bioinks are needed to be precisely optimized to suit the parameters of the corresponding bioprinting technology as well as to achieve high print fidelity and functionality. The properties of these said bioinks are essential for the maintenance of integrity of cells in the post-printed constructs. The material properties of a bioink, its printability, its degradation profile along with rheological parameters of viscosity, elasticity and gelation kinetics influence the overall characteristics of a bioink formulation [3, 5]. This chapter provides an insight into the quantification of the various aspects, which help in characterizing the nature of a bioink and how it can influence its overall behaviour.

2 Properties of Bioinks

A bioink is usually chosen in accordance with the employed bioprinting modality, and more importantly, a bioink's characteristics are required to conform to the cell biology of the target tissue. Finding the most optimum bioprinting conditions often prove to be quite challenging, as it requires tuning of the bioprinting parameters and the bioink properties consistently. Bioinks might be produced using common or engineered biomaterials alone, or a blend of two or more biomaterials. From the perspective of compatibility, an ideal bioink has to satisfy both the biological requirements of the chosen cell type and the physical parameters involved in the process of printing itself. Physically, it should bear characteristics like that of a gel or be aptly viscous for being dispensed as an independent thread or a droplet, without requiring additional support. However, too strong a gel strength may compel the use of larger shear forces, which can primarily result in gel fracture or cause cell death inadvertently [6]. A few common physiochemical parameters upon which the character of a bioink is dependent can be generalized as:

- Rheological parameters (viscosity, shear stress, shear strain, recovery rate)
- Strength of the biomaterial(s) for shape fidelity
- Material biocompatibility and biodegradability
- Miscibility of biomaterial blends for composite bioinks
- Permeability for nutrients, oxygen and wastes
- Maintenance of suspended cells and cellular aggregates
- Homogeneity in distribution of cells and cellular components
- Gelation mechanics for shape consistency (cross-linking mechanism)
- Chemical modifications of biomaterial structure for tissue-specific needs
- Reproducibility of composition for large-scale production

For the three primary types of bioprinting modalities, namely, extrusion-based bioprinting (EBB), laser-based bioprinting (LBB) and droplet-based bioprinting (DBB), the 3D constructs are designed in a computer system using CAD-CAM (computer-aided design–computer-aided manufacturing). Since the modalities are majorly different in their mode of action, the characteristic properties of a bioink are adjusted accordingly.

2.1 Bioink for Extrusion-Based Bioprinting

EBB is the most commonly employed bioprinting technique for tissue engineering, which can accommodate various print sets with different biomaterials in its composition, thereby permitting bioprinting with a wide range of biomaterials and cells. In EBB, a typical bioink is a blend of cells, cross-linking agents and biopolymers, which are extruded by means of a nozzle or multiple nozzles (multiple head deposition systems (MHDS)) [7]. In this process, hydrogels appear to be suitable, due

to their high-water retention and cell suspension capacity [8]. Naturally occurring hydrogels (e.g. gelatin, agarose, alginate, chitosan, fibrinogen, dextran, hyaluronic acid (HA), gellan gum (GG)) share structural similarities with extracellular matrix (ECM) containing signalling molecules, which facilitate cell adhesion. Synthetically derived hydrogels [e.g. polyacrylamide, poly(2-hydroxyethyl methacrylate) (pHEMA), poly(ethylene glycol) (PEG)] are also used for their high stiffness along with decreased variation when produced in multiple batches. Since cross-linking is extremely crucial in dictating the construct stability, both the strategies of pre-cross-linking or cross-linking the post-printed construct are necessary. This can be achieved by enzymatic cross-linking, ionic cross-linking, photochemical reactions, guest–host interactions or by altering the pH and temperature conditions [9–12]. Hereof, the cross-linking ability of both naturally occurring and synthetically derived hydrogels can be improved upon the addition of certain functional groups. For example, norbornene, tyramine, thiols, aldehydes, vinyl sulfone and methacrylate groups can alter gelatin and HA stability [13]. For the constructs to achieve high-shape fidelity, the window of the cross-linking action must also take place within a definite time span.

Bioinks for EBB are ought to be shear-thinning for convenient deposition. For this, solutions containing the building components for hydrogels, i.e. precursor gels or pregels are employed, which have lower viscosities compared with the final hydrogel obtained through the process of gelation. Due to hydrophobic, hydrogen or ionic interactions between polymeric chains, pregels help to create various meshed networks. For example, gelatin and methylcellulose rheology are determined by hydrophobic bonds [14] and alginate-based bioinks employ ionic cross-linking in the presence of Ca^{2+}, wherein the Ca^{2+} concentration modulates the viscoelasticity of the bioink [15]. Since the manufacturing of common hydrogels is less expensive, it leaves room for improvement of bioactivity through ubiquitous experimentation on modifications, i.e. tunable debasement and characteristic adjustment of mechanical attributes. The biggest hindrance to this technique, however, is that the cells experience high shear forces during extrusion and therefore enduring the resisting force may cause diminished construct functionality and cell viability. Another aspect is that EBB essentially generates filaments, limiting fabrication of intricate constructs with out-of-plane attributes [16].

Hydrogel selection on the basis of a specific function involves numerous considerations like gelation time, biocompatibility, cross-linkers, bioactivity, degradation profile and mechanical behaviour. Precise geometries are required to be bioprinted, particularly for tissues, which require bearing loads (articular ligament, muscle), the "fixable" inserts (platforms supplanting infarcts, expelled tumours, injury), and those with a specialized pliable capacity (ear, skin). Construct fidelity is an important characteristic that determines the capacity of any bioink to keep up the retained structure upon extrusion for subsequent application.

2.2 Bioink for Laser-Based Bioprinting

LBB uses nanosecond (ns) lasers under a fixed wavelength (UV or close to UV) as a means of depositing the bioink over a substrate. The bioink chosen for the large spectrum of LBB-based modalities (LIFT (laser-induced forward transfer), LGDW (laser-guidance direct writing), AFA-LIFT (absorbing film-assisted laser-induced forward transfer), MAPLE-DW (matrix-assisted pulsed laser evaporation direct writing), BioLP (biological laser processing)) should have high homogeneity and permeability [17]. The biggest advantage of LBB is that the bioprinting can be carried out without the requirement of a nozzle, which means that shear stress of a nozzle is not a limiting factor for the chosen components. Thus, delicate bioinks, for example, collagen and nanohydroxyapatite mixtures containing live cells can be employed for bone construct development [18]. Biomaterials like HA are major choices for this method, enabling fabrication with high resolution and maintaining high cell viability while printing at the speed of million cells per second [19].

As a major prerequisite for this technique, the bioink must meet the fundamental properties of biocompatibility and nontoxicity. Bioinks used for LBB are usually cells suspended in a mixture of sol, and the gelling of the viscous sol is desired only in the post-printing phase. For maintenance of nontoxicity and cell survival, pH value nearing neutral (ideally 7–7.4) under a cell-friendly range of temperature is warranted. As shown by Koch et al. [20], the basic mixture of bioink prepared for LBB consists of four major components. The first constituent should offer a fitting environment alongside providing proper nutrients for cell growth (e.g. addition of blood plasma). The second component optimizes the viscosity of the bioink. The third component involves the addition of growth factors for providing the required stimulus to the cells, and the fourth component involves the addition of a cross-linker, which can be added with the second component or sprayed after the bioink is printed. Using bioinks containing collagen, alginate and HA, various LBB bioprints have been produced alongside printing cells such as bovine pulmonary artery endothelial cells (BPAECs), human dermal fibroblasts (HDFs), mouse C2C12 myoblasts, rat neural stem cells and breast cancer (MCF-7) [20–25].

The bioink should also be compatible with the wavelength used in LBB. Most research groups employ ultraviolet rays with pulse spanning from 3 to 30 ns and the wavelengths used are 193, 248, 266, 337 nm or 355 nm [26]. These are favourable for polymers capable of absorption, since an individual UV photon embodies sufficient energy for promoting chemical reactions. Therefore, it disassembles solid polymers, subsequently scattering them as gases. Under the condition of the UV wavelength being below 300 nm, there is, however, a likelihood that the cells may get damaged. Visible light has been employed as photoinitiators for digital light processing (DLP) bioprinting. For example, Wang et al. [27] used eosin Y to photo-cross-link polyethylene glycol diacrylate (PEGDA) and gelatin methacrylate (GelMA), thus generating constructs with 50 μm resolution and more than 85% viability. Lim et al. [28] also employed GelMA to generate constructs with 90% viability, while Bernal et al. [29] showed the feasibility of photo-cross-linking to generate large constructs like

bone tissue models. Therefore, through a combinatorial manoeuvring of wavelength, viscosity and cell environment, the bioink for LBB can be carefully optimized.

2.3 Bioink for Droplet-Based Bioink

DBB is one of the simplest and versatile methods of bioprinting, which can dispense cell-laden droplets through a nozzle using thermal, sonic or pneumatic actuation. DBB allows for control over volume of deposition at pre-defined spots thus providing an opportunity to fabricate heterocellular constructs encouraging structural heterocellular builds. DBB is originated from inkjet printing, which predates as early as the 1950s. Elmqvist, one of the pioneers of the innovative inkjet printing, had licensed this technology from Siemens in 1951, which was later picked up by Sweet who was associated with Stanford University at the time, and henceforth in the 1960s, the improvement of consistent and standardized print framework of inkjet methodology was initiated. In 1987, the first instance of producing printed biologics was presented by Klebe where he had utilized an industrially accessible Hewlett Packard (HP) warm DOD (drop-on-demand) inkjet printer with fibronectin and collagen bioinks [30]. A short time later, in 2000, the first 'actual' 3D bioprinter based on inkjet technology was created by Objet Geometries. Later in 2003, Boland used a DOD printer to handle living cells within a proper scaffold, and this process ushered a new method of inkjet printing [31].

The bioink used for DBB must comprise of hydrogels or growth media, which can act as a medium for loading of various biologics, like cells, nucleic acids, growth factors or drugs along with showcasing characteristics of low viscosity, adequate biodegradability, material strength and cell adherence. For the different methods of DBB, the optimization of a DBB bioink varies. For example, the DOD method forces the biomaterial droplets through a very narrow nozzle, which can result in the damage of flowing cells, and therefore, cell density needs to be adjusted accordingly along with the viscosity. The electrohydrodynamic method, on the other hand, uses an electric field to ensure the smooth flow of the bioink, thus allowing less pressure and less damage on the live cells present in it. Securing the physical and biochemical properties of a bioink from the adversities of the bioprinting process is of utmost importance. The structural integrity, porosity, bonding and the elastic tension should be maintained and the live cells present should be viable [32]. Satisfying these characteristics has limited the number of truly usable biomaterials for DBB, which include alginate, fibrin, GelMA, collagen and PEG. These biomaterials can be used to form hydrogels whose cross-linking mechanisms are compatible with the DBB modalities and can ease the restraints in the process of ejection of the bioink [33].

Some of the common bioinks developed using naturally derived and synthetically derived biopolymers during the last decade are being shown in the following table (Table 1).

Table 1 Different bioink compositions, supporting molecules and their respective modalities

Bioink composition			Bioprinting modality	Result	References
Primary biomaterial	Additional biomaterial(s)/supporting molecules/modifications	Cells			
1. Agarose • (Advantage—simple gelation • Disadvantage—low stability)	Collagen (type I) Chitosan	Human stromal cells	EBB	Addition of collagen to agarose showed higher proliferation compared with addition of chitosan	Campos et al. [34]
2. Alginate • (Advantage—good gelation and stability • Disadvantage—low cellular interaction and degradation rate)	Fibrinogen PEG	Human umbilical vein endothelial cells (HUVECs), induced pluripotent cell-derived cardiomyocytes (iPSC-CMs)	EBB	Cell viability ranging from 80 to 90% after 14 days	Maullari et al. [35]
	Gelatin	(M231) human breast cancer cells	LBB	Cell viability >85% up to a 5-day period	Kingsley et al. [36]
	Polystyrene microbeads	3T3 mouse fibroblast cells	DBB	Cell concentration influences droplet formation	Xu et al. [37]
3. Collagen • (Advantage—promotes cell interaction • Disadvantage—low mechanical stability)	Gelatin nanoparticles Fibronectin VEGF growth factor	C2C12 (mouse myoblast cells)	EBB	96% post-printed cardiomyocyte cell viability	Lee et al. [38]
	Nanohydroxyapatite	Mesenchymal stem cells (MSCs)	LBB	High levels of osteogenic regeneration	Hakobyan et al. [18]

(continued)

Table 1 (continued)

Bioink composition			Bioprinting modality	Result	References
Primary biomaterial	Additional biomaterial(s)/supporting molecules/modifications	Cells			
	Gelatin Hyaluronic acid (HA)	INS1E β (rat insulinoma cell line)	DBB	~80% cell viability	Marchioli et al. [39]
4. Dextran • (Advantage—highly functionizable • Disadvantage—wide variability in source)	Fluorescein isothiocyanate (FITC) modified dextran Hyaluronan-methacrylate (HAMA) Gelatin GelMA	C2C12, bovine chondrocytes	EBB	Cell viability with gelatin and GelMA observed 98–92% with myotube formation; Cell viability with HAMA observed 90–92% over 21 days; porosity confirmed by dextran penetration	Kessel et al. [40]
	FITC modified dextran Alginate	Induced pluripotent stem cells (iPSCs), Human umbilical vein endothelial cells (HUVECs), MC3T3-E1 (mouse preosteoblast cell line)	DBB	HUVECs observed a reduced cell viability at a pressure >10 kPa compared with an average viability of 80–85%; HUVECs s and MC3T3-E1 bioinks showed good print resolution	Grottkau et al. [41]

(continued)

Table 1 (continued)

Bioink composition			Bioprinting modality	Result	References
Primary biomaterial	Additional biomaterial(s)/supporting molecules/modifications	Cells			
5. Gelatin • (Advantage—low antigenicity and inexpensive • Disadvantage—low stability)	Alginate	Immortalized mesenchymal stem cells (iMSCs)	EBB	Cell viability >90%	Koch et al. [42]
	Norbornene (NB)	human mesenchymal stem cells (hMSCs)	LBB	Uniform cell distribution and maintenance of viability up to 7 days	Dobos et al. [43]
6. GelMA • (Advantage—low antigenicity • Disadvantage—better mechanical properties than gelatin)		Human adipose-derived stem cells (hADSCs) and human dermal microvascular endothelial cells (HDMECs)	EBB	Osteogenic differentiation confirmed by bone-specific protein expression (Col I, FN and OPN)	Leucht et al. [44]
	Alginate	NIH-3T3 fibroblasts, SH-SY5Y (Human neuroblastoma cell line) and rabbit bone marrow-derived MSCs (rBMSC)	DBB	Three cell types showed viability >80% from 24 h to 7 days	Ji et al. [45]

(continued)

Table 1 (continued)

Bioink composition			Bioprinting modality	Result	References
Primary biomaterial	Additional biomaterial(s)/supporting molecules/modifications	Cells			
		NIH-3T3 fibroblasts	LBB	Cell viability > 80% after 4 days of culture	Wang et al. [46]
7. Gellan Gum (GG) • (Advantage—good mechanical properties • Disadvantage—average tissue tolerance)	Poly(lactic-co-glycolic acid) (PLGA)	3T3 murine fibroblasts	EBB	Cell viability retained between 80 and 90% after 24 h as well as 48 h	Pitarresi et al. [47]
8. Hyaluronic acid (HA) • (Advantage—good angiogenesis and cell interaction • Disadvantage—rapid degradation)	Gelatin Glycerol Fibrinogen Polyurethane (PU)	Human epidermal keratinocytes (KCs) and human dermal fibroblasts (HDFs)	EBB	Wound reduction <40% after 14 days of subcutaneous implantation; formation of dermis and epidermis layers	Seol et al. [48]
	GelMA	Chondrocytes isolated from 6 to 12-month-old domestic pigs	LBB	Chondrogenic differentiation confirmed by expression of cartilage-specific genes COL2A1 and ACAN after 14 days of printing	Lam et al. [49]

(continued)

Table 1 (continued)

Bioink composition			Bioprinting modality	Result	References
Primary biomaterial	Additional biomaterial(s)/supporting molecules/modifications	Cells			
9. Fibrin/fibrinogen • (Advantage—fast gelation and angiogenesis • Disadvantage—rapid clogging and stability issues)	Guggulsterone/polycaprolactone–microspheres Polyvinyl alcohol (PVA)	Human iPSC-derived neural progenitor cells (NPCs)	EBB	Cell viability 90–95% from Day 1 to Day 7; expression of TUJ1, FOXA2 markers after 15 days; expression of markers GFAP, OP, NURR1, PAX6, LMX1B and TH after 30 days indicating neural tissue differentiation	Sharma et al. [50]
	Thrombin Gelatin	Pellets of 3T3 fibroblast cell line	LBB	Cell viability ~83% with adequate cell to cell interaction	Hakam et al. [51]
	Collagen Thrombin	Dermal fibroblasts and epidermal keratinocytes	DBB	Reduced contraction rapid closure of wound closure, and quick re-epithelialization	Albanna et al. [52]
10. Chitosan • (Advantage—short time of gelation • Disadvantage—high viscosity)	Glycerophosphate Hydroxyethyl cellulose Cellulose nanocrystals (CNCs)	MC3T3-E1	EBB	Significant improvement in viscosity and mechanical properties with osteogenesis and ECM formation	Maturavongsadit et al. [53]

(continued)

Table 1 (continued)

Bioink composition			Bioprinting modality	Result	References
Primary biomaterial	Additional biomaterial(s)/supporting molecules/modifications	Cells			
11. Silk fibroin • (Advantage—good mechanical stability • Disadvantage—low cell interaction)	Hydroxypropyl methylcellulose	Bone marrow mesenchymal stem cells (BMSCs)	EBB	Proliferation increased after Day 10 and cartilage-specific gene Agg, Col II) Sox 9) expression observed after Day 14	Ni et al. [54]
	PEG	Bovine MSCs	DBB	Maintenance of shape for 6 weeks; high-shape fidelity and cell viability	Li et al. [55]
	Glycidyl methacrylate (GMA)	NIH-3T3 fibroblasts, chondrocytes	LBB	Increase in cell viability till Day 14 with maximum growth in 30% Sil-MA; chondrogenic differentiation observed till 4 weeks	Kim et al. [56]
12. Hydroxyapatite • (Advantage—high biological activity • Disadvantage—high cost)	Alginate	hMSCs	EBB	Cell viability ~85% through an in vitro culture period of 3 days	Wüst et al. [57]

(continued)

Table 1 (continued)

Bioink composition			Bioprinting modality	Result	References
Primary biomaterial	Additional biomaterial(s)/supporting molecules/modifications	Cells			
	Alginate	EA.hy926 (human endothelial cells)	LBB	Cells showed high viability up to Day 11	Guillemot et al. [23]
	Bioactive glass PEGDMA	hMSCs	DBB	Cell viability >86% and high ALP activity	Gao et al. [58]
13. PEG • (Advantage—easy modification and reproducibility • Disadvantage—low mechanical strength)	GelMA Polycaprolactone (PCL)	Rabbit bMSCs	EBB	Cells showed osteogenic and chondrogenic differentiation	Qiao et al. [59]
	GelMA	hMSCs	DBB	Cell viability > 80%; chondrogenic and osteogenic differentiation confirmed by expression of specific genes and analysis of protein expression	Gao et al. [60]
14. PCL • (Advantage—good mechanical property • Disadvantage—average cell adhesion)	HA Gelatin Heprasil Gelin-S	hMSCs	EBB	Formation of smooth muscles and cartilage observed	Ke et al. [61]
	Fibrin Pluronic F-127 Thrombin Collagen Type-1	Articular chondrocytes (rabbit)	DBB	Cell viability >80% up to a week with formation of ECM components	Xu et al. [62]

(continued)

Table 1 (continued)

Bioink composition			Bioprinting modality	Result	References
Primary biomaterial	Additional biomaterial(s)/supporting molecules/modifications	Cells			
		MG63 (human osteosarcoma cell line)	LBB	Cells proliferated after 2 weeks	Catros et al. [63]
15. Pluronic • (Advantage—functionally modifiable • Disadvantage—weak mechanical property and rapid degradation rate)	Alginate	HepG2/C3A cells (human hepatocellular carcinoma cells)	EBB	Synthesis of albumin, urea; expression of detoxifying CYP1A2 enzyme confirming liver-specific activity of the cells	Gori et al. [64]
16. pHEMA • (Advantage—allows high 0_2 and nutrient diffusion • Disadvantage—slow degradation rate)	RGD-poly-D-lysine (synthetic protein) modified	NIH-3T3 fibroblasts, primary dorsal root ganglion DRG (adult rat)	EBB	Scaffolds printed with RGD modified pHEMA formed structures resembling ganglions of DRG architecture	Badea et al. [65]

3 Characterization of Bioinks

In view of the bioprinting methods and the applicability of tissue constructs, a bioink requires satisfying multiple criteria, some of the important characterizations are discussed here.

3.1 Rheology

Rheology can be best described as the deformation experienced by a material upon application of force on it, wherein from the perspective of 3D bioprinting, the printability of the construct is governed by the corresponding rheological character of a bioink. Rheology is related to the bioink viscosity, which is consequently dictated by its concentration and molecular weight (MW) among other factors. Higher viscosity causes better print fidelity but requires higher shear stress, causing cell damage. The impact of cells and cellular components on rheological properties of a bioink are also important, which is required to be studied both before and after gelation [66]. The rheological parameters that determine the polymer architecture are shear thinning, yield stress and yield recovery.

Shear thinning is an important attribute of bioinks, which is essentially a property of a non-Newtonian fluid, which does not exhibit a linear relation between shear rate and shear stress. For different forms of bioinks, such as colloidal suspensions, melts and pregel solutions, the respective mechanism of shear thinning varies. For example, in colloidal suspensions like nanosilicates and cements of calcium phosphates, the shear thinning occurs through disruptive interactions between the suspended particles, wherein the positive interaction is again reinstated when the suspension comes at rest, i.e. in the post extrusion phase [67, 68]. Whereas, in case of melts or pregels, the shear thinning occurs with the disentangling of the polymeric chains under shear stress, which are again reoriented with the secondary cross-linking [69, 70]. Shear thinning is particularly pertinent to EBB, as for an impactful extrusion phase, the shear rates and the viscosity are required to be higher and lower respectively, and a high viscosity is warranted for the post-extrusion phase to add to the shape retention.

By definition, yield stress is the force that is necessary to overcome the threshold value for deformation. This requires outweighing the surface tension, capillary force and the force of gravity offered by the weight of the filaments. Yield stress is dependent on the property of viscoelasticity of the bioink, which is again related to the elastic modulus (responsible for shape retention) and the viscous modulus (responsible for the viscosity of flow), measured through oscillatory rheology. Raising the value of yield stress improves the formation of filaments, thereby adding to the rigidity of the printed construct. However, increasing the yield stress should be monitored on the basis of the internal resistance offered by the action of cross-linking of the filaments present in the bioink so as to avoid permanent deformation and also to

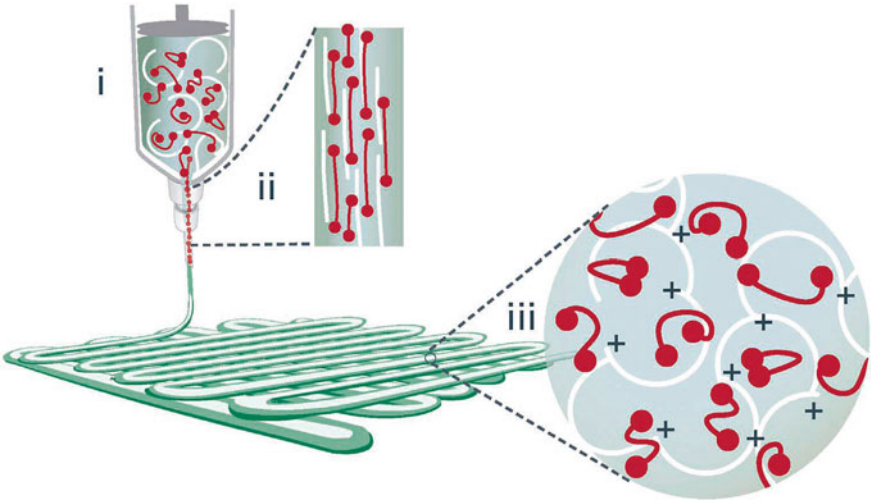

Fig. 1 Illustration of yield stress and shear thinning behaviour of gelMA/GG bioink, wherein the GG chains (represented in white) bear gel-like character prior dispensing (i) but during dispensing through the nozzle, the network between the GG chains becomes aligned and the hence the viscosity is reduced and (ii) and finally the polymeric network is again reinstated in the printed filament in the absence of shear stress, thereby solidifying the construct, reproduced with permission from [74]. Copyright John Wiley and Sons

avert cells loss. Some common materials to increase yield stress include GG, poloxamer 407, and GelMA which interact non-covalently or electrostatically with the components of the bioink, allowing for shear reversibility and increased viscosity when at rest [71, 72]. In a study, it was shown that in a PEG-Poloxamer-407-based hydrogel, an increased concentration of Poloxamer led to increased yield stress and decreased bending of the construct [73]. In another study, the influence of yield stress on shear thinning behaviour was shown using GelMA/GG bioink [74], as illustrated in Fig. 1.

Yield recovery is another aspect that determines the shape retention of the printed construct, which is again dependent upon the viscosity and the regaining of the shear modulus when the shear forces are withdrawn [75]. The dominance of either elastic modulus or the viscous modulus influences the yield recovery, wherein the prevalence of the former over the later indicates recoverable elastic deformation and the opposite indicates destructive deformation.

The rheological measurements are significant so as to control the arrangement of the platform structure. By employing mathematical models to derive data from a rheometer, the properties of flow behaviour, extent of shear thinning, yield stress and recovery and its effect on the cell viability of a bioink can be determined. Rheological studies enable optimization of material properties, which impacts the printability of the construct and the subsequent time for its fabrication [76].

3.2 Printability

Printability is a broad term that encompasses multiple parameters involved in the process of bioprinting to render a bioink "printable". These involve gelation strategies, time consumed by the printing process, cell feasibility and needle measurements [3]. The inspection of the significance of printability has led to many different iterations of its interpretation. For example, Atala and Murphy [77] have defined printability to be "the properties that facilitate handling and deposition by the bioprinter", while Noh and Gopinathan [78] depict printability to be reliant on, "the different parameters such as viscosity of the solution, surface tension of the bioink, the ability to cross-link on its own and surface properties of the printer nozzle". On the basis of multiple perspectives, a basic interpretation of printability can be comprehended as the potential of a biomaterial to produce a satisfactorily 3D-printed scaffold, depending upon its proper optimization suiting the different conditions of bioprinting. A wide assortment of tests have been practised by researchers to investigate the aspects of printability, which are, however, subjective to the type of bioink and their respective set of printing conditions. Depending upon the bioprinting modality, an analyst needs to essentially map the framework of the last build to remember for their distribution and repeat the process with alterations, thereby utilizing grouping frameworks to achieve conceivable printing outcomes. By characterizing the last construct, the print fidelity can be regularly improved by regulating the viscous flow and rigidity of bioink by modulating the degree of cross-linking between the nanofibers in the framework, which may influence cell growth [79].

There are multiple forums for the evaluation of printability, which encompasses the examination of the rheology and filament formation and its role in formation of multi-layered structures adding to the shape fidelity. For instance, in EBB, all the settings involving bioprinting incorporate feed rate, feed pressure, way plan, needle length, temperature and numerous other aspects. By providing a quantitative aspect to printability, it may be drastically impactful in bioink improvement. As shown by Schwab et al. [80], for rheological evaluation, multiple mathematical models are being used to empirically derive the shear thinning behaviour, based on the rheometer-derived data of viscosity under respective shear rates. Since most bioinks are time-independent, the most popular model is based on the Ostwald-de Waele equation, more commonly known as the 'power law' represented as:

$$\eta = k\dot{\gamma}^{n-1} \tag{1}$$

where η represents viscosity, k represents a constant of consistency index, n represents the behaviour index (shear thinning index) and $\dot{\gamma}$ represents shear rate. The behaviour index is determined by the nature of the fluid. For shear-thinning liquids, the value of n should ideally range between 0 and 1 ($0 < n < 1$), whereas for shear thickening liquids, the value of n should exceed 1 ($n > 1$) and for Newtonian fluids, the value of n should ideally be 1 ($n = 1$). k could be measured when the values of the other variables are unchanged. The velocity during the process of bioink dischargement can be calculated using Eq. (2).

$$\tau = \left(\frac{\delta v}{\delta r}\right)^{n} \tag{2}$$

where n is calculated from Eq. (1) as the parameter for shear-thinning, τ represents the shear rate, the velocity of the fluid discharge and the needle radius is represented by v and r, respectively. Due to the proportionality between shear stress, applied pressure and nozzle radius, the extrusion velocity for a large number of materials under respective printing conditions can be evaluated through the following (Eq. 3).

$$v = \frac{n}{n+1}\left(\frac{\Delta p}{2Lk}\right)^{\frac{1}{n}}\left(R^{\frac{n+1}{n}} - r^{\frac{n+1}{n}}\right) \tag{3}$$

where Δp represents the change in capillary pressure, L represents capillary distance of the flow, R represents the radius of the outer needle, r represents the flow radius. For a range of needle geometries and printing pressures, the average extrusion velocity can be calculated as

$$\dot{v} = \left(\frac{-\Delta p}{2Lk}\right)\left(\frac{n}{3n+1}\right)R^{\frac{n+1}{n}} \tag{4}$$

Under specific extrusion parameters such as the use of co-axial nozzle as shown by Yu et al. [81], the mathematical models may become modified, for example, the shear rate (τ) while using a coaxial nozzle can be represented as:

$$\tau = \left(-\frac{\Delta P}{L}\right)\frac{R}{2}\left(\xi - \frac{\lambda^2}{\xi}\right) \tag{5}$$

where ξ represents the ratio between r and R, λ represents a constant that locates the spot of maximum velocity of flow whose value depends on the parameter n from Eq. 1 and σ, defined as $r_{\min}$/R. The value of $-\Delta$P/L can be obtained by the following equation:

$$-\frac{\Delta P}{L} = \frac{Q}{\left(\frac{n\pi R^3}{3n+1}\right)\left(\frac{R}{4k}\right)^{\frac{1}{n}}\left\{\left(1-\lambda^2\right)^{\frac{n+1}{n}} - \sigma^{\frac{n-1}{n}}\left(\lambda^2-\sigma^2\right)^{\frac{n+1}{n}}\right\}}^{n} \tag{6}$$

where k is derived from Eq. (1) and Q is defined as the volumetric flow rate. Some of the more derivatives of nozzle-based mathematical models have been delineated by Koch et al. [42]

Though the power law can be used to simply predict printability, it is limited to a range of shear rates (10–10^4 s^{-1}) and produces the most accurate results only under the ideal conditions of the linear and steady flow of bioink, disregarding the reduced

viscosity at the inner walls of the nozzle. To rectify this problem, the Herschel–Bulkley mathematical model is employed which encompasses the regions having reduced shear rate and is represented as:

$$\tau = \tau_0 + k\dot{\gamma}^n \tag{7}$$

where τ is represented as shear stress τ_0 represented as yield stress, k is parameter for shear rate, and n represents the parameter for shear-thinning from Eq. (1). Besides the assessment of rheological parameters, printing settings are needed to be continuously tested to ensure uniformity in the linear extrusion of filaments, where the diameter of each extruded filament would approximately be the same. This can be estimated through tan (δ) or loss tangent, which correlates to the absorption and dispersion of energy by a bioink. Higher the value of tan (δ), better the uniformity of the filament. The post-printed deformation of the array of extruded filaments due to gravity and stresses can be assessed by calculating the deflection angle (θ). Derived from the area and the perimeter of the pore, the quantitative identification of filament circularity and filament fusion can be done using printability index represented as:

$$\mathrm{Pr} = \frac{L^2}{16A} \tag{8}$$

where L represents the length of the perimeter of the pore and A represents the area of the pore. $P_r = 1$ represents ideal square shaped pore geometry whereas $P_r > 1$ and $P_r < 1$ represent a more circular and irregular geometry, respectively. For other methods like stereolithography (SLA), the printability is significantly based on the regulation of photo-cross-linking of hydrogels under light irradiation, which adds to the shape fidelity. Unlike EBB, this modality does not mandate the influence of shear-thinning behaviour, wherein hydrogel precursors with low viscosity produce a better print resolution. Here, the printing resolution is dependent on the printing hardware, the concentration of the material for photo-initiation, absorbance of the irradiation wavelength, the function of point spread in a multiphoton event, reactive species diffusivity, depletion of the photo-generated radicals, the curing depth, which ensures the gelation in-between two successive layers and the presence of cells in the hydrogel precursors [82–84]. Finally, various imaging methods like 3D computed tomography (CT) and optical coherence tomography (OCT) are employed for the volumetric shape assessment of the post-printed constructs and for visualizing the inner microstructures and the pore volume. For modalities such as LBB and DBB which use high number of cells, the printability is ensured by the optical behaviour (refractive index) of a thermosensitive bioink, the distribution of the encapsulated cells inside the hydrogel and also the volume of the cell media and the concentration of the receiving substrate on which the drops are focused on. Besides these, laser radiation must also be precisely controlled as because thermoacoustic phenomenon, ablation, plasma generation are common occurrences.

As shown by Zhang et al. [85], for DBB, the dimensionless numbers and the ratios play a significant role in the formation of droplets. The Z number (jettability) and the Weber numbers are very important for preparing the graphical presentation of bioink distribution. The Weber number (W_e) is defined as the ratio between the inertial forces of deformation and the cohesive forces of a fluid given by:

$$W_e = \frac{8F_A}{C_w F_K} = (\rho v^2 L)/(\sigma) \tag{10}$$

where F_A is the fluid mechanical force, F_K is the cohesive force, C_w is the drag coefficient, L is the characteristic length scale, ρ represents the density, v represents the flow rate and σ represents the surface tension. The Z number is the reciprocal of the Ohnesorge numbers (O_h), which also decides the nature of fibres that are released by the bioinks. O_h is represented as:

$$O_h = \frac{\mu}{\sqrt{\rho \sigma L}} = \frac{\sqrt{W_e}}{R_e} \tag{11}$$

where μ represents the dynamic viscosity of the liquid, ρ represents the density of the liquid, σ represents the surface tension, L represents the characteristic length scale (drop diameter), R_e represents the Reynolds number ($Re = (\rho UL/\mu)$ and W_e represents the Weber number. Higher O_h values indicate dominant dissipation of internal viscous forces, which means that the formation of a droplet is critical and nearly impossible. On the contrary, the lower the O_h values, the weaker is the friction loss due to the viscous forces, which is a result of the conversion of most of the inserted energy into surface tension, and therefore a droplet can be formed [86]. When used within the range of $0.1 < O_h < 1$, the droplets can be aptly dispersed, and therefore the jettability (Z) of the bioink must range between 1 and 10 for proper droplet dispersion. The Weissenberg and Deborah numbers are of similar importance for non-Newtonian bioinks. The Deborah number (D_e) provides an idea of how a specific biomaterial will perform over a finite period of time, represented by:

$$D_e = \frac{\lambda}{T} = \sqrt{\frac{\lambda^2 \sigma}{\rho L^3}} \tag{12}$$

where T is a characteristic time for the process of deformation and λ is the time of relaxation. The Weissenberg number (W_i), which is dependent upon the Reynold's number (R_e), the flow speed (U), the parameters of Eq. 11 and the group ratios of elastic forces to viscous forces ($\lambda U/L$), is given by:

$$W_i = \lambda \dot{\gamma} \tag{13}$$

where $\dot{\gamma}$ is the rate of deformation estimated through L and velocity scales through U/L. During smaller scale expulsion, the Oldroyd model is used to portray the certain components of Herschel–Bulkley liquids, which is represented as:

$$O_d = \frac{\tau_y d^n}{k v_{nozzle}^n} \tag{14}$$

where v_{nozzle} represents the nozzle printing speed, d represents the outer diameter of the nozzle, and n, k and τ_y are parameters of the Herschel–Bulkley equation, which characterizes the flow dimensions of Herschel–Bulkley fluids inside the inner walls of a cylinder. Other than these, the capillary number ($C_a = \frac{\mu U}{\sigma}$) measures the relative effects of the forces of viscous drag due to capillary action of bioink and the elasto-capillary number ($E_c = \frac{\lambda \sigma}{\mu L}$) affects the flow of bioink with inconsistent stretches.

Therefore, to sum up, printability is the overall assessment of the formability of a bioink, which include tuning the material viscosities and rheology, manoeuvring the sol–gel conversion and setting up the most optimum printing parameters, so that the printed construct can maintain its functionality and biocompatibility. The idea is to provide the cells a natural ECM like environment, which mostly contains specialized proteins, structural proteins and proteoglycans. Therefore, it seems fitting that the chosen biomaterial must be inspired from the components of ECM and exhibits functional similarity with it, such that a particular cell can have a similar meshwork to grow on. For example, a known biomaterial such as HA is employed for bioprinting of chondrocytes because it is a regular component of cartilages, and therefore it ensures the biocompatibility and the functionality of the construct. Another factor that impacts the printability is the nature of the bioink, wherein hydrogels and tissue spheroids (discussed later in the chapter) provide the best printability among most due to their capability to provide the most viable cellular microenvironment for growth and proliferation. The factors influencing the gelation mechanics of different hydrogels (ion-sensitive, thermosensitive, photosensitive, pH-responsive or enzyme-sensitive) also have an impact on the printability of the bioink, wherein a handful of hydrogels made of naturally or synthetically derived biomaterials such as silk fibroin, alginate, fibrinogen, collagen, chitosan, GelMA, HA, PEO and PEG have been used, along with sacrificial hydrogel components such as agarose, gelatin or pluronics [87–90]. Newer methods of assessment of printability are under works, for example, machine learning-based strategy for designing printable bioink based on the rheological parameters has been demonstrated by Lee et al. [91] All in all, the assessment of the rheology and biocompatibility of newer sets of multicomponent compositions requires to be balanced with the printing parameters along with application of improved mathematical avenues for quantitative assessment of printability, which can stretch the boundaries of 3D bioprinting.

3.3 Biofabrication Window

The biofabrication window can be defined as the window of printability, or in other words, the overall approach for construct fabrication is to achieve the best shape fidelity for the exhibition of its biological functions. The concept of biofabrication window is illustrated in Fig. 2.

The biofabrication window acts as a method of characterization of bioinks since under a definite period of time, the bioink added is required to be optimized to produce the necessary texture, which essentially refers to obtaining the most favourable printing conditions to attain the correct shape. This is highly dependent upon some factors, which range from setting up of the printing parameters such as the velocity, the collector speed, printing pressures, the nozzle aperture diameter to the evaluation of rheology, the viscosity and the shear-thinning behaviour of the fluid using mathematical models and also the assessment of cell viability of the corresponding scaffold structure [80]. For example, in the assessment for the window of biofabrication, Paxton et al. [92] used the mathematical models for rheological evaluations of the bioink to demonstrate the dependency of the window upon the n and k (shear thinning coefficients) of the power law (Eq. 1), the shear rate, bioprinting viscosity and velocity. Through experimentally derived values, needle sizes, and printing pressure through velocity ranging from 1 to 40 mm s−1, the biofabrication window of multiple materials was determined (Fig. 2b), wherein poloxamer 407 (25% wt) displayed a narrow fabrication window (under printing pressure 1.2–2.8 bar) whereas 8% and 1% alginate showed a wide fabrication window. In this study, it was also shown how the concentration of a material is pertinent to its feasibility of printing with respect to the nozzle geometry, the print velocity, the machine operating parameters and the relation between the theoretical window of biofabrication and the practical printing conditions.

Biofabrication window also deals with providing the best shape fidelity under adequate cytocompatible conditions and with the minimum input of material content, which is a predominant focus in the field of 3D bioprinting. As depicted by Levato et al. [93], besides rheological evaluation, several strategies of chemical cross-linking have been studied to regulate the biofabrication window, which is an essential part of the bioink design. Step-growth reactions are a popularly employed mechanism of cross-linking where the hydrogel formation is regulated by fast movement of the active centres in the monomeric double bonds of carbon. Step-growth reaction has been studied in inks containing GelMA, gelatin modified with allyl groups (e.g. gelAGE), thiol groups (e.g. dithiothreitol DTT) [94], norbornene-functionalized (Gel-NB) and thiol-chemistry modified gelatin (Gel-SH) [95], modified alginate [96], or modified HA/ polyglycidols [97], and PEGs [98]. Another mechanism of in-situ photo-cross-linking causes the bioink to undergo photoinduced reactions to become cross-linked either during or after the deposition of the bioink. A few examples include cell-laden bioinks containing GelMA, PEGDA, norbornene-modified HA and methacrylated-HA [99]. Another photo-cross-linking mechanism that previously warranted the use of UV light to generate radicals from photointitators has

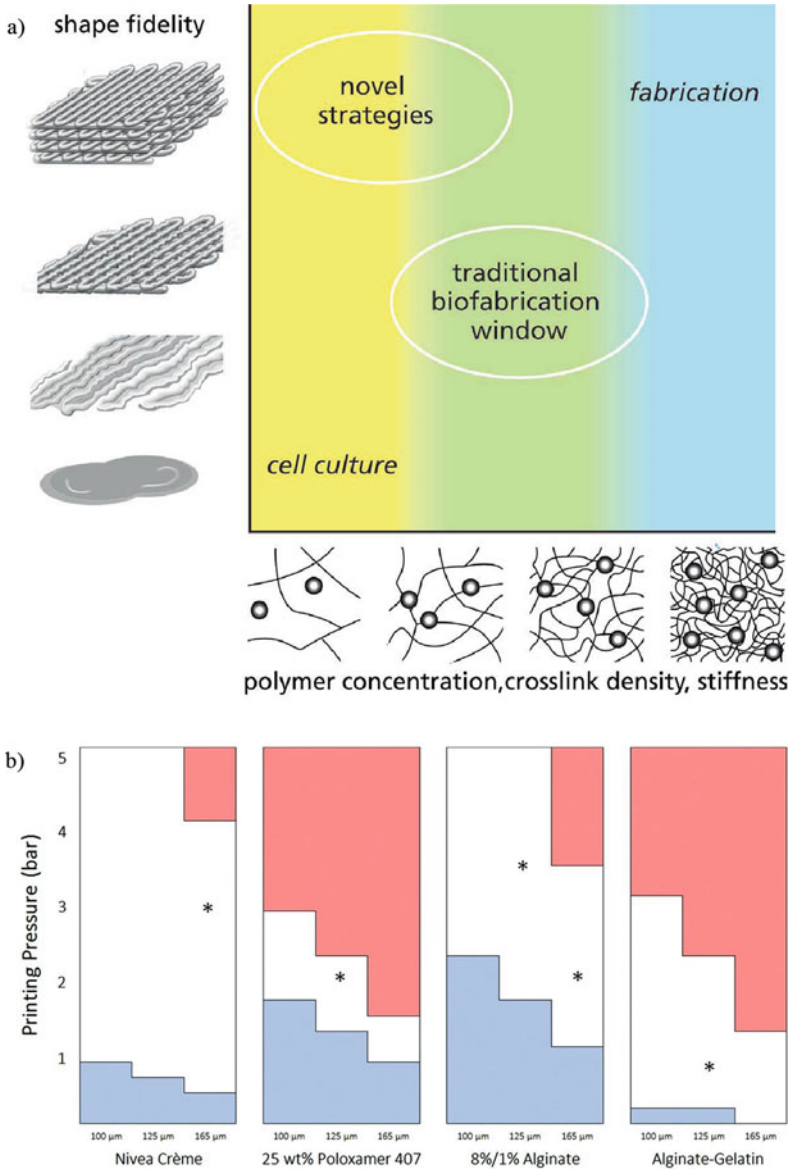

Fig. 2 **a** Illustration of the concept of biofabrication window, which requires the bioinks to possess a balance between the stiffness (to maintain shape fidelity) and soft hydrogels (to provide optimal cell growth conditions), reproduced with permission from [74]. Copyright John Wiley and Sons. **b** Bioprinting windows of different printable materials, where the red and the blue regions indicate too high and too low an extrusion velocity to support high print fidelity, and the white region between indicates the window of printability, reproduced from [92].

now been rendered functional under visible (near-UV) light through the fabrication of visible-light sensitive bioinks, which thereby results in improved cell viability. Some examples include ruthenium (Ru)/sodium persulfate (SPS) (Ru/SPS) [28], eosin Y [100] and lithium phenyl-2,4,6-trimethylbenzoylphosphinate (LAP) [101]. Pre-cross-linking strategies have also been found to ensure good rheological attributes and improve upon construct stability, as seen for horseradish peroxidase (HRP) and H_2O_2-mediated enzymatic cross-linking of tyramine-modified HA, followed by visible light cross-linking with eosin Y. To further ensure good viscoelastic properties, imine type low molecular cross-linkers such as hydrazide, semi-carbazide, alkoxy group have been studied to discard the use of secondary cross-linking altogether for an improved window of biofabrication. Besides cross-linking strategies, the selection of the material for gelation based on their intermolecular interactions is crucial to the expansion of the biofabrication window of the bioink. For example, hydrogels formed from polypeptides and proteins such as silk or silk-based protein provide good yield recovery during gelation because of the β-sheet formation, along with optimum shear thinning behaviour, biodegradation and improved cellular interaction due to the presence of RGD sequence, which thereby indicates the influence of bioink design on print shape fidelity and cell supportiveness [102].

Swerving through various fabrication mechanisms and by tuning the bioprinting parameters to the most optimum settings, the different characteristics of a bioink are observed to crucially impact the biofabrication window, wherein the material chemistry, its rheology and its interactions with the cross-linking materials attribute to the multi-layered stacking of a construct. This goes on to determine the cellular growth and attachment. To further improve upon the biofabrication window, several studies are being pursued on the incorporation of decellularized ECM particles such as peptides and other bioactive moieties to improve upon the cellular attachment with the bioink hydrogel and to form a favourable microenvironment for rapid cell growth and development [103]. Exact varieties of upgrades should be intended to prompt proliferation into well-defined and functional tissues.

3.4 Cell Density

Evaluating the optimum cell density prior bioprinting is a fundamental aspect of bioink characterization as it directly correlates to the viscosity and the rheological parameters of the bioink, thereby influencing its printability. Though the correlation between these parameters and cell density is apparent, however, it is fairly ambiguous and inconsistent, as some studies have indicated an increase in viscosity upon an increase in cell density in the cell-laden hydrogels, whereas some have shown a loss of viscosity with an increasing cell density as well as changes in other rheological parameters such as mechanism of gelation, stiffness and yield stress [104–107]. There can also be multiple damaging consequences for cell viability of the construct for having irregularity in cell density of cell-laden hydrogels, as it has been observed that too less of encapsulated cells can result in poor cell attachment and growth while

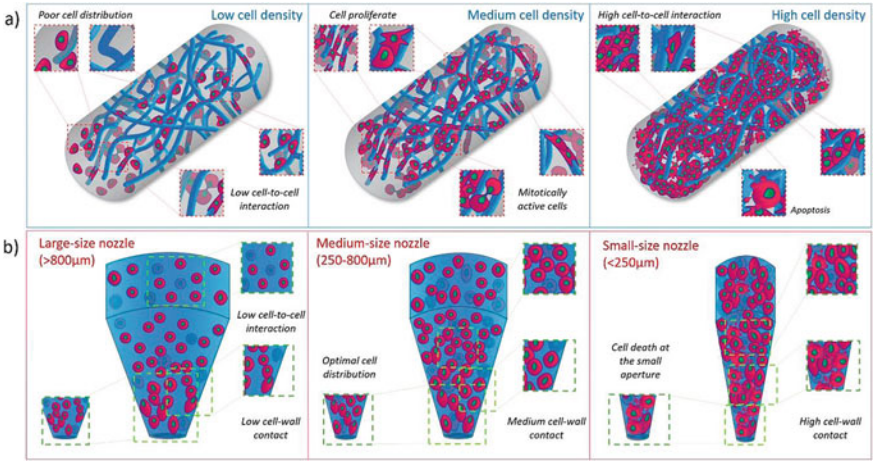

Fig. 3 **a** Influence of cell density and the concentration of polymers (indicated by dark blue polymeric chains) on the distribution and proliferation of viable cells (indicated by red circles), seeded in biomaterials; **b** Influence of the shape and diameter of the nozzle on cell density and subsequently on the cellular interactions, determining the viability of the final construct, reproduced from [109]

too high a number of cells can cause build-up of excess cellular aggregates in the construct deposition area, leaving no room for growth or proliferation of the cells, thus hindering tissue development (see Fig. 3a). Moreover, as shown in Fig. 3b, nozzle dimensions can also influence cell density and viability.

The characterization of cell density warrants repeated rheological evaluation using multiple cellular concentrations to find the optimum cell density. In an extensive study carried out by Gillispie et al. [108], the impact of cell density on rheology and the overall printing outcome has been assessed by using GelMA/GG composite bioink and MS1 endothelial murine cells wherein multiple cell densities (0, 5, 10, 20 and 40×10^6 cells per mL) were printed under a constant set of printing conditions (150 mm s^{-1} feed rate, 1.4 mm^3 flow rate, printing pressure 210–240 kPa) followed by rheological evaluation using mathematical models (Eq. 1) and under fixed values of parameters of a rheometer. While the shear-thinning behaviour (K and n) proved to be similar for all cell densities, an increase in both the loss modulus and storage modulus was observed in comparison to their acellular counterparts with an increase in cell density ascending from 20 to 40×10^6 cells per mL along with an observed variation in yield stress, which decreased with increase in cell density. In a separate study by Diamantides et al. [107], a more pronounced effect of cell density (primary chondrocytes) was observed on the printability wherein high cell densities (100×10^6 cells per ml) increased the viscosity of a collagen-based bioink and induced a post-gelation decrease in gelation rate and storage modulus with an increase in cell density, resulting in a more controlled deposition of cells in the construct. Therefore, it is safe to say that printability is dependent on cell densities as much as it is dependent on other parameters of material properties and rheology.

As a parameter of printability, cell viability is influenced heavily by cell density (see Fig. 3a), as depicted by Cidonio et al. [109], wherein lower cell density (<1 $\times$ 10^6 cells ml^{-1}) can achieve higher chances of cell survival during the process of printing but may present with lower proliferation rate due to poor distribution of cells. On one hand, high cell density (>5 $\times$ 10^6 cells ml^{-1}) may contribute to destructive interaction between cells due to increased cell saturation, resulting in lower cell viability. However, strand deposition is influenced by high cell concentration, which can either add to the strength or weaken the stiffness of the bioink depending upon the type of biomaterial used in it. For nozzle-based modalities like EBB, the geometry of the nozzle is a determinant factor in relation to the cell density assessment and the corresponding cell viability. It has been observed that cylindrically shaped nozzle affects cells under high shear stress at the region of luer-lock, which can decrease the cell viability of the printed construct up to 10 times its original concentration [106, 110]. In this regard, conical-shaped medium-sized nozzles (250–800 μm) have been found to provide the most favourable distribution of cells to ensure optimum cell survival and growth. Nozzle size below 250 μm may cause decreased cellular interactions, resulting in slow growth, whereas a nozzle size higher than 800 μm may induce cell hypoxia, apoptosis, and necrosis thereby reducing cell survival. The by-products of dead cell fragments can also impact the viability of the surrounding cells [111]. The extrusion pressure also accounts for determining the required initial cell density in the bioink, and it has a direct impact on the cell viability of the printed construct. It was shown by Nair et al. [112] that there was a significant reduction of viable cells (38.75%), which mostly experienced necrosis when the dispensing pressure rose from 5 to 40 psi. Under these accounts, it is important to choose an optimum cell density based on the nozzle geometry, dispensing pressure and the rheological behaviour of the bioink as well as its cell capsulation efficiency.

Therefore, cell density and its relation with rheology and cell viability are an essential criterion for bioink design whose characterization is crucial in the preparation of printing protocols and thereby requires more experimentations by tuning the properties of multiple formulations to be able to produce reproducible results.

3.5 Cytocompatibility and Functionality

In the line of testing for cell viability in pre- and post-printing process, the cytocompatibility of a bioink is crucial to its tissue regeneration capacity, as it essentially refers to the parameter for cell survival in both the bioink and the 3D-printed construct, and therefore decides the extent of cell growth and proliferation within the construct, which in turn reflects on its applicability. As a determinant parameter for construct functionality, a quantitative characterization method is warranted for the evaluation of cytocompatibility, as it is increasingly pertinent towards modern tissue engineering application where increased cell densities are required to produce functional mimics of multiple types of tissues. In a study by Dubbin et al. [113], the

characterization of cytocompatibility of a bioink (containing 3T3 mouse fibroblast cells) has been executed following a three-staged cell-based study.

In the first stage, the cell sedimentation assay was performed through confocal microscopy wherein the cells were labelled prior to encapsulation and incubated for 1 h. The resulting images were analyzed for cell counting using imaging software and the sedimentation coefficient was also determined using the mathematical model:

$$\delta = n\frac{\sum c_i^2}{(\sum c_i)^2} \tag{15}$$

where δ represents the sedimentation coefficient (δ = 1 indicates no sedimentation and uniform cell density across zones), n represents the zone number and c_i being the density of cells in individual zones. As shown in this study, prevention of cell sedimentation, either by using thickeners for bioinks in sol phase (e.g. PEGDA) or gel phase inks (e.g. GelMA) is a necessary step to ensure good printability, as excess accumulation cells cause the print head to clog and thereby hamper the printing process. The second stage involves the calculation of the viability of cells during the process of printing, which is required to be addressed because the Pouseille flow during the sol phase accounts for cell death/damage, the fragments of which congregate to hinder the growth of surrounding cells, thereby resulting in a decreased cell viability in the final construct [114]. After setting up an optimum range of flow rate and feed pressure, the cell viability of the print was readily assessed through live/dead assay (staining-based technique that identifies the live cells through green fluorescent labelling (calculated as shown in Eq. 16) to quantify the cell membrane damage, followed by imaging using confocal microscopy.

$$\text{Cell viability} = (\text{number of cells stained green}/\text{number of total cells}) \times 100\% \tag{16}$$

It is also important to ensure proper hydration of the prints for the cells to stay viable, and thereby the formulation can be printed on a PBS solution as shown in the study. The third stage involves calculation of cell viability after curing the bioink, which serves as the final step in the characterization of bioink cytocompatibility wherein the cell viability assays from the second stage can be repeated in the post-printed construct to comparatively evaluate the cell survival in multiple materials used in the bioink (e.g. PEGDA, GelMA, RAPID (Recombinant-protein Alginate Platform for Injectable Dual-cross-linked ink)). It is also important to perform the experiments in each stage in triplicates or more in order to evaluate the statistical significance of the accumulated data using statistical tests (e.g. ANOVA with Tukey posthoc test). By following these three-staged cell-based assays can help in determining the cytocompatibility of a bioink and also determine the cell density required in the process of printability.

Besides live/dead assay, MTT assay (colorimetric test based on the principle of reduction of yellow coloured tetrazolium salt to purple coloured formazan crystals

by metabolically active/live cells) can also be performed to quantify the cell viability in a bioink or in the construct, which can be calculated by evaluating the absorbance values and placing them in the equation:

$$\text{Cell viability}\,(\%) = \left(\frac{\text{At} - \text{Ab}}{\text{Ac} - \text{Ab}}\right) \times 100 \tag{17}$$

where At, Ab and Ac represent the absorbance of tested samples, medium only and untreated cells, respectively. Identification of apoptosis (activated caspase assay, Annexin V fluorescent conjugate staining, etc.) and necrosis (lactate dehydrogenase release assay, DNA binding assay using propidium iodide, etc.) can also provide a perspective into the cellular activities, which can call for the adjustment of the machine parameters of printability and material properties of the bioink. For the prediction of viable cells in relation to the material properties and process parameters of the bioink (shear forces), a quantitative model has been developed by Nair et al. [112] from the data generated in the process of bioprinting a number of encapsulated cells at various printing pressures. By considering D (the nozzle diameter) and P (dispensing pressure) as independent variables, the model is expressed as:

$$E(y) = \beta_0 + \beta_1 x_1 + \beta_2 x_2 + \beta_3 x_1 x_2 + \beta_4 x_1^2 + \beta_5 x_2^2 \tag{18}$$

where $E(y)$ is the mean value of the expected percentages of viable cells, injured cells and non-viable cells, and the x_1 and x_2 are the variables of nozzle diameter and pressure. The β_0, β_1, β_2, β_3, β_4 and β_5 are constants derived from the data generated from the live cell, the apoptotic and the necrotic assays across a range of parameters in the process.

The cytocompatibility of a bioink directly correlates to the functionality of the post-printed construct, which can be defined as the interdependency of multiple parameters such as cell type, cell density and material properties, to ensure that the construct possesses the biological properties of any targeted tissue it mimics and subsequently replaces. The identification of construct functionality deals with detection of certain cell-specific bioactive molecules or markers, which can confirm the presence of the respective tissue type in the construct. For instance, in a study by Yu et al. [81], the functionality of a construct formed using a bioink containing cartilage progenitor cells (CPCs) in an alginate solution was demonstrated by identifying specific genetic markers in CPCs, encoding for chondrocyte specific proteins. By decellularizing and isolating the RNA from post-printed cells, the expression levels of collagen type-II (responsible for the function and chondrocyte phenotype), ACAN (Aggrecan gene, codes for aggrecan found in cartilage ECM) and Sox-9 (transcription factor essential for chondrogenic differentiation) were evaluated using RT-PCR, where a plausible differentiation of CPCs to chondrocytes was confirmed, thereby deeming the bioink to be functional for printing of 3D constructs for its potential use as a cartilage replacement. In another study by Skardal et al. [115], the functionality of liver tissue-specific constructs formed by liver spheroid-laden hydrogel (containing

decellularized ECM components and growth factors) was tested with ELISA and colorimetric assay to detect and quantify the levels of albumin and urea respectively, the presence of which would thereby identify the healthy functionality of a construct mimicking the liver tissue, and therefore can be potentially implemented.

Aside from the identification of tissue-specific cellular activity, the functionality is also dependent on the level of oxygen and nutrient supply that can reach the cells, which is a primary need for its growth, proliferation and differentiation (in case of stem cells), and also on the extent of vascularization in the later stages. Vascularization is one of the most important challenges in the translational success of tissue grafts [116]. Therefore, aspects of material characterization (e.g. porosity, permeability) are also highly relevant to construct functionality and thereby on the parameters of printability [117]. In a study on the growth of neutral stem cells (NSCs), Banerjee et al. [118] found that increasing the elastic modulus of hydrogels led to a decrease in proliferation and also the expression of β-tubulin III (a marker used to identify NSCs activity by RT-PCR) was found to be the most prominent in the softer hydrogels, with elastic modulus similar to brain tissues. Therefore, the calibration of both the rheological and the cellular aspects in a bioink is crucial to the biological performance of the printed construct, which can be thereby evaluated through cytotoxicity assays, biochemical assays, colorimetric assays and biomolecular techniques.

3.6 Bioink Purity

The purity of a bioink refers to the accuracy in the composition of biomaterials and cells, which are responsible for adequate bioink functionality. Without the presence of any contamination, the biochemical purity needs to be consistent and with specific biomaterial blends and cells [119]. Absolute pure blends of biomaterials are not often desirable for bioprinting due to various reasons, giving rise to the need for bioink blending [120, 121]. For example, 100% complete collagen scaffold printing is hard due to its negligible density and rigidity and therefore is unsuitable as a construct [122]. On the other hand, unadulterated fibrinogen ends up being of low consistency in the preparation of a colloidal gel [123]. In pure form, gelatin is water soluble and yields a heat-sensitive colloidal gel, which goes through the process of sol–gel transition between 25 and 35 °C. Under any other temperature conditions, gelatin exhibits a poor consistency, rendering it unsuitable for bioprinting applications [124]. In case of silk, the significant impediment of its use in bioprinting is its high viscosity, which brings about nozzle blockage during bioprinting. Because of the excess shear effect inside the nozzle in the printing process, the silk β polypeptide chains crystallize inside the nozzle, which further hinders the flow [125]. An endeavour for improvement of the printing stability of constructs depends on mixing of blends of other biomaterials (e.g. chitosan with blended with different biopolymers to provide adequate mechanical strength [126]).

Along with using homogenized blends to obtain bioinks, various developmental factors such as hormones and activating molecules can be mixed in bioink, which

can help in cell segregation, differentiation and growth and may justifiably be used in cell types, tissues, and organs [72]. When all is said and done, certain groups of hormones follow up on many different morphologies of tissues, for example, the BMP family activates bone-related physiological cycles through VEGF and is known to positively influence the vascularization cycle [127, 128]. Hence, these are broadly utilized in tissue formation, either as immediate release factors or as a controlled delivery framework (e.g. microspheres). In a few investigations, hormones and activating factors were being supplemented and utilized to activate the bioprinted constructs. Bioinks containing insulin-like growth factor II (IGF-II), bone morphogenetic protein 2 (BMP-2), and fibroblast growth factor-2 (FGF-2) were imprinted on surfaces covered with fibrin using an inkjet affidavit framework. On these printed structures, cultivation of myogenic cells was carried out [129]. Desorption tests conducted with BMP-2 and IGF-II demonstrated a 10-day commencement of the development factors to be contained inside the medium containing serum.

3.7 Bioink Degradation

A determinant factor in the characterization of a bioink is the chosen biomaterial's ability to go under degradation in the bioprinted construct. Degradation can be defined as the trait of a biocompatible scaffold/construct to be able to disintegrate in the local site of implantation, so as to be replaced by the newly regenerated cells followed by vascularization. Delayed rate of degradation can cause various clinical issues following cytotoxicity in the body. Under ideal conditions, the degradation rate should be the same as the regeneration rate of a tissue, indicating the formation ECM components, which replaces the degenerating bioink material in the construct. The method of studying degradation involves measuring the dry weight of the scaffolds, periodically over a span of time and then the data from multiple timestamps are used to measure the rate of degradation. The in-vitro degradation in the printed scaffolds can be measured using the following equation:

$$\text{Weight remaining} = \left(\frac{W_t}{W_0}\right) \times 100\% \tag{19}$$

where the initial scaffold weight is represented by W_0 and the remaining scaffold weight is represented by W_t at predetermined timestamps 't'.

The degradation rate is dependent upon the material composition of the bioink and the architecture of the construct (CAD model), which may be modulated through a varied number of concentrations of the biomaterials involved. For example, through variations in the compositions of PCL and chitosan in a PCL/Chitosan hybrid scaffold, Dong et al. [130] showed that the degradation rate could be modulated between 15 and 60% within a period of 20 days, as shown in Fig. 4.

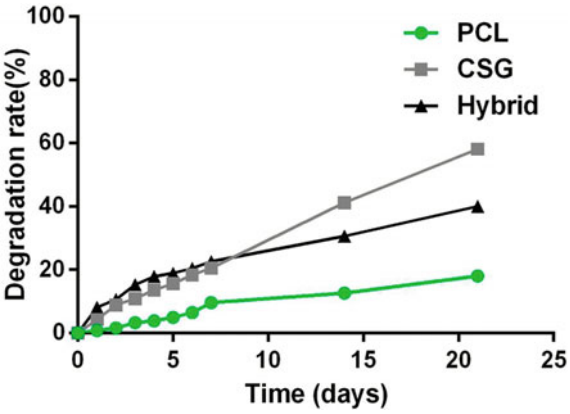

Fig. 4 Graph indicating the degradation rates of PCL (indicated in green), CSG (thermo-sensitive chitosan hydrogel) (indicated in grey) and PCL-CSG (indicated in black) scaffolds; For more than 3 weeks, the biodegradation rate for CSG scaffolds was the highest (60%), followed by the hybrid scaffold (40%) and the lowest being PCL (20%), reproduced from [130]

Similarly, in another study by Walker et al. [131], the degradation of poly(propylene fumarate) (PPF) scaffolds could be driven from 20% to nearly 70% by varying the architectural styles and the input molecular mass of the polymer. In this aspect, the molecular mass or the MW of the bioink has also been found to impact the degradation profile of the construct. This is further expanded in a study by Freeman et al. [132], where it was shown that 3D-printed alginate scaffolds with a much higher MW showed little degradation in the culture over a span of 21 days, whereas alginate scaffolds with low MW showed high degradation from Day 0 to Day 21. In this study, it was also shown that the choice of cross-linkers in the bioink also affects the degradability of a scaffold, as in case of alginate scaffolds with lower MW, which showed higher degradation with CaSO4 and CaCl2 cross-linking than with $CaCO_3$ cross-linking, thus indicating that the mechanism of ionic cross-linking can also impact the degradation profile. In another study by Gordon et al. [133], the cross-linking in collagen type II scaffolds by dehydrothermal treatment and ultraviolet radiation proved to be in favour of faster degradation due to low cross-linking. Alongside being regulated by ionic cross-linking, the degradation kinetics of bioinks can be controlled enzymatically and hydrolytically as well [134]. For example, early reports by Mann et al. [135] and Lutoff et al. [136] have shown that with the use of enzymes that are responsible for migration of cells, the PEG-peptide conjugates can be degraded to promote infiltration of cells. Scaffolds formed from naturally occurring polymers like collagen can also be enzymatically degraded [137]. Hydrolytic degradation has been well demonstrated by Diniz et al. [138] on Pluronic F-127 hydrogel, which proved to have a fast degradation rate facilitating the growth of dental pulp stem cells (DPSCs).

A relatively newer avenue for controlled degradation is through designing composite bioinks, which allows for individual components to interact with specific enzymes, thereby offering multiple mechanisms for manoeuvring the mechanical properties of the bioink. This has been well demonstrated by a novel form of bioink developed by Li et al. [139], which is a conjugate of polypeptides and DNA, wherein grafting complementary short sequences on the polypeptide backbone cross-links

the short DNA strands in the bioink. Therefore, the printed structure can be degraded by the action of both proteases and DNases without compromising the stability of the structure and can be printed using both the modalities of DBB and EBB. More interestingly, through a recent study performed by English et al. [140], the promise of smart bioinks has been shown to lead to programmable degradation of the construct by cleaving the DNA present in the hydrogels with the action of a CRISPR-Cas12a system, rendering changes in the material properties, thereby controlling degradation. Therefore, experimenting with the bioink components and by modulating the material properties, molecular mass, mechanism of cross-linking and also working with various architectural models, the design of bioink can be characterized based on its degradation kinetics. Also, by implementing novel formulations, the rate of degradation can be steered in line with the growth rate of healthy cells, forming the tissues for its intended applications. Moreover, micro-computer tomography can be a useful tool for characterizing the spatial degradation of bioprinted constructs [141].

3.8 Viscosity and Molecular Weight

As described earlier in the chapter, viscosity (measurement of resistance from a fluid's flow) of a bioink is a determinant factor of the rheology (yield stress and yield recovery) and the printability of the bioink that is monitored by its shear thinning behaviour, viscous modulus and the cell density of the ink, thereby exhibiting a profound effect on print fidelity and print resolution. The viscosity has an intricate relation with the MW of the biopolymer, the concentration of its residues, its degree of branching and the action of cross-linkers [15, 142]. As shown by Schuurman et al. [143], the addition of biomaterials also influences the viscosity of the bioink. GelMA solution with low viscosity could produce prints with good shape fidelity upon the inclusion of HA, as represented in Fig. 5.

Typically, biopolymers with a higher MW present with more viscosity due to increased chain entanglements [94]. The polymeric viscosity and the average MW (M_n) of the biopolymer are given by Mark–Houwink equation:

$$[\eta] = K_\eta M_\eta^\alpha \tag{20}$$

where K_η and α represent the parameters of Mark–Houwink equation and $[\eta]$ represents the intrinsic viscosity, which can be represented as:

$$\lim_{c \to 0} \frac{\eta - \eta_0}{c\eta_0} \tag{21}$$

where c represents the solute concentration and η_0 represents the solvent viscosity. Since most bioink has a multilateral composition, containing biopolymers whose polymerization is governed by the action of random interactions, the polymeric

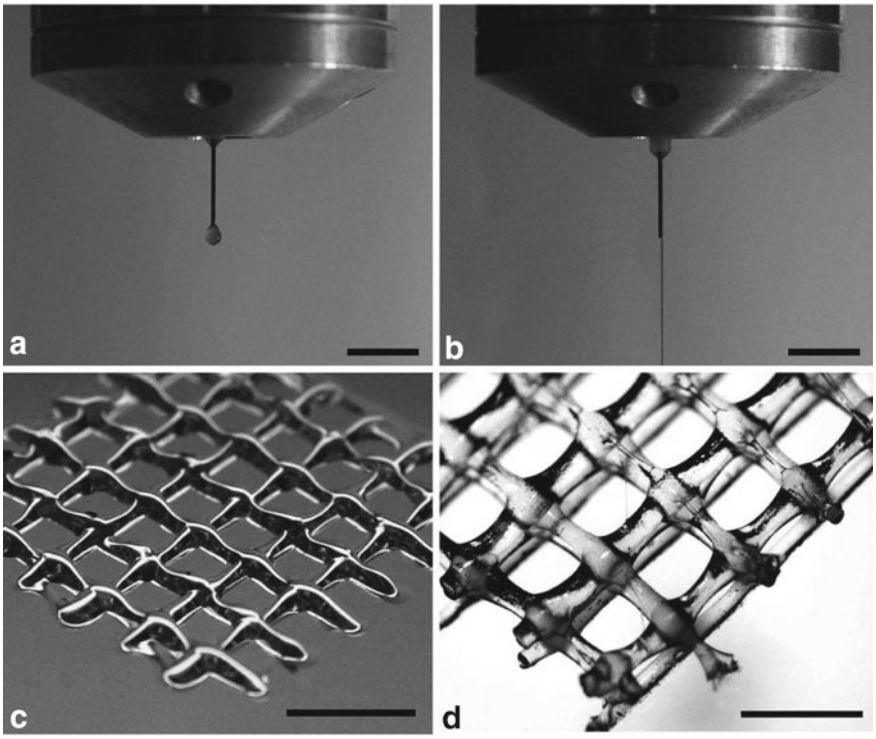

Fig. 5 20% GelMA formed droplets, aggregated at the tip of the nozzle (**a**), producing flat and spread outlines instead of a concrete fibre (**c**); addition of 2.4% of HA to GelMA produced strands (**b**) which formed fibres producing four layers of construct (**d**); (5 mm scale bar for A–C, 2 mm scale bar for D), reproduced with permission from [143] Copyright John Wiley and Sons

mixture develops chains of varying length and therefore a statistical average of the distribution of MW is required to be calculated instead of calculating the MW of a single substance. In this regard, the average MW is expressed as viscosity average MW in the following equation represented as:

$$\overline{M}_{\eta} = \left[\left(\sum_{i}^{N} N_i M_i^{\alpha+1}\right)/\left(\sum_{i}^{N} N_i M_i\right)\right]^{\frac{1}{\alpha}} = \left[\left(\sum_{i=1}^{N} w_i M_i^{\alpha}\right)/\left(\sum_{i=1}^{N} w_i\right)\right]^{\frac{1}{\alpha}} = \left[\left(\sum_{i=1}^{N} w_i M_i^{\alpha}\right)\right]^{\frac{1}{\alpha}} \quad (22)$$

where N_i and w_i are the total number of molecules and their weight fraction, respectively, with M_i being the MW of each molecule, and α being the weighting factor. Chromatography is a common means of measuring MW of a polymer (gel permeation chromatography and high-pressure liquid chromatography).

For bioinks based on hydrogels, the MW between cross-links is a parameter for characterization of the involved biomaterials. The extent of polymeric networking within the hydrogels decides the diffusional properties of the bioink, which is essentially one of the aspects for a complete evaluation of the hydrogel meshwork and has crucial impact on cell growth, cell migration and tissue permeability. Mathematical models have been developed in order to evaluate the relation between the cross-linking MW and diffusion of solutes within the gel [144–146]. The diffusion of solutes is proportional to $\left(\frac{M_c - M_{crit}}{M_n - M_{crit}}\right)^2$, where M_c represents the MW between cross-link, M_n represents the average MW of the uncross-linked polymer, and M_{crit} represents the MW between cross-links critical for the passage of solute. More studies on low MW hydrogels based on PEGDA by Jimenez-Vergara et al. [147] have helped to develop mathematical models to evaluate the MW between cross-links by following the previous models proposed by Peppas et al. [148], wherein the average MW between cross-links has been expressed as:

$$\left(\frac{1}{M_c}\right) = \left(\frac{2}{M_n}\right) + V_e \tag{23}$$

where M_c represents the MW between cross-link, M_n represents the average MW of the biopolymer and V_e represents the effective chain number/unit volume. This study has further delineated the mathematical relation between M_c and the cross-linking density (defined by chain density or segments connecting two parts of a polymer network, rather than the density of cross-link junctures) expressed as:

$$\rho_x = \frac{1}{\overline{v} M_c} \tag{24}$$

where $\overline{v}$ represents the volume of the biopolymer and ρ_x represents the cross-linking density. Using molecular size exclusion (MSE) for the individual hydrogel using the models developed by Watkins et al. [149], this study has also developed a new correlation between the mesh size and degree of swelling with M_n being a crucial parameter of the relation. An in-depth comparison between different mesh sizes using the correlation data and the MSE-generated experimental data proved MSE to be the most precise approach where the calculations of mesh size using MSE showed better correlation with changes in tensile modulus of the hydrogel.

There is a positive relation between viscosity and MW, as an increase in MW leads to an increased viscosity of the biopolymer. For example, preparing alginate hydrogels with a varied ratio of G (α-L-glucuronic acid) and M (β-D-mannuronic acid) through acid hydrolysis and gel permeation chromatography, Jiao et al. [150] showed that this variation in the content ratio changes the MW of the hydrogel, which significantly alters the rheological properties of the hydrogel, wherein samples with a high amount of M units and low MW showed higher viscosity compared with the ones with high amount of G units and high MW. Besides variation in the constituent ratios,

variation in the ratio of a biopolymer and its cross-linker can also influence the MW and the viscosity of the bioink. As shown by Freeman et al. [132], to print stable 3D constructs, a less viscous alginate hydrogel with lower MW of 28 kDa requires 2.5 times the cross-linker compared with the alginate hydrogels with a higher MW of 75 kDa. Another important aspect by which the viscosity of a bioink is influenced is through the mechanical consistency of the biopolymers, which is governed by its polydispersity index (PDI). PDI is reliant upon the MW of the biopolymer and determines the size distribution, wherein low PDI indicates similarity in length of the polymer thereby indicating consistency in mechanical properties. PDI is represented as:

$$PDI = (M_W / M_n) \tag{25}$$

where M_w and M_n represent the weight average and the number average of molar masses, respectively. Nuclear magnetic resonance (NMR) spectroscopy or attenuated total reflectance (ATR) can be used to identify biopolymer terminal groups and MW of the biopolymer.

Therefore, by modulating the viscosity, MW, cross-linking density and gelation kinetics, the characteristics of a biopolymer meshwork can be controlled to allow the diffusional properties to be in favour of ample nutrient supplementation, thereby influencing the cell behaviour. Along with this, the overall bioink printability can be improved by understanding the interplay between cellular stresses and the material chemistry of a bioink.

3.9 Bioink Homogeneity

As a fundamental criterion for the maintenance of the structural uniformity, in terms of mechanical property, MW distribution, regularity in viscosity, distribution of cells and other biologics, the homogeneity of a bioink is warranted, which essentially refers to the extent to which the components of a bioink are evenly dispensed in it. While the regularity in mechanical strength can be attained with the aid of various cross-linking mechanisms, the homogeneity is particularly relevant towards achieving an even distribution of cells as it is even more crucial that the cells are dispersed uniformly in the bioink so that it's functionality can follow suit in the 3D-printed constructs. For platforms like EBB that requires a constant force for extrusion of the bioink, homogeneity is a decisive factor to ensure the correct shape fidelity of the construct, as inhomogeneity caused due to particle aggregation in the bioink can cause fluctuations in the extrusion force leading to inconsistency in the settled filaments [80]. More importantly, as we are moving towards printing full-sized organs and large tissues, the cells are required to stay suspended for a large amount of time within the bioink due to long hours of print time, and therefore the biomaterial also has to comply well

with the process of cell encapsulation so as to count for the least possibility of cell sedimentation and thereby increase the homogeneity in the solution.

To achieve the homogeneity in bioink, the density of a biomaterial must match the density of the type of cell being employed, wherein the density of both the cells and the biomaterial must be considered. This has been demonstrated by Lin et al. [101] where the most efficient suspension of hADSCs in PEGDA-based hydrogel was achieved with 37.5% Percoll, indicating the most optimum density required to maintain homogeneity in the bioink. In another study by Jia et al. [142], it was shown that the finest homogeneous distribution of hADSCs occurs when the cells are suspended in an oxidized alginate hydrogel with a density of 1.05 gcm^{-3}, as verified by cell suspension assays through fluorescent labelling. Since density of a bioink correlates directly to its viscosity, homogenous distribution of cells also depends on the viscosity the bioink, which has been shown by Rutz et al. [151], where the cells encapsulated in hydrogels containing a blend of PEG and GelMA showed better homogeneous dispersion due to improved viscosity. More recently, Chen et al. [152] developed a novel method to increase homogenous cell dispersity by creating liquid interfaces through multi-layered modification to a GelMA-silk fibroin bioink, which increases interfacial retention and decreases cell sedimentation through the manipulation of the liquid interfaces.

Besides countering cell sedimentation, mechanical harm can also be caused to the cells being subjected to brutal mixing conditions during blending. A novel method for a semi-automated homogeneous mixing process has been suggested by Bhattacharyya et al. [153] using a twin-screw extruder (TSE) head, which can simultaneously function in mixing and bioprinting of ionic alginate gel, micro/nanoparticles of α-TCP (alpha-tricalcium phosphate) and osteoblast cells. This system displayed a higher cell distribution and lower cell damage due to its real-time nature of mixing and low sedimentation time.

Cross-linking strategies can also have a positive effect on the homogeneous distribution of a bioink. As shown by Dubbin et al. [154], dual cross-linked alginate hydrogels modified with peptide domains (P1) and engineered protein (C7) containing NIH 3T3s fibroblasts and hADSCs display better dispersion compared with ordinary alginate due to the protein and peptide-attachment sites being present.

All in all, the characterization of bioink homogeneity requires monitoring a set of parameters, which include bioink density (for both cell and biomaterial), bioink viscosity, the forces experienced by the bioink (e.g. gravity, buoyancy, friction), cross-linking strategies and the working duration of the printing process.

3.10 Solubility

The ability of the biomaterial component in a bioink to dissolve in a compatible solvent to add consistency to the bioink definition is defined as the solubility of a bioink. There are several factors that affect the solubility of a bioink, primarily the

nature of the biomaterial and the nature of the solvent. As water-friendly biopolymers provide better compatibility to the cellular microenvironment, most bioinks employed are hydrogels as they are capable of retaining high volumes of water within their structure. Therefore, the water solubility of biomaterials is crucial to the maintenance of the functionality and the rheological consistency of the bioink. Most of the naturally occurring biopolymers like HA and silk fibroin are water soluble but some are soluble under certain conditions. For example, both chitosan and collagen are only soluble in water under low pH conditions, gelatin is soluble in water only at a temperature above 35 °C, and the solubility of alginate depends upon its particle size. However, they also present with low solubility due to their high MW compared with synthetic water-soluble biomaterials like PVA and PEG [155]. Other synthetic biopolymers such as PCL and PLGA are soluble in organic solvents. Hence, the solubility is a crucial part of bioink characterization, as many inks use blends of naturally and synthetically derived polymers or both, and the phases have to be compatible with each other before attempting to make the rheological adjustments.

Solubility can be guided through monitoring the MW and the material concentration in the bioink. Along with this, the structural chemistry of a biomaterial including the number of repeating units and the nature of its polymeric branching also accounts for achieving the most optimum solubility. External factors for controlled solubility include maintenance of temperature, regulation of pH of the solvent and the addition of salts, which impacts the performance of the gel by influencing the cross-linking chemistry. For example, in the development of multicomponent bioinks based on alginate solutions, Piras et al. [15] showed that the addition of divalent cations (e.g. Ca^{2+} from salts such as $CaCl_2$, $CaSO_4$ and $CaCO_3$) at room temperature generates inter-chain ionic bridges, which regulates the solubility and the cross-linking in the gel. Since cross-linking influences the stiffness of the bioink, different solubilities also cause varied stiffness in the material. As found in the aforementioned study, a lower solubility of $CaSO_4$ resulted in a much stiffer filament formation and imparted a more uniform gelation compared with $CaCl_2$ and $CaSO_4$ led gelation. This goes to show that calcium ions with lower solubility render more homogeneous alginate bioink solution. The influence of temperature and concentration on the solubility of a bioink has been studied for other biomaterials like agarose where the optimum sol–gel transition takes place at a temperature of 40 °C, under a fixed concentration within the aqueous solution [156]. Through manoeuvring of temperature, the definitions of alginate gels can be adequately thickened with an elevated bulk modulus, which achieves better consistency and thereby encourages higher print goal/accuracy, wherein pressure and space testing also influences the solubility by showcasing the outcomes of modulus expansion in terms of alginate elasticity [157]. Other than this, the stirring speed and the size of the polymeric particles also influence solubility.

3.11 Spheroid Characterization

Spheroids are an arrangement of cell clusters in spherical formations, which provide a closer connectivity between the cells involved in the process of tissue formation, compared with the free cells suspended in a bioink. These are regarded as the frontiers of modern organ printing and regeneration as spheroids can truly achieve scaffold-free constructs, which then supports a higher ECM deposition due to dense packaging of cells causing elevated cellular interactions, homogeneous distribution and long hours of cell functionality [158]. However, there are several challenges in the way of using spheroids in bioinks, which mostly include the maintenance and reproducibility of spheroid size uniformity when using diverse cell types and also the positioning of these spheroids [159]. These challenges can be overcome by developing workflows, which fit the best-suited technique. The steps to forming spheroids are a part of a time-dependant process, which include compacting high density of cells, letting it proliferate and then using these multicellular aggregates as the bioink for 3D printing. As delineated by Khoshnood et al. [160], the common methods for spheroid formation include the following:

1. Magnetic levitation: This employs an outer magnetic field to drive the cells together into forming spheroids by using biocompatible magnetic labels (e.g. iron oxide) and paramagnetic agents (e.g. Gadobutrol, Gadodiamide and Gadoteric acid), which paramagnetizes the cellular environment. For example, formation of MSC spheroids using Fe3O4 nanoparticles [161]; formation of spheroids of NIH 3T3 mouse fibroblasts and HCC827 lung cancer cells using Gadolinium (III) chelates (paramagnetic agents) [162].
2. Hanging drop: This method leverages the contact area of a cell suspension placed onto a lid and which is then inverted upside down, only to let the gravity and surface tension of the attached cells result in the formation of spheroids. For example, fabrication of spheroids using pancreatic cancer cells with the addition of methylcellulose polymer [163].
3. Hydrogel microwells: This method employs microwells made out of hydrogels formed by different biopolymers wherein the cells are dropped into these microwells, which go on to form spheroids under the influence of gravity. For example, Agarose microwells are used to produce spheroids of hADSCs [164].
4. Spinner Flask: This method employs the stirring of cell suspension inside a spinner flask, which then results in the formation of spheroids. The stirring speed and the time of operation decide the size of the spheroids. For example, formation of spheroids using rBMSCs, bACs (bovine articular chondrocytes) [165].
5. Microfluidic systems: This method uses a lab-on-chip device with a limited number of inlets/outlets whose size can be adjusted to produce high number of accurately sized spheroids by depositing low amounts of multiple cell types in a single bulk. Compared with other methods, this method can achieve a higher printing accuracy within a reduced time of operation and provides more

protection to the cells, resulting in a better homogeneous aggregation and reproducibility, while also imparting a much higher geometrical accuracy to the spheroids. For example, microfluidic systems developed to produce spheroids using hepatoma cells [166].

The use of spheroids in a bioink is becoming increasingly popular, with the earliest instances dating back to early 2000s. For example, in a study by Jakab et al. [167], micropipettes were used as cartridges for the preparation, loading and printing of spheroids and pellets of Chinese hamster ovary cells (CHO). Since then, the preparation of spheroids and their application as bioinks has evolved through the developments of various methods as depicted earlier. However, the most prominent method to emerge in recent years is the stainless steel made microneedle-based method of bioprinting, developed by Nakayama et al. [168]. The "Kenzan" method, as it is called, helps in the growth and interaction between the cells in the spheroid. Instead of arbitrary positioning, it ensures that the microneedles are positioned in such a way that they help to strategically form agglomerates in the areas where it is needed. During the post-fusion stage of the spheroids, the microneedles are removed to achieve the 3D construct. In this method, a definite or multiple cell types are provided with an opportunity to be organized in three dimensions and demonstrate biologically active functions by also utilizing the extra cell culture after removal of the Kenzan. Several pieces of research involving the in vitro formation of a repertoire of tissue constructs using the Kenzan method and their subsequent implantation have been recorded. These include vascular grafts [169], liver mini-tissues [170], cardiac patches [171] and many more.

There are certain determinant factors to ensure the optimum functionality of the spheroids when used in a bioink in 3D bioprinting. The non-attaching setup for culturing the constituent cells of the spheroids plays a huge part in the process of forming cellular aggregates from the collective suspension. Besides this, the performance of the spheroids is dependent upon the characteristics of its outermost surface and its external shape, which is determined by the size and the nature of the blend of different cell types present in the spheroids. The characterization of spheroid morphology depends upon the method employed. For example, in a study of both the gravity-induced and centrifuge-induced formation of spheroids from BMSCs by Aguilar et al. [172], the Regenova 3D bioprinter (Cyfuse Biomedical K.K., Japan) was employed to measure the diameter, roundness and the smoothness of the spheroids. The roundness was evaluated repeatedly using the equation:

$$Roundness\,[\%] = \left[100 - \left(\frac{R-r}{R}\right)\right] \times 100 \tag{26}$$

where radius R is that of the smallest circle circumscribing the spheroid and radius r is that of an inscribed circle, which is in concentricity with the central circle, thereby connecting to the perimeter of the spheroid. The smoothness of the spheroid was determined through the following equation:

$$Smoothness\,[\%] = \left(\frac{DA}{SA}\right) \times 100 \tag{27}$$

where the DA is the area of the spheroidal parts that deviate from the average value of maximum and minimum contour, and SA is the total area of the spheroid.

The nature of the cell types also determines the nutrient uptake and the level of oxygen requirement, which, in turn, requires optimization of the spheroid thickness, thereby deciding the endurance and the viability of the cells inherent to the spheroids. Furthermore, the time period for the sustenance of the cells in the culture media for the formation and arrangement of spheroids also influences the functionality of the spheroids in the bioprinted construct. The addition of antixodiants has been shown to reduce shear-induced cell deaths in certain bioprinting process [173].

4 Conclusion and Future Prospects

As of late, dynamic 3D bioprinting strategies accompanied by multifaceted methods of bioink fabrication are still being studied to design artificial arrangement of local tissues. At present, manufacturing of multicomponent bioink involves using common engineered biomaterials, various kinds of cells and dissolvable components. Additionally, some supplementary nanobiomaterials to bioinks can embellish the process of imitation of intricate and complex local tissue morphology. A constant progression in innovation of various bioprinting modalities has empowered research on distinct materials to create multicomponent bioinks, resulting in ceaseless achievement of both vast and diminutive goals, thereby providing a quick and accurate remedy to the mind-boggling engineering of the local tissues. It has been observed that multicomponent bioinks have had an extraordinary impact in advancing biomimetic tissue engineering for restorative and pharmaceutical applications. However, there still stays much to be routed to empower the interpretation of the innovation to the facility.

Bioink improvement is hugely progressive in its application. Be that as it may, numerous difficulties still do stay ahead. For each bioink created, another arrangement of printing boundary must be upgraded separately for sorting of cell lines. Every cell type needs an exclusive arrangement of bioprinting boundaries, depending on which the bioink properties are to be modified. Improvement upon cell-explicit bioinks can be done through examination of the mechanical attributes of various cell types under printing pressure, which will be beneficial in building up a superior comprehension for additional upgrades [174]. A few investigations have revealed the attributes of different cell types carefully observed under atomic force microscopy, which have indicated a noteworthy assortment of the variety in mechanical qualities of multiple cell types.

Other than this, designed tissue scaffolds should be produced with a room for simultaneous detection of intercellular and intracellular network alongside the developmental design of the bioprinted tissue constructs or organ built. Monitoring the

capacity of cell development with time will help in building a superior comprehension of cellular network and adequacy to bolster such connections. This may lead to a road to foresee the improvement of printed structures for implantation. Maybe the existing advancements made is to screen cell movement as a component of time, for example, 'organ-on-a-chip' has ceaseless perfusion framework, which allows for checking the framework and be adjusted for 3D bioprinting of subsequent constructs [175, 176]. Additionally, the improvement of biomaterials alongside framework design would commit to venturing far into 3D bioprinting. There have been some acutely created 4D printing materials with changes in their shapes and properties formatted in the view of extrinsic upgrades [177, 178]. Comparative change in properties may also stimulate internal development in cell growth by reinforcing a better microenvironment and ideal conditions for its growth.

Besides this, the prospect of the printing process to scale up and produce huge and complex constructions (e.g. transplantation organs and large patches of tissues) needs experimentation. There are numerous difficulties faced in producing such structures, which involve adequate mechanical strength, time imperatives following cell suitability, mechanisms of supplement dissemination and vascularization and more. Therefore, the possibility of organ bioprinting needs inventive structure and techniques as well as reasonably equipped bioinks.

All in all, 3D bioprinted tissue constructs and organ framework must be cultivated through subjugation of the existing difficulties and comprehending the cellular bioprocesses that happen because of a given bioink/ECM. The pre-eminent test for bioink compatibility is the printability of bioinks in light of the fact that the initial move in manufacturing of complex arrangements is heavily dependent on printability. Characteristic printability of a bioink should be advanced for various cell lines and connections must be built up between the bioinks' microstructure and cell retention capacity. Bioinks having advanced diffusivity and printability must be created in order to promote the printing of large structures with proficient nourishment. A strong affiliation connecting the bioink boundaries and properties of bioink should be built up to decide the ideal circumstances for printing constructs retaining fitting shape and demonstrating optimal functionality.

References

1. Han S et al (2020) 3D bioprinted vascularized tumour for drug testing. Int J Mol Sci 21(8). https://doi.org/10.3390/ijms21082993.
2. Kang Y, Datta P, Shanmughapriya S, Ozbolat IT (2020) 3D bioprinting of tumor models for cancer research. ACS Appl Bio Mater 3(9):5552–5573. https://doi.org/10.1021/acsabm.0c00791. (American Chemical Society, 21 Sept 2020)
3. Datta P, Barui A, Wu Y, Ozbolat V, Moncal KK, Ozbolat IT (2018) Essential steps in bioprinting: from pre- to post-bioprinting. Biotechnol Adv 36(5):1481–1504. https://doi.org/10.1016/j.biotechadv.2018.06.003. (Elsevier Inc., 01 Sept 2018)
4. Unagolla JM, Jayasuriya AC (2020) Hydrogel-based 3D bioprinting: a comprehensive review on cell-laden hydrogels, bioink formulations, and future perspectives. Appl Mater Today 18:100479. https://doi.org/10.1016/j.apmt.2019.100479. (Elsevier Ltd., 01 Mar 2020)

5. O'Connell C et al (2020) Characterizing bioinks for extrusion bioprinting: printability and rheology. In: Methods in molecular biology, vol 2140. Humana Press Inc., pp 111–133
6. Li H, Tan C, Li L (2018) Review of 3D printable hydrogels and constructs. Mater Des 159:20–38. https://doi.org/10.1016/j.matdes.2018.08.023
7. Derakhshanfar S, Mbeleck R, Xu K, Zhang X, Zhong W, Xing M (2018) 3D bioprinting for biomedical devices and tissue engineering: a review of recent trends and advances. Bioact Mater 3(2):144–156. https://doi.org/10.1016/j.bioactmat.2017.11.008. (KeAi Communications Co., 01 Jun 2018)
8. Cui X et al (2020) Advances in extrusion 3D Bioprinting: a focus on multicomponent hydrogel-based bioinks. Adv Healthcare Mater 9(15):1901648. https://doi.org/10.1002/adhm.201901648
9. Rodell CB et al (2015) Shear-thinning supramolecular hydrogels with secondary autonomous covalent crosslinking to modulate viscoelastic properties in vivo. Adv Func Mater 25(4):636–644. https://doi.org/10.1002/adfm.201403550
10. Rodell CB, Kaminski AL, Burdick JA (2013) Rational design of network properties in guest-host assembled and shear-thinning hyaluronic acid hydrogels. Biomacromol 14(11):4125–4134. https://doi.org/10.1021/bm401280z
11. Petta D, Grijpma DW, Alini M, Eglin D, D'Este M (2018) Three-dimensional printing of a tyramine hyaluronan derivative with double gelation mechanism for independent tuning of shear thinning and postprinting curing. ACS Biomater Sci Eng 4(8):3088–3098. https://doi.org/10.1021/acsbiomaterials.8b00416
12. Choi DJ, Kho YJ, Park SJ, Kim YJ, Chung S, Kim CH (2019) Effect of cross-linking on the dimensional stability and biocompatibility of a tailored 3D-bioprinted gelatin scaffold. Int J Biol Macromol 135:659–667. https://doi.org/10.1016/j.ijbiomac.2019.05.207
13. Tytgat L et al (2020) High-resolution 3D bioprinting of photo-cross-linkable recombinant collagen to serve tissue engineering applications. Biomacromol 21(10):3997–4007. https://doi.org/10.1021/acs.biomac.0c00386
14. Demir Oğuz Ö, Ege D (2018) Rheological and mechanical properties of thermoresponsive methylcellulose/calcium phosphate-based injectable bone substitutes. Materials 11(4). https://doi.org/10.3390/ma11040604
15. Piras CC, Smith DK (2020) Multicomponent polysaccharide alginate-based bioinks. J Mater Chem B 8(36):8171–8188. https://doi.org/10.1039/d0tb01005g. (Royal Society of Chemistry, 28 Sept 2020)
16. de Ruijter M et al (2018) Out-of-plane 3D-printed microfibers improve the shear properties of hydrogel composites. Small 14(8). https://doi.org/10.1002/smll.201702773
17. Kérourédan O, Rémy M, Oliveira H, Guillemot F, Devillard R (2018) Laser-assisted bioprinting of cells for tissue engineering. In: Laser printing of functional materials Wiley-VCH Verlag GmbH & Co. KGaA, Weinheim, Germany, pp 349–373
18. Hakobyan D et al (2020) Laser-assisted bioprinting for bone repair. In: Methods in molecular biology, vol 2140. Humana Press Inc., pp 135–144
19. Detsch R, Blob S, Zehnder T, Boccaccini AR (2016) Evaluation of cell inkjet printing technique for biofabrication. BioNanoMaterials 17(3–4):185–191. https://doi.org/10.1515/bnm-2016-0007
20. Koch L, Deiwick A, Chichkov B (2018) Laser-based cell printing. In: 3D printing and biofabrication. Springer International Publishing, pp 303–329.
21. Ringeisen BR et al (2004) Laser printing of pluripotent embryonal carcinoma cells. Tissue Eng 10(3–4):483–491. https://doi.org/10.1089/107632704323061843
22. Barron JA, Wu P, Ladouceur HD, Ringeisen BR (2004) Biological laser printing: a novel technique for creating heterogeneous 3-dimensional cell patterns. Biomed Microdevice 6(2):139–147. https://doi.org/10.1023/B:BMMD.0000031751.67267.9f
23. Guillemot F et al (2010) High-throughput laser printing of cells and biomaterials for tissue engineering. Acta Biomater 6(7):2494–2500. https://doi.org/10.1016/j.actbio.2009.09.029
24. Gruene M, Unger C, Koch L, Deiwick A, Chichkov B (2011) Dispensing pico to nanolitre of a natural hydrogel by laser-assisted bioprinting. Biomed Eng Online 10(1):19. https://doi.org/10.1186/1475-925X-10-19

25. Lin Y, Huang Y, Chrisey DB (2009) Droplet formation in matrix-assisted pulsed-laser evaporation direct writing of glycerol-water solution. J Appl Phys 105(9):093111. https://doi.org/10.1063/1.3116724
26. Koch L, Brandt O, Deiwick A, Chichkov B (2017) Laser-assisted bioprinting at different wavelengths and pulse durations with a metal dynamic release layer: a parametric study. Int J Bioprinting 3(1):42–53. https://doi.org/10.18063/IJB.2017.01.001
27. Wang Z, Abdulla R, Parker B, Samanipour R, Ghosh S, Kim K (2015) A simple and high-resolution stereolithography-based 3D bioprinting system using visible light crosslinkable bioinks. Biofabrication 7(4):045009. https://doi.org/10.1088/1758-5090/7/4/045009
28. Lim KS et al (2016) New visible-light photoinitiating system for improved print fidelity in gelatin-based bioinks. ACS Biomater Sci Eng 2(10):1752–1762. https://doi.org/10.1021/acsbiomaterials.6b00149
29. Bernal PN et al (2019) Volumetric bioprinting of complex living-tissue constructs within seconds. Adv Mater 31(42):1904209. https://doi.org/10.1002/adma.201904209
30. Klebe RJ (1988) Cytoscribing: a method for micropositioning cells and the construction of two- and three-dimensional synthetic tissues. Exp Cell Res 179(2):362–373. https://doi.org/10.1016/0014-4827(88)90275-3
31. Wilson WC, Boland T (2003) Cell and organ printing 1: protein and cell printers. In: Anatomical record-part a discoveries in molecular, cellular, and evolutionary biology, vol 272, no 2, pp 491–496. https://doi.org/10.1002/ar.a.10057
32. Gu Z, Fu J, Lin H, He Y (2020) Development of 3D bioprinting: From printing methods to biomedical applications. Asian J Pharm Sci, 15(5):529–557. https://doi.org/10.1016/j.ajps.2019.11.003. (Shenyang Pharmaceutical University, 01 Sept 2020)
33. Gudapati H, Dey M, Ozbolat I (2016) A comprehensive review on droplet-based bioprinting: past, present and future. Biomaterials 102:20–42. https://doi.org/10.1016/j.biomaterials.2016.06.012. (Elsevier Ltd., 01 Sept 2016)
34. Campos DFD et al (2015) The stiffness and structure of three-dimensional printed hydrogels direct the differentiation of mesenchymal stromal cells toward adipogenic and osteogenic lineages. Tissue Eng Part A 21(3–4):740–756. https://doi.org/10.1089/ten.tea.2014.0231
35. Maiullari F et al (2018) A multi-cellular 3D bioprinting approach for vascularized heart tissue engineering based on HUVECs and iPSC-derived cardiomyocytes. Sci Rep 8(1):1–15. https://doi.org/10.1038/s41598-018-31848-x
36. Kingsley DM, Dias AD, Chrisey DB, Corr DT (2013) Single-step laser-based fabrication and patterning of cell-encapsulated alginate microbeads. Biofabrication 5(4):045006. https://doi.org/10.1088/1758-5082/5/4/045006
37. Xu C, Zhang M, Huang Y, Ogale A, Fu J, Markwald RR (2014) Study of droplet formation process during drop-on-demand inkjetting of living cell-laden bioink. Langmuir 30(30):9130–9138. https://doi.org/10.1021/la501430x
38. Lee A et al (2019) 3D bioprinting of collagen to rebuild components of the human heart. Science 365(6452):482–487. https://doi.org/10.1126/science.aav9051
39. Marchioli G et al (2015) Fabrication of three-dimensional bioplotted hydrogel scaffolds for islets of Langerhans transplantation. Biofabrication 7(2):025009. https://doi.org/10.1088/1758-5090/7/2/025009
40. Kessel B, Lee M, Bonato A, Tinguely Y, Tosoratti E, Zenobi-Wong M (2020) 3D bioprinting of macroporous materials based on entangled hydrogel microstrands. Adv Sci 7(18):2001419. https://doi.org/10.1002/advs.202001419
41. Grottkau BE, Hui Z, Pang Y (2020) A novel 3D bioprinter using direct-volumetric drop-on-demand technology for fabricating micro-tissues and drug-delivery. Int J Mol Sci 21(10):3482. https://doi.org/10.3390/ijms21103482
42. Koch F, Tröndle K, Finkenzeller G, Zengerle R, Zimmermann S, Koltay P (2020) Generic method of printing window adjustment for extrusion-based 3D-bioprinting to maintain high viability of mesenchymal stem cells in an alginate-gelatin hydrogel. Bioprinting 20:e00094. https://doi.org/10.1016/j.bprint.2020.e00094

43. Dobos A et al (2020) Thiol–gelatin–norbornene bioink for laser-based high-definition bioprinting. Adv Healthcare Mater 9(15):1900752. https://doi.org/10.1002/adhm.201900752
44. Leucht A, Volz AC, Rogal J, Borchers K, Kluger PJ (2020) Advanced gelatin-based vascularization bioinks for extrusion-based bioprinting of vascularized bone equivalents. Sci Rep 10(1):1–15. https://doi.org/10.1038/s41598-020-62166-w
45. Ji Y et al (2019) Improved resolution and fidelity of droplet-based bioprinting by upward ejection. ACS Biomater Sci Eng 5(8):4112–4121. https://doi.org/10.1021/acsbiomaterials.9b00400
46. Wang Z, Jin X, Dai R, Holzman JF, Kim K (2016) An ultrafast hydrogel photocrosslinking method for direct laser bioprinting. RSC Adv 6(25):21099–21104. https://doi.org/10.1039/c5ra24910d
47. Pitarresi G, Martorana A, Palumbo FS, Fiorica C, Giammona G (2020) New gellan gum-graft-poly(D, L-lactide-co-glycolide) copolymers as promising bioinks: Synthesis and characterization. Int J Biol Macromol 162:1653–1667. https://doi.org/10.1016/j.ijbiomac.2020.07.254
48. Seol YJ et al (2018) 3D bioprinted biomask for facial skin reconstruction. Bioprinting 10:e00028. https://doi.org/10.1016/j.bprint.2018.e00028
49. Lam T et al (2019) Photopolymerizable gelatin and hyaluronic acid for stereolithographic 3D bioprinting of tissue-engineered cartilage. J Biomed Mater Res B Appl Biomater 107(8):2649–2657. https://doi.org/10.1002/jbm.b.34354
50. Sharma R, Smits IPM, de La Vega L, Lee C, Willerth SM (2020) 3D bioprinting pluripotent stem cell derived neural tissues using a novel fibrin bioink containing drug releasing microspheres. Front Bioeng Biotechnol 8:57. https://doi.org/10.3389/fbioe.2020.00057
51. Hakam MS, Imani R, Abolfathi N, Fakhrzadeh H, Sharifi AM (2016) Evaluation of fibrin-gelatin hydrogel as biopaper for application in skin bioprinting: an in-vitro study. Bio-Med Mater Eng 27(6):669–682. https://doi.org/10.3233/BME-161617
52. Albanna M et al (2019) In situ bioprinting of autologous skin cells accelerates wound healing of extensive excisional full-thickness wounds. Sci Rep 9(1). https://doi.org/10.1038/s41598-018-38366-w
53. Maturavongsadit P, Narayanan LK, Chansoria P, Shirwaiker R, Benhabbour SR (2021) Cell-laden nanocellulose/chitosan-based bioinks for 3D bioprinting and enhanced osteogenic cell differentiation. ACS Appl Bio Mater. https://doi.org/10.1021/acsabm.0c01108
54. Ni T, Liu M, Zhang Y, Cao Y, Pei R (2020) 3D Bioprinting of bone marrow mesenchymal stem cell-laden silk fibroin double network scaffolds for cartilage tissue repair. Bioconjug Chem 31(8):1938–1947. https://doi.org/10.1021/acs.bioconjchem.0c00298
55. Li Z et al (2018) 3D-printed scaffolds with calcified layer for osteochondral tissue engineering. J Biosci Bioeng 126(3):389–396. https://doi.org/10.1016/j.jbiosc.2018.03.014
56. Kim SH et al (2018) Precisely printable and biocompatible silk fibroin bioink for digital light processing 3D printing. Nat Commun 9(1):1–14. https://doi.org/10.1038/s41467-018-03759-y
57. Wüst S, Godla ME, Müller R, Hofmann S (2014) Tunable hydrogel composite with two-step processing in combination with innovative hardware upgrade for cell-based three-dimensional bioprinting. Acta Biomater 10(2):630–640. https://doi.org/10.1016/j.actbio.2013.10.016
58. Gao G, Schilling AF, Yonezawa T, Wang J, Dai G, Cui X (2014) Bioactive nanoparticles stimulate bone tissue formation in bioprinted three-dimensional scaffold and human mesenchymal stem cells. Biotechnol J 9(10):1304–1311. https://doi.org/10.1002/biot.201400305
59. Qiao Z et al (2021) Bioinspired stratified electrowritten fiber-reinforced hydrogel constructs with layer-specific induction capacity for functional osteochondral regeneration. Biomaterials 266:120385. https://doi.org/10.1016/j.biomaterials.2020.120385
60. Gao G et al (2015) Improved properties of bone and cartilage tissue from 3D inkjet-bioprinted human mesenchymal stem cells by simultaneous deposition and photocrosslinking in PEG-GelMA. Biotech Lett 37(11):2349–2355. https://doi.org/10.1007/s10529-015-1921-2
61. Ke D et al (2020) Bioprinted trachea constructs with patient-matched design, mechanical and biological properties. Biofabrication 12(1). https://doi.org/10.1088/1758-5090/ab5354

62. Xu T et al (2013) Hybrid printing of mechanically and biologically improved constructs for cartilage tissue engineering applications. Biofabrication 5(1):015001. https://doi.org/10.1088/1758-5082/5/1/015001
63. Catros S et al (2012) Layer-by-layer tissue microfabrication supports cell proliferation in vitro and in vivo. Tissue Eng Part C Methods 18(1):62–70. https://doi.org/10.1089/ten.tec.2011.0382
64. Gori M et al (2020) Biofabrication of hepatic constructs by 3D bioprinting of a cell-laden thermogel: an effective tool to assess drug-induced hepatotoxic response. Adv Healthcare Mater 9(21). https://doi.org/10.1002/adhm.202001163
65. Badea A et al (2017) 3D-printed pHEMA materials for topographical and biochemical modulation of dorsal root ganglion cell response. ACS Appl Mater Interfaces 9(36):30318–30328. https://doi.org/10.1021/acsami.7b06742
66. Kyle S, Jessop ZM, Al-Sabah A, Whitaker IS (2017) "Printability" of candidate biomaterials for extrusion based 3D printing: state-of-the-art. Adv Healthcare Mater 6(16). https://doi.org/10.1002/adhm.201700264. (Wiley-VCH Verlag, 23 Aug 2017)
67. Ramirez Caballero SS et al (2019) 3-D printing of chitosan-calcium phosphate inks: rheology, interactions and characterization. J Mater Sci Mater Med 30(1):1–15. https://doi.org/10.1007/s10856-018-6201-y
68. Xu HHK et al (2017) Calcium phosphate cements for bone engineering and their biological properties. Bone Res 5. https://doi.org/10.1038/boneres.2017.56. (Sichuan University, 20 Dec 2017)
69. Mezger TG (2019) The rheology handbook. Vincentz Network
70. Ouyang L, Highley CB, Rodell CB, Sun W, Burdick JA (2016) 3D printing of shear-thinning hyaluronic acid hydrogels with secondary cross-linking. ACS Biomater Sci Eng 2(10):1743–1751. https://doi.org/10.1021/acsbiomaterials.6b00158
71. Mouser VHM, Melchels FPW, Visser J, Dhert WJA, Gawlitta D, Malda J (2016) Yield stress determines bioprintability of hydrogels based on gelatin-methacryloyl and gellan gum for cartilage bioprinting. Biofabrication 8(3):035003. https://doi.org/10.1088/1758-5090/8/3/035003
72. Chopin-Doroteo M, Mandujano-Tinoco EA, Krötzsch E (2021) Tailoring of the rheological properties of bioinks to improve bioprinting and bioassembly for tissue replacement. Biochimica et Biophysica Acta-General Subjects1865(2):129782. https://doi.org/10.1016/j.bbagen.2020.129782. (Elsevier B.V., 01 Feb 2021)
73. Ribeiro A et al (2018) Assessing bioink shape fidelity to aid material development in 3D bioprinting. Biofabrication 10(1). https://doi.org/10.1088/1758-5090/aa90e2
74. Malda J et al (2013) 25th anniversary article: engineering hydrogels for biofabrication. Adv Mater 25(36):5011–5028. https://doi.org/10.1002/adma.201302042
75. Highley CB, Song KH, Daly AC, Burdick JA (2019) Jammed microgel Inks for 3D printing applications. Adv Sci 6(1):1801076. https://doi.org/10.1002/advs.201801076
76. Tang G, Du B, Stadler FJ (2018) A novel approach to analyze the rheological properties of hydrogels with network structure simulation. J Polym Res 25(1):1–10. https://doi.org/10.1007/s10965-017-1352-y
77. Murphy SV, Atala A (2014) 3D bioprinting of tissues and organs. Nat Biotechnol 32(8):773–785. https://doi.org/10.1038/nbt.2958. (Nature Publishing Group, 05 Aug 2014)
78. Gopinathan J, Noh I (2018) Recent trends in bioinks for 3D printing. Biomater Res 22(1):1–15. https://doi.org/10.1186/s40824-018-0122-1. (BioMed Central Ltd., 06 Apr 2018)
79. P. S. Gungor-Ozkerim, I. Inci, Y. S. Zhang, A. Khademhosseini, and M. R. Dokmeci, "Bioinks for 3D bioprinting: An overview," *Biomaterials Science*, vol. 6, no. 5. Royal Society of Chemistry, pp. 915–946, May 01, 2018, doi: https://doi.org/10.1039/c7bm00765e.
80. Schwab A, Levato R, D'Este M, Piluso S, Eglin D, Malda J (2020) Printability and shape fidelity of bioinks in 3D bioprinting. Chem Rev 120(19):11028–11055. https://doi.org/10.1021/acs.chemrev.0c00084. (American Chemical Society, 14 Oct 2020)
81. Yu Y, Zhang Y, Martin JA, Ozbolat IT (2013) Evaluation of cell viability and functionality in vessel-like bioprintable cell-laden tubular channels. J Biomech Eng 135(9). https://doi.org/10.1115/1.4024575

82. Chu S, Maples MM, Bryant SJ (2020) Cell encapsulation spatially alters crosslink density of poly(ethylene glycol) hydrogels formed from free-radical polymerizations. Acta Biomater 109:37–50. https://doi.org/10.1016/j.actbio.2020.03.033
83. Li Z et al (2013) Initiation efficiency and cytotoxicity of novel water-soluble two-photon photoinitiators for direct 3D microfabrication of hydrogels. RSC Adv 3(36):15939–15946. https://doi.org/10.1039/c3ra42918k
84. Seck TM, Melchels FPW, Feijen J, Grijpma DW (2010) Designed biodegradable hydrogel structures prepared by stereolithography using poly(ethylene glycol)/poly(d, l-lactide)-based resins. J Control Release 148(1):34–41. https://doi.org/10.1016/j.jconrel.2010.07.111
85. Zhang Z et al (2018) Evaluation of bioink printability for bioprinting applications. Appl Phys Rev 5(4):041304. https://doi.org/10.1063/1.5053979
86. Li D (2008) Ohnesorge number. In: Encyclopedia of microfluidics and nanofluidics. Springer, US, pp 1513–1513
87. Kang HW, Lee SJ, Ko IK, Kengla C, Yoo JJ, Atala A (2016) A 3D bioprinting system to produce human-scale tissue constructs with structural integrity. Nat Biotechnol 34(3):312–319. https://doi.org/10.1038/nbt.3413
88. Gao G et al (2017) Tissue engineered bio-blood-vessels constructed using a tissue-specific bioink and 3D coaxial cell printing technique: a novel therapy for ischemic disease. Adv Func Mater 27(33):1700798. https://doi.org/10.1002/adfm.201700798
89. Lee W et al (2010) On-demand three-dimensional freeform fabrication of multi-layered hydrogel scaffold with fluidic channels. Biotechnol Bioeng 105(6):n/a–n/a. https://doi.org/10.1002/bit.22613
90. Heinrich MA et al (2019) 3D bioprinting: from benches to translational applications. Small 15(23):1805510. https://doi.org/10.1002/smll.201805510
91. Lee J, Oh SJ, An SH, Kim WD, Kim SH, Kim SH (2020) Machine learning-based design strategy for 3D printable bioink: elastic modulus and yield stress determine printability. Biofabrication 12(3):035018. https://doi.org/10.1088/1758-5090/ab8707
92. Paxton N, Smolan W, Böck T, Melchels F, Groll J, Jungst T (2017) Proposal to assess printability of bioinks for extrusion-based bioprinting and evaluation of rheological properties governing bioprintability. Biofabrication 9(4):044107. https://doi.org/10.1088/1758-5090/aa8dd8
93. Levato R et al (2017) The bio in the ink: cartilage regeneration with bioprintable hydrogels and articular cartilage-derived progenitor cells. Acta Biomater 61:41–53. https://doi.org/10.1016/j.actbio.2017.08.005
94. Bertlein S et al (2017) Thiol-ene clickable gelatin: a platform bioink for multiple 3D biofabrication technologies. Adv Mater 29(44):1703404. https://doi.org/10.1002/adma.201703404
95. Tytgat L et al (2019) Additive manufacturing of photo-crosslinked gelatin scaffolds for adipose tissue engineering. Acta Biomater 94:340–350. https://doi.org/10.1016/j.actbio.2019.05.062
96. Ooi HW, Mota C, Tessa Ten Cate A, Calore A, Moroni L, Baker MB (2018) Thiol-ene alginate hydrogels as versatile bioinks for bioprinting. Biomacromol 19(8):3390–3400. https://doi.org/10.1021/acs.biomac.8b00696
97. Stichler S et al (2017) Double printing of hyaluronic acid/poly(glycidol) hybrid hydrogels with poly (ϵ-caprolactone) for MSC chondrogenesis. Biofabrication 9(4):044108. https://doi.org/10.1088/1758-5090/aa8cb7
98. Xin S, Chimene D, Garza JE, Gaharwar AK, Alge DL (2019) Clickable PEG hydrogel microspheres as building blocks for 3D bioprinting. Biomater Sci 7(3):1179–1187. https://doi.org/10.1039/c8bm01286e
99. Ouyang L, Highley CB, Sun W, Burdick JA (2017) A generalizable strategy for the 3D bioprinting of hydrogels from nonviscous photo-crosslinkable inks. Adv Mater 29(8):1604983. https://doi.org/10.1002/adma.201604983
100. Shih H, Lin C-C (2013) Visible-light-mediated thiol-ene hydrogelation using eosin-y as the only photoinitiator. Macromol Rapid Commun 34(3):269–273. https://doi.org/10.1002/marc.201200605

101. Lin H et al (2013) Application of visible light-based projection stereolithography for live cell-scaffold fabrication with designed architecture. Biomaterials 34(2):331–339. https://doi.org/10.1016/j.biomaterials.2012.09.048
102. Panwar A, Tan L (2016) Current status of bioinks for micro-extrusion-based 3D bioprinting. Molecules 21(6):685. https://doi.org/10.3390/molecules21060685
103. Huettner N, Dargaville TR, Forget A (2018) Discovering cell-adhesion peptides in tissue engineering: beyond RGD. In: Trends in Biotechnol 36(4):372–383. https://doi.org/10.1016/j.tibtech.2018.01.008. (Elsevier Ltd., 01 Apr 2018)
104. Cheng J et al (2008) Rheological properties of cell-hydrogel composites extruding through small-diameter tips. J Manuf Sci Eng Trans ASME 130(2):0210141–0210145. https://doi.org/10.1115/1.2896215
105. Maisonneuve BGC, Roux DCD, Thorn P, Cooper-White JJ (2013) Effects of cell density and biomacromolecule addition on the flow behavior of concentrated mesenchymal cell suspensions. Biomacromol 14(12):4388–4397. https://doi.org/10.1021/bm401335g
106. Billiet T, Gevaert E, de Schryver T, Cornelissen M, Dubruel P (2014) The 3D printing of gelatin methacrylamide cell-laden tissue-engineered constructs with high cell viability. Biomaterials 35(1):49–62. https://doi.org/10.1016/j.biomaterials.2013.09.078
107. Diamantides N, Dugopolski C, Blahut E, Kennedy S, Bonassar LJ (2019) High density cell seeding affects the rheology and printability of collagen bioinks. Biofabrication 11(4). https://doi.org/10.1088/1758-5090/ab3524
108. Gillispie GJ et al (2020) The influence of printing parameters and cell density on bioink printing outcomes. Tissue Eng Part A 26(23–24):1349–1358. https://doi.org/10.1089/ten.tea.2020.0210
109. Cidonio G, Glinka M, Dawson JI, Oreffo ROC (2019) The cell in the ink: improving biofabrication by printing stem cells for skeletal regenerative medicine. Biomaterials 209:10–24. https://doi.org/10.1016/j.biomaterials.2019.04.009. (Elsevier Ltd., 01 Jul 2019)
110. Liu W et al (2017) Extrusion bioprinting of shear-thinning gelatin methacryloyl bioinks. Adv Healthcare Mater 6(12):1601451. https://doi.org/10.1002/adhm.201601451
111. Kawamoto Y, Nakajima YI, Kuranaga E (2016) Apoptosis in cellular society: communication between apoptotic cells and their neighbors. Int J Mol Sci 17(12). https://doi.org/10.3390/ijms17122144. (MDPI AG, 20 Dec 2016)
112. Nair K et al (2009) Characterization of cell viability during bioprinting processes. Biotechnol J 4(8):1168–1177. https://doi.org/10.1002/biot.200900004
113. Dubbin K, Tabet A, Heilshorn SC (2017) Quantitative criteria to benchmark new and existing bio-inks for cell compatibility. Biofabrication 9(4). https://doi.org/10.1088/1758-5090/aa869f
114. Aguado BA, Mulyasasmita W, Su J, Lampe KJ, Heilshorn SC (2012) Improving viability of stem cells during syringe needle flow through the design of hydrogel cell carriers. Tissue Eng Part A 18(7–8):806–815. https://doi.org/10.1089/ten.tea.2011.0391
115. Skardal A et al (2015) A hydrogel bioink toolkit for mimicking native tissue biochemical and mechanical properties in bioprinted tissue constructs. Acta Biomater 25:24–34. https://doi.org/10.1016/j.actbio.2015.07.030
116. Barua R, Giria H, Datta S, Roy Chowdhury A, Datta P (2020) Force modeling to develop a novel method for fabrication of hollow channels inside a gel structure. Proc Inst Mech Eng Part H J Eng Med 234(2):223–231. https://doi.org/10.1177/0954411919891654
117. Kim J, Kong JS, Han W, Kim BS, Cho D-W (2020) 3D cell printing of tissue/organ-mimicking constructs for therapeutic and drug testing applications. Int J Mol Sci 21(20):7757. https://doi.org/10.3390/ijms21207757
118. Banerjee A et al (2009) The influence of hydrogel modulus on the proliferation and differentiation of encapsulated neural stem cells. Biomaterials 30(27):4695–4699. https://doi.org/10.1016/j.biomaterials.2009.05.050
119. Grigoryan B et al (2021) Development, characterization, and applications of multi-material stereolithography bioprinting. Sci Rep 11(1):3171. https://doi.org/10.1038/s41598-021-82102-w

120. Datta S, Das A, Sasmal P, Bhutoria S, Roy Chowdhury A, Datta P (2020) Alginate-poly(amino acid) extrusion printed scaffolds for tissue engineering applications. Int. J Polym Mater Polym Biomater 69(2):65–72. https://doi.org/10.1080/00914037.2018.1539988
121. Datta S et al (2018) Alginate-honey bioinks with improved cell responses for applications as bioprinted tissue engineered constructs. J Mater Res 33(14):2029–2039. https://doi.org/10.1557/jmr.2018.202
122. Mazzocchi A, Devarasetty M, Huntwork R, Soker S, Skardal A (2019) Optimization of collagen type I-hyaluronan hybrid bioink for 3D bioprinted liver microenvironments. Biofabrication 11(1). https://doi.org/10.1088/1758-5090/aae543
123. Pal A, Tripathi K, Pathak C, Vernon BL (2019) Plasma-based fast-gelling biohybrid gels for biomedical applications. Sci Rep 9(1):1–10. https://doi.org/10.1038/s41598-019-47366-3
124. Xing Q, Yates K, Vogt C, Qian Z, Frost MC, Zhao F (2014) Increasing mechanical strength of gelatin hydrogels by divalent metal ion removal. Sci Rep 4(1):1–10. https://doi.org/10.1038/srep04706
125. Yucel T, Cebe P, Kaplan DL (2009) Vortex-induced injectable silk fibroin hydrogels. Biophys J 97(7):2044–2050. https://doi.org/10.1016/j.bpj.2009.07.028
126. Croisier F, Jérôme C (2013) Chitosan-based biomaterials for tissue engineering. Eur Polym J 49(4):780–792. https://doi.org/10.1016/j.eurpolymj.2012.12.009. (Elsevier Ltd., 01 Apr 2013)
127. Hu K, Olsen BR (2016) The roles of vascular endothelial growth factor in bone repair and regeneration. Bone 91:30–38, (Elsevier Inc., 01 Oct 2016). https://doi.org/10.1016/j.bone.2016.06.013
128. Benn A, Hiepen C, Osterland M, Schütte C, Zwijsen A, Knaus P (2017) Role of bone morphogenetic proteins in sprouting angiogenesis: Differential BMP receptor-dependent signaling pathways balance stalk vs. tip cell competence. FASEB J 31(11):4720–4733. https://doi.org/10.1096/fj.201700193RR
129. Miller E, Phillippi J, Fisher G, Campbell P, Walker L, Weiss L (2009) Inkjet printing of growth factor concentration gradients and combinatorial arrays immobilized on biologically-relevant substrates. Comb Chem High Throughput Screen 12(6):604–618. https://doi.org/10.2174/138620709788681907
130. Dong L, Wang SJ, Zhao XR, Zhu YF, Yu JK (2017) 3D-printed poly (ϵ-caprolactone) scaffold integrated with cell-laden chitosan hydrogels for bone tissue engineering. Sci Rep 7(1). https://doi.org/10.1038/s41598-017-13838-7
131. Walker JM et al (2017) Effect of chemical and physical properties on the in vitro degradation of 3D printed high resolution poly(propylene fumarate) scaffolds. Biomacromol 18(4):1419–1425. https://doi.org/10.1021/acs.biomac.7b00146
132. Freeman FE, Kelly DJ (2017) Tuning alginate bioink stiffness and composition for controlled growth factor delivery and to spatially direct MSC Fate within bioprinted tissues. Sci Rep 7(1):1–12. https://doi.org/10.1038/s41598-017-17286-1
133. Gordon TD, Schloesser L, Humphries DE, Spector M (2004) Effects of the degradation rate of collagen matrices on articular chondrocyte proliferation and biosynthesis in vitro. Tissue Eng 10(7–8):1287–1295. https://doi.org/10.1089/ten.2004.10.1287
134. Chimene D, Lennox KK, Kaunas RR, Gaharwar AK (2016) Advanced bioinks for 3D printing: a materials science perspective. Ann Biomed Eng 44(6):2090–2102. https://doi.org/10.1007/s10439-016-1638-y. (Springer New York LLC, 01 Jun 2016)
135. Mann BK, Gobin AS, Tsai AT, Schmedlen RH, West JL (2001) Smooth muscle cell growth in photopolymerized hydrogels with cell adhesive and proteolytically degradable domains: Synthetic ECM analogs for tissue engineering. Biomaterials 22(22):3045–3051. https://doi.org/10.1016/S0142-9612(01)00051-5
136. Lutolf MP et al (2003) Synthetic matrix metalloproteinase-sensitive hydrogels for the conduction of tissue regeneration: engineering cell-invasion characteristics. Proc Natl Acad Sci USA 100(9):5413–5418. https://doi.org/10.1073/pnas.0737381100
137. Mano JF et al (2007) Natural origin biodegradable systems in tissue engineering and regenerative medicine: present status and some moving trends. J R Soc Interface 4(17):999–1030. https://doi.org/10.1098/rsif.2007.0220. (Royal Society, 22 Dec 2007)

138. Diniz IMA et al (2015) Pluronic F-127 hydrogel as a promising scaffold for encapsulation of dental-derived mesenchymal stem cells. J Mater Sci Mater Med 26(3):1–10. https://doi.org/10.1007/s10856-015-5493-4
139. Li C et al (2015) Rapid formation of a supramolecular polypeptide-DNA Hydrogel for in situ three-dimensional multilayer bioprinting. Angewandte Chemie Int Edn 54(13):3957–3961. https://doi.org/10.1002/anie.201411383
140. English MA et al (2019) Programmable CRISPR-responsive smart materials. Science 365(6455):780–785. https://doi.org/10.1126/science.aaw5122
141. Datta S, Jana S, Das A, Chakraborty A, Chowdhury AR, Datta P (2020) Bioprinting of radiopaque constructs for tissue engineering and understanding degradation behavior by use of Micro-CT. Bioactive Mater 5(3):569–576. https://doi.org/10.1016/j.bioactmat.2020.04.015
142. Jia J et al (2014) Engineering alginate as bioink for bioprinting. Acta Biomater 10(10):4323–4331. https://doi.org/10.1016/j.actbio.2014.06.034
143. Schuurman W et al (2013) Gelatin-methacrylamide hydrogels as potential biomaterials for fabrication of tissue-engineered cartilage constructs. Macromol Biosci 13(5):551–561. https://doi.org/10.1002/mabi.201200471
144. Canal T, Peppas NA (1989) Correlation between mesh size and equilibrium degree of swelling of polymeric networks. J Biomed Mater Res 23(10):1183–1193. https://doi.org/10.1002/jbm.820231007
145. Reinhart CT, Peppas NA (1984) Solute diffusion in swollen membranes. Part II. Influence of crosslinking on diffusive properties. J Membr Sci 18(C):227–239. https://doi.org/10.1016/S0376-7388(00)85036-X
146. Amsden B (1998) Solute diffusion within hydrogels. Mechanisms and models. Macromolecules 31(23):8382–8395. https://doi.org/10.1021/ma980765f
147. Jimenez-Vergara AC, Lewis J, Hahn MS, Munoz-Pinto DJ (2018) An improved correlation to predict molecular weight between crosslinks based on equilibrium degree of swelling of hydrogel networks. J Biomed Mater Res B Appl Biomater 106(3):1339–1348. https://doi.org/10.1002/jbm.b.33942
148. Peppas NA, Merrill EW (1977) Crosslinked poly(vinyl alcohol) hydrogels as swollen elastic networks. J Appl Polym Sci 21(7):1763–1770. https://doi.org/10.1002/app.1977.070210704
149. Watkins AW, Anseth KS (2005) Investigation of molecular transport and distributions in poly(ethylene glycol) hydrogels with confocal laser scanning microscopy. Macromolecules 38(4):1326–1334. https://doi.org/10.1021/ma0475232
150. Jiao W et al (2019) Effects of molecular weight and guluronic acid/mannuronic acid ratio on the rheological behavior and stabilizing property of sodium alginate. Molecules (Basel, Switzerland) 24(23). https://doi.org/10.3390/molecules24234374
151. Rutz AL, Hyland KE, Jakus AE, Burghardt WR, Shah RN (2015) A Multimaterial bioink method for 3D printing tunable, cell-compatible hydrogels. Adv Mater 27(9):1607–1614. https://doi.org/10.1002/adma.201405076
152. Chen N et al (2020) Using multilayered hydrogel bioink in three-dimensional bioprinting for homogeneous cell distribution. J Vis Exp 2020(159):e60920. https://doi.org/10.3791/60920
153. Bhattacharyya A, Janarthanan G, Tran HN, Ham HJ, Yoon JH, Noh I (2021) Bioink homogeneity control during 3D bioprinting of multicomponent micro/nanocomposite hydrogel for even tissue regeneration using novel twin screw extrusion system. Chem Eng J 415:128971. https://doi.org/10.1016/j.cej.2021.128971
154. Dubbin K, Hori Y, Lewis KK, Heilshorn SC (2016) Dual-stage crosslinking of a gel-phase bioink improves cell viability and homogeneity for 3D bioprinting. Adv Healthcare Mater 5(19):2488–2492. https://doi.org/10.1002/adhm.201600636
155. Munaz A, Vadivelu RK, st John J, Barton M, Kamble H, Nguyen NT (2016) Three-dimensional printing of biological matters. J Sci Adv Mater Devices 1(1):1–17. https://doi.org/10.1016/j.jsamd.2016.04.001. (Elsevier B.V., 01 Mar 2016)
156. Graham S, Marina PF, Blencowe A (2019) Thermoresponsive polysaccharides and their thermoreversible physical hydrogel networks. Carbohydr Polym 207:143–159. https://doi.org/10.1016/j.carbpol.2018.11.053. (Elsevier Ltd., 01 Mar 2019)

157. Chung JHY et al (2013) Bio-ink properties and printability for extrusion printing living cells. Biomater Sci 1(7):763–773. https://doi.org/10.1039/c3bm00012e
158. Yu Y et al (2016) Three-dimensional bioprinting using self-Assembling scalable scaffold-free 'tissue strands' as a new bioink. Sci Rep 6(1):1–11. https://doi.org/10.1038/srep28714
159. Murata D, Arai K, Nakayama K (2020) Scaffold-free bio-3D printing using spheroids as 'Bio-Inks' for tissue (Re-)construction and drug response tests. Adv Healthcare Mater 9(15):1901831. https://doi.org/10.1002/adhm.201901831
160. Khoshnood N, Zamanian A (2020) A comprehensive review on scaffold-free bioinks for bioprinting. Bioprinting 19:e00088. https://doi.org/10.1016/j.bprint.2020.e00088. (Elsevier B.V., 01 Sept 2020)
161. Lewis EEL et al (2016) A quiescent, regeneration-responsive tissue engineered mesenchymal stem cell bone marrow niche model via magnetic levitation. ACS Nano 10(9):8346–8354. https://doi.org/10.1021/acsnano.6b02841
162. Türker E, Demirçak N, Arslan-Yildiz A (2018) Scaffold-free three-dimensional cell culturing using magnetic levitation. Biomater Sci 6(7):1745–1753. https://doi.org/10.1039/c8bm00122g
163. Ware MJ et al (2016) Generation of homogenous three-dimensional pancreatic cancer cell spheroids using an improved hanging drop technique. Tissue Eng Part C: Methods 22(4):312–321. https://doi.org/10.1089/ten.tec.2015.0280
164. Tsai CC, Hong YJ, Lee RJ, Cheng NC, Yu J (2019) Enhancement of human adipose-derived stem cell spheroid differentiation in an: In situ enzyme-crosslinked gelatin hydrogel. J Mater Chem B 7(7):1064–1075. https://doi.org/10.1039/c8tb02835d
165. He H, He Q, Xu F, Zhou Y, Ye Z, Tan WS (2019) Dynamic formation of cellular aggregates of chondrocytes and mesenchymal stem cells in spinner flask. Cell Prolif 52(4):12587. https://doi.org/10.1111/cpr.12587
166. Li Y, Zhang T, Pang Y, Li L, Chen ZN, Sun W (2019) 3D bioprinting of hepatoma cells and application with microfluidics for pharmacodynamic test of Metuzumab. Biofabrication 11(3). https://doi.org/10.1088/1758-5090/ab256c
167. Jakab K, Neagu A, Mironov V, Markwald RR, Forgacs G (2004) Engineering biological structures of prescribed shaped using self-assembling multicellular systems. Proc Natl Acad Sci USA 101(9):2864–2869. https://doi.org/10.1073/pnas.0400164101
168. Moldovan NI, Hibino N, Nakayama K (2017) Principles of the kenzan method for robotic cell spheroid-based three-dimensional bioprinting. Tissue Eng Part B: Rev 23(3):237–244. https://doi.org/10.1089/ten.teb.2016.0322
169. Itoh M et al (2019) Development of an immunodeficient pig model allowing long-term accommodation of artificial human vascular tubes. Nat Commun 10(1):1–8. https://doi.org/10.1038/s41467-019-10107-1
170. Yanagi Y et al (2017) In vivo and ex vivo methods of growing a liver bud through tissue connection. Sci Rep 7(1):1–15. https://doi.org/10.1038/s41598-017-14542-2
171. Ong CS et al (2017) Biomaterial-free three-dimensional bioprinting of cardiac tissue using human induced pluripotent stem cell derived cardiomyocytes. Sci Rep 7(1):1–11. https://doi.org/10.1038/s41598-017-05018-4
172. Aguilar IN et al (2019) Scaffold-free bioprinting of mesenchymal stem cells using the Regenova printer: spheroid characterization and osteogenic differentiation. Bioprinting 15. https://doi.org/10.1016/j.bprint.2019.e00050
173. Datta S, Das A, Chowdhury AR, Datta P (2019) Bioink formulations to ameliorate bioprinting-induced loss of cellular viability. Biointerphases 14(5):051006. https://doi.org/10.1116/1.5111392
174. Hospodiuk M, Dey M, Sosnoski D, Ozbolat IT (2017) The bioink: a comprehensive review on bioprintable materials. Biotechnol Adv 35(2):217–239. https://doi.org/10.1016/j.biotechadv.2016.12.006. (Elsevier Inc., 01 Mar 2017)
175. Yu F, Choudhury D (2019) Microfluidic bioprinting for organ-on-a-chip models. Drug Discov Today 24(6):1248–1257. https://doi.org/10.1016/j.drudis.2019.03.025. (Elsevier Ltd., 01 Jun 2019)

176. Miri AK, Mostafavi E, Khorsandi D, Hu SK, Malpica M, Khademhosseini A (2019) Bioprinters for organs-on-chips. Biofabrication 11(4):042002. https://doi.org/10.1088/1758-5090/ab2798. (Institute of Physics Publishing, 20 Sept 2019)
177. Ashammakhi N et al (2018) Advances and future perspectives in 4D bioprinting. Biotechnol J 13(12). https://doi.org/10.1002/biot.201800148. (Wiley-VCH Verlag, 01 Dec 2018)
178. Wan Z, Zhang P, Liu Y, Lv L, Zhou Y (2020) Four-dimensional bioprinting: current developments and applications in bone tissue engineering. Acta Biomaterialia, 101:26–42. https://doi.org/10.1016/j.actbio.2019.10.038. (Acta Materialia Inc., 01 Jan 2020)

Chapter 3
3D Printing of Hydrogel Constructs Toward Targeted Development in Tissue Engineering

Alexandra I. Cernencu

Abstract The venture to design a biomaterial to be functional and compatible to human physiology faces numerous challenges in shaping its properties to emulate the macro- and microstructural organization of the natural tissue. Hydrogels are widely considered the closest possible assemblies that could be bioengineered into complex artificial tissues due to their ability to cope more efficiently with the imposed mechanical, morphological, and biological requirements. The use of the three-dimensional (3D) printing technology for the fabrication of biological models facilitated further developments in tissue engineering. These computer-aided techniques enable the design and fabrication of complex structures to meet user-specified requirements. Research on printable formulations really took off in the late decade and there is still an increased interest in discovering most appropriate biomaterial ink. This chapter provides an overview of the latest developments in hydrogel-based inks and describes the factors that are generally considered to have the most influential effect over the printing process. Herein, current 3D printing ink formulations intended for tissue engineering are discussed in hand with printing strategies, focusing on the correlation of the fluid properties of polymeric hydrogel precursors with key control factors and printing performance. The chapter highlights the exhilarating capability of hydrogels to be fabricated as 3D accurate constructs by surveying the representative advances in designing hydrophilic 3D networks for biomedical application.

Keywords 3D printing · Polymeric hydrogels · Printing performance · Tissue engineering · Biofabrication

1 Introduction

Tissue engineering, as a subfield of regenerative medicine, became a far-reaching branch of knowledge that combines cutting-edge research from chemistry, biology, medicine, and engineering in the pursue to reconstruct damaged tissues or whole organs**.** With the rising of life expectancy and a worldwide aging population

A. I. Cernencu (✉)
Advanced Polymer Materials Group, University Politehnica of Bucharest, Bucharest, Romania

A. Kumar et al. (eds.), *3D printable Gel-inks for Tissue Engineering*, Gels Horizons: From Science to Smart Materials, https://doi.org/10.1007/978-981-16-4667-6_3

trend, there is an escalating demand for biosynthetic materials able to recreate the complexity of human tissue and thus to replace the tedious and expensive tissue/organ grafts [1]. The field of tissue engineering aims to provide the scientific ground base and the technologies needed for the development of biological substitutes able to promote endogenous regeneration that further will not only mitigate the critical shortage of donor organs but also provide therapies for patients not in need for a transplant, but with severe chronic conditions that affect the heart, liver, bones, skin, etc. [2].

Spectacular advances have been made over the past 20 years to harness the innate ability of tissues to regenerate and thus, nowadays, various bioartificial materials in the form of skin grafts, bone grafts, cartilage, and even whole trachea graft have already been experimentally implanted in patients and some are already FDA approved [3]. Bright results were achieved concerning also the more complex organ tissues such as heart, lung, and liver tissue, as researchers succeeded to fully recreate the tissue in the laboratory and even reconstruct the whole organ [4]. Nonetheless, the clinical use is limited, the cost of the procedures is exceedingly expensive and there is still enormous work to be done to achieve full functionality and reproducibility of complex tissues to answer the medical need.

Thus far, with a huge potential to genuinely improve the quality of life over the next decades, tissue engineering field has gradually broadened focusing on all prevalent conditions that engage tissue regeneration and increasing research efforts have been devoted to create bioartificial tissue. Scaffold-based strategy is the most appealing approach to generate effective constructs for tissue engineering since it comes with an existent three-dimensional (3D) porous structure that facilitates cells ingrowth and passage of nutrients leading to the formation of new tissue [5, 6]. In need of a 3D network able to maintain a distinct structure, provide support for cells and best mimic the extracellular matrix (ECM), various types of materials were envisioned for scaffold design.

Of all, hydrogels proved to be the leading class of materials best suited to design biosynthetic tissue since they are highly hydrated assemblies of polymer chains that ensure the 3D microenvironment required for cell survival, adhesion, and migration and can act as a template to organize cells and guide the formation of desired tissue. Depending on the intended application, the required properties of the hydrogel scaffold will significantly vary to meet the ones of the tissue of interest. For several years of research, hydrogels were conventionally considered materials with weak mechanical properties and suitable only for soft tissues [7]. Recent advances, nonetheless, proved that their physical and chemical properties can be tremendously modulated not only through chemistry and composition but also through sophisticated architectures. Thus, since it dictates the entire biological and physical behavior of the material, a thoughtful design of the underlying polymeric hydrogel scaffold is crucial and will require advanced fabrication methods to gain spatial control over the physicochemical characteristics and architecture of the hydrogel.

3D printing technology outstands among fabrication techniques through precision, ease, and flexibility of design, delivering complex 3D hydrogel structures with

well-defined and controlled properties. Since its inception, 3D printing truly revolutionized the field of tissue engineering and significant progress has been made due to the capacity of this technique to reproduce any 3D design that further enables the possibility to create patient-specific constructs [8, 9]. By the use of 3D printing, highly porous architectures can be attained, on which tissue engineering extensively relies on, in order to ensure the appropriate microenvironment for tissue regeneration. Moreover, the ability to fabricate hydrogel scaffolds with controlled shape, size, surface morphology, and internal porosity could surpass challenges such as neovascularization, growth factors delivering, and multiple cell lines seeding.

Whereas 3D printing is the first-rate tool to accurate control the fabrication process of functional biomaterial scaffolds, this technique is vitally defined by the material ink properties. The selection of biomaterials to achieve printable formulations comes with new requirements in addition to biological and mechanical characteristics and thus the potential pool of biomaterials significantly narrows [10]. The printability of a material is based on the flowing behavior, liquid-to-solid transition, and the stiffness of the network [11]. On these grounds, polymeric hydrogels are the most convenient class of biomaterial inks also from the rheological point of view. 3D printing technology exploits the ability of hydrogels to undergo a sol–gel transition with respect to specific stimuli and the possibility to tune their rheological response to achieve printable formulations.

Ergo, tissue engineering field greatly benefits from the progress of the fabrication technologies which in turn has a huge impact over the development of biomaterials. With the development of 3D printing, new generation of biomaterials hydrogels ink are designed to be bioactive, bioresorbable, printable, and suitable from the mechanical and architectural points of view.

2 3D Printing Technologies for Hydrogel Inks

The fabrication of hydrogel-based scaffolds as frameworks for tissue development has explored various techniques particularly focusing on computer-assisted approaches due to their capacity to accurately replicate the complexity of the native 3D structures. The concept of layer-by-layer fabrication dates from 1980s, and ever since, the development of the 3D printing technologies really took off. In contrast to the methods not making use of computer control, such as freeze-drying, electrospinning, gas-foaming, etc., computer-aided methods allow the control of the internal architecture at micro- and nanoscale levels [12]. By using a computer software, a 3D structure is defined by user and sliced into transverse-plane images. Each image is created as an individual layer and by stacking them one over the other (layer-by-layer) the object is reconstructed from bottom to top. The software translates each layer into printing instructions (g-code) that further dictates the machine movement in *XYZ* directions. Medical imaging techniques such as computer tomography (CT) or magnetic resonance imaging (MRI) are used to create digital tissue models to fabricate 3D printed models as personalized scaffolds for defect site or even as organ

models [13]. Ergo, with the use of this technology, the high complexity of hydrogel structures is guided by virtual 3D designs so that they can be fabricated on-demand to replicate the cellular and subcellular levels of tissues.

Several strategies to process hydrogels into organized 3D structures are available nowadays and are rapidly advancing, so that understanding the working principle of each is the key to make the most appropriate choice regarding the hydrogel's components and properties toward application. The computer-aided fabrication techniques feasible to manipulate water-rich compositions, bioactive compounds and cells can be divided in three main groups based on the printing mechanism: light-assisted direct-printing inkjet printing and direct dispensing. Despite the freedom of design enabled by 3D printing in general, each printing strategy has its own limitations and its own requirements regarding the biomaterial ink properties.

2.1 Light-Assisted Direct-Printing

The light-assisted 3D printing methods makes use of light energy to initiate a chain reaction over a layer of either monomer or polymers solution in a predesigned pattern and are applicable to print 3D hydrogel constructs out of photocurable precursors [12, 14]. Illustration describing the working principle for light-assisted direct-printing techniques are depicted in Fig. 1.

The first 3D printing technology that has been developed, was using the photopolymerization concept and it was patented in 1986 as *stereolithography (SLA)* [15, 16]. Although first designed to process "photocurable plastics", with the technology advancements throughout the years, SLA technique exceeded by far its original applications being able to fabricate geometries of high complexity out of a broader array of materials The conventional SLA system is build up of a laser source (generally UV light source) attached to a device controlling the laser beam movement on XY-axes and a fabrication platform in the shape of a container that includes a mechanism to control movement on the Z-direction. In the fabrication process, the focal point is

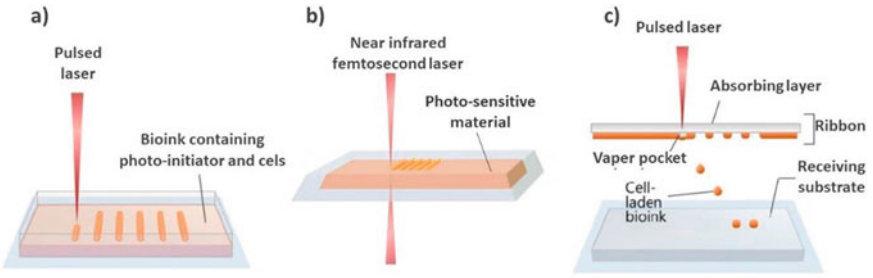

Fig. 1 Illustration describing the working principle for light-assisted direct-printing techniques: **a** stereolithography, **b** two-photon polymerization, and **c** laser-induced forward transfer. Adapted from [30] (licensed under CC BY-NC 4.0)

raster-scanned on the *XY*-direction creating a layer by crosslinking or polymerize the liquid precursor. Then, it moves in the *Z*-direction to print a new layer onto the previous one. In this manner, the focused UV laser beam is spatially manipulated using a computer-designed pathway to build layer by layer a solid object out of photocurable systems. Based on this principle, SLA processes perfected achieving high printing resolutions (10–150 μm) and can further be categorized based on the incident light direction or method of irradiation [17]. SLA technologies were successfully employed to encapsulate cells into 3D hydrogel structures based on poly(ethylene glycol) dimethacrylate or poly(ethylene oxide) combined with poly(ethylene glycol)dimethacrylate, achieving good results in terms of cell viability and toxicity of photoinititor [18].

Using a similar mechanism to induce photopolymerization or to create photo-induced polymer crosslinks, the *two-photon polymerization technique* (referred to as TPP or 2PP) is able to fabricate 3D structures by using light emitted from a near-infrared femtosecond laser. The working principle of TPP is based on the combination of the energies of two individual photons to attain the energy required to activate the curing reaction. This approach leads to a very precise area of excitation, called volume pixel or voxel and makes possible that the laser focus be pointed inside the photosensitive material bath and create the 3D structure within the liquid volume, not only on the surface. By the use of TPP, very high printing resolutions can be attained, as 3D constructs can be build with spatial resolutions down to 100 nm and roughness bellow 10 nm [19]. Although this technique is limited to fabricate geometries in the mm range, it is suitable to build structures appropriate for studying cell–material interactions [20].

Both these technologies are able to create complex 3D structures, but neither SLA nor TPP involve material deposition. Thus, specific requirements are imposed regarding hydrogel properties, especially in terms of chemical functionality and viscosity. Thus, the variety of photopolymerizable hydrogel-based biomaterials suitable for fabrication of constructs for TE by means of SLA and TPP is much more limited.

Laser-induced forward transfer (LIFT) technology is also a direct-writing technique that use a laser light energy to print free form patterns and can fabricate complex structures with a submicron resolution. Its working principle is, nonetheless, more particular since it is a nozzle-free printing technique that involves biomaterial deposition onto a collector substrate. The LIFT setup is typically made of three components: a focused pulsed laser source, one donor, and one acceptor substrate [21]. The LIFT technology has been all along applied to solid donor films, especially for the deposition of various metals, but the same working principle is now applicable to ink liquid films as well. Therefore, this fabrication method is well suited for deposition of a broad range of either liquid or solid materials, extending from metallic inks to cell-containing biomaterials [21–23]. During the printing process, the energy-absorbing material (e.g., hydrogels) that covers the donor slide is propelled toward the acceptor slide due to the local evaporation induced by laser pulses. As such, using the energy of the incident laser pulse, the material is deposited as successive voxels on the acceptor substrate creating 2D and 3D complex patterns. Optimization

of structures, materials, and process parameters will achieve resolutions well below 1 μm. With few restrictions regarding the rheological properties of ink material, this nozzle-free approach became a very competitive biofabrication technique as it allows integration of different types of cells and biological factors in a single-step multilayer-printing process to emulate tissues heterogeneity [24–26]. Technological progress gave rise to several variants of LIFT processes and also to combination of LIFT with other processing methods, so that it became a very interesting cell-printing tool for TE applications. Bioprinting of several cell types such as mesenchymal stem cells (MSCs), human adipose-derived stem cells (hASCs), as well as simultaneous bioprinting of different cells, was successfully performed using LIFT-based technologies without damaging cells phenotype [27–29].

2.2 Inkjet Printing

Inkjet printing is non-contact technique able to fabricate tissue constructs out of hydrogels and living cells by dispensing small volume ink droplets into computer-designed 3D patterns. The printing system is driven by either a thermal or piezoelectrical actuator that generate pulses to produce individual picoliter volume droplets. The process can be configured to run in two modes, drop-on demand jetting, and continuous inkjet printing, where the droplets are generated either using heat to create a pulse caused by ink evaporation or by applying voltage to produce a shock wave that create direct mechanical pulse. In inkjet printing systems, hydrogels structures can be fabricated through a precise droplet-deposition of either hydrogel precursor or crosslinker onto a reactive substrate. The drop-on-demand jetting configuration allows deposition of individual droplets of predefined volumes to be deposited with high speed on a substrate or in a cross-liking bath. The continuous inkjetting, on the other hand, employs a printhead nozzle from which, electrically charged ink droplets are expelled, and precisely directed onto the substrate by the electrical field. Illustration describing the working principle for inkjet printing technique are depicted in Fig. 2.

Inkjet printing technologies can deliver 3D constructs with high speed and with high printing resolutions in a range from 50 to 300 μm, being best suited for printing low-viscosity inks (3.5–10 mPa.s) [31, 32]. Various types of cells (such as mouse myoblasts, bovine chondrocytes, human osteoblasts, human articular chondrocytes, and human microvascular endothelial cells) were loaded in polymeric hydrogels and accurately deposited with high cell viability rates using inkjetting technique [33, 34]. Recent studies surmount the challenges in predicting the relationship between motion control and gelation as well as the difficulties encountered in multicomponent deposition encouraging biofabrication of high-complexity tissue structures using inkjet printing [35, 36].

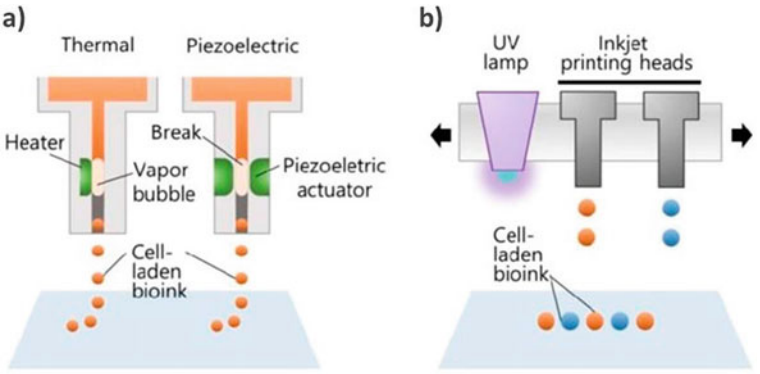

Fig. 2 Illustration describing the working principle for **a** inkjet printing technique and **b** multi-jet modeling. Reproduced from [30] (licensed under CC BY-NC 4.0)

2.3 Direct Dispensing

The most widely exploited technique in biofabrication is from far the direct dispensing that allows the direct deposition of biomaterials to build clinically relevant 3D structures. As highlighted is numerous reviews, complex tissue-like constructs can be fabricated out of cell-embedded polymeric solutions, ECM-derived hydrogels, cell suspensions, or cell aggregates (spheroids) by the use of extrusion-based technology. Its operation principle is based on using pressure as the driving force to extrude the printing formulation as a continuous filament from a syringe barrel throughout a nozzle [31, 37, 38]. The 3D dispensing instrument typically includes one or more dispensing systems, a building platform, and a computer-controlled robotic stage that guides their movement in *XYZ*-directions. The versatility of this fabrication technique arise from the multiple setup options that enables the use of printing formulations with a viscosity within a broad range (from 30 to even above 6×10^7 mPa.s) to build constructs in a layer-by-layer fashion [39, 40]. Ergo, the robotic dispensing process could involve the use of either pneumatic, mechanic, or solenoid system to extrude the biomaterial through the nozzle and deposit a continuous strand onto construction platform (Fig. 3). The printing material require specifically designed properties for each driving mechanism of dispensing so that the strut breakeup to be avoided.

The pneumatic systems operate using pressurized air and can be configured as valve-free or valve-based system. Hydrogels best perform in pneumatic-based extrusion printing given their shear-thinning behavior and thus the ability maintain filament shape upon deposition. Due to its ease of use, the direct dispensing technique is widely preferred to fabricate 3D hydrogel constructs, yet a more precise control of hydrogel deposition is attained when the pneumatic pressure is assisted by a microvalve. The air pressure is additionally regulated by setting up the valve opening time, enabling a better control of filament formation. The mechanically driven systems

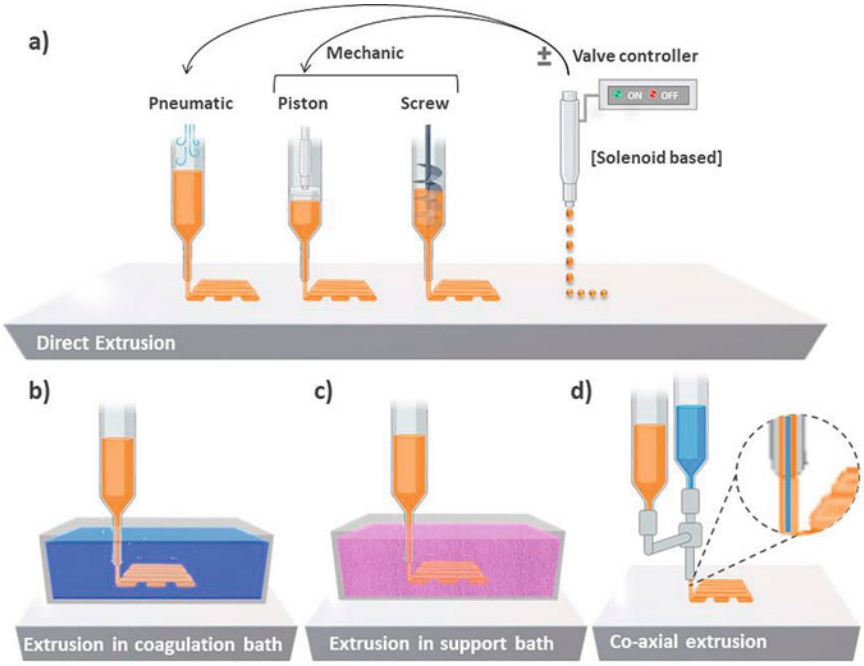

Fig. 3 The direct dispensing process could be driven by either pneumatic or mechanic (piston or screw) forces and may be assisted by a solenoid system (**a**), while the filament may be deposited by direct extrusion, in a coagulation bath, in a support bath or using co-axial extrusion

control the flow by the use of a screw or a piston. Screw-driven systems are best suited for high viscosity bioinks, where the formulation's extrusion is manipulated by screw design and rotation speed. Yet, the use of large pressure may decrease cell viability. Piston-based approaches allow a better control over ink deposition in comparison with pneumatic systems, where air volume compression could induce a significant delay of strands printing. However, both piston and pneumatic dispensing methods perform at cell-appropriate pressures and high cell viability rates were reported toward their use in bioprinting. In solenoid systems, ink flow is controlled by electrical pulses and it is more suitable for low-viscosity inks that do not require temperature control. The use of an electromagnetic valve nonetheless impose a good control over the surrounding conditions since it is more sensitive to several factors (such as variation of temperature and/or viscosity) consequently affecting the accuracy and reproducibility of the printing process [41]. Nonetheless, the robotic dispensing systems can easily accommodate additional modules to enable temperature control of the environment, barrel, and/or needle, to allow in situ crosslinking or to permit multi-material printing in a sequential or co-axial fashion.

The printing resolution is the feature that best accounts the 3D printing performance of each technology. In extrusion-based printing, achieving high-quality printing is still a challenge since resolutions bellow 200 μm are hard to attain.

Table 1 Summarized comparison of (bio) printing technologies

Bioprinter type	Light-assisted printing	Inkjet printing	Direct dispensing
Material viscosities	1–300 mPa.s	3.5–10 mPa.s	30 mPa.s to above 6×10^7 mPa.s
Printing speed	Medium to fast	Fast	Slow
Printing resolution	High	High	Moderate
Printer cost	Low to High	Low	Medium
Cell densities	Medium, 10^8 cells/ml	Low < 10^6 cells/ml	High (cell spheroids)
Cell viability	<85%	80–95%	40–90%

Although the resolution of printing attained by direct dispensing techniques is considered low in comparison with the one of inkjet and light-assisted printing, the fabrication speed and its versatility with respect to equipment configuration, and biomaterial ink selection and design, ranks it as the foremost exploited biofabrication method. To date, artificial liver tissue constructs, adipose tissue sustitutes, and a variety of 3D constructs in the shape of pyramid, hemisphere, hollow cylinder up to nose and ear models were bioprinted by use of direct dispensing without affecting cell viability [42–46].

In Table 1 are summarized the main characteristics of aforementioned printing technologies.

3 Trends and Strategies in Designing Hydrogel-Based Inks

Hydrogel-based inks are the most promising printable materials with the ability to cope efficiently with the requirements of biofabrication technologies and clinical applications. To develop scaffolds for TE, they are designed out of either of natural or synthetic hydrophilic polymers to assembly 3D networks and to accommodate cells and/or bioactive factors. Considering the new perspectives that 3D printing technologies open by gaining control over the shape, porosity, morphology, and dimensions of a construct, the adequate selection, and design of hydrogel precursor have become more and more specific regarding preferred properties with respect to application. In addition to targeting ideal biological and physicochemical properties (such as gel formation, mechanical performance, degradation, diffusion, cell interaction), the rheological response of polymeric solutions became a fundamental aspect in formulating hydrogel-based inks. Ergo, the gold standard in biomaterial ink formulation features: (i) the ability to generate tissue-like constructs with appropriate mechanical strength and robustness; (ii) tunable rheological response including the liquid–solid phase transition to aid printability and post-printing stability of constructs; (iii) biocompatibility and, if required, bioresobability; (iv) functionality and conjugation-binding ability to promote specific tissue/cell-type targeting; (v) high reproductibility toward large-scale construct fabrication.

Although the biomaterial inks for 3D constructs fabrication developed exponentially, starting from single-component inks to multicomponent cell-interactive inks, to date, the advancements in printing formulations have not outperform the progress of the fabrication technologies.

3.1 Single-Component Hydrogel Inks

Single-component inks consist of only one hydrogel-forming compound of natural or synthetic origin and not many studies report the use of sole constituents in formulating printable aqueous environment. Tailoring the properties of a single-network hydrogel is challenging since very few macromolecules impart alone cell adhesion motifs, relevant mechanical properties, and rheological behavior appropriate for 3D printing. The single-component hydrogel inks are considered to be rudimentary, and in most cases, the features in between biocompatibility and shape fidelity are compromised. Yet, successful printing of single-component hydrogel inks able to load cell was accomplished and a summary of reported single-component hydrogel inks for 3D printing is presented as tabulated data (see Table 2).

3.2 Bi-Component Hydrogel Inks

The most frequent reported hydrogel inks are based on proteins (collagen, gelatin, fibrin, Matrigel), polysaccharides (cellulose, alginate, chitosan, hyaluronic acid. agarose, gellan gum), and protein–polysaccharide complexes (chondroitin sulfate), counting on their ability to efficiently accomodate the imposed tissue complexity. However, the natural components partially meet alone the requirements of tissue engineering, concurrently failing to provide appropriate mechanical properties and to permit printing of well-defined 3D constructs. Therefore, various hetero-assembling hydrogel strategies have been proposed to formulate polymeric blends suitable for 3D bioprinting, while more advanced hydrogel inks are designed as interpenetrating networks. The urge to find the most appropriate ink for biofabrication led to a huge number of research papers describing naturally derived or natural/synthetic bi-component hydrogels inks. The literature reviews have extensively covered in several different formats the most frequently employed components in ink formulations, their numerous combinations, and variations and their applicability as bioinks in TE. Table 3 briefly surveys bi-component hydrogel ink for 3D printing.

Table 2 Summary of reported single-component hydrogel inks for 3D printing

3D printing techniques	Biomaterial inks	Application	Refs.
Light-assisted printing	Polyethylene glycol dimethacrylate (PEGDMA)	Tissue engineering, formation of immobilized cell and protein arrays, Tissue constructs, artificial ECM	[47–49]
	Methacrylate-modified gelatin (GelMA)	Bone replacement materials	[50]
	Collagen	Skin tissue engineering	[51, 52]
Inkjet printing	Collagen	Tissue engineering, colony patterning applications	[53]
	Fibrinogen	Tissue engineering, neuronal tissue	[54]
	Gelatin	Endothelial cell attachment	[55]
Direct dispensing	Collagen	Adipose, bone, skin tissue engineering	[56, 57]
	Gelatin	Liver tissue	[58]
	Methacrylate-modified gelatin (GelMA)	Tissue engineering, placental model	[59]
	Alginate	Tissue engineering	[60, 61]
	Chondroitin sulfate	Cartilage regeneration	[62]
	Methacrylate-modified pectin	generation of biomimetic skin constructs	[63]
	Methyl cellulose	Cardiac tissue	[64]
	Nanocellulose	Wound healing, regeneration, and tissue repair	[65]

3.3 Nanocomposite Hydrogel Inks

The macro- and micro-mechanical characteristics of hydrogel-based inks are critical features in defining their performance as tissue scaffolding materials. Ideally, the mechanical properties of hydrogels should be closely comparable with those of targeted tissue, particularly with regard to stiffness and viscoelastic behavior. For instance, soft tissue substitutes should be able to undergo same compression levels as surrounding tissue without shattering. In bioprinting, hydrogels must be capable of maintain their shape after extrusion and withstand deposition of subsequent layers with minimal deformation. Apart from the macroscopic features, cell behavior toward tissue regeneration is genuinely influenced by micromechanical and structural properties of hydrogels such as network stiffness and elastic modulus along with pore size distribution and interconnectivity. When compared to most of biomaterials, hydrogels used in tissue engineering exhibit lower elastic modulus, spanning in the

Table 3 Summary of reported bi-component hydrogel inks for 3D printing

3D printing techniques	Biomaterial inks	Application	Refs.
Light-assisted printing	Methacrylated gelatin/methacrylated hyaluronic acid	Cartilage tissue	[66]
	Polyethylene oxide/polyethylene glycol dimethacrylate,	Cartilage tissue	[67]
	Methacrylated gelatin/polyethylene glycol dimethacrylate	Nerve tissue regeneration	[68]
Inkjet printing	Collagen/fibrin	Skin tissue	[69, 70]
	Collagen/Alginate	Tissue engineering	[71]
	Alginate/fibrin	Tissue engineering	[72]
	RGD-Alginate	Liver tissue/organ	[73]
Direct dispensing	Collagen/methacrylated gelatin	Skin tissue	[74]
	Collagen/alginate	Bone and cartilage tissue	[75]
	Collagen/agarose	Corneal tissue	[76]
	Methacrylated collagen/alginate	Corneal tissue	[77]
	Methacrylated collagen/hyaluronic acid	Liver tissue	[78]
	Gelatin/fibrinogen	Liver tissues; vascular channel	[79]
	Gelatin/chitosan	Liver tissue	[80]
	Gelatin/alginate	Liver and cartilage tissue, vascular networks	[81–83]
	Gelatin/methacrylated gelatin	Tissue engineering	[84, 85]
	Methacrylated gelatin/alginate	Cardiac tissue	[86]
	Methacrylated gelatin/methacrylated hyaluronic acid	Heart valve, tissue engineering	[87, 88]
	Methacrylated gelatin/Methylcellulose	Bone tissue	[89]
	Methacrylated gelatin/polyethylene glycol dimethacrylate	Tissue regeneration	[90]
	Alginate/methyl cellulose	Regeneration and tissue repair	[91, 92]
	Alginate/Chitosan	Tissue constructs	[93]

(continued)

Table 3 (continued)

3D printing techniques	Biomaterial inks	Application	Refs.
	Alginate/polyethylene glycol	Cardiac tissue	[94]
	Alginate/gellan gum	Tissue engineering	[95]
	Polyvinyl acohol/κ-carrageenan	Bone tissue	[96]

range of 0.001 ÷ 1 mPa as a consequence of their large water content [97]. Considering that hydrogel precursor inks should ensure both structural support and cellular signaling while providing a good printing resolution, conventional hydrogel-based inks fail to meet these requirements. Aiming to improve the printability and mechanical properties of single- and bi-component inks by increasing polymer content and/or crosslinking density, the porosity, and subsequently, the permeability required by cells are usually compromised. The next-generation hydrogel inks make use of nanomaterials to dissipate mechanical energy, designing advanced biomaterial ink formulations with improved mechanical properties and high print fidelity along with a cell-interactive environment. Nanomaterials already validated for biomedical applications alongside with different ink reinforcement techniques have been employed to channel the biophysical and biochemical features of the hydrogel network. A wide array of nanostructured compounds such nanoclays, calcium phosphates, magnetic particles, carbonaceous nanomaterials, and polymeric nanoparticles or nanofibers have been most frequently used to reinforce polymeric hydrogels. Understanding the correlations between structure, property, and function of hydrogel networks and the mechanism behind their reinforcement, advanced designs of hydrogel inks were elaborated. Table 4 summarizes in brief nanocomposite 3D printing hydrogel inks.

3.4 Multicomponent Hydrogel Inks

Biomaterial inks design dramatically increased in complexity following the gradually broadening knowledge on all prevalent conditions that engage tissue regeneration. Most recent research studies have focused on the development of multicomponent hydrogel inks to simultaneously improve several features and reach out the gold standard in biomaterial ink formulation. A successful combination of more than two components will concurrently improve the biofunctionality, the mechanical stability and the biofabrication window of hydrogel inks.

Multicomponent hydrogel-based inks come with the ability to get the rheological and biological properties into balance and thus to provide 3D printed tissue constructs with a high functionality and complexity. Ergo, multicomponent hydrogel-based systems have become a leading strategy to develop tissue-specific bioinks. One of the

Table 4 Summary of reported nanocomposite hydrogel inks for 3D printing

3D printing techniques	Biomaterial inks	Reinforcement material	Application	Refs.
Light-assisted printing	Polyethylene glycol dimethacrylate	Hydroxyapatite	Bone and cartilage tissue	[98, 99]
Inkjet printing	Gellan/Xanthan Gum	Carbone nanotube	General tissue	[100]
	Chitosan Alginate/Methacrylated gelatin	Nanocellulose	Skin tissue mimics	[101]
Direct dispensing	Collagen	β-TCP		[102]
		Nano-sized mesoporous bioactive glasses	Bone and cartilage tissue	[103]
		Nanocellulose	General tissue	[104]
	Gelatin	Nanocellulose	General tissue	[65]
		Hydroxyapatite/graphene oxide	Bone tissue	[105]
	Methacrylated gelatin	Nanoclay	Epithelial tissue	[99]
		Hydroxyapatite	Bone tissue	[106]
		Nanocellulose	Wound healing	[107]
	Methacrylated gelatin/Methylcellulose	Laponite®	Connective tissue	[108]
	Alginate/Gelatin	Bioglass	Bone tissue	[109]
		Hydroxyapatite		[110]
	Alginate/gelatin/Polyethylene glycol dimethacrylate	Laponite®	General tissue	[111]

(continued)

Table 4 (continued)

3D printing techniques	Biomaterial inks	Reinforcement material	Application	Refs.
	Polyethylene glycol/Alginate	Nanoclay	Medical device	[112]
	Methacrylated chitosan	Graphene oxide	Growth of electroresponsive cells	[113]
		Hydroxyapatite	Bone tissue	[114]
	Thiol-modified hyaluronic acid	Gold nanoparticle	Vessel tissue	[115]
	Alginate/Methylcellulose	Laponite®	Bone tissue	[116]
	Alginate/Carboxymethyl cellulose	Nanocellulose/NiCu nanoparticles	General tissue	[117]
	Alginate	Nanocellulose	Cartilage tissue	[118, 119]
	Pectin	Nanocellulose	General tissue	[120]

most common approach is to design a base polymeric hydrogel network that accommodate auxiliary compounds such as a secondary polymer, nanofibers, or nanoparticles to enhance both the biophysical and biochemical response. Natural polymers are preponderantly considered as primary polymers within the hydrogel-based inks due to their various bioactive motifs and cell-interactive behavior that can enhance cell motility and induce proliferation and differentiation of cells [121]. Among the 3D fabrication techniques, the direct dispensing is from far the most exploited technology since more sophisticated and clinically relevant 3D hydrogels structures can be achieved using extrusion-based printing. In addition to the nanocomposite inks, Table 5 summarizes recently developed multicomponent bioinks for 3D bioprinting.

3.5 Cell-Embedding and the Bio-Printability Window

Cell-laden hydrogel inks are currently a critical topic of focus given the recent highly encouraging research studies on fabrication of functional tissue constructs [144, 145]. To date, the design and development of hydrogel-based inks became an active field of research, especially since the advancements in biofabrication remain limited by the lack of bioprintable formulations. Despite decades of research, the definition of the term "bioink" continues to be debated among researchers. Yet, in the view of a recent in-depth road map of the term evolution within the field of biofabrication, bioinks are generally stated as cell-laden formulation that can be processed by a computer-assisted fabrication technique [10]. Cell-encapsulating biomaterials are commonly used, but not generally required as an auxiliary component, considering also that the concept of bioink was first introduced as a formulation consisting aggregated cells in the form of cell spheroids or microtissues [146, 147]. Ergo, a bioink will compulsory consist of a cell suspension, whereas formulations containing only bioactive components would not count as bioinks.

The role of the hydrogel ink components within the 3D printed construct guided the classification of bioinks into four groups: (i) support bioinks—engineered to integrate cells and to provide a suitable matrix for cell attachment and proliferation; (ii) fugitive bioinks—configured as sacrificial materials that can generate pores or channels within a printed construct upon removal; (iii) structural bioinks—designed to provide permanent or temporary intrinsic mechanical strength to the printed structure; and (iv) functional bioinks—bioengineered to integrate biochemical cues that guide the post-printing cellular behavior within the 3D construct [10]. Regardless of their role in the biofabrication process, the design of performant hydrogel inks faces several challenges since they must almost simultaneously provide a microenvironment that emulate the physical and chemical properties of native extracellular matrix, exhibit viscoelastic behavior that ensure a high printing resolution and a sufficient fluidity for cell safety during printing and then preserve both the shape and cells viability post-printing. Therefore, a more targeted design is required when cell embedding is envisioned, given the multiple factors and critical properties that must be considered. These conflicting conditions gave rise to the conceptualization of the

Table 5 Summary of recently developed multicomponent bioinks for 3D bioprinting

3D printing techniques	Biomaterial inks	Application	Refs.
Light-assisted printing	Polyethylene glycol dimethacrylate/polyethylene glycol diacrylate/tetrapeptide Arg–Gly–Asp–Ser (RGDS)	Soft tissue	[122]
Inkjet printing	Aminoacricone-alginate or Aminofluorescein-alginate/pluronic PE6800 Alginate/polyethylene glycol/transglutaminase	General tissue	[35]
Direct dispensing	Gelatin/alginate/fibrinogen	Vascularized liver, adipose, and cardiac tissues	[123–125]
	Polycaprolactone/gelatin/fibrinogen/hyaluronic acid/glycerol	Bone, cartilage, and skeletal muscle tissues	[126]
	Agarose/methacrylated gelatin/methacrylated hyaluronic acid	Meniscus tissue	[127]
	Alginate/Engineered protein	General tissue	[128]
	Alginate/Agarose/Chitosan	General tissue	[129]
	Alginate/Pluronic—F127/Gelatin	Bone tissue	[130]
	Alginate/Hyaluronic Acid/DNA/Polycaprolactone	Bone tissue	[131]
	Alginate/Hyaluronic acid/Fibrinogen	General tissue	[132]
	Collagen/Chitosan/Graphene Oxide	Cartilage tissue	[133]
	Decellularized extracellular matrix/Vitamin B2	cardiac tissue	[134]
	Decellularized extracellular matrix/Alginate	Vascular tissue	[135]
	Gelatin/glycerol/Hyaluronic acid	Skin tissue	[136]
	methacrylated gelatin/Alginare/CS-AEMA	Embryonic tissues	[137]
	methacrylated gelatin/Alginate/HEMA	Cartilage tissue	[138]
	Hyaluronic acid/N-polyethylene glycol–isopropylacrylamide–N-(2-hydroxypropyl)methacrylamide-cysteine	General tissue	[139]

(continued)

Table 5 (continued)

3D printing techniques	Biomaterial inks	Application	Refs.
	oxidized hyaluronate/glycol chitosan/adipic acid dihydrazide	Cartilage tissue	[140]
	Matrigel/Alginate	Cortical tissue	[141]
	Silk/Gelatin/Glycerol	Soft tissue	[142]
	polyethylene glycol/peptides	General tissue	[143]

bioprintability window that will guide the selection of material properties suited both for high-fidelity printing and high cell viability. In biofabrication processes, as the direct interaction between materials and cells is already foreseen, the biocompatible nature of ink components is a standard requirement. Thereby, the current research in bioprinting predominately focus on the investigation of rheological behavior and crosslinking strategies to tailor the biofabrication window of hydrogel-based inks and better preserve cell viability throughout the printing process. There has been a conceptual change away from single-component inks which have seen a trade-off between printing accuracy and biocompatibility toward more advanced inks rationally engineered to have superior biocompatibility with excellent shape fidelity (see Fig. 4).

Recent developments in bioink efficiency and printing techniques have extended the biofabrication window through new key strategies that enable effective control over bioprinting process. Nonetheless, a wide and comprehensive knowledge of key parameters that guide the performance of hydrogel-based inks is fundamental in designing scaffolds for tissue engineering.

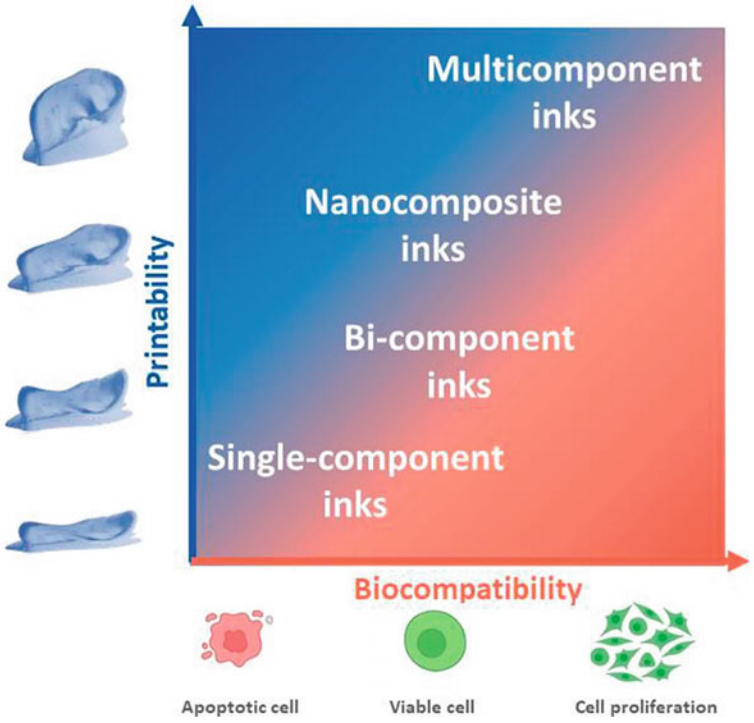

Fig. 4 Graphical representation of biofabrication window. Adapted with permission [148]. Copyright 2016, Springer

4 Key Parameters in Designing Printable Hydrogel Formulation

More and more complex approaches and strategies to tweak material properties continue to emerge toward developing the hydrogel-based materials as cell-delivery matrices seeking to fulfill the more stringent requirements of the cell-laden formulations in contrast with basic demands for a biomaterial ink. To develop clinically relevant constructs for TE, hydrogel-based inks are engineered to accommodate cells and/or bioactive factors, while they assembly a 3D network in a layer-by-layer fashion. New insights were opened in 3D printing technology by gaining influence over a construct's form, porosity, morphology, and proportions. Thus, the fabrication of tissue constructs have become more and more precise with respect to the preferred ink properties and processing conditions. Yet, the design of hydrogel-based formulations suitable for both 3D fabrication and cell culture is still challenging and key factors to be considered when fabricating tissue constructs refer to both material and fabrication parameters. The suitability of a hydrogel for a particular bioprinting process primarily rely on the materials physical and chemical features since each technology imparts specific processing conditions. Among material properties, the rheological behavior and gelation mechanism are the key parameters that govern the printability of a hydrogel ink particularly with respect to printing instrument. While the material characteristics already envision specific fabrication processes (e.g., high-viscosity inks perform best in extrusion-based systems vs low-viscosity inks which are most suitable for ink-jet printing), the fabrication parameters have a tremendous effect over the printing resolution, shape fidelity, and equally important—cells viability.

Several computer-aided fabrication techniques, counting light-assisted direct-printing, inkjet printing, and direct dispensing are being pursued with the aim to create biosynthetic tissues. Although each bioprinting technology depends on a cell-containing bioink, a precise bioink criteria differ based on the printing mechanism. Thus, despite the freedom of design enabled by 3D printing in general, each printing strategy has its own limitations and its own requirements regarding the biomaterial ink properties. Among them, superior advancements have been achieved in extrusion-based printing where the demands on ink properties are high but clearly specified and coherent.

Most relevant factors to be considered when designing performant hydrogel-based inks are summarized in 0. The material and fabrication parameters are interdependent and both require optimization to ensure high cell viability and to achieve accurate 3D printed models with sufficient mechanical stability (see Fig. 5).

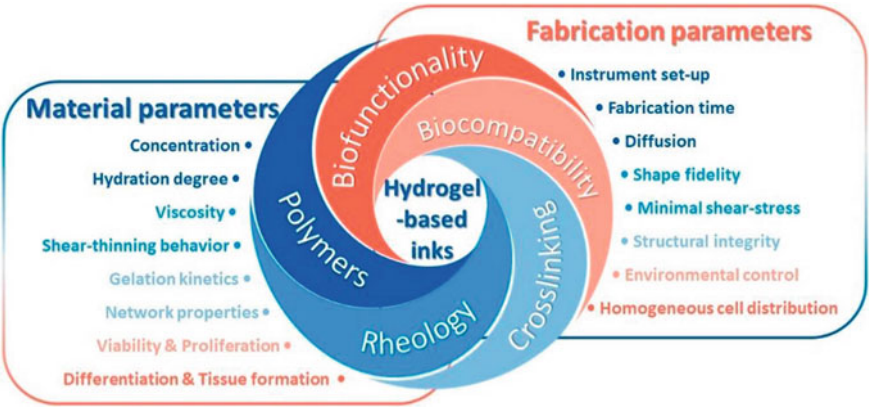

Fig. 5 Key factors to be considered when designing performant hydrogel-based inks

4.1 Material Parameters

It is crucial that the desired functional and mechanical characteristics of effective hydrogel inks be closely related to the native tissue. A successful, printable hydrogel-based ink must have appropriate features to preserve cell integrity during and post-printing while maintaining the pre-designed macro- and microstructure. It is widely known that different phenotypes of cells are vulnerable to even slight changes in the microenvironment's mechanical properties and as such, bioinks have been developed and engineered for specific cell types. Cell behavior can be swayed to promote tissue functional recovery by tunning the physical and chemical characteristics of the extracellular matrix (ECM). It is therefore essential to properly select the polymers as ink components that can sustain and enhance the tissue regeneration from a temporospatial point of view. A variety of polymers are exploited as a hydrogel inks to grant the tunability required to stimulate the interactions of cells and to ensure the motility, proliferation, and differentiation of cells.

For a hydrogel ink to be truly efficient, a genuine material science approach to design the printable formulation is crucial since understanding how polymer characteristics affect printing effectiveness and cytocompatibility is compulsory. Polymeric hydrogels employed as "bioinks" for tissue 3D printing, rely both on natural and synthetic polymers and consequently on their variations. In contrast with synthetic polymers, natural polymeric hydrogels may grant an adequate microenvironment for cells, particularly stem cells, to attach, proliferate, and/or differentiate within. The most popular design parameters are related to the rheological behavior since it governs the printed structure features, or polymer behavior in solution, as it determines the printing efficiency. Other parameters, such as sustainability, cost, and storability of a polymer, are also essential determinants of components selection [149].

4.1.1 Polymer Concentration

Apart from selecting polymers that exhibit biocompatibility and cell-interactive features, their concentration within the ink formulation is a main determinant of several features with high impact over printability and functional capability of a 3D constructs. In particular, the network density, viscosity, cell viability, and degradation rate are predominantly determined by polymer concentration. The traditional strategy to enhance the printability of a hydrogel ink formulation was based on increasing polymer concentration since a denser network and a high dry content will led to stiff hydrogels able to maintain shape upon deposition. Yet, high polymer concentration is detrimental to cells viability, migration, and growth and, as well, to hydrogel degradation rate. Advanced designs of printable formulations focus on using rather hydrogel precursors with low polymer concentration and rely on auxiliary components to optimize their printability [150].

4.1.2 Hydration Degree

In determining the applicability of polymers to the development of particular tissues, physical properties of polymers, such as *hydrophilicity and surface energy*, influence cellular behavior and are essential parameters in designing printable formulations. *Hydration degree* of the polymeric network is one characteristic that can significantly change the viscosity of the hydrogel ink. The hydration capacity and consequently the induced porosity influence the mechanical properties and viscoelasticity, while upon printing, it minimizes the shear stress. In addition, oxygen and nutrient flow within hydrogel network is a compulsory property for an efficient engineered tissue. Several natural polymers and water-soluble synthetic polymers (e.g., PLGA and PEG), are commonly employed in the development of hydrogel inks to fabricate complex tissue constructs such as blood vessels since material fluidity makes it simple to process, while inherent hydration properties could effectively imitate natural tissue environment. Nevertheless, between the hydration degree and network stiffness a compromise has to be made since high water content will decrease the hydrogel modulus [151].

4.1.3 The Rheological Behavior

The rheological behavior of a polymer aqueous solution is a critical physicochemical feature when assessing its printability. Rheology is the study of a matter's flow and deformation upon external forces and is extremely relevant to processes that involve material direct deposition. Despite high number of studies that describe novel printable formulations, the significance of their rheological behavior is often overlooked and the direct correlation between the rheological behavior and deposition process is speculative.

In deciding its flow behavior, the *viscosity* of a hydrogel ink is a crucial feature and is one of the most frequently measured value during the optimization phase of the bioink. The effects of viscosity can be conflicting with respect to ink efficiency to yield functional tissue constructs: highly viscous formulation provide shape fidelity and mechanical stability particularly advantageous to printing larger structures and yet could led to apoptosis via high shear stress generated during the printing process. Specifically, it has been reported that shear stresses can cause morphological modifications, cytoskeleton reorientation, reactive oxygen species generation, and even alteration of the expression of genes and proteins. These effects depend nonetheless on the cells phenotype and density along with the degree and period of shear stress. Moreover, a high flow resistance can also obstruct the outlet, leading to nonuniform ink deposition. Conversely, low viscosity inks limits the fabrication of tall structures and the cell distribution may be nonhomogeneous since cells are prone to sedimentation. The factors that predominantly determine the viscosity of hydrogel inks are the concentration and molecular weight of polymers, ion content, temperature, and encapsulated cell density [97].

Shear thinning is a rheological phenomenon beneficial in bioprinting in which, the increase of shear rate induces a decrease in viscosity due to polymer chains alignment along the flow path. Therewith, owing to the lower shear stresses at which embedded cells are exposed to, high printing fidelity along with high cell viability can be attained. Shear-thinning behavior is more pronounced in high-molecular weight polymers and larger concentrations. Flow models such as the power-law model, the Herschel–Bulkley model, or Carreau equation can be used to predict and characterize the hydrogel behavior upon printing [120, 152–155]. Although shear thinning is a valuable characteristic that is highly exploited and various strategies are employed to enhance the phenomenon, once deposited, the hydrogel ink does not regain its initial high viscosity right away. Hence, *the shear recovery* becomes as significant post-printing. Recent studies have highlighted the importance of a rapid shear recovery toward printing fidelity [111, 150, 152]. This effect is especially noticeable when tall constructs are built, where the weight of subsequent layer is soon borne by bottom layers. The shape recovery capacity can be assessed through peak hold tests to simulate the shear deformation and recovery of hydrogel inks during the printing process [156, 157].

4.2 Crosslinking Strategies

Crosslinking strategy is essential to attain the desired biomechanical features of printed architectures as it governs the future behavior and performance of the 3D construct. In bioprinting, the solution of polymer is shaped into a 3D structure where the structural integrity is preserved via crosslinking. The gelation mechanism is a key material parameter that greatly affects the mechanical and physicochemical properties of the printed structures and the behavior of cells they mature in. Hydrogel-based inks must be formulated to attain the appropriate biochemical features and structural

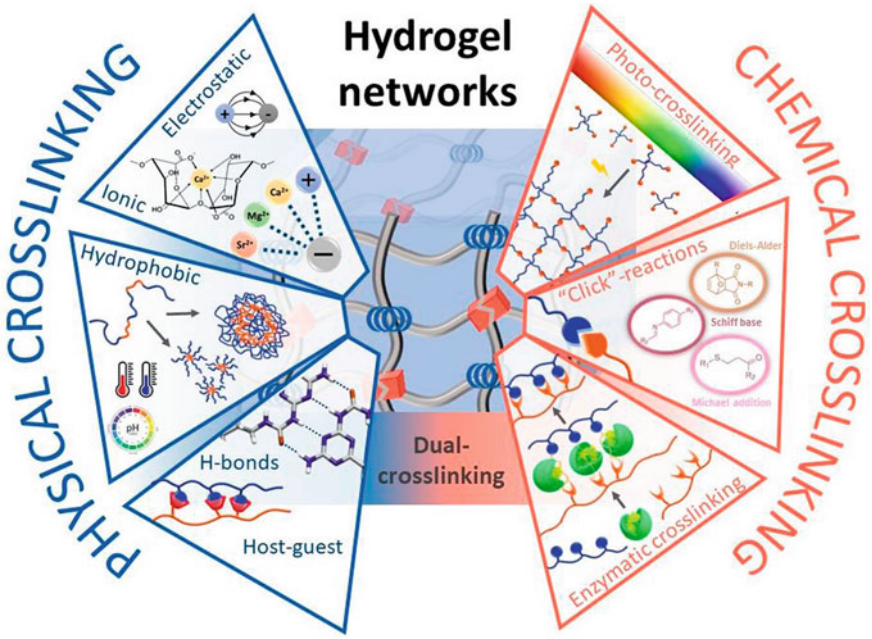

Fig. 6 Crosslinking strategies employed in 3D printing of hydrogels

stability for rapid shear recovery during and post-printing and to support simultaneously the cell differentiation, migration, and proliferation. Therefore, ink formulations will be optimized to undergo crosslinking by using either specific stimuli (e.g., temperature, light) or crosslinking agents within the printing blend or in a crosslinking bath. Based on the on the polymer's nature and the type of functional groups present in its structure, hydrogel ink formulations may be crosslinked using different approaches that can be physical, chemical, enzymatic, or even combination of them (see Fig. 6).

4.2.1 Physical Crosslinking Strategies

Physical crosslinking strategies commonly employed in fabrication of 3D hydrogel structures occur through noncovalent interactions such as ionic, electrostatic, hydrophobic, or H-bonds [158]. The main drawback of this approach is that physical hydrogels are generally weak from the mechanical point of view and yet they ensure a more appropriate environment for cells when compared to covalently crosslinked hydrogels. Several strategies have been employed to address this limitation, among which the most common ones involve the use of nanofillers or introduction of functional groups onto polymer backbone [159]. To ensure the structural integrity of the 3D construct, the crosslinking density is as important as the gelation mechanism.

There seems to be a fine balance between the crosslinking extent and printability as a low degree of crosslinking will facilitate flowing while a high degree will lead to stiffer structure and may impede printing.

Ionic interaction is one of the most popular approaches employed for the crosslinking of hydrogels used throughout 3D fabrication and it typically requires the presence of multivalent cations in a polymer solution to cause gelation. Since this crosslinking process is highly efficient for a rapid gelation, can occur under physiological conditions and don't involve extreme factors that can destroy cells, it became an appealing strategy in printing hydrogel 3D structures. It does have certain inconveniences, however, including mechanical weakness, poor stacking capacity, and a high probability of metal ions to be released shortly after implantation. The gelation based on ionic interaction is widely considered as an efficient crosslinking strategy for 3D bioprinting of polymers bearing carboxyl groups (such as alginate, carboxymethyl cellulose, tempo-oxidized nanocellulose, low methoxylated pectin) [158]. Here, the polymer solution concentration as well as the number of carboxylate groups are the main factors that dictate the physicochemical and mechanical characteristics of hydrogels. Nonetheless, the type of multivalent cation, its concentration, and addition strategy to polymer solution has an important effect on the hydrogel printability. Although various metal ions such as calcium, barium, magnesium, ferric, and strontium where exploited as ionic crosslinkers, more consistent, and promising results are attained when calcium was used [160, 161]. There are three main methods where multivalent cation can induce gelation of polymers comprised in a hydrogel-based inks: direct printing of polymer solution into a bath containing crosslinking agent; spraying crosslinking solution on an underlying polymer solution; and pre-crosslinking method where the crosslinker is incorporated into ink formulation [152]. It was found that, when employing ionic crosslinking it is important to select an appropriate ionic crosslinker concentration. Even if this approach prevents exposure of cells to severe conditions, high calcium concentration, or long-time exposure to metal ions may still cause cell damage [114, 162, 163]. The strategy of adding metal ions to hydrogel inks has a direct influence on both the ink consistency, printing performance, and cell viability.

Electrostatic interactions may also lead to formation of hydrogel networks, where ionic crosslinks are established between two oppositely charged functional groups present in the backbone of polymer chains. In the absence of metal ions, this approach becomes more cell-friendly, and it has been employed in bioprinting of several ionic charge-containing hydrogels. With respect to ionic charge, hydrophilic polymers can be classified as anionic (e.g., alginate, xanthan, kappa (κ)-carrageenan), cationic (e.g., gelatin, chitosan), and non-ionic or neutral (e.g., dextran). Reversible character of the electrostatic gelation provides high flexibility for 3D printing processes as most of hydrogel inks that can establish electrostatic interactions exhibit a shear-thinning behavior during fabrication and fast internal structure restructuring forming a thixotropic hydrogel. Consequently, the hydrogel-based ink can be easily extruded with minimum shear stress. Yet, blends of polycation inks with polyanionic inks are likely to form inhomogeneous crosslinked hydrogels as stronger interactions may occur at the interface. As a consequence of a gradient in the crosslinking density of

the 3D printed hydrogel, the biomechanical properties may be not only inconsistent but generally poor. To overcome this issue and to preserve the integrity of 3D printed structures, a second crosslinking process is usually employed. Another strategy to enhance the biomechanical features of 3D printed structures is the incorporation of an ionically charged filler. This approach would lead to the formation of additional electrostatic interactions and thus both shear thinning behavior and final mechanical properties of the hydrogel are likely to be improved.

Hydrophobic interactions play a critical role in both the formation of large biological systems and 3D printing as this strategy lead to a rapid formation of elastically effective crosslinks between water-soluble polymers bearing hydrophobic end groups or side chains. Thus, homogeneous hydrogel networks exhibiting high strength and resilience, environmental responsiveness, and even self-healing properties can be formed by hydrophobic associations. There are two methods that can generate hydrophobic interactions: one implies a change in temperature and other an ultrasonic treatment. For bioprinting applications, thermo-responsive inks are highly advantageous as the rapid sol–gel transition can ensure high shape fidelity during the printing process. Several polymers of natural (gelatin, cellulose, k-carrageenan) and synthetic (poly(N-isopropylacrylamide) (pNIPAAm), Pluronics® or Poloxamers) origin were exploited as printing formulations due to their thermo-responsive properties [164, 165]. The conformational changes taking place at a certain temperature (referred to as the critical solution temperature) facilitate hydrophobic interactions among macromolecules, which in turn leads to gelation. Two main groups of hydrogels can be distinguished based on their behavior: (i) Upper Critical Solution Temperature (UCST) hydrogels also considered positive thermo-sensitive hydrogels, where the sol–gel transition occurs by cooling below UCST (e.g., gelation, agarose); and (ii) Lower Critical Solution Temperature (LCST) hydrogels or negative thermo-sensitive hydrogels, where gelation take place upon heating above LCST (e.g., methylcellulose, PolyNIPAM, Pluronic F127) [37]. There are several benefits of using thermo-sensitive hydrogels in 3D printing since the non-covalent interactions occur without using crosslinkers, they allow an easy handling and flow, and most important the shape stability is ensured upon heating or cooling. Nonetheless, only a limited number of polymers exhibit sol–gel transition at physiologically relevant temperatures that can further facilitate incorporation of cells or biomolecules [166]. Several papers rather describe the hydrophobic interactions as a secondary network within hydrogels since it can additionally provide structural stability and stimuli-responsive properties [167–170].

Other noncovalent interactions arise via hydrogen bonds [171–173], self-assembling peptides and peptide–DNA conjugation [158, 174] and host–guest interactions [175, 176]. Despite the low binding energy, multiple interactions are sufficient to sustain the polymeric network so that they are the emerging candidates as additional crosslinking strategies in 3D printing of hydrogels.

4.2.2 Chemical Crosslinking Strategies

Chemical crosslinking strategies involve the formation of covalent bonds between polymer chains which are usually strong and nonreversible, leading to hydrogel networks that are more stable under physiological conditions and with excellent mechanical features if compared with physical hydrogels. Thus far, several crosslinking methods were employed in fabrication of 3D hydrogel structures, most of them relying on free radical polymerization, Diels–Alder "click" reaction, Schiff base formation, Michael-type addition, or enzymatic reactions [165]. Various functionalization methods were explored in the interest to qualify specific polymers to specific crosslinking mechanism and thus to gain control over the gelation kinetics. The timescale of the sol–gel transition is essential as the ink should easily flow throughout the nozzle, while the proper shape stability during and after printing must be ensured.

Photo-crosslinking is of particular interest in 3D printing uses as it is a straightforward approach to yield hydrogel-based 3D materials. Photo-induced crosslinking mechanisms are cost-effective strategies since they can be done under ambient temperature and require fewer resources than other techniques. Numerous 3D bioprinting technologies including direct extrusion and light-assisted direct-printing have been using photocurable bioinks to build complex 3D architectures [158]. There are several parameters to consider when approaching a photo-crosslinking process in 3D printing. First, one should consider hydrophilic polymers that present or can be functionalized with photo-crosslinkable groups, and also exhibit biocompatibility and adequate rheological behavior at low concentrations. Equally important is the selection of initiator, whose performance in terms of cytocompatibility and network stiffness will depend on the nature of reactive species, solubility, concentration, and exposure type and time. Thus, this approach is focused on the use of photocurable polymers which can be crosslinked by chain-growth, step-growth, or redox-based reaction mechanisms. Photo-initiated systems rely on the presence of unsaturated groups, the most commonly used in 3D printing being the (meth)acrylate compounds such as poly(ethylene glycol) diacrylate, gelatin methacryloyl, and methacrylate hyaluronic acid [177–182]. The formation of photo-crosslinked hydrogel networks implies nonetheless the use of photo-initiators, compounds that can form reactive species when exposed to light at a specific wavelength. By absorbing photons, the photo-initiator can generate either free radicals, cations, or anions, among which the radical photo-initiators are most popular in the development of hydrogel-based bioinks. Based on the mechanism of reactive species formation, two main categories of radical photo-initiators arise: photo-cleavable (Type-I) that include Irgacure® (e.g., Irgacure 2959, Irgacure 1173, Irgacure 819, Irgacure 651) and lithium acyl phosphinate (LAP) and bimolecular (Type-II) that include camphorquinone, fluorescein, and eosin Y [183]. Although a broad range of photo-initiators can be used to produce photo-crosslinked hydrogels, the selection of an appropriate photo-initiator is essential to achieve an optimal cross-linking rate and to improve overall performance of the hydrogel bio-construct [184]. Among several key characteristics such as absorption spectrum, water solubility, efficiency, and cytocompatibility, the latter must be first

addressed when designing photo-curable hydrogel inks, especially if cell-embedding is envisioned. Several research works showed that the photo-initiators exhibit excellent biocompatibility at concentrations below 0.01% (w/w) while ensuring sufficient hydrogel stiffness [107, 177, 185]. Nonetheless, all these parameters must be optimized to limit irradiation exposure as there are still some concerns regarding cell damage.

Usage of "*click chemistry*" on design and fabrication of hydrogels developed rapidly after 2001 since this type of chemical reactions comes with various benefits such as high specificity and selectivity that lead to high yields with few and less toxic byproducts [165]. A broad range of functional groups may serve as desirable candidates for the fabrication of complex hydrogel scaffolds and most popular strategies include (i) Diels–Alder, (ii) Schiff base, and (iii) Michael-type addition. *(i) The Diels–Alder* (DA) reaction is a thermoreversible [4 + 2] cycloaddition between a conjugated diene and a dienophile that overcome the disadvantage of using coupling agents, catalysts, or photo-initiators. While they are widely used in organic chemistry, DA reactions have more recently found application in tissue engineering as they can also be employed to obtain chemically crosslinked hydrogels under mild conditions [186]. The range of polymeric hydrogel materials is yet narrow, furan-modified polymers being the most commonly used to react with poly(ethylene glycol) dimaleimide for hydrogel formation. Nonetheless, while furan–maleimide reactions may exhibit a too slow gelation in physiologically relevant conditions, strategies to enhance the reaction rate were developed by using substituted furans and fulvenes [187, 188]. *(ii) Schiff base reactions* conventionally take place between amino and aldehyde groups forming dynamic covalent imine bonds that can even provide hydrogels some self-healing properties. This crosslinking approach is based on a simple, reversible, pH-sensitive, and biocompatible mechanism that has great prospects in the field of biomedicine. Hydrogel networks formed by Schiff base linkages can be fabricated under physiological conditions and their properties can be easily tuned to fulfil the particular requirements of various tissues [189]. Various polymer such as hyaluronic acid, alginate, or chitosan were modified with hydrazide or aldehyde groups and used to formulate bioinks based on Schiff base reaction [190–192]. *(iii) Michael-type addition* is a facile and spontaneous reaction between an electron-deficient olefin (Michael acceptor) and a nucleophile (Michael donor). Although either amines or enolates can be used as Michael donors, one of the most frequently used Michael reaction is the addition of thiols to α,β-unsaturated carbonyl polymers. It has become a popular approach to design tissue mimicking hydrogel networks as the crosslinking processes based on the mechanism of thiol-Michael addition exhibit a favorable reaction rate, a high degree of chemical selectivity, high conversion, and also occurs under mild conditions that facilitate the encapsulation of biomolecules and/or cells. Moreover, as the thiol groups exist in the sidechain of cysteine, proteins can be coupled with either acrylates or vinyl sulfones to generate functional hydrogel inks. Nonetheless, the reaction time is a critical parameter as there is limited control over the reaction initiation and kinetics. Extensive research focused on designing Michael-type hydrogels and some examples include using derivatized hyaluronic acid (e.g., thiolated hyaluronic acid, acrylamide-functionalized, and acrylated hyaluronic acid),

derivatized collagen (e.g., maleilated collagen), poly(ethylene glycol) derivatives and derivatized Pluronic F127 [193–196].

The *enzyme-mediated crosslinking strategies* have recently gained a fresh interest in formulation of 3D printable hydrogel inks as they be employed to facilitate covalent bonding under cell-friendly environments with high specificity. Enzymes can be used to initiate the crosslinking either by generating new reactive functional groups or by acting as catalyst to form amide bonds. By excluding harsh conditions in terms of temperature, solvents, or compounds that can cause chemical denaturation, enzymes are excellent auxiliaries to provide bio-orthogonal control of the gelation phase and to tune the viscoelastic and degradation properties of the bioink formulation [197]. To date, few studies exploited enzymatic crosslinking of hydrogel-based inks, where enzymes such as transglutaminase, tyrosinase, lysyl oxidase, plasma amine oxidase, phosphopantetheinyl transferase, peroxidases, and horseradish peroxidase have been most commonly used to crosslink bioinks based on collagen, gelatin, fibrinogen, or silk fibroin [198, 199]. Although it is very promising toolkit in 3D bioprinting, enzymatic crosslinking is not a straightforward strategy since specific substrate sequences are required and cost-effective production of biotechnologically relevant enzymes is still a challenge.

Multiple crosslinking strategies need to be thoroughly studied and their effects carefully assessed so that they can lead to the formation of more heterogeneous 3D structures able to replicate native tissues. There is an inherent challenge to formulate hydrogel bioinks since these cell-embedded formulations would be subjected to the printing process and would then be expected to retain dimensional stability. The difficulty to simultaneously improve the interactions between polymers and also the interactions between polymers and cells while maintaining the high printability persists as a major milestone that marks the developments in 3D bioprinting.

4.3 Fabrication Parameters

The fabrication parameters, also referred to as printing parameters, require a rigorous optimization to attain performant 3D hydrogel structures. They must be clearly defined for each formulation with respect to the printing technology, material properties, crosslinking strategy, type of embedded cells, and scaffold design. Although the bioprinting technique will first guide the selection of hydrogel ink formulation in terms of polymer choice, rheological behavior, and gelation kinetics, process parameters are indisputably important in creating functional constructs. The instrument setup must be flexibly optimized to minimize fabrication time, diffusion, and shear stress while providing shape fidelity, structural integrity, environmental control, and a homogeneous cell distribution. The quality of the printed construct relies as much on materials as it does on the equipment and the design and slicing of the 3D model.

4.3.1 Light-Assisted Printing Processes

Light-assisted printing processes address to photocurable hydrogel precursors and their competence in creating high-quality 3D constructs with fine features (thin walls, sharp corners) made them highly competitive biofabrication techniques. In SLA processes, the control knobs refer to layer thickness, light power and exposure time, lift speed, object orientation, and aliasing [200]. The layer thickness has a direct influence over the printing quality and time: a thinner layer will preserve better the details but at the same time by decreasing the layer thickness the number of layers increases which will consequently increase the printing time. The printing quality is also dependent on the irradiation type, intensity, and time and these parameters must be adjusted as a function of material properties and, if the case, cells sensitivity. The speed of which the build plate is lifted to the adjacent layer can damage the structure if too high or increase the printing time if too low. Moreover, the orientation of the 3D virtual model in a different direction will produce significant differences in the printing quality. By choosing the most appropriate orientation for the slicing process, the surface quality and the structural integrity will be considerably enhanced. Also, the anti-aliasing function will smooth object edges and remove artifacts. TPP processes are more difficult to control since they require an intimate knowledge of optics. The main fabrication parameters refer to laser power, exposure time, and the numerical aperture (NA) of the objective and they must be evaluated only with respect to chemical reaction kinetics [20, 201]. The printing resolution is directly proportional with the initiator's effectiveness so by selecting an appropriate laser-pulse energy and exposure time, voxels of any small size can be obtained. The laser focal point control is critical and often the threshold condition the printing resolution. Understanding the laser–material interaction is crucial for gaining control over the entire printing process. Nonetheless, in LIFT processes, the rheological, optical, and thermal properties of the ink formulations as well as the wetting properties of the receiving substrate are first to be considered for a better control of the printing quality. Laser parameters such as wavelength, spot size, or pulse width will define, however, the size and the pressure of the gas bubble. By modifying the laser fluence or the gap between the donor and acceptor substrate, the size of the printed droplets can be tuned to achieve high-quality outputs [21]. Printing time is always one of the essential aspects in setting up the fabrication process, and LIFT makes no exception. Yet, the printing speed is herein determined by the laser repetition rate and can range up to millions deposits per second, therefore, it can surpass most of the current technologies in terms of speed. Is it nonetheless worth to mention that pulses at very high repetition rates may compromise the printing process if the time delay between laser pulses is shorter than the evaporation time of the material [21, 22].

4.3.2 Inkjet Printing Processes

Inkjet-printing processes are best suited for printing low-viscosity inks where droplets of 300 down to 20 μm can be generated by using either drop-on demand

jetting or continuous inkjet printing mode [202]. Here, the printing performance relies on fabrication parameters nearly as much as it does on ink properties. Although a limited range of ink formulations can be printed using this method, considering the restrictions in terms of surface tension and viscosity of the inks, the droplet stability can be influenced by fabrication parameters. These include nozzle dimensions, driving parameters (the pulse amplitude and width), dot distance, printing height, applied temperature gradient, and surface properties of the substrate [203, 204].

The droplet dimensions directly impact the printing output and minimizing the droplet size will enhance printing quality and resolution. The nozzle diameter is the main factor that affects droplet dimension, and it is important to keep in mind that the final printed width is usually larger than the nozzle gauge. Although reducing the nozzle dimensions will lead to the formation of smaller droplets, when dispersions are used as printing inks, the selection of the nozzle must consider only diameters sufficiently larger than the particles size to avoid clogging. The droplet size is also influenced by jetting voltage and frequency. Smaller droplet can be generated by decreasing the voltage level, but droplet size and pulse amplitude are linearly dependent only above the minimum voltage required for droplet formation. Conversely the jetting frequency exhibit a more complex and fluctuating influence as an increase of the pulse width may produce disturbances and affect the droplet stability [205].

Another critical parameter in inkjet printing is the distance between two adjacent droplets as it will determine the characteristics of the printed structure. A too large distance between droplets will not allow them to merge and form a continuous feature, while a too small spacing will lead to the formation of a continuous film. The droplet dimensions after impact at a surface are to be considered when setting dot spacing in both *X*- and *Y*-directions. It is essential in line forming and there is also a linear dependence between the distance between droplets and the width and height of the subsequent printed lines.

Other parameters such as substrate temperature or the nozzle-to-substrate distance can be adjusted to higher values to decrease the droplet dimensions by stimulating the evaporation of solvent. To accommodate cells and ensure a high viability toward fabrication process while printing with high resolution, all these parameters must be flexibly optimized for the best possible outcome [203].

4.3.3 Direct Dispensing Processes

Direct dispensing processes can efficiently work with relatively high-viscous inks or high cell densities (above 1×10^6 cells/mL) and therefore are compatible with a wide range of ink formulation designs [206]. Ergo, various hydrogel-based inks were developed to perform in extrusion-based printing techniques and the benefits of using this printing technique to fabricate constructs for tissue engineering application still prevail among the others (see Sect. 0). Beside the stringent requirements for ink properties, the operating parameters are easier to manipulate and their influence over the printing quality is more predictable. The biomechanical properties of the 3D construct can be augmented by adjusting the strand width via (i) needle variables; (ii)

pressure; (iii) speed; (iv) offset and delay; (v) temperature control system (for nozzle, platform, or environment); and (vi) virtual model design [207]. Printing parameters optimized exclusively considering the printing fidelity may not efficiently cope with the conditions that ensure high cell viability. For most tissue engineering applications, a compromise should be found between conditions that support high printing fidelity and those that favor high cell viability.

The characteristics of the needle tip are key aspects in process optimization. Its diameter, length, geometry, and even the material the needle is made of, will significantly influence not only the printing pressure and speed and but also the printing resolution and cells viability. For instance, higher printing resolution can be attained using a needle of a smaller inner diameter, but at the same time, the pressure required for extrusion increases leading to a higher shear stress that will affect cells viability. Moreover, both the extrusion rate and layer height will decrease with decreasing nozzle diameter resulting in a longer fabrication time. The bioprinting processes focus on minimizing the shear stress encountered by the cells so that shorter needles are usually preferred. Nonetheless, longer needles can be highly effective when printing directly into well plates or when using freeform reversible embedding of suspended hydrogels, also referred to as the FRESH method. The needle can have either cylindrical or conical geometry and under identical operating conditions the two types can have very different effects on printing pressure and viability of cells. Both plastic and metal needles can be used for printing hydrogels [208].

Printing pressure is the most critical factor affecting the printing process. It has a direct influence over the line width, and it is highly dependent on the ink viscosity and the surface tension in the nozzle. Although high-viscosity inks will require higher pressures, it is best to optimize the process to the lowest possible value so that the shear stress to be minimal [209]. Printing speed is strongly reliant on printing pressure and nozzle diameter and is one of the main factors that determine the fabrication time as well. Typically, with increasing the feed rate, the printed filament will become thinner as the material will stretch, up to a point when the deposition becomes non-uniform. The offset, described as the distance from the nozzle to the building platform, will affect the line width and angles shapes as a wide range of filament dimensions can be attained when modulating this parameter. Also, depending on material properties and type of applied pressure, a printing delay may be required in order to compensate a potential response lag and to ensure a continuous, uniform deposition. Controlling the temperature during the process has much to do with the material properties and particularly with the crosslinking strategy. Therefore, accessories can be used to control the temperature of the needle and/or of the printing platform. When considering printing with cell-embedded formulations, it is beneficial to have control over the environmental temperature as well.

As important as the operating parameters is the virtual model design. The infill density, angles shapes, and layer thickness will influence the printing stability and fidelity. Therefore, with respect to line width, the overlapping, and diffusion rate can be minimized by avoiding sharp angles, setting a sufficient distance between printed lines, and reducing as much as possible line intersection at the same printing level. Hydrogel-based inks most commonly experience expansion after extrusion

and gravitational collapse after deposition. Consequently, the line width is bigger and the line height smaller when compared to nozzle inner diameter. The filament dimensions should be individually evaluated and then optimized since the error of the line width or layer height will accumulate with every subsequent printed layer, up to the point when printing process fails. The duration of the printing process in determined concomitantly by filament dimensions, printing speed, and the characteristics of the virtual model. As the period of exposure to printing conditions is critical to cells viability, the printing resolution is frequently compromised in favor of shorter biofabrication time.

4.4 Investigation of Printability

The 3D printability is an individualizing characteristic for hydrogels as they can be designed to mimic the architecture and the biomechanical properties of native tissues only when the material is able to form and maintain the pre-defined structure. However, the 3D construct is rarely printed one to one and therefore it is particularly critical to evaluate the differences between the CAD model and the printed scaffold. Given the complexity and specificity of natural tissues, the printing precision, shape fidelity, and the reproducibility are vital aspects in biofabrication. Thus, it became of prime importance to find methods to associate numbers with the physical qualities so that they will describe the printability of hydrogels and will enable fair comparisons between different formulations. Despite its ubiquity and significance, there is little consensus among researchers on how to measure printability and what can actually be measurable. Many different methods proposed to predict and evaluate the printability of various biomaterials with the goal of providing a better understanding of the correlation between material and fabrication parameters are summarized in Table 6.

A majority of studies focus first on the investigation of ink properties considering closely the flowing behavior of hydrogels to identify the printability potential [87, 97, 118, 149, 236–239]. The predictive methods so far include rheological tests to measure the viscosity, shear thinning behavior, shear storage, and loss moduli or gelation time which can further use flow models as the power-law model, the Herschel–Bulkley model, or Carreau equation to predict and characterize the hydrogel behavior upon printing [152–155]. In addition, flow simulation, ink consistency tests, injectability, and the glass flip test were used for a preliminary investigation of biomaterial printability (see Table 6).

In an effort to demonstrate printability of various hydrogel-based formulations, the literature reports a number of experimental studies that can be broadly classified as qualitative and quantitative methods. Up to date, it is still very common for research works presenting novel hydrogel-based inks to provide qualitative descriptions of printability based on photographs of filaments, strands, and up to 3D constructs. Also, imaging techniques such as optical microscopy, SEM, or Micro-CT were used to emphasize the printability aspects which on top provide semi-quantitative measurements. Although these approaches offer valuable insights on printability, quantitative

Table 6 Summary of methods used alone or combined to evaluate inks printability

Measurement method			Quantifiable outcomes	Refs.
Ink properties	Predictive	Rheological tests and bioink flow models	Flowing properties	[97, 150]
		Flow simulation	Determination of the ideal flow rate	[65]
		Ink consistency tests	Variations in extrusion force, ink homogeneity	[120, 210]
		Glass flip test	Investigation the process printing window	[211]
Filament quality	Qualitative	Filament drop test	Filament/drop formation	[85, 209, 212]
		Strand formation test	Determination of optimal material/fabrication parameters	[211, 213–215]
		Line printing		[120, 209, 216]
		S-test		[217]
	Quantitative	Filament deposition	Filament width and height	[218]
		Filament width	Extrusion uniformity	[212, 219]
		Mathematical models relating measurements	Strand printability, Pore printability	[207, 212, 213, 220, 221]
			Uniformity factor, pore factor	[222]
Shape fidelity and printing accuracy	Qualitative	Comparison based on images (digital camera, optical microscopy, SEM images, Micro-CT)	Dimensional stability	[107, 212, 223–225]
			Strand thickness and pore size	[226, 227]
			Object height	[219, 228–230]
			Printability	[209, 210, 222]
	Quantitative	Filament fusion test	Evaluation of printing resolution	[211, 213, 227]
		Filament collapse test	Deflection angle of unsupported filament	
		Mathematical models relating measurements	Diffusion rate (%) and Printability (%)	[211, 216]
			Printability and deformation (%)	[231]
			Aspect ratio	[229]

(continued)

Table 6 (continued)

Measurement method		Quantifiable outcomes	Refs.
Print viability	Live/dead assays	Cell viability and proliferation	[181, 224, 225, 230, 232–236]
		Cell aggregation and differentiation	
		Cell morphology and distribution	
		Tissue formation	
	Specific biochemical analysis	Tissue formation	[181, 234]

studies are more objective and facilitate comparisons of inks and printing conditions. Nonetheless, the development and improvement of quantitative descriptions of printable materials greatly contributed to bioink advancement which, in turn, further enhanced bioprinting toward clinically relevant applications. A hybrid approach to data collection is preferable because each method has its limitations, and quantitative and qualitative approaches can help mitigate those drawbacks when used together. Effective evaluation methods inevitably contribute to a deeper comprehension of the fundamental processes that influence printability. Hereby, we refer the readers to an excellent review for more detailed information on representative printability measurements [240].

One of the important functions of hydrogel-based inks is to preserve cells viability, but it is a more complicated process since the formulation must fulfill stringent requirements to accommodate and homogenize the cell pellet while maintaining its printability. Therefore, a clear identification of material bioprintability window is crucial in assessing cell viability toward printing process. Both quantitative and qualitative methods are widely used to evaluate cell distribution, viability, proliferation up till differentiation, and tissue formation [181, 234].

Despite the fact that many experiments have been conducted on the printability of various biomaterials, the true image and concept of printability remain elusive, and basic questions regarding how to chart the relationships between printability and other interrelated variables such as biomaterial and fabrication remain unanswered. Standardized methods to ascertain the principles of printing can pave the way for greater knowledge of bioink behaviors, which can then be used to make more accurate parallels between bioinks.

5 Evolution to 4D Printing

Combining biomimetics and 3D printing has been schemed as sustainable resolution for the fabrication of unrivaled architectures for the development of tissue engineering constructs in the tangible future. Nature-inspired structures often incorporate complex combinations of micro- and macrofeatures that work together to provide effective biomechanical features [241]. In the field of personalized medicine, 3D printing techniques have proven to provide freedom of design despite the geometrical complexity. Yet, the state of the art in 3D printing still lacks the ability to obtain fringe resolutions from optimal materials, limiting the scope for scalability. 3D fabrication technologies today achieve sub-micrometer accuracy, but nanometric features of the extracellular matrix are not reproducible using printing techniques alone [242]. Customized outer shapes of a 3D construct are now easily possible to fabricate at acceptable costs, but inner architecture design is more limited and generally fails to reach clinical standards.

Four-dimensional (4D) printing introduces the dimension of time to 3D printed objects, which gives greater relevance to the design process. 4D-printed designs must be meticulously configured depending on the design of tunable biomaterials with properties that change over time relying on a controlable deformation mechanism [243]. 4D printing allows for the development of adaptive constructs made of smart materials that can cover the limitations of time when coupled with external stimuli [244]. The feature-changing prints are generated by modulating a smart material in response to a predefined stimulus such as humidity, thermal energy, electromagnetic fields (light, electricity, magnetic fields), osmotic pressure, mechanical stimuli, chemical catalysts, or biological triggers, all of which are a cumulation of other variables [245]. Under stimulation, triggers, or stresses, set off the predesigned behavior, allowing the print to evolve into a superior tridimensional object over time. Materials enclosing distinct micro- or nanoarchitectures that are intimately cohered can support various cell lineages for tissue regeneration while targeted biodegradation of the print is another aspect of time dependency found in 4D printing [246]. Intrinsically active implants with a controlled drug release encompass an inherent mechanism to soften tissue adjustments [247]. In brief, 4D printing consists of post-fabrication optimization of prefabricated objects in a 4D itinerary or additive manufacture with space and time constraint resolutions.

So far, the research community has begun to explore 4D printing from the viewpoint of biologically inspired shapemorphism found in plant motion. The range of hydrogel-based biomaterials used as 3D-printing inks to fabricate constructs relevant for tissue engineering offers a wide array of options to extent their application in 4D printing, detailed in recent review papers [245, 248]. Until conducting “first in human” studies on printed tissue-like constructs, comprehensive preclinical research would be needed. However, if they fail, the consequences can be highly detrimental and, as a result, the bar for clinical trials is set high. There has been no human trials of a whole bio-engineered organ to date. Meanwhile, clinical trials were conducted for engineered valves, as well as synthetic and biologic matrices [249].

However, a better coordination of 3D printing technologies and material smart design is expected to launch future printed biomaterials into various fields of bioengineering and creative industries.

References

1. Tibbitt MW, Rodell CB, Burdick JA, Anseth KS (2015) Progress in material design for biomedical applications. Proc Natl Acad Sci 112(47):14444–14451. https://doi.org/10.1073/pnas.1516247112
2. Furth ME, Atala A (2014) Tissue Engineering: Future Perspectives. In: Principles of Tissue Engineering. Elsevier, pp 83–123
3. Kaoud HAE-S (2018) Introductory chapter: concepts of tissue regeneration. In: Tissue Regeneration. IntechOpen
4. Kupfer Molly E., Lin Wei-Han, Ravikumar Vasanth, Qiu Kaiyan, Wang Lu, Gao Ling, Bhuiyan Didarul B., Lenz Megan, Ai Jeffrey, Mahutga Ryan R et al (2020) In situ expansion, differentiation, and electromechanical coupling of human cardiac muscle in a 3D bioprinted, chambered organoid. Circulation Research 127(2):207–224. https://doi.org/10.1161/CIRCRESAHA.119.316155
5. Ovsianikov A, Khademhosseini A, Mironov V (2018) The synergy of scaffold-based and scaffold-free tissue engineering strategies. Trends Biotechnol 36(4):348–357
6. O'brien FJ (2011) Biomaterials & scaffolds for tissue engineering. Mater Today 14(3):88–95
7. Zhu J, Marchant RE (2011) Design properties of hydrogel tissue-engineering scaffolds. Expert Rev Med Devices 8(5):607–626
8. Derby B (2012) Printing and prototyping of tissues and scaffolds. Science 338(6109):921–926
9. Bittner SM, Guo JL, Melchiorri A, Mikos AG (2018) Three-dimensional printing of multilayered tissue engineering scaffolds. Mater Today 21(8):861–874
10. Groll J, Burdick JA, Cho D-W, Derby B, Gelinsky M, Heilshorn SC, Juengst T, Malda J, Mironov VA, Nakayama K (2018) A definition of bioinks and their distinction from biomaterial inks. Biofabrication 11(1):013001
11. Corker A, Ng HC-H, Poole RJ, García-Tuñón E (2019) 3d printing with 2d colloids: designing rheology protocols to predict 'printability' of soft-materials. Soft Matter 15(6):1444–1456
12. Hribar KC, Soman P, Warner J, Chung P, Chen S (2014) Light-assisted direct-write of 3D functional biomaterials. Lab Chip 14(2):268–275
13. Yan Q, Dong H, Su J, Han J, Song B, Wei Q, Shi Y (2018) A review of 3D printing technology for medical applications. Engineering 4(5):729–742
14. Benjamin AD, Abbasi R, Owens M, Olsen RJ, Walsh DJ, LeFevre TB, Wilking JN (2019) Light-based 3D printing of hydrogels with high-resolution channels. Biomed Phys Eng Express 5(2):025–035
15. Ngo TD, Kashani A, Imbalzano G, Nguyen KT, Hui D (2018) Additive manufacturing (3D printing): a review of materials, methods, applications and challenges. Compos B Eng 143:172–196
16. Hull CW (1986) Apparatus for production of three-dimensional objects by stereolithography. US 4,575,330 Patent
17. Schmidleithner C, Kalaskar DM (2018) Stereolithography. In: IntechOpen
18. Mota C, Puppi D, Chiellini F, Chiellini E (2015) Additive manufacturing techniques for the production of tissue engineering constructs. J Tissue Eng Regen Med 9(3):174–190
19. Takada K, Sun H-B, Kawata S (2005) Improved spatial resolution and surface roughness in photopolymerization-based laser nanowriting. Appl Phys Lett 86(7):071–122
20. Raimondi MT, Eaton SM, Nava MM, Laganà M, Cerullo G, Osellame R (2012) Two-photon laser polymerization: from fundamentals to biomedical application in tissue engineering and regenerative medicine. J Appl Biomater Funct Mater 10(1):56–66

21. Serra P, Piqué A (2019) Laser-induced forward transfer: fundamentals and applications. Adv Mater Technol 4(1):1800099
22. Theodorakos I, Kalaitzis A, Makrygianni M, Hatziapostolou A, Kabla A, Melamed S, de la Vega F, Zergioti I (2019) Laser-induced forward transfer of high viscous, non-Newtonian silver nanoparticle inks: jet dynamics and temporal evolution of the printed droplet study. Adv Eng Mater 21(10):1900605
23. Piqué A, Serra P (2018) Laser printing of functional materials: 3D microfabrication, electronics and biomedicine. John Wiley & Sons
24. Guillemot F, Souquet A, Catros S, Guillotin B, Lopez J, Faucon M, Pippenger B, Bareille R, Rémy M, Bellance S (2010) High-throughput laser printing of cells and biomaterials for tissue engineering. Acta Biomater 6(7):2494–2500
25. Barron JA, Krizman DB, Ringeisen BR (2005) Laser printing of single cells: statistical analysis, cell viability, and stress. Ann Biomed Eng 33(2):121–130
26. Guillemot F, Souquet A, Catros S, Guillotin B (2010) Laser-assisted cell printing: principle, physical parameters versus cell fate and perspectives in tissue engineering. Nanomedicine 5(3):507–515
27. Hopp B, Smausz T, Kresz N, Barna N, Bor Z, Kolozsvári L, Chrisey DB, Szabó A, Nógrádi A (2005) Survival and proliferative ability of various living cell types after laser-induced forward transfer. Tissue Eng 11(11–12):1817–1823
28. Gruene M, Deiwick A, Koch L, Schlie S, Unger C, Hofmann N, Bernemann I, Glasmacher B, Chichkov B (2011) Laser printing of stem cells for biofabrication of scaffold-free autologous grafts. Tissue Eng Part C Methods 17(1):79–87
29. Sorkio A, Koch L, Koivusalo L, Deiwick A, Miettinen S, Chichkov B, Skottman H (2018) Human stem cell based corneal tissue mimicking structures using laser-assisted 3D bioprinting and functional bioinks. Biomaterials 171:57–71
30. Choi Y-J, Yi H-G, Kim S-W, Cho D-W (2017) 3D cell printed tissue analogues: a new platform for theranostics. Theranostics 7(12):3118
31. Li H, Tan C, Li L (2018) Review of 3D printable hydrogels and constructs. Mater Des 159:20–38
32. Malda J, Visser J, Melchels FP, Jüngst T, Hennink WE, Dhert WJ, Groll J, Hutmacher DW (2013) 25th anniversary article: engineering hydrogels for biofabrication. Adv Mater 25(36):5011–5028
33. Cui X, Boland T, DD'Lima D, K Lotz M (2012) Thermal inkjet printing in tissue engineering and regenerative medicine. Recent Pat Drug Deliv Formul 6(2):149–155
34. Saunders RE, Derby B (2014) Inkjet printing biomaterials for tissue engineering: bioprinting. Int Mater Rev 59(8):430–448
35. Negro A, Cherbuin T, Lutolf MP (2018) 3D inkjet printing of complex, cell-laden hydrogel structures. Sci Rep 8(1):1–9
36. Teo MY, Kee S, RaviChandran N, Stuart L, Aw KC, Stringer J (2019) Enabling free-standing 3D hydrogel microstructures with microreactive inkjet printing. ACS Appl Mater Interfaces 12(1):1832–1839
37. Unagolla JM, Jayasuriya AC (2020) Hydrogel-based 3D bioprinting: a comprehensive review on cell-laden hydrogels, bioink formulations, and future perspectives. Appl Mater Today 18:100479. https://doi.org/10.1016/j.apmt.2019.100479
38. Li J, Wu C, Chu PK, Gelinsky M (2020) 3D printing of hydrogels: rational design strategies and emerging biomedical applications. Mater Sci Eng R Rep 140:100543. https://doi.org/10.1016/j.mser.2020.100543
39. Jungst T, Smolan W, Schacht K, Scheibel T, Groll Jr (2016) Strategies and molecular design criteria for 3D printable hydrogels. Chem Rev 116(3):1496–1539
40. Pedde RD, Mirani B, Navaei A, Styan T, Wong S, Mehrali M, Thakur A, Mohtaram NK, Bayati A, Dolatshahi-Pirouz A (2017) Emerging biofabrication strategies for engineering complex tissue constructs. Adv Mater 29(19):1606061
41. Hospodiuk M, Moncal KK, Dey M, Ozbolat IT (2016) Extrusion-based biofabrication in tissue engineering and regenerative medicine. Springer International Publishing, Cham

42. Ozbolat IT, Hospodiuk M (2016) Current advances and future perspectives in extrusion-based bioprinting. Biomaterials 76:321–343
43. Billiet T, Gevaert E, De Schryver T, Cornelissen M, Dubruel P (2014) The 3D printing of gelatin methacrylamide cell-laden tissue-engineered constructs with high cell viability. Biomaterials 35(1):49–62
44. Pati F, Jang J, Lee JW, Cho D-W (2015) Extrusion bioprinting. In: Essentials of 3D biofabrication and translation. Elsevier, pp 123–152
45. Melchels FP, Dhert WJ, Hutmacher DW, Malda J (2014) Development and characterisation of a new bioink for additive tissue manufacturing. J Mater Chem B 2(16):2282–2289
46. Kesti M, Eberhardt C, Pagliccia G, Kenkel D, Grande D, Boss A, Zenobi-Wong M (2015) Bioprinting: bioprinting complex cartilaginous structures with clinically compliant biomaterials. Adv Funct Mater 25(48):7397–7397
47. Warner J, Soman P, Zhu W, Tom M, Chen S (2016) Design and 3D printing of hydrogel scaffolds with fractal geometries. ACS Biomater Sci Eng 2(10):1763–1770
48. Hahn MS, Taite LJ, Moon JJ, Rowland MC, Ruffino KA, West JL (2006) Photolithographic patterning of polyethylene glycol hydrogels. Biomaterials 27(12):2519–2524
49. Ovsianikov A, Gruene M, Pflaum M, Koch L, Maiorana F, Wilhelmi M, Haverich A, Chichkov B (2010) Laser printing of cells into 3D scaffolds. Biofabrication 2(1):014104
50. Schuster M, Turecek C, Weigel G, Saf R, Stampfl J, Varga F, Liska R (2009) Gelatin-based photopolymers for bone replacement materials. J Polym Sci Part A Polym Chem 47(24):7078–7089
51. Koch L, Deiwick A, Schlie S, Michael S, Gruene M, Coger V, Zychlinski D, Schambach A, Reimers K, Vogt PM (2012) Skin tissue generation by laser cell printing. Biotechnol Bioeng 109(7):1855–1863
52. Michael S, Sorg H, Peck C-T, Koch L, Deiwick A, Chichkov B, Vogt PM, Reimers K (2013) Tissue engineered skin substitutes created by laser-assisted bioprinting form skin-like structures in the dorsal skin fold chamber in mice. PloS One 8(3):e57741
53. Roth EA, Xu T, Das M, Gregory C, Hickman JJ, Boland T (2004) Inkjet printing for high-throughput cell patterning. Biomaterials 25(17):3707–3715
54. Xu T, Gregory CA, Molnar P, Cui X, Jalota S, Bhaduri SB, Boland T (2006) Viability and electrophysiology of neural cell structures generated by the inkjet printing method. Biomaterials 27(19):3580–3588
55. Lee VK, Kim DY, Ngo H, Lee Y, Seo L, Yoo S-S, Vincent PA, Dai G (2014) Creating perfused functional vascular channels using 3D bio-printing technology. Biomaterials 35(28):8092–8102
56. Lode A, Meyer M, Brüggemeier S, Paul B, Baltzer H, Schröpfer M, Winkelmann C, Sonntag F, Gelinsky M (2016) Additive manufacturing of collagen scaffolds by three-dimensional plotting of highly viscous dispersions. Biofabrication 8(1):015015
57. Yoon H, Lee J-S, Yim H, Kim G, Chun W (2016) Development of cell-laden 3D scaffolds for efficient engineered skin substitutes by collagen gelation. RSC Adv 6(26):21439–21447
58. Wang X, Yan Y, Pan Y, Xiong Z, Liu H, Cheng J, Liu F, Lin F, Wu R, Zhang R (2006) Generation of three-dimensional hepatocyte/gelatin structures with rapid prototyping system. Tissue Eng 12(1):83–90
59. Ding H, Illsley NP, Chang RC (2019) 3D Bioprinted GelMA based models for the study of trophoblast cell invasion. Sci Rep 9(1):1–13
60. Freeman FE, Kelly DJ (2017) Tuning alginate bioink stiffness and composition for controlled growth factor delivery and to spatially direct MSC fate within bioprinted tissues. Sci Rep 7(1):1–12
61. Yu Y, Zhang Y, Martin JA, Ozbolat IT (2013) Evaluation of cell viability and functionality in vessel-like bioprintable cell-laden tubular channels. J Biomech Eng 135(9):091–011
62. Abbadessa A, Blokzijl M, Mouser V, Marica P, Malda J, Hennink W, Vermonden T (2016) A thermo-responsive and photo-polymerizable chondroitin sulfate-based hydrogel for 3D printing applications. Carbohyd Polym 149:163–174

63. Pereira RF, Sousa A, Barrias CC, Bártolo PJ, Granja PL (2018) A single-component hydrogel bioink for bioprinting of bioengineered 3D constructs for dermal tissue engineering. Mater Horiz 5(6):1100–1111
64. Negrini NC, Bonetti L, Contili L, Farè S (2018) 3D printing of methylcellulose-based hydrogels. Bioprinting 10:e00024. https://doi.org/10.1016/j.bprint.2018.e00024
65. Xu X, Zhou J, Jiang Y, Zhang Q, Shi H, Liu D (2018) 3D printing process of oxidized nanocellulose and gelatin scaffold. J Biomater Sci Polym Ed 29(12):1498–1513
66. Lam T, Dehne T, Krüger JP, Hondke S, Endres M, Thomas A, Lauster R, Sittinger M, Kloke L (2019) Photopolymerizable gelatin and hyaluronic acid for stereolithographic 3D bioprinting of tissue-engineered cartilage. J Biomed Mater Res B Appl Biomater 107(8):2649–2657
67. Cui X, Breitenkamp K, Finn M, Lotz M, D'Lima DD (2012) Direct human cartilage repair using three-dimensional bioprinting technology. Tissue Eng Part A 18(11–12):1304–1312
68. Zhu W, Tringale KR, Woller SA, You S, Johnson S, Shen H, Schimelman J, Whitney M, Steinauer J, Xu W (2018) Rapid continuous 3D printing of customizable peripheral nerve guidance conduits. Mater Today 21(9):951–959
69. Skardal A, Mack D, Kapetanovic E, Atala A, Jackson JD, Yoo J, Soker S (2012) Bioprinted amniotic fluid-derived stem cells accelerate healing of large skin wounds. Stem Cells Transl Med 1(11):792–802
70. Albanna M, Binder KW, Murphy SV, Kim J, Qasem SA, Zhao W, Tan J, El-Amin IB, Dice DD, Marco J (2019) In situ bioprinting of autologous skin cells accelerates wound healing of extensive excisional full-thickness wounds. Sci Rep 9(1):1–15
71. Pataky K, Braschler T, Negro A, Renaud P, Lutolf MP, Brugger J (2012) Microdrop printing of hydrogel bioinks into 3D tissue-like geometries. Adv Mater 24(3):391–396
72. Nakamura M, Iwanaga S, Henmi C, Arai K, Nishiyama Y (2010) Biomatrices and biomaterials for future developments of bioprinting and biofabrication. Biofabrication 2(1):014–110
73. Faulkner-Jones A, Fyfe C, Cornelissen D-J, Gardner J, King J, Courtney A, Shu W (2015) Bioprinting of human pluripotent stem cells and their directed differentiation into hepatocyte-like cells for the generation of mini-livers in 3D. Biofabrication 7(4):044–102
74. Shi Y, Xing T, Zhang H, Yin R, Yang S, Wei J, Zhang W (2018) Tyrosinase-doped bioink for 3D bioprinting of living skin constructs. Biomed Mater 13(3):035008
75. Yang X, Lu Z, Wu H, Li W, Zheng L, Zhao J (2018) Collagen-alginate as bioink for three-dimensional (3D) cell printing based cartilage tissue engineering. Mater Sci Eng C 83:195–201
76. Duarte Campos DF, Rohde M, Ross M, Anvari P, Blaeser A, Vogt M, Panfil C, Yam GHF, Mehta JS, Fischer H (2019) Corneal bioprinting utilizing collagen-based bioinks and primary human keratocytes. J Biomed Mater Res Part A 107(9):1945–1953
77. Isaacson A, Swioklo S, Connon CJ (2018) 3D bioprinting of a corneal stroma equivalent. Exp Eye Res 173:188–193
78. Mazzocchi A, Devarasetty M, Huntwork R, Soker S, Skardal A (2018) Optimization of collagen type I-hyaluronan hybrid bioink for 3D bioprinted liver microenvironments. Biofabrication 11(1):015003
79. Xu W, Wang X, Yan Y, Zheng W, Xiong Z, Lin F, Wu R, Zhang R (2007) Rapid prototyping three-dimensional cell/gelatin/fibrinogen constructs for medical regeneration. J Bioact Compat Polym 22(4):363–377
80. Yan Y, Wang X, Pan Y, Liu H, Cheng J, Xiong Z, Lin F, Wu R, Zhang R, Lu Q (2005) Fabrication of viable tissue-engineered constructs with 3D cell-assembly technique. Biomaterials 26(29):5864–5871
81. Yan Y, Wang X, Xiong Z, Liu H, Liu F, Lin F, Wu R, Zhang R, Lu Q (2005) Direct construction of a three-dimensional structure with cells and hydrogel. J Bioact Compat Polym 20(3):259–269
82. Zhang T, Yan KC, Ouyang L, Sun W (2013) Mechanical characterization of bioprinted in vitro soft tissue models. Biofabrication 5(4):045010
83. Yao R, Zhang R, Yan Y, Wang X (2009) In vitro angiogenesis of 3D tissue engineered adipose tissue. J Bioact Compat Polym 24(1):5–24

84. Yin J, Yan M, Wang Y, Fu J, Suo H (2018) 3D bioprinting of low-concentration cell-laden gelatin methacrylate (GelMA) bioinks with a two-step cross-linking strategy. ACS Appl Mater Interfaces 10(8):6849–6857
85. Schuurman W, Levett PA, Pot MW, van Weeren PR, Dhert WJ, Hutmacher DW, Melchels FP, Klein TJ, Malda J (2013) Gelatin-methacrylamide hydrogels as potential biomaterials for fabrication of tissue-engineered cartilage constructs. Macromol Biosci 13(5):551–561
86. Colosi C, Shin SR, Manoharan V, Massa S, Costantini M, Barbetta A, Dokmeci MR, Dentini M, Khademhosseini A (2016) Microfluidic bioprinting of heterogeneous 3D tissue constructs using low-viscosity bioink. Adv Mater 28(4):677–684
87. Duan B, Kapetanovic E, Hockaday LA, Butcher JT (2014) Three-dimensional printed trileaflet valve conduits using biological hydrogels and human valve interstitial cells. Acta Biomater 10(5):1836–1846
88. Skardal A, Zhang J, McCoard L, Xu X, Oottamasathien S, Prestwich GD (2010) Photocrosslinkable hyaluronan-gelatin hydrogels for two-step bioprinting. Tissue Eng Part A 16(8):2675–2685
89. Rastin H, Ormsby RT, Atkins GJ, Losic D (2020) 3D bioprinting of methylcellulose/gelatin-methacryloyl (MC/GelMA) bioink with high shape integrity. ACS Appl Bio Mater 3(3):1815–1826
90. Ma Y, Ji Y, Huang G, Ling K, Zhang X, Xu F (2015) Bioprinting 3D cell-laden hydrogel microarray for screening human periodontal ligament stem cell response to extracellular matrix. Biofabrication 7 (4):044105
91. Schütz K, Placht AM, Paul B, Brüggemeier S, Gelinsky M, Lode A (2017) Three-dimensional plotting of a cell-laden alginate/methylcellulose blend: towards biofabrication of tissue engineering constructs with clinically relevant dimensions. J Tissue Eng Regen Med 11(5):1574–1587
92. Li H, Tan YJ, Leong KF, Li L (2017) 3D bioprinting of highly thixotropic alginate/methylcellulose hydrogel with strong interface bonding. ACS Appl Mater Interfaces 9(23):20086–20097
93. Liu Q, Li Q, Xu S, Zheng Q, Cao X (2018) Preparation and properties of 3D printed alginate–chitosan Polyion complex hydrogels for tissue engineering. Polymers 10(6):664
94. Hockaday L, Kang K, Colangelo N, Cheung P, Duan B, Malone E, Wu J, Girardi L, Bonassar L, Lipson H (2012) Rapid 3D printing of anatomically accurate and mechanically heterogeneous aortic valve hydrogel scaffolds. Biofabrication 4(3):035005
95. Akkineni AR, Ahlfeld T, Funk A, Waske A, Lode A, Gelinsky M (2016) Highly concentrated alginate-gellan gum composites for 3D plotting of complex tissue engineering scaffolds. Polymers 8(5):170
96. Jiang P, Yan C, Guo Y, Zhang X, Cai M, Jia X, Wang X, Zhou F (2019) Direct ink writing with high-strength and swelling-resistant biocompatible physically crosslinked hydrogels. Biomater Sci 7(5):1805–1814
97. Chimene D, Kaunas R, Gaharwar AK (2020) Hydrogel bioink reinforcement for additive manufacturing: a focused review of emerging strategies. Adv Mater 32(1):1902026
98. Castro NJ, O'brien J, Zhang LG (2015) Integrating biologically inspired nanomaterials and table-top stereolithography for 3D printed biomimetic osteochondral scaffolds. Nanoscale 7(33):14010–14022
99. Zhu W, Holmes B, Glazer RI, Zhang LG (2016) 3D printed nanocomposite matrix for the study of breast cancer bone metastasis. Nanomed Nanotechnol Biol Med 12(1):69–79
100. Heurtematte A, Small WR, Paunov VN (2007) Inkjet printed water sensitive transparent films from natural gum–carbon nanotube composites. Soft Matter 3(7):840–843
101. Yoon S, Park JA, Lee HR, Yoon WH, Hwang DS, Jung S (2018) Inkjet–spray hybrid printing for 3D freeform fabrication of multilayered hydrogel structures. Adv Healthcare Mater 7(14):1800050
102. Kim W, Kim G (2019) Collagen/bioceramic-based composite bioink to fabricate a porous 3D hASCs-laden structure for bone tissue regeneration. Biofabrication 12(1):015007

103. Montalbano G, Borciani G, Cerqueni G, Licini C, Banche-Niclot F, Janner D, Sola S, Fiorilli S, Mattioli-Belmonte M, Ciapetti G (2020) Collagen hybrid formulations for the 3D printing of nanostructured bone scaffolds: an optimized genipin-crosslinking strategy. Nanomaterials 10(9):1681
104. Lohrasbi S, Mirzaei E, Karimizade A, Takallu S, Rezaei A (2020) Collagen/cellulose nanofiber hydrogel scaffold: physical, mechanical and cell biocompatibility properties. Cellulose 27(2):927–940
105. Nosrati H, Sarraf-Mamoory R, Le DQS, Canillas Perez M, Bunger CE (2020) Physical evaluation of 3D printed gelatin-hydroxyapatite-reduced graphene oxide nanocomposite as a bone tissue engineering scaffold. J Tissues Mater 3(1):1–11
106. Gao Q, Niu X, Shao L, Zhou L, Lin Z, Sun A, Fu J, Chen Z, Hu J, Liu Y (2019) 3D printing of complex GelMA-based scaffolds with nanoclay. Biofabrication 11(3):035006
107. Xu W, Molino BZ, Cheng F, Molino PJ, Yue Z, Su D, Wang X, Willför S, Xu C, Wallace GG (2019) On low-concentration inks formulated by nanocellulose assisted with gelatin methacrylate (gelma) for 3D printing toward wound healing application. ACS Appl Mater Interfaces 11(9):8838–8848
108. Adib AA, Sheikhi A, Shahhosseini M, Simeunović A, Wu S, Castro CE, Zhao R, Khademhosseini A, Hoelzle DJ (2020) Direct-write 3D printing and characterization of a GelMA-based biomaterial for intracorporeal tissue engineering. Biofabrication 12(4):045006
109. Wang X, Tolba E, Schröder HC, Neufurth M, Feng Q, Diehl-Seifert B, Müller WE (2014) Effect of bioglass on growth and biomineralization of SaOS-2 cells in hydrogel after 3D cell bioprinting. PLoS One 9(11):e112497
110. Luo Y, Li Y, Qin X, Wa Q (2018) 3D printing of concentrated alginate/gelatin scaffolds with homogeneous nano apatite coating for bone tissue engineering. Mater Des 146:12–19
111. Jin Y, Liu C, Chai W, Compaan A, Huang Y (2017) Self-supporting nanoclay as internal scaffold material for direct printing of soft hydrogel composite structures in air. ACS Appl Mater Interfaces 9(20):17456–17465
112. Hong S, Sycks D, Chan HF, Lin S, Lopez GP, Guilak F, Leong KW, Zhao X (2015) 3D printing of highly stretchable and tough hydrogels into complex, cellularized structures. Adv Mater 27(27):4035–4040
113. Sayyar S, Gambhir S, Chung J, Officer DL, Wallace GG (2017) 3D printable conducting hydrogels containing chemically converted graphene. Nanoscale 9(5):2038–2050
114. Demirtaş TT, Irmak G, Gümüşderelioğlu M (2017) A bioprintable form of chitosan hydrogel for bone tissue engineering. Biofabrication 9(3):035003
115. Skardal A, Zhang J, McCoard L, Oottamasathien S, Prestwich GD (2010) Dynamically crosslinked gold nanoparticle–hyaluronan hydrogels. Adv Mater 22(42):4736–4740
116. Ahlfeld T, Cidonio G, Kilian D, Duin S, Akkineni A, Dawson J, Yang S, Lode A, Oreffo R, Gelinsky M (2017) Development of a clay based bioink for 3D cell printing for skeletal application. Biofabrication 9(3):034103
117. Milojević M, Gradišnik L, Stergar J, Klemen MS, Stožer A, Vesenjak M, Dubrovski PD, Maver T, Mohan T, Kleinschek KS (2019) Development of multifunctional 3D printed bioscaffolds from polysaccharides and NiCu nanoparticles and their application. Appl Surf Sci 488:836–852
118. Markstedt K, Mantas A, Tournier I, Hc MÁ, Hagg D, Gatenholm P (2015) 3D bioprinting human chondrocytes with nanocellulose–alginate bioink for cartilage tissue engineering applications. Biomacromol 16(5):1489–1496
119. Nguyen D, Hägg DA, Forsman A, Ekholm J, Nimkingratana P, Brantsing C, Kalogeropoulos T, Zaunz S, Concaro S, Brittberg M (2017) Cartilage tissue engineering by the 3D bioprinting of iPS cells in a nanocellulose/alginate bioink. Sci Rep 7(1):1–10
120. Cernencu AI, Lungu A, Stancu I-C, Serafim A, Heggset E, Syverud K, Iovu H (2019) Bioinspired 3D printable pectin-nanocellulose ink formulations. Carbohyd Polym 220:12–21
121. Cui X, Li J, Hartanto Y, Durham M, Tang J, Zhang H, Hooper G, Lim K, Woodfield T (2020) Advances in extrusion 3D bioprinting: a focus on multicomponent hydrogel-based bioinks. Adv Healthc Mater 9(15):1901648

122. Arcaute K, Mann B, Wicker R (2010) Stereolithography of spatially controlled multi-material bioactive poly (ethylene glycol) scaffolds. Acta Biomater 6(3):1047–1054
123. Li S, Yan Y, Xiong Z, Zhang CWR, Wang X (2009) Gradient hydrogel construct based on an improved cell assembling system. J Bioact Compat Polym 24(1_suppl):84–99
124. Li S, Xiong Z, Wang X, Yan Y, Liu H, Zhang R (2009) Direct fabrication of a hybrid cell/hydrogel construct by a double-nozzle assembling technology. J Bioact Compat Polym 24(3):249–265
125. Xu M, Wang X, Yan Y, Yao R, Ge Y (2010) An cell-assembly derived physiological 3D model of the metabolic syndrome, based on adipose-derived stromal cells and a gelatin/alginate/fibrinogen matrix. Biomaterials 31(14):3868–3877
126. Kang H-W, Lee SJ, Ko IK, Kengla C, Yoo JJ, Atala A (2016) A 3D bioprinting system to produce human-scale tissue constructs with structural integrity. Nat Biotechnol 34(3):312–319
127. Bahcecioglu G, Hasirci N, Bilgen B, Hasirci V (2019) Hydrogels of agarose, and methacrylated gelatin and hyaluronic acid are more supportive for in vitro meniscus regeneration than three dimensional printed polycaprolactone scaffolds. Int J Biol Macromol 122:1152–1162
128. Dubbin K, Hori Y, Lewis KK, Heilshorn SC (2016) Dual-stage crosslinking of a gel-phase bioink improves cell viability and homogeneity for 3D bioprinting. Adv Healthcare Mater 5(19):2488–2492
129. Gu Q, Tomaskovic-Crook E, Lozano R, Chen Y, Kapsa RM, Zhou Q, Wallace GG, Crook JM (2016) Stem cell bioprinting: functional 3d neural mini-tissues from printed gel-based bioink and human neural stem cells. Adv Healthcare Mater 5(12):1428–1428
130. Zhang W, Feng C, Yang G, Li G, Ding X, Wang S, Dou Y, Zhang Z, Chang J, Wu C (2017) 3D-printed scaffolds with synergistic effect of hollow-pipe structure and bioactive ions for vascularized bone regeneration. Biomaterials 135:85–95
131. Cunniffe GM, Gonzalez-Fernandez T, Daly A, Sathy BN, Jeon O, Alsberg E, Kelly DJ (2017) Three-dimensional bioprinting of polycaprolactone reinforced gene activated bioinks for bone tissue engineering. Tissue Eng Part A 23(17–18):891–900
132. Ning L, Zhu N, Mohabatpour F, Sarker M, Schreyer DJ, Chen X (2019) Bioprinting Schwann cell-laden scaffolds from low-viscosity hydrogel compositions. J Mater Chem B 7(29):4538–4551
133. Cheng Z, Landish B, Chi Z, Nannan C, Jingyu D, Sen L, Xiangjin L (2018) 3D printing hydrogel with graphene oxide is functional in cartilage protection by influencing the signal pathway of Rank/Rankl/OPG. Mater Sci Eng C 82:244–252
134. Jang J, Kim TG, Kim BS, Kim S-W, Kwon S-M, Cho D-W (2016) Tailoring mechanical properties of decellularized extracellular matrix bioink by vitamin B2-induced photo-crosslinking. Acta Biomater 33:88–95
135. Gao G, Lee JH, Jang J, Lee DH, Kong JS, Kim BS, Choi YJ, Jang WB, Hong YJ, Kwon SM (2017) Tissue engineered bio-blood-vessels constructed using a tissue-specific bioink and 3D coaxial cell printing technique: a novel therapy for ischemic disease. Adv Func Mater 27(33):1700798
136. Jorgensen AM, Varkey M, Gorkun A, Clouse C, Xu L, Chou Z, Murphy SV, Molnar J, Lee SJ, Yoo JJ (2020) Bioprinted skin recapitulates normal collagen remodeling in full-thickness wounds. Tissue Eng Part A 26(9–10):512–526
137. Ouyang L, Yao R, Chen X, Na J, Sun W (2015) 3D printing of HEK 293FT cell-laden hydrogel into macroporous constructs with high cell viability and normal biological functions. Biofabrication 7(1):015010
138. Costantini M, Idaszek J, Szöke K, Jaroszewicz J, Dentini M, Barbetta A, Brinchmann JE, Święszkowski W (2016) 3D bioprinting of BM-MSCs-loaded ECM biomimetic hydrogels for in vitro neocartilage formation. Biofabrication 8(3):035002
139. Boere KW, Blokzijl MM, Visser J, Linssen JEA, Malda J, Hennink WE, Vermonden T (2015) Biofabrication of reinforced 3D-scaffolds using two-component hydrogels. J Mater Chem B 3(46):9067–9078
140. Kim SW, Kim DY, Roh HH, Kim HS, Lee JW, Lee KY (2019) Three-dimensional bioprinting of cell-laden constructs using polysaccharide-based self-healing hydrogels. Biomacromol 20(5):1860–1866

141. Salaris F, Colosi C, Brighi C, Soloperto A, de Turris V, Benedetti MC, Ghirga S, Rosito M, Di Angelantonio S, Rosa A (2019) 3D bioprinted human cortical neural constructs derived from induced pluripotent stem cells. J Clin Med 8(10):1595
142. Rodriguez MJ, Brown J, Giordano J, Lin SJ, Omenetto FG, Kaplan DL (2017) Silk based bioinks for soft tissue reconstruction using 3-dimensional (3D) printing with in vitro and in vivo assessments. Biomaterials 117:105–115
143. Echalier C, Levato R, Mateos-Timoneda MA, Castano O, Déjean S, Garric X, Pinese C, Noël D, Engel E, Martinez J (2017) Modular bioink for 3D printing of biocompatible hydrogels: sol–gel polymerization of hybrid peptides and polymers. RSC Adv 7(20):12231–12235
144. Wang K, Ho C-C, Zhang C, Wang B (2017) A review on the 3D printing of functional structures for medical phantoms and regenerated tissue and organ applications. Engineering 3(5):653–662
145. Poomathi N, Singh S, Prakash C, Subramanian A, Sahay R, Cinappan A, Ramakrishna S (2020) 3D printing in tissue engineering: a state of the art review of technologies and biomaterials. Rapid Prototyp J 27(7):1313–1334
146. Mironov V (2003) Printing technology to produce living tissue. Taylor & Francis
147. Mironov V, Markwald RR, Forgacs G (2003) Organ printing: self-assembling cell aggregates as "Bioink." Sci Med 9(2):69–71
148. Chimene D, Lennox KK, Kaunas RR, Gaharwar AK (2016) Advanced bioinks for 3D printing: a materials science perspective. Ann Biomed Eng 44(6):2090–2102
149. Murphy SV, Skardal A, Atala A (2013) Evaluation of hydrogels for bio-printing applications. J Biomed Mater Res Part A 101(1):272–284
150. Kyle S, Jessop ZM, Al-Sabah A, Whitaker IS (2017) 'Printability" of candidate biomaterials for extrusion based 3d printing: state-of-the-art.' Adv Healthcare Mater 6(16):1700264
151. Carrow JK, Kerativitayanan P, Jaiswal MK, Lokhande G, Gaharwar AK (2015) Polymers for bioprinting. In: Essentials of 3D biofabrication and translation. Elsevier, pp 229–248
152. Paxton N, Smolan W, Böck T, Melchels F, Groll J, Jungst T (2017) Proposal to assess printability of bioinks for extrusion-based bioprinting and evaluation of rheological properties governing bioprintability. Biofabrication 9(4):044107
153. Melchels FP, Blokzijl MM, Levato R, Peiffer QC, De Ruijter M, Hennink WE, Vermonden T, Malda J (2016) Hydrogel-based reinforcement of 3D bioprinted constructs. Biofabrication 8(3):035004
154. Sarker M, Chen X (2017) Modeling the flow behavior and flow rate of medium viscosity alginate for scaffold fabrication with a three-dimensional bioplotter. J Manuf Sci Eng 139(8):081002
155. Kosik-Kozioł A, Costantini M, Bolek T, Szöke K, Barbetta A, Brinchmann J, Święszkowski W (2017) PLA short sub-micron fiber reinforcement of 3D bioprinted alginate constructs for cartilage regeneration. Biofabrication 9(4):044105
156. Chimene D, Peak CW, Gentry JL, Carrow JK, Cross LM, Mondragon E, Cardoso GB, Kaunas R, Gaharwar AK (2018) Nanoengineered ionic–covalent entanglement (NICE) bioinks for 3D bioprinting. ACS Appl Mater Interfaces 10(12):9957–9968
157. Peak CW, Stein J, Gold KA, Gaharwar AK (2018) Nanoengineered colloidal inks for 3D bioprinting. Langmuir 34(3):917–925
158. GhavamiNejad A, Ashammakhi N, Wu XY, Khademhosseini A (2020) Crosslinking strategies for 3D bioprinting of polymeric hydrogels. Small 16(35):2002931
159. Hribar KC, Choi YS, Ondeck M, Engler AJ, Chen S (2014) Digital plasmonic patterning for localized tuning of hydrogel stiffness. Adv Func Mater 24(31):4922–4926
160. Kesti M, Eberhardt C, Pagliccia G, Kenkel D, Grande D, Boss A, Zenobi-Wong M (2015) Bioprinting complex cartilaginous structures with clinically compliant biomaterials. Adv Func Mater 25(48):7406–7417
161. Sarker M, Izadifar M, Schreyer D, Chen X (2018) Influence of ionic crosslinkers (Ca2+/Ba2+/Zn2+) on the mechanical and biological properties of 3D Bioplotted Hydrogel Scaffolds. J Biomater Sci Polym Ed 29(10):1126–1154

162. Khalil S, Sun W (2009) Bioprinting endothelial cells with alginate for 3D tissue constructs. J Biomech Eng 131(11):111002
163. Sapir Y, Kryukov O, Cohen S (2011) Integration of multiple cell-matrix interactions into alginate scaffolds for promoting cardiac tissue regeneration. Biomaterials 32(7):1838–1847
164. Chatterjee S, Hui PC-l, Kan C-W (2018) Thermoresponsive hydrogels and their biomedical applications: Special insight into their applications in textile based transdermal therapy. Polymers 10(5):480
165. Hu W, Wang Z, Xiao Y, Zhang S, Wang J (2019) Advances in crosslinking strategies of biomedical hydrogels. Biomater Sci 7(3):843–855
166. Klouda L (2015) Thermoresponsive hydrogels in biomedical applications: a seven-year update. Eur J Pharm Biopharm 97:338–349
167. Lim W, Kim GJ, Kim HW, Lee J, Zhang X, Kang MG, Seo JW, Cha JM, Park HJ, Lee M-Y (2020) Kappa-carrageenan-based dual crosslinkable bioink for extrusion type bioprinting. Polymers 12(10):2377
168. Tuncaboylu DC, Argun A, Algi MP, Okay O (2013) Autonomic self-healing in covalently crosslinked hydrogels containing hydrophobic domains. Polymer 54(23):6381–6388
169. Roehm KD, Madihally SV (2017) Bioprinted chitosan-gelatin thermosensitive hydrogels using an inexpensive 3D printer. Biofabrication 10(1):015002
170. Lee JB, Wang X, Faley S, Baer B, Balikov DA, Sung HJ, Bellan LM (2016) Development of 3D microvascular networks within gelatin hydrogels using thermoresponsive sacrificial microfibers. Adv Healthcare Mater 5(7):781–785
171. Zhai X, Ma Y, Hou C, Gao F, Zhang Y, Ruan C, Pan H, Lu WW, Liu W (2017) 3D-printed high strength bioactive supramolecular polymer/clay nanocomposite hydrogel scaffold for bone regeneration. ACS Biomater Sci Eng 3(6):1109–1118
172. Wang H, Zhu H, Fu W, Zhang Y, Xu B, Gao F, Cao Z, Liu W (2017) A high strength self-healable antibacterial and anti-inflammatory supramolecular polymer hydrogel. Macromol Rapid Commun 38(9):1600695
173. Tan Z, Parisi C, Di Silvio L, Dini D, Forte AE (2017) Cryogenic 3D printing of super soft hydrogels. Sci Rep 7(1):1–11
174. Li C, Faulkner-Jones A, Dun AR, Jin J, Chen P, Xing Y, Yang Z, Li Z, Shu W, Liu D (2015) Rapid Formation of a Supramolecular Polypeptide–DNA Hydrogel for In Situ Three-Dimensional Multilayer Bioprinting. Angew Chem 127(13):4029–4033
175. Ouyang L, Highley CB, Rodell CB, Sun W, Burdick JA (2016) 3D printing of shear-thinning hyaluronic acid hydrogels with secondary cross-linking. ACS Biomater Sci Eng 2(10):1743–1751
176. Wang Q, Han G, Yan S, Zhang Q (2019) 3D printing of silk fibroin for biomedical applications. Materials 12(3):504
177. Choi JR, Yong KW, Choi JY, Cowie AC (2019) Recent advances in photo-crosslinkable hydrogels for biomedical applications. Biotechniques 66(1):40–53
178. Levato R, Webb WR, Otto IA, Mensinga A, Zhang Y, van Rijen M, van Weeren R, Khan IM, Malda J (2017) The bio in the ink: cartilage regeneration with bioprintable hydrogels and articular cartilage-derived progenitor cells. Acta Biomater 61:41–53
179. Zhai X, Ruan C, Ma Y, Cheng D, Wu M, Liu W, Zhao X, Pan H, Lu WW (2018) 3D-bioprinted osteoblast-laden nanocomposite hydrogel constructs with induced microenvironments promote cell viability, differentiation, and osteogenesis both in vitro and in vivo. Adv Sci 5(3):1700550
180. Ma Y, Ji Y, Zhong T, Wan W, Yang Q, Li A, Zhang X, Lin M (2017) Bioprinting-based PDLSC-ECM screening for in vivo repair of alveolar bone defect using cell-laden, injectable and photocrosslinkable hydrogels. ACS Biomater Sci Eng 3(12):3534–3545
181. Mouser VH, Melchels FP, Visser J, Dhert WJ, Gawlitta D, Malda J (2016) Yield stress determines bioprintability of hydrogels based on gelatin-methacryloyl and gellan gum for cartilage bioprinting. Biofabrication 8(3):035003
182. Poldervaart MT, Goversen B, De Ruijter M, Abbadessa A, Melchels FP, Öner FC, Dhert WJ, Vermonden T, Alblas J (2017) 3D bioprinting of methacrylated hyaluronic acid (MeHA) hydrogel with intrinsic osteogenicity. PLoS One 12(6):e0177628

183. Qin X-H, Ovsianikov A, Stampfl J, Liska R (2014) Additive manufacturing of photosensitive hydrogels for tissue engineering applications. BioNanoMaterials 15(3–4):49–70
184. Chen G, Kawazoe N, Ito Y (2018) Photo-crosslinkable hydrogels for tissue engineering applications. In: Photochemistry for biomedical applications. Springer, pp 277–300
185. Bryant SJ, Nuttelman CR, Anseth KS (2000) Cytocompatibility of UV and visible light photoinitiating systems on cultured NIH/3T3 fibroblasts in vitro. J Biomater Sci Polym Ed 11(5):439–457
186. Kirchhof S, Brandl FP, Hammer N, Goepferich AM (2013) Investigation of the Diels-Alder reaction as a cross-linking mechanism for degradable poly (ethylene glycol) based hydrogels. J Mater Chem B 1(37):4855–4864
187. Smith LJ, Taimoory SM, Tam RY, Baker AE, Binth Mohammad N, Trant JF, Shoichet MS (2018) Diels-Alder click-cross-linked hydrogels with increased reactivity enable 3D cell encapsulation. Biomacromol 19(3):926–935
188. Madl CM, Heilshorn SC (2019) Rapid diels–alder cross-linking of cell encapsulating hydrogels. Chem Mater 31(19):8035–8043
189. Xu J, Liu Y, Hsu S-h (2019) Hydrogels based on Schiff base linkages for biomedical applications. Molecules 24(16):3005
190. Wang LL, Highley CB, Yeh YC, Galarraga JH, Uman S, Burdick JA (2018) Three-dimensional extrusion bioprinting of single-and double-network hydrogels containing dynamic covalent crosslinks. J Biomed Mater Res, Part A 106(4):865–875
191. Hafeez S, Ooi HW, Morgan FL, Mota C, Dettin M, Van Blitterswijk C, Moroni L, Baker MB (2018) Viscoelastic oxidized alginates with reversible imine type crosslinks: self-healing, injectable, and bioprintable hydrogels. Gels 4(4):85
192. Li C, Wang K, Zhou X, Li T, Xu Y, Qiang L, Peng M, Xu Y, Xie L, He C (2019) Controllable fabrication of hydroxybutyl chitosan/oxidized chondroitin sulfate hydrogels by 3D bioprinting technique for cartilage tissue engineering. Biomed Mater 14(2):025006
193. Hao Y, Fowler EW, Jia X (2017) Chemical synthesis of biomimetic hydrogels for tissue engineering. Polym Int 66(12):1787–1799
194. Li R, Cai Z, Li Z, Zhang Q, Zhang S, Deng L, Lu L, Li L, Zhou C (2017) Synthesis of in-situ formable hydrogels with collagen and hyaluronan through facile Michael addition. Mater Sci Eng C 77:1035–1043
195. Zhang Z, Loebus A, de Vicente G, Ren F, Arafeh M, Ouyang Z, Lensen MC (2014) Synthesis of poly (ethylene glycol)-based hydrogels via amine-michael type addition with tunable stiffness and postgelation chemical functionality. Chem Mater 26(12):3624–3630
196. Berry DR, Díaz BK, Durand-Silva A, Smaldone RA (2019) Radical free crosslinking of direct-write 3D printed hydrogels through a base catalyzed thiol-Michael reaction. Polym Chem 10(44):5979–5984
197. Teixeira LSM, Feijen J, van Blitterswijk CA, Dijkstra PJ, Karperien M (2012) Enzyme-catalyzed crosslinkable hydrogels: emerging strategies for tissue engineering. Biomaterials 33(5):1281–1290
198. Valot L, Martinez J, Mehdi A, Subra G (2019) Chemical insights into bioinks for 3D printing. Chem Soc Rev 48(15):4049–4086
199. Włodarczyk-Biegun MK, Del Campo A (2017) 3D bioprinting of structural proteins. Biomaterials 134:180–201
200. Martínez-Pellitero S, Castro M, Fernández-Abia AI, González S, Cuesta E (2017) Analysis of influence factors on part quality in micro-SLA technology. Procedia manufacturing 13:856–863
201. Pearre BW, Michas C, Tsang J-M, Gardner TJ, Otchy TM (2019) Fast micron-scale 3D printing with a resonant-scanning two-photon microscope. Addit Manuf 30:100887
202. Miri AK, Mirzaee I, Hassan S, Oskui SM, Nieto D, Khademhosseini A, Zhang YS (2019) Effective bioprinting resolution in tissue model fabrication. Lab Chip 19(11):2019–2037
203. Li X, Chen J, Liu B, Wang X, Ren D, Xu T, Ovsianikov A, Yoo J, Mironov V (2018) Inkjet printing for biofabrication. 3D printing and biofabrication reference series in biomedical engineering. Ovsianikov A, Yoo J, Mironov V (eds), pp 1–19

204. Zhong Y, Fang H, Ma Q, Dong X (2018) Analysis of droplet stability after ejection from an inkjet nozzle. J Fluid Mech 845:378
205. Liu Y-F, Tsai M-H, Pai Y-F, Hwang W-S (2013) Control of droplet formation by operating waveform for inks with various viscosities in piezoelectric inkjet printing. Appl Phys A 111(2):509–516
206. Placone JK, Engler AJ (2018) Recent advances in extrusion-based 3D printing for biomedical applications. Adv Healthcare Mater 7(8):1701161
207. Naghieh S, Sarker M, Sharma N, Barhoumi Z, Chen X (2020) Printability of 3D printed hydrogel scaffolds: influence of hydrogel composition and printing parameters. Appl Sci 10(1):292
208. Li M, Tian X, Schreyer DJ, Chen X (2011) Effect of needle geometry on flow rate and cell damage in the dispensing-based biofabrication process. Biotechnol Prog 27(6):1777–1784
209. He Y, Yang F, Zhao H, Gao Q, Xia B, Fu J (2016) Research on the printability of hydrogels in 3D bioprinting. Sci Rep 6(1):1–13
210. Chung JH, Naficy S, Yue Z, Kapsa R, Quigley A, Moulton SE, Wallace GG (2013) Bio-ink properties and printability for extrusion printing living cells. Biomater Sci 1(7):763–773
211. Cai FF, Heid S, Boccaccini AR (2020) Potential of laponite incorporated oxidized alginate–gelatin (ADA-GEL) composite hydrogels for extrusion-based 3D printing. J Biomed Mater Res Part B Appl Biomater 109(8):1090–104
212. Jin Y, Chai W, Huang Y (2017) Printability study of hydrogel solution extrusion in nanoclay yield-stress bath during printing-then-gelation biofabrication. Mater Sci Eng C 80:313–325
213. Habib A, Sathish V, Mallik S, Khoda B (2018) 3D printability of alginate-carboxymethyl cellulose hydrogel. Materials 11(3):454
214. Zhu F, Cheng L, Yin J, Wu ZL, Qian J, Fu J, Zheng Q (2016) 3D printing of ultratough polyion complex hydrogels. ACS Appl Mater Interfaces 8(45):31304–31310
215. Wilson SA, Cross LM, Peak CW, Gaharwar AK (2017) Shear-thinning and thermo-reversible nanoengineered inks for 3D bioprinting. ACS Appl Mater Interfaces 9(50):43449–43458
216. Di Giuseppe M, Law N, Webb B, Macrae RA, Liew LJ, Sercombe TB, Dilley RJ, Doyle BJ (2018) Mechanical behaviour of alginate-gelatin hydrogels for 3D bioprinting. J Mech Behav Biomed Mater 79:150–157
217. Gatenholm P, Martinez H, Karabulut E, Amoroso M, Kölby L, Markstedt K, Gatenholm E, Henriksson I (2016) Development of nanocellulose-based bioinks for 3D bioprinting of soft tissue. 3D printing and biofabrication, reference series in biomedical engineering, Springer, Cham, pp 1–23
218. Göhl J, Markstedt K, Mark A, Håkansson K, Gatenholm P, Edelvik F (2018) Simulations of 3D bioprinting: predicting bioprintability of nanofibrillar inks. Biofabrication 10(3):034105
219. Gao T, Gillispie GJ, Copus JS, Pr AK, Seol Y-J, Atala A, Yoo JJ, Lee SJ (2018) Optimization of gelatin–alginate composite bioink printability using rheological parameters: a systematic approach. Biofabrication 10(3):034106
220. Smith PT, Basu A, Saha A, Nelson A (2018) Chemical modification and printability of shear-thinning hydrogel inks for direct-write 3D printing. Polymer 152:42–50
221. Ouyang L, Yao R, Zhao Y, Sun W (2016) Effect of bioink properties on printability and cell viability for 3D bioplotting of embryonic stem cells. Biofabrication 8(3):035020
222. Soltan N, Ning L, Mohabatpour F, Papagerakis P, Chen X (2019) Printability and cell viability in bioprinting alginate dialdehyde-gelatin scaffolds. ACS Biomater Sci Eng 5(6):2976–2987
223. Blaeser A, Duarte Campos DF, Weber M, Neuss S, Theek B, Fischer H, Jahnen-Dechent W (2013) Biofabrication under fluorocarbon: a novel freeform fabrication technique to generate high aspect ratio tissue-engineered constructs. BioRes Open Access 2(5):374–384
224. Müller M, Becher J, Schnabelrauch M, Zenobi-Wong M (2015) Nanostructured Pluronic hydrogels as bioinks for 3D bioprinting. Biofabrication 7(3):035006
225. Müller M, Öztürk E, Arlov Ø, Gatenholm P, Zenobi-Wong M (2017) Alginate sulfate–nanocellulose bioinks for cartilage bioprinting applications. Ann Biomed Eng 45(1):210–223
226. Ojansivu M, Rashad A, Ahlinder A, Massera J, Mishra A, Syverud K, Finne-Wistrand A, Miettinen S, Mustafa K (2019) Wood-based nanocellulose and bioactive glass modified gelatin–alginate bioinks for 3D bioprinting of bone cells. Biofabrication 11(3):035010

227. Ribeiro A, Blokzijl MM, Levato R, Visser CW, Castilho M, Hennink WE, Vermonden T, Malda J (2017) Assessing bioink shape fidelity to aid material development in 3D bioprinting. Biofabrication 10(1):014102
228. Jiang Y, Xv X, Liu D, Yang Z, Zhang Q, Shi H, Zhao G, Zhou J (2018) Preparation of cellulose nanofiber-reinforced gelatin hydrogel and optimization for 3D printing applications. BioResources 13(3):5909–5924
229. Rutz AL, Hyland KE, Jakus AE, Burghardt WR, Shah RN (2015) A multimaterial bioink method for 3D printing tunable, cell-compatible hydrogels. Adv Mater 27(9):1607–1614
230. Duarte Campos DF, Blaeser A, Korsten A, Neuss S, Jäkel J, Vogt M, Fischer H (2015) The stiffness and structure of three-dimensional printed hydrogels direct the differentiation of mesenchymal stromal cells toward adipogenic and osteogenic lineages. Tissue Eng Part A 21(3–4):740–756
231. Azam RS, Zhang M, Bhandari B, Yang C (2018) Effect of different gums on features of 3D printed object based on vitamin-D enriched orange concentrate. Food Biophys 13(3):250–262
232. Li Z, Huang S, Liu Y, Yao B, Hu T, Shi H, Xie J, Fu X (2018) Tuning alginate-gelatin bioink properties by varying solvent and their impact on stem cell behavior. Sci Rep 8(1):1–8
233. Lee J-S, Kim BS, Seo D, Park JH, Cho D-W (2017) Three-dimensional cell printing of large-volume tissues: application to ear regeneration. Tissue Eng Part C Methods 23(3):136–145
234. Abbadessa A, Mouser VH, Blokzijl MM, Gawlitta D, Dhert WJ, Hennink WE, Malda J, Vermonden T (2016) A synthetic thermosensitive hydrogel for cartilage bioprinting and its biofunctionalization with polysaccharides. Biomacromol 17(6):2137–2147
235. Cohen DL, Lo W, Tsavaris A, Peng D, Lipson H, Bonassar LJ (2011) Increased mixing improves hydrogel homogeneity and quality of three-dimensional printed constructs. Tissue Eng Part C Methods 17(2):239–248
236. Jia J, Richards DJ, Pollard S, Tan Y, Rodriguez J, Visconti RP, Trusk TC, Yost MJ, Yao H, Markwald RR (2014) Engineering alginate as bioink for bioprinting. Acta Biomater 10(10):4323–4331
237. Zhao Y, Li Y, Mao S, Sun W, Yao R (2015) The influence of printing parameters on cell survival rate and printability in microextrusion-based 3D cell printing technology. Biofabrication 7(4):045002
238. Lim KS, Schon BS, Mekhileri NV, Brown GC, Chia CM, Prabakar S, Hooper GJ, Woodfield TB (2016) New visible-light photoinitiating system for improved print fidelity in gelatin-based bioinks. ACS Biomater Sci Eng 2(10):1752–1762
239. Blaeser A, Duarte Campos DF, Puster U, Richtering W, Stevens MM, Fischer H (2016) Controlling shear stress in 3D bioprinting is a key factor to balance printing resolution and stem cell integrity. Adv Healthcare Mater 5(3):326–333
240. Gillispie G, Prim P, Copus J, Fisher J, Mikos AG, Yoo JJ, Atala A, Lee SJ (2020) Assessment methodologies for extrusion-based bioink printability. Biofabrication 12(2):022003
241. Miao S, Castro N, Nowicki M, Xia L, Cui H, Zhou X, Zhu W, Lee S-j, Sarkar K, Vozzi G (2017) 4D printing of polymeric materials for tissue and organ regeneration. Mater Today 20(10):577–591
242. Trujillo-de Santiago G, Alvarez MM, Samandari M, Prakash G, Chandrabhatla G, Rellstab-Sánchez PI, Byambaa B, Abadi PPSS, Mandla S, Avery RK (2018) Chaotic printing: using chaos to fabricate densely packed micro-and nanostructures at high resolution and speed. Mater Horiz 5(5):813–822
243. Momeni F, Liu X, Ni J (2017) A review of 4D printing. Mater Des 122:42–79
244. Mohamed MA, Fallahi A, El-Sokkary AM, Salehi S, Akl MA, Jafari A, Tamayol A, Fenniri H, Khademhosseini A, Andreadis ST (2019) Stimuli-responsive hydrogels for manipulation of cell microenvironment: from chemistry to biofabrication technology. Prog Polym Sci 98:101147
245. Champeau M, Heinze DA, Viana TN, de Souza ER, Chinellato AC, Titotto S (2020) 4D printing of hydrogels: a review. Adv Func Mater 30(31):1910606
246. Gao B, Yang Q, Zhao X, Jin G, Ma Y, Xu F (2016) 4D bioprinting for biomedical applications. Trends Biotechnol 34(9):746–756

247. Devillard CD, Mandon CA, Lambert SA, Blum LJ, Marquette CA (2018) Bioinspired multi-activities 4d printing objects: a new approach toward complex tissue engineering. Biotechnol J 13(12):1800098
248. Ashammakhi N, Ahadian S, Zengjie F, Suthiwanich K, Lorestani F, Orive G, Ostrovidov S, Khademhosseini A (2018) Advances and future perspectives in 4D bioprinting. Biotechnol J 13(12):1800148
249. Taylor DA, Parikh RB, Sampaio LC (2017) Bioengineering hearts: simple yet complex. Current Stem Cell Rep 3(1):35–44

Chapter 4
Three-Dimensional Self-healing Scaffolds for Tissue Engineering Applications

Durgalakshmi Dhinasekaran, Mohanraj Jagannathan, and Anuj Kumar

Abstract Self-healing property is the most important inherent quality of the living system. For the synthetic materials used as tissue engineering scaffolds, in addition to the basic supportive structure, added self-healing capability is also necessary. If the structure is having self-healing property the patient will bet the benefit of a quick recovery and these supports reduce the need for revision surgery. For tissue engineering applications, polymer scaffolds were highly suitable for the incorporation of cells and growth-stimulating hormones in the native tissue. Even though hydrogels were the first man-made biomaterial, the material optimization was much restricted for tissue engineering applications. With the discoveries of supramolecular chemistry, a lot of self-assembled structuring was explored. And also, by understanding the systems chemistry, bioinspired polymerization-based self-healing hydrogels were being explored. The field of supramolecular chemistry is old as 50 decades, however, the application of polymerization by non-covalent interaction of biomedical applications was explored lesser compare to other optoelectronic and mechanical applications. This book chapter will be give details about the need for self-healing scaffolds, prepared by supramolecular polymerization for 3D structuring towards tissue engineering applications is discussed in detail. The discussion of supramolecular bonding includes hydrogen bonding, electrostatic interaction, metal–ligand, host–guest interaction and π–π interaction. Also, a comparative outline of the need for tissue-engineering scaffolds properties in terms of rheology, mechanical property and shape memory effect of these polymerization interactions was amended.

Keywords Hydrogels · Supramolecules · Tissue engineering · Drug delivery · Living polymerization

D. Dhinasekaran (✉) · M. Jagannathan
Department of Medical Physics, Anna University, Chennai 600025, India

A. Kumar
School of Chemical Engineering, Yeungnam University, Gyeongsan 38541, South Korea

A. Kumar et al. (eds.), *3D printable Gel-inks for Tissue Engineering*, Gels Horizons: From Science to Smart Materials, https://doi.org/10.1007/978-981-16-4667-6_4

1 Introduction

Nature is a beautiful and mysterious creator in creating a complex structure, one such example is our human body. Healthy living is mostly addressed by the absence of disease; however, it is also true in quick recovery from any disease condition [1]. The quick recovery condition is variable for the individual and depends on their self-regeneration potentialities. Due to ageing, medical complications and chronic conditions, human beings are limited in depending completely on the self-regeneration of the human system and in need of external stimuli and supportive biomaterial for the treatment of diseases and defects. These biomaterials were greatly helped to fulfil the need of human beings. From the first generation of biomaterials, where it was meant to be there just for supporting the defects, now we are in the fourth generation of biomaterials that deal with biomimetic tissue regeneration [2]. As most of modern medicines are following the Greek concept of treatment, tissue regeneration is also old as those concepts, which starts with the story of the Prometheus liver tissue regeneration after it was fed to the eagle every day [3]. During the major post-war years between 1960 and 1970, there was a much need for implant materials to treat the defective and disease parts of the body, and in those years based on the goal of achieving bio-inertness with in vivo conditions, first-generation biomaterials were widely fulfilled human needs [4]. After trying to understand the interaction between the implant material and the extracellular matrix, research and development related to the second-generation bioactive materials were developed since the 1970s. Later from 2000, third-generation biomaterials having the potentialities of bio-resorption and regeneration were explored [5, 6]. To mimic the structural and bioactivity of the tissues, three-dimensional (3D) structures with molecular tailoring to the localized microenvironment were the field of interest for the present researchers.

Later in the 1970s, van der Waals interaction based 3D hydrogels were prepared and suggested for biomedical applications [7]. This polymeric hydrogel material can swell in water/physiological medium without dissolving in the water medium. (William Dictionary) [8]. Initially, most of the hydrogels were prepared for soft lens applications, as an alternative to silicone rubber [9]. For this purpose, poly (hydroxyethyl methacrylate) hydrogels were developed first with water absorption of 30% [10]. Later copolymer-based hydrogels were developed by the United States with an increase in water absorption of over 60% [4]. However, these hydrogels were mostly bioactive and limited in bio-resorption and regeneration properties.

In the mid-twentieth century, the organic chemist innovated the concept of molecular information and recognition, which turned into the field of supramolecular chemistry [11]. In this, the molecular system has the capability of well-defined functional assemblies with the possibility to form complexes [12]. This process is termed as ‘lock-and-key’ mechanism by Lichtenthaler [13]. For the invention and contribution in this field, the Nobel prize award for the year 1987 was given to Huang and Anslyn [14]. Based on the concept given by these Nobel persons, Daniel E. Koshland formulated the ‘induced fit’ concept, where he added that the lock-and-key concept occurs explicitly only after the changes in the three-dimensional substrate, during

the relationship of the amino acids at the active cites in enzymatic reactions [15]. The concepts of supramolecular chemistry are the platform for understanding the self-organization and self-healing principles of polymer structure, can be used for biomedical applications, more specifically for tissue engineering applications. This self-organization through the supramolecular chemical structure can behold in terms of molecules and can have good integrity with cells and tissue growth as it has the ability for progressive unravelling the complexity of the matter.

2 Understanding Nature's Method of Self-healing

Nature is the best teacher to teach us the process of self-organization in forming beautiful creatures and organizing dissipative structures at a different time frame. The process of self-organization can be seen in many facets with the different time frames of formation; from the development of the foetus to a baby in the mothers' womb is the best example, which remains as an exclamatory to understand nature. Another best example is a systemic process of self-healing in some disease and inflammatory conditions. Self-organization can be achieved by self-assembly, self-patterning, and self-driven morphogenesis, which are individually a different process. Self-organization is a powerful inherent characteristic of cells that can be adapted finely but not over-engineered to construct new tissues or organs. For suggesting biomaterials for tissue engineering applications, rather than bio-inert and bioactive scaffolding, three-dimensional (3D) structure support with physio-chemical mimetic to the targeted in vivo region and influencing self-organization can be highly compatible [16, 17]. Even though a lot of 3D microporous scaffolding is reported and in use, the needs of the scaffolding are much more for regeneration [18]. For example, mechanical forces mimicking the development of tissues through biomaterial support can contribute to self-driven morphogenesis for the specifically targeted tissue regeneration and can contribute to the self-healing process [19, 20].

This self-healing process can be achieved if self-assembled polymers are used for tissue engineering applications. The concept of self-healing from molecular structuring to planetary arrangements was discussed elaborately by Whitesides and Grzybowski [21]. They also defined the self-assembly process as 'a reversible association of distinct entities out of a disordered system that can be controlled by the rational design of those entities'. This order out of chaos concept is the emergent property of nature, includes a lot of environmental factors, and the reductionistic simplicity fails here, except in mimetic the concepts.

To understand the importance of suggesting a self-assembled structure for tissue engineering application, first, we need to understand some of the concepts of bone and healing mechanism [22, 23]. Briefly, when a bone underwent a heavy fracture, the sharp ends of the fractured bones will also tear muscles and blood vessels in the affected region. Within a moment, that region is surrounded with blood and that induces blood clot, fibrinogenesis and muscular debris within followed by swelling in the region. At the region of the fracture site and in the surrounding regions, all

structural and functional processes will flow for repair. A small region of muscle in the region within a period change their structure and function similar to cartilage to accomplish the common task. Later, this soft cartilage transforms into strong osseous tissue, and the damaged muscles and blood vessels will heal simultaneously with the association of the number of chemicals, nervous, circulatory and structural phenomena. Instead, the process of bones adapts to their dynamic mechanical surroundings over the time period [24]. and potentially leading to a predictable relationship between structure and function, as described by 'Wolff's law' [25, 26], where this law mostly deals with the direction of the principal stresses and the phenomena occur through 'self-regulating' reaction mechanisms in response to mechanical forces acting upon bone tissues.

As we know, the skin is the largest organ in the body that consist of superposed sheets of flat cells (i.e. the epithelial cells). These cells lie on soft and elastic connective tissue layers having small blood vessels. When a small region of the skin is exposed, the bottom of the wound is identified with fatty tissue and muscles. After 3–4 days, the damaged surface becomes smooth, glistening and red, because of the contraction of new tissue covering the wound site. Simultaneously, the skin cells start gliding over the red surface as a white fringe. Moreover, they cover its entire surface area, resulting in the formation of a definitive scar. This scar is due to the participation of two tissue types: (1) the connective tissue that fills the wound, and (2) the epithelial cells that proceed over its surface from the boundary. Connective tissue is responsible for the wound contraction and epithelial tissues for the membrane that ultimately covers it. The rate of healing (i.e. Cicatrization) in the superficial wounds can be measured by Lecomte du Nouy's formulas. Notably, they have formulated the cicatrization index (i) as the ratio between the rate expressed in function of the total area with the square root of the age of the wound [27–29]. If one of the regenerating mechanisms fails, it is replaced by the other. The result alone is invariable. Similarly, in the tissue engineering process, the healing process between the supporting biomaterials and the new tissue formation needs to compensate each other. Biological tissues have repairing or regenerative ability in response to their minor damage or injury [30]. Inspired by this, various self-healing materials based on natural polymers have widely been fabricated [31]. The incorporation of self-healing properties into material development has not only extended the shelf-life of materials but has also decreased the utilization of limited natural resources.

3 Self-healing Supramolecular Hydrogels

A 3D polymeric network composed of natural or synthetic polymers containing high water amounts with a high degree of flexibility is called hydrogel [32, 33]. Hydrogels have characteristics properties that include defined functionality, reversibility, stabilizability and biocompatibility that fulfill the need of both material and biological requirements during tissue regeneration [34, 35]. Hydrogels can be classified based on their sources, method of preparation, nature of swelling, nature of the

crosslinking process, rate of biodegradation, etc. Most of the hydrogel synthesis methodologies were achieved by physical processes that include hydrophobic association, hydrogen bonding, aggregation or complexion of polymer chains and crystallization [36]. On the other hand, hydrogels can also prepared by a chemical process that involves chemical covalent crosslinking [37]. A dual-network hydrogel is formed through electrostatic interaction achieved by combining the aforementioned physically and chemically crosslinked hydrogels [38]. This type of dual network with the aid of nanomaterials was recently shown to have self-healing properties with superior mechanical properties [39].

With the advent of self-healing hydrogels, in addition to fulfilling the needs of the biomaterials, we can also achieve quick recovery and after injury. These self-healing hydrogels as biomaterials for tissue engineering applications with high biocompatibility and biodegradability, under specific circumstances can lead to the rapid autonomous reconfiguration of the network, concerning the in vivo conditions [40–42]. As the production of self-healing polymer hydrogels is often mediated by diverse bonding, the initiation of a crack in a material through a break in covalent or non-covalent bonds can be reformed. Other than suggesting self-healing materials for biomedical applications, it is widely suggested to make electronic components, i.e. plastic transistors and photovoltaics [43–45]. The large-scale load-bearing materials as self-healing materials have been prepared by composite preparation of adding microcapsules or microvascular networks filled with self-healing hydrogels incorporated into base materials as composites [46]. During damages, the gels will be released in situ and the repair process will be done, this also prevents further damage to the material.

The chemistry of self-healing polymerization can be understood from the concept of supramolecular chemistry. Where the non-covalent bonding and its dynamic concept were involved, which gave birth to the idea of self-healing materials. The non-covalent interactions in the supramolecular self-healing polymers can be realized through various binding mechanisms and designed by altering the important parameters such as [47]

K_{eq}—equilibrium association constants,

K_a—the rate of association,

k_d—the rate of dissociation,

c—concentration of the functionality and binding dynamics.

The degree of polymerization (DP) can be determined from the strength of the end group interaction in the polymer chain, and it is also absolutely governed by the association constant (Ka) and the concentration of the monomer(s) (Fig. 1) [48]. In general, the equilibrium constant directly affects the degree of association of the supramolecular compound. There is a complex interplay between each of these parameters within dynamically crosslinked polymeric hydrogels, in addition to more traditional parameters such as molecular weight of the polymer, the concentration of the polymer, and the crosslink density, [49]. Even, on considering the general type

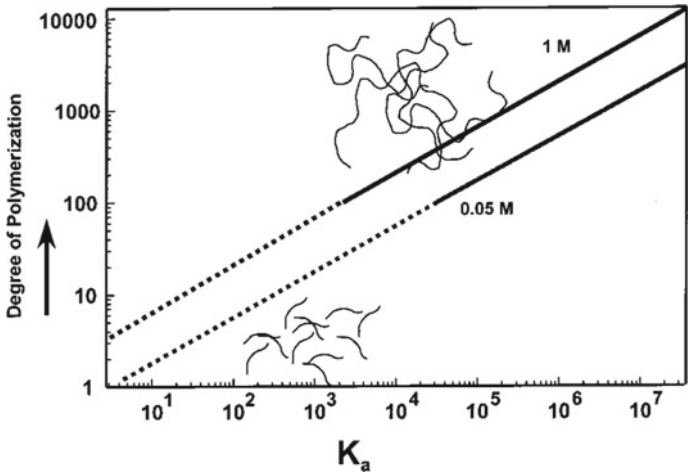

Fig. 1 Plot representing the theoretical relationship between the rate of the dissociation constant (Ka) and Degree of polymerization (DP) [48]

of interaction (e.g. hydrogen bonding), each of these specific parameters must be considered to develop a system by taking full advantage of the specific non-covalent interactions used.

4 Self-assembled Hydrogels for Tissue Engineering and Drug Delivery Applications

The research on tissue engineering carries considerable assurance for the restoration and regeneration of the damaged or disease tissues. The advancement in developing tissue engineering scaffolds is always a learning process as a subject of great attraction in the biomedical area [50]. As the synthetic materials always aimed to mimetic the native tissue functionality, it is hard to achieve due to the complexity of the latter [51]. Hydrogels have shown promising tissue regenerative potentialities due to their biocompatibility and similarities to the native extracellular matrix. The essential notable qualities noted to the design hydrogel scaffold, include swelling ratio, mimicking native tissue mechanical property, degradation, and diffusion [52]. These properties are closely related to the crosslinked hydrogel structure, which is controlled through various suitable processing conditions and hybrid structuring [53]. Out of the desired properties, the main lacuna in hydrogels is its inadequate mechanical and porosity properties. And hence the hydrogel scaffolds with remarkable mechanical performance and self-healing capability affords a favourable aid to repair load-bearing tissues beneath a dynamic 3D microenvironment [54]. A work on poly(L-glutamic acid) (PLGA)-based hydrogels with appropriate toughness and self-healing capability have been fabricated by filling soft self-healing hydrogels

right into a hard porous hydrogel skeleton [55]. Type of composite hydrogels could be a favourable biomaterial for the restoration of load-bearing tissues. Recently oxidized alginate-based hydrogels have drawn significant interest as biodegradable materials for tissue engineering applications. This type of oxidized alginate hydrogels possesses a faster degradation rate, as it consists of more reactive groups as compared to native alginate [56].

Compare to dry scaffolds, the hydrogels have the possibility of encapsulating cells in biodegradable hydrogels. This gives numerous attractive functions for tissue engineering, which include ease of compatibility of cells to grow in a tissue-like environment and the potential to quick acceptance of the in vivo tissue [57]. Self-healing supramolecular hydrogels have emerged as a novel elegance of biomaterials that integrate hydrogels with supramolecular chemistry to increase incredibly functional biomaterials with advantages including native tissue mimicry, biocompatibility and injectability. These properties are endowed through the reversibly crosslinked polymer network of the hydrogel. Even though, these hydrogels have excellent capability, as the concept is new a lot of regulations needs to be tested and hence it is yet to be available for clinically translated tissue engineering treatments [58]. The family of the supramolecular hydrogels that comply with the dynamic nature constituents includes supramolecular bonding motifs that depend on hydrogen bonding, electrostatic interactions, π–π bonding, host–guest interactions, hydrophobic interactions or metal coordination act as dynamic crosslinks among hydrophilic polymers to shape memory hydrogels. The form of supramolecular building blocks opens the possibility for the development of a numerous variety of biomaterials that provide promise as scaffolds for tissue engineering. Moreover, depending on the target tissue, the self-healing hydrogels are predicted to comply with an extensive variety of properties which include electric, biological and mechanical. Notably, the incorporation of nanomaterials into double-network hydrogels is showing excellent promise as a possible way to generate self-healable hydrogels with the above-stated attributes.

In addition to the support and regeneration essential properties of the tissue engineering scaffolds, the in situ drug deliverable property is also expected [59]. To achieve this, the deliberately engineered self-assemble peptides that can represent diverse supramolecular nanostructures for target-specific drug delivery have been developed. For this, the bottom-up approach is successfully employed widely to carry amphiphilic drugs with high loading, low leakage and high permeability via bio-membranes into the target cells [60]. Furthermore, the stimuli-sensitive property of self-assemble scaffolds allows the controllable release of the therapeutics. The characteristic of peptide hydrogels can easily be modified through the attachment of chemical or bioactive motifs to immobilize drug molecules via physical or covalent interactions. Also, the therapeutic release can be adjusted through the mesh size and network degradation. The injectable hydrogel promotes macrophage infiltration and polarization through macrophage-material interactions without generating a proinflammatory environment. These self-assembled peptide hydrogels have been applied to transfer brain, cardiovascular, bone, and anticancer drugs for a sustained releasing condition [61].

For tissue engineering biocompatible assessment, in vitro two-dimensional culture is the broadly used procedure for drug screening and disease modelling before animal tests. However, the cells grown on flat and difficult plastic surfaces cannot reflect the important characteristics of the proliferation because of lacking to mimic the complex and dynamic cell-cellular communications in addition to cell–matrix interactions. Rather, 3D cultures have been advanced to recapitulate the features in the in vivo microenvironment. The biomimetic 3D models offer spatial intensity in addition to cell connectivity and hence have a better in vivo physiology for drug screening and disease modelling. In the fabrication of hydrogels-based 3D tissue engineering support, 3D bioprinting is a potential technology for its capability to create a 3D assemble at a shorter time [62]. Also, the 3D assemblies prepared by the hydrogels can have the possibility of comprising more than one cell type and bioactive moieties with a unique distribution. As this field of research is new, there is a lack of suitable bioinks that constrains the improvement of bioprinting. The concept of supramolecular self-assembled polymer hydrogels based bio-inks and its fabricated 3D assemblies is expected to show substantial efficiency for accumulating remarkable biocompatibility, biodegradability, self-healing, stimuli-sensitive gelation, and shape memory properties collectively.

5 Supramolecular Chemistry

Supramolecular polymeric hydrogels can be achieved both by covalent and non-covalent interaction. However, the self-healing polymers have more relied on non-covalent interaction and hence the latter will be discussed in detail in subsequent sections. In this chapter, non-covalent method of supramolecular self-healing polymer preparation accomplished by H-bonding, metal–ligand coordination, ionic host–guest complexation, and electrostatic interactions will be discussed. The bonding mechanism involved in the supramolecular polymers disused in this chapter is given in Fig. 2.

5.1 Hydrogen Bonding

Hydrogen bonding mechanism is the most common driving force for the self-assembly of supramolecules. Especially, this method of bonding is prime in a lot of important biological and synthetic supramolecular systems. Biological tissue is not only capable of successful self-restore of the damaged tissue but is also very difficult and resilient. The ‘secrets’ of some biological mechano-responsive strategies that enhance biomaterials have recently been unveiled. However, such insight remains undiscovered or undeveloped for man-made self-healing materials. A prominent example is the stiffness of the channelled whelk. The egg-capsule wall of a channelled whelk effectively absorbs shock with a high degree of reversible extensibility

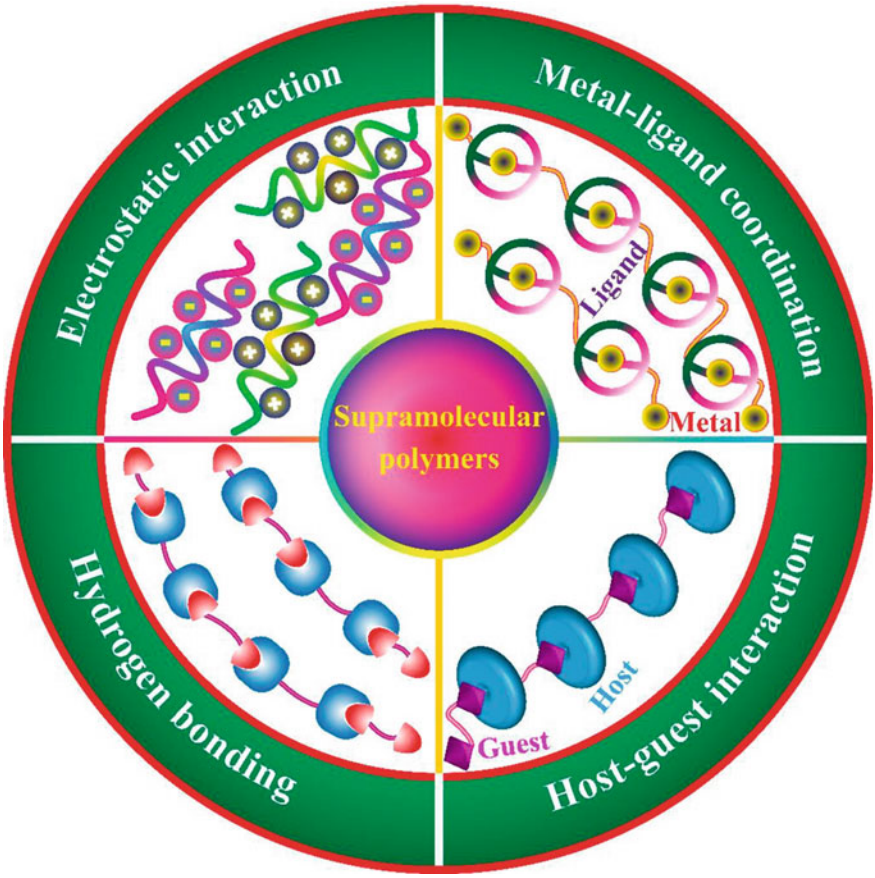

Fig. 2 Self-healing supramolecular bonding mechanism between polymers and polymer hybrids for tissue engineering applications

and stiffness. The structure segments proteins, undergo reversible α-helix to β-sheet structural transitions with internal-electricity modifications when loaded. After the removal of stress, energy relaxation consequences in the healing of the structure. As another example, the toughening and shape memory of spider silk is the result of the organization and the density of the intermolecular hydrogen bonds in silk crystals that are adjusted through the spinning rate from the spider's secretion gland [63].

The inspiring example for hydrogen bonding in nature is the evolution of DNA and RNA and its formation into the three-dimensional assembly, where the process also involves directionality and specificity in assembling the nucleotides through hydrogen bonding in association with π–π stacking. Due to this similar type of numbers bonding in a biological system, conventionally supramolecular were named by the term, "living polymers". The hydrogen bonding in supramolecules shows liquid crystallinity and is hence mentioned as a liquid crystalline polymer (LCP).

Even though hydrogen bonding is relatively weak bonds with energy in the range of 10^{-65} kJ mol^{-1} because of their novel directionality and specificity in boding, added with ease of design and synthesis capabilities to accept or donate or both multiple hydrogen (H) bonds simultaneously, it is greatly explored in numerous applications. Lehn and his group were the first people to develop a supramolecular main-chain polymer through triple hydrogen bonding. A notable work contribution was given by Cates and his group on developing physical models for understanding the relationship between rheological parameters information of the supramolecular. As with single H-bonds, the strength of the emerged interactions is affected by various factors: (a) the nature of the donors and acceptors (i.e. rate of association, nature of organic functional group bonding), (b) the choice of solvent and (c) the configuration of the donor(D)–acceptor(A) sites (e.g. arrays of DDD-AAA has a maximum number of secondary interactions compare to ADA-DAD arrays, similarly, arrays of DAAD vs. DADA provide differing binding strengths through secondary interactions opens the possibility of tautomerization).). A bottom-up approach for the development of bioactive mesh made by electrospinning method using hydrogen-bonded supramolecular polymers combined with ECM-peptides shows a promising application for supporting living renal membranes [64].

Earlier reports on the self-healing supramolecular hydrogels prepared by hydrogen bonding with in vivo evidence of tissue engineering applications are given in Table 1.

Self-healing hydrogels with N-carboxyethyl chitosan (CEC) and oxidized sodium alginate (OSA) for the treatment of neurological diseases can create the aid of floating live cells suspension in the hydrogel precursors are it can also be injected into the target site simultaneously. The reaction mechanism for the preparation of the hydrogels by Schiff base reaction and the procedure of insertion of the transparent gels loaded with cells to the lesion cavity is depicted in Fig. 3. A composite structure of cytosine (C) and guanosine (G) modified hyaluronic acid (HA) by hydrogen bonding shows good self-healing properties and has also shown pH-sensitive responses suggested for tissue engineering applications [65]. Self-adhesive gels in an aqueous medium prepared by gelatin methacrylate (GelMA) contributes to the possibility of sutureless skin and stomach after surgery [66]. Polyurethane elastomers prepared with multiple hydrogen bonds show good shape recovery property and with the incorporation of phosphorous in polyurethanes there occurs an increase in the mechanical property of the hydrogels [67]. The antibacterial need of the tissue engineering gels was also be rectified by incorporating suitable antibacterial element with the gels, that does not alter the polymerization of the hydrogels. Studies on zinc ions incorporated carboxymethyl chitosan (CMCh) hydrogels validate it as a potential candidate for antibacterial self-healing supramolecular gels [68].

5.2 Metal–Ligand Coordination Complexation

The formation of metal–ligand coordination complexes is constructively achieved if polymer chains can form effective coordination bonds with metal ions. The metal

Table 1 Self-healing hydrogels prepared by Hydrogen bonding interaction for tissue engineering applications

S. no	Polymers	Force	Elongation	Healing efficacy	Load	Application	Refs.
1	CMCh-Zn hydrogels	0.1–100 rad/s		0.1–200%	~110000 Pa	Antibacterial activity	[69]
2	Polysaccharide	0.1 rad/s		1600 s	100–1000 Pa	Neural stem cells	[69]
3	HA-HMDA-C, HA-HMDA-G, and HA-HMDA-C/G hydrogels	1–100 rad/s		–	10 Pa	Suggested for pH-sensitive tissue engineering scaffold	[65]
4	Glycogen	–	1420%	97%	1.12 MPa	Gly-sensor	[70]
5	Gelatin methacrylate	1–100 rad/s		90%	3.2 Pa–4.6 MPa	In vivo wound healing, in vitro cell viability	[66]
6	polyurethane elastomer		702%	91.8%	37.11 MPa	Suggested for self-healing tissue engineering applications	[71]

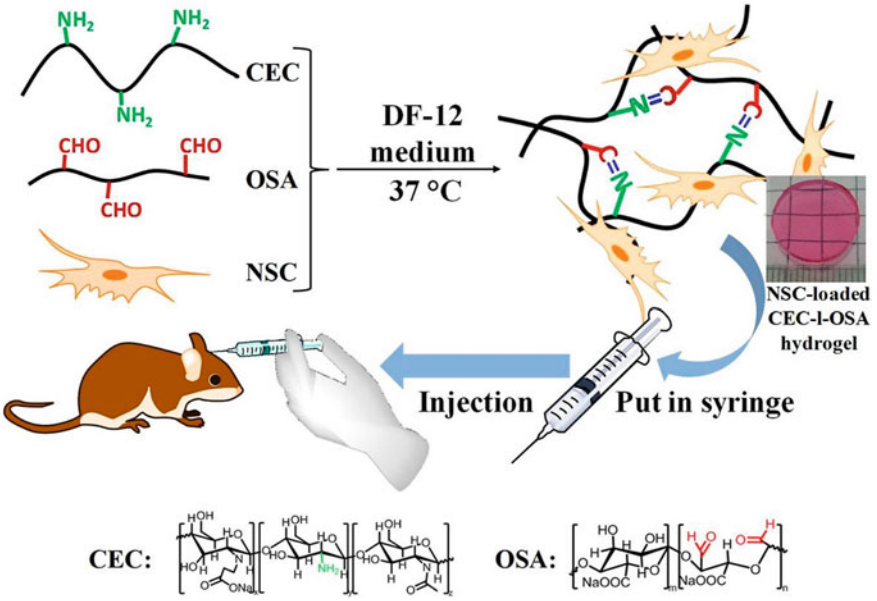

Fig. 3 Self-healing hydrogels prepared using CEC-l-OSA for treatment of neurological diseases [69]

coordinates help to form one-dimensional structure from supramolecular polymers. Because of its complex dynamic properties, it is widely used in developing self-healable materials. The preparation of metal–ligand complexation can be tuned to adopt both in aqueous as well as organic media. In the mechanism of non-covalent bonding, based on the choice of several ligands, bonding can form between polymer electron pairs to the outer empty orbits of the metal ions. Some of the metal–ligand coordination with lesser dynamic properties such as Ru (II) based complexes is also possible and used similarly as covalent bond like polymer applications. This type of bonding was also used as UV treated structural modifiable polymers and used as biocompatible resigns. Nature-inspired mechanically enhanced self-healing materials were widely explored by metal-ligand coordination complexation. Medical adhesives, applied to wet tissue bonding were prepared by self-healing hydrogel using metal–ligand coordinates, where the process is inspired by understanding the chemistry of aquatic mussels. A detailed review by Balkenende et al. emphasizes various methods of preparing medical adhesives inspired by marine animals [68]. Also, the review by Janarthanan et al. elaborates the metal–ligand supramolecular hydrogels for tissue engineering and biomedical applications [67]. Notable work on nature-inspired functionalized PEG-based hydrogels as sealants for amniotic sac was reported by Messersmith and his group at the University Hospital Zurich. In mussels, the strong bonding is mediated by a high concentration of 3,4-dihydroxypheny-l-alanine (DOPA) as explained by Waite et al. in 1981. In synthetic adhesive materials, Fe^{3+} were added with DOPA, which creates coordination bonds between them and

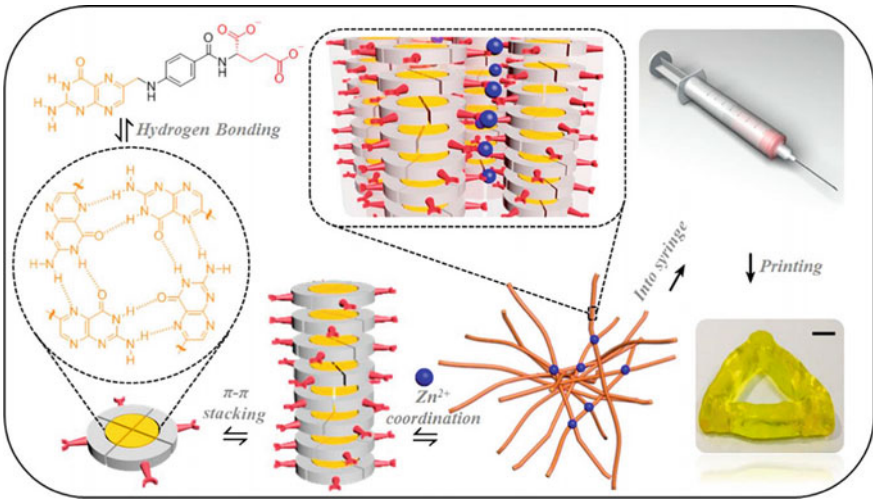

Fig. 4 Preparation schema of the metal(Zn+)/folate biopolymer, which can be printable to desire structure [81].

enhances the touchiness property. Other than Fe, the most common metal ions used for metal–ligand coordinated supramolecular systems are Mn, Fe, Ru, Os, Co, Ir, Ni, Pt, Cu, Ag, Zn, Cd and Hg. The choice of the metal ions was being used at a low oxidation state to maintain the stability of the supramolecular system (Fig. 4).

Self-healing hydrogels prepared by metal–ligand coordination possess a modifiable rheological property by varying the Equilibrium constants (Keq) various metal–ligand coordination bonds. A detailed review of various equilibrium constants for metal ligands is given in the review by Shi et al. [72]. The hydrogels prepared using Ni (II) and imidazole—polyaspartamide units, evidences the self-healing behaviour with good adhesion property even under wet surface conditions [73]. The self-healing property of metal–ligand hydrogels can be modifiable under ultrasound-mediated conditions, which can induce needed chemical alteration in the in vivo aqueous condition [74]. The ligand molecule can also be used from natural polymers such as silk fibroin, hybrid with calcium phosphate compounds for bone tissue engineering applications. The self-healing hydrogel for bone regeneration prepared using calcium phosphate (CaP) and mSF (CaP@mSF) hybrid with biopolymer binder (Am-HA-BP) to form a composite Am-HA-BP·CaP@mSF hydrogel has the capability for bone regeneration and hence curing rat cranial critical defect [75]. A sequential hybrid structuring of metal–ligand and π−π stacking can be developed as a robust injectable and printable gel, using which various three-dimensional structures can be structured (Fig. 3). In this type of supramolecular hydrogels, with the addition of suitable metal ions, it can be modifiable as pH-responsive shape memory structuring and for antibacterial applications [76]. Some of the other potential applications of this metal–ligand supramolecules for therapy and diagnosis applications is elaborated by Zhang et al., in which in the nanoparticles hybrid this type of supramolecular

Table 2 Self-healing hydrogels prepared by metal–ligand coordinates for tissue engineering applications

S. no	Polymers	Force	Load	Application	Refs.
1	CS-Ca2 + /PAA and CS-Ca2 + /PAA-Fe3 + DN hydrogels	12.2 MPa and 1292%,	1.65–1.54 Mpa	Anti-fatigue	[78]
2	Elastomeric vitrimers	–	–	Supramechanical robustness and retentive malleability	[79]
3	SN and DN hydrogels	–	–	Biomedical applications	[80]
4	[PEG-Dopa]4	–	1030-45 Pa	Drug delivery	[74]
5	Hierarchical folate/zinc supramolecular hydrogels	–	–	Printable biomaterials and bioengineering applications	[81]
6	Silk-fibroin-based Hydrogel	–	–	Bone regeneration applications	[75]
7	PHEA-his-metal coordination gel	–	–	Biomedical applications and antibacterial activity	[82]
8	HA-BP and Ag + ions hydrogel	–	–	Regenerative wound treatment	[83]
9	PHEA-API gels	–	–	Biomedical and drug delivery applications	[84]
10	Agar/CMC–metal ions DN gels	–	–	Soft electronic based biosensing applications	[76]

were also explored [77]. Some of the earlier reports on the self-healing supramolecular hydrogels prepared by metal–ligand bonding with in vivo evidence of tissue engineering applications are given in Table 2.

5.3 Electrostatic Interaction

Electrostatic interactions of supramolecular comprise attractive or repulsive interactions between charged molecules. Mostly, electrostatic interactions are combined with other interactions for material repair. Hydrogels prepared by electrostatic interactions display the ability of strong and multivalent non-covalent interactions to form extremely strong or stimuli-sensitive materials. Most of the electrostatic interactions

in supramolecular were obtained by polyelectrolytes and results in phase separation. However, the incorporation of a neutral hydrophilic block to the polyelectrolyte chain results in the formation of a hydrogel. There is only a limited number of self-healing polymers were explored by electrostatic interaction, due to the less reversibility and dynamic properties. Wei and his group reported on the development of self-healing hydrogels by electrostatic interactions using poly (acrylic acid) (pAA) polymer as the backbone with free iron ions. This process was, however, similar to metal–ligand interaction and an increase in Fe^{3+} concentration improves the self-healing efficiency. Self-healing hydrogels based on short peptides forms ordered nanostructures in an aqueous medium can be obtained by electrostatic interaction mediated self-assembled systems. This array of peptide interactions arrangement is depending on the amino acid sequencing, which can also form stable β-strand or β-sheet structures that can lead to self-assembled hydrogel scaffolds.

3D printable self-healing scaffolds for cartilage repair and regeneration were achieved by a combination of silica/poly-tetrahydrofuran/poly-ε-caprolactone hybrids, which can also mimic the mechanical property of the articular cartilage. In addition to the self-healing property, poly (N,N-dimethylaminoethyl methacrylate) (PDMAEMA) and poly(itaconic anhydride-co-3,9- divinyl-2,4,8,10-tetraoxaspiro[5.5] undecane) (PITAU) based hydrogels prepared by electrostatic interactions possess the capability of in situ drug delivery applications [85]. Some of the natural polymers and natural inspired polymer structures such as cellulose [86]-, chitosan [87, 88]- and collagen [89]-based hydrogels also show promising application as self-healing tissue engineering applications during hybrid structuring with additional molecules. A combination of two natural polymers, i.e. oxidized konjac glucomannan with chitosan shows good antibacterial and adhesion properties with excellent biocompatibility (Fig. 5). These hydrogels were also showing shortened wound healing time and could significantly accelerate the re-epithelialization of damaged tissues [90]. Some of the earlier reports on the self-healing supramolecular hydrogels prepared by electrostatic interactions with in vivo evidence of tissue engineering applications are given in Table 3.

5.4 Host–Guest Interactions

Next to hydrogen bonding, host–guest interaction is widely explored for supramolecular hydrogel preparation due to its dynamic properties. In host–guest interaction, the binding affinity, specificity and molecular recognition are mediated by complementary shapes and hence highly suitable for designing self-healing materials. The 'host' molecule typically has external characteristics that interact with the solvent and internal characteristics that promote binding of a 'guest' via either a specific shape or a favourable circumstance. Several macrocyclic compounds (e.g. crown ethers, cucurbit[n]urils, calix[n]arenes, pillar[n]arenes and cyclodextrins (CDs)) have been applied as host molecules for host–guest interactions to prepare self-healing materials. In these interactions, a stronger binding occurs between a hydrophobic guest

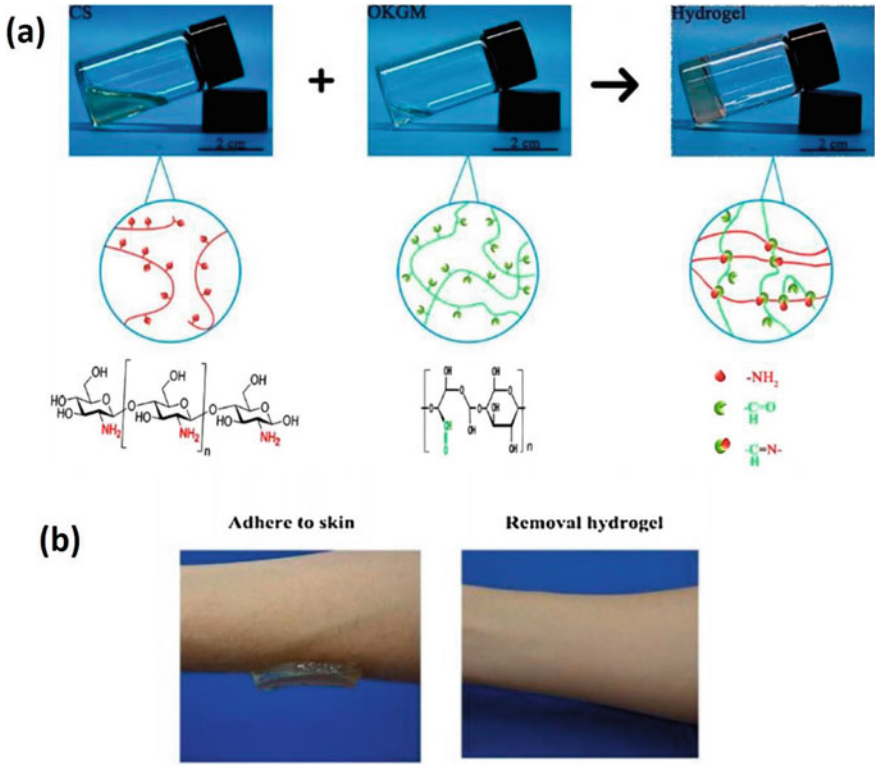

Fig. 5 **a** Schematic representation of the synthesis of self-healing hydrogel from natural polymers chitosan(cs) with oxidized konjac glucomannan (OKGM). **b** Pictorial representation of Image of adherence of hydrogel to the skin surface [90]

sequestered into the hydrophobic inner cavity of a host, such as cyclodextrins (a-, b- and g-CD) or cucurbit[n]urils (CB[n], n = 5–8 and 10), in water through favourable solvophobic interactions. The inclusion of complex formation changes the physical and chemical properties of the guest molecule and generally exhibits improved water solubility. Scherman and co-workers reported in 2010 the first example of a supramolecular polymeric hydrogel based on CB[n] host–guest inclusion complexes. Owing to their low price, good availability and the ability to form the inclusion complexes with high water solubility, CDs have been demonstrated to be highly useful compounds in broad areas, such as analytical science, pharmacy, improved separation techniques, catalysis, food, textile and cosmetic industries. On the other hand, Cucurbit[n]urils (CB[n], n = 5–8, 10), named after the genus Cucurbita (genus in the gourd family Cucurbitaceae) due to its structural resemblance, are macrocyclic oligomers composed of repeating units of glycoluril (monomer) by having the hydrophobic cavity and the polar carbonyl groups surrounding the portals. Several concerted intermolecular interactions promote the binding of guests by CB[n]s [96].

Table 3 Self-healing hydrogels prepared by electrostatic interaction for tissue engineering applications

S. no	Polymers	Force	Healing efficacy	Load	Application	Refs.
1	Dextran 1. HD/LAP-5 2. HD/LAP-1 3. HD	–	–	8 kPa 2.3 kPa 1.9lPa	New bone regeneration and mineralization	[91]
2	SiO_2/PTHF/PCL-diCOOH		5 s	Pre-142 kPa and post-113 kPa	Cartilage regeneration	[92]
3	Cordycepin/chitosan	1 rad/s	–	–	Wound healing	[93]
4	Collagen	1 Hz	–	–	Wound healing	[89]
5	Sequential-IPN gels	5 rad/s	30 s Resotring-60 s	5 Pa and 3000 Pa	in vivo biocompatibility and in vivo somatic antinociception	[85]
6	Hydroxyethyl cellulose	1.25 MPa	92.64% in stress and 88.23% in strain	23 MPa-32 MPa	Conductivity measurement	[86]
7	Xanthan and chitosan	0.1–100 rad/s	1–180%, 330% and 800%		Abdominal wall defect model and drug release	[88]
8	CS-OKGM hydrogels	10 rad/s	300% with 30 min	35 Pa	Antibacterial, wound closure and histological studies	[90]
9	SHZPU compound		60% and 100 min		Shape memory	[88]
10	CNCs@P4VP		85.9% in 6 h	6.6 MPa		[94]
11	Chitosam/GO		900%		Biocompatibility, cell proliferation and viability study	[95]

A detailed review of the host–guest supramolecular polymers for biomedical application is given by Bai et al. [97] and Jing et al. [98]. Recently, self-healing macrocyclic host–guest materials using elastomer approach has comparable or even higher mechanical properties with other supramolecular self-healing materials were widely explored due to the flexible bonding between host and guest molecules. These kinds of polymers were highly suitable for 3D printing to create a defined structure with high surface reactive functional properties. A detailed review by Pramod et al. on bioprinting of hydrogel for various soft and hard tissue engineering applications [99].

With the aid of host–guest interaction excellent biocompatibility and enhanced mechanical property can be achieved by UV-initiated polymerization (Fig. 6), in the presence of host (isocyanatoethyl acrylate modified b-cyclodextrin) and guest (2-(2-(2-(2-(adamantyl-1-oxy)ethoxy)ethoxy)ethoxy)ethanol acrylate) to form "three-arm" shows its possibility towards soft-tissue engineering applications [100]. A host–guest reaction between β-cyclodextrin (CD) and adamantane (AD) on modified gelatin shows excellent cell delivery for stem-cell-based tissue engineering applications [101]. Through this type of interaction an even complex and extracellular matrix-like 3D electroactive matrix can be achieved, in which cyclodextrin-adamantane acts as a host–guest module. The self-healing duration of this gelwas also quick within the 60 s. A modification of this base structure as 3,4-ethylene dioxythiophene: adamantyl-modified sulfated alginate /poly-β-cyclodextrin (PEDOT:S-Alg-Ad/Pβ-CD) hydrogels shows good mechanical and electrical properties [102]. Similarly, an electroactive degradable bio elastomer by the micropatterning method using poly (glycerol sebacate) (PGS) copolymerized with aniline trimer (AT) promotes cellular elongation and is suggested for cardiac tissue engineering applications [103]. Some of the earlier reports on the self-healing supramolecular hydrogels prepared by host–guest interaction with in vivo evidence of tissue engineering applications are given in Table 4.

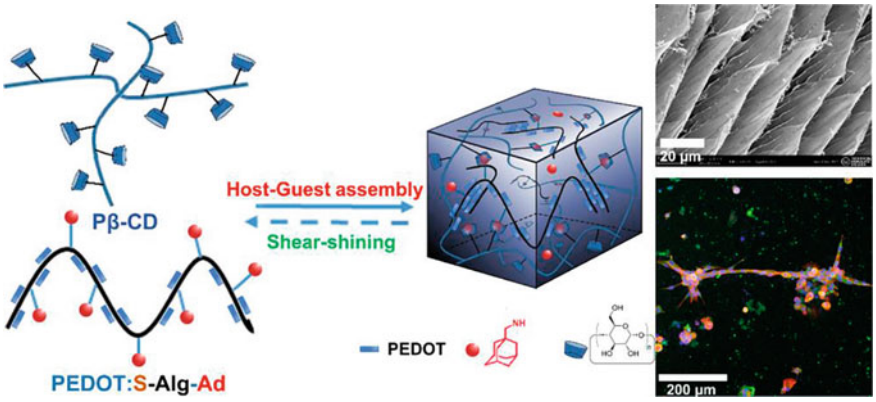

Fig. 6 Schematic representation on the reaction bonding mechanism of the host–guest supramolecular conductive hydrogel formed using that can mimic three-dimensional extracellular matrix-like structuring for tissue engineering applications [102]

Table 4 Self-healing hydrogels prepared by electrostatic interaction for tissue engineering applications

S. no vb	Polymers	Force	Elongation	Healing Efficacy	Load	Application	Refs.
1	Poly (glycerol sebacate)-aniline trimer elastomer			150%	2.4 MPa	Cardiac tissue engineering	[103]
2	PEDOT:S-Alg-Ad/Pβ-CD hydrogel		1%	1 min		3D cell culture	[102]
3	Gelatin hydrogels	10 rad/s	400%	~5 min	~400 and ~10 Pa	Localized therapeutic cell delivery	[101]
4	Poly (L-glutamic acid)		0-30%	80%	0.51 MPa	Load-bearing tissues	[55]

6 π–π Interactions

The words 'π–π stacking' or, more commonly, 'π–π interactions' are also used when unsaturated organic groups are engaged in non-covalent interactions. To date, no readily available or intuitive model has been proposed. π–π stacking is a phenomenon for larger structures except for some improvement in understanding the basic principles [104]. When extended structures are built out of building blocks with aromatic moieties, they may create self-assembly or molecular recognition processes. Therefore, from massive biological structures to comparatively small molecules, π–π interactions differ [105]. In a greater number of chemical, physical and biological processes, non-covalent interactions involving π schemes are vital. In the case of proteins, the function of aromatic π interactions is evident, considering that in their side chains there are plenty of amino acids arrangements with the aromatic ring structure. In particular, interactions influencing the protein's structure and function, these aromatic side chains may be involved and behaving in a way unique to aliphatic amino acids. These phenomena also regulate the vertical base–base interactions that balance DNA's double-helical structure, the intercalation of drugs into DNA, and the crystal packing of aromatic molecules. The more notable contribution next to DNA structuring is the assembly of tertiary protein structures, which includes polyaromatic macrocycle conformation preferences based on binding properties, functionalization in many host–guest systems, and porphyrin aggregations.

To understand the mechanism of the π–π interaction, a basic electrostatic model that considers several of the experimental results to represent the energy of the interaction between two molecules is given as

$$\mathbf{E_{total}} = \mathbf{E_{electrostatic}} + \mathbf{E_{induction}} + \mathbf{E_{dispersion}} + \mathbf{E_{repulsion}}$$

The main contributions to the energy of interaction come from the factors of electrostatic and van der Waals, induction being a second-order concept generally. Where this term is often desirable for interplanar separations of interest (greater than 3.4 Å). The interaction of van der Waals between molecules of the kind is approximately proportional to the region of π overlap. The π–π interactions between two aromatic entities can be roughly categorized into three groups based on geometry: edge-to-face T-shape, parallel displacement, and parallel co-facial stacking. Edge-to-face T-shaped geometry is favoured by the thin, unsubstituted aromatic compounds, while substituted and large multi-ring aromatic compounds favour parallel displaced geometry. It is very unusual to find co-facial parallel layered geometry [106]. In the arrangement of aromatic rings, a stacked arrangement will usually be distinguished from an edge- or point-to-face, T-shaped conformation [106]. A C-H … π interaction is the T-shaped conformation. Stacking may not have to be a complete face-to-face atom alignment, but it could also be a slipped or offset bundle. In aromatic interactions, both face-to-face and T-shaped conformations are constraining modes. In each of these, as π–π interactions, the stacked arrangements are of special interest.

To clarify the nature of π–π interactions, a large number of theoretical and experimental experiments have been carried out. While there is substantial scientific proof on the structural property of these relationships that influence their character, their true existence is indeed a matter of some concern [105].

Figure 7 shows a basic model of a π-system; it comprises a positively charged σ-framework sandwiched between two π-electron clouds that are negatively charged [107]. Currently, the interaction between two such π systems (i.e. an enticing interaction) is counter-intuitive since the repulsion of the two nearest approaching ~ clouds would be the dominant interaction. The σ-electrons must be viewed separately from the framework when the separation of the two π-systems is equal to their thickness [108].

A much more understanding can be obtained from the earlier computation results of the π–π complex stacked systems [109]. For π–π complexes, a displacement layered configuration matching the structure of the multiple layers in graphite is the most favourable relative orientation. The most favourable configuration of σ–π dimers is the same arrangement, while the most favourable geometry in the case of aliphatic σ–σ dimers is the fully stacked one, with one molecule only on top of another. As the size of the system grows, the key factor favouring the durability of aromatic dimers over aliphatic ones is linked to the existence of the aromatic structures. Changes in molecular properties as the aromatic system expand due to greater electron delocalization contribute to an increase in the contribution of dispersion to stability, which is absent in aliphatic dimers. Moreover, in π–π dimers linked to the softening of the repulsive wall, additional stability is found that enables shorter intermolecular distances. Compared to complexes containing aliphatic species, the combination of these two effects makes π–π dimers more and more stable as the system size increases [110].

In terms of a quadruple moment with partial negative electrostatic potential above both the aromatic faces and a partial positive electrostatic potential for the benzene form of molecules around the periphery, Sanders and Hunters have clarified π–π interactions. They have already shown that two such quadruple moments in proximity

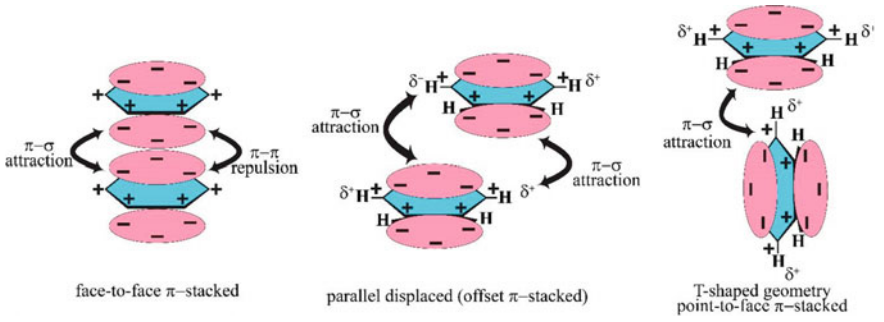

Fig. 7 Schematic illustration on the basic models of electrostatic attraction between σ framework and the π electron density by face-to-face π-stacked, parallel displaced and by T-typed geometry

can favour edge-to-face T-shaped or parallel displacement over co-facial geometry. If strong electron-donating groups are added to the aromatic ring (e.g. hexafluoro benzene), polarization happens in the opposite direction, resulting in a quadruple moment with a partial positive electrostatic potential above both the aromatic faces and a partial negative electrostatic potential along the periphery. Now, whenever one such aromatic electron-deficient ring gets next to an aromatic electron-rich ring, an electrostatic attraction takes place between the two opposite quadrupole moments, and the co-facial parallel stacked geometry is followed by the structures. In this type of assembly, due to lowering in the highest occupied molecular orbital (HOMO) (from the electron-rich aromatic compound)—Lowest unoccupied molecular orbital (LUMO) (from electron-deficient aromatic compound) distance, a charge transfer complex is sometimes formed. As Hunter and Sanders have stated, however, charge transfer is not the driving force for this complimentary stacking of π–π but is a consequence of this interaction.

Even though the field of π–π-stacking is old as five decades, the synthesis of supramolecular polymerization for biomedical application is limited. A work on romantic π–π-stacking between the π electron-deficient diimide groups and the π electron-rich pyrenyl units is consistent with an elastomeric, healable, supramolecular polymer mix containing a chain-folding polyimide and a telechelic polyurethane with pyrenyl end groups. More than 95% of the tensile modulus, 91% of the elongation to crack, and 77% of the hardness modulus of the pristine composite were reproducibly regained by a broken sample of this material [111]. Other than this, chain-folding co-polymers that contain π electron-deficient diimide units in the backbone are described in several recent papers. Spectroscopic and crystallographic studies of these polyimides and associated model compounds have shown that chain-folded conformations can be introduced to associate with π-electron-rich aromatic molecules, folded conformations that increase the number of complementary π–π stacking interactions. As a consequence of the thermo-reversibility of non-covalent interactions, a novel supramolecular polymer structure in which the terminal pyrenyl groups of a polyamide intercalate into the chain-folds of a polyimide through electronically-complementary π–π stacking shows both improved mechanical properties relative to those of its components and simple healing characteristics [112].

7 Bioinspired Systems Chemistry

Learning from nature on the self-organization and autonomous functioning of my mode of chemical interactions has opened the way to the new exploring field called ‘systems chemistry’. In this field of research, much focus is emphasized on the emergent properties of the formation of the complex systems from simple solutions and the mote of interactions between the molecules. As this topic of research is new, a lot more properties on creating synthetic polymerization through biomimetic approaches are being examined.

When observing nature, the structure and functionalities of the biological systems have precise control, which follows a temporal programme by utilizing a cascade of enzymes. To achieve a biomimetic material with similar properties like biological systems, more understanding is needed for the system chemist in the concepts of interconnection bonding, thermodynamics, photo interactions, etc. [113]. Specifically, for developing the higher complex supramolecular system, the concepts of bioinspired fuel-driven systematic enzyme reactions need to be targeted. In this, nature has employed much sensitivity, selectivity and specificity in the choice of interaction followed by its transient changes in each stage of life. The validation for this type of reaction can be found in microtubules. In which, the duration of the assembly of adenosine triphosphate (ATP) is controlled by the presence of guanosine triphosphate (GTP) as fuel [57]. Also in mitochondria, to maintain thermodynamic equilibrium for cell relaxation, the actin filaments utilize ATP and systematically the microtubules utilize GTP to control the independent variations in the formation and decay kinetics. Recently, integration in the synthetic systems under far-from-equilibrium conditions was developed to mimetic the individual characteristics of life that include, compartmentalization, replication and metabolism. However, the synthesis process is complicated with the requirement of advanced equipment needs that are limited to the small-scale structure. This concept in the future may be advanced in developing nano- or microscale self-synthesizing energy-efficient compounds that has the potential of regulating and repairing themselves [114].

The thermodynamic principles for supramolecules as proposed by George et al. are given in Fig. 8 [115]. The figure adopted here depends on the bioinspired living polymerization followed by aggregated at higher transient state concerning variation in Gibbs free energy. In the energy, the pathway has been distinct by four distinct thermodynamic states. Out of these states, three initial states were found in living supramolecular polymerization that includes non-dissipative kinetically trapped ($G >> K_BT$), non-dissipative metastable ($G \sim K_BT$) and thermodynamic equilibrium state. These states also can be represented as an activated molecule, kinetic dormmate state and thermodynamic assembled state in discussing bioinspired self-assemble structure. Above the equilibrium states, again there is an uphill in the energy level that results in dissipative polymerization structuring. Amongst the three states of living polymerization, the thermodynamic equilibrium energy level is the most stable state. And hence, for the development of supramolecular systems, often this thermodynamic equilibrium state is intended to achieve. However, in some polymerizations, this method of achieving polymerization resist reorganization with time and remains kinetically and thermodynamically stable [116]. In the recent past, the focus has shifted from the thermodynamic stable state to the development of non-dissipative kinetically trapped structures. Where the modifications were done through mass inputs and energy shifts towards non-dissipative states from the states of thermodynamic equilibrium. The controlled preparation modalities are difficult to achieve which involves complex pathways and non-uniform assemble rates. However, by a proper understanding of the kinetic models of the specific compound, the competing pathways can be modifiable in desired directions [117].

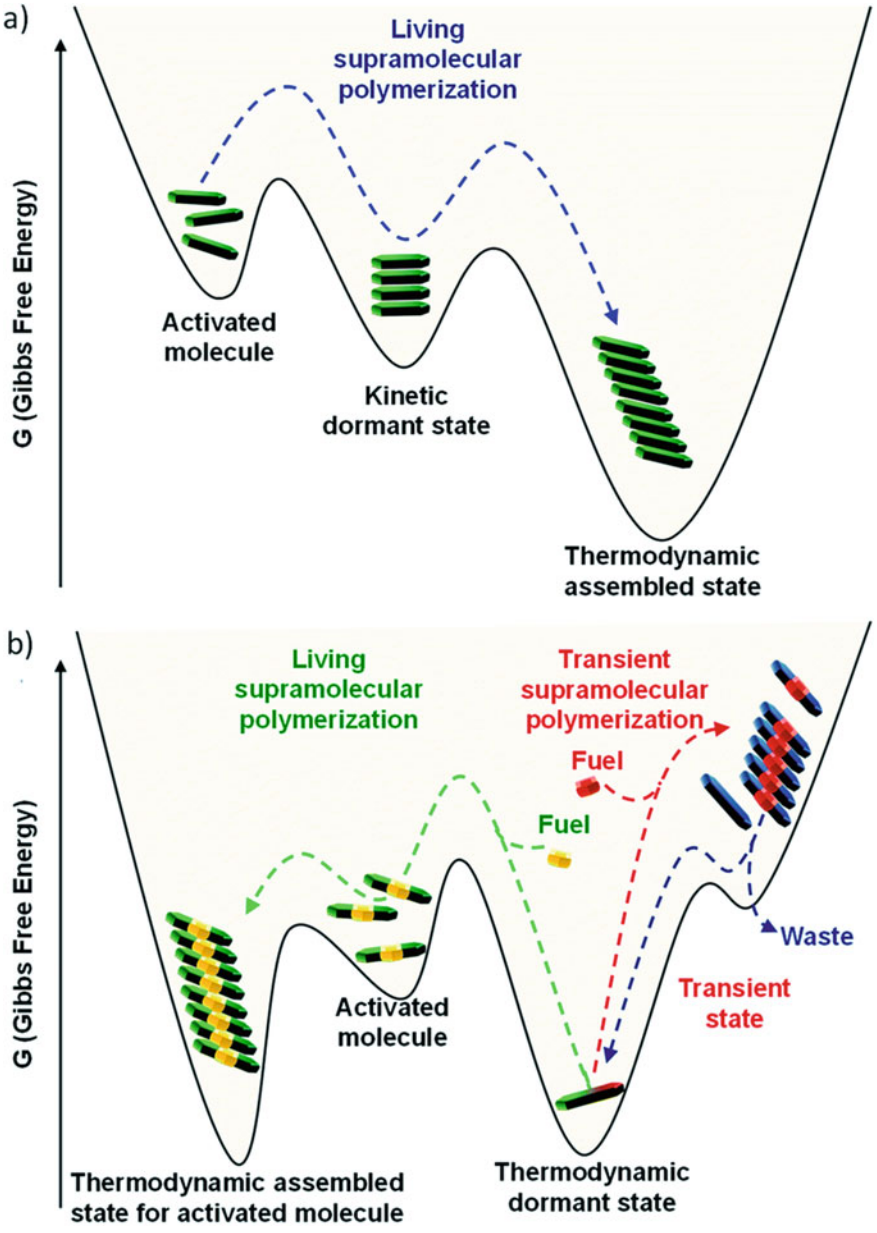

Fig. 8. **a** Energy pathway landscape of supramolecular polymerization. **b** Energy landscape for the aggregation pathways associated with bioinspired fuel-driven supramolecular polymerization follows transient self-assembly with the dissipative non-equilibrium condition [57]

In a biological system, the living supramolecular polymerization can be evidenced from 'protein-only' hypothesis. This involves the formation of abnormal protein aggregates, observed in prion infection. More specifically, the process involves the transformation of porphyrin-based supramolecular assembly from a nanoparticle to nanofibre upon addition of a very small amount of pathogen (i.e. nanofibre solution). Where the protein is inert and kinetically stable in normal conditions, but in the presence of a pathogenic environment, it results in abnormal polymerization due to structural rearrangements and aggregation [115, 118]. Figure 8b can also be represented concerning the energy landscape pathway of porphyrin dye, the kinetically stable state on the left side is called as 'isodesmic' process with lesser or negligible aggregates (J-aggregates). And upon crossing the active barrier, there occurs polymerization by the formation of—π-stacking interactions and thereby results in one-dimensional aggregates (H-aggregates) with lesser dispersity [119]. Meijer et al. reported a lot of works on these types of supramolecular aggregation and this pathway complexity. A lot of studies all show that there is the possibility of a repeated polymerization process in the given system [115]. Notable work has been reported on the synthesis of bis(pyrene) derivatives, BP1 and BP2 [120]. By altering the thermodynamical states, they have achieved J-type aggregates with almost 30-fold fluorescence enhancement compared to H-type aggregates. This J-aggregates also shows potentialities as functioning as nanoprobes for lysosome-targeted imaging in living cells with negligible cytotoxicity. The similar type of fluorescence property in organic supramolecular self-assembles in platinum(II) supramolecular structures containing BODIPY-based bridging ligands opens the possibility of these types of assembled structures for theragnostic applications [121]. In the future, the development of this type of assemblies is expected in the area of tissue engineering applications.

8 Conclusion

The progress in the development of self-healing scaffolds mimicking the structural and functional property of the tissue condition still has lots of topics that need to get explored. However, the recent research developments in understanding supramolecular chemistry in π–π interaction, π–π-gelators, bioinspired polymerization, nanostructure mediated synthesis were promising in enhancing the property of the self-healing hydrogels. By making the supramolecular self-healing hydrogels with suitable hybrid or composite structure, it will help make the hydrogel to be a shape memory scaffold, that can also modifiable using the 3D printing method to obtained customized structure for the need of the treatment conditions. In future, DNA hybrid self-healing gels, biomimetic gels, hydrogels with precultured cells that defining specific organs is giving hope towards the positive growth of this research area for the need of human beings.

Acknowledgements One of the authors D. Durgalakshmi gratefully acknowledges DST-INSPIRE Faculty Fellowship under the sanction DST/INSPIRE/04/2016/000845 for their funding.

References

1. Pleasant A, Rudd RE, O'Leary C, Paasche-Orlow MK, Allen MP, Alvarado-Little W, Myers L, Parson K, Rosen S (2016) Considerations for a new definition of health literacy. National Academy of Medicine Washington, DC
2. Sachot N, Mateos-Timoneda MA, Planell JA, Velders AH, Lewandowska M, Engel E, Castano O (2015) Towards 4th generation biomaterials: a covalent hybrid polymer–ormoglass architecture. Nanoscale 7:15349–15361
3. Tiniakos DG, Kandilis A, Geller S (2010) Tityus: a forgotten myth of liver regeneration. J Hepatol 53:357–361
4. Park J, Lakes RS (2007) Biomaterials: an introduction. Springer Science & Business Media
5. Ratner BD, Hoffman AS, Schoen FJ, Lemons JE (2013) Biomaterials science: an evolving, multidisciplinary endeavor. Elsevier
6. Ning C, Zhou L, Tan G (2016) Fourth Gener Biomed Mater 19:2–3
7. Utech S, Boccaccini AR (2016) A review of hydrogel-based composites for biomedical applications: enhancement of hydrogel properties by addition of rigid inorganic fillers. J Mater Sci 51:271–310
8. Williams DF (1999) The Williams dictionary of biomaterials. Liverpool University Press
9. Hron P (2003) Hydrophilisation of silicone rubber for medical applications. Polym Int 52:1531–1539
10. Pedley DG, Skelly PJ, Tighe B (1980) Hydrogels in biomedical applications. Adv Drug Deliv Rev 12:99–110
11. Lehn JM (1993) Supramolecular chemistry. Science 260:1762–1764
12. Korevaar PA, George SJ, Markvoort AJ, Smulders MM, Hilbers PA, Schenning AP, De Greef TF, Meijer E (2012) Pathway complexity in supramolecular polymerization. Nature 481:492–496
13. Lichtenthaler FW (1995) 100 Years "Schlüssel-Schloss-Prinzip": what made emil fischer use this analogy? Angew Chem Int Ed 33:2364–2374
14. Huang F, Anslyn EV (2015) Introduction: supramolecular chemistry. Chem Rev
15. Bosshard HR (2001) Molecular recognition by induced fit: how fit is the concept? News Physiol Sci 16:171–173
16. Nikolova MP, Chavali MS (2019) Recent advances in biomaterials for 3D scaffolds: a review. Bioact Mater 4:271–292
17. Chen FM, Liu X (2016) Advancing biomaterials of human origin for tissue engineering. Prog Polym Sci 53:86–168
18. Spicer CD (2020) Hydrogel scaffolds for tissue engineering: the importance of polymer choice. Polym Chem 11:184–219
19. Cai P, Hu B, Leow WR, Wang X, Loh XJ, Wu YL, Chen X (2018) Biomechano-interactive materials and interfaces. Adv Mater 30:1800572
20. Abdulghani S, Mitchell GR (2019) Biomaterials for in situ tissue regeneration: a review. Biomolecules 9:750
21. Whitesides G, Mathias J, Seto CJS (1991) Science 254:1312. [Crossref], [PubMed], [CAS], [Google Scholar]. (b) Whitesides GM, Grzybowski B (2002) 295:2418
22. Fazzalari N (2011) Bone fracture and bone fracture repair. Osteoporos Int 22:2003–2006
23. McKibbin B (1978) The biology of fracture healing in long bones. J Bone Joint Surg Br 60:150–162
24. Ulstrup AK (2008) Biomechanical concepts of fracture healing in weight-bearing long bones. Acta Orthop Belg 74:291
25. Cowin SC (1986) Wolff's law of trabecular architecture at remodeling equilibrium. J Biomech Eng
26. Frost HM (1994) Wolff's Law and bone's structural adaptations to mechanical usage: an overview for clinicians. Angle Orthod 64:175–188
27. du Noüy PL (1916) Cicatrization of wounds, III. J Exp Med 24:461

28. Du Noüy PL (1916) Cicatrization of wounds: II mathematical expression of the curve representing cicatrisation. J Exp Med 24:451–460
29. du Noüy PL (1919) Cicatrization of wounds: X a general equation for the law of cicatrization of surface wounds. J Exp Med 29:329
30. Gurtner GC, Werner S, Barrandon Y, Longaker MT (2008) Wound repair and regeneration. Nature 453:314–321
31. Hager MD (2017) Self-healing materials. In: Handbook of solid state chemistry, pp 201–225
32. Ahmed EM (2015) Hydrogel: preparation, characterization, and applications: a review. J Adv Res 6:105–121
33. Bargavi P, Ramya R, Chitra S, Vijayakumari S, Chandran RR, Durgalakshmi D, Rajashree P, Balakumar S (2020) Bioactive, degradable and multi-functional three-dimensional membranous scaffolds of bioglass and alginate composites for tissue regenerative applications. Biomater Sci 8:4003–4025
34. Rosiak JM, Yoshii F (1999) Hydrogels and their medical applications. Nucl Instrum Methods Phys Res Sec B Beam Interact Mater Atoms 151:56–64
35. Kumar A, Matari IAI, Choi H, Kim A, Suk YJ, Kim JY, Han SS (2019) Development of halloysite nanotube/carboxylated-cellulose nanocrystal-reinforced and ionically-crosslinked polysaccharide hydrogels. Mater Sci Eng C 104:109983
36. Voorhaar L, Hoogenboom R (2016) Supramolecular polymer networks: hydrogels and bulk materials. Chem Soc Rev 45:4013–4031
37. Maitra J, Shukla VK (2014) Cross-linking in hydrogels-a review. Am J Polym Sci 4:25–31
38. Moura MJ, Faneca H, Lima MP, Gil MH, Figueiredo MM (2011) In situ forming chitosan hydrogels prepared via ionic/covalent co-cross-linking. Biomacromol 12:3275–3284
39. Ullah F, Othman MBH, Javed F, Ahmad Z, Akil HM (2015) Classification, processing and application of hydrogels: a review. Mater Sci 57:414–433
40. Billiet T, Vandenhaute M, Schelfhout J, Van Vlierberghe S, Dubruel P (2012) A review of trends and limitations in hydrogel-rapid prototyping for tissue engineering. Biomaterials 33:6020–6041
41. Talebian S, Mehrali M, Taebnia N, Pennisi CP, Kadumudi FB, Foroughi J, Hasany M, Nikkhah M, Akbari M, Orive G (2019) Self-healing hydrogels: the next paradigm shift in tissue engineering? Adv Sci 6:1801664
42. Durgalakshmi D, Balakumar S (2015) Analysis of solvent induced porous PMMA–Bioglass monoliths by the phase separation method–mechanical and in vitro biocompatible studies. Phys Chem Chem Phys 17:1247–1256
43. Kang J, Tok JB-H, Bao Z (2019) Self-healing soft electronics. Nat Electr 2:144–150
44. Someya T, Bao Z, Malliaras GG (2016) The rise of plastic bioelectronics. Nature 540:379–385
45. Babu SS, Prasanthkumar S, Ajayaghosh A (2012) Self-assembled gelators for organic electronics. Angew Chem Int Ed 51:1766–1776
46. Zhu DY, Rong MZ, Zhang MQ (2015) Self-healing polymeric materials based on microencapsulated healing agents: from design to preparation. Prog Polym Sci 49:175–220
47. Thordarson P (2011) Determining association constants from titration experiments in supramolecular chemistry. Chem Soc Rev 40:1305–1323
48. Brunsveld L, Folmer B, Meijer EW, Sijbesma R (2001) Supramolecular polymers. Chem Rev 101:4071–4098
49. Steed JW, Turner DR, Wallace K (2007) Core concepts in supramolecular chemistry and nanochemistry. Wiley
50. Kumar A, Han SS (2017) PVA-based hydrogels for tissue engineering: A review. Int J Polym Mater Polym Biomater 66:159–182
51. Chen J, Zou X (2019) Self-assemble peptide biomaterials and their biomedical applications. Bioact Mater 4:120–131
52. Kumar A, Rao KM, Han SS (2017) Synthesis of mechanically stiff and bioactive hybrid hydrogels for bone tissue engineering applications. Chem Eng J 317:119–131
53. Nicodemus GD, Bryant SJ (2008) Cell encapsulation in biodegradable hydrogels for tissue engineering applications. Tissue Eng Part B Rev 14:149–165

54. Annabi N, Nichol J, Zhong X, Ji C, Koshy S, Khademhosseini A, Dehghani F (2010) Controlling the this article is licensed under a creative commons attribution-noncommercial 3.0 unported licence. Porosity and microarchitecture of hydrogels for tissue engineering. Tissue Eng. Part B 16:371–383
55. Zhang W, Zhang K, Yan S, Wu J, Yin J (2018) A tough and self-healing poly (L-glutamic acid)-based composite hydrogel for tissue engineering. J Mater Chem B 6:6865–6876
56. Reakasame S, Boccaccini AR (2018) Oxidized alginate-based hydrogels for tissue engineering applications: a review. Biomacromol 19:3–21
57. Dhiman S, Sarkar A, George SJ (2018) Bioinspired temporal supramolecular polymerization. RSC Adv 8:18913–18925
58. Mehrali M, Thakur A, Pennisi CP, Talebian S, Arpanaei A, Nikkhah M, Dolatshahi-Pirouz A (2017) Nanoreinforced hydrogels for tissue engineering: biomaterials that are compatible with load-bearing and electroactive tissues. Adv Mater 29:1603612
59. Rao KM, Kumar A, Han SS (2017) Polysaccharide based bionanocomposite hydrogels reinforced with cellulose nanocrystals: drug release and biocompatibility analyses. Int J Biol Macromol 101:165–171
60. Majumder S, Ranjan Dahiya U, Yadav S, Sharma P, Ghosh D, Rao GK, Rawat V, Kumar G, Kumar A, Srivastava CM (2020) Zinc oxide nanoparticles functionalized on hydrogel grafted silk fibroin fabrics as efficient composite dressing. Biomolecules 10:710
61. Liu Y, Hsu S-H (2018) Synthesis and biomedical applications of self-healing hydrogels. Front Chem 6:449
62. Kumar A, Matari IAI, Han SS (2020) 3D printable carboxylated cellulose nanocrystal-reinforced hydrogel inks for tissue engineering. Biofabrication 12:025029
63. Eom Y, Kim S-M, Lee M, Jeon H, Hwang SY, Park J, Oh D (2020) Mechano-responsive hydrogen-bonding array of thermoplastic polyurethane elastomer captures both strength and self-healing. Nat Res
64. Dankers PY, Boomker JM, Huizinga-van der Vlag A, Wisse E, Appel WP, Smedts FM, Harmsen MC, Bosman AW, Meijer W, van Luyn MJ (2011) Bioengineering of living renal membranes consisting of hierarchical, bioactive supramolecular meshes and human tubular cells. Biomaterials 32:723–733
65. Ye X, Li X, Shen Y, Chang G, Yang J, Gu Z (2017) Self-healing pH-sensitive cytosine-and guanosine-modified hyaluronic acid hydrogels via hydrogen bonding. Polymer 108:348–360
66. Liu B, Wang Y, Miao Y, Zhang X, Fan Z, Singh G, Zhang X, Xu K, Li B, Hu Z (2018) Hydrogen bonds autonomously powered gelatin methacrylate hydrogels with super-elasticity, self-heal and underwater self-adhesion for sutureless skin and stomach surgery and E-skin. Biomaterials 171:83–96
67. Yang S, Wang S, Du X, Du Z, Cheng X, Wang H (2020) Mechanically robust self-healing and recyclable flame-retarded polyurethane elastomer based on thermoreversible crosslinking network and multiple hydrogen bonds. Chem Eng J 391:123544
68. Wahid F, Zhou Y-N, Wang H-S, Wan T, Zhong C, Chu L-Q (2018) Injectable self-healing carboxymethyl chitosan-zinc supramolecular hydrogels and their antibacterial activity. Int J Biol Macromol 114:1233–1239
69. Wahid F, Zhou YN, Wang HS, Wan T, Zhong C, Chu LQ (2018) Injectable self-healing carboxymethyl chitosan-zinc supramolecular hydrogels and their antibacterial activity. Int J Biol Macromol 114:1233–1239
70. Wei Z, Zhao J, Chen YM, Zhang P, Zhang Q (2016) Self-healing polysaccharide-based hydrogels as injectable carriers for neural stem cells. Sci Rep 6:37841
71. Hussain I, Ma X, Luo Y, Luo Z (2020) Fabrication and characterization of glycogen-based elastic, self-healable, and conductive hydrogels as a wearable strain-sensor for flexible e-skin. Polymer, 122961
72. Balkenende DW, Winkler SM, Messersmith PB (2019) Marine-inspired polymers in medical adhesion. Eur Polym J 116:134–143
73. Janarthanan G, Noh I (2020) Recent trends in metal ion based hydrogel biomaterials for tissue engineering and other biomedical applications. J Mater Sci Technol

74. Shi L, Ding P, Wang Y, Zhang Y, Ossipov D, Hilborn J (2019) Self-healing polymeric hydrogel formed by metal-ligand coordination assembly: design fabrication, and biomedical applications. Macromol Rapid Commun 40:1800837
75. Tran NB, Moon JR, Jeon YS, Kim J, Kim J-H (2017) Adhesive and self-healing soft gel based on metal-coordinated imidazole-containing polyaspartamide. Colloid Polym Sci 295:655–664
76. Huang W-C, Ali F, Zhao J, Rhee K, Mou C, Bettinger CJ (2017) Ultrasound-mediated self-healing hydrogels based on tunable metal–organic bonding. Biomacromol 18:1162–1171
77. Shi L, Wang F, Zhu W, Xu Z, Fuchs S, Hilborn J, Zhu L, Ma Q, Wang Y, Weng X (2017) Self-healing silk fibroin-based hydrogel for bone regeneration: dynamic metal-ligand self-assembly approach. J Adv Funct Mater 27:1700591
78. Yan K, Xu F, Wang C, Li Y, Chen Y, Li X, Lu Z, Wang D (2020) A multifunctional metal-biopolymer coordinated double network hydrogel combined with multi-stimulus responsiveness, self-healing, shape memory and antibacterial properties. Biomater Sci
79. Zhang H, Kang L, Zou Q, Xin X, Yan X (2019) Coordination-assembled supramolecular nanoplatforms: structural modulation and theranostic applications. Curr Opin Biotechnol 58:45–52
80. Wang X-H, Song F, Xue J, Qian D, Wang X-L, Wang Y-Z (2018) Mechanically strong and tough hydrogels with excellent anti-fatigue, self-healing and reprocessing performance enabled by dynamic metal-coordination chemistry. Polymer 153:637–642
81. Wu S, Fang S, Tang Z, Liu F, Guo B (2020) Design bioinspired design of elastomeric vitrimers with sacrificial metal-ligand interactions leading to supramechanical robustness and retentive malleability. Mater Sci, 108756
82. Li S, Wang L, Yu X, Wang C, Wang Z (2018) Synthesis and characterization of a novel double cross-linked hydrogel based on Diels-Alder click reaction and coordination bonding. Mater Sci Eng C 82:299–309
83. Liu K, Zang S, Xue R, Yang J, Wang L, Huang J, Yan Y (2018) Coordination-triggered hierarchical folate/zinc supramolecular hydrogels leading to printable biomaterials. ACS Appl Mater Interfaces 10:4530–4539
84. Moon JR, Jeon YS, Kim YJ, Kim J-H (2019) Adhesive, self-healing and antibacterial properties of Cu-coordinated soft gel based on histamine-conjugated polyaspartamide. J Polym Res 26:12
85. Shi L, Zhao Y, Xie Q, Fan C, Hilborn J, Dai J, Ossipov DA (2018) Moldable hyaluronan hydrogel enabled by dynamic metal–bisphosphonate coordination chemistry for wound healing. J Adv Healthc Mater 7:1700973
86. Tran NB, Moon JR, Jeon YS, Kim J, Kim JH (2017) Adhesive and self-healing soft gel based on metal-coordinated imidazole-containing polyaspartamide. Coll Polym Sci 295:655–664
87. Nita LE, Chiriac AP, Rusu AG, Bercea M, Ghilan A, Dumitriu RP, Mititelu-Tartau L (2019) New self-healing hydrogels based on reversible physical interactions and their potential applications. Eur Polymer J 118:176–185
88. Hussain I, Sayed SM, Liu S, Oderinde O, Kang M, Yao F, Fu G (2018) Enhancing the mechanical properties and self-healing efficiency of hydroxyethyl cellulose-based conductive hydrogels via supramolecular interactions. Eur Polym J 105:85–94
89. Song R, Zheng J, Liu Y, Tan Y, Yang Z, Song X, Yang S, Fan R, Zhang Y, Wang Y (2019) A natural cordycepin/chitosan complex hydrogel with outstanding self-healable and wound healing properties. Int J Biol Macromol 134:91–99
90. Huang J, Deng Y, Ren J, Chen G, Wang G, Wang F, Wu X (2018) Novel in situ forming hydrogel based on xanthan and chitosan re-gelifying in liquids for local drug delivery. Carbohyd Polym 186:54–63
91. Ding C, Yang Q, Tian M, Guo C, Deng F, Dang Y, Zhang M (2020) Novel collagen-based hydrogels with injectable, self-healing, wound-healing properties via a dynamic crosslinking interaction. Polym Int
92. Chen H, Cheng J, Ran L, Yu K, Lu B, Lan G, Dai F, Lu F (2018) An injectable self-healing hydrogel with adhesive and antibacterial properties effectively promotes wound healing. Carbohyd Polym 201:522–531

93. Zhang Y, Chen M, Dai Z, Cao H, Li J, Zhang W (2020) Sustained protein therapeutics enabled by self-healing nanocomposite hydrogels for non-invasive bone regeneration. Biomater Sci 8:682–693
94. Tallia F (2018) co-workers, Mater, Horiz
95. Song R, Zheng J, Liu Y, Tan Y, Yang Z, Song X, Yang S, Fan R, Zhang Y, Wang Y (2019) A natural cordycepin/chitosan complex hydrogel with outstanding self-healable and wound healing properties. Int J Biol Macromol 134:91–99
96. Wen H, Chen S, Ge Z, Zhuo H, Ling J, Liu Q (2017) Development of humidity-responsive self-healing zwitterionic polyurethanes for renewable shape memory applications. RSC Adv 7:31525–31534
97. Bai L, Jiang X, Sun Z, Pei Z, Ma A, Wang W, Chen H, Yang H, Yang L, Wei D (2019) Self-healing nanocomposite hydrogels based on modified cellulose nanocrystals by surface-initiated photoinduced electron transfer ATRP. Cellulose 26:5305–5319
98. Jing X, Mi H-Y, Napiwocki BN, Peng X-F, Turng L-S (2017) Mussel-inspired electroactive chitosan/graphene oxide composite hydrogel with rapid self-healing and recovery behavior for tissue engineering. Carbon 125:557–570
99. Appel EA, del Barrio J, Loh XJ, Scherman OA (2012) Supramolecular polymeric hydrogels. Chem Soc Rev 41:6195–6214
100. Loh XJ (2014) Supramolecular host–guest polymeric materials for biomedical applications. Mater Horiz 1:185–195
101. Rodell CB, Mealy JE, Burdick JA (2015) Supramolecular guest–host interactions for the preparation of biomedical materials. Bioconjug Chem 26:2279–2289
102. Dorishetty P, Dutta NK, Choudhury NR (2020) Bioprintable tough hydrogels for tissue engineering applications. Adv Coll Interface Sci, 102163
103. Wang Z, Ren Y, Zhu Y, Hao L, Chen Y, An G, Wu H, Shi X, Mao C (2018) A rapidly self-healing host-guest supramolecular hydrogel with high mechanical strength and excellent biocompatibility. Angew Chem 130:9146–9150
104. Sisso AM, Boit MO, DeForest CA (2020) Self-healing injectable gelatin hydrogels for localized therapeutic cell delivery. J Biomed Mater Res, Part A 108:1112–1121
105. Xu Y, Cui M, Patsis PA, Günther M, Yang X, Eckert K, Zhang Y (2019) Reversibly assembled electroconductive hydrogel via a host-guest interaction for 3D cell culture. ACS Appl Mater Interfaces 11:7715–7724
106. Hu T, Wu Y, Zhao X, Wang L, Bi L, Ma PX, Guo B (2019) Micropatterned, electroactive, and biodegradable poly (glycerol sebacate)-aniline trimer elastomer for cardiac tissue engineering. Chem Eng J 366:208–222
107. Grimme S (2008) Do special noncovalent π–π stacking interactions really exist? Angew Chem Int Ed 47:3430–3434
108. Jeffrey GA, Jeffrey GA (1997) An introduction to hydrogen bonding. Oxford University Press, New York
109. Thakuria R, Nath NK, Saha BK (2019) Design, the nature and applications of π–π interactions: a perspective. Crystal Growth 19:523–528
110. Hunter CA, Sanders JK (1990) The nature of pi-pi. Interactions. J Am Chem Soc 112:5525–5534
111. Claesson H, Malmström E, Johansson M, Hult A (2002) Synthesis and characterisation of star branched polyesters with dendritic cores and the effect of structural variations on zero shear rate viscosity. Polymer 43:3511–3518
112. Martinez CR, Iverson BL (2012) Rethinking the term "pi-stacking." Chem Sci 3:2191–2201
113. Cabaleiro-Lago EM, Rodríguez-Otero JS (2018) On the nature of σ–σ, σ–π, and π–π stacking in extended systems. ACS Omega 3:9348–9359
114. Burattini S, Greenland BW, Merino DH, Weng W, Seppala J, Colquhoun HM, Hayes W, Mackay ME, Hamley IW, Rowan SJ (2010) A healable supramolecular polymer blend based on aromatic π−π stacking and hydrogen-bonding interactions. J Am Chem Soc 132:12051–12058

115. Burattini S, Colquhoun HM, Fox JD, Friedmann D, Greenland BW, Harris PJ, Hayes W, Mackay ME, Rowan SJ (2009) A self-repairing, supramolecular polymer system: healability as a consequence of donor–acceptor π–π stacking interactions. Chem Commun, 6717–6719
116. Cremaldi JC, Bhushan B (2018) Bioinspired self-healing materials: lessons from nature. Beilstein J Nanotechnol 9:907–935
117. Ashkenasy G, Hermans TM, Otto S, Taylor AF (2017) Systems chemistry. Chem Soc Rev 46:2543–2554
118. Ogi S, Sugiyasu K, Manna S, Samitsu S, Takeuchi M (2014) Living supramolecular polymerization realized through a biomimetic approach. Nat Chem 6:188
119. Dhiman S, Sarkar A (2018) RSC Adv 8:18913–18925; (b) Dhiman S, George SJ (2018) Bull Chem Soc Jpn 91:687–699
120. Sorrenti A, Leira-Iglesias J, Markvoort AJ, de Greef TF, Hermans TM (2017) Non-equilibrium supramolecular polymerization. Chem Soc Rev 46:5476–5490
121. Mukhopadhyay RD, Ajayaghosh A (2015) Living supramolecular polymerization. Science 349:241–242
122. Würthner F (2014) Living it up. Nat Chem 6:171–173

Chapter 5
Gel-Inks for 3D Printing in Corneal Tissue Engineering

Songul Ulag, Sumeyye Cesur, Ecem Dogan, Mustafa Sengor, Nazmi Ekren, Cem Bulent Ustundag, and Oguzhan Gunduz

Abstract Corneal transplantation from donor tissue is one of the primary healing of cornea diseases. However, the scarcity of donor tissue is a serious problem. Tissue engineering approaches offer an alternative recourse for corneal regeneration. Corneal tissue engineering (CTE) can provide tissue substitute to preserve and enhance corneal functions combining cells, bioactive molecules, and three-dimensional scaffolds for native cornea transplantation. 3D printing is a novel and rising process for constructing layer-by-layer fabrication of these materials in clinical applications. Among the different materials, gel-based inks are remarkable materials to use as ink in the 3D printing. In view of the printability feature of the inks, the processing abilities of the gel-ink formulation is an important parameter to consider. Furthermore, to produce gel-ink with transparency, non-toxicity, and mechanical properties almost identical to the human cornea have a vital role in replacing corneal tissues. Herein, the desired properties for selecting gel-inks and combination and characterization of inks for 3D printing in CTE are presented in detail.

Keywords Corneal tissue engineering · Hydrogel · Ink · 3D printing · Corneal regeneration

H factors of the authors Oguzhan Gunduz: web of science 15
Cem Bulent Ustundag: web of science 8

S. Ulag · S. Cesur · E. Dogan · M. Sengor · N. Ekren · C. B. Ustundag · O. Gunduz (✉)
Center for Nanotechnology and Biomaterials Application and Research (NBUAM), Marmara University, Istanbul, Turkey
e-mail: ucemogu@ucl.ac.uk

S. Ulag · S. Cesur · M. Sengor · O. Gunduz
Faculty of Technology, Department of Metallurgical and Materials Engineering, Marmara University, Istanbul, Turkey

E. Dogan · C. B. Ustundag
Faculty of Chemical and Metallurgical Engineering, Department of Bioengineering, Yildiz Technical University, Istanbul, Turkey

A. Kumar et al. (eds.), *3D printable Gel-inks for Tissue Engineering*, Gels Horizons: From Science to Smart Materials, https://doi.org/10.1007/978-981-16-4667-6_5

1 Introduction

1.1 Structure of the Cornea

The cornea is a transparent, multi-layered avascular tissue that preserves the eye against infections and acts as a structural boundary [1]. Since the cornea is a non-vascular structure, there is no blood vessel to feed it or protect it against infection. The oxygenation and nutrition of the cornea are provided by tear secretion on the outside and intraocular vision fluid on the inside. Together with the tear film, it provides an appropriate pre-refraction surface for the eyes. The cornea has 11–12 mm horizontal length and 9–11 mm vertical length in adults. The mean corneal diameter is 11.77 $\pm$ 0.37 mm in men and 11.64 $\pm$ 0.47 mm in women [2, 3]. Corneal tissue consists of five basic layers (Fig. 1), front to back, each of which has an important function. These are stroma, epithelium, Descemet's and Bowman's layers, and endothelium. The Bowman and Descemet layers are the acellular layers. Stroma, endothelium, and epithelium are the cellular layers [4].

1.1.1 Epithelium

The epithelium is the outmost region of the cornea and comprises of a homogeneous cell layer. It makes up about 10% of the tissue thickness. It is smooth, uniform and consists of non-keratinized squamous epithelial cells [5]. The epithelium is loosely attached to the underlying base layer and Bowman's membrane. The corneal epithelium, like most epithelium, spreads cells into the environment. This is a strategy that possibly prevents the progression of pathogens to relatively immunologically deficient stromal tissue [6]. Corneal epithelium differs from conjunctural epithelium in that it has no mucin and goblet cells but contains protein-bound to glycogen. There

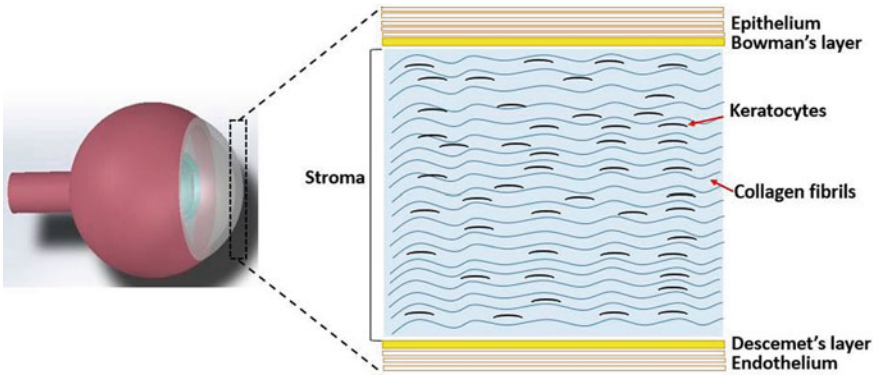

Fig. 1 Structural anatomy of the cornea with its layers

is a symbiotic relationship between the epithelium and the tear film covering it. The mucin layer of the tear film, which is in direct connection with the epithelium, is manufactured by the conjunctival goblet cells [7]. Corneal epithelial cells undergo apoptosis, desquamation, and evolution.

The lifetime is 7–10 days. There are three kinds of cells in the epithelium: basal cells, wing cells, and superficial cells. Superficial cells consist of flat polygonal cells approximately 2–6 μm (thickness) and 40–60 μm (diameter) values. The epithelial layer consists of small light cells and large dark cells. Desmosomes form the tight junction between superficial cells, and these are placed in the lateral tissue layers of all epithelial cells to hold the epithelial cells attached. Basal cells with abundant organelles are the only cubic or columnar layer of the epithelium. The deepest cell layer (about 20 μm high) of the epithelium compromises. Basal cells are the origin of the wing and superficial cells and the solely corneal epithelial cells adequate to do mitosis. The basement membrane consists of type IV collagen and lamine released from basal cells. It is 40–60 nm thick. Lamina densa and lamina lucida form the basement membrane. In addition, the basal membrane is required to adjust cellular signal and traffic between stroma and epithelium, and for adhesion and polarity of epithelial cells [8].

1.1.2 Bowman's Layer

It is the acellular layer known as the Bowman layer or Bowman membrane. This clear layer is nearly 12–18 μm thick in persons and supports the cornea to retain its form. It does not renew when injured and may end in scarring. If these scars are centrally located and large, some vision loss may occur. The Bowman layer gets thinner with aging [9]. It can be thought about a special area of the prior stroma that mediates transactions with the epithelium [10]. This region consists of strong layered protein fibers called collagen with very small diameters around 18-30 nm. Collagen fibers are synthesized and released from stromal keratocytes. Collagen type I and type III in this layer are smaller than collagen fibers found in the stroma [11]. The Bowman layer comprises anchoring complexes consisting of anchor plates containing collagen IV and anchoring fibrils containing collagen VII, except for collagen fibrils [12]. Once the Bowman layer is broken, it will not regenerate, and its absence does not affect corneal function [13]. In recent studies, it has been successfully reported that the Bowman layer is removed from a cadaver donor and transplanted to recipients with significant anterior corneal scars [14].

1.1.3 Stroma

Stroma is the primary component of the cornea and forms more than ninety percent of the cornea thickness. It comprises principally of 78% water, 16% collagen and doesn't comprise blood vessels. Stroma differs from other collagen structures in terms of its biomechanical properties. It provides sufficient strength, transparency, and stability

[8]. The stroma has a transparent structure due to the well-defined arrangement of stromal fibers and extracellular matrix (ECM). Cornea stroma consists of ECM and keratocytes. ECM comprises collagen (Type I, III, V, VI) and glycosaminoglycans [15]. Glucosaminoglycans form chondroitin sulfate, dermatan sulfate, keratan sulfate. Glucosaminoglycans predominantly contain keratan sulfate. The corneal stroma has keratocytes and about 300 collagen lamellas. Keratocytes are the dominant cellular parts of the stroma, and most are found in the anterior stroma. They preserve the ECM surroundings [16]. They are dispersed between the stroma lamellae. The stroma consists of collagen fibrils with the parallel array. Proper spacing and alignment of collagen fibers in the stroma are very critical on the transparency of the cornea.

Cell Classifications in the Corneal Stroma

1. Keratocytes
Keratocytes consist of about 10% of stroma by volume. They are responsible for protecting the extracellular matrix environment and the development of the stroma [17]. Keratocytes direct and regulate the deposition of collagen fibrils. Some of the main functions of the corneal crystals in the keratocytes in the cornea are to reduce the amount of reflection of the rays coming to the cornea and to contribute to the preservation of the transparent structure of the cornea. Keratocytes synthesize and store crystals at a high rate in their cytoplasm. This accumulation of crystals stored in the keratocyte promotes the transparency of the stroma, similar to cells in the natural lens [18]. The three-dimensional keratocyte arrangement can be examined with confocal biomicroscopy, light microscopy, and scanning electron microscopy.

2. Stem Cells
Adult stem cells are placed in the limbal stromal region of the corneal stroma [19]. These adult cells are usually detected in specific places or positions in the body. Adult stem cells, glial fibrils, and chondrocytes can develop into different cell lines, including acidic protein-expressing cells [20]. Glial fibrillary acidic protein (GFAP) is a protein that is indicated by many cell kinds of the central nervous system. It is a familiar neural factor and can play a role for herpes simplex virus-1 (HSV-1) infection in the cornea. Adult stem cells can also be expanded as keratocytes that can regenerate stromal tissue. Stem cell habitats are often effective at changing lost cells to regenerate them when tissue is injured or loses function. Treating corneal wounds and infections is currently limited. Therefore, the recognition and isolation of stem cells have attracted great notice. Recognition of stem cells has the capability for the healing of injured cornea tissue [21].

3. Dendritic Cells
These are specialized hema-topoetic cells, and they are a sub-set of immune-regulating antigen-giving cells [22]. It plays a vital role between acquired and adaptive immunity. They are nonhomogenous inhabitants of bone marrow acquired cells

along with the cornea [23]. The dendritic cells in the cornea are main players in epithelial wound healing and response to infection. When dendritic cells are exhausted, recovery is reduced [24].

ECM of the Cornea

The structural arrangement of the stroma is critical for transparency of the whole cornea. Transparency depends on the uniform packaging of uniform, small diameter collagen fibrils. Fibrils are packed equidistantly [18]. The diameter of the fibrils is generally between 25–35 nm and varies according to the species. In the corneal stroma, collagen I is the dominant kind of fibril-forming collagen. In addition, the extracellular matrix and corneal stroma structure are generally not determined by the type of collagen present [25].

1. Collagen
The most abundant element of the extracellular matrix (ECM) in tissues is collagen [26]. Collagen accounts for more than seventy percent of the dry mass of the cornea. The collagen in the corneal fibrils are types I, II, III, V and XI that possess a continuous triple helix area of approximately 300 nm and provide the greatest tensile strength to the cornea. Type I collagen is a plentiful protein in the stroma [1]. Type V and type VI collagen are also remarked in relatively large amounts. Collagen V constitutes 10–20% of the fibril forming collagen, and it is responsible for modification of the fibril diameter. Type III is normally found at low rates but can be increase related to inflammation, wound healing, and pathological situations. In addition, collagen III is extensively found in many organs, involving the skin, blood vessels, intestine, and uterus. Collagen XI can be found in the slightest degree. Type XII collagen combines with the top of collagen fibrils and changes their possessions [27].

1.1.4 Descemet's Layer

Descemet's membrane (5–10 μm) is the basic layer of the cornea endothelium. In humans, its thickness value slowly rises from birth to maturity [28]. It is a superior base membrane in terms of both size and composition. Descemet's membrane behaves like a defensive boundary under the stroma against infections and damages. Easily regenerated after injury [29]. Descemet's membrane consists of fibronectin, laminin, and proteoglycans, including heparan, keratan and dermatan sulphates. The content and qualities of proteoglycans are essential for tissue hydration. Structurally, Descemet's membrane comprises collagen, type IV and VIII. Type IV collagen is a familiar element of the basal lamina part of basement tissue layers. Type VIII collagen is scarce in other parts of the body but is found in high concentrations in Descemet's membrane [8].

1.1.5 Endothelium

The corneal endothelium is a single honeycomb-like cell layer on the cornea. It comprises a single hexagonal layer (5 μm) of 400.000 cells [30]. The endothelium places on a thick basement and Descemet's membranes. Endothelial cells are not easy to regenerate. Age-related and layer damage can be compensated by surrounding cells. But there is a limit to the endothelium's ability to compensate [31]. If too many endothelial cells are destroyed, corneal edema, corneal swelling and blindness occur. In case of damage or loss of corneal endothelial cells, water absorption by the cornea stroma increases. Endothelial cells comprise ion transport structures that prevent water from being absorbed into the stroma. Endothelial cells are essential for keeping the cornea clean. Endothelial cells act as a barrier preventing fluid from entering the cornea. Endothelial cells prevent overhydration of the stroma by moving water and ions from the stroma [32]. In other words, it pumps the excess liquid out of the stroma through ionic pumps and auxiliary carriers. If this pumping system does not exist, the stroma will swell with water and become cloudy opaque. Therefore, the endothelium is of paramount importance in preserving the nutrition and transparency of the cornea through this "pump-leak" system [33]. In a healthy eye, there is a perfect match between the fluid pumped from the cornea and the fluid moving to the cornea [33].

1.2 Desired Qualities for Cornea Replacement

Tissue engineering is one of the new advances in treating corneal disorders beginning from the epithelium to the stroma and endothelial layers. The epithelium is thin layers that make up about 10% of the thickness of the cornea, respectively, and the endothelium, about 1%. Stroma is a dense layer with a regular form [34]. Accordingly, in order to heal the injured tissue; 2D and/or 3D cell transportation methods have been employed according to the natural structure of each layer [35]. 2D scaffolds provide suitable fibrillar structure and mechanical properties for epithelial and endothelial layers and cultured cells, but cannot imitate the complex 3D form of stroma tissue. Transplantation technique is significant for improving ocular surface defects. Delivery methods such as non-invasive growth factor/limbal stem cell injection are preferred to an operation known as incursive manipulation with the soft corneal surface [36]. In scaffold-based cell delivery techniques, scaffold properties such as surface topology, stiffness, cytocompatibility, and degradation behaviour have a significant effect on cell growth and differentiation [37]. The mechanical properties mimic the native tissue microenvironment and influence cell distinction. The swelling rate relies on the hydrophilicity and hardness of the pier. Water capacity is important for biocompatibility and cell growth. Because it is related to hydrophilicity and is inversely proportional to the mechanical resistance of the carrier. The transparency of the cornea relies on the size and ordered distribution of the stromal collagen fibres. Therefore, suitable surface topology can increase cell

proliferation and differentiation in stromal tissue regeneration [38]. Biomaterials are separated into two classifications, natural and synthetic biomaterials. Natural ones are important in cornea regeneration due to their biocompatibility, and suitable cell adhere positions. However, high degradation rate and poor mechanical properties are drawbacks of naturally obtained biomaterials.

On the other hand, synthetic biomaterials have a low degradation rate, suitable mechanical strength, and adjustable geometry. Hydrogel-based scaffolds in 3D structures contain cross-linked polymeric materials that retain important quantities of water. Non-hydrogel scaffolds are other kinds of scaffolds, such as films and electrospun mats [39].

2 Corneal Regeneration in Tissue Engineering

2.1 Scaffold-Based Tissue Engineering for Corneal Regeneration

Tissue engineering proposes a distinctive solution for transplantation because of the donor corneas deficiency. Tissue engineering-based inserts may diminish the probability of refusal and complexities emerging from the operation, comprising bacterial disease, enzymatic degradation of encompassing tissue, and destitute balance [40]. The main components in deciding the ability to manufacture tissue to precisely replicate innate tissue are the type of material (Fig. 2). Scaffolds give a functional synthetical intercellular substance to permit a tissue to create. The various scaffold types are stromal scaffolds, decellularized scaffolds, nanomaterial-based scaffolds,

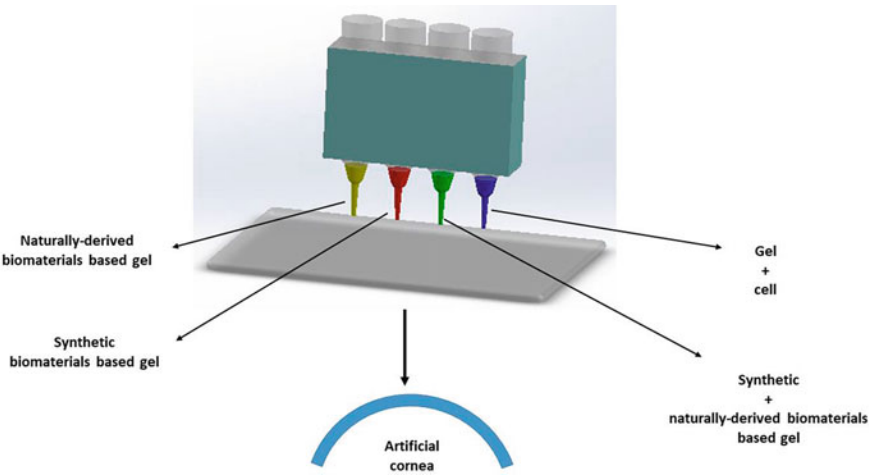

Fig. 2 Combinations of the materials to form gel-inks for corneal transplantation

and bioprinted scaffolds. Physical possessions, cytocompatibility, degradation, and optical features are the critical parameters for choosing a proper scaffold material. The size and number of the pores and surface area are the significant factors for cell migration, growth, and new tissue development [41]. Mechanical qualities of the scaffolds have to be suitable for the native cornea. Recent progress in materials manufacture methods such as bioprinting, electrospinning, and diverse collagen arrangement strategies, permit constructs to be created that more precisely simulate the nature of the corneal stroma [42]. The impacts of corneal cell multiplication and migration on the substance have to be taken into account in selecting suitable material as a scaffold for utilizing in corneal tissue designing [43].

When planning a scaffold for corneal regeneration, one of the key components to remember is how it would be implemented. On the sort of required scaffold, the sort of surgery which is required has a noteworthy impact. Depending upon the kind of damage or therapeutic disorder, various procedures or keratoplasties can be employed to repair sight. Penetrating keratoplasty (PKP) includes the expulsion of the total thickness of the cornea. Alternative techniques are deep anterior lamellar keratoplasty (DALK), anterior lamellar keratoplasty (ALK), Descernet's stripping endothelial keratoplasty (DSEK), and Descemet's membrane endothelial keratoplasty (DMEK) [44]. Cell culture before transplantation is necessary and important when using endothelial cells. In cases where cells are transplanted into scaffolds, the origin and phenotype of the cells are important [1]. ECM molecules must have the ability to renew the structure when the scaffold degrades. Scaffolds can be designed as a fixed implant that does not make variety with the period. As a corneal substitute, scaffolds have more potential that supports remodelling and regeneration. The biocompatibility of the scaffolds is critical for their surviving after implantation and also the materials and their degradation products that used to fabricate the scaffolds must not be noncytotoxic and not cause an immune response from the host. The light transmission of the cornea is an important factor when producing scaffolds. The cornea permits light to pass across the observable light spectrum (wavelength 400–780 nm) [42].

2.2 Synthetic Biomaterials for Corneal Regeneration

Biomaterials include natural and synthetic polymers that allow the required properties for customization [45]. There are adequate mechanical power, quick polymerization, low degradation rate, and synthetic biomaterial configurable geometry features [46]. Since the structure and biological substitution can be organized, synthetic polymers are beneficial for making extremely verified cellular areas [47–50]. Synthetic materials can be solid-like materials which are non-water soluble polymers formulated into fibres [51, 52], sponges [53] or layers [54] and hydrogels. Hydrogels are largely utilized in tissue engineering due to their elevated water amount, 3D shape, changeable possessions, and large mass deliver. Non-hydrogel based scaffolds are a convenient option in regenerative medicine due to their greater mechanical power

[39]. A diversity of synthetic substances contain poly(vinyl alcohol) (PVA) [55], poly(2-hydroxyethyl methacrylate) (PHEMA) [56], polyethylene (glycol) Diacrylate (PEGDA) [57], poly(lactic-co-glycolic acid) (PLGA) [58] and poly(ethylene glycol)/poly(acrylic acid) (PEG/PAA)-based hydrogels [58, 59] use in corneal tissue engineering as a substrate or corneal substitutes. PEG that is used the loss of corneal endothelial cells disease is a biocompatible synthetic polymer and has a proper mechanical property. The disadvantage of this polymer is a lack of cell integration [60]. PEGDA with the same properties and disadvantages as PEG is used for corneal wound disease [61]. PCL that is used dysfunction or loss of epithelial stem cell diseases is a biocompatible synthetic polymer and has a proper mechanical property. The disadvantage of this polymer is a low degradation rate [62]. PEG + PAA combination that is used epithelial defect and corneal thinning diseases has the same properties as PEG, PEGDA, and PCL. The disadvantage of this combination is inducing inflammatory response [63]. PVA that is used corneal blindness is a biocompatible synthetic polymer and has a proper mechanical property. Disadvantages of this polymer are a low degradation rate and a lack of cell integration [64]. PLGA that is used limbal deficiency disease has proper mechanical properties. The disadvantage of this polymer is the lack of cell integration [61].

2.3 Corneal Regeneration Using Naturally Derived Biomaterials

Natural biopolymers have essential features such as strong biocompatibility, biodegradability, low immunogenicity, noncytotoxic degradation products, easily adjusted biological system degradation rates, and overall material availability [65]. They are also an effective choice for tissue regeneration due to their proper cell-binding area [39]. Weak mechanical power and high degradation rate are drawbacks of natural biomaterials [40]. Collagen consists of 70 percent of the cornea's dry weight [66, 67]. Hydrogels, films and sponges are used to fabricate different collagen scaffolds for corneal tissue engineering [68]. Collagen films can be used for various purposes in corneal tissue engineering such as transplantation of endothelial or epithelial cells [69, 70] or stacked to produce laminal layers [71]. Gelatin is a protein obtained from the hydrolysis of collagen [72]. This material has features such as biocompatibility, low cost, and low immunogenicity, and these factors make gelatin a favourable material [73, 74]. Besides, gelatin can make bioadhesive hydrogels fix and repair the cornea after damage without the sutures [75, 76]. Fibrin that has been utilized as an option to suturing for keratoplasties is created by combining fibrinogen and thrombin. Fibrin uses to close corneal wounds and leaks after surgery due to damage caused by trauma [77]. Fibrin has been used for corneal development in conjunction with agarose [78, 79]. The existence of agarose mechanically stabilized the hydrogel and enhanced transparency [79]. Chitosan is has been used

to utilize to create scaffolds for different types of tissues. This material has advantages such as nontoxic biodegradability, antimicrobial and anti-inflammatory properties, low toxicity, immunogenicity and biocompatibility [80]. However, chitosan also has disadvantages such as poor mechanical properties and quick degradation. For cornea engineering to obtain scaffolds, chitosan is used with gelatin or gelatine and hyaluronic acid to create layers to culture and transplant limbal and epithelial cells and with silk fibroin to fabricate a corneal stromal substitute in previous studies [81, 82]. Alginate is a natural polymer obtained from seaweed, and it has been utilized with gelatin nanofibers to fabricate a cornea stroma [83]. Hyaluronic acid is a nonsulfated glycosaminoglycan (GAG) and has a critical role in wound healing and used as a scaffold for cornea engineering.

Hyaluronic acid has been used to culture corneal epithelial cells and as a potential carrier for endothelial cells [84–86]. All of these materials were given in Table 1 with their advantages and disadvantages.

3 Corneal Regeneration Using Gel-Based Scaffolds

3.1 Desired Properties of Gel-Inks for 3D Printing in Corneal Tissue Engineering

Hydrogels can be a good candidate for smart or stimuli-sensitive biotechnology stages due to their unique properties. They can differ from a liquid to gel as a reaction to a stimulus [87]. Furthermore, hydrogels have a similar structure with the extracellular matrix and three-dimensional models that support cell spread and viability. Therefore, hydrogels have important suitable qualities for cornea regeneration [87] which are summarized in Fig. 3.

Several important facts should be considered to fabricate the novel hydrogels for ocular operations, such as physical nature, elasticity, surface structure, water capacity, and oxygen permeableness [87]. Transparency, refractive power, and protection are the parameters that a synthetic cornea should have [87].

One of the most critical qualities of the human cornea is optical transparency and optical density. This property can be impressed by some conditions such as curvature nature of cornea and mechanical strength against the intraocular pressure [88]. Therefore, these properties should be considered together to fabricate the native cornea-like tissue. Collagen fibril alignment in the stroma has an essential role in the transparency of the cornea. These narrow (∼32 nm) and separated collagen fibrils run parallel to each other in lamellae composed of cross-oriented stacked layers. Innate collagen fibrils have the alternating space and overlap fields along the fibril (D-periodicity). This is coming from the organization of collagen molecules. The periodic order is important for generating heterotypic forms having in it fibrillar collagens and non-collagenous macromolecules. Proteoglycans hold to particular parts along the fibrils, and they have an important role in a matrix organization and

Table 1 The naturally derived and synthetic biomaterials for cornea tissue replacement

Scaffolds	Material type	Advantages	Disadvantages
Poly (ethylene glycol) (PEG)	Synthetic	Biocompatible Proper mechanical property	Lack of cell integration
Polyethylene (glycol) Diacrylate (PEGDA)	Synthetic	Biocompatible Proper mechanical property	Lack of cell integration
Polycaprolactone (PCL)	Synthetic	Biocompatible Proper mechanical property	Low degradation rate
Poly(ethylene glycol)/Poly(acrylic acid) (PEG + PAA)	Synthetic	Biocompatible Proper mechanical property	Inducing inflammatory response
Poly(vinyl alcohol) (PVA)	Synthetic	Biocompatible Proper mechanical property	Low degradation rate Lack of cell integration
Poly(lactic-co-glycolic acid) (PLGA)	Synthetic	Proper mechanical property	Lack of cell integration
Collagen	Natural	Biodegradable Biocompatible	Difficult to sterilize without alterations
Gelatin	Natural	Biocompatible Low cost Low immunogenicity	Poor mechanical strength High degradation rate
Fibrin	Natural	Low cost Availability Good tolerance to cells	Poor mechanical strength High degradation rate
Chitosan	Natural	Nontoxic biodegradability Low toxicity Biocompatibility	Poor mechanical properties Quick degradation
Alginate	Natural	Biocompatibility Low cost Low immunogenicity	Stability Llack of binding sites
Hyaluronic acid	Natural	Easy to produce and modify nonadhesive Biodegradable	Poor mechanical strength High degradation rate

indirectly affect the corneal transparency [89]. The transparency of the cornea can be affected negatively when this highly organized alignment is disrupted. Another important effect on transparency is the cells in the stroma. ALDH1A1 and ALDH3A1 are the crystalline proteins in the cytoplasm and can decrease keratocyte capability to scatter light. The passage of light is going to disrupt when these cells are activated [90].

Corneal mechanical strength properties are changed with corneal thickness, curvature geometry of cornea, and corneal biomechanical factors [91]. Corneal stroma has

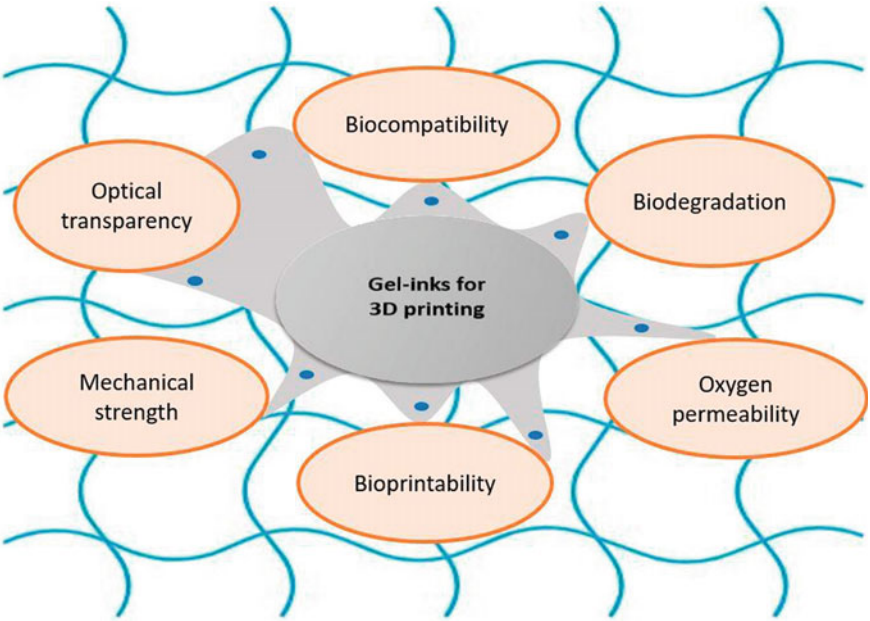

Fig. 3 Desired properties of gel-inks for cornea tissue replacement

an important role in biomechanical (viscoelastic, viscous, structural strength, elasticity, and integrity) properties of the cornea due to its highly aligned collagen fibrils structure. Biomechanical properties of the eye can also be impacted by microstructural changes in the cornea. Since the external forces in the cornea can form resistance and cause the deformation, corneal mechanical properties should be considered in the artificial cornea developments [92].

Briefly, stiffness of the cornea can be different between the people devolving on the strain, age, and place.

Following ex vivo results confirmed the biomechanical properties of the cornea [88].

1. At high strains, the cornea demonstrates a non-linear stress/strain feedback with continuous rigidify.
2. Different alignment and amount of collagen fibrils affect strain and deformation properties of the cornea due to its regional in-plane variation. The central cornea is softer than paracentral and peripheral cornea due to this variation.
3. Corneal elastic strength depends on the deepness with reducing stress from the prior to the ulterior stroma. Elastic modulus is changed from prior human cornea (82–530 kPa) to ulterior stroma (28–162 kPa) by indentation at 245–209 kPa, 100–61 kPa, respectively.

4. Corneal hardness is raised with the time, and it was determined that this value is 200 kPa for 50–65 years old and 700 kPa for 80–95 years old at 15 mmHg physiological intraocular pressure.

Biocompatibility can be operated by the interface between host living cells, tissues and foreign materials. Chemical structures of the polymers (e.g., hydrophilicity) used for artificial cornea stroma can affect the biocompatibility properties of the corneal stromal tissues. Chemical properties can determine the architecture of the tissues (porous nature, number of pores, and size). These possessions enhance the hydrophilicity of the matrix and diffusion of nutrient fluids and gases, which induces the cell attachment. The materials to fabricate the corneal scaffolds should not be cytotoxic and generate a host immune reaction. Since cornea has no blood or lymphatic vessels, keratoplasties are generally used due to its low immune rejection properties. However, it is still wrong for the immune reaction and suffers to rejection [90].

3.2 Biocompatible 3D-Printing Techniques for Bioinks Design

3D bioprinting is a developing technology used in regenerative medicine. With this technique, complex tissue constructs are developed to form native organ and tissue-like structures. It contains cell-laden biomaterials with designed geometry to fabricate functional tissues or organs in a layer by layer concept. Live cells, biomaterials, and controlled machine systems are combined to produce complex structures in this technique. It is more practical than other methods due to its ability to construct complex geometry, controllable porosity, and mechanical properties.

The thickness and curvature of the cornea are the key parameters for corneal refractive power. This special geometry of the cornea is important to build the personalized artificial cornea, and 3D bioprinting is an ideal method using the 3D model. 3D bioprinting provides to build a multi-material integration and constructs high strength scaffolds which contain bioinks with complex structures. Furthermore, the control of the surface property can be acquired during the fabrication system.

Multicell corneal patterns, cornea microstructure constructs and cornea regeneration are developed by 3D bioprinting. Since 3D printing provides to fabricate flexible models, with this technique multilayered, multicell, cell particular organization of curved structures can be achieved easily. 3D printing is the method to build all cornea layers with bioinks. There are four types of 3D bioprinting techniques to fabricated the cornea tissue, which are extrusion-based bioprinting, fused deposition modelling, inkjet printing, and laser-induced forward transfer (LIFT) (Fig. 4).

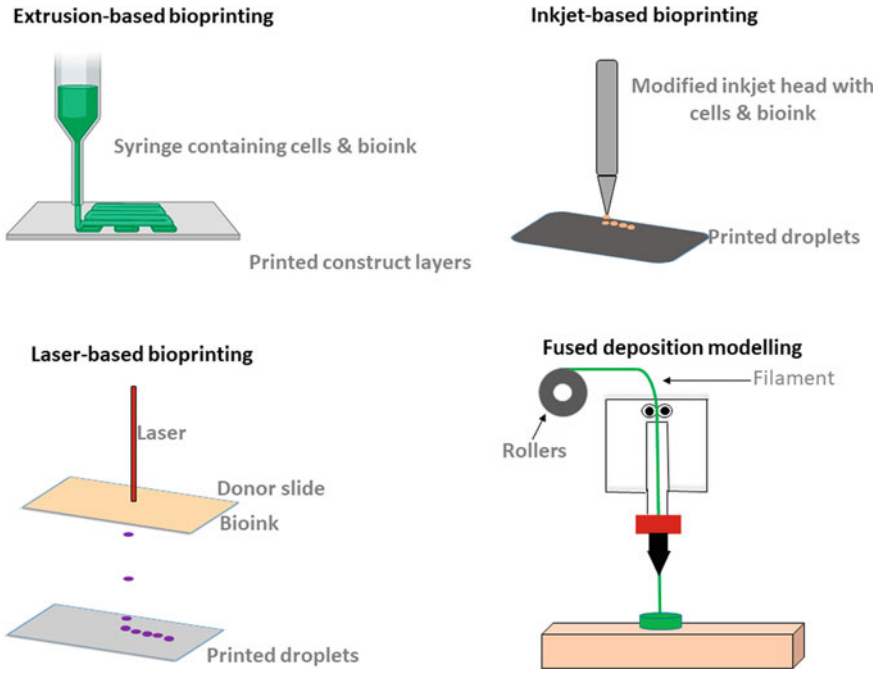

Fig. 4. 3D bioprinting techniques for construction of corneal stroma tissue

3.2.1 Extrusion-Based-Bioprinting

A continuous bioink stream is a part of micro-extrusion based bioprinting (Fig. 4). With this technique, constant accumulation of bioink enables superior structural integrity. In this printing technique, the cells with biomaterials are dispensed through needles or nozzles. The microextrusion head collects the material into the platform employing commands from design programs. Firstly, the drops are placed in the x–y control, and then extrusion control is started to move on the z-axis. This method allows using of the broad range of bioinks because micro nozzle sizes permit to fabricate high viscosity bioinks. The driven powers of the extrusion bioprinting are the screw, piston, or pneumatic pressures. The primary benefit of this method is that the high density of cells can be used with a quick fabrication rate.

On the other hand, this method also has the disadvantage that shear force arises in the cells. In the pressure-based system, the printing pressure can affect cell viability. Another factor impresses the viability is the nozzle diameter. Among these parameters, the critical optimization parameters are the concentration of the compounds, nozzle diameter, and pressure to solve these mentioned problems.

3.2.2 Inkjet Printing

This printing technique computer-based data or image is used, and this model is fabricated onto a substrate using ink drops (Fig. 4). This method has been widely used in electronics to construct electronic materials. It has a disadvantage because of its lower resolution than the lithographic process (20–250 mm). On the other hand, it also has various advantages. It is contact-free, mask-less, and direct designing model. Furthermore, it has 2–10 pL small deposition, decreased contamination due to the non-contact nature of the process. It has elastic, low precise, and amenable to ranging technique [93].

Thermal or acoustic forces are applied to fabricate the constructs that contain biological materials in specific locations during inkjet bioprinting. In thermal inkjet printing, the ink is sent away from the nozzle through air pressure created by heated components in the device.

Another inkjet printing is the acoustic inkjet systems, and in this system, ultrasound or piezoelectric actuators are used to generate the pulses. There are many advantages of this printing method, such as high construction speeds, 20–100 μm resolution, and low price. The drawbacks of this printing system are the low cell densities and low precision of droplet localization [94].

3.2.3 Laser-Induced Forward Transfer (LIFT)

LIFT is a nozzle-free and no contact printing method that shows great capacity with high resolution (Fig. 4). This printing technique permits to fabricate bioinks which have high viscosity, high resolution (<10 pL droplets), and high cell density without impressing viability of the cells. It is needed to use small nozzles (<100 μm diameter) to obtain high-resolution printing, this provides high cell concentration due to shear force on the cells. Moreover, it is possible to carry out the spatial structure of cells and employ various cell kinds in the same design [95].

Since LIFT can build micropatterning of a diversity of materials which can be inks, semiconductors, metals, oxides, organic materials, biomaterials, and other materials, it is a possible method for additive fabrication. Laser light is the driven force for this technique, and it is absorbed from the laser beam of a donor substance or sacrificed layer. This absorption causes the laser-induced change such as melting, heating, and ablation. High temperature and/or pressure and laser-induced transfer are used to induce a temporary excitation area. Temperature and/or pressure at high level moves the donor substance towards a receiver substratum [96].

3.2.4 Fused Deposition Modeling

One of the fast methods is the fused deposition modeling (FDM) which construct any design by the consecutive deposit of materials layer by layer (Fig. 4). This method uses heated thermoplastic filaments. Layer thickness (A), alignment (B), lattice angle

(C), lattice width (D), and lattice to lattice gap (E) are the main control factors that affect the strength of FDM. The details about these factors were given in below [97]:

(a) Orientation: It signifies to the tendency of the component in a build stand with X, Y, Z axis.
(b) The thickness of layer: It represents the thickness of layer sedimented by the nozzle, and it relies on the nozzle types.
(c) Lattice angle: It is a way of lattice related to the x-axis of build board.
(d) Lattice width: Width of the lattice model employed to load inner areas of part curves.
(e) Lattice to lattice distance: It is the distance between two neighbouring lattices on the exact layer.

4 Combination and Characterization of Gel-Inks for in Corneal Regeneration

This part will investigate the combination and characterization techniques of all studies found in the literature on produced gel-inks for 3D printing of corneal tissue given in Table 2 with material combinations and cells and in Fig. 5 with their images.

4.1 Rheological and Printability Examinations

Printability strongly depends on viscosity which affects the extrusion ability of the materials. It should be small enough to permit easy extrusion and be high to be stackable on organized layers.

Rheology properties of the gel inks are one of the required parameters for the gel-inks design. Viscosity is one of the test technique used to determine the rheological possessions of the inks. The viscosity values of the bioinks can directly affect the shape fidelity of printing and required pressure to distribute the material, which is essential for the cell viability. Cell viability and spread are also impressed by high amounts of shear force during the printing stage at long and immediate term.

Extrudability is another criterion for gel-inks printability. The adequate flow rate or print speed is important for achieving extrusion with dispensing pressure. In the cell-based 3D printing, checking the shear stress during the extrusion force has significance because different cell types have different sensitivity. A quantitative connection has not been created before between storage, loss modulus, and needed extrusion pressure. Furthermore, an ordinary technique to develop the bioink printability does not occur, yet [98].

In Campos et al. work [99], 3D corneal stromal models were fabricated with drop-on-demand bioprinting technique. Bioink was produced with a combination of corneal stromal keratocytes and collagen-based composite, and in vitro culture was

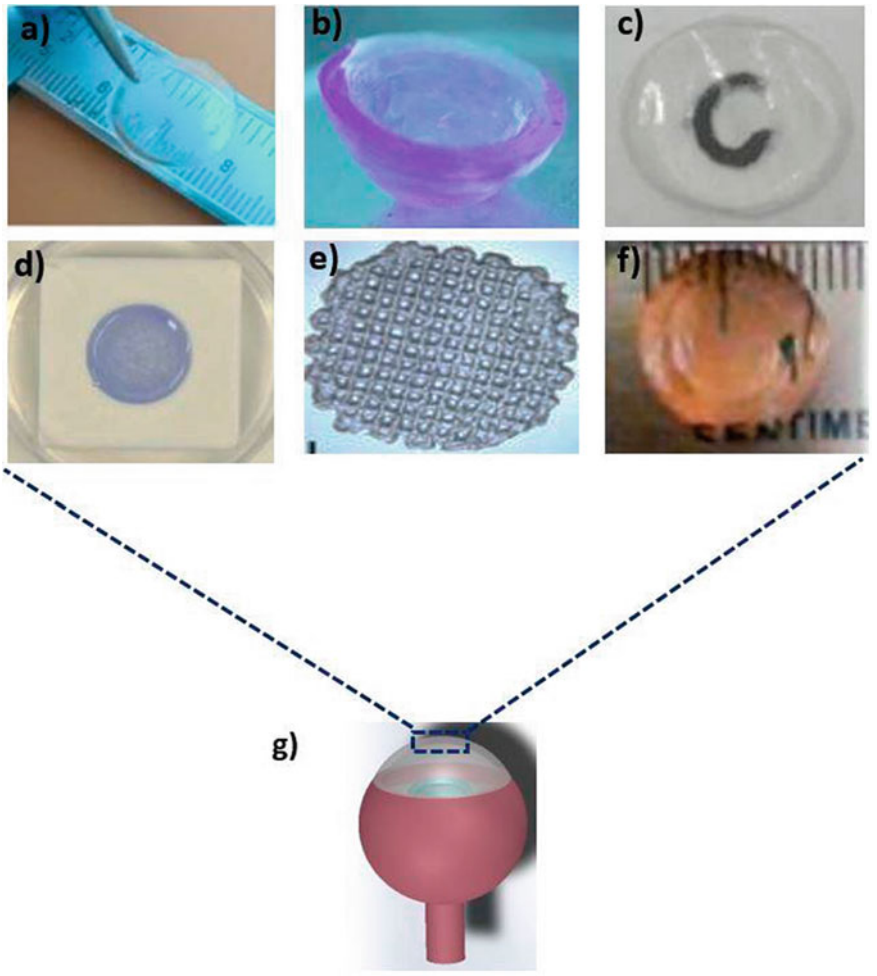

Fig. 5 The fabricated corneal tissues using 3D printing/bioprinting process: PVA/CS cornea stroma construct (**a**), CSK loaded bioprinted corneal stroma (**b**), the cornea stroma contaning gelatin type B, sodium alginate, and type I collagen (**c**), 3D bioprinted corneal structure consisted of collagen based bioink (**d**), 3D bioprinted cornea consisted of GELMA hydrogel (**e**), 3D printed cornea structure formed with GELMA hydrogel (**f**), te representative image of the eye (**g**)

carried out to decide the usefulness of the bioprinted constructs (Table 2). In this research, rotational rheometer with 4° rotational cone plate was utilized to quantify the rheological properties of nonprintable 0.3% collagen type I gel and bioprintable agarose (0.5%) with collagen (0.2%) gel mixes at 37 °C, 0.01–1 s^{-1} shear rates interval. According to the results, they found that bioinks had higher thickness compared with the neat collagen bioink. It had quicker gelation time, which shows that it is more precise bioprinting than pure collagen bioinks.

Within the Kim et al. work [100], they built a corneal stroma tissue containing corneal decellularized extracellular lattice (Co-dECM) and cells by 3D bioprinting process (Table 2). Progressed Rheometric Extension Framework was utilized to examine the rheological properties of 0.5, 1.0, 1.5, and 2% of Co-dECM gels. To calculate the thickness of the Co-dECM gel, the relentless shear clear examination was carried out at 15 °C. To supply the printable bioink for the 3D cell printing, the viscosity values of the inks ought to be over than 10 Pa.s. According to this study, Co-dECM gel with various concentrations showed shear-thinning behaviours in 1–1000 s^{-1} shear stress range, and larger viscosity range at 1 s^{-1} shear rate was observed for higher amount Co-dECM gel.

The viscosity values were 2.35, 3.83, 22.51, and 64.99 Pa.s for 0.5, 1, 1.5, and 2.0% Co-dECM, respectively, in their studies. The time for the gelatin were 2201, 1151, 504, and 252 s for 0.5, 1.0, 1.5, and 2.0% Co-dECM bioinks, respectively. This can be explained with that larger concentrations which can provide the easy crosslinking of gel which causes the shorter gelation time. It is found in this study that the time difference of gelation between the lowest and largest concentrations of the Co-dECM gels was 8.7-times.

In Kutlehria et al. work [101], they used high-throughput 3D bioprinting to fabricate the cornea stroma. To fabricate the cornea stroma, gelatin (type B), sodium alginate, and collagen (type I) were blended (Table 2). Rheological behaviours of the gels were examined with a rheometer. First of all, the gel-inks were incubated at 37 °C for 10 min. Then they were put into the plate and adjusted to 4 °C to arrive a steady form. The extra gel was removed from the plate before the conducting test. Oscillation temperature was changed from 4 to 40 °C with a 5 °C/min rate and 10.0 rad/s angular frequency. According to their reports, gelatin melted at the printing temperature higher than 37 °C and storage modulus of the bio-ink was decreased above this temperature value. Then again, printing temperature lower than 20 °C results in the high-pressure requirement to extrude the filament. This situation caused more pressure on the cells, and this is not suitable.

4.2 Light Transmission Examination

Light transmittance is another parameter that should be taken into about when three-dimensional scaffolds are produced for cornea regeneration. The central and peripheral regions of the cornea had different transmittance ability of UV light, which can cause damage to the retina. The curvature nature of the cornea can negatively affect the focusing of light, which can lead to vision decreased vision. Collagen fibril structure is a crucial effect on corneal transparency. Small and aligned collagen fibrils are the parts of the cornea stroma. This well-organized arrangement is critical for light to pass between the fibrils. If an injury or damage results in this arrangement, this causes a reduction in transparency. Another factor for transparency is the cells in the stroma. ALDH1A1 and ALDH3A1 are the crystalline proteins which decrease the

capacity of keratocytes to distribute light. The cells disordered the transition of light when the cells are actuated, which causes the reduction of proteins [90].

In Bektas et al. work [102], both cell-laden (1×106) and cell-free GELMA hydrogels were analyzed within the extend of 250–700 nm wavelength employing a UV spectrophotometer for 1, 7, 14, and 21 days. The background is scanned with a growth medium in the well. Transmittance values of the constructs were calculated from the subtraction of mean values of blanks from the constructs readings. They found about 75% transmittance value at 700 nm for cell-laden hydrogels on day 1. With the increment of culture time, the transmittance value of the hydrogels raised to around 83%. During the three weeks in culture, the transparency of cell-free and cell-loaded hydrogels showed 80% transmittance near the transparence value of the innate cornea (85%). In Ulag et al. study, PVA and Chitosan were combined to construct the artificial cornea (Table 2) using 3D printing, and light transmittance rate of the 3D-printed corneal stroma structures in this study was examined utilizing UV/VIS Spectrophotometer in the visible region. Before the measurement, the baseline was taken to minimize the background in the measurement, and the experiment was performed in the air. According to results in their study, all tests appeared about the same transmittance values, and with Chitosan addition, transmittance values reduced a bit [103].

Kim et al. created bioinks which have decellularized corneal extracellular matrix (Co-dECM) hydrogel and differentiated keratocytes [100]. In this work, light transmittance measurement was tested employing a microplate reader to decide the corneal transmittance values of the created structures. To begin with, of all, all samples were put into the plate, and extra fluid on the samples was taken off. The human cornea was decided as a control group of the test, and they were dehydrated in glycerol. 200-μm thickness value was decided for all samples, and the test was performed within the run of 300–700 nm wavelength. Each measurement was performed triplicate for each one, and the blank well was used as a reference.

In vivo, transparency was performed with ten healthy male rabbits (8 weeks old, 2 kg). 15 mg/mL ketamine and 5 mg/mL rumpun were used to anaesthetize the rabbits. According to their result, 25G corneal matrix samples showed enhanced transmission of the light in the visible region compare with Co-dECM hydrogel and the native cornea on day 28. This might be because newly synthesized ECMs perpendicularly stacked for 25G- constructs are different from original collagen fibrils. This circumstance enables more light rays to transfer over all wavelengths homogeneously. 25G implanted cornea demonstrated a more transparent structure in vivo than NP transplantation in this study.

In Mahdavi et al. study [39], Gelatin Methacrylate (GELMA) was blended with corneal stromal cells to manufacture bioink for corneal stroma equivalent (Table 2). The transparency features were analysed after cell encapsulation into the bioprinted scaffolds for 1, 3, and 7 days. The absorbance values of the samples were examined at four different wavelength range (450, 490, 570, 630 nm) with ELISA reader. The founded absorbance values in this test were used to find the transmission percentage of the samples using the Eq. (1).

$$\text{Transmission (\%)} = (10 - \text{absorbance}) \cdot 100 \quad (1)$$

Transmission range was recorded for both edge and centre of the bioprinted samples. Results appeared that innate cornea tissue had different transmittance values that change from 80 to 94% within the run of 450–600 nm wavelength and 95 to 98% within the extend of 600–1000 nm. The fabricated 12.5% GELMA had optical transmittance values of 80–95% (edge) and 78–90% (centre). The 7.5% GELMA demonstrated lower transmittance value than the native cornea for the centre and edge regions. However, the transmittance values found in this study still had less variation at the 700–1000 nm range [39].

In Kim et al. research, they built the corneal stroma tissue comprising decellularized extracellular matrix (Co-dECM) gel encapsulated with cells. A microplate reader was employed to evaluate the transparency possessions of the samples in this study. PG and samples produced with 25G nozzle were put into the plate to arrange nearly the same height of innate cornea, which is nearly 0.5 mm. Innate cornea dehydration with glycerol was selected as a control in the 300–700 nm wavelength interval in the transmittance test. Then, the samples were incubated in white media for 28 days. According to the results, PG had less transparency than 25GN (over than 75%, similar to the native cornea). They concluded that the aliened cells in 25GN enhance the light to transmit the human cornea [100].

In Kutlehria et al. study [101], microplate reader was used to examining the light transmittance values of the samples of wavelength at 300–700 nm. The bioink was dissolved at 37 °C and poured into a 48-well plate to coordinate the thickness and height values of the human cornea before the experiment. The blank was utilized as a reference to adjust the transmittance values. Results appeared that the transmittance of inks was an extend from 75 to 90%.

4.3 Mechanical Characterizations

Another important parameter for the cornea stroma engineering is the mechanical properties of the gel-inks. Intraocular pressure, eyelid and tear film motions are the physiological forces that the cornea should be highly enough to withstand across these forces.

The material hardness should not be very high, which can cause deformation when under stress and bringing a lack of harmony in strain. The viscoelastic properties of the cornea should be considered as these affect the behaviour of the cornea under force. It is ideal to obtain scaffolds which mechanical possessions should fit the innate corneas. Tissue anisotropy, various testing techniques, and donor variance can change the modulus of elasticity and tensile stress of cornea between researches (modulus of elasticity ≈100 kPa to 57 MPa; stress ≈3–6 MPa) [90].

In Bektas et al. study [102], 5 N load cell was used in the compression test with 1 mm/min displacement rate. The compressive modulus of the scaffolds was found from Harley, Leung, and Gibson method after samples arrived at the equilibrium

swelling capacity. This method suggested a technique that used the angle of the linear area of the stress–strain graph and calculated the compressive modulus using the Eqs. (2, 3, 4):

$$\text{Stress: } \sigma = F/A \tag{2}$$

$$\text{Strain: } \in = \Delta l/l \tag{3}$$

$$\text{Modulus of compression: } \sigma/\varepsilon \tag{4}$$

F is the force, A represents the area at the cross-sectional region, the initial length of the samples is l, and displacement is labelled as Δl.

According to their results, GELMA hydrogels had lower compressive modulus than native corneas, ranging from 403 to 624 kPa. However, it was reported that their results had still potential.

Uniaxial tensile testing was performed in Ulag et al. study [103] to find the mechanical possessions of the dry 3D-printed stroma constructs. In this test, both non-degradable and degrade 3D-printed corneal stroma samples were placed between the jaws. They found that fabricated corneal stroma constructs had enough tensile strength value, even the degraded samples.

Campos et al. also performed the compression testing to measure the stiffness off Agarose and Collagen tip I gel-inks (Table 2). In this test, discs (diameter 15 mm, height 20 mm) were fabricated for agarose (0.5%) and Type I collagen (0.2%) mold. 4 mm/min cross-speed was applied in the test, and samples were put onto the device platform and compressed until the break. In the elastic region (20% strain), the tangent of the stress/strain graph was employed to estimate the compressive modulus. In their results, compressive modulus of the produced bioink blends was 18.1 ± 3.5 kPa. According to the previous studies, it is known that native cornea has ~ 300 kPa compressive modulus value, and this work should be further enhanced to reach this value [99].

4.4 Biocompatibility Assessment

Biocompatibility is an important parameter to fabricate the corneal tissue equivalent and could occupy with native tissue without any immune problem [92]. The biocompatibility of the corneal stroma constructs can be determined by the LIVE/DEAD Viability/Cytotoxicity Kit. Sorkio et al. fabricated three parts of the cornea layers. The first layer consisted of corneal epithelium using hESC-LESCs. The second layer is the corneal stroma using hASCs and acellular layers of bioink, and cornea stroma construct stroma and epithelial portions (Table 2). LIVE/DEAD® Viability/Cytotoxicity Kit and PrestoBlue™ reagent were employed to determine the

Table 2 The fabricated gel-inks, cells and their fabrication techniques studied in the literature

Researchers	Gel-inks	Cells	Method
Bektas et al. [102]	Methacrylated gelatin (GELMA)	Human corneal keratocytes (HKs)	3D Bioprinting
Bektas et al. [102]	Methacrylated gelatin (GelMA) and poly(2-hydroxyethyl methacrylate) (pHEMA)	Human corneal keratocytes (HKs)	3D Bioprinting
Campos et al. [99]	Collagen tip I and agarose	Corneal stromal keratocytes (CSKs)	3D Bioprinting
Ulag et al. [103]	Polyvinyl-alcohol (PVA) and chitosan (CS)	Human adipose-derived mesenchymal stem cell (hADSCs)	3D Printing
Sorkio et al. [95]	–	Human embriyonic stem cell derived limbal epithelial stem cells (hESC-LESC) and human adipose tissue derived stem cells (hASCs)	Laser-assisted 3D bioprinting
Mahdavi et al. [39]	Methacrylated gelatin (GELMA) hydrogel	Corneal stromal cells	Stereolithography 3D Bioprinting
Kim et al. [80]	Corneal decellularized extracellular matrix (Co-dECM)	Human turbinate derived mesenchymal stem cells (hTMSCs)	3D cell printing
Kim et al. [100]	Corneal decellularized extracellular matrix (Co-dECM)	Human turbinate derived mesenchymal stem cells (hTMSCs)	3D cell printing
Kutlehria et al. [101]	Sodium alginate, gelatin type B, and type I collagen	Human corneal keratocyte (HCK)	High-throughput 3D bioprinting

cell viability of the constructs. Firstly, the hESC-LESC viability was carried out after three and seven days. After that hASCSs viability on the constructs were analysed. The PrestoBlueTM assay was performed with hESC-LESCs for one and seven days, and hASCs viability on 2D patterns was carried out for one and four days. 3D stromal structures were cultured at one, four, and seven days. The phase-contrast microscope was employed to see the cell morphology daily up to culture period. Immunofluorescence (IF) staining was applied to investigate the cell migration, cell morphology, and tissue morphology after culturing. In the cell culture method, DPBS was utilized to clean the corneal structures, and for fixation of the cells, 4% PFA was used during 1 h at room temperature.

Later, PBS was used to wash the samples and samples were incubated in + 4 °C with 20% sucrose solution during the night. They were cultured in Tissue-Tek OCT after incubation, and they were frozen in liquid at 80 °C. To prepare the samples to

the IF and histological stainings, samples were cut in the diameter of 7 mm. After that, they dried at air condition for 1 h at room temperature. Afterwards, they were cultured in BSA (3%) and Triton-X-100 (0.1%) for 1.5 h at 37 °C. According to their results, 3D bioprinted constructs showed high cell viability after printing, and just a few dead cells were observed. Also, they reported that laser-printed hESC-LESCs displayed epithelial cell morphology.

Cell culture protocol in Ulag et al. work [103] was performed with the human-derived adipose cells. In this procedure, the MTT assay was carried out with corneal structures for one, three, and seven days. Before the MTT assay, the constructs were purified by UV in the plate overnight. 4×10^4 cells and DMEM supported with 10% FBS and 0.1 mg/ml penicillin/streptomycin were cultured together for half an hour. Then, remaining liquid was thrown out with micropipette, and all constructs were collected. Cytotoxicity was carried out with a cytotoxicity detection kit in this method. The absorbance values were determined with ELISA reader (560 nm). The morphologies of the MSCs on the 3D-printed constructs were examined under a fluorescence microscope.

In the DAPI staining protocol, the growth medium was discarded from the plates and constructed with PBS. The fixation was performed with formaldehyde (4%) for half an hour. Then they were rinsed again. To dye the nucleus of the cells, DAPI (Invitrogen, 1 μg/ml) staining was applied, and they were incubated at room temperature for 20 min. As a final step, DAPI was taken off, and corneal structures were analysed by an inverted fluorescence microscope (Leica). SEM was utilized to remark the cell morphology on the constructs after fixation protocol. In the preparation step, the growth medium was taken and samples were stabled with 4% glutaraldehyde. After, they were rinsed with ethanol and dried in room conditions. According to the MTT results, they found that 3D-printed corneal constructs have the promising potential for the viability of MSCs. Moreover, SEM analysis also proved that hASCs were capable of adhering the surface of the 3D printed cornea constructs. These results reported that the combination of the materials could build the cornea stroma tissue cultured with stem cells.

Collagen tip I and agarose are the bioinks in Campos et al. study that were cultured with CSKs to analyse the live/dead cells on the gel-inks [99]. In this assay, cells (10^6 cells/ml) were trypsinized from the plates and they were embedded in bioinks added with agarose (0.5%) and type I Collagen (0.2%). Live/dead cells received by fluorescent staining (5% fluorescein diacetate, 5% propidium iodide) after one and seven days bioprinting and examined with a laser scanning microscope. Ti:Sapphire pulsed laser (800 nm) was used, and images were taken in the x–y axis and gathered at 1 μm. CSK-laden collagen was used as a control. To observe the CSK viability after the bioprinting, the corneal stromal constructs were put into the incubator for one and seven days. They were stained with FDA/PI to point outlive and dead cells, respectively. The results reported that most cells were viable after finishing of bioprinting. To reinforce the phenotype of CSK in bioprinted inks, lumican, keratocan, and smooth muscle actin antibodies were used to perform the immunocytochemical stainings. According to their results, CSK morphology in bioinks showed

the elongated structure of cells and parallel to each other to mimic the innate cornea tissue.

Bektas et al. [102] performed the cytotoxicity test with live/dead cell viability kit on the GELMA discs for 1, 2, 7, and 21 days. First of all, the growth medium was taken away from the plate, and constructs were double-dyed with calcein and ethidium homodimer for half an hour. Then, all samples were rinsed with PBS and investigated under confocal microscopy. The number of live and dead keratocytes in the hydrogels was determined via ImageJ NIH software according to the Eq. (5):

$$\text{Cell vability} = (\text{Live Cells (Green)})/(\text{Total Cells (Green} + \text{Red)}) \cdot 100. \quad (5)$$

Firstly, to stain the cells with DRAQ5 and Phalloidin, the medium into the GELMA hydrogel discs was throw away, and discs were resolved with 4% (w/v) paraformaldehyde for 30 min.

Triton X-100 was applied for five minutes at room temperature to permeabilize the cell membranes on the samples, and BSA was incubated with samples for 30 min. FITC-labelled Phalloidin was used to stain the cytoskeleton and put in an incubator. Then, the samples were rinsed with 0.1%BSA and DRAQ5 was used to dye the cells. Preparing the samples to the CLSM analysis, the samples were washed and stored in it. The primary antibodies, which are Collagen types I and V, biglycan, and decorin, were prepared in the immunofluorescence staining protocol. Then samples were cultured at 4 °C with these antibodies overnight. After that, samples were incubated with anti-rabbit/anti-mouse 488 secondary antibody. Then, DRAQ5 was applied to the nuclei of the cells at room temperature and waited in the incubator for 1 h. During the intensity measurements, the threshold was not applied. Normalized fluorescence intensity was calculated using the Eq. (6):

$$\text{Normalized Fluorescence Intensity} = I_{Ab}/I_{\text{DNA}} \quad (6)$$

I_{Ab} represents the intensity of the antibody, and I_{DNA} demonstrates the intensity of the DNA.

According to the biocompatibility results of this study, it was found that the cell counts in the structures didn't exchange importantly during the culture time. On the other hand, for GELMA15 hydrogels, cell numbers declined notably from 7th to 14th day. Moreover, they observed that loaded HKs in 3D printed hydrogels generally had round shapes.

Kutlehria et al. analyzed the viability of the cells for 1, 7, and 14 days with live/dead viability/cytotoxicity assay, which contained the 1% calcein and 4% ethidium bromide II. First of all, the medium was taken away, and the constructs were cleaned with HBSS (Hanks' Balanced Salt Solution). As a final stage, live/dead assay liquid was added to bioprinted corneal structures, then the plate was put into the incubator at 37 °C for half an hour. The samples were visualized with a fluorescent microscope, and Image J1 program was utilized to calculate the viability of the

cells on the samples. According to the live/dead test results, the percentages of cell viability were 96% on day 1 and 86% on day 14.

Kutlehria et al. [101] performed the Alamar blue test to examine the cell count/proliferation on the constructs. Firstly, HBSS was applied to clean the corneas, then Alamar blue dye was put into the wells. After that, the plates were kept into the CO_2 incubator for 4 h. In the following step, 100 μl medium was taken and put into the well plate. The fluorescent intensity was obtained at 590 nm, 560 nm, and 570 nm using a microplate reader. They analyzed the cell viability for 1, 10, 14 days in their studies. They found that maximum cell viability obtained from the optimum combination of collagen and gelatin. They managed to keep the cells alive for two weeks.

4.5 Oxygen Permeability

The advance of materials with essential oxygen permeability, most importantly hydrogels, strict gas permeables and silicone hydrogels, gives an increasing range of choices to support clinicians avoid hypoxia outcomes [104]. In Ulag et al. study, oxygen permeability test on the 3D-printed cornea stroma structures (13%PVA, 13%PVA/(1, 3, 5)%CS) was carried out with perm O2 single cell. In this test, the corneal structures were put onto a metal surface using epoxy glue. The test was done at 23 °C, 60% room humidity conditions with 100% oxygen gas from both sides. According to their results, they found no noticeable changes in oxygen permeability values of the constructs [103].

5 Conclusion and Future Perspectives

The main objective of cornea tissue regeneration is to design and fabricate an artificial cornea. Both naturally-derived and synthetic biomaterials and their gel forms combining with cells have been utilized to renew the pathological corneas. Naturally derived corneal constructs have advantages for a long-continued outcome to reach human clinical examinations. Additionally, cell-based advances may also be reasonable choices for both cornea regeneration. To build full-thickness artificial cornea with complex structure, 3D bioprinting is an ideal and developing technology which permits the study of cornea tissue-like constructs using gel-inks. In this chapter, many works related to three-dimensional artificial cornea formed with gel-inks and their characterizations were reviewed and discussed. Researches reported that synthetic and naturally derived biomaterials, and their combinations can potentially be gel-inks for cornea tissue replacement. However, more additional efforts should be performed to combine the materials with systems to mimic the human cornea, both physiologically and morphologically and enable enough time to the implants to regenerate the damaged cornea effectively.

Acknowledgements The authors thank Marmara University Scientific Research Committee (Project Numbers: FDK-2020-10117) for their support.

References

1. Chen Z, You J, Liu X, Cooper S, Hodge C, Sutton G, Wallace GG (2018) Biomaterials for corneal bioengineering. Biomed Mater 13(3):032002
2. Rüfer F, Schröder A, Erb C (2005) White-to-white corneal diameter: normal values in healthy humans obtained with the Orbscan II topography system. Cornea 24(3):259–261
3. Fares U, Otri AM, Al-Aqaba MA, Dua HS (2012) Correlation of central and peripheral corneal thickness in healthy corneas. Cont Lens Anterior Eye 35(1):39–45
4. Sridhar MS (2018) Anatomy of cornea and ocular surface. Indian J Ophthalmol 66(2):190
5. DelMonte DW, Kim T (2011) Anatomy and physiology of the cornea. J Cataract Refract Surg 37(3):588–598
6. Streilein JW (1990) Anterior chamber associated immune deviation: the privilege of immunity in the eye. Surv Ophthalmol 35(1):67–73
7. Smelser GK, Ozanics V (1965) New concepts in anatomy and histology of the cornea. In: The Cornea World Congress. London (pp 1–20)
8. Eghrari AO, Riazuddin SA, Gottsch JD (2015) Overview of the cornea: structure, function, and development. In: Progress in molecular biology and translational science, vol 134. Academic Press, pp 7–23
9. Germundsson J, Karanis G, Fagerholm P, Lagali N (2013) Age-related thinning of Bowman's layer in the human cornea in vivo. Invest Ophthalmol Vis Sci 54(9):6143–6149
10. Kermani O, Fabian W, Lubatschowski H (2008) Real-time optical coherence tomography-guided femtosecond laser sub-Bowman keratomileusis on human donor eyes. Am J Ophthalmol 146(1):42–45
11. Linsenmayer TF, Fitch JM, Gordon MK, Cai CX, Igoe F, Marchant JK, Birk DE (1998) Development and roles of collagenous matrices in the embryonic avian cornea. Prog Retin Eye Res 17(2):231–265
12. Tisdale AS, Spurr-Michaud SJ, Rodrigues M, Hackett J, Krachmer J, Gipson IK (1988) Development of the anchoring structures of the epithelium in rabbit and human fetal corneas. Invest Ophthalmol Vis Sci 29(5):727–736
13. Wilson SE (2020) Bowman's layer in the cornea–structure and function and regeneration. Exper Eye Res 108033
14. Tong CM, van Dijk K, Melles GR (2019) Update on Bowman layer transplantation. Curr Opin Ophthalmol 30(4):249–255
15. Sayers Z, Koch MH, Whitburn SB, Meek KM, Elliott GF, Harmsen A (1982) Synchrotron X-ray diffraction study of corneal stroma. J Mol Biol 160(4):593–607
16. Meek KM, Boote C (2004) The organization of collagen in the corneal stroma. Exp Eye Res 78(3):503–512
17. Hassell JR, Birk DE (2010) The molecular basis of corneal transparency. Exp Eye Res 91(3):326–335
18. Jester JV (2008) Corneal crystallins and the development of cellular transparency. In: Seminars in cell & developmental biology, vol 19, no 2. Academic Press, pp 82–93
19. Pinnamaneni N, Funderburgh JL (2012) Concise review: stem cells in the corneal stroma. Stem cells 30(6):1059–1063
20. Espana EM, Birk DE (2020) Composition, structure and function of the corneal stroma. Exper Eye Res 108137
21. Hertsenberg AJ, Funderburgh JL (2015) Stem cells in the cornea. In" Progress in molecular biology and translational science, vol 134. Academic Press, pp 25–41

22. Ginhoux F, Guilliams M (2016) Tissue-resident macrophage ontogeny and homeostasis. Immunity 44(3):439–449
23. Steinman RM (2012) Decisions about dendritic cells: past, present, and future. Annu Rev Immunol 30:1–22
24. Gao N, Yin J, Yoon GS, Mi QS, Fu-Shin XY (2011) Dendritic cell–epithelium interplay is a determinant factor for corneal epithelial wound repair. Am J Pathol 179(5):2243–2253
25. Birk DE, Brückner P (2011) Collagens, suprastructures, and collagen fibril assembly. In: The extracellular matrix: an overview. Springer, Berlin, Heidelberg, pp 77–115
26. Raghunathan V, McKee C, Cheung W, Naik R, Nealey PF, Russell P, Murphy CJ (2013) Influence of extracellular matrix proteins and substratum topography on corneal epithelial cell alignment and migration. Tissue Eng Part A 19(15–16):1713–1722
27. Smith SM, Birk DE (2012) Focus on molecules: collagens V and XI. Exp Eye Res 98(1):105
28. Feneck EM, Lewis PN, Meek KM (2020) Identification of a Primary Stroma and Novel Endothelial Cell Projections in the Developing Human Cornea. Invest Ophthalmol Vis Sci 61(6):5–5
29. Jeang L, Cha BJ, Birk DE, Espana EM (2020) Endothelial–stromal communication in murine and human corneas. The Anatomical Record
30. Noske W, Levarlet B, Kreusel KM, Fromm M, Hirsch M (1994) Tight junctions and paracellular permeability in cultured bovine corneal endothelial cells. Graefes Arch Clin Exp Ophthalmol 232(10):608–613
31. Cardozo OL (1979) Cellular density of normal corneal endothelium. Doc Ophthalmol 46(2):201–206
32. Bonanno JA (2012) Molecular mechanisms underlying the corneal endothelial pump. Exp Eye Res 95(1):2–7
33. Roy O, Leclerc VB, Bourget JM, Thériault M, Proulx S (2015) Understanding the process of corneal endothelial morphological change in vitro. Invest Ophthalmol Vis Sci 56(2):1228–1237
34. Ghezzi CE, Rnjak-Kovacina J, Kaplan DL (2015) Corneal tissue engineering: recent advances and future perspectives. Tissue Eng Part B Rev 21(3):278–287
35. Duval K, Grover H, Han LH, Mou Y, Pegoraro AF, Fredberg J, Chen Z (2017) Modeling physiological events in 2D vs. 3D cell culture. Physiology 32(4), 266–277
36. Shaharuddin B, Meeson A. (2015) Current perspectives on tissue engineering for the management of limbal stem cell deficiency. J Stem Cells Res Rev Rep
37. El-Sherbiny IM, Yacoub MH (2013) Hydrogel scaffolds for tissue engineering: Progress and challenges. Glob Cardiol Sci Pract 2013(3):38
38. Kishore V, Alapan Y, Iyer R, Mclay R, Gurkan UA (2016) Application of hydrogels in ocular tissue engineering. In GELS HANDBOOK: fundamentals, properties and applications volume 2: applications of hydrogels in regenerative medicine, pp 137–164.
39. Mahdavi SS, Abdekhodaie MJ, Mashayekhan S, Baradaran-Rafii A, Djalilian AR (2020) Bioengineering approaches for corneal regenerative medicine. Tissue Eng Regener Med 1–27
40. Wang JH, Hung CH, Young TH (2006) Proliferation and differentiation of neural stem cells on lysine–alanine sequential polymer substrates. Biomaterials 27(18):3441–3450
41. Chen G, Ushida T, Tateishi T (2002) Scaffold design for tissue engineering. Macromol Biosci 2(2):67–77
42. Duan X, Sheardown H (2006) Dendrimer crosslinked collagen as a corneal tissue engineering scaffold: mechanical properties and corneal epithelial cell interactions. Biomaterials 27(26):4608–4617
43. Orwin EJ, Hubel A (2000) In vitro culture characteristics of corneal epithelial, endothelial, and keratocyte cells in a native collagen matrix. Tissue Eng 6(4):307–319
44. Park CY, Lee JK, Gore PK, Lim CY, Chuck RS (2015) Keratoplasty in the United States: a 10-year review from 2005 through 2014. Ophthalmology 122(12):2432–2442
45. Chen FM, Liu X (2016) Advancing biomaterials of human origin for tissue engineering. Prog Polym Sci 53:86–168

46. Lutolf MP, Hubbell JA (2005) Synthetic biomaterials as instructive extracellular microenvironments for morphogenesis in tissue engineering. Nat Biotechnol 23(1):47–55
47. Benoit DS, Schwartz MP, Durney AR, Anseth KS (2008) Small functional groups for controlled differentiation of hydrogel-encapsulated human mesenchymal stem cells. Nat Mater 7(10):816–823
48. Singh A, Zhan J, Ye Z, Elisseeff JH (2013) Modular multifunctional poly (ethylene glycol) hydrogels for stem cell differentiation. Adv Func Mater 23(5):575–582
49. Seliktar D (2012) Designing cell-compatible hydrogels for biomedical applications. Science 336(6085):1124–1128
50. Saraf A, Lozier G, Haesslein A, Kasper FK, Raphael RM, Baggett LS, Mikos AG (2009) Fabrication of nonwoven coaxial fiber meshes by electrospinning. Tissue Eng Part C Methods 15(3):333–344
51. Moutos FT, Freed LE, Guilak F (2007) A biomimetic three-dimensional woven composite scaffold for functional tissue engineering of cartilage. Nat Mater 6(2):162–167
52. Rnjak-Kovacina J, Wray LS, Burke KA, Torregrosa T, Golinski JM, Huang W, Kaplan DL (2015) Lyophilized silk sponges: a versatile biomaterial platform for soft tissue engineering. ACS Biomater Sci Eng 1(4):260–270
53. Dahlin RL, Kinard LA, Lam J, Needham CJ, Lu S, Kasper FK, Mikos AG (2014) Articular chondrocytes and mesenchymal stem cells seeded on biodegradable scaffolds for the repair of cartilage in a rat osteochondral defect model. Biomaterials 35(26):7460–7469
54. Kobayashi H (2007) Surface modified poly (vinyl alcohol) nanofiber for the artificial corneal stroma. In: Key engineering materials, vol 342. Trans Tech Publications Ltd., pp. 209–212
55. Zainuddin BZ, Keen I, Hill DJ, Chirila TV, Harkin DG (2008) PHEMA hydrogels modified through the grafting of phosphate groups by ATRP support the attachment and growth of human corneal epithelial cells. J Biomater Appl 23(2):147–168
56. Yanez-Soto B, Liliensiek SJ, Murphy CJ, Nealey PF (2013) Biochemically and topographically engineered poly (ethylene glycol) diacrylate hydrogels with biomimetic characteristics as substrates for human corneal epithelial cells. J Biomed Mater Res Part A 101(4):1184–1194
57. Kim EY, Tripathy N, Cho SA, Lee D, Khang G (2017) Collagen type I-PLGA film as an efficient substratum for corneal endothelial cells regeneration. J Tissue Eng Regen Med 11(9):2471–2478
58. Zhang Q, Fang Z, Cao Y, Du H, Wu H, Beuerman R, Xu R (2012) High refractive index inorganic–organic interpenetrating polymer network (IPN) hydrogel nanocomposite toward artificial cornea implants. ACS Macro Lett 1(7), 876-881
59. Hartmann L, Watanabe K, Zheng LL, Kim CY, Beck SE, Huie P, Frank CW (2011) Toward the development of an artificial cornea: improved stability of interpenetrating polymer networks. J Biomed Mater Res B Appl Biomater 98(1):8–17
60. Ozcelik B, Brown KD, Blencowe A, Ladewig K, Stevens GW, Scheerlinck JPY, Qiao GG (2014) Biodegradable and biocompatible poly (ethylene glycol)-based hydrogel films for the regeneration of corneal endothelium. Adv Healthcare Mater 3(9):1496–1507
61. Ortega Í, Deshpande P, Gill AA, MacNeil S, Claeyssens F (2013) Development of a microfabricated artificial limbus with micropockets for cell delivery to the cornea. Biofabrication 5(2):025008
62. Sharma S, Mohanty S, Gupta D, Jassal M, Agrawal AK, Tandon R (2011) Cellular response of limbal epithelial cells on electrospun poly-ε-caprolactone nanofibrous scaffolds for ocular surface bioengineering: a preliminary in vitro study. Mol Vis 17:2898
63. Luo Zheng L, Vanchinathan V, Dalal R, Noolandi J, Waters DJ, Hartmann L, Ta CN (2015) Biocompatibility of poly (ethylene glycol) and poly (acrylic acid) interpenetrating network hydrogel by intrastromal implantation in rabbit cornea. J Biomed Mater Res Part A 103(10):3157–3165
64. Fenglan X, Yubao L, Xiaoming Y, Hongbing L, Li Z (2007) Preparation and in vivo investigation of artificial cornea made of nano-hydroxyapatite/poly (vinyl alcohol) hydrogel composite. J Mater Sci Mater Med 18(4):635–640

65. Stoppel WL, Ghezzi CE, McNamara SL, Black LD III, Kaplan DL (2015) Clinical applications of naturally derived biopolymer-based scaffolds for regenerative medicine. Ann Biomed Eng 43(3):657–680
66. Meek KM (2009) Corneal collagen—its role in maintaining corneal shape and transparency. Biophys Rev 1(2):83–93
67. Robert L, Legeais JM, Robert AM, Renard G (2001) Corneal collagens. Pathol Biol (Paris) 49(4):353–363
68. Ahearne M, Fernández-Pérez J, Masterton S, Madden PW, Bhattacharjee P (2020) Designing scaffolds for corneal regeneration. Adv Funct Mater 1908996
69. Palchesko RN, Funderburgh JL, Feinberg AW (2016) Engineered basement membranes for regenerating the corneal endothelium. Adv Healthcare Mater 5(22):2942–2950
70. Liu Y, Liu X, Wu M, Ji P, Lv H, Deng L (2019) A collagen film with micro-rough surface can promote the corneal epithelization process for corneal repair. Int J Biol Macromol 121:233–238
71. Kilic C, Girotti A, Rodriguez-Cabello JC, Hasirci V (2014) A collagen-based corneal stroma substitute with micro-designed architecture. Biomater Sci 2(3):318–329
72. Echave CM, Burgo L, Pedraz LJ, Orive G (2017) Gelatin as biomaterial for tissue engineering. Curr Pharm Des 23(24):3567–3584
73. Rose JB, Pacelli S, Haj AJE, Dua HS, Hopkinson A, White LJ, Rose FR (2014) Gelatin-based materials in ocular tissue engineering. Materials 7(4):3106–3135
74. Sun M, Sun X, Wang Z, Guo S, Yu G, Yang H (2018) Synthesis and properties of gelatin methacryloyl (GelMA) hydrogels and their recent applications in load-bearing tissue. Polymers 10(11):1290
75. Sani ES, Kheirkhah A, Rana D, Sun Z, Foulsham W, Sheikhi A, Annabi N (2019) Sutureless repair of corneal injuries using naturally derived bioadhesive hydrogels. Sci Adv 5(3):eaav1281
76. Guhan S, Peng SL, Janbatian H, Saadeh S, Greenstein S, Al Bahrani F, Melki SA (2018) Surgical adhesives in ophthalmology: history and current trends. Br J Ophthalmol 102(10):1328–1335
77. Scalcione C, Ortiz-Vaquerizas D, Said DG, Dua HS (2018) Fibrin glue as agent for sealing corneal and conjunctival wound leaks. Eye 32(2):463–466
78. Rico-Sánchez L, Garzón I, González-Andrades M, Ruíz-García A, Punzano M, Lizana-Moreno A, Sanchez-Pernaute R (2019) Successful development and clinical translation of a novel anterior lamellar artificial cornea. J Tissue Eng Regen Med 13(12):2142–2154
79. Alaminos M, Sánchez-Quevedo MDC, Munoz-Ávila JI, Serrano D, Medialdea S, Carreras I, Campos A (2006) Construction of a complete rabbit cornea substitute using a fibrin-agarose scaffold. Invest Ophthalmol Vis Sci 47(8):3311–3317
80. Kim CH, Park SJ, Yang DH, Chun HJ (2018) Chitosan for tissue engineering. In: Novel biomaterials for regenerative medicine. Springer, Singapore, pp 475–485
81. de la Mata A, Nieto-Miguel T, López-Paniagua M, Galindo S, Aguilar MR, García-Fernández L, Calonge M (2013) Chitosan–gelatin biopolymers as carrier substrata for limbal epithelial stem cells. J Mater Sci Mater Med 24(12):2819–2829
82. Guan L, Ge H, Tang X, Su S, Tian P, Xiao N, Liu P (2013) Use of a silk fibroin-chitosan scaffold to construct a tissue-engineered corneal stroma. Cells Tissues Organs 198(3):190–197
83. Tonsomboon K, Oyen ML (2013) Composite electrospun gelatin fiber-alginate gel scaffolds for mechanically robust tissue engineered cornea. J Mech Behav Biomed Mater 21:185–194
84. Chen D, Qu Y, Hua X, Zhang L, Liu Z, Pflugfelder SC, Li DQ (2017) A hyaluronan hydrogel scaffold-based xeno-free culture system for ex vivo expansion of human corneal epithelial stem cells. Eye 31(6):962–971
85. Lai JY, Cheng HY, Ma DHK (2015) Investigation of overrun-processed porous hyaluronic acid carriers in corneal endothelial tissue engineering. PLoS One 10(8):e0136067
86. Lu PL, Lai JY, Ma DHK, Hsiue GH (2008) Carbodiimide cross-linked hyaluronic acid hydrogels as cell sheet delivery vehicles: characterization and interaction with corneal endothelial cells. J Biomater Sci Polym Ed 19(1):1–18

87. Tummala GK, Lopes VR, Mihranyan A, Ferraz N (2019) Biocompatibility of nanocellulose-reinforced PVA hydrogel with human corneal epithelial cells for ophthalmic applications. J Funct Biomater 10(3):35
88. Fuest M, Yam GHF, Mehta JS, Duarte Campos DF (2020) Prospects and challenges of translational corneal bioprinting. Bioengineering 7(3):71
89. Hayes S, Lewis P, Islam MM, Doutch J, Sorensen T, White T, Meek KM (2015) The structural and optical properties of type III human collagen biosynthetic corneal substitutes. Acta Biomater 25:121–130
90. Ahearne M, Fernández-Pérez J, Masterton S, Madden PW, Bhattacharjee P (2020) Designing scaffolds for corneal regeneration. Adv Funct Mater 1908996
91. Pešić S, Jovanović S, Mitrašević M, Vuletić B, Jovanović M, Jovanović Z (2017) The impact of silicone hydrogel contact lenses on the measurement of intraocular pressure using non-contact tonometry. Vojnosanit Pregl 74(8):763–766
92. Zhang B, Xue Q, Li J, Ma L, Yao Y, Ye H, Yang H (2019) 3D bioprinting for artificial cornea: challenges and perspectives. Med Eng Phys 71:68–78
93. Saunders RE, Derby B (2014) Inkjet printing biomaterials for tissue engineering: bioprinting. Int Mater Rev 59(8):430–448
94. Prina E, Mistry P, Sidney LE, Yang J, Wildman RD, Bertolin M, Dua HS (2017) 3D microfabricated scaffolds and microfluidic devices for ocular surface replacement: a review. Stem Cell Rev Rep 13(3):430–441
95. Sorkio A, Koch L, Koivusalo L, Deiwick A, Miettinen S, Chichkov B, Skottman H (2018) Human stem cell based corneal tissue mimicking structures using laser-assisted 3D bioprinting and functional bioinks. Biomaterials 171:57–71
96. Narazaki A, Oyane A, Komuro S, Kurosaki R, Kameyama T, Sakamaki I, Miyaji H (2019) Bioactive micropatterning of apatite immobilizing cell adhesion protein by laser-induced forward transfer with a shock absorber. Optic Mater Express 9(7):2807–2816
97. Sood AK, Ohdar RK, Mahapatra SS (2010) Parametric appraisal of mechanical property of fused deposition modelling processed parts. Mater Des 31(1):287–295
98. Gao T, Gillispie GJ, Copus JS, Pr AK, Seol YJ, Atala A, Lee SJ (2018) Optimization of gelatin–alginate composite bioink printability using rheological parameters: a systematic approach. Biofabrication 10(3):034106
99. Campos DF, Rohde M, Ross M, Anvari P, Blaeser A, Vogt M, Walter P (2019) Corneal bioprinting utilizing collagen-based bioinks and primary human keratocytes. J Biomed Mater Res Part A 107(9):1945–1953
100. Kim H, Jang J, Park J, Lee KP, Lee S, Lee DM, Cho DW (2019) Shear-induced alignment of collagen fibrils using 3D cell printing for corneal stroma tissue engineering. Biofabrication 11(3):035017
101. Kutlehria S, Dinh TC, Bagde A, Patel N, Gebeyehu A, Singh M (2020) High-throughput 3D bioprinting of corneal stromal equivalents. J Biomed Mater Res Part B Appl Biomater
102. Bektas CK, Hasirci V (2020) Cell loaded 3D bioprinted GelMA hydrogels for corneal stroma engineering. Biomater Sci 8(1):438–449
103. Ulag S, Ilhan E, Sahin A, Yilmaz BK, Ekren N, Kilic O, Gunduz O (2020) 3D printed artificial cornea for corneal stromal transplantation. Eur Polym J 109744
104. Papas EB (2014) The significance of oxygen during contact lens wear. Cont Lens Anterior Eye 37(6):394–404

Chapter 6
Three Dimensional (3D) Printable Gel-Inks for Skin Tissue Regeneration

Simin Nazarnezhad, Sara Hooshmand, Francesco Baino, and Saeid Kargozar

Abstract Recent and rapid progression in three-dimensional (3D) printing techniques has revolutionized conventional therapies in medicine; 3D printed constructs are gradually being recognized as common substitutes for the replacement of skin wounds. As gel-inks, large numbers of natural and synthetic (e.g., collagen and polyurethane, respectively) substances were used to be printed into different shapes and sizes for managing both acute and chronic skin wounds. The resultant 3D printed scaffolds not only provide physical support but also act as supporting niches for improving immunomodulation and vascularization and subsequent accelerated wound healing. Recently, the use of thermosensitive and pH-responsive gels has made it possible to prepare 3D printed constructs with the ability to facilitate in situ crosslinking within the biopolymer and with native wound edge tissue as well as to fill the exact shape of wound damage. In this chapter, we aim to introduce the current state of 3D printable gel-inks utilized for skin wound treatment and illustrate future prospects in this amazing area of science.

Keywords Three dimensional (3D) printing · Additive manufacturing · Gel-inks · Skin tissue engineering · Wound healing

S. Nazarnezhad · S. Kargozar (✉)
Tissue Engineering Research Group (TERG), Department of Anatomy and Cell Biology, School of Medicine, Mashhad University of Medical Sciences, 917794-8564 Mashhad, Iran
e-mail: kargozarsaeid@gmail.com

S. Hooshmand
Pharmacological Research Center of Medicinal Plants, Mashhad University of Medical Sciences, 917794-8564 Mashhad, Iran

Faculty of Medicine, Department of Pharmacology, Mashhad University of Medical Sciences, 917794-8564 Mashhad, Iran

S. Hooshmand
e-mail: s_hooshmand@yahoo.com

F. Baino
Institute of Materials Physics and Engineering, Applied Science and Technology Department, Politecnico di Torino, Corso Duca degli Abruzzi 24, 10129 Torino, Italy
e-mail: francesco.baino@polito.it

A. Kumar et al. (eds.), *3D printable Gel-inks for Tissue Engineering*, Gels Horizons: From Science to Smart Materials, https://doi.org/10.1007/978-981-16-4667-6_6

1 Introduction

The skin, the largest organ of the human body, forms nearly 15% of total body weight in human adults. Similar to other organs, the skin is composed of extracellular matrix (ECM) and various cell types, which exert structural and functional activities. In fact, the skin makes the outermost layer of the body (covering other tissues and organs) and plays pivotal roles in the protection (UV light absorption, mechanical support, and immune surveillance), perception (temperature, pain, and touch), and regulatory mechanisms (hemostasis, thermal, hydration, and excretory) of the body [1]. Human skin comprises two major layers, the epidermis and the dermis, and a third region called subcutaneous tissue. The major constituents of the epidermal layer are keratinocytes, which generate a stratified epithelium and undergo terminal differentiation to generate functional mature keratinocytes [2, 3]. This layer resides onto the basement membrane, separating the epidermis from the dermis. The dermis is made of ECM, containing mostly collagen synthesized by fibroblasts [4].

The skin is the outermost tissue of the body which is highly susceptible to environmental stresses, leading to a wide range of skin injuries generated by acute trauma, thermal, mechanical, chemical, microbial, and radiation issues. Furthermore, skin injuries can be caused by genetic disorders, surgical interventions, and chronic wounds [5, 6]. Depending on the extension and depth of skin damage, the epidermis or dermis may be affected, especially in third-degree burns and full-thickness wounds, which could lead to high morbidity and mortality [7].

Numerous skin substitutes and wound care products have been developed to be used in managing different types of skin injuries. Traditional therapeutics rely on utilizing the epidermal, dermal, or dermo-epidermal substitutes by processing auto-, allo-, and xenografts that provide a highly resemble replacement for damaged tissue [8]. However, there are a few limitations with these biological substitutes, including their time-consuming fabrication, lack of donor tissue, and the risk of immunological rejection and pathogen transmission. Therefore, advanced bioengineered constructs with high regenerative capacity have emerged as promising alternatives to the traditional substitutes. Regarding skin nature, the use of biocompatible polymers (natural and synthetic) resulted in the best clinical outcomes. Collagen, gelatin, and alginate are among the widely used natural polymers for skin wound healing, whereas poly(ε-caprolactone) and polyurethane are extensively applied for managing dermal injuries. In order to take optimal results, the mentioned biopolymers should be utilized as three dimensional (3D) constructs; 3D printed polymeric scaffolds are excellent patient-specific substitutes for skin tissue engineering. A series of 3D printing methods (e.g., extrusion-, laser-assisted routes) was well-used for fabricating effective skin replacements. Apart from the method, the type of printable gel-inks is of utmost importance as to their critical roles in determining physico-chemical, mechanical, and biological properties of the final products. In this chapter, skin tissue is initially introduced structurally, and functionality and then different printable polymeric gel-inks are presented and discussed.

2 Skin: A Histological Overview

Understanding the anatomical and physiological functions of the skin is of great importance for researchers aiming to prepare tissue substitutes used in the repair and regeneration of skin wounds. The skin tissue has a very complex multi-layered structure containing ECM components, capillary networks, nerves, appendages (e.g., hair follicles and sweat glands), and various cells. It is well known that the ECM is the most constituent of the skin, contributing to the formation of an integrated tissue both structurally and functionally. In particular, the ECM components can provide a favorable substrate for cell attachment and migration, as well as nutrient and metabolite exchanges. Furthermore, the polysaccharides, proteins, and water available in the ECM contribute to the tensile strength and elasticity of the skin as a result of generating a gel-like network [9].

As shown in Fig. 1, the skin is structurally made of three distinct layers, i.e., the epidermis, dermis, and hypodermis (also named subcutaneous tissue). The main constituents of these layers are summarized in Table 1 and will be discussed in the details in the following sections.

2.1 Epidermis

The epidermis is a stratified squamous epithelium with a high proliferation capacity which can regenerate itself routinely. The epidermis is mostly composed of keratinocytes (up to 95%) (Fig. 1a), while other cell types are found in this layer, including small populations of Langerhans cells, melanocytes, Merkel cells, and unmyelinated axons. Keratinocytes originate from the cells located in the stratum basal and migrate up toward the stratum corneum and progressively differentiate. According to the differentiation stage of keratinocytes, the epidermis is divided into four functionally separate layers, including the stratum basal (basal layer), the stratum spinosum (spinous layer), the stratum granulosum, and the stratum corneum (cornified layer) (from deep to superficial) (Fig. 2). The stratum basal is generally made of a monolayer of cells that are settled on the underlying basement membrane. The basal layer possesses a subpopulation of stem cells, which may have a critical role in the high regenerative potential of the skin tissue. Post-mitotic keratinocytes are located on the top of the stratum basal and migrate from the spinous layer (containing the youngest cells) to the oldest cornified layer during terminal differentiation. Keratinization is initiated in the stratum spinusom (8–10 layers of cells) when columnar basal cells differentiate into polygonal keratinocytes. These cell types then synthesize keratins, insoluble proteins, causing a hydrophobic and impermeable barrier. Thus, the cells in the spinous layer contain a high concentration of keratin and are attached to each other by desmosomes (intercellular junctions) [12]. The spinous cells transform into a more squamous shape and acquire keratohyaline granules and generate the stratum granulosum (1–3 layers of cells). Further differentiation of

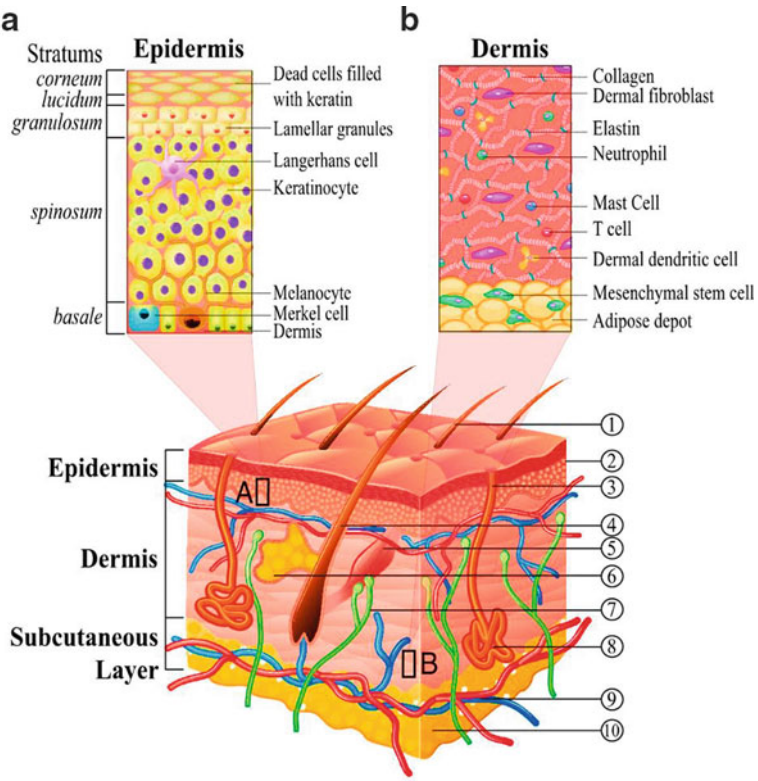

Fig. 1 A schematic representation of microanatomy of the skin tissue with underlying cells in the epidermis and dermis layers. The epidermis consists of five distinct layers, including basal, spinous, granulosum, lucidum, and corneum layer (from the deep to the superficial). Keratinocytes are the major cell type of the epidermis that undergo terminal differentiation to generate the stratified skin. The dermis is mostly composed of fibroblasts, which are distributed in collagen fibers. Other components are discussed in detail in the text. Adapted from [10]

granular cells leads to losing their nucleus and organelles via lysosomic processes considered as dead cells and make up the stratum corneum (almost 10–15 layers of flattened cells). The turnover rate of the corneum cell layer is estimated at about 30 days. The resulted keratinization may lead to the generation of an impermeable barrier that avoids water loss and entry of pathogens detrimental molecules to the body. Furthermore, keratinocytes also produce various cytokines and growth factors (GFs), playing a role in the repair and regeneration process. These bioactive molecules include transforming growth factor (TGF-β), interleukins (IL-1, IL-6, IL-8), interferons (IFN-α and IFN-β), platelet-derived growth factor (PDGF), fibroblast growth factor (FGF), tumor necrosis factor (TNF-α), and granulocyte–macrophage colony-stimulating factor (GM-CSF) [13].

In addition to keratinocytes, the epidermal layer contains melanocytes that are randomly distributed in the basal layer. Melanocytes are primarily responsible for

Table 1 The major components of the three layers of the skin [11]

Components	Function(s)
Epidermis	
Keratinocytes	Making a protective barrier against pathogens, UV radiation, heat, and water loss
Melanocytes	Producing the pigment melanin, which protects against UV-B light exposure
Merkel cells	Associated with tactile sensation
Langerhans cells	Antigen-presenting cells of the skin tissue
Dermis	
Collagens	Fibrous proteins responsible for mechanical support and elasticity of the skin
Fibroblasts	Synthesizing ECM ingredients and collagens and possessing a fundamental role in wound healing
Mast cells	Wound healing, angiogenesis, allergy response, and anaphylaxis
Hypodermis	
Fibroblasts	Synthesizing ECM ingredients and collagens and possessing a fundamental role in wound healing
Adipocytes	Fat formation with the aim of energy storage
Macrophages	Phagocytosis, wound healing, immune response

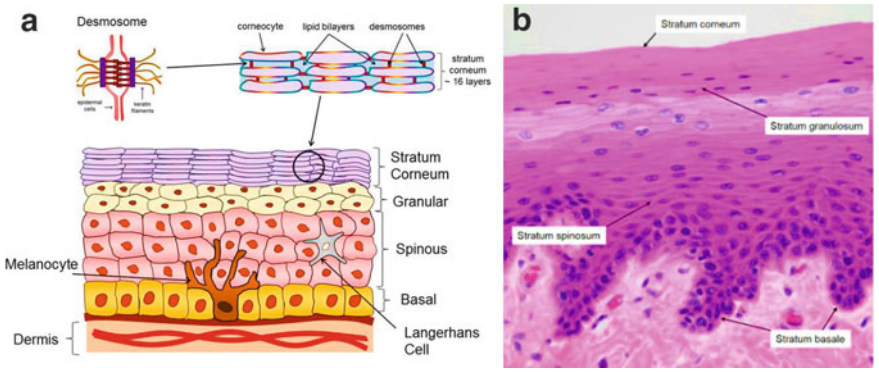

Fig. 2 Various layers of the epidermis and its underlying cells. **a** Schematic representation of major cells constituting the epidermis, including basal, spinous, granular, and corneal layers. Keratinocytes are major cellular components of the epidermal layer in which desmosomes (intercellular connecting proteins) are highlighted. Other cell types include Langerhans cells and melanocytes. **b** Histological demonstration of epidermal layer stained with hematoxylin and eosin (H & E). Adapted from [14]

the skin color via producing the pigment melanin (UV-protective pigment). Melanin is encapsulated within organelles named melanosomes, followed by transitioning to the adjacent keratinocytes [15]. Once the pigments have reached the keratinocyte cytoplasm, they arrange in a well-orchestrated manner to protect the nucleus from detrimental UV irradiation. Scientific evidence shows that UV induces melanization

via promoting the p53 pathway through synthesizing melanin stimulating hormone (MSH) by keratinocytes. In addition, the p53 pathway would initiate apoptosis of keratinocytes possessing inadequate pigmentation to prevent side effects of UV exposure (e.g., defective and premalignant mutations) [16]. Langerhans cells are mainly recognized as epidermal dendritic cells and participate in the immune response. They mostly reside in the spinous layer and constitute up to 2–4% of epidermal cells. Another important cell type in the epidermis is Merkel cells located in the basal layer. These cells are possibly responsible for the sensation by generating synaptic junctions with peripheral nerve endings [17].

2.2 Basement Membrane

The basement membrane (BM), also called the basal lamina, immediately lies beneath the epidermal layer and serves as a boundary between the epidermis and the underlying connective tissues. Although BM is mostly composed of collagen IV, it has a very complex molecular structure. The cells residing in the stratum basal could communicate with the components of BM through hemidesmosomes (anchoring plaques containing collagen XVII). BM could be separated into two specific layers, including lamina densa and lamina Lucida. The first one is the superficial portion just beneath the epidermis and mostly made of collage IV, while the latter is considered the deep part and constructed from laminin and other glycoproteins. The lamina densa is connected to the dermal layer via epidermal-dermal anchoring proteins (mainly collagen VII) [17].

2.2.1 Dermis

The dermis is an intricate and dynamic microenvironment that conveys blood vessels, nerves, hair follicles, sweat glands, and sebaceous glands. The dermis plays a vital role in maintaining the elasticity and integrity of the skin; providing mechanical and structural support to the epidermis; immunosurveillance; cutaneous nutrition; sensory perception; and regulating the body temperature [17]. The dermal layer is divided into two functionally and structurally distinct layers, i.e., the papillary dermis and the reticular dermis. The papillary dermis forms the superficial layer and contains loosely woven fibers, including collagen-I, -III, anchoring fibrils of collagen-VII, and elastin fibers. On the other hand, the reticular dermis makes the deep layer that is composed of compacted fibers of collagen-I (diameter of 100 μm) arranged in parallel to the skin surface [18].

In normal physiological conditions, the dermis contains a broad range of specialized cells, including fibroblasts, endothelial cells (ECs), monocyte/macrophage, dermal DCs, mast cells, lymphocytes, Schwan cells, pericytes, and mesenchymal stem cells (MSCs). These cells are harbored within a complex and acellular matrix mainly composed of collagen and glycosaminoglycans (GAGs).

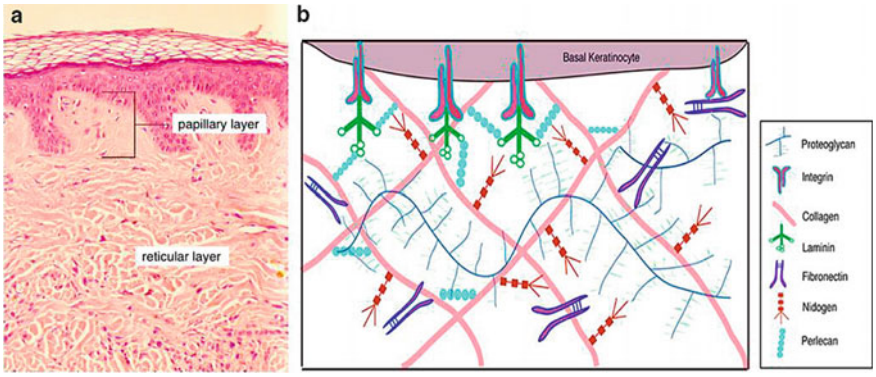

Fig. 3 **a** Histological illustration of the papillary and reticular dermis. **b** A schematic representation of major components of skin ECM including proteins (e.g., collagen), glycoproteins (like fibronectin), and proteoglycans. Adapted from [19]

Fibroblasts are the major cell type of the dermal layer, which synthesize dermis' ECM components, including collagen (the most abundant fibers) and elastic fibers, GAGs, and proteoglycans that are incorporated within the ground substance. It has been indicated that the papillary dermis is prevailed by loosely woven collagen-III, while the reticular dermis is dominated by dense and compacted bundles of collagen-I (Fig. 3a). Altogether, the ratio of collagen-I to collagen-III is 4:1 in normal physiological conditions. In addition to structural proteins like collagens, the ground substance is mainly composed of GAGs such as hyaluronic acid. These polysaccharide molecules are bound to the peptide chains to generate high molecular weight combinations named proteoglycans (Fig. 3b). Table 2 summarizes a collection of peptide- and saccharide-based components of skin components.

Epidermal and dermal cells supply their nutrition and metabolite exchanges through the blood vessels located in the dermis. The lumen of dermal microvessels are lined by ECs which express vascular markers, such as CD31, CD34, and CD144 [29]. The dermal vascular microenvironment is surrounded by a collection of immune cells, e.g., macrophages, DCs, and mast cells. Generally, these cells participate in initiating the immune response and triggering inflammation and hemostasis. Dendritic cells can serve as antigen-presenting cells (APCs) and play a phagocytic role. These cells express a class of epitopes like CD34 (hematopoietic progenitor marker) and factor VIIIa (activated fibrin stabilizing factor), which may have a vital role in the early stages of wound healing.

3 Skin Wound Healing: What We Know and Need to Know

In the normal physiological condition, the skin shows self-healing property with a dynamic and well-orchestrated cascade of wound healing signaling pathways leading to advance repair and/or regeneration. It is well known that efficient wound

Table 2 Some major constituents of skin ECM

Constituent	Function(s)	Ref(s)
Proteins		
Collagen	The main structural constituent of the dermis	[20]
	Promotes tensile strength of the skin	
Elastin	Provides elasticity of the skin	[21]
Glycosaminoglycans (GAGs)		
Hyaluronic acid	High water absorption capacity which leads to greater compression resistance and proangiogenic potential	[22]
Heparin sulfate	Promotes mechanical strength of the skin	[23]
	Contributing to cell adhesion, proliferation, and migration, collagen fiber formation, granulation tissue formation, and basement membrane regeneration in connection with wound healing	
Glycoproteins		
Fibrillin	Providing integrity and elasticity of the skin	[24]
Fibronectin	Modulating the interaction between cells and ECM components and promoting angiogenesis	[25, 26]
Laminin	Providing stable attachment of epidermis and dermis	[27, 28]
	Facilitating the assembly of basement membrane leading to promoted wound healing	
	Promoting re-epithelialization, angiogenesis, and cell migration in the wound healing process	

healing results in the restoration of skin both structurally and functionally. Although the skin regeneration process reconstitutes an identical copy of the injured tissue without scarring in some species (e.g., fish, salamanders, and spiny mice) [30], it usually causes fibrosis and scarring in adult humans [31]. This process contains a complex interaction of cells and bioactive molecules that can be classified into four overlapping stages: (1) hemostasis (clotting), (2) inflammation, (3) proliferation, and (4) tissue remodeling [31]. Some of the major bioactive molecules involved in the wound healing process have been summarized in Table 3. All these stages are comprehensively discussed in the following section.

Hemostasis is a phenomenon happening immediately after happening the injury to the skin; it occurs in a few hours and causes coagulation and formation of a fibrin network. This clot suppresses hemorrhaging and provide a temporary scaffold (mainly composed of fibrin, fibronectin, and collagen) for cellular adhesion and migration. From a molecular mechanism point of view, clotting is initiated by the attachment of the von Willebrand factor to the subject tissue resulting in the aggregation of platelets along the damaged endothelium. The platelets contribute to clot formation by producing thrombin and releasing pro-inflammatory factors, including PDGF and TGF- β [31, 49]. PDGF initiates the recruitment of neutrophils, macrophages, fibroblasts, and endothelial cells (ECs), playing vital roles in the

Table 3 Major GFs and cytokines involved in the skin wound healing process

Bioactive molecule	Primary function	Ref(s)
Epidermal growth factor (EGF)	Proliferation of keratinocytes and fibroblasts	[32]
FGF-1, -2, and -4	Promoting angiogenesis and fibroblast proliferation	[33]
PDGF	Recruitment of macrophages and fibroblasts, macrophage activation, fibroblast proliferation, and ECM synthesis	[34]
Insulin-like growth factor (IGF-1)	Fibroblast and EC proliferation	[35]
Vascular endothelial growth factor (VEGF)	Promotes angiogenesis, granulation tissue formation, and re-epithelialization	[36]
Hepatocyte growth factor (HGF)	Migration, differentiation, and maturation of keratinocytes	[37–39]
	Scarless wound healing	
TGF-β	Keratinocyte migration, recruitment of macrophages and fibroblasts	[40, 41]
	Scarless wound healing	
IL-1	Activating GF expression in keratinocytes, fibroblasts, and macrophages	[42]
IL-4	Migration and differentiation of fibroblasts	[43, 44]
	ECM synthesis	
IL-10	Modulating fibroblast and endothelial progenitor cell (EPC) in differentiation	[45–47]
	Modifying inflammatory response	
IL-12	Early inflammatory response and angiogenesis	[48]
	Modulating GF synthesis	
TNF-α	Activating GF expression in keratinocytes, fibroblasts, and macrophages	[42]

following steps. TGF-β contributes to macrophage infiltration into the wound site and secretion of FGF, IL-1 (acute inflammatory response), TNF-α (acute inflammatory response), and more PDGF from macrophages. In addition, TGF-β also promotes the recruitment of fibroblasts and ECs [31].

The inflammatory phase initiates with the infiltration of neutrophils into the wound bed and lasts for about 2–5 days in a normal condition [31]. Neutrophils release cytokines such as TNF-α, IL-1β, and IL-6 to exert the first line of defense against pathogens and strengthen the immune response. After approximately three days,

monocytes migrate to the wound site and differentiate into macrophages in order to phagocyte pathogens and cellular debris. Moreover, macrophages release bioactive molecules including IL-1, PDGF, TGF-β, TGF-α, FGF, IGF-1, and VEGF, which play pivotal roles in the recruitment of fibroblasts and transitioning from inflammation to proliferation phase [50].

The proliferation phase is recognized by main features, including re-epithelialization, angiogenesis, and granulation tissue formation. The re-epithelialization begins within the first hours after the injury and provide a covering onto the wound surface [51]. Residing cells at the wound edge secret various GFs, including EGF, keratinocyte growth factor (KGF), and TGF-β, to evoke keratinocytes and fibroblasts to migrate into the wound site. In fact, keratinocytes stimulate fibroblasts to produce and secrete GFs, which in turn trigger keratinocyte proliferation. Later, the proliferation of fibroblasts promotes the production of GFs in fibroblasts in a synergistic manner [52]. Furthermore, stem cells residing in the hair follicle bulge can differentiate into the epidermal progenitor lineages and facilitate the restoration of the epidermis [53, 54]. Angiogenesis, also known as neovascularization, provide nutrients and metabolites exchanges for the newly formed tissue. Sprouting of existing blood vessels occurs by the attachment of VEGF, PDGF, bFGF, and thrombin to the receptors on the ECs. Matrix metalloproteinase (MMPs) secreted by vascular ECs triggers the migration of vascular branches toward the wound site that consequently differentiate to new mature vessels [55]. Finally, the granulation tissue is formed about four days after the injury. At this stage, secreted PDGF, TGF-β, and FGF stimulate fibroblasts to convert the provisional fibrin matrix with newly formed collagen type III and ECM components such as fibronectin, GAGs, and proteoglycans [49]. In addition, some fibroblasts could be differentiated into myofibroblasts (i.e., contractile cells) leading to better wound healing via improved mechanical strength [56, 57]. This stage of healing can be followed by both macroscopically and microscopically, i.e., via wound closure rate and monitoring re-epithelialization, granulation tissue, density of dermal collagen fibers, leukocyte infiltration, respectively.

The remodeling phase is considered as the last phase of wound healing; this stage commonly initiates during 2–3 weeks after the injury and may last for several months. This includes remodeling of the granulation tissue into a mature scar via MMPs and other collagenases secreted by fibroblasts and macrophages. In addition, the remaining fibroblasts begin to differentiate into myofibroblasts [49]. It is worth noting that collagen type III found in the granulation tissue is replaced by bundles of collagen type I and further cross-linked by lysyl oxidase with a parallel orientation with the skin surface. This substitution of collagens increases the tensile strength of ECM from 25 to 80% [58].

Based on the etiology, the process of wound healing could be affected by the type of wound, i.e., acute or chronic. In acute conditions (e.g., burns), excessive contraction of myofibroblasts occurs as a result of the poor apoptotic rate at the remodeling phase and lead to ECM degradation and fibrotic scar formation [59]. While in chronic wounds (e.g., diabetic ulcers), the healing process remains in a

prolonged inflammation phase that leads to the overactivation of proteases (e.g., MMPs, elastase, plasmin, and thrombin) as well as reactive oxygen species (ROS) degrading the ECM [60–62]. One of the marked differences between chronic wounds and acute wounds is the epidermis diameter. In chronic wounds, the epidermal layer is thicker and highly keratinized, and often it is detached. Furthermore, the newly formed sin tissue in chronic wounds possesses less vasculature [63].

4 Bioengineered Skin Substitutes

Although many traditional and modern wound dressings have been found effective substances for managing various skin wounds, the use of tissue-engineered (TE) skin substitutes has gained much attention over the last years [64]. In general, an ideal skin substitute should have specific features including the ability to immediately replace injured epidermis and dermis, the capability of preventing and suppressing infection, avoiding water loss, reducing inflammation, enduring the shear forces, the lack of antigenicity, affordability, long-term stability, and availability [65]. Here, we summarized a collection of epidermal and dermal substitutes as well as advanced bioengineered grafts, including electrospun meshes and 3D bio-printed grafts.

4.1 Epidermal Substitutes

Epidermal substitutes are utilized for managing superficial skin injuries to repair and/or regenerate the epidermal layer. They were initially reported in 1981 for large full-thickness burns. Generally, a skin biopsy with an extension of 2–5 cm^2 is taken from the patient, which is called a skin autograft, followed by the separation of the epidermis from the dermis. After that, keratinocytes are isolated and cultured in the presence of fibroblasts that serve as a feeder layer. Since this process usually takes three weeks, the wounds are initially covered and treated with a provisional dressing to protect the wound bed and stimulate the healing [5, 66].

Despite several advantages, such as the lack of allogenic rejection, epidermal substitutes have some limitations, including long-term fabrication time, variable engraftment rates, expensive to use, and laborious handling due to their thin and fragile nature [66]. Direct cell spraying to the lesion can be considered as an alternative to the cultured keratinocytes as it shorts the fabrication time of the construct. In this strategy, obtained epidermal cells from a biopsy are locally sprayed at the wound site and consequently facilitate the epithelialization. ReCell® (Avita Medical, Perth, Australia) and Spray®XP (Graco, MN, USA) are two examples of available cell spray products for autologous re-epithelization [67, 68].

4.2 Dermal Substitutes

Dermal constructs provide suitable substitutes for full-thickness wounds in which both the epidermis and dermis are affected. The main advantages of dermal constructs could be summarized as good mechanical properties, availability in various thicknesses and compositions, and the lack of wound contraction [69]. Dermal substitutes are made of either natural or synthetic materials [70, 71] and are covered by a permanent epidermal graft [69]. Consequently, the substitutes undergo colonization and neovascularization, resulting in the formation of an autologous new dermis [66]. Dermagraft® (Advanced BioHealing, LaJolla, CA, USA) is a good example of a synthetic commercial dermal substitute, which is composed of a bioabsorbable polyglactin mesh seeded with allogeneic neonatal fibroblasts. Dermagraft® is utilized as a provisional or temporary coverage for burns, chronic wounds, and diabetic ulcers [72, 73].

4.3 Dermo-Epidermal Substitutes

Comparing the epidermal and dermal substitutes, dermo-epidermal substitutes are the most skin-imitating constructs and made of keratinocytes and fibroblasts in underlying ECM to generate a temporary dressing [5]. In spite of a close resemblance to the skin construction, dermo-epidermal substitutes possess high production costs and may result in a lack of permanent wound closure due to the risk of allogenic cell rejection by the host [5]. Apligraft® (Organogenesis, Inc., Canton, MA, USA, and Novartis Pharmaceuticals Corp., East Hanover, NJ, USA) is a well-known artificial bilayered skin equivalent, which is made of allogenic keratinocytes and neonatal fibroblasts in a type I bovine collagen matrix. This product should be freshly applied and has a shelf-life of five days at room temperature [73, 74]. The major application of Apligraft® is to heal partial to full-thickness burns, chronic wounds, diabetic ulcers, and Epidermolysis Bullosa [72].

With respect to major limitations of available skin substitutes (e.g., high production cost, poor engraftment rate, long fabrication time, rejection possibility of allogeneic cells, etc.), advanced bioengineering strategies have offered permanent and affordable alternatives to the existing ones. The following sections are focused on some of these advanced strategies, and their advantages and disadvantages are further discussed.

5 Advanced Strategies for Skin Repair and Regeneration

Advanced skin regeneration strategies propose an efficient and viable alternative to overcome the major obstacles of currently available skin substitutes (mainly allografts). These strategies incorporate biomaterials, cells, bioactive molecules, and novel fabrication techniques to generate a highly biomimetic skin construct. Two primary strategies could be noted regarding top-down or bottom-up approaches [75–78]. The top-down or scaffold-based approaches rely on the utilization of provisional scaffolds that provide a temporary environment for underlying cells to facilitate the attachment, proliferation, and secretion of their own ECM, leading to the promoted new tissue formation. In addition, the temporary scaffold provides physical support to guide and organize the formation of new skin tissue [75, 79, 80]. In contrast, the bottom-up approaches are considered as scaffold-free strategies and rely on the use of cells or cell-aggregates to generate a tissue-engineered construct [81, 82]. Accordingly, tissue-engineered constructs can be fabricated by self-assembled aggregation, fabrication of cell sheets, microfabrication of cell-laden hydrogels, or direct bio-printing [83].

5.1 Top-Down Approaches for Skin Regeneration

Top-down approaches are performed based on the fabrication of porous, biocompatible, and biodegradable scaffolds containing mammalian cells in the presence or absence of bioactive molecules (like GFs). The assembled 3D constructs are further maturated in a bioreactor [82, 84]. Scaffolds are generally made of natural, synthetic, or combination biomaterials to imitate the natural skin ECM both structurally and functionally [85, 86]. In fact, the skin ECM is comprised of structural proteins (e.g., collagen and elastin), specialized proteins (e.g., fibronectin and laminin), and proteoglycans (e.g., hyaluronic acid (HA) and heparin sulfate), which are well-orchestrated in desired skin layers [87]. For instance, the dermal layer is constituted of a 3D fibrillary network, mostly composed of collagen fibers, with dimensions of submicron to nanoscale ranges to provide mechanical strength and structural integrity to the skin tissue [88, 89]. In order to regenerate a skin tissue similar to a healthy counterpart, either structurally and mechanically or functionally, the bioengineered constructs should be capable of resembling the microscale and nanoscale organization of the natural components of the skin as well as providing an ideal ambient for cell attachment, proliferation, and differentiation [90, 91]. In this regard, several strategies have been developed to fabricate such constructs, such as electrospinning, self-assembly techniques, template synthesis, and phase separation [90, 92]. Among the mentioned approaches, electrospun nanofibers have emerged as promising scaffolds capable of resembling microscale and nanoscale organization of natural skin ECM, providing a desirable substrate for cell adhesion, proliferation, and differentiation [93, 94]. Furthermore, electrospun nanofibers can be used as

delivery vehicles for a wide range of bioactive molecules, including GFs, cytokines, and adhesive peptides [95–97]. An electrospinning apparatus is fundamentally composed of a capillary tube containing polymeric solution, a high voltage supply, a grounded collector, and a syringe pump for a controlled jet of solution. In brief, the electrospinning process is initiated by the charged jet of a polymeric solution as a consequence of applied high voltage. The solvent is then evaporated, and nanofibers are finally deposited on the collector [98, 99]. It is well known that the morphology of nanofibers could be affected by a number of parameters, including molecular weight and viscosity of the polymeric solution, the applied voltage, capillary tip to collector distance, and capillary diameter [100]. A wide range of natural polymers (e.g., collagen, gelatin, and chitosan) [101, 102] and synthetic ones (e.g., poly(lactic-co-glycolic) acid (PLGA), poly(lactic acid) (PLA), and poly(ethylene glycol) (PEG)) [103, 104], and combinations of both natural and synthetic polymers [105, 106] have been utilized to fabricate electrospun mats for promoted skin regeneration. These constructs benefit from a high surface to volume ratio and make an appropriate environment for cellular interaction and promoted angiogenesis [107]. In addition, the desired porosity of electrospun mats allows oxygen and nutrition exchange, which is necessary for prohibiting necrosis and failed skin wound healing [89]. Most importantly, the fiber dimensions of nanofibrous mats are in the range of natural ECM components and is mentioned a key parameter in accelerating the wound healing processes [90, 108]. Moreover, electrospun nanofibers can be utilized as drug delivery systems for sequential and controlled release of bioactive molecules (e.g., GFs, natural chemicals, and small molecules) at the wound site [109–112]. As an illustration, bFGF-loaded nanofibrous mats composed of PEG-PLA revealed a sustained release of bFGF for four weeks facilitating fibroblast cell adhesion, proliferation, and ECM synthesis. When implanted into diabetic wounds of rat, the constructs promoted re-epithelialization and maturation of skin appendages (hair and sebaceous glands) [110]. Still, poor mechanical strength, poor integrity to the body, and non-uniform thickness distribution are stated as the major drawbacks of electrospun constructs for skin regeneration applications [97].

In addition to electrospun fibrous scaffolds, experimental studies emphasize the use of hydrogels in managing a broad range of skin wounds as regards their capability of absorbing large amounts of liquids at the injured sites. Hydrogels can be described as 3D networks of hydrophilic polymers possessing hydrophilic chains allowing them to swell extensively. Accordingly, hydrogels offer a class of permanent or temporary dressings for regenerating the epidermis and/or dermis in damaged skin [113]. Moreover, it is feasible to load different cell types, growth factors, and other therapeutic agents to hydrogels for boosting the healing process [114]. Hydrogels could be made of both natural (e.g., gelatin and alginate) and synthetic (e.g., PVA) polymers, as well as their composites [115]. They are commonly categorized based on their crosslinking nature, i.e., chemical or physical hydrogels. Chemical hydrogels entail the formation of covalent bonds between the polymer chains, whereas physical

hydrogels involve physical interactions between polymer chains (e.g., ionic interactions, hydrogen bonds, and molecular entanglement) [116, 117]. Major advantages of hydrogels as wound dressing materials include (1) promoting wound debridement and absorbing wound exudates, (2) providing an optimum moist environment to accelerate the healing process, (3) permeable to oxygen and other soluble factors, (4) inhibiting bacterial infection, and (5) poor adhesion to the wound site which prevent trauma formation after its detachment from the wound bed [8]. Hydrogels can be loaded with both keratinocytes and fibroblasts [118, 119]. Despite their ease of fabrication, affordability, and good control over the scaffold properties, they lack sufficient mechanical strength, and they are unable to load individual cells at specific regions throughout the scaffold [120]. Hence, they are being improved as advanced biomaterials capable of encapsulating various cells and bioactive molecules, which are called gel bioinks.

5.2 *Bottom-Up Approaches for Skin Regeneration*

Bottom-up approaches utilize cells or cell-aggregates to generate tissue-engineered constructs without administration of scaffolds as supporting substrates [121]. These approaches generally entail three fundamental components: (I) a bioink containing the cell suspensions to be printed, (II) a biopaper, providing a temporary substrate for the deposited bio-inks, and (III) a bioprinter. The 3D bioprinting strategy, an advanced branch of the 3D printing technique, has been widely used in tissue engineering and regenerative medicine for fabricating substitutes with a maximum resemblance to human tissues and organs [122]. It is fairly well accepted that 3D constructs often provide more accurate physiological situations than two dimensional (2D) counterparts since many functions naturally happen in the 3D condition of the human body.

Based on the main principles of casting, current 3D bioprinting strategies basically include laser-assisted, drop-based (inkjet), extrusion, stereolithography, electrohydrodynamic, and microfluidic bioprinting techniques [123–125]. Although all these methods are used as the fabrication route, it should be emphasized that printing a construct with a well-controlled and precise geometry is of utmost importance for efficient living cells and reconstruction of human tissues and organs in the laboratory [126]. In the following sections, the above-mentioned methods are briefly introduced, and then suitable gel-inks for fabricating 3D skin replacements will be presented.

5.3 *Laser-Assisted 3D Bioprinting*

Two separate main approaches of laser-induced forward transfer (LIFT) and laser-guided direct writing have been validated in laser-based bioprinting. To align and focus the laser, the device consists of a focusing system, a pulsed laser beam to

induce the transfer of bioink, a ribbon as the absorbing layer, and a substrate for the bioink layer [127]. A laser source is used in this bioprinting technique, which is based on the LIFT model to irradiate high energy focused laser pulses at high precision onto thin substrates coated with a layer of laser absorbing material. The resulted bioink produces a high-pressure bubble to remove the cells and biomaterial from the substrate and deposit them onto the platform [128], where the scaffold is formed layer by layer [129]. Two layers are normally involved in this process: the energy absorbing layer (upper glass slide), which receives the pulsed laser, and the cell-containing layer of biomaterials (on the bottom). After ejecting the cell-containing hydrogel precursor toward the platform, the final 3D structure will be shaped through the movement of the platform [130]. Some advantages have been reported for this method, including high cell viability (>90%), variety of printable bioinks with high viscosity, and nozzle-free and non-contact (between the bioink and processing device), which provides a mechanical stress-free medium for normal cellular activity [131]. On the other hand, the drawbacks of low cell density, complexity, low repeatability of the resulted droplet, time-consuming, high cost, and relatively low flow rate of crosslinking due to the fast gelation, which is essential for attaining a highly precise shape but can limit the applications of laser bioprinting approach, have addressed the researchers' focus on optimizing this method, which needs further study [132].

5.4 Drop-Based Bioprinting

As a highly versatile, rapid, simple, and cost-effective technique introduced in the early 2000s [133], drop-based bioprinting is compatibly capable of depositing pico-liter droplets of various low viscous biological material inks (3.5–12 mPa/s) to avoid clogging in a precisely controlled way with high resolution and no contact between the substrate and the nozzle. Similar to laser-based bioprinting, this method faces some limitations, including non-uniformity of the droplets and inconsistent encapsulation of cells, as well as a restricted structural and mechanical integrity in bioprinted concepts. On the other hand, since it is difficult to control the porosity and vascularization, the size of the constructs can be restricted by cross-contamination of bioinks [134, 135]. Drop-based bioprinting has been classified into three main types of acoustic, micro-valve, and layer-by-layer inkjet bioprinting. The acoustic-droplet method produces the droplets from the bioinks through acoustic waves in an open pool without applying any heat, high voltage, or pressure. Micro-valve bioprinters generate droplets under pneumatic pressure through the opening and closing of a microvalve. Moreover, the inkjet technique, as the most common system of drop-based bioprinting, includes electrodynamic, drop-on-demand, and continuous-inkjet bioprinting. These systems use mechanical, thermal, and piezoelectric pulses to produce small (picoliter-volume) bioink droplets which can affect the cell viability in inkjet bioprinted microstructures [136]. By controlling the parameters affecting the ultrasound, including time, pulse, and amplitude, the inkjet technique as the first organ printing approach is capable of adjusting the desired size of ejected droplets,

which is known as the primary advantage of this method [137]. Furthermore, the possibility of using multiple printing heads on the device allows different cells to be printed faster (1–104 drops/s) at the same time. However, possible thermal damage to cells and weak mechanical stability of the 3D-bioprinted structures, as well as the challenge of the drying process of droplets on the substrate, are the main issues to be solved. Additionally, this technique often leads to the construction of weak skin structures since high concentrations of cells and high viscous biomaterials cannot be used due to the low driving pressure of the nozzles, which should be considered in future studies [138].

5.5 Extrusion-Based Bioprinting

Extrusion bioprinting technique is evolved from inkjet technology and uses physical forces of pneumatic pressure, metal screw, or piston systems to selectively dispense the biomaterials with high geometric complexity through a mechanically driven nozzle where the extrusion head moves in three directions of x, y, and z to form 3D architectures of biomaterial on the substrate platforms. This technique has been branded as the most suitable for fabricating soft tissues among different bioprinting approaches [139]. In spite of its lower accuracy compared to laser-based and inkjet techniques, this technique allows the extrusion of different biomaterials, including hydrogels, cell-spheroids, cell-laden bioink, and high viscous polymeric thermoplastics with various viscosity ranges of 6–30 $\times$ 10^7 mPa/s and the resolution of 100 μm-millimeter [140]. The ability to be installed in a multi-head system is the key benefit of applying this bioprinting technique, which provides printing one or more biomaterials simultaneously. These complex and quickly manufactured 3D tissue structures could mimic the human body both biologically and morphologically, verifying the extrusion technique as one of the most promising available clinical approaches [141]. While pneumatic systems use compressed gases to provide a continuous extrusion pressure to dispense bioinks, two other systems of piston and screw dispense bioinks through a pump using mechanical forces without any gases. With the help of the simple and low-cost extrusion bioprinting device, it is possible to fabricate a wide range of biostructures similar to skin tissues. However, bioink cells can potentially be damaged due to exposure upon external mechanical forces, which needs to be reduced as much as possible [142]. The use of extrusion-based 3D bioprinting in skin wound healing has been validated in recent studies [143, 144].

5.6 Stereolithography-Based Bioprinting

Photolithography techniques use photons/light to transfer the geometric shapes of a mask to a light-sensitive surface and are being effectively employed for constructing 3D scaffolds for tissue engineering applications. These techniques are generally

divided into three main methods, including mask-based photolithography, multi-photon lithography, and stereolithography. As a notable 3D bioprinting technique, stereolithography uses a projected light source of the laser, infrared radiation, or an ultraviolet bulb to photolytically crosslink bioinks selectively in a layer-by-layer process to form highly precise 3D structures (commonly acrylics and epoxies) [145]. Stereolithography bioprinting systems consist of a light source, a digital mirror device, an elevator system, and a photopolymer reservoir with the biocompatible liquid photocurable resin as well as a print head which has to move only in one direction through an up and down movement [146]. While this method has been traditionally used to fabricate cell scaffolds [147], currently, it is applied in 3D printing of bioink with cells with high efficiency [148]. Compared to other 3D bioprinting techniques, stereolithography provides the advantages of high cell viabilities (>90%), high printing accuracy and resolution (<100 μm), short printing time (<1 h), as well as being simple and easy to control device [149]. However, this technique suffers from some drawbacks, including a high cost for system installation, the lack of available and useable photosensitive resins, and cytotoxicity of the photocurable resins, which can reduce the viability of embedded cells [150].

5.7 Electrohydrodynamic-Based Bioprinting

As a newly emerging 3D bioprinting technique, electrohydrodynamic printing has been applied in the controlled fabrication of 3D micro/nano-scale constructions [151, 152]. Combining the principles of electrohydrodynamics and layer-by-layer additive production makes this technique mainly appropriate for fabrication and biomimetic structural organization of artificial tissue models on a similar scale to that of living cells or native extracellular matrix, which proves its great potential to precisely regulate tissue regeneration [153] and control cellular behaviors [154].

5.8 Microfluidic-Based Bioprinting

Microfluidic 3D bioprinters employ a micro-printing apparatus based on microfluidic technology. They are different from traditional bioprinters (laser, inkjet, extrusion, and stereolithography) as to their capability of artificial printing tissues, for example, the skin, in a shorter period of time [155]. Microfluidic print heads use the combination with bioprinter to enable precise patterning of a biomaterial and cells in 3D. In addition, choosing the right bioink and design for your print is essential to create a functional 3D tissue. Bioink selection is of great importance since a bioink incorporates both cells and biomaterials. So, software (e.g., ASPECT®-Studio) is being used to specifically design a 3D structure [156]. One of the main benefits of microfluidic 3D bioprinting is the ability to pattern tissues on the microscale. Moreover, it is feasible to encapsulate different types of cells and materials as core–shell and concentrically

multilayered fibers mimicking tissue interfaces. The size of microarchitectures and features may finally be controlled by microfluidics.

Although this system cannot entirely model all features of human skin, including hair follicles and pigmentation, it is capable of stimulating wound regeneration by printing a large amount of artificial transplantable skin in a fairly short time [157].

6 Natural 3D Printable Gel-Inks for Skin Regeneration

In general, 3D printable gel-inks could be originally categorized as natural and synthetic polymers. It should be pointed out that their combinations have also been reported as a reasonable strategy for having an enhanced biological and mechanical property [158]. In spite of their shortage of mechanical stability, naturally-derived polymers are the main source of around 90% of polymeric substrates employed in 3D bioprinting applications [159]. The reason for the high usage of natural polymers is related to their inherent benefits, including high similarity to human extracellular matrix (ECM) composition, which mimics cell native microenvironment and subsequently facilitates cells' attachment, proliferation, migration, and differentiation [160, 161]. Among a broad range of natural polymers, alginate, collagen, decellularized ECM (dECM), and gelatin inks have been extensively applied in skin tissue engineering. Natural protein-based inks, collagen, dECM, and gelatin-based polymers have shown remarkable potential in the regeneration of the epithelial layer of skin tissue [162].

6.1 Alginate

Alginate (known as alginic acid) is an anionic polysaccharide found in the cell walls of brown algae. This biopolymer has been widely utilized in various 3D bioprinting applications due to its rapid gelation post-printing and high shear-thinning [163]. Hydrated alginate can form a viscous gel as to its hydrophilic property, meeting the needs of physicochemical features suitable for 3D bioprinting. Due to its good biocompatibility and structural similarity to native ECM, alginate has been widely using as a wound dressing material [164]. Additionally, being directly polymerized by multivalent cations (e.g., Ca^{2+} and Ba^{2+}), alginate can generate a proper cell-compatible hydrogel ink for the bioprinting of human skin [165]. However, some limitations, including crosslinking delay, can reduce the shape fidelity of the alginate-based bioprinted constructs as it may adversely affect cell viability. Therefore, biomedical scientists have considered new ways to enhance alginate viscosity or extrude it using chemical crosslinkers (e.g., Ca^{+2}) to control the low shape fidelity of simple alginate solutions [166]. On the other hand, in order to increase cell viability without affecting alginate printability, researchers have conducted attempts to reduce alginate viscosity by using honey [167]. Future studies are also required to enhance

alginate cell adhesion due to their poor cell adhesion properties without altering its suitable physicochemical characteristics for 3D bioprinting applications.

6.2 Collagen

Collagen is another natural printable polymer which extensively utilized for skin wound healing applications. This biopolymer is known as the most plentiful protein in the human body and contains proline and glycine residues in its structure with a triple-helix polypeptide arrangement [168]. Among various types of collagen available in connective tissues (e.g., skin) [169, 170], collagen type I is the most abundant and also the most commonly used in 3D bioprinting applications [171]. Although collagen hydrogels are found to be printed in a desirable biodegradability level without using any chemical crosslinkers, the collagen direct 3D bioprinting approach is still restricted to collagen solutions. Collagen has revealed exceptional microstructures of macropores as well as a desirable shape consistency at 37 °C to stimulate cellular attachment and proliferation [172]. However, incorporating cells or tissue spheroids may cause a reduced printability as well as a significantly longer recovery time [165]. These issues were further solved by a series of interventions including (I) adding chitosan [173], fibrinogen and thrombin [174], and fibrillar collagen [172] to collage; (II) using low concentrations (2–4%) of collagen [175]; and (III) controlling cell suspensions and densities [176] instead of using chemical crosslinking agents. In the case of thin structures, the protein gelation in a matrix of collagen could be controlled by temperature, pH, or both, while gelled and non-gelled regions are observed in thick structures (1–3 mm) as a result of diffusion and thermal conveyance limitations. Moreover, high levels of temperature and pH may severely harm cells' viability [176].

Collagen-based bioinks have been considered as extremely promising biomimetic materials due to their ability to increase cell attachment and proliferation using asparagine-glycine-aspartic acid residues as well as their low toxicity and immunological reactions [177]. However, the key benefit of applying collagen-based bioinks is implanting living cells within biochemical materials and ECM components. On the other hand, due to their crosslinking property, it is essential to use a temperature-dependent gelation process to form 3D concepts. Moreover, in order to improve mechanical properties and printability, collagen is combined with biocomposite including agarose [178], alginate [179], chitosan [180], and fibrin [181] to control the viscosity of the collagen contents.

6.3 Gelatin

Gelatin is a partially hydrolyzed form of native collagen with a broad range of applications in tissue engineering and regenerative medicine. Regarding its cost

economy, gelatin is being used in experiments rather than collagen. Gelatin shows proper compatibility with living systems (human tissues and organs) and supports cell adhesion, growth, and proliferation due to its RGD sequence with abundant integrin-binding motifs [182]. In addition, this biopolymer displays good water solubility, low immunogenicity, adhesiveness, and safe degradation in the body.

The capability of gelatin in forming transparent gels under specific conditions makes it a suitable candidate for additive manufacturing of tissue substitutes. In spite of high rheological properties, gelatin hydrogels possess zero viscosity at temperatures above 27 ± 1 °C and weak mechanical strength [183], encouraging the use of different crosslinking agents for optimal outcomes [166, 184–187]. Although gelatin keeps its thermo-sensitive properties by dissolving in water, it forms a reversible low viscous soluble phase at human body temperature [188]. All the drawbacks mentioned above indicate that the pure gelatin does not seem a suitable substrate for 3D bioprinting; its composites with alginate [189], chitosan hydrogel [190], fibrin [191], hyaluronic acid [192], and silk [193, 194] have been developed to overcome low formability. Also, to enable photocrosslinkable properties of polymers and modify structural stabilization after bioprinting, researchers have widely used gelatin methacrylate as a potential advanced wound healing bioink. Indeed, gelatin methacrylate shows exceptional biological features, including improved biodegradability, enhanced cell adhesion and migration, as well as high thermal sensitivity and photo-crosslinking capability. For instance, the mixture of gelatin methacrylate and 2-hydroxy-1-(4-(hydroxyethoxy) phenyl)-2-methyl-1-propanone (Irgacure 2959) as the photoinitiator to form an applicable combined material which leads to a fast crosslinking after extrusion under UV light (360–480 nm) to improve suitable rheological properties with the desired quality [195]. Furthermore, gelatin methacrylate has been used to induce its high mechanical stability and shape fidelity after UV crosslinking in natural-based bioinks, such as silk sericin [196] and cellulose nanofibrils [184].

6.4 Chitosan

Chitosan (CS) is the main derivative of chitin, a polysaccharide usually derived from shells of aquatic animals (e.g., crabs and shrimps). CS is actually a polycationic polymer owning free acetamide groups and hydroxyl functions linked to the glucopyranose rings, making it susceptible to react through a nucleophilic attack. Therefore, a broad range of CS functionalizations could be carried out via selective modifications of the free amino groups. CS has no mutagenic effects and is recognized as a biocompatible material for biomedical applications. This biodegradable polymer is being widely employed in different areas of science (drug and cell delivery as well as tissue engineering) thanks to its excellent properties, including antibacterial and mucoadhesive activities. For example, CS is currently being administrated for dermal tissue engineering regarding its capability of making hemostasis, which may provide a suitable condition for inducing collagen formation and subsequent tissue

regeneration. In addition, CS could promote polymorphonuclear neutrophils (PMNs) migration and improve the granulation process by inducing dermal fibroblasts' proliferation. In general, CS has introduced an effective remedy playing positive roles in all the wound repair stages [197].

Up to now, various CS-based constructs (gels, films, and scaffolds) were successfully prepared via different production methods and showed great promises in wound healing. Currently, the use of CS as a suitable ink for additive manufacturing has attracted much attention as regards the possibility of making CS-based 3D scaffolds having the precise adjustment of porosity size and shape, fiber size, suitable interconnectivity of pores [198]. Extrusion-based 3D printing, FDM, single-arm robotic printing, two-photon-induced micro stereolithography, the 3D printer with jet dispenser have been used to print CS and its composites for preparing suitable constructs in tissue engineering [198]. For example, porous 3D-printed scaffolds with the film of CS at the base were successfully fabricated by the FDM-3D printing technique, which could support cell attachment and spreading in vitro and improve wound healing in rat models of diabetes [199]. Blending CS with other polymers (e.g., gelatin) was also examined for preparing gel-inks, and outcomes indicated an improvement in printability of gels through the extrusion-based process as well as cellular enhancement behaviors (adhesion, growth, and proliferation) [200, 201]. In order to prepare potential bioadhesive dressing aiming wound healing purposes, 3D printed films based on CS were also reported in which genipin (GE) and glycerol (GLY) or polyethylene glycol 600 (PEG) were used as crosslinker with either as a plasticizer, respectively [202].

6.5 Silk Fibroin

Silk fibroin (SF) is a natural polymeric protein made by a variety of insects, mostly derived from tame *Bombyx mori*. This polymer displays fascinating biological properties (high biocompatibility and biodegradability) and is being employed as an FDA approved material for imaging, drug delivery, and reconstructive applications [203]. From the tissue engineering point of view, SF may provide a suitable substrate for cell adhesion and growth as well as causing minimal immune responses due to its natural biopolymeric features [204]. SF-based biomaterials have shown excellent thermal and mechanical stability and validated cell adhesion and good fibroblast proliferation along with enhanced neovascularization leading to tissue healing and complete regeneration of wounds [205]. Up to now, a series of fabrication methods, including electrospinning, solvent casting, and gas foaming, were applied to make SF-based 3D scaffolds with the ability to use in managing skin injuries [206, 207]. However, lack of the desired fiber orientation, predefined internal architecture, and pore size are unsolved drawbacks of the mentioned traditional techniques.

Due to its fascinating properties like tunable biodegradability, biocompatibility, elasticity, and mechanical robustness, SF is being considered a promising bioink

material for 3D printer machines [208]. SF exhibits high printability, proper mechanical strength, shear-thinning, and cytocompatible gelation behaviors, which verifying its usability for bioprinting application [209, 210]. Moreover, SF, as a polymeric protein bioink, possesses the ability to physically self-crosslinking through hydrophobic interactions without any additional chemical reactions or additives to stabilize the materials [211]. Still, the slow degradation rate of SF is considered as the main concern; the incorporation of other rapid-degrading materials (e.g., gelatin) during the initial process of the scaffold fabrication is suggested as a reasonable and effective strategy. SF has been successfully printed by extrusion-, inkjet-, and laser-based 3D bioprinting [212].

Hydrogel bioinks are an excellent type of matrix for 3D bioprinting as a highly influential technology in tissue engineering to obtain a fast and precise 3D pattern of growth factors, cells, and biomaterials. In order to get rapid printing time and high spatial resolution of compound, stereolithographic bioprinting by using digital light processing (DLP) has recently been applied to develop a novel SF-based bioink that has been widely used in biomedical fields due to its positive biological and biochemical properties as biomaterials [213]. Although regenerated SF (RSF) has revealed high-strength mechanical properties and excellent biocompatibility, it can hardly be applicable in 3D bioprinting in the traditional form to fabricate artificial implants. A printable 3D RSF hydrogel with remarkably improved mechanical properties has been recently reported, which is formed by a weak, two-step chemically crosslinking method, including a ripening process. With a maximum compressive modulus of 2.5 MPa, this RSF hydrogel reached the same order of magnitude as natural elastomers such as cartilage. The gelation mechanism exposed that this chemically cross-linked network could form a dense and uniform physical network through constraining the growth of β-sheet structures of RSF to provide high strength and good resilience of RSF hydrogels. Therefore, due to both excellent mechanical properties and high biocompatibility, this double-network hydrogel owns great potential in generating 3D bioprinted scaffolds for tissue engineering applications [214]. As gelatin-based hydrogels with tuned mechanical properties have shown outstanding cytocompatibility profile appropriate enough for tissue engineering applications, a tailorable hydrogel of gelatin with silk fibroin has been recently designed with different loading concentrations of silk fibroin. In order to explore the effect of silk fibroin loading, biological, chemical, and physico-mechanical properties of the tailored matrix was tested. β-sheet formation of silk was enhanced applying ethanol treatment and led to deployed carbodiimide coupling, which covalently cross-linked the matrix. A considerable increase in cohesive energy was also observed with increasing the concentration of silk fibroin in the gel matrix as well as tuned surface properties to reach the maximum cell adhesion and proliferation confirmed by Rhodamine-DAPI staining. Additionally, MTT assay results verified a certain increase in mitochondrial activity of L929 fibroblast cells for silk fibroin-containing matrix as compared to the bare model making it a reasonable alternative in regenerative medicine [215].

6.6 Decellularized Extracellular Matrix (dECM)

dECM-based inks are another class of naturally-driven materials used as suitable substrates for 3D bioprinting applications. These substances are usually produced by decellularization of specific types of tissues (e.g., the amnion) and show amazing promises in tissue engineering due to their inherent properties for providing a tissue-specific microenvironment for mammalian regrowth cells. Indeed, including glycoprotein, proteoglycans, and collagenous protein, which can uphold native structures through supporting cell migration [216]. Different dECM-based bioinks have been validated to perform specific functions with different printability properties for target-specific skin [217], vessel [158], kidney [218], liver [219], and bone [220] tissue applications where all represent distinctive features of temperature-responsive gelation in physiological environments [221]. dECM-based bioinks can be fabricated through an applicable protocol and reprocessed as a scaffold in tissue regeneration [222]. According to the results of a comparative study by Kim et al., ECM-derived porcine skin equivalent bioinks could successfully enhance epidermal organization through promoting dermal compartment stabilization, compared to collagen bioinks in vitro. In addition, using this dECM-based 3D skin, a promotion in re-epithelialization and neovascularization was observed as well as a satisfying wound closure in in vivo studies [223].

7 Synthetic 3D Printable Gel-Inks for Skin Regeneration

Although natural hydrogels or polymers provide a desirable microenvironment mimicking the tissue interfaces for cell activities, their tunable properties are quite low [224]. It is also of interest to mention that synthetic polymers are favorable candidates to adjust the characteristics to improve the printability, cross-linking, and mechanical properties [225]. Among synthetic polymers, Pluronics and poly(ethylene glycol) (PEG) are the most commonly used polymers to produce 3D printable bioinks, but they are not specifically applied to the field of skin regeneration [226, 227]. From a general viewpoint, synthetic polymers can support the 3D printed tissue structures and fully degrade after being implanted without any side effects. Here, we describe a set of biocompatible synthetic polymers, including thermoplastic polycaprolactone (PCL), poly(lactic acid) (PLA), and polyurethane, which have the Food and Drug Administration (FDA) approval for use in the human body with special reference to skin regeneration and are broadly applied in 3D bioprinting field of tissue engineering [228–231].

7.1 Poly(ε-caprolactone) (PCL)

Poly(ε-caprolactone) (PCL) is a linear aliphatic polyester, which has been extensively used in biomedical applications. This polymer is hydrophobic and semicrystalline (50%), showing good biocompatibility and relatively slow degradability in the human body. The usefulness of PCL, either alone or in combination with other polymers (e.g., collagen and gelatin), in managing different skin wounds has been previously reported [232–234]. Indeed, poor hydrophilicity and slow degradation lead to designing and using PCL composites in tissue engineering applications.

PCL, as a thermoplastic polymer, shows several desirable features, including good stability under ambient conditions and ease of processability (thermal and solution) and makes it an appropriate candidate for 3D bioprinting [235, 236]. PCL superior printability stems from its low melting temperature and glass transition temperature. Furthermore, it is an applicable biomaterial clinically approved by the FDA as a biodegradable and biocompatible polymer [237]. One of the challenges in employing 3D biomaterials is their degradation rate that should be carefully taken into consideration before the construction of the tissue-engineered target-specific structures. Quick degradation of 3D scaffolds leads to a possible mechanical deficiency and subsequently a rapid degradation of implants in the body. In this regard, PCL can act beneficial by controlling the degradation rate of bioinks through merging different ratios of the polymer and copolymers [238, 239]. The degradation mechanism of the PCL runs through a bulk erosion hydrolysis process in which no toxic components are released [240, 241]. Therefore, due to these useful benefits, PCL is actively utilized as an efficient bioprinting material. In a recently published study, copolymers PCL-block-poly(1,3-propylene succinate) (PCL-PPSu) containing silver particles were prepared to provide a lower processing temperature ink as compared to neat PCL [242]. This approach could enhance the degradation behavior and render antibacterial features without any adverse effects on human dermal fibroblast (HDF) viability. Applying this approach, the inclusion of temperature-sensitive bioactive reagents into 3D printable inks might be realized. The possibility of hot-melt extrusion of PCL containing Ag, Cu, and Zn elements was also shown for 3D printing of antibacterial personalized wound dressings [243].

7.2 Poly(Lactic Acid) (PLA)

Poly(lactic acid) (PLA), known as polylactide, is an aliphatic polyester with a broad range of applications in biomedical engineering [244]. This polymer shows good biocompatibility and degradation without remaining toxic byproducts in the body. In addition, PLA has tailorable features and well-established processing technologies, including injection molding and extrusion [245]. However, some drawbacks are mentioned for PLA, such as its poor toughness, slow degradation rate, and hydrophobicity. Regarding tissue repair and regeneration approaches, PLA could be

successfully applied as a wound-healing material in different shapes and forms [246–248]. Electrospun composites of PLA (e.g., cellulose–PLA, PCL-PLA, and PGA-PLA) have been the most widely prepared and used constructs for skin regeneration applications.

Due to its accessible thermoplastic properties, PLA has been used as a potent biomaterial in frequency 3D bioprinting applications [249]. Despite some molecular weight-dependent differences, PLA owns quite high mechanical properties with an approximate tensile strength of 50–70 MPa and tensile modulus of 3 GPa [250]. Although the molecular weight plays a major role in biodegradability, PLA with high molecular weight may cause infection and inflammation in vivo [251]. Thus, molecular weight properties should be carefully considered before 3D bioprinting due to the effects on the mechanical properties of the target tissues.

7.3 Polyurethane (PU)

Polyurethane (PU) is a thermoset polymer made of urethane links and is considered a versatile material for biomedical setting due to its appropriate biocompatibility, biodegradation, good oxygen and carbon dioxide permeability, mechanical integrity, toughness, durability, and moldable properties. PU either alone or blended with other polymers has been employed for skin repair and regeneration; there several commercially available PU-based dressings for managing wounds, including OpSite®, 3M® Tegaderm®, Medifoam® N, and Bioclusive® [252, 253]. Most of these constructs are commonly used as thin films; however, the use of PU-based composites has also shown promise in treating various skin injuries (e.g., full-thickness wounds) [254].

Using advanced 3D bioprinting techniques, PU can be processed closely into the native ECM of human tissues and organs to achieve improved tissue healing [255]. This polymer has been assessed in different bioprinting systems to create 3D scaffolds with uniform pore patterns and precise control over pore size, shape, and dimensions [256].

8 Conclusion

Over the last two decades, a range of 3D printing technologies have been successfully applied to prepare wound dressings based on both natural and synthetic polymers in the attempt to promote skin regeneration even in very dramatic cases, like diabetic ulcers or severe and wide burns. Man-made polymers allow fine-tuning of the physico-chemical and mechanical properties of the final product as compared to natural substances. Furthermore, their use in tissue-engineered constructs permits overcoming the limitations associated to autologous and allogenic skin grafts. Polymers can be used alone either as thin films or as micropatterned porous structures (scaffolds); some of these products (e.g., beased on polyurethane) have received

FDA approval for clinical used and are currently marketed all around the world and available to clinicians. A special set of advanced manufacturing strategies, collectively called 3D bioplotting, allows the simultaneous printing of both polymeric gels and cells, thus yielding ready-to-use cell-laden constructs; sterilization, commercialization, and storage of such products still remain partially open issues.

Polymeric gels, being soft and sometimes exhibiting thermoreversible properties, are ideal biomaterials to produce printable inks. However, not all biocompatible polymers are inherently functional for promoting skin regeneration from a "biological viewpoint". In other words, while some natural polymers exhibit alone key properties for skin repair, such as pro-angiogenic (e.g., hyaluronic acid) or antibacterial functions (e.g., chitosan), synthetic polymers often do not elicit any beneficial "active" action, apart from wound protection and passive support to host tissue. Regenerative functions can be provided to polymeric gel inks by incorporating cells, therapeutic ions having, for example, a pro-angiogenic (Cu^{2+}) or antimicrobial effect (Ag^{+}), or bioactive inclusions such as bioactive glasses. The last option is highly versatile and opens new horizons in the field of wound healing, while carrying new technological challenges related to the design and actual printability of polymer-based inks that contain rigid micro- or nano-particles inside.

References

1. Boyce ST (2001) Design principles for composition and performance of cultured skin substitutes. Burns 27(5):523–533
2. Tobin DJ (2006) Biochemistry of human skin—our brain on the outside. Chem Soc Rev 35(1):52–67
3. Parenteau NL et al (1992) The organotypic culture of human skin keratinocytes and fibroblasts to achieve form and function. Cytotechnology 9(1–3):163–171
4. Supp DM, Boyce ST (2005) Engineered skin substitutes: practices and potentials. Clin Dermatol 23(4):403–412
5. Groeber F et al (2011) Skin tissue engineering—in vivo and in vitro applications. Adv Drug Deliv Rev 63(4–5):352–366
6. Shevchenko RV, James SL, James SE (2010) A review of tissue-engineered skin bioconstructs available for skin reconstruction. J R Soc Interface 7(43):229–258
7. Volk SW, Iqbal SA, Bayat A (2013) Interactions of the extracellular matrix and progenitor cells in cutaneous wound healing. Adv Wound Care 2(6):261–272
8. Pereira RF et al (2017) Advances in bioprinted cell-laden hydrogels for skin tissue engineering. Biomanufacturing Reviews 2(1):1
9. Ennis WJ, Hill D (2016) Wound healing: a comprehensive wound assessment and treatment approach. Skin Tissue Eng Regen Med 239:75–81
10. Gaur M, Dobke M, Lunyak VV (2017) Mesenchymal stem cells from adipose tissue in clinical applications for dermatological indications and skin aging. Int J Mol Sci 18(1):208
11. McGrath J, Eady R, Pope F (2004) Anatomy and organization of human skin. Rook's Textb Dermatol 1:3.2–3.80
12. Weinstein GD, McCullough JL, Ross P (1984) Cell proliferation in normal epidermis. J Invest Dermatol 82(6):623–628
13. Steinhoff M, Brzoska T, Luger TA (2001) Keratinocytes in epidermal immune responses. Curr Opin Allergy Clin Immunol 1(5):469–476

14. Visscher M, Narendran V (2014) Neonatal infant skin: development, structure and function. Newborn Infant Nurs Rev 14(4):135–141
15. Cichorek M et al (2013) Skin melanocytes: biology and development. Adv Dermatol Allergol/Postępy Dermatologii I Alergologii 30(1):30
16. Johnson J et al (2005) P53 family activities in development and cancer: relationship to melanocyte and keratinocyte carcinogenesis. J Investig Dermatol 125(5):857–864
17. Nguyen D, Orgill D, Murphy G (2009) The pathophysiologic basis for wound healing and cutaneous regeneration. Biomaterials for treating skin loss. Elsevier, pp 25–57
18. Fenner J, Clark R (2016) Anatomy, physiology, histology, and immunohistochemistry of human skin. In: Skin tissue engineering and regenerative medicine, vol 1
19. Bhattacharjee O et al (2019) Unraveling the ECM-immune cell crosstalk in skin diseases. Front Cell Dev Biol 7:00068
20. Reed CC, Iozzo RV (2002) The role of decorin in collagen fibrillogenesis and skin homeostasis. Glycoconj J 19(4–5):249–255
21. Oxlund H, Manschot J, Viidik A (1988) The role of elastin in the mechanical properties of skin. J Biomech 21(3):213–218
22. Nyman E et al (2013) Hyaluronic acid, an important factor in the wound healing properties of amniotic fluid: in vitro studies of re-epithelialisation in human skin wounds. J Plast Surg Hand Surg 47(2):89–92
23. Gallo RL et al (2015) The potential role of topically applied heparan sulfate in the treatment of photodamage. J Drugs Dermatol 14(7):669–674
24. Olivieri J, Smaldone S, Ramirez F (2010) Fibrillin assemblies: extracellular determinants of tissue formation and fibrosis. Fibrogenesis Tissue Repair 3(1):24
25. Fyrand O (1979) Studies on fibronectin in the skin. Arch Dermatol Res 266(1):33–41
26. Johnson MB et al (2017) Topical fibronectin improves wound healing of irradiated skin. Sci Rep 7(1):1–10
27. Nishiyama T et al (2000) The importance of laminin 5 in the dermal–epidermal basement membrane. J Dermatol Sci 24:S51–S59
28. Iorio V, Troughton LD, Hamill KJ (2015) Laminins: roles and utility in wound repair. Adv Wound Care 4(4):250–263
29. Duda DG et al (2007) A protocol for phenotypic detection and enumeration of circulating endothelial cells and circulating progenitor cells in human blood. Nat Protoc 2(4):805
30. Erickson JR, Echeverri K (2018) Learning from regeneration research organisms: the circuitous road to scar free wound healing. Dev Biol 433(2):144–154
31. Gurtner GC et al (2008) Wound repair and regeneration. Nature 453(7193):314–321
32. Marikovsky M et al (1993) Appearance of heparin-binding EGF-like growth factor in wound fluid as a response to injury. Proc Natl Acad Sci USA 90(9):3889–3893
33. Werner S et al (1992) Differential splicing in the extracellular region of fibroblast growth factor receptor 1 generates receptor variants with different ligand-binding specificities. Mol Cell Biol 12(1):82–88
34. Eriksson A et al (1992) PDGF alpha- and beta-receptors activate unique and common signal transduction pathways. Embo j 11(2):543–550
35. Rappolee DA et al (1988) Wound macrophages express TGF-alpha and other growth factors in vivo: analysis by mRNA phenotyping. Science 241(4866):708–712
36. Losi P et al (2013) Fibrin-based scaffold incorporating VEGF-and bFGF-loaded nanoparticles stimulates wound healing in diabetic mice. Acta Biomater 9(8):7814–7821
37. Schmitt S et al (2013) Stathmin regulates keratinocyte proliferation and migration during cutaneous regeneration. PLoS One 8(9):e75075
38. Bevan D et al (2004) Diverse and potent activities of HGF/SF in skin wound repair. J Pathol 203(3):831–838
39. Jackson WM, Nesti LJ, Tuan RS (2012) Mesenchymal stem cell therapy for attenuation of scar formation during wound healing. Stem Cell Res Ther 3(3):20
40. Madlener M et al (1996) Regulation of the expression of stromelysin-2 by growth factors in keratinocytes: implications for normal and impaired wound healing. Biochem J 320(2):659–664

41. Frank S, Madlener M, Werner S (1996) Transforming growth factors beta1, beta2, and beta3 and their receptors are differentially regulated during normal and impaired wound healing. J Biol Chem 271(17):10188–10193
42. Hübner G et al (1996) Differential regulation of pro-inflammatory cytokines during wound healing in normal and glucocorticoid-treated mice. Cytokine 8(7):548–556
43. Salmon-Ehr V et al (2000) Implication of interleukin-4 in wound healing. Lab Invest 80(8):1337–1343
44. Mattey DL (1997) Interleukin-4 induces myofibroblast differentiation is synovial fibroblasts. Biochem Soc Trans 25(2):290s
45. Peranteau WH et al (2008) IL-10 overexpression decreases inflammatory mediators and promotes regenerative healing in an adult model of scar formation. J Invest Dermatol 128(7):1852–1860
46. Krishnamurthy P et al (2011) Interleukin-10 deficiency impairs bone marrow-derived endothelial progenitor cell survival and function in ischemic myocardium. Circ Res 109(11):1280–1289
47. King A et al (2014) Regenerative Wound Healing: The Role of Interleukin-10. Adv Wound Care (New Rochelle) 3(4):315–323
48. Matias MA et al (2011) Accelerated wound healing phenotype in Interleukin 12/23 deficient mice. J Inflamm (Lond) 8:39
49. Clark RA (2014) Wound repair: basic biology to tissue engineering. Principles of tissue engineering. Elsevier, pp 1595–1617
50. Schultz GS, Wysocki A (2009) Interactions between extracellular matrix and growth factors in wound healing. Wound repair and regeneration 17(2):153–162
51. Wu Y, Tredget E (2014) Pathology of tissue regeneration repair: skin regeneration pp 558–566
52. Babu PS, Danilovich N, Sairam M (2001) Hormone-induced receptor gene splicing: enhanced expression of the growth factor type I follicle-stimulating hormone receptor motif in the developing mouse ovary as a new paradigm in growth regulation. Endocrinology 142(1):381–389
53. Levy V et al (2007) Epidermal stem cells arise from the hair follicle after wounding. FASEB J 21(7):1358–1366
54. Ito M et al (2005) Stem cells in the hair follicle bulge contribute to wound repair but not to homeostasis of the epidermis. Nat Med 11(12):1351–1354
55. Brodsky S et al (2001) Plasmin-dependent and-independent effects of plasminogen activators and inhibitor-1 on ex vivo angiogenesis. Am J Physiol-Heart Circulatory Physiol 281(4):H1784–H1792
56. Velnar T, Bailey T, Smrkolj V (2009) The wound healing process: an overview of the cellular and molecular mechanisms. J Int Med Res 37(5):1528–1542
57. Diegelman R, Evans M (2004) Wound healing: an overview of acute, fibrotic and delayed. Front Biosci 9:283–289
58. Madden JW, Peacock EE Jr (1971) Studies on the biology of collagen during wound healing. 3. Dynamic metabolism of scar collagen and remodeling of dermal wounds. Ann Surgery 174(3):511–520
59. Hinz B (2016) The role of myofibroblasts in wound healing. Curr Res Transl Med 64(4):171–177
60. Guo SA, DiPietro LA (2010) Factors affecting wound healing. J Dental Res 89(3):219–229
61. Menke NB et al (2007) Impaired wound healing. Clin Dermatol 25(1):19–25
62. Moseley R et al (2004) Comparison of oxidative stress biomarker profiles between acute and chronic wound environments. Wound Repair Regener 12(4):419–429
63. Herrick S et al (1992) Sequential changes in histologic pattern and extracellular matrix deposition during the healing of chronic venous ulcers. Am J Pathol 141(5):1085
64. Halim AS, Khoo TL, Yussof SJM (2010) Biologic and synthetic skin substitutes: an overview. Indian J Plast Surgery: Off Publ Assoc Plast Surgeons India 43(Suppl):S23
65. Shores JT, Gabriel A, Gupta S (2007) Skin substitutes and alternatives: a review. Adv Skin Wound Care 20(9):493–508

66. Böttcher-Haberzeth S, Biedermann T, Reichmann E (2010) Tissue engineering of skin. Burns 36(4):450–460
67. Zweifel C et al (2008) Initial experiences using non-cultured autologous keratinocyte suspension for burn wound closure. J Plast Reconstr Aesthet Surg 61(11):e1–e4
68. Gravante G et al (2007) A randomized trial comparing ReCell® system of epidermal cells delivery versus classic skin grafts for the treatment of deep partial thickness burns. Burns 33(8):966–972
69. Philandrianos C et al (2012) Comparison of five dermal substitutes in full-thickness skin wound healing in a porcine model. Burns 38(6):820–829
70. van der Veen VC et al (2011) New dermal substitutes. Wound Repair Regener 19:s59–s65
71. Milan PB et al (2016) Accelerated wound healing in a diabetic rat model using decellularized dermal matrix and human umbilical cord perivascular cells. Acta Biomater 45:234–246
72. Van der Veen VC et al (2010) Biological background of dermal substitutes. Burns 36(3):305–321
73. Hansen SL et al (2001) Using skin replacement products to treat burns and wounds. Adv Skin Wound Care 14(1):37–46
74. Pham C et al (2007) Bioengineered skin substitutes for the management of burns: a systematic review. Burns 33(8):946–957
75. Bártolo PJ et al (2011) Biofabrication strategies for tissue engineering. Advances on Modeling in Tissue Engineering. Springer, pp 137–176
76. Nichol JW, Khademhosseini A (2009) Modular tissue engineering: engineering biological tissues from the bottom up. Soft Matter 5(7):1312–1319
77. Du Y et al (2008) Directed assembly of cell-laden microgels for fabrication of 3D tissue constructs. Proc Natl Acad Sci 105(28):9522–9527
78. Khademhosseini A et al (2006) Microscale technologies for tissue engineering and biology. Proc Natl Acad Sci 103(8):2480–2487
79. Bartolo P et al (2012) Biomedical production of implants by additive electro-chemical and physical processes. CIRP Ann 61(2):635–655
80. Bártolo P et al (2009) Biomanufacturing for tissue engineering: present and future trends. Virtual Phys Prototyping 4(4):203–216
81. Melchels FP et al (2012) Additive manufacturing of tissues and organs. Prog Polym Sci 37(8):1079–1104
82. Guillotin B, Guillemot F (2011) Cell patterning technologies for organotypic tissue fabrication. Trends Biotechnol 29(4):183–190
83. Jakab K et al (2004) Engineering biological structures of prescribed shape using self-assembling multicellular systems. Proc Natl Acad Sci 101(9):2864–2869
84. Censi R et al (2012) Hydrogels for protein delivery in tissue engineering. J Control Release 161(2):680–692
85. de Amorim Almeida H, da Silva Bártolo PJ (2010) Virtual topological optimisation of scaffolds for rapid prototyping. Med Eng Phys 32(7):775–782
86. Hosseinkhani H et al (2006) Enhanced angiogenesis through controlled release of basic fibroblast growth factor from peptide amphiphile for tissue regeneration. Biomaterials 27(34):5836–5844
87. Mohamed A, Xing MM (2012) Nanomaterials and nanotechnology for skin tissue engineering. Int J Burns Trauma 2(1):29
88. Smith L, Ma P (2004) Nano-fibrous scaffolds for tissue engineering. Colloids Surf B 39(3):125–131
89. Zhong S, Zhang Y, Lim C (2010) Tissue scaffolds for skin wound healing and dermal reconstruction. Wiley Interdisc Rev: Nanomed Nanobiotechnol 2(5):510–525
90. Chandrasekaran AR et al (2011) Fabrication of a nanofibrous scaffold with improved bioactivity for culture of human dermal fibroblasts for skin regeneration. Biomed Mater 6(1):015001
91. Nazarnezhada S et al (2020) Alginate hydrogel containing hydrogen sulfide as the functional wound dressing material: in vitro and in vivo study. Int J Biol Macromol 164:3323–3331

92. Heunis T, Dicks L (2010) Nanofibers offer alternative ways to the treatment of skin infections. J Biomed Biotechnol 2010:510682
93. Ranjbar Mohammadi M et al (2020) An excellent nanofibrous matrix based on gum tragacanth-poly (Ɛ-caprolactone)-poly (vinyl alcohol) for application in diabetic wound healing. Polym Degradat Stab 174:109105
94. Salehi M et al (2020) Porous electrospun poly(ε-caprolactone)/gelatin nanofibrous mat containing cinnamon for wound healing application: in vitro and in vivo study. Biomed Eng Lett 10(1):149–161
95. Zahedi P et al (2010) A review on wound dressings with an emphasis on electrospun nanofibrous polymeric bandages. Polym Adv Technol 21(2):77–95
96. Mitchella GR, Ahnb K-H, Davisb FJ (2011) The potential of electrospinning in rapid manufacturing processes. Virtual and Physical Prototyping 6(2):63–77
97. Cunha C, Panseri S, Antonini S (2011) Emerging nanotechnology approaches in tissue engineering for peripheral nerve regeneration. Nanomed: Nanotechnol Biol Med 7(1):50–59
98. Bhardwaj N, Kundu SC (2010) Electrospinning: a fascinating fiber fabrication technique. Biotechnol Adv 28(3):325–347
99. Lee JKY et al (2018) Polymer-based composites by electrospinning: Preparation & functionalization with nanocarbons. Prog Polym Sci 86:40–84
100. Zhang Y et al (2007) Biomimetic and bioactive nanofibrous scaffolds from electrospun composite nanofibers. Int J Nanomed 2(4):623
101. Dhandayuthapani B, Krishnan UM, Sethuraman S (2010) Fabrication and characterization of chitosan-gelatin blend nanofibers for skin tissue engineering. J Biomed Mater Res B Appl Biomater 94(1):264–272
102. Powell H, Boyce S (2008) Fiber density of electrospun gelatin scaffolds regulates morphogenesis of dermal–epidermal skin substitutes. J Biomed Mater Res Part A: Offl J Soc Biomater Japanese Soc Biomater Austr Soc Biomater Korean Soc Biomater 84(4):1078–1086
103. Cui W et al (2009) Evaluation of electrospun fibrous scaffolds of poly (dl-lactide) and poly (ethylene glycol) for skin tissue engineering. Mater Sci Eng C 29(6):1869–1876
104. Kumbar SG et al (2008) Electrospun poly (lactic acid-co-glycolic acid) scaffolds for skin tissue engineering. Biomaterials 29(30):4100–4107
105. Chen H et al (2011) Electrospun chitosan-graft-poly (ε-caprolactone)/poly (ε-caprolactone) cationic nanofibrous mats as potential scaffolds for skin tissue engineering. Int J Biol Macromol 48(1):13–19
106. Zhou Y et al (2008) Electrospun water-soluble carboxyethyl chitosan/poly (vinyl alcohol) nanofibrous membrane as potential wound dressing for skin regeneration. Biomacromol 9(1):349–354
107. Nazarnezhad S et al (2020) Electrospun nanofibers for improved angiogenesis: promises for tissue engineering applications. Nanomaterials 10(8):1609
108. Yildirimer L, Thanh NT, Seifalian AM (2012) Skin regeneration scaffolds: a multimodal bottom-up approach. Trends Biotechnol 30(12):638–648
109. Choi JS, Leong KW, Yoo HS (2008) In vivo wound healing of diabetic ulcers using electrospun nanofibers immobilized with human epidermal growth factor (EGF). Biomaterials 29(5):587–596
110. Yang Y et al (2011) Promotion of skin regeneration in diabetic rats by electrospun core-sheath fibers loaded with basic fibroblast growth factor. Biomaterials 32(18):4243–4254
111. Shalumon K et al (2011) Sodium alginate/poly (vinyl alcohol)/nano ZnO composite nanofibers for antibacterial wound dressings. Int J Biol Macromol 49(3):247–254
112. Suganya S et al (2011) Herbal drug incorporated antibacterial nanofibrous mat fabricated by electrospinning: an excellent matrix for wound dressings. J Appl Polym Sci 121(5):2893–2899
113. Tavakoli S, Klar AS (2020) Advanced hydrogels as wound dressings. Biomolecules 10(8):1169
114. Gupta P, Vermani K, Garg S (2002) Hydrogels: from controlled release to pH-responsive drug delivery. Drug Discovery Today 7(10):569–579

115. Ahmed EM (2015) Hydrogel: Preparation, characterization, and applications: a review. J Adv Res 6(2):105–121
116. Pereira RF, Bártolo PJ (2014) Photopolymerizable hydrogels in regenerative medicine and drug delivery. Fut Med 6–28
117. Yang J-A et al (2014) In situ-forming injectable hydrogels for regenerative medicine. Prog Polym Sci 39(12):1973–1986
118. Hunt NC, Shelton RM, Grover L (2009) An alginate hydrogel matrix for the localised delivery of a fibroblast/keratinocyte co-culture. Biotechnol J 4(5):730–737
119. Lootens L et al (2013) Keratinocytes in the treatment of severe burn injury: an update. Int Wound J 10(1):6–12
120. Mironov V et al (2009) Organ printing: tissue spheroids as building blocks. Biomaterials 30(12):2164–2174
121. Mironov V et al (2003) Organ printing: computer-aided jet-based 3D tissue engineering. Trends Biotechnol 21(4):157–161
122. Zhang YS et al (2017) 3D bioprinting for tissue and organ fabrication. Ann Biomed Eng 45(1):148–163
123. Guillotin B et al (2010) Laser assisted bioprinting of engineered tissue with high cell density and microscale organization. Biomaterials 31(28):7250–7256
124. Unkovskiy A et al (2019) Additive manufacturing: a comparative analysis of dimensional accuracy and skin texture reproduction of auricular prostheses replicas. J Prosthodont 28(2):e460–e468
125. Hakimi N et al (2018) Handheld skin printer: in situ formation of planar biomaterials and tissues. Lab Chip 18(10):1440–1451
126. Sun W et al (2020) The bioprinting roadmap. Biofabrication 12(2):022002
127. Michael S et al (2013) Tissue engineered skin substitutes created by laser-assisted bioprinting form skin-like structures in the dorsal skin fold chamber in mice. PloS One 8(3):e57741
128. Koch L et al (2013) Laser assisted cell printing. Curr Pharm Biotechnol 14(1):91–97
129. Seol Y-J et al (2018) 3D bioprinted biomask for facial skin reconstruction. Bioprinting 10:e00028
130. Obata K et al (2013) High-aspect 3D two-photon polymerization structuring with widened objective working range (WOW-2PP). Light: Sci Appl 2(12):e116–e116
131. Malda J et al (2013) 25th anniversary article: engineering hydrogels for biofabrication. Adv Mater 25(36):5011–5028
132. Singh D, Singh D, Han SS (2016) 3D printing of scaffold for cells delivery: advances in skin tissue engineering. Polymers 8(1):19
133. Peng W, Unutmaz D, Ozbolat IT (2016) Bioprinting towards physiologically relevant tissue models for pharmaceutics. Trends Biotechnol 34(9):722–732
134. Seol Y-J et al (2014) Bioprinting technology and its applications. Eur J Cardiothorac Surg 46(3):342–348
135. Gudapati H, Dey M, Ozbolat I (2016) A comprehensive review on droplet-based bioprinting: past, present and future. Biomaterials 102:20–42
136. Li K et al (2018) Controllable printing droplets on demand by piezoelectric inkjet: applications and methods. Microsyst Technol 24(2):879–889
137. Matai I et al (2020) Progress in 3D bioprinting technology for tissue/organ regenerative engineering. Biomaterials 226:119536
138. Mandrycky C et al (2016) 3D bioprinting for engineering complex tissues. Biotechnol Adv 34(4):422–434
139. McCormack A et al (2020) 3D printing in suspension baths: keeping the promises of bioprinting afloat. Trends Biotechnol 38(6):584–593
140. Shim J-H et al (2012) Bioprinting of a mechanically enhanced three-dimensional dual cell-laden construct for osteochondral tissue engineering using a multi-head tissue/organ building system. J Micromech Microeng 22(8):085014
141. Gao G et al (2019) Recent strategies in extrusion-based three-dimensional cell printing toward organ biofabrication. ACS Biomater Sci Eng 5(3):1150–1169

142. Khalil S, Sun W (2007) Biopolymer deposition for freeform fabrication of hydrogel tissue constructs. Mater Sci Eng C 27(3):469–478
143. Tigner TJ et al (2019) Comparison of photo cross linkable gelatin derivatives and initiators for three-dimensional extrusion bioprinting. Biomacromol 21(2):454–463
144. Turner PR et al (2020) Peptide chitosan/dextran core/shell vascularized 3D constructs for wound healing. ACS Appl Mater Interf 12(29):32328–32339
145. Yue Z et al (2016) Advances in printing biomaterials and living cells: implications for islet cell transplantation. Curr Opin Organ Transplant 21(5):467–475
146. Wang Z et al (2015) A simple and high-resolution stereolithography-based 3D bioprinting system using visible light crosslinkable bioinks. Biofabrication 7(4):045009
147. Zhou X et al (2020) Three-dimensional printing biologically inspired dna-based gradient scaffolds for cartilage tissue regeneration. ACS Appl Mater Interf 12(29):33219–33228
148. Lin H et al (2013) Application of visible light-based projection stereolithography for live cell-scaffold fabrication with designed architecture. Biomaterials 34(2):331–339
149. Melchels FP, Feijen J, Grijpma DW (2010) A review on stereolithography and its applications in biomedical engineering. Biomaterials 31(24):6121–6130
150. Donderwinkel I, Van Hest JC, Cameron NR (2017) Bio-inks for 3D bioprinting: recent advances and future prospects. Polym Chem 8(31):4451–4471
151. Liang Y et al (2019) Direct electrohydrodynamic patterning of high-performance all metal oxide thin-film electronics. ACS Nano 13(12):13957–13964
152. He J et al (2020) High-resolution electrohydrodynamic bioprinting: a new biofabrication strategy for biomimetic micro/nanoscale architectures and living tissue constructs. Biofabrication 12(4):042002
153. Gao D, Zhou JG (2019) Designs and applications of electrohydrodynamic 3D printing. Int J Bioprint 4(6):309
154. Mao M et al (2020) Multi-directional cellular alignment in 3D guided by electrohydrodynamically-printed microlattices. Acta Biomater 101:141–151
155. Sutterby E et al (2020) Microfluidic skin-on-a-chip models: toward biomimetic artificial skin. Small 16(39):2002515
156. Xu J et al (2020) Advances in the research of bioinks based on natural collagen, polysaccharide and their derivatives for skin 3D bioprinting. Polymers 12(6):1237
157. Au AK et al (2016) 3D-printed microfluidics. Angew Chem Int Ed 55(12):3862–3881
158. Gao G et al (2017) Tissue engineered bio-blood-vessels constructed using a tissue-specific bioink and 3D coaxial cell printing technique: a novel therapy for ischemic disease. Adv Func Mater 27(33):1700798
159. Montero FE et al (2019) Development of a smart bioink for bioprinting applications. Front Mech Eng 5:56
160. Gopinathan J, Noh I (2018) Recent trends in bioinks for 3D printing. Biomater Res 22(1):11
161. Valot L et al (2019) Chemical insights into bioinks for 3D printing. Chem Soc Rev 48(15):4049–4086
162. Smandri A et al (2020) Natural 3D-printed bioinks for skin regeneration and wound healing: a systematic review. Polymers 12(8):1782
163. Colosi C et al (2016) Microfluidic bioprinting of heterogeneous 3D tissue constructs using low-viscosity bioink. Adv Mater 28(4):677–684
164. Aderibigbe BA, Buyana B (2018) Alginate in wound dressings. Pharmaceutics 10(2):42
165. Pourchet LJ et al (2017) Human skin 3D bioprinting using scaffold-free approach. Adv Healthcare Mater 6(4):1601101
166. Liu P et al (2019) 3D bioprinting and in vitro study of bilayered membranous construct with human cells-laden alginate/gelatin composite hydrogels. Colloids Surf B 181:1026–1034
167. Datta S et al (2018) Alginate-honey bioinks with improved cell responses for applications as bioprinted tissue engineered constructs. J Mater Res 33(14):2029–2039
168. Hunt NC, Grover LM (2010) Cell encapsulation using biopolymer gels for regenerative medicine. Biotech Lett 32(6):733–742

169. Skardal A et al (2012) Bioprinted amniotic fluid-derived stem cells accelerate healing of large skin wounds. Stem Cells Transl Med 1(11):792–802
170. Augustine R (2018) Skin bioprinting: a novel approach for creating artificial skin from synthetic and natural building blocks. Prog Biomater 7:77–92
171. Xue Z, Yang M, Xu D (2019) Nucleation of biomimetic hydroxyapatite nanoparticles on the surface of type I collagen: molecular dynamics investigations. J Phys Chem C 123(4):2533–2543
172. Nocera AD et al (2018) Development of 3D printed fibrillar collagen scaffold for tissue engineering. Biomed Microdevice 20(2):26
173. Heidenreich AC et al (2020) Collagen and chitosan blends for 3D bioprinting: A rheological and printability approach. Polymer Test 82:106297
174. Albanna M et al (2019) In situ bioprinting of autologous skin cells accelerates wound healing of extensive excisional full-thickness wounds. Sci Rep 9(1):1–15
175. Osidak EO et al (2019) Viscoll collagen solution as a novel bioink for direct 3D bioprinting. J Mater Sci Mater Med 30(3):31
176. Lee V et al (2014) Design and fabrication of human skin by three-dimensional bioprinting. Tissue Eng Part C Methods 20(6):473–484
177. Kim JE, Kim SH, Jung Y (2016) Current status of three-dimensional printing inks for soft tissue regeneration. Tissue Eng Regen Med 13(6):636–646
178. Ulrich TA et al (2010) Probing cellular mechanobiology in three-dimensional culture with collagen–agarose matrices. Biomaterials 31(7):1875–1884
179. Kim G et al (2011) Coaxial structured collagen–alginate scaffolds: fabrication, physical properties, and biomedical application for skin tissue regeneration. J Mater Chem 21(17):6165–6172
180. Ma L et al (2003) Collagen/chitosan porous scaffolds with improved biostability for skin tissue engineering. Biomaterials 24(26):4833–4841
181. Han C-M et al (2010) Application of collagen-chitosan/fibrin glue asymmetric scaffolds in skin tissue engineering. J Zhejiang Univ Sci B 11(7):524–530
182. Shin J-Y, Jeong S-J, Lee W-K (2019) Fabrication of porous scaffold by ternary combination of chitosan, gelatin, and calcium phosphate for tissue engineering. J Ind Eng Chem 80:862–869
183. Choi DJ et al (2018) Effect of the pore size in a 3D bioprinted gelatin scaffold on fibroblast proliferation. J Ind Eng Chem 67:388–395
184. Xu W et al (2019) On low-concentration inks formulated by nanocellulose assisted with gelatin methacrylate (gelma) for 3D printing toward wound healing application. ACS Appl Mater Interf 11(9):8838–8848
185. Shi L et al (2018) Three-dimensional printing alginate/gelatin scaffolds as dermal substitutes for skin tissue engineering. Polym Eng Sci 58(10):1782–1790
186. Huang L et al (2019) Bacterial cellulose nanofibers promote stress and fidelity of 3D-printed silk based hydrogel scaffold with hierarchical pores. Carbohyd Polym 221:146–156
187. Chen C-S et al (2018) Three-dimensionally printed silk-sericin-based hydrogel scaffold: a promising visualized dressing material for real-time monitoring of wounds. ACS Appl Mater Interf 10(40):33879–33890
188. Wang X et al (2006) Generation of three-dimensional hepatocyte/gelatin structures with rapid prototyping system. Tissue Eng 12(1):83–90
189. Ouyang L et al (2016) Effect of bioink properties on printability and cell viability for 3D bioplotting of embryonic stem cells. Biofabrication 8(3):035020
190. Roehm KD, Madihally SV (2017) Bioprinted chitosan-gelatin thermosensitive hydrogels using an inexpensive 3D printer. Biofabrication 10(1):015002
191. Sharma R et al (2020) 3D bioprinting pluripotent stem cell derived neural tissues using a novel fibrin bioink containing drug releasing microspheres. Front Bioeng Biotechnol 8:57
192. Shin JH, Kang H-W (2018) The development of gelatin-based bio-ink for use in 3D hybrid bioprinting. Int J Precis Eng Manuf 19(5):767–771
193. Xiong S et al (2017) A gelatin-sulfonated silk composite scaffold based on 3D printing technology enhances skin regeneration by stimulating epidermal growth and dermal neovascularization. Sci Rep 7(1):1–12

194. Das S et al (2015) Bioprintable, cell-laden silk fibroin–gelatin hydrogel supporting multilineage differentiation of stem cells for fabrication of three-dimensional tissue constructs. Acta Biomater 11:233–246
195. Gauvin R et al (2012) Microfabrication of complex porous tissue engineering scaffolds using 3D projection stereolithography. Biomaterials 33(15):3824–3834
196. Chen X et al (2019) Development of rhamnose-rich hydrogels based on sulfated xylorhamnouronic acid toward wound healing applications. Biomater Sci 7(8):3497–3509
197. Patrulea V et al (2015) Chitosan as a starting material for wound healing applications. Eur J Pharm Biopharm 97:417–426
198. Pahlevanzadeh F et al (2020) Three-dimensional printing constructs based on the chitosan for tissue regeneration: state of the art, developing directions and prospect trends. Materials (Basel, Switzerland) 13(11):2663
199. Intini C et al (2018) 3D-printed chitosan-based scaffolds: an in vitro study of human skin cell growth and an in-vivo wound healing evaluation in experimental diabetes in rats. Carbohyd Polym 199:593–602
200. Ng WL, Yeong WY, Naing MW (2016) Polyelectrolyte gelatin-chitosan hydrogel optimized for 3D bioprinting in skin tissue engineering. Int J Bioprint 2(1):53–62
201. Ng WL, Yeong WY, Naing MW (2016) Development of polyelectrolyte chitosan-gelatin hydrogels for skin bioprinting. Procedia Cirp 49:105–112
202. Hafezi F et al (2019) 3D printed chitosan dressing crosslinked with genipin for potential healing of chronic wounds. Int J Pharm 560:406–415
203. Gholipourmalekabadi M et al (2020) Silk fibroin for skin injury repair: where do things stand? Adv Drug Deliv Rev 153:28–53
204. Jao D, Mou X, Hu X (2016) Tissue regeneration: a silk road. J Funct Biomater 7(3):22
205. Kamalathevan P, Ooi PS, Loo YL (2018) Silk-based biomaterials in cutaneous wound healing: a systematic review. Adv Skin Wound Care 31(12):565–573
206. Wang F et al (2020) Tunable biodegradable polylactide–silk fibroin scaffolds fabricated by a solvent-free pressure-controllable foaming technology. ACS Appl Bio Mater 3(12):8795–8807
207. Keirouz A et al (2020) High-throughput production of silk fibroin-based electrospun fibers as biomaterial for skin tissue engineering applications. Mater Sci Eng C 112:110939
208. Egan PF (2019) Integrated design approaches for 3D printed tissue scaffolds: review and outlook. Materials 12(15):2355
209. Chawla S et al (2018) Silk-based bioinks for 3D bioprinting. Adv Healthcare Mater 7(8):1701204
210. Wang Q et al (2019) 3D printing of silk fibroin for biomedical applications. Materials 12(3):504
211. Zheng Z et al (2018) 3D bioprinting of self-standing silk-based bioink. Adv Healthcare Mater 7(6):1701026
212. Gupta S et al (2020) Evaluation of silk-based bioink during pre and post 3D bioprinting: a review. J Biomed Mater Res Part B: Appl Biomater 109(2):279–293
213. Kim SH, Lim TH, Park CH (2020) Silk fibroin bioinks for digital light processing (DLP) 3D bioprinting. Bioinspired biomaterials. Springer, pp 53–66
214. Gong D et al (2020) Preparing 3D-printable silk fibroin hydrogels with robustness by a two-step crosslinking method. RSC Adv 10(45):27225–27234
215. Kulkarni G et al (2020) Tailorable hydrogel of gelatin with silk fibroin and its activation/crosslinking for enhanced proliferation of fibroblast cells. Int J Biol Macromol 164:4073–4083
216. Kim BS et al (2017) Decellularized extracellular matrix: a step towards the next generation source for bioink manufacturing. Biofabrication 9(3):034104
217. Kim BS et al (2019) 3D cell printing of perfusable vascularized human skin equivalent composed of epidermis, dermis, and hypodermis for better structural recapitulation of native skin. Adv Healthcare Mater 8(7):1801019

218. Ali M et al (2019) A photo-crosslinkable kidney ECM-derived bioink accelerates renal tissue formation. Adv Healthcare Mater 8(7):1800992
219. Lee H et al (2017) Development of liver decellularized extracellular matrix bioink for three-dimensional cell printing-based liver tissue engineering. Biomacromol 18(4):1229–1237
220. La W-G et al (2016) Systemically replicated organic and inorganic bony microenvironment for new bone formation generated by a 3D printing technology. RSC Adv 6(14):11546–11553
221. Jang J et al (2018) Biomaterials-based 3D cell printing for next-generation therapeutics and diagnostics. Biomaterials 156:88–106
222. Dzobo K, Motaung KSCM, Adesida A (2019) Recent trends in decellularized extracellular matrix bioinks for 3D printing: an updated review. Int J Mol Sci 20(18):4628
223. Kim BS et al (2018) 3D cell printing of in vitro stabilized skin model and in vivo pre-vascularized skin patch using tissue-specific extracellular matrix bioink: a step towards advanced skin tissue engineering. Biomaterials 168:38–53
224. Burdick JA, Prestwich GD (2011) Hyaluronic acid hydrogels for biomedical applications. Adv Mater 23(12):H41–H56
225. Guvendiren M, Burdick JA (2013) Engineering synthetic hydrogel microenvironments to instruct stem cells. Curr Opin Biotechnol 24(5):841–846
226. Kang H-W et al (2016) A 3D bioprinting system to produce human-scale tissue constructs with structural integrity. Nat Biotechnol 34(3):312–319
227. Hockaday L et al (2012) Rapid 3D printing of anatomically accurate and mechanically heterogeneous aortic valve hydrogel scaffolds. Biofabrication 4(3):035005
228. Jeong H-J et al (2020) 3D bioprinting strategies for the regeneration of functional tubular tissues and organs. Bioengineering 7(2):32
229. Sabir MI, Xu X, Li L (2009) A review on biodegradable polymeric materials for bone tissue engineering applications. J Mater Sci 44(21):5713–5724
230. Wu W, DeConinck A, Lewis JA (2011) Omnidirectional printing of 3D microvascular networks. Adv Mater 23(24):H178–H183
231. Kim BS et al (2016) Three-dimensional bioprinting of cell-laden constructs with poly-caprolactone protective layers for using various thermoplastic polymers. Biofabrication 8(3):035013
232. He J et al (2020) Anti-oxidant electroactive and antibacterial nanofibrous wound dressings based on poly (ε-caprolactone)/quaternized chitosan-graft-polyaniline for full-thickness skin wound healing. Chem Eng J 385:123464
233. Dodero A et al (2020) Multilayer alginate-polycaprolactone electrospun membranes as skin wound patches with drug delivery abilities. ACS Appl Mater Interf 12(28):31162–31171
234. Yang S et al (2020) Multifunctional chitosan/polycaprolactone nanofiber scaffolds with varied dual-drug release for wound-healing applications. ACS Biomater Sci Eng 6(8):4666–4676
235. Mondal D, Griffith M, Venkatraman SS (2016) Polycaprolactone-based biomaterials for tissue engineering and drug delivery: current scenario and challenges. Int J Polym Mater Polym Biomater 65(5):255–265
236. Borkar T, Goenka V, Jaiswal AK (2020) Application of poly-ε-caprolactone in extrusion-based bioprinting. Bioprinting 21:e00111
237. Li Z, Tan BH (2014) Towards the development of polycaprolactone based amphiphilic block copolymers: molecular design, self-assembly and biomedical applications. Mater Sci Eng C 45:620–634
238. Woodruff MA, Hutmacher DW (2010) The return of a forgotten polymer—Polycaprolactone in the 21st century. Prog Polym Sci 35(10):1217–1256
239. Guo B, Ma PX (2014) Synthetic biodegradable functional polymers for tissue engineering: a brief review. Science China Chem 57(4):490–500
240. Lam CX et al (2009) Evaluation of polycaprolactone scaffold degradation for 6 months in vitro and in vivo. J Biomed Mater Res Part A: Off J Soc Biomater Japanese Soc Biomater Austr Soc Biomater Korean Soc Biomater 90(3):906–919
241. Lam CX et al (2008) Dynamics of in vitro polymer degradation of polycaprolactone-based scaffolds: accelerated versus simulated physiological conditions. Biomed Mater 3(3):034108

242. Afghah F et al (2020) 3D printing of silver-doped polycaprolactone-poly (propylene succinate) composite scaffolds for skin tissue engineering. Biomed Mater 15(3):035015
243. Muwaffak Z et al (2017) Patient-specific 3D scanned and 3D printed antimicrobial polycaprolactone wound dressings. Int J Pharm 527(1):161–170
244. Patrício T et al (2014) Fabrication and characterisation of PCL and PCL/PLA scaffolds for tissue engineering. Rapid Prototyping 20(2):145–156
245. Casalini T et al (2019) A perspective on polylactic acid-based polymers use for nanoparticles synthesis and applications. Front Bioeng Biotechnol 7:259
246. Foong CY et al (2018) Influence of poly (lactic acid) layer on the physical and antibacterial properties of dry bacterial cellulose sheet for potential acute wound healing materials. Fibers Polym 19(2):263–271
247. Nguyen TTT et al (2013) Characteristics of curcumin-loaded poly (lactic acid) nanofibers for wound healing. J Mater Sci 48(20):7125–7133
248. Ren Y et al (2020) Stereocomplexed electrospun nanofibers containing poly (lactic acid) modified quaternized chitosan for wound healing. Carbohydrate Polym 247:116754
249. Zhang B et al (2016) 3D printing of high-resolution PLA-based structures by hybrid electrohydrodynamic and fused deposition modeling techniques. J Micromech Microeng 26(2):025015
250. Farah S, Anderson DG, Langer R (2016) Physical and mechanical properties of PLA, and their functions in widespread applications—a comprehensive review. Adv Drug Deliv Rev 107:367–392
251. Liu S et al (2020) Current applications of poly (lactic acid) composites in tissue engineering and drug delivery. Comp Part B: Eng 199:108238
252. Nair LS, Laurencin CT (2007) Biodegradable polymers as biomaterials. Prog Polym Sci 32(8):762–798
253. Lee SM et al (2016) Physical, morphological, and wound healing properties of a polyurethane foam-film dressing. Biomater Res 20(1):15
254. Bankoti K et al (2017) Accelerated healing of full thickness dermal wounds by macroporous waterborne polyurethane-chitosan hydrogel scaffolds. Mater Sci Eng, C 81:133–143
255. Eppa Ł et al (2018) Deposition of mannose-binding lectin and ficolins and activation of the lectin pathway of complement on the surface of polyurethane tubing used for cardiopulmonary bypass. J Biomed Mater Res B Appl Biomater 106(3):1202–1208
256. Hung K-C, Tseng C-S, Hsu S-H (2016) 3D printing of polyurethane biomaterials. Advances in Polyurethane Biomaterials. Elsevier, pp 149–170

Chapter 7
Biofunctional Inks for 3D Printing in Skin Tissue Engineering

Elif Ilhan, Esma Ahlatcioglu Ozerol, Saadet Alpdagtas, Mustafa Sengor, Cem Bulent Ustundag, and Oguzhan Gunduz

Abstract Three-dimensional (3D) bioprinting, consisting of computer-controlled deposition of scaffolds and cells into designed patterns, is an innovative and promising biofabrication strategy for creating artificial tissues and organs. Bioprinted skin has the potential for clinical transplantation, drug testing, cosmetic assaying as well as fundamental researches. Remarkable advancements have been done over the past decades in the improvement of engineered substitutes that mimic skin by applying the advances in polymer engineering, bioengineering, and nanomedicine. Prior to the printing stage, the pre-design of the process, selection of cell, and biofunctional inks are significant steps for the successful fabrication of 3D bioprinted skin constructs. It is crucial to seek and decide on an appropriate source of biofunctional ink capable of stimulating and supporting printed cells for tissue development. Based on this perspective, this chapter deals with the skin and wound structure, skin tissue engineering, the performance and properties of a broad range of biofunctional inks available for 3D bioprinting technologies to produce skin structures. Besides, the current challenges and advances in designing and developing biofunctional inks with desired properties are overviewed.

E. Ilhan · S. Alpdagtas · M. Sengor · C. B. Ustundag · O. Gunduz (✉)
Center for Nanotechnology and Biomaterials Application and Research (NBUAM), Marmara University, Istanbul, Turkey
e-mail: ucemogu@ucl.ac.uk

E. Ilhan
Faculty of Engineering, Department of Bioengineering, Marmara University, 34722 Istanbul, Turkey

E. A. Ozerol · C. B. Ustundag
Faculty of Chemical and Metallurgical Engineering, Department of Bioengineering, Yildiz Technical University, Istanbul, Turkey

S. Alpdagtas
Faculty of Science, Department of Biology, Van Yuzuncu Yil University, Van, Turkey

M. Sengor · O. Gunduz
Faculty of Technology, Department of Metallurgical and Materials Engineering, Marmara University, Istanbul, Turkey

A. Kumar et al. (eds.), *3D printable Gel-inks for Tissue Engineering*, Gels Horizons: From Science to Smart Materials, https://doi.org/10.1007/978-981-16-4667-6_7

Keywords Skin tissue engineering · 3D printing · Biofunctional ink · Biofabrication · Tissue regeneration · Biomaterial

Graphical Abstract

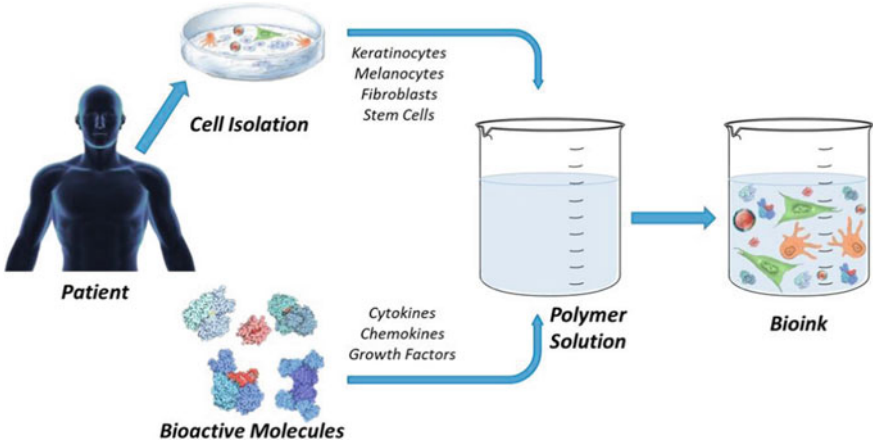

1 Introduction

Skin is one of the most significant part of the human body, acting as a barrier with protective, sensorial, and immunologic functions. Kind of external interventions on the skin tissue may result in various wounds [142]. As one of the most common injuries, skin wounds affect millions of people worldwide [10, 36, 72]. Due to the increment of diabetes and venous/arterial insufficiencies, the cases suffering from chronic wounds have been rising dramatically [101]. Indirect results of skin defects frequently cause bacterial infections, dehydration, and some serious complications which target the homeostasis and thereby the integrity of the skin [30].

To preserve the immediate reactions of the skin, wounds should be recovered or regenerated right after the injury as soon as possible [167]. Tissue engineering approaches suggest many promising treatments to overcome the devastating injuries via combining therapeutic agents, cells, and biomaterials in several methods [26, 40, 121]. As one of the eminent techniques, biofabrication, has emerged as a powerful and novel strategy to develop complex three-dimensional (3D) structures mimicking injured organs and tissues in the skin tissue engineering or outputs used as the basis for regenerative medicine [46, 77]. 3D bioprinting is an advanced biofabrication process that benefits from the computer-controlled deposition of biocompatible materials to produce living and functional 3D tissue constructs. To regenerate or substitute one of the body components, these constructs can be used in the body [23, 83]. 3D

printing technology has paved the way for patient treatment plans that can best fit individual needs [191]. It has numerous advantages including the ability to design different kinds of porous natures [33], complex structures [195], combine growth factors [33], and multiple cells [99] mimicking native tissues. Bioink is the most critical parameter to reach the desired goals in mimicking the skin tissue. Depending on the technique used under biofabrication, bioinks can vary and deserves broad research. Applications of 3D printing are limited by the type of utilized bioinks. Numerous researchers have improved new bioinks to provide their utilization for characteristic 3D bioprinting [83].

Bioinks are the main building blocks for 3D bioprinted constructs [122, 197]. They are termed as cell-laden liquid materials that can include additional components like growth factors and/or signaling molecules in addition to the specific cells, to fabricate native-like structures [196]. To design and fabricate complex biofunctional inks, the bioinks should have critical features, like biodegradability, mechanical durability, biocompatibility, viscoelasticity, non-immunogenicity, and nontoxicity [20]. In addition, for maintaining cell viability, and induce/prevent cellular response, biofunctional ink materials have to be determined based on their mechanical, chemical, biological, and rheological features with best fitting one of the bioprinting techniques [136, 165].

In this chapter, a comprehensive overview of appropriate biofunctional inks utilized in 3D bioprinting for skin tissue engineering is provided. Finally, current challenges and advances in the development of biofunctional inks are also outlined.

2 The Structure and Function of Skin

The skin tissue covers 15% of body weight and 1.8 m^2 of the body area [3, 171]. It performs primarily as a barrier protecting the inner organs from the outer effects such as ultraviolet radiation, abrasion, and pathogens, also fulfills some functions like sensation, vitamin D synthesis, temperature/fluid homeostasis, immune protection, and self-healing [45, 98]. From outer to inner, the skin is composed of three main layers: epidermis, dermis, and hypodermis [6] (Fig. 1). The dermis is largely comprised of elastic and collagen fibrils found in a glycosaminoglycan structure, while the epidermis contains numerous cells [145]. The epidermis layer essentially consists of keratinocytes (95%) and also includes melanocytes, Merkel cells, and antigen-presenting dendritic Langerhans cells. The keratinocytes grow rapidly to transport urea and water throughout aquaporins, repair wounds, and play role in immunity via antimicrobial peptide secretion of the Langerhans cells. Also, they acquire skin color pigment, melanin, from melanocytes to filter out ultraviolet radiation from sunlight [21, 22, 175]. The epidermis has no intrinsic vascular network; therefore, it is nourished from microvascular networks of the dermal layer [6, 117]. The structures localized in the epidermis from the bottom to top are stratum basale (SB), stratum spinosum (SS), stratum granulosum (SG), stratum lucidum (SL), and the stratum corneum (SC) [145]. Generally, the differentiated cubic basal

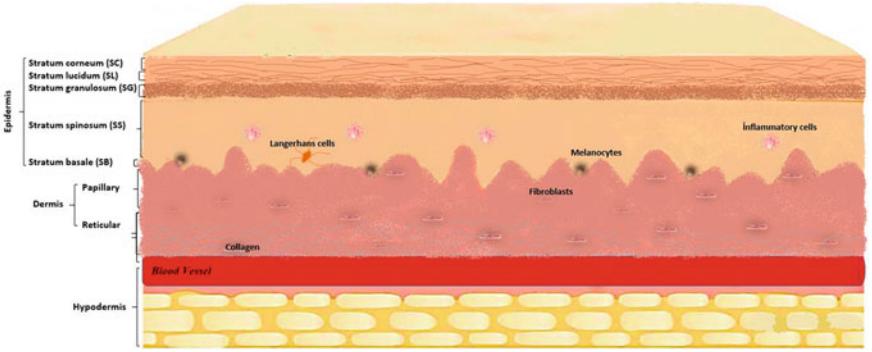

Fig. 1 The schematic structure of skin tissue

keratinocytes migrate from the bottom layer through the apical layers every 28 days [179]. Thus, they progressively get an ovoid shape, lose their nuclei, and ultimately detach from the epidermis [57]. During this process, lipids and keratin ensue which then undergoes terminal differentiation to constitute the upper layer (SC) [2]. This layer prevents the entry of foreign objects and microorganisms into the body [22]. This structure has two separate layers, consisting of the upper part, stratum disjunctum, and the lower part, stratum compactum [47, 51]. The latter layer is composed of 4–6 cell layers of the SC and includes solid components that provides a diffusion barrier. The more loosely structured upper part consists of ca. 8–15 cell layers with only lateral cell–cell junctions. Both of these sublayers maintain the cohesion of the stratum corneum [29, 53]. SB includes phospholipids while the upper epidermal layers are rich in lipid lamellae [55]. As a non-cellular layer, stratum basale includes fibrils, proteoglycans, and glycoproteins like laminin, collagen type IV, and VII. Under this structure, a reticular lamina including high concentrations of collagen type III is present [15]. Besides, the epidermis has various invaginations, including hair follicles connected to sweat glands and sebaceous glands (pilosebaceous units). The epithelial stem cells, changing into basal keratinocytes, are present in this pilosebaceous unit [21]. Then, as keratinocytes move towards the skin surface, they differentiate and mature. The keratinized cell layer on the skin contributes to the barrier function of the skin [22].

On the other hand, as the thickest layer, the dermis is located beneath the epidermis. It is a connective tissue including extracellular matrix (ECM), vascular endothelial cells, fibroblasts, hair follicles, sebaceous glands, sweat glands, nerve endings, and blood vessels [22]. The loose connective tissue layer is positioned under the epithelium. It harbors scarce cells with a high amount of the matrix material. Just beneath this layer, the dense connective layer is present. It includes collagen in high concentrations and sparse cells, typically single type-fibroblasts [145]. Fibroblasts are the most abundant cells in this layer and synthesize the ECM [6]. It is made of interconnected protein structures (elastin, fibronectin, collagen, and laminin), proteoglycans (chondroitin sulfate, heparan sulfate, and keratan sulfate), and glycosaminoglycans

[128]. The ECM is like a scaffold providing flexibility and physical strength to the skin via extracellular structural proteins and glycosaminoglycans. In addition, it plays role in the hydration of tissue due to the high water-binding capacity of the hyaluronic acid component [3, 6, 166]. The lymphatic system in the dermal layer has various functions such as pressure maintenance in tissue by removal of interstitial fluid, waste byproducts, and also the regulation of immune responses [4, 56, 70, 80, 153]. On the other hand, the blood vessels are responsible for transferring oxygen and nutrients to the skin cells [8, 143]. The thin collagen fibers on the surface (superficial/papillary dermis) and much thicker collagen fibers in the deep (reticular dermis) provide mechanical strength to the skin [18]. Hair follicle stem cells are anticipated to be fundamental for the repairment of skin and regeneration of hair follicles, including specification into several types of hair follicle epithelial cells, epidermal cells, and sebaceous gland cells [109]. Moreover, sweat glands contribute to skin repair and are responsible for the thermo-regulation of the body [201].

The innermost layer of the skin is the hypodermis, underlying the reticular dermis [6]. The hypodermis consists of loose connective tissues and lipids, which provides insulation from cold and heat as a thermo-regulator. It also has several endocrine functions involved in inflammation, angiogenesis, food intake, glucose homeostasis, and lipid metabolism [45, 163].

3 Wound Types and Wound Healing Process

Damage or loss of integrity in skin layers can be caused by wounds. The wounds that resulted from blood circulation problems, burns, aging, surgical processes, or mechanical trauma, may disrupt the several functions of the skin [45]. They are grouped into chronic or acute wounds related to their underlying consequences and causes [92]. Skin damages often result in acute skin wounds. Acute wounds are healed through an organized repair process, and restoration of anatomical and functional integrity is provided to the tissue [50]. However, depending on the increment of the depth and size of a wound, the healing process may not complete properly, causing improper or delayed wound closure [157]. The wounds which do not progress through appropriate reparation of functional and structural integrity frequently result in chronic wounds [190]. Some factors like the presence of autoimmune/metabolic diseases, ongoing drug therapies, and patient age may influence the wound healing process and cause chronic wounds [106]. To restore the skin functions properly, rapid and exact wound healing are crucial.

The wound healing process includes closure of the wound to prevent infection, suppress pain, and recover the functionality of the skin. The epidermis has the capability for self-healing due to the presence of stem cells. However, in severe injuries, the healing mechanism is not adequate, thus resulting in a chronic wound [190]. Based on the injury's depth, the wounds are categorized into four main groups consisting of epidermal, superficial partial-thickness (lose a part of the epidermis), deep partial-thickness (damage in deeper dermal layers and epidermis), and full-thickness skin

wounds (damage in deeper tissue and subcutaneous fat) [135, 167]. The first two types are generally restored via self-healing processes. However, in the rest of the wound types, self-healing cannot be performed due to the destruction of the epithelial regenerative elements [152]. The healing process is a complex cascade system consisting of individual but overlapping stages. These are inflammation, hemostasis, proliferation, and remodeling (maturation) phases [25, 171] (Fig. 2). These dynamic and continuous processes are performed by various cellular components and molecular pathways and include the interactions of cells, ECM components, cytokines, and growth factors involved in repairing the wound [164]. The hemostasis phase reveals in a few seconds or minutes after the skin injury and is essentially mediated by platelets [145]. In this stage, the intravascular platelets are exposed to the subendothelial collagen by the skin injury, and thrombin is produced [177]. Then, in average patient profiles, fibrinogens are converted into fibrin fibers to prevent blood loss and form a fibrous scaffold for clotting blood. This blood plug temporarily prevents the loss of fluid and entry of pathogens [145, 190]. Besides, some cytokines and growth factors, such as epidermal growth factor (EGF), platelet-derived growth factor (PDGF), heparin-binding EGF-like growth factor, vascular endothelial growth factor (VEGF), insulin-like growth factor-1 (IGF-1), transforming growth factor, alpha (TGF-α) and beta (TGF-β), are produced by activated platelets [16, 41, 105]. Then, the above-mentioned growth factors and cytokines diffuse into surrounding tissues and induce the migration of neutrophils and monocytes into the wound, within the first 24 h after the injury. Neutrophiles produce proteases and antimicrobial compounds [73, 145]. The monocytes differentiate into macrophages, and then the macrophages and also lymphocytes are attracted to the damaged layers to begin the inflammation

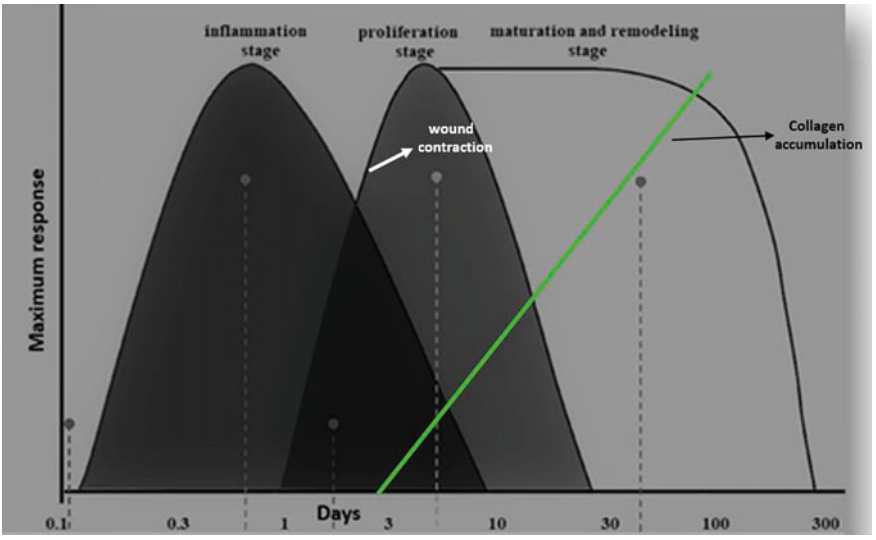

Fig. 2 Timeline for skin wound healing

phase [137, 145]. They digest the remaining matrix, cellular debris, and microorganisms to prevent infections (after about 48 h of injury) [21]. The blood circulation and expression of several pro-inflammatory factors, like colony-stimulating factor-1 (CSF-1) and tumor necrosis factor (TNF), are stimulated by these inflammatory cells. These molecules trigger the proliferation and migration of smooth muscle cells, keratinocytes, endothelial cells, and fibroblasts [146]. During this stage, collagen production is induced by the latter cells, and dead cells are surrounded by phagocytes [49, 104, 156]. The inflammatory phase prepares the damaged tissue for healing through restoring homeostasis and providing a barrier against pathogens [61, 114]. Production of novel tissue and angiogenesis (formation of blood vessels) begin with the third stage, namely, the proliferation phase. In this stage, due to the proliferation of the keratinocytes, re-epithelialization of the injured tissue occurs. Also, increased VEGF induces angiogenesis to generate the vascularized tissue [21]. The quantity of inflammatory cells is reduced during this stage, and PDGF and TGF-β chemotactically attract fibroblasts into the wound site [192]. Fibroblast growth factor (FGF) is continuously released by macrophages, and it induces the proliferation and activation of fibroblasts. ECM is produced by the latter cells [162]. Some proliferated fibroblasts produce type III collagen and glycosaminoglycans, like chondroitin-4-sulfate, heparin sulfate, dermatan sulfate, and hyaluronic acid [21, 168], which form a gel in which collagen fibers are deposited. The ECM is essential for the formation of novel tissue and formed by collagen and fibronectin [69]. Also, some fibroblasts change into myofibroblasts. The latter cells with their contractile function, reduce the wound size, and finally, contribute to the wound closure process [189]. In the final phase, the maturation (remodeling) stage, the ECM composition is changed by the reconstruction of collagen fibers type III to I. These changes and direction of fibers provide mechanical durability of the skin [67]. Besides, to reduce the blood vessel density and dermal cellularity, most of the cells that come from the previous stage encounter apoptosis. After all of these stages, by healing, the tissue gets its final appearance [21]. This phase is longer than the others, and generally begins 3 weeks post-injury and may continue for 2 years [145].

This native healing process gets severely destroyed in some pathophysiological cases. Because such critical cases result in loss of the skin tissue and this result in the interruption of wound healing [155]. Clinical treatments can be used in such situations to provide wound repair, and regeneration includes skin substitutes, allografts, autografts, cell therapy, and cytokine therapy [5, 17, 43, 133, 159]. Nevertheless, these conventional techniques are usually impeded by a small repair range, the availability of donor skin for grafting, high treatment cost, immune rejection, secondary injuries, and long healing time [59, 68]. Such situations can be overcome with current biofabrication techniques.

4 Skin Tissue Engineering

Damage to the function of skin integrity due to injuries and diseases represents a significant imbalance of physiological processes leading to disability. Common causes of skin damage include acute trauma, burns, chronic wounds, infections, genetic disorders, and surgical interventions [13]. Damages on the skin can be categorized according to their different thickness. These can be classified as epidermal, superficial partial-thickness, deep partial-thickness, and full-thickness skin wounds. The epidermis has an enormous wound healing capacity. However, there are situations where normal regeneration is insufficient and large areas of the epidermis need to be replaced. The regeneration capacity of the dermis is very low. The scar tissue formed in the absence of the dermis lacks the flexibility, elasticity, and strength of the natural dermis, also causes pain, limits movement, and is esthetically poor. There is a need for the development of engineering applications that mimic human skin for use as graft material after damage and wound, to restore skin function and facilitate wound healing [188]. Autologous grafts (autografts) taken from the patient's own body are used to return the skin barrier to its normal function, facilitate wound healing after damage or injury, and prevent immune rejection. Unfortunately, autografts are insufficient for healing and wound closure of large and severe wounds or burns [111, 134, 158]. Skin tissue engineering develops applications to meet this need and to produce artificial skin using in vitro methods. The major important aim of skin tissue engineering is to regenerate the normal physiology and anatomy of natural skin [11]. Also, in skin tissue engineering, it is necessary to achieve effective recovery and full simulation of physiological skin, close to natural mechanical properties, without immune rejection or host toxicity. Artificial skin produced for skin regeneration should have a structural architecture to reinstitute the skin pigmentation, nerve, vascular plexus, and adnexa [89]. In recent years, researches have increased in skin tissue engineering applications, with the latest studies in materials science and the demand for artificial skin. The primary objective of skin tissue engineering is to produce a structure that provides skin regeneration and wound healing using various tissue engineering methods using suitable cells and biomaterials. Scaffolds that are produced for skin should have important properties such as biocompatibility, biodegradability, and non-toxic nature, and suitable mechanical properties [118]. Besides, skin tissue engineering scaffolds should be cost-effective and elicit minimal scarring and minimal inflammatory response [193]. Artificial skin, which is expected to replace and completely mimic the natural skin, is tried to be produced with many tissue engineering applications, including the three-dimensional bioprinting method.

5 Overview of 3D Bioprinting

The main aim of tissue engineering is to design cell-laden 3D structures that mimic natural tissue. So, designing and building biomaterial-based scaffolds is one of the

most crucial parameters in tissue engineering [113]. Three-dimensional bioprinting (3D bioprinting), also known as additive manufacturing, steers novelties in many fields like engineering, manufacturing, medicine, art, and education. 3D bioprinting is an advanced manufacturing platform that enables the predefined deposition of living cells, biomaterials, and growth factors to manufacture customizable scaffolds via a layer-by-layer printing process using computer-aided design (CAD) [125]. The three-dimensional bioprinting technique has arisen as an alternative and easily applicable technique, especially in tissue engineering applications. With its broader definition, three-dimensional bioprinting can be defined as the computer-aided layer-by-layer modeling of bioinks, known as cells, DNA, drugs, growth factors, and biomaterials. This approach also includes toxicology studies and drug screening for the clinical use of artificial tissues created by the 3D printing method [119, 140].

Three-dimensional bioprinting can be described as a state-of-the-art product that aims to produce structures that are used for biological tissues with suitable and ideal hierarchical architecture. Living and functional tissues, which are much needed in tissue and organ transplantation, can be developed artificially. From this perspective, printing technologies are overwhelmingly accepted by researchers around the world as an alternative option to improve the lives of patients suffering from a disease [113]. Macro-scale architectures that can be achieved with bioprinting technology can perfectly mimic the natural extracellular matrix (ECM). Thus, it allows multiple cell types to bind and multiply at the same time [66]. Structures obtained by 3D printing method also have advantages such as adjustment of desired dimensional properties, mechanical strength, and simple drug loading [81]. The exact shapes and complex geometries of the desired tissues can be mimicked with the 3D bioprinting technology [178].

Generally, the 3D bioprinting process is separated into three main stages; pre-bioprinting (modeling), bioprinting, and post-bioprinting. Pre-bioprinting modeling is the process of designing the desired 3D model in a digital platform. It also includes the selection of bioink and biomaterials according to the desired tissue to be created and the type of 3D bioprinting model. Collecting complex tomography that will mimic natural tissue architecture is precisely composed using CAD software and stored as stereolithography (stl) files [147]. The designs of the printers are different from each other. In some printers, the 3D material file can be uploaded directly to the device, while in some printers, it is transferred to the printer after being converted into G-Code in the slicing program. The slicing program divides the shape into a stack of cross-sections and creates it by integrating it with the programmed fill pattern. After the printer reads the stl file, it deposits a layer of material to create the 3D model [34]. The bioprinting stage is the process of creating the desired structure with the desired features after making the necessary adjustments of many parameters. For tissue engineering applications, the printing process is divided according to two different procedures, with and without incorporated living cells. Printing with 3D printers is divided into three main categories according to their working strategies: extrusion-based, droplet-based, and laser-assisted bioprinting (mentioned in Sect. 5.2) [204]. Finally, post-printing is an important step in improving the mechanical support and biological functionality of generated structures [120]. Even more importantly, in vitro

culture (inside in a bioreactor), in vivo implantation, and even in situ bioprinting can be used to improve the structure; hence, transform the formed structures into functional tissues [131].

5.1 3D Bioprinting Technologies

Scaffolds used in tissue engineering can be prepared according to two different approaches: bottom-up or top-down. Depending on the basic working principles for fabricating tissue structures, there are many different bioprinting strategies, such as inkjet bioprinting, laser-assisted bioprinting, pressure-supported (extrusion)-based bioprinting, acoustic bioprinting, stereolithography-based bioprinting, and magnetic bioprinting. These bioprinting methods can be applied with different combinations or alone, depending on the production goal [116]. Nowadays, in 3D bioprinters, three major methods are applied mostly: extrusion, droplet, and laser-based bioprinting (Fig. 3). The technique should be preferred depending on the characteristics of the cells and biomaterials to be used, the required sensitivity and speed, or the size and properties of the tissue to be printed.

5.1.1 Extrusion-Based 3D Bioprinting

The extrusion-based bioprinting technique is the most widespread application, especially due to its ability to produce greater extent 3D structures. This is the basis of all bioprinting techniques. The extrusion-based bioprinting technique is a combination of the fluid dispensing system and robotic system for bioprinting. Biological printing is distributed by the deposition system with the help of computer control. It results in precise deposition of encapsulated cells within cylindrical filaments of desired 3D-shaped structures. Thanks to this technique, the filaments are constantly deposited, which provides structural integrity [132]. During bioprinting, the dispensing head is moved along the X and Y axes to place the bioink onto a stage. As specified in CAD models, it is moved up and down along the Z-axis to create the scaffold by accumulating different layers [186]. Biological materials are extruded from the dispenser by pneumatic, mechanical (piston or screw assisted), or solenoid-based dispensing techniques [141]. Extrusion-based bioprinting is a suitable method for high viscosity materials that provide mechanical support, and low viscosity materials that support cellular bioactivity. This technique can print a very large class of biomaterials and cells, including both natural and synthetic hydrogel polymers, cell aggregates, and decellularized extracellular matrices. Compared to other bioprinting methods, it is more possible to deposit biomaterials with physiological cell density with the extrusion-based bioprinting technique. It can be preferred to produce large-scale scaffolds because it provides fast deposition speed [127]. Apart from the advantages provided by the extrusion-based bioprinting method, there are also some negative aspects. As higher pressures and smaller diameter nozzles are used in extrusion-based

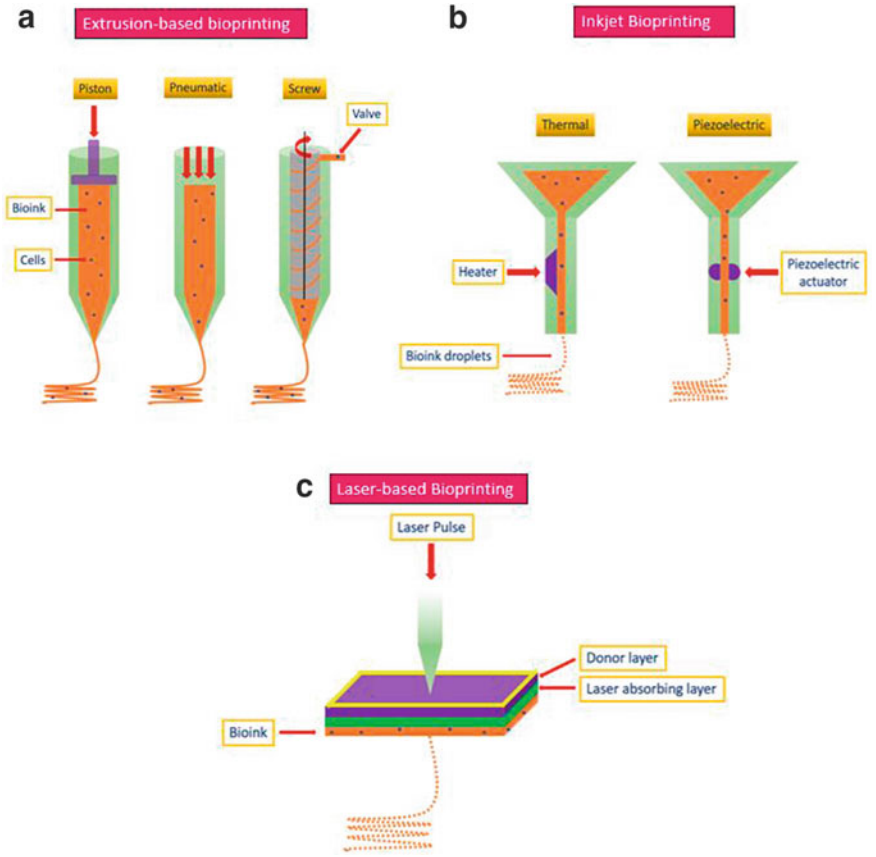

Fig. 3 Schematic illustration of different bioprinting techniques; **a** Extrusion-based bioprinting. **b** Inject bioprinting. **c** Laser-based bioprinting

bioprinting, a decrease in cell viability has been observed due to process-induced stress [173]. In this technique, nozzle clogging caused by biomaterial solidification can completely interrupt the integrity of the created structure compared to nozzle-less techniques [127]. The other disadvantages are the lower resolution ($\geq$100 μm) and less accuracy than other techniques [35].

5.1.2 Droplet-Based 3D Bioprinting

The droplet-based bioprinter was first presented in 1980s as the foundation of biological printing technologies [94]. The core of the droplet-based bioprinter is inkjet technology (also known as drop-on-demand printers). Inkjet printing is a technology derived from traditional 2D desktop inkjet printers. Inkjet printers that deliver controlled volumes of fluid to predefined locations are the widely preferred

type of printer for non-biological and biological processes [182]. This non-contact bioprinting process relies on the formation and exact positioning of droplets on a computer-controlled substrate [151]. It has the same mechanism as the extrusion-based bioprinting technique [107]. The accumulated droplets create 3D scaffolds with the help of different chemical and physical cross-linking agents like pH, ultraviolet (UV) radiation, and cross-binding agents. With this method, cell viability is at least 70%, and this rate can be further increased by applying various procedures [64]. In inkjet bioprinters, drops created by heat and mechanical compression are often smaller than 30 μm, resulting in high resolution. Inkjet bioprinting sprays droplets onto the substrate using thermal, piezo, or acoustic forces.

A thermal inkjet bioprinter includes a heating element and an ink chamber with a nozzle. Thermal inkjet printers work by electrically heating the printhead to generate pressure pulses [24]. The thermal inkjet technique is more preferred because it is efficient, simple, and more economical. However, clogging of the nozzle due to bioink gelation disrupts the manufacturing of evenly sized drops and smooth printing operations [58]. Besides, the risk of exposing cells and materials to thermal and mechanical stress, low droplet orientation, non-uniform droplet size, unreliable cell encapsulation are major disadvantages [125]. In another technique, piezoelectric inkjet, the pressure pulse is produced by mechanically actuating piezoelectric crystals. Internal vibrations press the bioink droplet out of the nozzle. The pressure required to eject the droplets from the nozzle is achieved by using a voltage to the piezoelectric material, causing a quick change in structure [58]. Other inkjet printers can spray liquid droplets with the aid of the acoustic radiation force found in the ultrasound field. Acoustic inkjet printers have the advantages of generating and controlling a uniform droplet size and ejection directionality, as well as preventing cells from being exposed to heat and pressure stressors [150]. The main advantages of inkjet bioprinting are better resolution, affordable price, and the ability to easily model complex geometries. The main disadvantages are the lower viscosity range, longer printing time, which limits the bioink composition. Additionally, the technique used by the actuator to generate the drops can affect cell viability, especially the thermal mode [188].

5.1.3 Laser-Based 3D Bioprinting

Laser-based bioprinters are also called laser-assisted printers and laser direct printers. Although laser-based bioprinting systems are less popular compared to other printer techniques, over time they have been used more and more in tissue engineering applications. Laser-based printers have an ultraviolet (UV) laser, a hydrogel focusing principle that is made light-sensitive by the addition of a photoinitiator [95]. With the energy provided by the UV laser, covalent bonds are formed between neighboring polymer chains and allow the liquid to solidify [115]. This technology that is based on conventional laser-induced forward transfer is a nozzle-free technique. Laser-based printers include a pulsed laser beam, focusing system, donor slide, and collector substrate slide. The donor slide is covered with a laser-absorbing layer and bioink

layer containing the biomaterials and cells to be transferred. The collector slide, which acts as the printing bed, is placed at distances ranging from millimeters to micrometer. Several lasers can be used in this technique to increase the printing speed. The main advantage of this method is that it has high sensitivity. The laser-based bioprinting technique allows more printing on small tissue surfaces and operates with lower viscosities (1–300 mega pascal-second [mPa · s]) than extrusion-based prints [65, 97, 154]. Because laser-assisted printers are a nozzle-free technique, it eliminates the risk of nozzle clogging and contamination, very widespread difficulties with nozzle-based bioprinting techniques [198]. Thanks to laser-based printers, high-resolution 2D and 3D patterns can be designed and different cell lines can be combined [163]. The most important advantage of laser-based printers is that cell encapsulated hydrogels accumulate high cell density (1×10^8 cells/ml) and high cell viability (>90%) at high print resolutions (80–140 mm) [96]. The desired mechanical performance in the produced structures is achieved by applying processes such as heating or photo-curing to fabricated parts. In laser-based printers, the thickness of each layer varies according to the exposure time to light energy. However, the laser-based printing technique is somewhat slow and costly compared to other techniques. The curing process and reaction kinetics are more complex. Besides, limited material types can be used in printing with this technique [12]. The use of metallic laser energy-absorbing layer in laser-based printers poses a high risk of metallic particle contamination. It is less efficient compared to other printing applications, and therefore the adaptation of this technique to the fabrication scale is limited [110].

6 3D Skin Bioprinting

It has now become possible to imitate and manufacture the skin, which is the body's most complex, largest, and multi-layered organ, with 3D bioprinting applications. Tissue-engineered 3D skin structures have great potential as a graft for burnt skin replacement, in vitro human skin models, and wound healing for drug analysis [31]. Many researches so far have explored skin bioprinting methods to reconstruct functional skin tissue. The advantages of manufacturing skin structures with 3D bioprinting method are more than other traditional tissue engineering strategies. Especially with the skin bioprinting method, automation, standardization, and high sensitivity in the accumulation of cells can be achieved for clinical application. Although traditional tissue engineering applications, such as culturing cells in a scaffold and maturing in a bioreactor, achieve bioprinting-like results, there are many trends of the skin that require improvement in the manufacturing methods, including long production times to achieve larger areas. In situ bioprinting and in vitro bioprinting are two different strategies for how to apply print skin in wound treatments [187].

In situ bioprinting is the process of directly printing pre-cultured cells onto the wound site for wound healing. It is a mobile skin bioprinting system that includes a hand-held 3D scanner to determine the size and topography of the wound. The use

of in situ bioprinting for wound regeneration allows for the precise accumulation of cells on the wound [131, 194]. In in vitro bioprinting, a skin structure (usually the dermis and epidermis) is made in vitro. The printed skin structure is then kept in a bioreactor for maturation. It is then transferred to the wound area of the patient or experimental animal [14]. The schematic illustration of 3D skin bioprinting is demonstrated in Fig. 4.

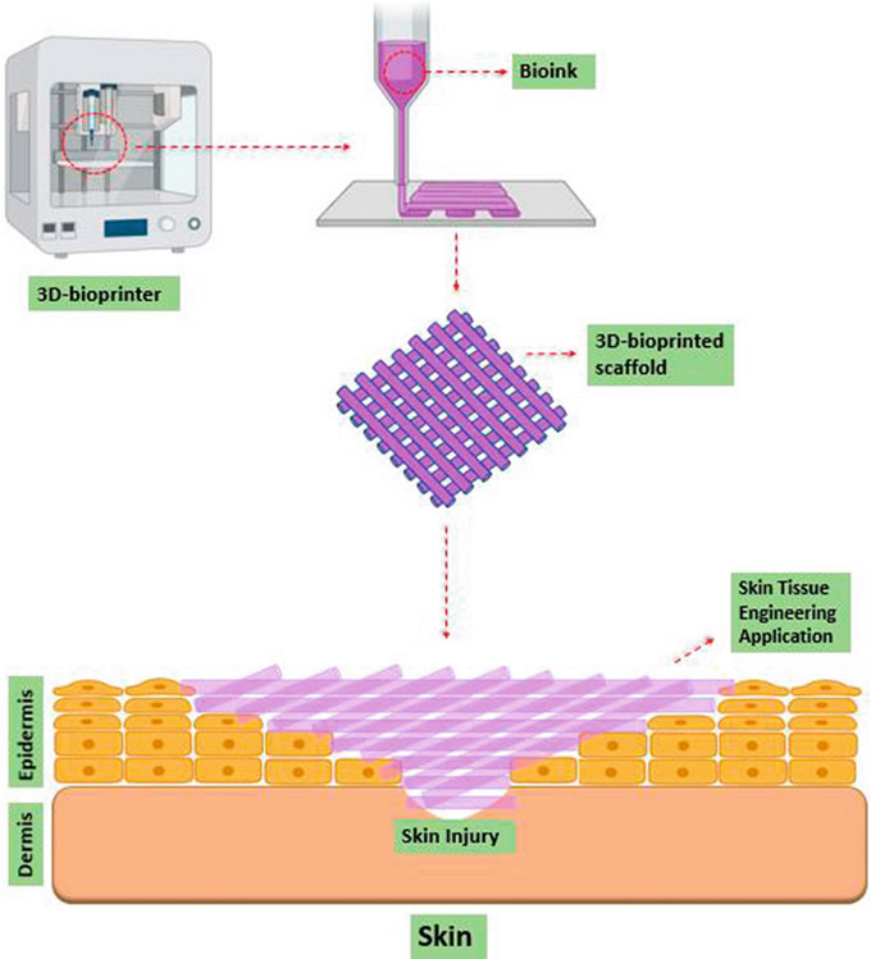

Fig. 4 The basic representation of the 3D bioprinter, fabrication of 3D bioprinted scaffold, and skin tissue engineering application

6.1 Design Considerations for Skin Bioprinting

6.1.1 Bio-Ink Development

The selection of bioink is an important parameter in skin bioprinting because it should provide the spectrum of biochemical (i.e., adhesion factors, growth factors, or signaling proteins, chemokines) and physical (i.e., interstitial flow, mechanical and structural properties of extracellular matrix) cues [63].

The bioink to be used must match the printability, biocompatibility, and mechanical strength properties of natural skin. The biomaterial to be used must have a fast gelation time for good quality bioprinting. The biomaterial to be used must have a fast gelation time for high throughput bioprinting. The complexity of natural ECM needs to be mimicked well enough to support cellular binding and proliferation. In addition, the deposition of thin bioink layers (1–2 mm) simplifies significant cell–cell interactions between adjacent printed cell layers. It is a considerable point in reducing cell sedimentation (Fung and Skalak 1982; [78]). There are different categories in the selection of bioink: cellular/non-cellular biomaterials as printing ink (functional scaffold bioprinting) and using only cells as printing ink (scaffold-free bioprinting) [125]. The produced biomaterial structures act as the extracellular matrix (ECM) that regulates tissue reconstruction. Other basic factors such as porosity, interconnection, pore sizes, and biological degradation kinetics are also taken into account in scaffolding [34].

6.1.2 Cell Sources and Selection

The proliferation of bioprinted cells is an important point when creating a 3D structure that will mimic the natural tissue most closely. There are two important parameters for cell selection; the first is how much the physiological state of bio-imprinted cells overlap with the cells of the natural tissue. The second is to what extent cells can maintain or improve their function in the optimized microenvironment [125]. Natural skin tissue contains multiple types of cells with specific and biological functions. Often choosing autologous cells minimizes the potential risk of rejection. Primary cells such as fibroblasts, melanocytes, and keratinocytes can be obtained from biopsies and can be used in bioprinting applications. The use of stem cells provides advantages in terms of differentiation and adaptation to natural tissue in skin bioprinting as in different areas [1, 102, 174].

7 Biofunctional Inks for Bioprinting in Skin Tissue Engineering

Three-dimension bioprinting is the important latest technology for the production of 3D structures for tissue engineering applications and regenerative medicine [62, 123]. Biofabrication is a powerful tool for developing biologically functional constructs [123]. The bioprinting consists of layer-by-layer deposition of living cells using computer-aided transfer processes to generate functional tissues and organs [62, 180].

The bioink properties are very important for choosing bioprinting techniques. Bioink formulations are the most important point in bioprinting process in aspect of rheological and biological properties to reach good printability [44]. Natural biomaterials are widely used in tissue engineering because of biodegradability, tunable properties, biocompatibility, abundantly available, and minimal inflammatory response in vivo [44, 87].

7.1 Natural Bioinks

The design and selection of ideal bioinks are important parameters for the bioprinting process. Bioink is a formulation of cells convenient for processing by an automated biofabrication technology. Biocompatibility, non-immunogenicity, nontoxicity, viscoelasticity, high mechanical integrity, convenient degradability are crucial parameters for providing ideal bioinks. Alginate, agarose, collagen, extracellular matrix derived from a special tissue, gelatin, or fibrin can be given as examples of natural bioinks [129].

7.1.1 Bioinks Based on Alginate

Alginate is an anionic linear copolymer polysaccharide consisting of (1,4)-linked α-l-guluronic acid (G) and β-d-mannuronic acid (M) residues harvested from Brown algae [20, 129]. The concentration of polymer, molecular weight, average chain subunit ratio, molecular weight distribution, pH of solution are critical parameters in the aspect of the viscosity of alginate [20, 27]. For cell bioprinting applications, the alginate is a remarkable material because of providing mechanical properties to the cell, biocompatibility, non-immunogenicity. Beside this, the gelation time is fast, and it is enable to fast encapsulation of cells and to hold water and other molecules, providing diffusion throughout the structure [20, 129]. Increasing the concentration of HMW alginates in bioink to increase structural stiffness is a common approach. If bioink material is modified with some parameters like viscosity, the concentration of alginate, and temperature, it will allow the user to optimize this material during several bioprinting techniques [20]. Despite its advantages, alginate has a

relatively slow and unpredictable degradation rate [129]. To support cell adhesion and bioactivity, alginate is widely modified with functional groups, such as Arginyl-glycylaspartic acid peptides or blended with other polymers, such as collagen due to its bioinert nature [20]. Alginate was blended with different polymers such as hydroxyapatite [193], gelatin [193], polycaprolactone [37, 84, 160], and poloaxamer [7] to obtain different 3D printed structures for tissue engineering applications. For the first time, induced human pluripotent stem cells and human embryonic stem cells were bioprinted with alginate as bioink by Faulkner-Jones et al. [52]. In the other work, the effect of different combinations of HMW and LMW agaroses in creating 3D structures and supporting fibroblast cells was investigated by Park et al. The results showed that for bioprinting application area, combination of 2:1 ratio high molecular weight and LMW agarose polymer was good in aspect of its cell viability and process ability investigations for tissue engineering [138]. Nguyen et al. used hyaluronate-based nano fibrillated cellulose composite bioink and alginate-based nano fibrillated cellulose composite bioinks, it is also used to induce pluripotent stem cells for 3D bioprinting of cartilage tissue construct and compared with each other. The bioinks based on alginate with nanofibrillated cellulose composite presented higher cell proliferation [126].

7.1.2 Bioinks Based on Agarose

Agarose is a linear polysaccharide chain. It is obtained from seaweed. It is most commonly used in the bioprinting process among other natural polymers. Due to its advantageous gelation properties, it is used in a wide range of bioprinting applications. Agarose forms a hydrogel through hydrogen bonding, resulting in a gelled structure that will thermally degrade and cross-link naturally. Because of the gelation structure, the resulting bioink has high viscosity. This situation is a negative effect in the aspect of 3D printing. It can be used to lower viscosity bioinks, which are inherently less mechanically stable to overcome this problem. Agarose can be modified with, blended with different polymers, or bioactive groups to support biological activity and cell adhesion [20, 27]. Agarose-based bioink with collagen and agarose-based bioink with fibrinogen were used by Kreimendahl et al. It was reported that these agarose-based blend biomaterials were able to stable 3D structure and to support fibroblast and endothelial cell growth [100]. Another similar study was from Yang et al. for cartilage tissue engineering application. They used agarose collagen composition with sodium alginate as bioink. The results showed that the mechanical properties of biomaterial improved without affecting the gelling behavior [200]. Because of the advantageous properties of agarose, such as perfect gelation, biocompatibility, and rheological properties, it is a promising material for 3D bioprinting applications [82]. Daly et al. reported chemically modified agorose (carboxylated agarose) as a bioink for developing mechanically tunable 3D tissue structure. They used human mesenchymal stem cells for its evaluation. The results showed that the carboxylated agarose constructs yielded remarkable cell viability up to 95% according to the native agarose gel. The carboxylation degree may be changeable for obtainment

of different gels with changing mechanical properties [37]. Daly et al. also reported Agorose was used to compare a range of commonly used hydrogel bioinks such as alginate, GelMA, and BioINK (loaded with mesenchymal stem cells) for their 3D printing biocompatibility properties for cartilage tissue engineering [38].

7.1.3 Bioinks Based on Collagen

Collagen is widely used for tissue engineering application area. Because its physiological properties of native skin and the main component of Extracellular Matrix are similar to each other [161, 185]. Besides this, because of its excellent biocompatible properties and low immunogenicity [112, 135], it is widely used in 3D bioprinting applications [62]. The basis of collagen bioink is a collagen hydrogel which is produced from the protein mass in the connective tissues of mammals [60, 130]. Collagen can be crosslinked with the change of temperature or changing of pH value or using vitamin Riboflavin [20, 62]. The mechanical properties of crosslinked collagen are better than the uncrosslinked one [54, 124]. Moreover, by adding various amounts of different polymers, for using it in 3D bioprinting, the mechanical properties of the collagen materials may be improved [62]. Bioink based on Collagen with sodium alginate was used to develop 3D structure by Yang et al. According to their report, the mechanical properties of the 3D structure suggest that alginate-collagen can be chosen for the field of cartilage tissue engineering. [199]. The other works about improving mechanical properties and biological activity were collagen-based, cell-loading bioink for 3D bioprinting application. The study showed increased biological activity and mechanical properties by adding of collagen [202]. Stratesteffen et al. used collagen with gelatin for producing 3D construct. It showed the ability of this collagen–gelatin combination to obtain stable 3D construct with good rheological properties and high biological activity [170].

7.1.4 Bioinks Based on Decellularized Extracellular Matrix

Extracellular Matrix (ECM) is a three-dimensional network of extracellular macromolecules such as collagen type II, glycosaminoglycans, chondroitin sulfate, elastin, fibronectin, laminin, tenascin, thrombospondin, vitronectin, fibrillin. Decellularized extracellular matrix (dECM) is obtained by removing the cells from desired organs or tissues by a sequential procedure leaving the ECM intact [62, 88]. The obtained components are pulverized, then dissolved in a suitable buffer solution. Moreover, several polymeric hydrogels can be added to this solution to improve the printability of the Decellularized Extracellular Matrix-based bioink [62]. However, there are some disadvantages about using of DECM for bioprinting applications. Because, the decellularization step is time-consuming and its use in organs or tissues is limited [20]. Variant polymeric hydrogels can be added to the solution for the increment of the printability of the Decellularized Extracellular Matrix-Based bioinks. For example,

poly (caprolactone) was used to improve the printability of the Decellularized Extracellular Matrix-Based bioinks obtained from different type of tissues by Pati et al. The result of this work showed that good functionality of construct and high cell viability was obtained after the bioprinting [139]. For another work is related to 3D bioprinting for developing the cell-loading construct of tissue engineering applications. With controlling of heating and pH of the bioinks, they obtained 3D system which enable them to obtain the gelling form at 37 °C during 3D bioprinting [19].

7.1.5 Bioinks Based on Hyaluronic Acid

Hyaluronic acid (hyaluronan, HA) is a linear polysaccharide composed of d-glucuronic acid and N-acetyl-d-glucosamine. Hyaluronic acid is the basic component of Extracellular Matrix of cartilage and connective tissues [203]. Hyaluronic acid has remarkable properties for use in 3D bioprinting applications. These properties are non-immunogenic, biodegradable, and biocompatible [183, 185]. However, hyaluronic acid alone is not a viable polymer for 3D printing. Because Hyaluronic Acid has slow gelation time and its mechanical properties are not good. Because of this reason, there are a lot of studies in the literature about 3D printing application of HA blend-based bioinks. One of the works was to blend methacrylate with hyaluronic acid to form cross-linkable bioink by photo-crosslinking mechanism to increase mechanical properties and high stability after bioprinting [144]. The other study was declared by Stichler et al. They used hyaluronic acid with different synthetic polymers for producing a stable 3D construct with good cell viability. The ability of the hybrid 3D printed structures to improve chondrogenesis using a thiol-linked hyaluronic acid and polyglycidols gel with polycaprolactone [169]. There are a lot of works about the hyaluronic acid combination with synthetic polymers for 3D biorinting and various tissue engineering applications [74, 176].

7.1.6 Bioinks Based on Fibrin

Fibrin hydrogels are gelled by the enzymatic reaction of thrombin and fibrinogen [85, 185]. Thrombin and fibrinogen are the key proteins involved in blood clotting. It is an Extracellular Matrix part of the skin that promotes cell proliferation, vascularization, and differentiation [42]. Fibrin is highly biocompatible, biodegradable, and has capacity to bind cells, growth factors, and other Extracellular Matrix proteins [129]. Because of these promising properties, for tissue engineering applications, it is extensively used in 3D bioprinting. However, it has low viscosity and poor mechanical properties. Because of this reason, fibrin is widely blended with other polymers like HA, and during blending, the viscosity of bioink increases to provide the ability of 3D bioprinting [48]. The techniques have been based on the crosslinking of the other materials such as alginate, gelatin to generate 3D structures [108, 184]. For skin bioprinting applications, a bioink based on fibrin–gelatin blended hydrogel was declerated for using of a bio-paper. The results showed that fibrin–gelatin blended

hydrogel ensures a natural scaffold for fibroblast embedding and culturing [71]. England et al. used fibrin combined with Hyaluronic acid to encapsulate Schwann cells for the aim of 3D printing. For supporting nerve generation, they researched both capabilities of bioink and in vitro characterizations [48].

7.1.7 Bioinks Based on Silk

Silk is a naturally derived hydrogel that includes ECM proteins, and it is used extensively to print different tissues. Silk fibroin is obtained from spiders or silkworm. Because of promising properties, such as tissue integration, biocompatibility, and cell permeability, it is widely used in tissue engineering applications area. Similar to the other polymer, fibrin can be often blended with other polymers. In the literature, there are various works about the blending of silk with other polymers. For example, Das et al. demonstrated a bioink based on silk–gelatin for investigation of 3D bioprinting application. Mesenchymal progenitor cells were used for the bioink formulation. The combination of silk and gelatin was crosslinked by sonication and enzymatic crosslinking methods [39]. Another similar study belongs to Rodriguez et al. They also used silk–gelatin blend for bioink application with the aim of increasing biocompatibility, tissue integration, and cell permeability in soft tissue integration, and in this work, glycerol was used for physical crosslinker [148]. The other blending method for silk with a polymer is silk and alginate combination. In this work, silk and alginate were crosslinked, thanks to calcium chloride [28]. Xiong et al. carried out the mechanism and efficiency of gelatin–silk-based ink to regenerate skin. In this study, they added fibroblast growth factor-2 in the ink before printing, and it is shown that there was an increment of the granulation and tissue regeneration in vitro and in vivo [181].

7.2 Bioinks Based on Synthetic Polymers

Natural polymer or hydrogels have many advantages such as the desired microenvironment mimicking the native Extracellular Matrix about proliferation and cell attachment for 3D bioprinting as bioinks. However, the tunable properties of the natural polymer are poor. Because of this reason, the natural polymer is used with synthetic or another natural polymer. Synthetic polymers are excellent candidates used in bioink formulations to improve printability, cross-linking, and mechanical properties [62].

7.2.1 Poly (Ethylene Glycol) (PEG)

PEG is a linear hydrophilic polyether compound and bioinert polymer. It is most widely used in 3D bioprinting. Polyethylene glycol may be functionalized with

dimethacrylate and diacrylate to obtain the photo-cross-linkable Poly (ethylene glycol) diacrylate (PEGDA) and Poly (ethylene glycol) dimethacrylate (PEGDMA) [129]. Bioink-based poly(ethylene glycol) is used as polyethylene glycol-diacrylate and polyethylene glycol methacrylate in extrusion-based 3D bioprinting applications [32, 79]. Because poly (ethylene glycol) alone does not form a hydrogel [86]. It has a relatively low viscosity, and because of this reason, it is restricted to bioprint alone. As natural polymers-based bioinks, PEG can be used with different materials such as alginate, collagen, etc., for the aim of blending for 3D bioprinting applications to form different bioinks and to increase mechanical properties [75, 76, 86, 149]. Hockaday et al. used a Polyethlene-diacrylate with alginate blend as bioinks for printing aortic heart valve [75].

7.2.2 Pluronic®

Pluronic® is a block copolymer which consists of poly (ethylene oxide-b-propylene oxide-b-ethylene oxide). It is a hopeful bioink based on polymer type. Pluronic® is biocompatible with cells and tissues and is gel form at room temperature, and it is convenient for extrusion-based 3D bioprinting [86]. Pluronic® does not specifically support cell viability in long-term cell culture. However, there are some methods to improve the cell viability of Pluronic®-based bioinks. Khattak et al. reported that in the situation of Pluronic® with hydrocortisone, glucose, and glycerol as membrane-stabilizing agents, the viability of cells encapsulated in the matrix was increased [91]. Actually, Pluronic is not a bioink, technically due to their limited cell supporting capacity. However, it can be used as supporting ink [90].

7.2.3 Poly (N-isopropylacrylamide) (PNIPAAM)

Poly (N-isopropyl acrylamide) can be used in bioink area. PNIPAAM is a gel structure and thermoresponsive polymer. Poly (N-isopropyl acrylamide) has poor biodegradability and biocompatibility. In 3D bioprinting applications, PNIPAAM can be used in combination with different biopolymers and bioinks like HA and alginate [93, 172].

8 Current Challenges and Advances in Developing of Biofunctional Inks in Skin Tissue Engineering

There was a remarkable improvement in 3D bioprinting for the last few years to produce cellular constructs for skin tissue engineering. In the manufacture of artificial organs and tissues, the combination of bioinks based on natural or synthetic polymers and 3D bioprinting has significant potential for tissue engineering. For 3D bioprinting, the selection and design of bioinks are critical steps. Bioinks area

consists of choosing of special cells and convenient materials designed for processing 3D structure. For producing tissue structure easily, 3D bioprintings have the remarkable properties. Nevertheless, bioinks need further improvement in the aspect of commercialization of the 3D printed products and developing more complex specific 3D constructs based on specific patients for an urgent medical situation.

In this chapter, different types of bioinks, the various selection parameters for bioinks, and properties of different bioinks types were discussed. The cell-loading hydrogels are widely preferred for the improvement of 3D structures during 3D bioprinting. 3D bioprinting methods have numerous advantages such as using special cell types, controlling biodegradation, adjusting mechanical properties, and design flexibility. For creating complex tissue structures, skin bioprinting has excellent advantages. It is a very promising alternative method, especially for correcting complex skin imperfections that are difficult to heal by normal clinical means.

The obtainment of a fully functional skin equivalent is the fundamental aim of 3D bioprinting, and it is transplanted and anastomosed with native blood circulation [9]. Another exciting development will be the 4D print [44]. Smart materials sensitive to stimuli can also provide special properties to bioprinted skin structures like triggered shape memory.

9 Conclusion

The skin, which is the body's largest organ, has many functions such as protecting against toxins and microorganisms. There is no artificial skin model that mimics the natural skin and contains all its features. Therefore, one of the main goals of tissue engineering is to produce a universal skin substitute for skin damage. Three-dimension bioprinting is the important latest technology with excellent properties for the production of 3D structures among all tissue engineering techniques. Bioink formulations and properties are the most important points in the bioprinting process in aspects of rheological and biological properties to reach good printability. Bioink can be classified basically into two parts which are natural and synthetic. Natural bioinks have some good properties such as biocompatibility, viscoelasticity, high mechanical integrity, appropriate degradability, nontoxicity, and non-immunogenicity crucial for providing ideal bioinks. In this chapter, alginate, agarose, collagen, gelatin, decellularized matrix, fibrin-based bioink, hyaluronic acid-based bioink, silk-based bioink were given as natural types of bioink for skin bioprinting. The tunable properties of the natural polymer are poor. Because of this reason, the natural polymer is used with synthetic or another natural polymer. Synthetic polymers are excellent candidates used in bioink formulations to improve printability, cross-linking, and mechanical properties. The details of synthetic bioinks of Poly (Ethylene Glycol) (PEG), Pluronic®, and Poly (N-isopropyl acrylamide) (PNIPAAM) are given. This chapter deals with reviewing the utilization of bioinks for 3D bioprinting in skin tissue engineering, and experimental studies in the literature related to bioinks used for 3D bioprinting in tissue engineering were given.

Acknowledgements The authors have declared no conflict of interest.

References

1. Abbott RD, Kaplan DL (2015) Strategies for improving the physiological relevance of human engineered tissues. Trends Biotechnol 33(7):401–407
2. Abdo JM, Sopko NA, Milner SM (2020) The applied anatomy of human skin: a model for regeneration. Wound Med 28:100179
3. Albanna M, Holmes IV JH (2016) Skin tissue engineering and regenerative medicine. Academic Press
4. Alderfer L, Wei A, Hanjaya-Putra D (2018) Lymphatic tissue engineering and regeneration. J Biol Eng 12(1):32
5. Ali JM, Catarino P, Dunning J, Giele H, Vrakas G, Parmar J (2016, October) Could sentinel skin transplants have some utility in solid organ transplantation? In Transplantation proceedings, vol 48, no 8. Elsevier, pp 2565–2570
6. Amirsadeghi A, Jafari A, Eggermont L, Hashemi SS, Bencherif SA, Khorram M (2020) Vascularization strategies for skin tissue engineering. Biomater Sci 8(15):4073–4094
7. Armstrong JP, Burke M, Carter BM, Davis SA, Perriman AW (2016) 3D bioprinting using a templated porous bioink. Adv Healthcare Mater 5(14):1724–1730
8. Arroyo JA, Winn VD (2008, June) Vasculogenesis and angiogenesis in the IUGR placenta. In: Seminars in perinatology, vol 32, no 3. WB Saunders, pp 172–177
9. Augustine R (2018) Skin bioprinting: a novel approach for creating artificial skin from synthetic and natural building blocks. Prog Biomater 7(2):77–92
10. Balieva F, Kupfer J, Lien L, Gieler U, Finlay AY, Tomás-Aragonés L, ... Halvorsen JA (2017) The burden of common skin diseases assessed with the EQ5D™: a European multicentre study in 13 countries. British J Dermatol 176(5):1170–1178
11. Bannasch H, Föhn M, Unterberg T, Bach AD, Weyand B, Stark GB (2003) Skin tissue engineering. Clin Plast Surg 30(4):573–579
12. Bedir T, Ulag S, Ustundag CB, Gunduz O (2020) 3D bioprinting applications in neural tissue engineering for spinal cord injury repair. Mater Sci Eng: C110:110741
13. Bhardwaj N, Chouhan D, Mandal BB (2018) 3D functional scaffolds for skin tissue engineering. In: Functional 3D tissue engineering scaffolds. Woodhead Publishing, pp 345–365
14. Binder KW, Zhao W, Aboushwareb T, Dice D, Atala A, Yoo JJ (2010) In situ bioprinting of the skin for burns. J Am Coll Surg 211(3):S76
15. Bouwstra JA, Pilgram GS, Ponec M (2006) Structure of the skin barrier. Skin barrier. Taylor & Francis, New York, pp 65–96
16. Braund R, Hook S, Medlicott NJ (2007) The role of topical growth factors in chronic wounds. Curr Drug Deliv 4(3):195–204
17. Brock WD, Bearden W, Tann T III, Long JA (2003) Autogenous dermis skin grafts in lower eyelid reconstruction. Ophthalmic Plast Reconstr Surg 19(5):394–397
18. Brown TM, Krishnamurthy K (2018) Histology, dermis. In: StatPearls [Internet]. StatPearls Publishing
19. Burdick JA, Prestwich GD (2011) Hyaluronic acid hydrogels for biomedical applications. Adv Mater 23(12):H41–H56
20. Camacho P, Busari H, Seims KB, Tolbert JW, Chow LW (2019) Materials as bioinks and bioink design. In: 3D bioprinting in medicine. Springer, Cham, pp 67–100
21. Casado-Díaz A, Quesada-Gómez JM, Dorado G (2020) Extracellular vesicles derived from mesenchymal stem cells (MSC) in regenerative medicine: applications in skin wound healing.Front Bioeng Biotechnol 8

22. Chen D, Hou Q, Zhong L, Zhao Y, Li M, Fu X (2019) Bioactive molecules for skin repair and regeneration: progress and perspectives. Stem Cells Int 2019:6789823
23. Chimene D, Lennox KK, Kaunas RR, Gaharwar AK (2016) Advanced bioinks for 3D printing: a materials science perspective. Ann Biomed Eng 44(6):2090–2102
24. Choi CH, Lin LY, Cheng CC, Chang CH (2015) Printed oxide thin film transistors: a mini review. ECS J Solid State Sci Technol 4(4):P3044
25. Chouhan D, Dey N, Bhardwaj N, Mandal BB (2019) Emerging and innovative approaches for wound healing and skin regeneration: current status and advances. Biomaterials, 216:119267
26. Chua AWC, Khoo YC, Tan BK, Tan KC, Foo CL, Chong SJ (2016) Skin tissue engineering advances in severe burns: review and therapeutic applications. Burns Trauma 4:1–14
27. Chung JH, Naficy S, Yue Z, Kapsa R, Quigley A, Moulton SE, Wallace GG (2013) Bio-ink properties and printability for extrusion printing living cells. Biomater Sci 1(7):763–773
28. Compaan AM, Christensen K, Huang Y (2017) Inkjet bioprinting of 3D silk fibroin cellular constructs using sacrificial alginate. ACS Biomater Sci Eng 3(8):1519–1526
29. Cork MJ, Robinson DA, Vasilopoulos Y, Ferguson A, Moustafa M, MacGowan A, ... Tazi-Ahnini R (2006). New perspectives on epidermal barrier dysfunction in atopic dermatitis: gene–environment interactions. J Allergy Clin Immunol 118(1):3–21
30. Coyer F, Gardner A, Doubrovsky A, Cole R, Ryan FM, Allen C, McNamara G (2015) Reducing pressure injuries in critically ill patients by using a patient skin integrity care bundle (InSPiRE). Am J Crit Care 24(3):199–209
31. Cubo N, Garcia M, Del Cañizo JF, Velasco D, Jorcano JL (2016) 3D bioprinting of functional human skin: production and in vivo analysis. Biofabrication 9(1):015006
32. Cui X, Breitenkamp K, Finn MG, Lotz M, D'Lima DD (2012) Direct human cartilage repair using three-dimensional bioprinting technology. Tissue Eng Part A 18(11–12):1304–1312
33. Cui H, Zhu W, Nowicki M, Zhou X, Khademhosseini A, Zhang LG (2016a) Hierarchical fabrication of engineered vascularized bone biphasic constructs via dual 3D bioprinting: integrating regional bioactive factors into architectural design. Adv Healthcare Mater 5(17):2174–2181
34. Cui H, Nowicki M, Fisher JP, Zhang LG (2017) 3D bioprinting for organ regeneration. Adv Healthcare Mater 6(1):1601118
35. Dababneh AB, Ozbolat IT (2014) Bioprinting technology: a current state-of-the-art review. J Manuf Sci Eng 136(6)
36. Dalgard FJ, Gieler U, Tomas-Aragones L, Lien L, Poot F, Jemec GB, ... Evers AW (2015) The psychological burden of skin diseases: a cross-sectional multicenter study among dermatological out-patients in 13 European countries. J Invest Dermatol 135(4):984–991
37. Daly AC, Critchley SE, Rencsok EM, Kelly DJ (2016a) A comparison of different bioinks for 3D bioprinting of fibrocartilage and hyaline cartilage. Biofabrication 8(4):045002 (b)
38. Daly AC, Cunniffe GM, Sathy BN, Jeon O, Alsberg E, Kelly DJ (2016b) 3D bioprinting of developmentally inspired templates for whole bone organ engineering. Adv Healthcare Mater 5(18):2353–2362 (a)
39. Das S, Pati F, Choi YJ, Rijal G, Shim JH, Kim SW, ... Ghosh S (2015) Bioprintable, cell-laden silk fibroin–gelatin hydrogel supporting multilineage differentiation of stem cells for fabrication of three-dimensional tissue constructs. Acta Biomaterialia 11:233–246
40. Das S, Baker AB (2016) Biomaterials and nanotherapeutics for enhancing skin wound healing. Front Bioeng Biotechnol 4:82
41. Delavary BM, van der Veer WM, van Egmond M, Niessen FB, Beelen RH (2011) Macrophages in skin injury and repair. Immunobiology 216(7):753–762
42. De Luca AC, Lacour SP, Raffoul W, Di Summa PG (2014) Extracellular matrix components in peripheral nerve repair: how to affect neural cellular response and nerve regeneration? Neural Regen Res 9(22):1943
43. Demidova-Rice TN, Hamblin MR, Herman IM (2012) Acute and impaired wound healing: pathophysiology and current methods for drug delivery, part 2: role of growth factors in normal and pathological wound healing: therapeutic potential and methods of delivery. Adv Skin Wound Care 25(8):349–370

44. Dorishetty P, Dutta NK, Choudhury NR (2020) Bioprintable tough hydrogels for tissue engineering applications. Adv Colloid Interf Sci 102163
45. Dussoyer M, Michopoulou A, Rousselle P (2020) Decellularized scaffolds for skin repair and regeneration. Appl Sci 10(10):3435
46. Dzobo K, Thomford NE, Senthebane DA, Shipanga H, Rowe A, Dandara C, ... Motaung KSCM (2018) Advances in regenerative medicine and tissue engineering: innovation and transformation of medicine. Stem Cells Int 2018:2495848
47. Elias PM, Feingold KR (2005) Stratum corneum barrier function: definitions and broad concepts. In: Skin barrier. CRC Press, pp 21–24
48. England S, Rajaram A, Schreyer DJ, Chen X (2017) Bioprinted fibrin-factor XIII-hyaluronate hydrogel scaffolds with encapsulated Schwann cells and their in vitro characterization for use in nerve regeneration. Bioprinting 5:1–9
49. Enoch S, Leaper DJ (2008) Basic science of wound healing. Surgery (Oxford) 26(2):31–37
50. Erickson JR, Echeverri K (2018) Learning from regeneration research organisms: the circuitous road to scar free wound healing. Dev Biol 433(2):144–154
51. Fartasch M (1997) Ultrastructure of the epidermal barrier after irritation. Microsc Res Tech 37(3):193–199
52. Faulkner-Jones A, Fyfe C, Cornelissen DJ, Gardner J, King J, Courtney A, Shu W (2015) Bioprinting of human pluripotent stem cells and their directed differentiation into hepatocyte-like cells for the generation of mini-livers in 3D. Biofabrication 7(4):044102
53. Feingold KR, Elias PM (2014) Role of lipids in the formation and maintenance of the cutaneous permeability barrier. Biochimica et Biophysica Acta (BBA)-Molecular Cell Biol Lipids 1841(3):280–294
54. Ferreira AM, Gentile P, Chiono V, Ciardelli G (2012) Collagen for bone tissue regeneration. Acta Biomater 8(9):3191–3200
55. Freinkel RK, Woodley DT (eds) (2001) The biology of the skin. CRC Press
56. Frueh FS, Sanchez-Macedo N, Calcagni M, Giovanoli P, Lindenblatt N (2018) The crucial role of vascularization and lymphangiogenesis in skin reconstruction. Eur Surg Res 59(3–4):242–254
57. Gantwerker EA, Hom DB (2012) Skin: histology and physiology of wound healing. Clin Plast Surg 39(1):85–97
58. Gao Q, He Y, Fu JZ, Liu A, Ma L (2015) Coaxial nozzle-assisted 3D bioprinting with built-in microchannels for nutrients delivery. Biomaterials 61:203–215
59. Gautam S, Chou CF, Dinda AK, Potdar PD, Mishra NC (2014) Surface modification of nanofibrous polycaprolactone/gelatin composite scaffold by collagen type I grafting for skin tissue engineering. Mater Sci Eng C 34:402–409
60. Gelse K, Pöschl E, Aigner T (2003) Collagens—structure, function, and biosynthesis. Adv Drug Deliv Rev 55(12):1531–1546
61. Gonzalez ACDO, Costa TF, Andrade ZDA, Medrado ARAP (2016) Wound healing—a literature review. An Bras Dermatol 91(5):614–620
62. Gopinathan J, Noh I (2018) Recent trends in bioinks for 3D printing. Biomaterials research 22(1):11
63. Griffith LG, Swartz MA (2006) Capturing complex 3D tissue physiology in vitro. Nat Rev Mol Cell Biol 7(3):211–224
64. Gudapati H, Dey M, Ozbolat I (2016) A comprehensive review on droplet-based bioprinting: past, present and future. Biomaterials 102:20–42
65. Guillemot F, Souquet A, Catros S, Guillotin B, Lopez J, Faucon M, ... Chabassier P (2010) High-throughput laser printing of cells and biomaterials for tissue engineering. Acta Biomaterialia 6(7):2494–2500
66. Guillotin B, Guillemot F (2011) Cell patterning technologies for organotypic tissue fabrication. Trends Biotechnol 29(4):183–190
67. Guo SA, DiPietro LA (2010) Factors affecting wound healing. J Dent Res 89(3):219–229
68. Gupta SK, Dinda AK, Potdar PD, Mishra NC (2013) Fabrication and characterization of scaffold from cadaver goat-lung tissue for skin tissue engineering applications. Mater Sci Eng, C 33(7):4032–4038

69. Haas AF (1995) Wound healing. Dermatol Nurs 7(1):28–74
70. Hagura A, Asai J, Maruyama K, Takenaka H, Kinoshita S, Katoh N (2014) The VEGF-C/VEGFR3 signaling pathway contributes to resolving chronic skin inflammation by activating lymphatic vessel function. J Dermatol Sci 73(2):135–141
71. Hakam MS, Imani R, Abolfathi N, Fakhrzadeh H, Sharifi AM (2016) Evaluation of fibrin-gelatin hydrogel as biopaper for application in skin bioprinting: an in-vitro study. Bio-Med Mater Eng 27(6):669–682
72. Hall AH, Mathieu L, Maibach HI (2018) Acute chemical skin injuries in the United States: a review. Crit Rev Toxicol 48(7):540–554
73. Hart J (2002) Inflammation 2: its role in the healing of chronic wounds. J Wound Care 11(7):245–249
74. Hemshekhar M, Thushara RM, Chandranayaka S, Sherman LS, Kemparaju K, Girish KS (2016) Emerging roles of hyaluronic acid bioscaffolds in tissue engineering and regenerative medicine. Int J Biol Macromol 86:917–928
75. Hockaday LA, Kang KH, Colangelo NW, Cheung PYC, Duan B, Malone E, ... Chu CC (2012) Rapid 3D printing of anatomically accurate and mechanically heterogeneous aortic valve hydrogel scaffolds. Biofabrication 4(3):035005
76. Hong S, Sycks D, Chan HF, Lin S, Lopez GP, Guilak F, ... Zhao X (2015) 3D printing of highly stretchable and tough hydrogels into complex, cellularized structures. Adv Mater 27(27):4035–4040
77. Horch RE, Weigand A, Wajant H, Groll J, Boccaccini AR, Arkudas A (2018) Biofabrikation–neue Ansätze für den artifiziellen Gewebeersatz.Handchirurgie·Mikrochirurgie Plastische Chirurgie 50(2):93–100
78. Horváth L, Umehara Y, Jud C, Blank F, Petri-Fink A, Rothen-Rutishauser B (2015) Engineering an in vitro air-blood barrier by 3D bioprinting. Sci Rep 5(1):1–8
79. Hribar KC, Soman P, Warner J, Chung P, Chen S (2014) Light-assisted direct-write of 3D functional biomaterials. Lab Chip 14(2):268–275
80. Huethorst E, Krebber MM, Fledderus JO, Gremmels H, Xu YJ, Pei J, ... Cheng C (2016) Lymphatic vascular regeneration: the next step in tissue engineering. Tissue Eng Part B: Rev 22(1):1–14
81. Ilhan E, Cesur S, Guler E, Topal F, Albayrak D, Guncu MM, ... Oktar FN (2020) Development of Satureja cuneifolia-loaded sodium alginate/polyethylene glycol scaffolds produced by 3D-printing technology as a diabetic wound dressing material. Int J Biol Macromol 161:1040–1054
82. Jakus AE, Rutz AL, Shah RN (2016) Advancing the field of 3D biomaterial printing. Biomed Mater 11(1):014102
83. Jammalamadaka U, Tappa K (2018) Recent advances in biomaterials for 3D printing and tissue engineering. J Funct Biomater 9(1):22
84. Jang CH, Ahn SH, Yang GH, Kim GH (2016) A MSCs-laden polycaprolactone/collagen scaffold for bone tissue regeneration. RSC Adv 6(8):6259–6265
85. Janmey PA, Winer JP, Weisel JW (2009) Fibrin gels and their clinical and bioengineering applications. J R Soc Interface 6(30):1–10
86. Ji S, Guvendiren M (2017) Recent advances in bioink design for 3D bioprinting of tissues and organs. Front Bioeng Biotechnol 5:23
87. Jia J, Richards DJ, Pollard S, Tan Y, Rodriguez J, Visconti RP, ... Mei Y (2014) Engineering alginate as bioink for bioprinting. Acta Biomaterialia 10(10):4323–4331
88. Kabirian F, Mozafari M (2020) Decellularized ECM-derived bioinks: prospects for the future. Methods 171:108–118
89. Kamel RA, Ong JF, Eriksson E, Junker JP, Caterson EJ (2013) Tissue engineering of skin. J Am Coll Surg 217(3):533–555
90. Kang SW, Kim JS, Park KS, Cha BH, Shim JH, Kim JY, ... Lee SH (2011) Surface modification with fibrin/hyaluronic acid hydrogel on solid-free form-based scaffolds followed by BMP-2 loading to enhance bone regeneration. Bone 48(2):298–306

91. Kang HW, Lee SJ, Ko IK, Kengla C, Yoo JJ, Atala A (2016) A 3D bioprinting system to produce human-scale tissue constructs with structural integrity. Nat Biotechnol 34(3):312–319
92. Karimi K, Odhav A, Kollipara R, Fike J, Stanford C, Hall JC (2017) Acute cutaneous necrosis: a guide to early diagnosis and treatment. J Cutan Med Surg 21(5):425–437
93. Kesti M, Müller M, Becher J, Schnabelrauch M, D'Este M, Eglin D, Zenobi-Wong M (2015) A versatile bioink for three-dimensional printing of cellular scaffolds based on thermally and photo-triggered tandem gelation. Acta Biomater 11:162–172
94. Klebe RJ (1988) Cytoscribing: a method for micropositioning cells and the construction of two-and three-dimensional synthetic tissues. Exp Cell Res 179(2):362–373
95. Knowlton S, Yenilmez B, Anand S, Tasoglu S (2017) Photocrosslinking-based bioprinting: examining crosslinking schemes. Bioprinting 5:10–18
96. Koch L, Kuhn S, Sorg H, Gruene M, Schlie S, Gaebel R, ... Vogt PM (2010) Laser printing of skin cells and human stem cells. Tissue Eng Part C: Methods 16(5):847–854
97. Koch L, Gruene M, Unger C, Chichkov B (2013) Laser assisted cell printing. Curr Pharm Biotechnol 14(1):91–97
98. Kolarsick PA, Kolarsick MA, Goodwin C (2011) Anatomy and physiology of the skin. J Dermatol Nurses' Assoc 3(4):203–213
99. Kolesky DB, Homan KA, Skylar-Scott MA, Lewis JA (2016) Three-dimensional bioprinting of thick vascularized tissues. Proc Natl Acad Sci 113(12):3179–3184
100. Kreimendahl F, Köpf M, Thiebes AL, Duarte Campos DF, Blaeser A, Schmitz-Rode T, ... Fischer H (2017) Three-dimensional printing and angiogenesis: tailored agarose-type I collagen blends comprise three-dimensional printability and angiogenesis potential for tissue-engineered substitutes. Tissue Eng Part C: Methods 23(10):604–615
101. Kuehn BM (2007) Chronic wound care guidelines issued. Jama 297(9):938–939
102. Kumar A, Starly B (2015) Large scale industrialized cell expansion: producing the critical raw material for biofabrication processes. Biofabrication 7(4):044103
103. Langer R, Vacanti JP (1993) Tissue engineering. Sci 260(5110):920–926
104. Laurens N, Koolwijk P, de Maat MP (2006) Fibrin structure and wound healing. J Thrombosis Haemostasis: JTH 4(5):932–939
105. Lawrence WT (1998) Physiology of the acute wound. Clin Plast Surg 25(3):321–340
106. Lazarus GS, Cooper DM, Knighton DR, Margolis DJ, Percoraro RE, Rodeheaver G, Robson MC (1994) Definitions and guidelines for assessment of wounds and evaluation of healing. Wound Repair Regen 2(3):165–170
107. Le HP (1998) Progress and trends in ink-jet printing technology. J Imaging Sci Technol 42(1):49–62
108. Lee YB, Polio S, Lee W, Dai G, Menon L, Carroll RS, Yoo SS (2010) Bio-printing of collagen and VEGF-releasing fibrin gel scaffolds for neural stem cell culture. Exp Neurol 223(2):645–652
109. Leirós GJ, Kusinsky AG, Drago H, Bossi S, Sturla F, Castellanos ML, ... Balañá ME (2014) Dermal papilla cells improve the wound healing process and generate hair bud-like structures in grafted skin substitutes using hair follicle stem cells. Stem Cells Transl Med 3(10):1209–1219
110. Li J, Chen M, Fan X, Zhou H (2016) Recent advances in bioprinting techniques: approaches, applications and future prospects. J Transl Med 14(1):271
111. Loss M, Wedler V, Künzi W, Meuli-Simmen C, Meyer VE (2000) Artificial skin, split-thickness autograft and cultured autologous keratinocytes combined to treat a severe burn injury of 93% of TBSA. Burns 26(7):644–652
112. Lynn AK, Yannas IV, Bonfield W (2004) Antigenicity and immunogenicity of collagen. J Biomed Mater Res Part B: Appl Biomater: Off J Soc Biomater Japanese Soc Biomater Austr Soc Biomater Korean Soc Biomater 71(2):343–354
113. Matai I, Kaur G, Seyedsalehi A, McClinton A, Laurencin CT (2020) Progress in 3D bioprinting technology for tissue/organ regenerative engineering. Biomaterials 226:119536
114. Mayet N, Choonara YE, Kumar P, Tomar LK, Tyagi C, Du Toit LC, Pillay V (2014) A comprehensive review of advanced biopolymeric wound healing systems. J Pharm Sci 103(8):2211–2230

115. Melchels FP, Feijen J, Grijpma DW (2010) A review on stereolithography and its applications in biomedical engineering. Biomaterials 31(24):6121–6130
116. Melchels FP, Domingos MA, Klein TJ, Malda J, Bartolo PJ, Hutmacher DW (2012) Additive manufacturing of tissues and organs. Prog Polym Sci 37(8):1079–1104
117. Menon GK, Dryer L, Kalafsky R (2009) Approaches to the development of cosmetic products to counter the effects of skin aging. In: Skin aging handbook. William Andrew Publishing, pp 265–290
118. Metcalfe AD, Ferguson MW (2007) Tissue engineering of replacement skin: the crossroads of biomaterials, wound healing, embryonic development, stem cells and regeneration. J R Soc Interf 4(14):413–437
119. Mironov V, Kasyanov V, Drake C, Markwald RR (2008) Organ printing: promises and challenges. Future Med 3(1):93–103
120. Mironov V, Kasyanov V, Markwald RR (2011) Organ printing: from bioprinter to organ biofabrication line. Curr Opin Biotechnol 22(5):667–673
121. Mohammadi MH, Heidary Araghi B, Beydaghi V, Geraili A, Moradi F, Jafari P, ... Sanati-Nezhad A (2016) Skin diseases modeling using combined tissue engineering and microfluidic technologies. Adv Healthcare Mater 5(19):2459–2480
122. Montero FE, Rezende RA, Silva JVL, Sabino MA (2019) Development of a smart bioink for bioprinting applications. Front Mech Eng 5:56
123. Morgan FL, Moroni L, Baker MB (2020) Dynamic bioinks to advance bioprinting. Adv Healthcare Mater 1901798
124. Mori H, Shimizu K, Hara M (2013) Dynamic viscoelastic properties of collagen gels with high mechanical strength. Mater Sci Eng, C 33(6):3230–3236
125. Murphy SV, Atala A (2014) 3D bioprinting of tissues and organs. Nat Biotechnol 32(8):773–785
126. Nguyen D, Hägg DA, Forsman A, Ekholm J, Nimkingratana P, Brantsing C, ... Lindahl A (2017) Cartilage tissue engineering by the 3D bioprinting of iPS cells in a nanocellulose/alginate bioink. Sci Rep 7(1):1–10
127. Ning L, Chen X (2017) A brief review of extrusion-based tissue scaffold bio-printing. Biotechnol J 12(8):1600671
128. Norouzi M, Boroujeni SM, Omidvarkordshouli N, Soleimani M (2015) Advances in skin regeneration: application of electrospun scaffolds. Adv Healthcare Mater 4(8):1114–1133
129. Nulty J, Schipani R, Burdis R, Kelly DJ (2019) Bioinks and their applications in tissue engineering. In: Polymer-based additive manufacturing. Springer, Cham, pp 187–218
130. Osidak EO, Kozhukhov VI, Osidak MS, Domogatskiy SP (2020) Collagen as bioink for bioprinting: a comprehensive review. Int J Bioprint 6(3)
131. Ozbolat IT (2015) Bioprinting scale-up tissue and organ constructs for transplantation. Trends Biotechnol 33(7):395–400
132. Ozbolat IT, Hospodiuk M (2016) Current advances and future perspectives in extrusion-based bioprinting. Biomaterials 76:321–343
133. Pajardi G, Rapisarda V, Somalvico F, Scotti A, Russo GL, Ciancio F, ... Trabucchi E (2016) Skin substitutes based on allogenic fibroblasts or keratinocytes for chronic wounds not responding to conventional therapy: a retrospective observational study. Int Wound J 13(1):44–52
134. Papageorgiou SK, Kouvelos EP, Favvas EP, Sapalidis AA, Romanos GE, Katsaros FK (2010) Metal–carboxylate interactions in metal–alginate complexes studied with FTIR spectroscopy. Carbohyd Res 345(4):469–473
135. Papini R (2004) Management of burn injuries of various depths. BMJ 329(7458):158–160
136. Parak A, Pradeep P, du Toit LC, Kumar P, Choonara YE, Pillay V (2019) Functionalizing bioinks for 3D bioprinting applications. Drug Discov Today 24(1):198–205
137. Park JW, Hwang SR, Yoon IS (2017a) Advanced growth factor delivery systems in wound management and skin regeneration. Molecules 22(8):1259
138. Park J, Lee SJ, Chung S, Lee JH, Kim WD, Lee JY, Park SA (2017b) Cell-laden 3D bioprinting hydrogel matrix depending on different compositions for soft tissue engineering: characterization and evaluation. Mater Sci Eng: C 71:678–684

139. Pati F, Jang J, Ha DH, Kim SW, Rhie JW, Shim JH, ... Cho DW (2014) Printing three-dimensional tissue analogues with decellularized extracellular matrix bioink. Nat Commun 5(1):1–11
140. Peng W, Unutmaz D, Ozbolat IT (2016) Bioprinting towards physiologically relevant tissue models for pharmaceutics. Trends Biotechnol 34(9):722–732
141. Peng W, Datta P, Ayan B, Ozbolat V, Sosnoski D, Ozbolat IT (2017) 3D bioprinting for drug discovery and development in pharmaceutics. Acta Biomater 57:26–46
142. Pereira RF, Barrias CC, Granja PL, Bartolo PJ (2013) Advanced biofabrication strategies for skin regeneration and repair. Nanomedicine 8(4):603–621
143. Pittman RN (2011, April) Regulation of tissue oxygenation. In: Colloquium series on integrated systems physiology: from molecule to function, vol 3, no 3. Morgan & Claypool Life Sciences, pp 1–100
144. Poldervaart MT, Goversen B, De Ruijter M, Abbadessa A, Melchels FP, Öner FC, ... Alblas J (2017) 3D bioprinting of methacrylated hyaluronic acid (MeHA) hydrogel with intrinsic osteogenicity. PLoS One 12(6):e0177628
145. Rahmati M, Blaker JJ, Lyngstadaas SP, Mano JF, Haugen HJ (2020) Designing multigradient biomaterials for skin regeneration. Mater Today Adv 5:100051
146. Reinke JM, Sorg H (2012) Wound repair and regeneration. Eur Surgical Res. Europaische chirurgische Forschung. Recherches chirurgicales europeennes 49(1):35–43
147. Rengier F, Mehndiratta A, Von Tengg-Kobligk H, Zechmann CM, Unterhinninghofen R, Kauczor HU, Giesel FL (2010) 3D printing based on imaging data: review of medical applications. Int J Comput Assist Radiol Surg 5(4):335–341
148. Rodriguez MJ, Brown J, Giordano J, Lin SJ, Omenetto FG, Kaplan DL (2017) Silk based bioinks for soft tissue reconstruction using 3-dimensional (3D) printing with in vitro and in vivo assessments. Biomaterials 117:105–115
149. Rutz AL, Hyland KE, Jakus AE, Burghardt WR, Shah RN (2015) A multimaterial bioink method for 3D printing tunable, cell-compatible hydrogels. Adv Mater 27(9):1607–1614
150. Saunders R, Bosworth L, Gough J, Derby B, Reis N (2004) Selective cell delivery for 3D tissue culture and engineering. Eur Cells Mater 7(Suppl 1):84–5.*ls*
151. Saunders RE, Derby B (2014) Inkjet printing biomaterials for tissue engineering: bioprinting. Int Mater Rev 59(8):430–448
152. Savoji H, Godau B, Hassani MS, Akbari M (2018) Skin tissue substitutes and biomaterial risk assessment and testing. Front Bioeng Biotechnol 6:86
153. Schaupper M, Jeltsch M, Rohringer S, Redl H, Holnthoner W (2016) Lymphatic vessels in regenerative medicine and tissue engineering. Tissue Eng Part B Rev 22(5):395–407
154. Schiele NR, Corr DT, Huang Y, Raof NA, Xie Y, Chrisey DB (2010) Laser-based direct-write techniques for cell printing. Biofabrication 2(3):032001
155. Seavey JG, Masters ZA, Balazs GC, Tintle SM, Sabino J, Fleming ME, Valerio IL (2016) Use of a bioartificial dermal regeneration template for skin restoration in combat casualty injuries. Regen Med 11(1):81–90
156. Shah JMY, Omar E, Pai DR, Sood S (2012) Cellular events and biomarkers of wound healing. Indian J Plast Surgery: Off Publ Assoc Plast Surgeons India 45(2):220
157. Shamloo A, Sarmadi M, Aghababaie Z, Vossoughi M (2018) Accelerated full-thickness wound healing via sustained bFGF delivery based on a PVA/chitosan/gelatin hydrogel incorporating PCL microspheres. Int J Pharm 537(1–2):278–289
158. Sheridan R (2009) Closure of the excised burn wound: autografts, semipermanent skin substitutes, and permanent skin substitutes. Clin Plast Surg 36(4):643–651
159. Shi C, Zhu Y, Su Y, Cheng T (2006) Stem cells and their applications in skin-cell therapy. Trends Biotechnol 24(1):48–52
160. Shim JH, Lee JS, Kim JY, Cho DW (2012). Bioprinting of a mechanically enhanced three-dimensional dual cell-laden construct for osteochondral tissue engineering using a multi-head tissue/organ building system. J Micromech Microeng 22(8):085014
161. Shoulders MD, Raines RT (2009) Collagen structure and stability. Ann Rev Biochem 78:929–958

162. Singer AJ, Clark RA (1999) Cutaneous wound healing. N Engl J Med 341(10):738–746
163. Singh D, Singh D, Han SS (2016) 3D printing of scaffold for cells delivery: advances in skin tissue engineering. Polymers 8(1):19
164. Sinno H, Prakash S (2013) Complements and the wound healing cascade: an updated review. Plast Surgery Int 2013:146764
165. Skardal A (2018) Perspective:"Universal" bioink technology for advancing extrusion bioprinting-based biomanufacturing. Bioprinting 10:e00026
166. Smith MM, Melrose J (2015) Proteoglycans in normal and healing skin. Adv Wound Care 4(3):152–173
167. Sorg H, Tilkorn DJ, Hager S, Hauser J, Mirastschijski U (2017) Skin wound healing: an update on the current knowledge and concepts. Eur Surg Res 58(1–2):81–94
168. Stadelmann WK, Digenis AG, Tobin GR (1998) Physiology and healing dynamics of chronic cutaneous wounds. Am J Surgery 176(2):26S-38S
169. Stichler S, Böck T, Paxton N, Bertlein S, Levato R, Schill V, ... Groll J (2017) Double printing of hyaluronic acid/poly (glycidol) hybrid hydrogels with poly (ε-caprolactone) for MSC chondrogenesis. Biofabrication 9(4):044108
170. Stratesteffen H, Köpf M, Kreimendahl F, Blaeser A, Jockenhoevel S, Fischer H (2017) GelMA-collagen blends enable drop-on-demand 3D printablility and promote angiogenesis. Biofabrication 9(4):045002
171. Talikowska M, Fu X, Lisak G (2019) Application of conducting polymers to wound care and skin tissue engineering: a review. Biosens Bioelectron 135:50–63
172. Tan R, She Z, Wang M, Fang Z, Liu Y, Feng Q (2012) Thermo-sensitive alginate-based injectable hydrogel for tissue engineering. Carbohyd Polym 87(2):1515–1521
173. Tanzeglock T, Soos M, Stephanopoulos G, Morbidelli M (2009) Induction of mammalian cell death by simple shear and extensional flows. Biotechnol Bioeng 104(2):360–370
174. Tasoglu S, Demirci U (2013) Bioprinting for stem cell research. Trends Biotechnol 31(1):10–19
175. Ter Horst B, Chouhan G, Moiemen NS, Grover LM (2018) Advances in keratinocyte delivery in burn wound care. Adv Drug Deliv Rev 123:18–32
176. Tirella A, Orsini A, Vozzi G, Ahluwalia ARTI (2009) A phase diagram for microfabrication of geometrically controlled hydrogel scaffolds. Biofabrication 1(4):045002
177. Traversa B, Sussman G (2001) The role of growth factors, cytokines and proteases in wound management. Primary Intent: Austr J Wound Manag 9(4):161
178. Ulag S, Ilhan E, Sahin A, Yilmaz BK, Ekren N, Kilic O, ... Gunduz O (2020). 3D printed artificial cornea for corneal stromal transplantation. Eur Polym J 109744
179. Usui ML, Mansbridge JN, Carter WG, Fujita M, Olerud JE (2008) Keratinocyte migration, proliferation, and differentiation in chronic ulcers from patients with diabetes and normal wounds. J Histochem Cytochem 56(7):687–696
180. Xia Z, Jin S, Ye K (2018) Tissue and organ 3D bioprinting. SLAS Technol: Transl Life Sci Innov 23(4):301–314
181. Xiong S, Zhang X, Lu P, Wu Y, Wang Q, Sun H, ... Ouyang H (2017) A gelatin-sulfonated silk composite scaffold based on 3D printing technology enhances skin regeneration by stimulating epidermal growth and dermal neovascularization. Sci Rep 7(1):1–12
182. Xu T, Kincaid H, Atala A, Yoo JJ (2008) High-throughput production of single-cell microparticles using an inkjet printing technology. J Manuf Sci Eng 130(2)
183. Xu X, Jha AK, Harrington DA, Farach-Carson MC, Jia X (2012) Hyaluronic acid-based hydrogels: from a natural polysaccharide to complex networks. Soft Matter 8(12):3280–3294
184. Xu Y, Wang X (2015) Fluid and cell behaviors along a 3D printed alginate/gelatin/fibrin channel. Biotechnol Bioeng 112(8):1683–1695
185. Xu J, Zheng S, Hu X, Li L, Li W, Parungao R, ... Song K (2020) Advances in the research of bioinks based on natural collagen, polysaccharide and their derivatives for skin 3d bioprinting. Polymers 12(6):1237
186. Valkenaers H, Vogeler F, Voet A, Kruth JP (2013) Screw extrusion based 3D printing, a novel additive manufacturing technology. Mater Sci

187. Varkey M, Visscher DO, van Zuijlen PP, Atala A, Yoo JJ (2019) Skin bioprinting: the future of burn wound reconstruction? Burns Trauma 7:s41038–s42019
188. Velasco Bayón D, Quílez López C, García Díez M Cañizo López JFD, Jorcano Noval JL (2018) 3D human skin bioprinting: a view from the bio side. J 3D Print Med 2(3): 141–162
189. Velnar T, Bailey T, Smrkolj V (2009) The wound healing process: an overview of the cellular and molecular mechanisms. J Int Med Res 37(5):1528–1542
190. Vig K, Chaudhari A, Tripathi S, Dixit S, Sahu R, Pillai S, ... Singh SR (2017). Advances in skin regeneration using tissue engineering. Int Journal Molecular Sci 18(4):789
191. Vlăsceanu GM, Iovu H, Ioniţă M (2019) Graphene inks for the 3D printing of cell culture scaffolds and related molecular arrays. Compos B Eng 162:712–723
192. Wahl SM, Wong H, McCartney-Francis N (1989) Role of growth factors in inflammation and repair. J Cell Biochem 40(2):193–199
193. Wang X, Tolba E, Schröder HC, Neufurth M, Feng Q, Diehl-Seifert B, & Müller WE (2014). Effect of bioglass on growth and biomineralization of SaOS-2 cells in hydrogel after 3D cell bioprinting. PLoS One 9(11):e112497
194. Wang M, He J, Liu Y, Li M, Li D, Jin Z (2015) The trend towards in vivo bioprinting. Int J Bioprint 1(1)
195. Wang X, Rijff BL, Khang G (2017) A building-block approach to 3D printing a multichannel, organ-regenerative scaffold. J Tissue Eng Regen Med 11(5):1403–1411
196. Whitford WG, Hoying JB (2016) A bioink by any other name: terms, concepts and constructions related to 3D bioprinting. Future Sci OA 2(3):141–162
197. Williams D, Thayer P, Martinez H, Gatenholm E, Khademhosseini A (2018) A perspective on the physical, mechanical and biological specifications of bioinks and the development of functional tissues in 3D bioprinting. Bioprinting 9:19–36
198. Yan WC, Davoodi P, Vijayavenkataraman S, Tian Y, Ng WC, Fuh JY, ... Wang CH (2018) 3D bioprinting of skin tissue: from pre-processing to final product evaluation. Adv Drug Delivery Rev 132:270-295
199. Yang X, Lu Z, Wu H, Li W, Zheng L, Zhao J (2018) Collagen-alginate as bioink for three-dimensional (3D) cell printing based cartilage tissue engineering. Mater Sci Eng, C 83:195–201
200. Yang R, Yang S, Zhao J, Hu X, Chen X, Wang J, ... Xiong K (2020) Progress in studies of epidermal stem cells and their application in skin tissue engineering. Stem Cell Res Therapy, 11(1), 1-13
201. Yao B, Xie J, Liu N, Yan T, Li Z., Liu Y, ... Fu X (2016) Identification of a new sweat gland progenitor population in mice and the role of their niche in tissue development. Biochemical and Biophysical Res Commun 479(4):670–675
202. Yeo M, Lee JS, Chun W, Kim GH (2016) An innovative collagen-based cell-printing method for obtaining human adipose stem cell-laden structures consisting of core–sheath structures for tissue engineering. Biomacromol 17(4):1365–1375
203. Yoo HS, Lee EA, Yoon JJ, Park TG (2005) Hyaluronic acid modified biodegradable scaffolds for cartilage tissue engineering. Biomaterials 26(14):1925–1933
204. Zhang X, Zhang Y (2015) Tissue engineering applications of three-dimensional bioprinting. Cell Biochem Biophys 72(3):777–782

Chapter 8
Bioceramic-Starch Paste Design for Additive Manufacturing and Alternative Fabrication Methods Applied for Developing Biomedical Scaffolds

Andreea Maidaniuc and Florin Miculescu

Abstract Additive manufacturing has gained considerable attention for building biomedical scaffolds due to its presumed ability to provide porous structures adequate for inflow and ingrowth of blood and tissues that facilitate bone regeneration. Various paste designs, consisting of mixtures of polymers with various ceramic or glass particles were proposed as additive manufacturing inks. However, proper paste design is still an open research subject as the link between the paste performance and various properties such as solids loading ability, homogenization, jellification, or particle morphology needs further characterization. This chapter explores the possibilities of using starch gels in combination with various bioceramics for producing biomedical scaffolds for bone regeneration using either additive manufacturing methods or more cost-effective alternative methods. Next, an integrated technological solution for manufacturing biomimetic implants for filling large bone defects is presented in the chapter, as a practical alternative to the current additive manufacturing attempts. This solution aims to solve the challenges related to tissue vascularization and mechanical stability associated with bone scaffolds by creatively using low-cost, natural, and biocompatible sintering additives such as starch. Various three-dimensional test samples prepared with bioceramics and starch gels by applying this technology are evaluated, with good perspectives for clinical application.

Keywords Additive manufacturing · Robocasting ink · Ceramics · Starch gels · Medical scaffolds · Hydroxyapatite

1 Introduction

A simple search on Science Direct with the terms "medical scaffold" yields more than 11,000 literature reviews and more than 33,000 research articles on this topic. That is a vast amount of peer-reviewed literature dedicated to these promising devices.

A. Maidaniuc · F. Miculescu (✉)
Department of Metallic Materials Science, Physical Metallurgy, Faculty of Material Science and Engineering, Politehnica University of Bucharest, Bucharest, Romania

A. Kumar et al. (eds.), *3D printable Gel-inks for Tissue Engineering*, Gels Horizons: From Science to Smart Materials, https://doi.org/10.1007/978-981-16-4667-6_8

Medical scaffolds are porous structures, built from biomaterials, used to provide the appropriate environment for regeneration of various tissues and organs, thus acting as a template for new tissue formation. Their use is closely related to the field of tissue engineering (also known as regenerative medicine) which aims to regenerate damaged tissues instead of replacing them, by pivoting from tissue grafts to advanced biomaterials able to restore and possibly improve tissue function [1].

A part of this field is related to bone tissue engineering. Bones are organs that compose the skeleton in animals. Besides ensuring the mobility and structure of the body, the bones also protect other organs, store minerals, and are involved in red and white blood cell production. By their permanent interaction with body fluids, the bones are capable to regenerate through processes of remineralization and resorption. In this way, bones grow and repair themselves if their integrity is affected [2, 3].

When bones substantially lose their integrity through accidents, pathologies with major bone loss, or due to non-union fractures, their regeneration needs to be supported and stimulated for repairing the bone defects with minimum distress for the patients. If bone defects are as large as a few centimeters, the bone tissue cannot regenerate itself in optimal conditions, and its integrity is restored using bone substituents. The relation between the concepts related to the use of bone addition materials is schematically represented in Fig. 1. Ideally, these bone substituents shall ensure: (1) proper inflow of body fluids while avoiding tissue necrosis at the defect extremities; (2) bone stability within the local biomechanical environment; and (3) stimulation of bone regeneration through osteoconduction and osteoinduction mechanisms.

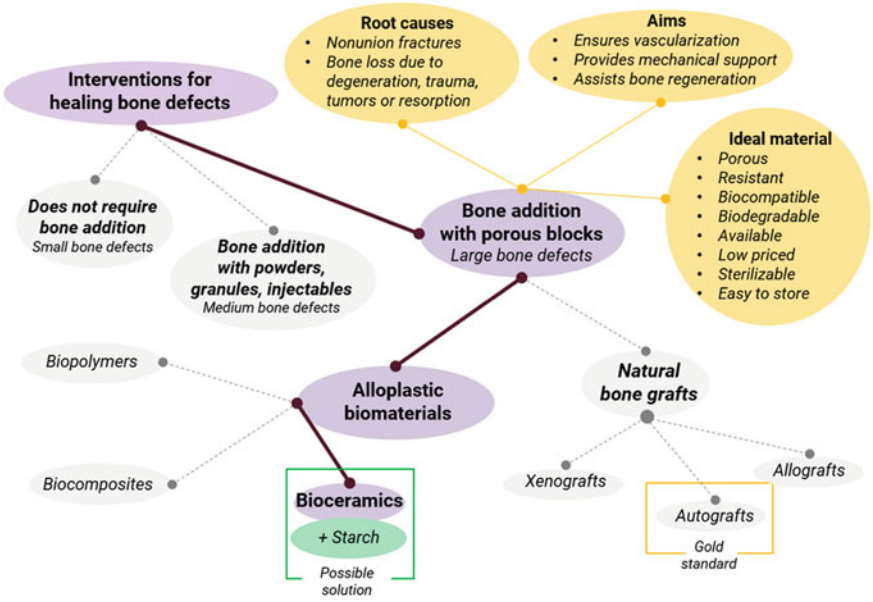

Fig. 1 Bioceramic-starch pastes among solutions for bone reconstruction

Currently, the standard material used for bone repair is the autologous/autogenous bone graft, also named bone autograft. The graft represents a part of bone tissue harvested from the patient from an area with reduced mechanical loads (such as the iliac crest or the mandibular bone). By being harvested directly from the patient, the bone autograft is completely compatible with the bone that needs reparation. Unfortunately, a bone autograft can only be collected in small quantities which are usually not sufficient for repairing large bone defects. Also, bone graft harvesting requires additional medical interventions besides the actual bone reconstruction, (which usually induce more discomfort to the patient) and prolongs the recuperation [4, 5].

Biomaterials science and engineering constantly test alloplastic biomaterials and products intended for bone reconstruction. If adequate, the synthetic biomaterials can be supplied in large quantities, with varied and tunable properties, and can eliminate the risks associated with natural bone grafts [6, 7]. But, although these materials and products should be similar to the bone tissues at an affordable price, most of the alloplastic solutions currently available for bone reconstruction are costly, does not provide complete integration with the bone, have irregular biological activity, and cannot be used for reconstruction of large bone defects.

Ideally, an alloplastic product for bone reconstruction should be designed considering the structure and function of the natural bone tissue, from biocompatible and biodegradable materials with high availability. These products should have a chemical composition similar to the original bone tissue, with adequate porosity to ensure the inflow and ingrowth of body fluids and bone cells respectively, and with adapted mechanical properties that match the loads from the implantation area to support the affected tissue during regeneration. Also, while bone regeneration takes place, the implanted biomaterial should degrade at a suitable rate into non-toxic and metabolizable by-products. In the end, to be clinically relevant, these materials and products should be easy to process at low costs, resistant to sterilization, and easy to store [8–10].

Based on all these requirements, the ceramic biomaterials emerged as a reasonable alternative for the fabrication of bone scaffolds. Their main limitations, such as brittleness, can be alleviated through combination with other materials—such as biopolymers, for preparing composite scaffolds. Starch, a natural, cheap, and biodegradable polymer used intensively in the food industry, has been tested in combination with bioceramics and other biopolymers for producing scaffolds. But although there is a substantial amount of data available related to bioceramic-starch combination, their use with modern technologies such as additive manufacturing is still very limited.

This chapter aims to describe the current research developments related to the fabrication of scaffolds for bone regeneration using starch gels with bioceramics, in an attempt to evaluate if starch-bioceramics pastes are adequate for additive manufacturing. Some topics will be discussed only briefly, as comprehensive information is available in the referenced works (Table 1).

Considering that full development of bioceramic-starch inks for tridimensional printing has not been achieved yet, the final part of the chapter presents a practical alternative: a conventional fabrication technology for bone scaffolds which

Table 1 Useful references related to the key concepts of this chapter

Topic	References
Bone as a material	[2, 3]
Bone grafts and bone substitutes	[4, 5]
Bioceramics and their applications	[11–13]
Ceramic processing and sintering	[14, 15]
Additive manufacturing of bioceramics	[16–19]
Bioceramic-starch formulations	[20–22]

was developed based on fundamental research and engineering best practices. The prototypes which were developed by applying this technology were fabricated from bone-derived hydroxyapatite, starch, and water. The product design strategy and the morphological characterization for the prototypes are discussed in detail.

2 Starch

Starch is a natural polysaccharide extracted from plants. The key concepts related to starch are represented in Fig. 2. In plants, starch is deposited as particles (granules)

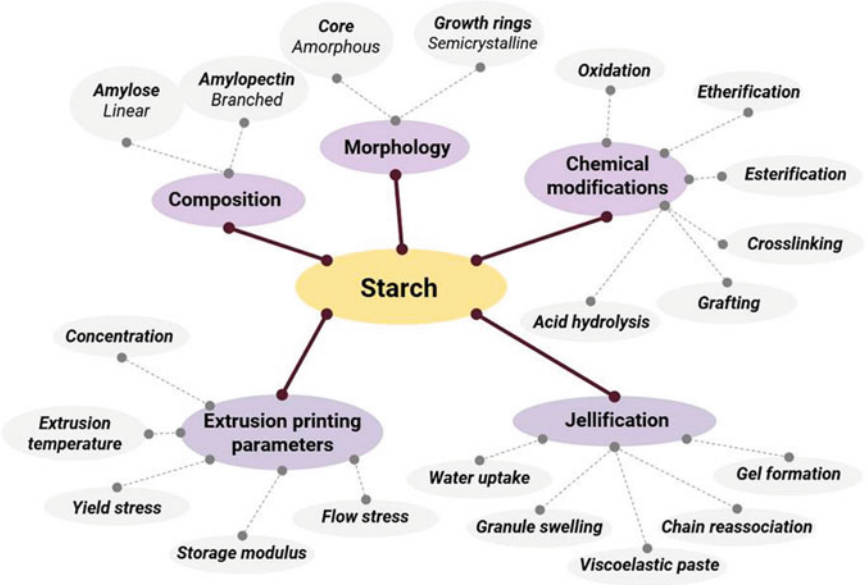

Fig. 2 Key-concepts related to the use of starch with bioceramics

which are insoluble in cold water. Starch mainly consists of 2 polymers: the linear amylose (amorphous), and the highly branched amylopectin (semicrystalline). The typical starch composition is 20–30% amylose and 70–80% amylopectin, depending on the source of extraction. Both constituents are built on glucan chains, which are glucose-based polymers. Many starch characteristics such as granule structure and morphology, water-solubility, swelling, and gelling ability depend on the source of extraction [20, 23].

A starch granule composed of an amorphous core area surrounded by concentric growth rings. The amorphous core is composed mainly of amylose chains. The size of the amorphous core depends on the amylose content of starch, that is why the maize starch granules have a small core compared to high amylose maize starch (which has the largest core) [24].

Given that starch is easily formed by simple processing techniques such as blowing, extrusion, and molding, its use for scaffold fabrication has been documented mainly for conventional methods such as salt particle leaching, solvent casting, and extrusion with blowing agents. Some of these methods use starches which were subjected to chemical modifications such as oxidation, etherification, esterification, crosslinking, grafting, and cationization [25].

Starch can form colloidal solutions by acid hydrolysis. The reaction occurs in aqueous or alcoholic solutions of hydrochloric or sulfuric acid, at temperatures between 55–85 °C [20]. Another useful characteristic for choosing starch in various medical applications (such as adhesives, bone cement, bone waxes, or drug-delivery systems [21]) is its ability to form gels in aqueous solutions. When heated at temperatures between 60–80 °C, an aqueous solution of starch is subjected to various changes, which involve water uptake, granule swelling, the formation of a viscoelastic paste during heating, reassociation of dispersed starch chains on cooling, and formation of a gel. All these changes influence starch functionality, which is important for controlling moisture, viscosity, texture, consistency, and shelf-life of starch-based products.

When starch is heated in the presence of water and subsequently cooled, amylose and amylopectin can reassociate into a different structure in a process named retrogradation. Retrogradation involves rapid recrystallization of amylose molecules followed by slow recrystallization of amylopectin molecules. Starch retrogradation is also accompanied by physical changes such as increased viscosity, gel formation, water exudation, and increased crystallinity. The outcomes of starch retrogradation depend on the starch type: the gel formed after retrogradation of waxy starches is firmer than the one formed by nonwaxy ones. This is further explained by the starch composition: high-amylose starches are usually stronger and provide elasticity and strength against deformation. Low-content amylose gels are softer gels with a weaker network and this leads to easier penetrability and greater stickiness and adhesiveness [24].

Its use as a biomaterial is limited by difficult processing, poor mechanical properties, and water sensibility. To overcome these limitations, starch is chemically modified [26], combined in starch blends with other polymers [27, 28], or combined in composites with ceramic materials.

The first uses of starch in ceramic technology were related to its binding abilities—starch firstly replaced plastic clay as a binder in ceramic mixtures. After that, starch was used as a pore-forming agent based on its complete thermal degradation at high temperatures. In 1998, the gelling ability of starch inspired the development of the starch consolidation method, in which the starch gel supports the ceramic body in the forming stage of a sintering program [29]. Starch gels can also be used in gel-mediated ceramic powder synthesis. Within these methods, starch acts as an eco-friendly chelating/ gelling agent (preventing the agglomeration of the synthesized ceramic particles) and as a highly energetic fuel that provides energy during combustion-based synthesis methods [30].

3 Bioceramics-Starch Pastes

3.1 Oxide Ceramics and Starch

Oxide ceramics are part of the first generation of biomaterials (along with the majority of metallic biomaterials and with some polymers such as silicone rubber and acrylic resins) which were developed in the 1950s. Oxide ceramics are considered *inert biomaterials*, meaning they can substitute bone or teeth without reacting with living tissues. Despite this inertness, all biomaterials elicit a response from the surrounding living tissue after implantation. This response consists of forming fibrous tissue of various thicknesses around the implanted material [11].

Oxide ceramics are constantly evolving into a wide range of materials that can be used as stand-alone biomaterials or as part of bioceramic composites [31]. The most popular oxide ceramics are aluminum oxide (alumina, Al_2O_3) and zirconium oxide (zirconia, ZrO—which is used as a biomaterial mainly in its yttria-stabilized tetragonal zirconia polycrystal (3Y-TZP) form). Other popular oxide ceramics include allotropic carbon-based materials such as graphene oxide (GO) and reduced graphene oxide (rGO).

Aluminum oxide (alumina, Al_2O_3) is characterized by strong ionic and covalent chemical bonds between Al^{3+} and O^{2-}. These bonds lead to chemical inertness high melting point and hardness. Alumina has a high wettability due to a layer of hydroxy groups attached at its surface, which leads to good scratching resistance. Starting from these characteristics, alumina is a suitable candidate for arthroprostheses joints with low wear. However, due to the same characteristics, alumina is difficult to process during casting and machining, and apart from hardness and scratch resistance, its mechanical properties do not match the target properties of bone. The improvement of alumina's characteristics is currently achieved by surface modification or functionalization with different ions and functional groups, and by mixing or coating with bioactive materials [11].

The use of starch with alumina is well documented. The successful use of the starch consolidation casting in alumina technology depends on the size and shape

characterization of starch, the rheology of ceramic-starch suspension, the swelling kinetics, and the burnout behavior of starch [22].

Starch consolidation was also combined with other methods for inducing porosity in alumina components. Notable examples are the combination with the sacrificial porogen method—in which pore formers such as poppy seeds were burnt for generating additional porosity [32] and with the biological foaming—in which a combination of yeast and sugar was used to generate foams at ~80 °C (at which starch is jellified in presence of water), followed by drying and sintering to remove the non-ceramic fraction from the green body [33].

Zirconia (zirconia, ZrO) is an oxide ceramic material with excellent mechanical properties, ionic conductivity, thermal and chemical stability. Its good biocompatibility and degradation resistance make it suitable as a biomaterial. Due to its esthetic characteristics, zirconia, and especially yttrium stabilized zirconia (YSZ), is currently used in dental clinical practice in crowns, bridges, implants, or veneers [34].

Given its intensive use, a wide range of conventional fabrication methods are currently used with zirconia, while the fabrication of zirconia components via additive manufacturing has been increasingly investigated. However, since the full potential of additive manufactured zirconia components has yet to be achieved, the use of conventional fabrication methods or hybrid approaches with additive manufacturing remains a more reliable solution for production [35]. Within the conventional fabrication methods, starch has been tested mostly as a pore-forming agent both for zirconia (via tape-casting [36] or thermoplastic co-extrusion [37]) and alumina–zirconia composites [38, 39].

Graphene oxide (GO) and reduced graphene oxide (rGO), are very popular 2D carbon-based materials with outstanding physical, chemical, and biological properties. Both are part of a larger group of carbon-based materials currently tested in tissue engineering that includes: graphite (three-dimensional), graphene (two-dimensional), nanowires (one-dimensional), nanotubes (one-dimensional), and fullerenes (zero-dimensional).

Both GO and rGO can be used to enhance the physical, chemical, and mechanical properties of various biomaterials due to their high specific surface area and mechanical strength. They can also improve the biological performance of the biomaterials, as they have been shown to influence the differentiation of stem cells, improve its bioactivity. Also, both can be functionalized or modified to deliver drugs, growth factors, or other active compounds useful in regenerative and reconstructive dentistry and medicine [40].

The main challenges currently faced by graphene composites are dealing with their poor dispersibility in water solution, low biocompatibility, inadequate in vivo biodistribution, and fast clearance from the body. Modification with various polysaccharides, including starch, was proposed for improving their water solubility and reducing the toxicity [41].

3.2 Glasses and Glass–Ceramics and Starch

Bioglasses were developed in the 1970s as part of the second generation of biomaterials (along with calcium phosphates and many synthetic and natural biodegradable polymers) and were considered revolutionary biomaterials due to their ability to form a chemical bond at the bone interface. This reaction, called *bioactive fixation*, involves growing a carbonated apatite layer on the glass surface. The bond can reach a mechanical strength similar to bone in 3–6 months after implantation.

One of the most studied bioglasses for bone substitution and regeneration is Bioglass 45S5 which is part of the Na_2O–Ca–SiO_2–P_2O_5 system [42–45]. Some bioglasses can interact with soft tissues during the reactions which take place between the bone and the glass [46, 47].

Some bioglasses are capable to stimulate bone formation by releasing ionic dissolution products such as Si^{4+}, Ca^{2+}, or PO^{3-} in critical concentrations. These ions activate the osteoprogenitor cells thus acting like chemical stimulants. Based on this idea, it is argued that the development of carbonated apatite layer at the bone interface is not mandatory (although it is useful), as the key phenomenon in bone regeneration is the material's ability to tune cellular events that take place near the implantation site [48].

The main bioglass advantages reported so far are (i) the high rate of cellular proliferation in the presence of ionic products from bioglasses; (ii) their capacity to stimulate angiogenesis and neovascularization (which promotes bone regeneration); and (iii) the antibacterial capacity of some bioglasses, which can inhibit bacterial proliferation at implantation site by increasing the pH and Ca concentration [49, 50]. The angiogenic potential is the main reason why bioglasses and especially Bioglass 45S5 are used in scaffolds [51]. The current trend in bioglasses research is to modify 45S5 composition by adding or removing ions to obtain adequate biomaterials for clinical applications [48].

Bioglasses may be combined with biodegradable polymers [52] or ceramic materials [48] for preparing composites with medical applications. Their use with starch has gained modest interest in the preparation of medical scaffolds. The main works have been reviewed in ref. [20]. Briefly, Bioglass 45S5 was mostly studied when interacting with various starch types, including modified starches such as SEVA-C (starch with ethylene–vinyl alcohol), SPLA (starch-poly (lactic acid)) or SPLC (starch-poly (epsilon-caprolactone)). Different fabrication techniques (twin-screw extrusion, sponge method, compression molding, etc.) were used for incorporating glass particles or glass fibers into starch matrices. Formation of the carbonated apatite layers was the most studied aspect in bioglass-starch research, with good results in most studies. Also, good in vitro testing results were achieved so far [53] as well as improved mechanical properties of the composites after bioglass addition [54, 55].

3.3 Calcium Phosphates and Starch

Calcium phosphates are currently used as biomaterials due to their similarity with the mineral components of animal and human bones and teeth. The history of using synthetic calcium phosphates as biomaterials started in the 1920s [56] and evolved considerably in the 1970s [57]. Although somehow hindered by the impressive evolution of polymeric materials with medical destinations, the use of calcium phosphates is a viable solution for managing the high demands for bone regeneration products [58].

Biological apatite, sometimes named "dahlite" is the mineral component of animal bones and teeth and is the most important natural calcium phosphate. In contrast to the geological apatite, which presents a hexagonal crystalline structure, the bone apatite crystallizes in the monoclinic system. The crystalline structure includes multiple substitutions [59]: Ca^{2+} may be substituted by Sr^{2+}, Ba^{2+}, Mg^{2+}, Na^{+} si K^{+}; also, PO_4^{3-} may be substituted by CO_3^{2-} (B-type substitution) or $(OH)^{-}$ may be substituted by CO_3^{2-} (A-type substitution), F^{-}, Cl^{-} or its position may be vacant [58].

Hydroxyapatite (HA) is the most popular calcium phosphate used in bone reconstruction because it is similar to the biological apatite [60]. Hydroxyapatite can be prepared from synthetic or natural sources. Synthetic hydroxyapatite is prepared by solid-state reactions, sol–gel methods, precipitation, emulsion synthesis, hydrothermal reactions, mecano-chemical methods, hydrolysis of other calcium phosphates, or chemical vapor deposition [61]. Natural-derived hydroxyapatite can be prepared from different plants, animals, or minerals by chemical treatment of natural calcium carbonates or calcium phosphates, by thermal decomposition of bones, or by a combination of thermal and chemical methods [62]. The different raw materials and preparation methods will lead to differences in the morphology, crystallinity, and biological affinities of the resulted hydroxyapatite.

The stoichiometric hydroxyapatite has the chemical formula $Ca_5(PO_4)_3(OH)$, but this is usually written $Ca_{10}(PO_4)_6(OH)_2$ to highlight that its crystalline cell includes two entities. The molar ratio between calcium and phosphorus, Ca/P is 1.667 and it is frequently used for fast identification of HA among other calcium phosphates [8, 63–65].

This material has proven its osteoconductive properties. It is claimed that HA is also able to promote bone formation in vivo, hence it is also osteoinductive [66]. However, this claim is still under debate because osteoinductivity depends on the chemical composition, crystallinity, stoichiometry, solubility, surface chemistry, microporosity, and roughness. Since no other material is more osteoinductive than the bone autograft, biomaterial researchers try to stimulate bone osteogenesis by inducing biologically active entities (bone morphogenetic proteins, growth factors, or osteogenic cells) into the scaffolds [58].

Tricalcium phosphate (TCP) has the chemical formula $Ca_3(PO_4)_2$ and is a bioactive calcium phosphate that dissolves rapidly within the biological environment. This

allows bone tissue development after scaffold implantation. TCP has four known polymorphs, from which the most popular are α-TCO and β-TCP [8].

β-TCP is bioresorbable, bioactive, and comparable with bone apatite in terms of chemical composition and crystallinity [67]. It is usually prepared by thermal decomposition of HA and can also be prepared from natural sources such as animal bones [60]. Although its fabrication via starch consolidation was limited [68], β-TCP can be processed via starch-assisted methods alone or in combination with other calcium phosphates by following the practices described for hydroxyapatite.

Along with alumina, hydroxyapatite had received more attention as part of starch-based formulations for preparing scaffolds or developing other medical applications. Two reviews discuss extensively the use of starch with hydroxyapatite [20, 21].

Starch and hydroxyapatite were used in simple formulations or combination with other biomaterials such as gelatin, chitosan, silk fibroin, or starch blends. Various preparation strategies were tested. Hydroxyapatite-starch composites can be obtained by the crystallization of hydroxyapatite in starch gels, simple mixing, and heating, electrospinning, or precipitation. These composites had good results as potential adhesives, bone cement, bone waxes, or drug delivery systems.

The most popular starch-based method for the preparation of scaffolds consists of using the starch gel as a consolidation agent in the forming stage of a sintering program, followed by its complete removal during the firing stage. In this way, besides its role in consolidation, starch also acts as a porogen agent (leading to porous hydroxyapatite scaffolds) because it is completely degradable at high temperatures. The pores formed during firing are interconnected and correspond with the quantity and shape of the starch gel network formed in the hydroxyapatite green body. This process, although is a simple and affordable solution for producing hydroxyapatite porous structures, has also some major limitations.

The main challenge with producing porous hydroxyapatite (or other bioceramics) is preparing a well-dispersed starch suspension. The type and quantity of dispersant (usually water), the bioceramic particle size, and the type and quantity of additives are the main factors that have to be taken into account in designing a starch-bioceramic paste, slurry, or suspension. In the conventional fabrication of hydroxyapatite and starch mixtures, the main additives used were acetone, ammonium polycarbonate, and sodium polycarbonate as dispersing agents, while sodium lauryl sulfate and foam bath were used as foaming agents [21]. While these additives seem to resolve the problems associated with conventional methods, their translation to modern additive manufacturing needs further readjustment.

Another major challenge is related to the starch's ability to form a gel in a limited temperature range: 60–80 °C. At lower temperatures, the starch does not dissolve completely in water, while at higher temperatures the starch gel becomes liquid. This limitation has to be taken into account when designing fabrication technologies based on extrusion, as the high shear stress usually leads to a local increase in temperature which may degrade the starch-bioceramic paste.

Finally, it is difficult to predict if starch can solve the porosity vs. mechanical properties scaffold dilemma. The starch-based methods allow the incorporation of a large quantity of gel in the bioceramic paste with excellent consolidation. The

limitation arises in the debinding stage, when the porous structures prepared after starch removal may lose their integrity if proper ceramic particle consolidation is not achieved during sintering. While a lower quantity of starch gel may help to achieve the targeted mechanical strength, it is usually not enough for ensuring the interconnected porosity required for scaffold vascularization.

4 Conventional Methods for Bioceramic Scaffold Fabrication

In conventional manufacturing, ceramics are often manufactured by sintering after green body formation. Ceramic green bodies can be formed from *dry* ceramic powder, *a suspension* of ceramic powder, or *a paste* prepared with ceramic powder and a low quantity of solvent. Dry ceramic powders are formed by various types of pressing (dry pressing, isostatic pressing, etc.) or by ramming or stamping. The classic methods for forming ceramic suspensions include slip casting, filter pressing, dip coating, and tape casting. Ceramic pastes are formed usually by extrusion or injection molding. Regardless of the forming method, the main objective is to achieve a green body that is uniformly packed because the differences in packing density will lead to cracking during sintering.

The forming methods applied more frequently for starch and bioceramic formulations are described very briefly below, and the reader is referred to [15] for an in-depth description of each forming method.

- **Slip casting** uses a mold to shape the green body. The mold is filled with the ceramic suspension and the ceramic is dewatered by different means. In the process called drain casting, a highly diluted suspension is poured and a part of the water is absorbed by the porous mold while the rest is removed by drying. Solid casting uses thicker suspensions which are poured into the mold and left there until they are dewatered.
- **Tape casting** is used for forming thin sheets of ceramic suspension. After drying, the sheets can be processed into a desired shape and sintered for producing the ceramic object.
- **Extrusion and injection molding** are intensively used in polymer processing. In extrusion, the ceramic paste is pushed through a die. The high shear stress imposed upon the ceramic paste can increase the temperature high enough to soften or even melt the polymeric binder. Injection molding works similarly, with the extrudate flowing into a mold until complete filling.

The use of ceramic blocks in bone reconstruction is based on ensuring a porosity which will fulfill the requirements for bone cell adhesion, proliferation, and vascularization at the implantation site. Preparation of porous ceramics is possible by direct methods, although more versatile methods, which allow the control of porosity, pores size, and their interconnection can be used for producing bioceramics:

- **Direct sintering methods** involve partial sintering of pressed powders or sintering of powdered mixtures which will lead to pore formation through various solid-state reactions. These methods provide a low porosity with pores distributed irregularly within the ceramic structure.
- **Polymeric sponge methods** use a highly porous polymeric structure for inducing pores in the ceramic material. The polymeric sponge is impregnated with the ceramic suspension and removed by pyrolysis. The method ensures a high pore interconnection. The successful application of this method depends on the rheologic properties of the ceramic suspension and its adhesion to the polymeric sponge.
- **Sacrificial porogen methods** lead to the formation of open pores with different morphologies. The primary step is porogen removal by pyrolysis, evaporation, or sublimation. Slow removal of the porogen may lead to fewer cracks in the ceramic structure. The materials prepared by this method have a superior mechanical resistance compared to the polymeric sponge method, but the pore interconnectivity can be low when low quantities/ small particles of porogen are used.
- **Foaming methods** produce pores within the product by directly incorporating air bubbles into the ceramic suspension, thus removing the pyrolysis step from the sintering program. The stabilization and solidification of the ceramic suspension are imperative for good application of this method (surfactants are usually used in the suspension). The porous ceramics prepared by foaming methods have also had better mechanical resistance than the ones prepared by polymeric replica techniques [69].

5 Additive Manufacturing for Bioceramic Scaffold Fabrication

Additive manufacturing, initially popularized as *tridimensional printing* is currently a hot topic in engineering. The intense technological advancements led to the development of multiple printing methods, researchers adopted them quickly for their tasks, and international committees such as ASTM and ISO still make efforts to standardize this field so product manufacturers could deliver performant and safe printed products to their users as soon as possible. Additive manufacturing is discussed in great detail in multiple literature reviews which became a source of inspiration for the research community. Various topics such as general engineering [18], general biomaterials [16], ceramics [70], and bioceramics (alumina, zirconia, and hydroxyapatite) [17, 71] are linked with additive manufacturing in an attempt to solve the challenges associated with the materials, equipment, and application of these methods.

Additive manufacturing is the term used by the standardization committees to define the methods which use computer-generated models for constructing detailed components with complex geometries from small units (usually layers) which increase gradually into a printed product. Additive manufacturing, which was also

named *additive layer manufacturing, layer(ed) manufacturing, (solid) freeform fabrication, rapid tooling, direct writing,* or *biofabrication* is now the general term used to describe a large number of printing methods [19, 72–77].

There are three main stages in additive manufacturing:

- **the computer-aided design,** in which a tridimensional model is conceived by classic design or reverse engineering (such as scanning another object),
- **the production stage,** in which a 3D printer builds material layers until the design is brought to form
- **the post-production stage,** which involves additional processing or surface finishing as well as the removal of excess material from the printed part.

When dealing with additive manufacturing of medical applications such as bone scaffolds, the design stage could use raw anatomical data from medical imaging techniques such as computed tomography (CT) or magnetic resonance imaging (MRI) to draw a personalized medical solution based on the patient needs. In this way, it could be possible to identify the exact shape of a bone defect using the imaging techniques and then to model a bone substitution product with the shape that the patient needs, like a missing puzzle piece. The CAD design could be transferred to a printer, which could build the scaffold, which could be implanted at the site of the bone defect. This seems a simple and efficient solution, but multiple challenges still need to be addressed to make personalized medicine a reality for the patients.

An important observation was discussed recently in a review dedicated to the additive manufacturing of hydroxyapatite-based materials, one of the most popular bioceramics proposed for bone substitution [71]. This discussion points out the fact that 3D printing produces stable architectures while the natural systems in which those products will be used are dynamic and complex. As a response to the challenges associated with natural organisms, 4D printing (in which the fourth dimension is time) is introduced as a potential solution to provide biomaterials that are more compatible with dynamic tissues subjected to regeneration [78]. A five-axis printing technology (5D printing) is also expected to print complex products with curved surfaces in multiple dimensions; its potential application has been discussed for orthopedics [79].

Until the full development of 4D and 5D printing, several additive manufacturing solutions were proposed for printing bioceramic scaffolds. The main challenge that needs to be addressed by these methods is the high-temperature melting point of bioceramics, which are generally difficult to process. Ceramic materials have complex phase diagrams which show that new phase formation or unexpected properties change (including biocompatibility) are possible after melting if this point can be achieved during manufacturing. Moreover, high-temperature processing of bioceramics could lead to pores and cracks. If the materials are intended for bone replacement, the pores must be interconnected to promote cellular proliferation, and implant fixation and crack formation need to be prevented [80, 81].

Some of the printing solutions include laser-based methods such as selective laser sintering, selective laser melting, or laser cladding. These methods use a laser beam which scans a powder ceramic bed and induces the local sintering of the particles.

Currently, the attempts to use laser-based methods for producing bioceramic scaffold include direct laser processing of hydroxyapatite, tricalcium phosphate, glasses, and oxides (with modest results), as well as laser processing of combinations between bioceramics and different polymeric materials such as polycaprolactone (PCL), or poly(D,L-lactic acid) (PDLLA) for producing scaffolds [16].

The second approach in additive manufacturing relates to ink-based methods. Based on findings from other industries [82–84], these methods could be suitable for bioceramic-starch formulations but there are still many challenges to be solved. A popular method for ink-based printing of bioceramic scaffolds is the robocasting method, also known as direct ink writing, which uses material extrusion to build tridimensional parts which should be able to self-sustain their shape after printing. This technique was patented in 2000 [85]. Robocasting is based on computer-controlled extrusion of a suspension with high ceramic particle loading. The suspension, usually called ink, is extruded by a small nozzle which creates material filaments that are deposited layer by layer. After material deposition, the ceramic printed part shall be densified by sintering.

The robocasting ink should have proper rheological behavior and be able to transform from a pseudoplastic material into a dilatable one when is extruded in air. Usually, the ceramic inks incorporate ~ 40%vol. of ceramic particles and less than 3% vol. dispersing agents. This is a major advantage of robocasting compared with other additive manufacturing methods that use high quantities of binders, which may lead to cracking of the structures due to excessive shrinkage during densification by sintering [80].

The ceramic particles and the binder (usually water or polymers) are the main ingredients of a bioceramic ink. Various additives such as surfactants or functionalization agents are usually included in the formulation. Some examples of bioceramic ink formulations used with extrusion-based techniques such as Robocasting are presented in Table 2.

Until now, there were very few attempts to develop suitable robocasting inks using bioceramics with starch [86, 87], ink design should take into consideration several factors which are related to [80, 86]:

- **solid fraction (bioceramic powder)**– the particle quantity, size, and morphology are some of the most important ceramic-related parameters when designing robocasting inks. Highly refined powders with large particle size distribution allow the formulation of higher ceramic loading of inks. Wider particle size distribution could also improve the mechanical properties of the printed parts after sintering. The particle morphology could influence the rheological properties of the ink, as inks with irregular particle morphologies are more susceptible to shear flow than the ones prepared from spherical particles. Nonetheless, the solid content is crucial for producing performant robocasted products—40–50%vol is the recommended proportion of solid particles in a robocasting ink (min. 30%.vol) for good dimensional and geometric predictability after sintering.
- **rheological properties**—the main challenge is related to the stabilization of colloidal suspension, which is achieved by electrostatic or steric stabilization

Table 2 Robocasting ink formulations tested as bioceramic scaffolds

Bioceramic	Solvent	Dispersant	Binder	Jellifying agent/Coagulant	References
Yttria-stabilised tetragonal zirconia	UV resins	–	–	–	[88]
Alumina	Deionized water	Pluronic F-127	Bermocoll	PEI	[89]
Alumina + magnesium oxide	Deionized water	Dolapix CA	–	Alginic acid	[90]
Bioactive glass 45S5	Water	–	CMC	–	[91]
Silicate glass (in- house)	Ice bath	Pluronic F-127	–	–	[92]
BCP	Water	PAA	HCPM	PEI	[93]
β-TCP + $CaCO_3$	Water	Darvan C	HCPM	PEI	[94]
HA + β-TCP	Water	Pluronic F-127	–	Food grade corn syrup	[95]
HA	Water	PAA + NaOH	HCPM	PEI	[96]
HA	Water + PVA	Darvan C	HCPM	PEI	[94]
Si-HA	Distilled water	Darvan C	HCPM	PEI	[97]
Si-HA	Distilled water	–	–	Gelatin	[98]

Where: **HA** = Hydroxyapatite; **BCP** = Biphasic calcium phosphate; **β-TCP** = Beta-tricalcium phosphate; **$CaCO_3$** = calcium carbonate; **Si-HA** = Silicon-doped HA; **UV** = Ultraviolet; **PVA** = Polyvinyl alcohol; **PAA** = Polyacrylic acid; **NaOH** = Sodium hydroxide; **Darvan C** = Ammonium polymethacrylate; **Pluronic F-127** = Polyol-type surfactant; **Bermocoll** = Ethylhydroxyethylcellulose; **Dolapix CA** = polyelectrolite basic anionic dispersant; **HCPM** = 2-hydroxy-3-cardanylpropyl methacrylate; **CMC** = Carboxymethyl cellulose; **PEI** = Polyethylenimine.

(or a combination of both). Some additives, such as charge binders are added in the stabilized suspension to control the flocculation. Although starch suspensions were not used in robocasting yet, there is available data regarding its rheological behavior for conventional manufacturing [99–101]. Also, since starch is capable to undergo reversible hydration, it could promote seamless hydrogel ejection in additive manufacturing methods based on extrusion (such as robocasting). For these applications, the viscoelastic properties of starch rely on five main variables: concentration, extrusion temperature, yield stress (τy), storage modulus (G'), and flow stress (τf). The first three characterize the extrudability of the ink, and the last two characterize the hydrogel's potential to withstand its weight when printed in successive layers. Shortly, an adequate starch ink for heat extrusion additive manufacturing should exhibit a moderate to high G' and τy in combination with a low τf. However, these ideal printing parameters are currently discussed mainly

for food-related printing applications, so printing specifications should firstly be translated for the fabrication of bone scaffolds [23].

- **robocasting processing parameters**—the specific robocasting equipment parameters that need to be taken into account are the extrusion temperature (very important for starch, which forms gels in a limited temperature range), feed speed, extruding pressure, and moving speed. Also, drying, debinding and sintering parameters such as heating rate, heating temperature, heating environment, and soaking time are essential for post-processing and densification of robocasted parts.

6 Bone Scaffold Prototype with Hydroxyapatite and Starch

6.1 Technology Description

The scientific literature offers a wide range of solutions for producing hydroxyapatite from various raw materials. It also describes countless methods of obtaining scaffolds with or without polymers or metals. However, the current paradigm of innovation-driven research shows little interest in combining the available knowledge and expertise to achieve actual physical products which could be translated to clinical practice. Starting from this idea, we developed a scaffold fabrication technology using hydroxyapatite and starch. This technology was built on previous fundamental research by implementing the best practices in ceramic preparation and processing.

The technology described here uses hydroxyapatite prepared from bovine bones and starch gels for producing bone scaffold prototypes. Its main steps are represented in Figs. 1, 2 and 3. All steps of this technology use simple and affordable equipment and are familiar to ceramic practitioners. During 2014–2020, each step of the technology was studied individually and the results were documented in dedicated works, which are referenced in the text.

The fabrication of bone scaffold prototypes using starch involves:

(a) preparation of medical-grade hydroxyapatite from bovine bones using three-step thermal processing: boiling, heat treatment for organics removal, and heat treatment for ceramic recrystallization [62, 102–108]. These procedures are applied by following legal and standard requirements regarding medical devices manufactured using tissues of animal origin to provide TSE-free biomaterials (such as Commission Regulation no. 722/2012 and ISO 22442 standard series) [109, 110].

(b) preparation of ceramic powders by comminution of the ceramic blocks prepared from bovine bones, using grinding with agate mortar and pestle and/or milling in agate ball mills, followed by granulometric sorting by vibratory sieving [111, 112];

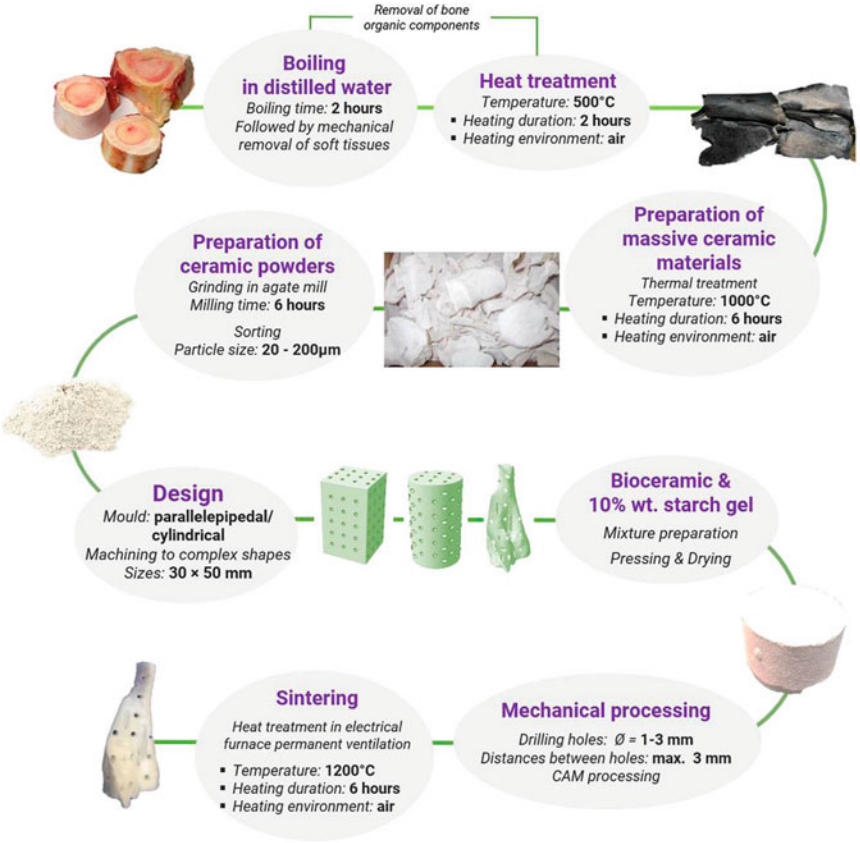

Fig. 3 Fabrication of bone scaffold prototypes using bovine-derived hydroxyapatite and starch gels

(c) mixing of hydroxyapatite powders with starch gels: this step was inspired by the starch consolidation method, in which the gel-forming ability of heated aqueous starch solutions is used for improving the mechanical characteristics of various bioceramics. The starch gel is used for preparing consolidated green bodies which can be easily processed to the desired shape. The optimal quantity of starch was established considering the need for processability, the required mechanical resistance, and the pore-forming ability. After mechanical processing and drying, the green body was sintered and starch acted as a pore-forming agent [86].

Briefly, after producing and evaluating the hydroxyapatite powders, the technology aimed to produce scaffold prototypes from hydroxyapatite-starch composites which are easy to process by conventional machining and advanced printing techniques. Lastly, a sintering step was included in the fabrication process to achieve suitable mechanical characteristics.

6.2 Raw Ceramic Preparation

Bovine bone is one of the most popular natural sources for producing calcium phosphates because it is similar to the human bone and it is available in large quantities as a by-product from other industries, especially the food industry—more than 68 million tons of cattle meat (beef and buffalo) are produced worldwide, in a single year, for human consumption [113].

Currently, a search for "bovine bone" in Web of Science generates approximately 800 results directly related to the production of calcium phosphates. The preparation of ceramic materials from bovine bone is based on the bone composition, which is a composite material consisting of an organic and a ceramic phase. Calcium phosphates are obtained by isolating the natural bone apatite from the organic phase (more than 90% collagen). This can be achieved, broadly, by chemical or thermal treatments. The chemical treatment of various types of bones is, historically, the first method employed for apatite isolation. The chemical treatment aims to react with the organic phase of the bone and to separate it from the bone apatite by generating byproducts which could be easily eliminated. A history of using bones for producing medical-grade materials [114] presents how initially, these materials were prepared by immersing animal bones in liquids such as chloroform, methanol, or hydrogen peroxide [115]. These procedures had to be constantly improved, especially during 1980–1990, when researchers and practitioners had to overcome various challenges, such as negative reviews of approved bone-derived products [116] or the transmissible spongiform encephalopathy (TSE) outbreak which imposed more stringent biosecurity requirements.

As a safer and more efficient alternative, the second approach—the thermal treatment, aims to completely degrade the organic phase of the bone by combustion. It can be employed with or without chemical treatment, as it is proved that it can provide biologically safe materials. Thermal treatment allows the preparation of various types of calcium phosphates. Mainly, hydroxyapatite (HA) and beta-tricalcium phosphate (β-TCP) can be obtained by this method. Alpha-tricalcium phosphate (α-TCP) could potentially be prepared by further thermal treatment of beta-tricalcium phosphate, although this was not achieved at temperatures below 1200 °C and there is insufficient data regarding the bone behavior at higher temperatures.

Preparation of biphasic calcium phosphates (BCP), with various proportions of HA and β-TCP, is a more recent strategy adopted by the researchers who use thermal treatment of bones in their work. The fine-tuning of the ratio between HA (bioactive) and β-TCP (resorbable) is one of the key-solutions for achieving performant biomaterials for bone scaffolds and one of the great challenges with which the scientific community is currently confronted. This fine-tuning depends strongly on some characteristics of the raw materials, such as the substitutions from the crystalline lattice of the biological apatite, the elemental species included in the structure and the interaction between these during thermal treatment. Despite this variability, a carefully managed thermal treatment program could lead to reproducible results in terms of materials morphology, structure, and properties.

The main aspects that need to be managed are the thermal treatment temperature, environment, heating rate, soaking time, and cooling conditions. Some of these parameters, such as the heating rate and soaking time, are at least partially established. Many of the thermal treatments performed on bovine bones are performed for at least 2 h, at heating rates of 10 °C/min or 5 °C/min [117, 118].

The thermal treatment temperature is, clearly, one of the critical parameters of the thermal treatment because it influences most of the bone characteristics. Heating of bones leads to water evaporation, organic combustion, apatite recrystallization, and partial degradation of the apatite into other products. While water evaporation is usually complete at approx. 120 °C, organic degradation is achieved at 500–600 °C. During these stages, the organic phase of the bone acts as a thermal shield for the poorly crystallized apatite [119]. As a consequence, bone apatite usually starts its transformation if the bone is heated above 600 °C. This transformation, called diffusion, has three stages, identified as lattice diffusion (500–750 °C), surface diffusion (750–900 °C), and grain boundary diffusion (900–1000 °C) [120]. After this stage, the bone apatite is transformed into nonstoichiometric hydroxyapatite which can partially degrade into β-TCP, calcium oxide (CaO) [117], or tetracalcium phosphate TTCP [121].

The heating environment is the parameter that governs the degradation of bone-derived hydroxyapatite into other materials when subjected to high-temperature treatments. Some environments, such as air or CO_2, ensure the thermal stability of hydroxyapatite up to 1200 °C [122], while more inert atmospheres such as argon lead to HA degradation into β-TCP at ~1200 °C. Also, the cooling conditions could influence further degradation of β-TCP. Given that β-TCP → α-TCP is reversible at slow cooling, the choice of a rapid cooling method such as quenching could preserve α-TCP into the final material [123].

The ceramic material presented in this chapter was prepared from the central component of bovine femurs (without joints). Since the bones were purchased from local slaughterhouses (Bucharest, Romania), they are safe starting materials and considered appropriate regarding their potential contamination with TSE infectious agents, per CE (EU) No 722/2012 [109].

Bones were cut and stored frozen until thermal processing. Distilled water was used in the preparation. All processing was realized by exclusively thermal routes following European legislation, to eliminate the risks of biological contamination. First, the cleaned bovine bones were heat-treated for producing raw ceramic blocks by removing the native organic components of the bone. The bones were boiled in water twice (for 2 h each round) and then were heat-treated in an electrical furnace at 500 °C, for 2 h, in an air atmosphere with constant ventilation. Next, an exclusively thermal route was applied to remove or inactivate TSE infectious agents—namely, it is necessary to perform heat treatments at above 850 °C to ensure safe TSE removal. The raw ceramic pieces were heat-treated at 1000 °C, for 6 h, with a 10 °C/min heating rate, in air atmosphere. This treatment was performed for transforming the poorly-crystalized apatite from the raw ceramic pieces into a more crystallized (non-stoichiometric) hydroxyapatite [102–104, 107, 108, 124, 125].

6.3 Powder Preparation and Processing

Regardless of the chosen fabrication method, ceramic scaffolds are usually produced from powders. The main parameters which will influence the characteristics of final ceramic products are related to powders quality and their interaction with other additives used in fabrication [126]. The particle size has proven influences upon the physical and biological properties of the ceramic products [127–130] and upon the efficiency of some fabrication procedures, notably additive manufacturing [131–133]. Additive manufacturing has more stringent requirements for particle size, with adequate dimensions between 15–35 μm, given that a printed layer will usually have 30–150 μm [134]. Particle shape also influences the biological properties [127], as well as the porosity and mechanical properties of sintered scaffolds [135–137].

To produce the ceramic powders, raw hydroxyapatite blocks produced from bovine bone were ground in an agate ball mill, for 6 h, at 450 rot/min. After grinding, the powders were sorted with a granulometric vibration sorting device using woven with 20–200 μm wire mesh sieves (Impact Test Equipment Ltd.). This grinding method yield 40% particles with 40–100 μm and equal parts (27%) of particles sized 100–200 μm and 20–40 μm. Only a small quantity (5–6%) of particles sized <20 μm was obtained, with further reduction possible by repeated grinding or complementary reduction methods. The estimation of particle size distribution was performed by weighing a total amount of 9500 g sorted powders.

Two types of powders were used in the experiments: a) sorted powder with 100–200 μm particle size and b) mixed powder prepared from equal parts of powders with <20 μm, 20–40 μm, 40–100 μm, and 100–200 μm particle size (Fig. 4). For ensuring a homogenous particle size distribution, the mixed powders were blended for 15 min using a tumbler mixer (Bioengineering Inversina, 2L).

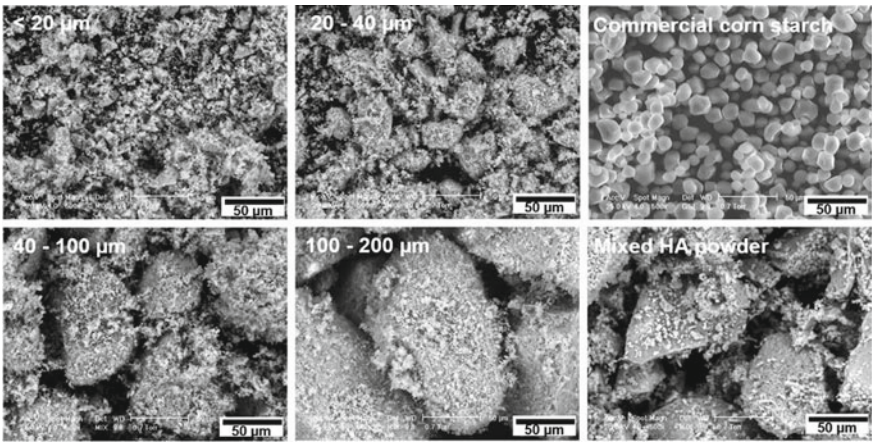

Fig. 4 Raw powders morphology—sorted HA with different particle sizes. The powders with 100–200 μm particles were used for preparing the first set of prototypes. An equal mix of all types of sorted powders (mixed HA powder) was used for preparing the second set of prototypes

Figure 4 presents the morphology of the sorted powders. The powders sized less than 40 μm consist of polyhedral particles with irregular shapes, sharp edges, and rough surfaces. The larger particles have rounder edges and smoother particles. Some agglomerations of small ceramic particles were observed on the surfaces of the larger ones. The particles are porous, with pores formed due to bone organics removal. All granulometric sorts are visible in the mixed powder. The commercial corn starch powder used in the experiments consists of spherical particles sized 10–20 μm in diameter, with smooth surfaces, without pores of defects.

6.4 Scaffold Design

Scaffold design is a stage in which the medical product is sketched considering its target use. A bone scaffold prototype should aim to provide a performant alternative to current bone grafts, by being successfully usable in clinical practice. Most of the current design strategies aim to mimic the bone microenvironment by ensuring a vascularized porous structure while reaching for the target mechanical properties able to ensure the stability required during scaffold degradation and bone regeneration. Many times, inspiration is found in nature, so many works are dedicated to describing natural architectures which can act as templates for tissue engineering and regenerative medicine [138, 139].

The basic design requirements include (i) selection of a biomaterial with a degradation rate compatible with bone healing rate which also provides adequate mechanical support; (ii) development of product concepts which fulfill the porosity requirements for bone inflow and ingrowth; and (iii) development of fabrication technologies which bring the product concepts to clinical reality [10, 140, 141].

Detailed design requirements include targets for:

- **Biocompatibility**—non-toxic material as defined by dedicated standards such as ISO 10993 series [142];
- **Biodegradability**—degradation rate adapted to local bone regeneration rate [143];
- **Surface chemistry and surface patterning**—adequate for cells attachment, proliferation, and differentiation [144];
- **Porosity and related characteristics**—bioceramic scaffolds are used as-prepared as osteoconductive platforms that nurture and sustain the bone regeneration or are loaded with medication (as drug delivery agents) or osteoinductive agents (cells, proteins, or growth factors) [145]. The main targets for scaffold porosity are inspired by the bone porosity, which is 5–3% for cortical bone and 30–90% for cancellous bone[146] These applications require pore diameters of 100–200 μm for hosting bone cells, 75–100 μm for the development of nonmineralized osteoid tissue and 10–75 μm for ingrowth of the fibrous tissue responsible for vascularization and mechanical support [145, 147, 148]. Pore interconnection (also called mesoporosity) is mandatory for all types of bioceramic scaffolds, because,

depending on the application, it allows the ingrowth of blood vessels and bone cells or the uniform distribution of drugs within the drug delivery device [149].

- **Mechanical properties**—ideally, a bioceramic scaffold should have the mechanical characteristics of the substituted tissue. Currently, achieving these targets while fulfilling the porosity requirements is the most important challenge associated with the fabrication of bone scaffolds. Compressive strength is usually the first mechanical characteristic evaluated for a scaffold—its target value is 130 -180 MPa for the cortical bone and 4–12 MPa for the cancellous bone [3]. Other characteristics, such as bending strength, tensile strength, or elastic modulus may be evaluated based on the specific destination of the scaffold.

This technology was developed for calcium phosphate powders prepared from bovine bone or other natural sources [125, 150–152]. The product concept was built around the ability of bone-derived hydroxyapatite to safely interact with a starch gel used as a binder for consolidating green bodies and as a pore former in a conventional sintering routine. Considering that bone-derived ceramics preserve an intrinsic microporosity resulted from organics thermal degradation, the design strategy aimed to ensure an adequate macroporosity by using different granulometric sorts of ceramic powder and by drilling macro channels which shall ensure an adequate distribution of macropores within the product. The macro channels were designed for scaffold irrigation with body fluids, which offers a surgical advantage by eliminating the risk of tissue necrosis after implantation.

The ceramic products were designed in multiple versions. Figure 5 represents a technical drawing of one of these versions. It is a parallelepipedal scaffold with a square base with a side $l = 30$ mm and height $h = 50$ mm. The macro channels distribution was designed so each channel has a diameter of $Ø = 2$ mm and the distance between any two adjacent channels is $d = 3$ mm. To achieve this design, 51 channels were designed within the product.

6.5 Forming, Processing, and Sintering

The aqueous starch solution was prepared by mixing starch with water in 1:4 proportion at approx. 70 °C. For prototype fabrication, the ceramic powder (sorted or mixed) was poured in the aqueous solution of starch (which contained 10%wt. starch relative to hydroxyapatite powder). Starch was used as an additive due to its capacity of forming a gel when its aqueous solution is heated at approx. 70 °C.

Initially, hydroxyapatite was mixed with different gels, corresponding to various starch concentrations (0–50 wt.% relative to the hydroxyapatite). A complete structural and mechanical characterization of these materials was already published—briefly, regardless of starch concentration, materials jellification occurred without significant structural changes and mechanical processing was possible in the green body stage [86].

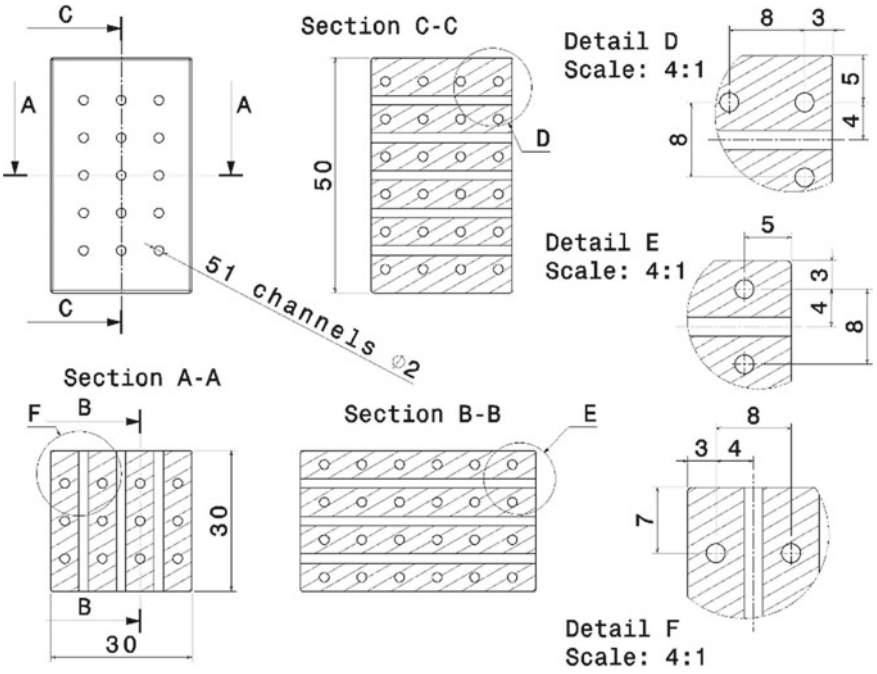

Fig. 5 Technical drawing for a parallelepipedal scaffold prototype

Starch gel influence upon the visual appearance of the green bodies can be observed from Fig. 6a. The addition of starch gel in the hydroxyapatite powder led to an easier shaping of the samples. Higher concentrations of starch (10–50%wt.) allowed the shaping of green parts with smoother surfaces and with accurate preservation of the edges. Next to samples photographs, Fig. 6a presents the morphology of the green samples, as depicted by SEM.

A blank sample without starch is presented for reference. The blank morphology consists of ceramic particles sized 100–200 μm (the granulometric sort selected for display). The particles have the typical polyhedral shape with rough edges and are well packed within the green body. As starch concentration increases, the starch gel network formed surrounding the ceramic particles becomes more visible. In the samples with 25–50% wt. starch, the ceramic particles are nearly suspended in a dense network of starch gel, in which the starch particles are still differentiated.

After sintering, the starch particles from the green bodies were completely degraded and the areas in which starch was located were transformed into pores. The visual aspect and the morphology of the samples, as depicted by SEM, are presented in Fig. 6b. From the photographs, it can be observed that the addition of larger quantities of starch into the green bodies affected the samples' integrity after sintering. The strongest influence was observed for the samples prepared with 50%wt. starch which

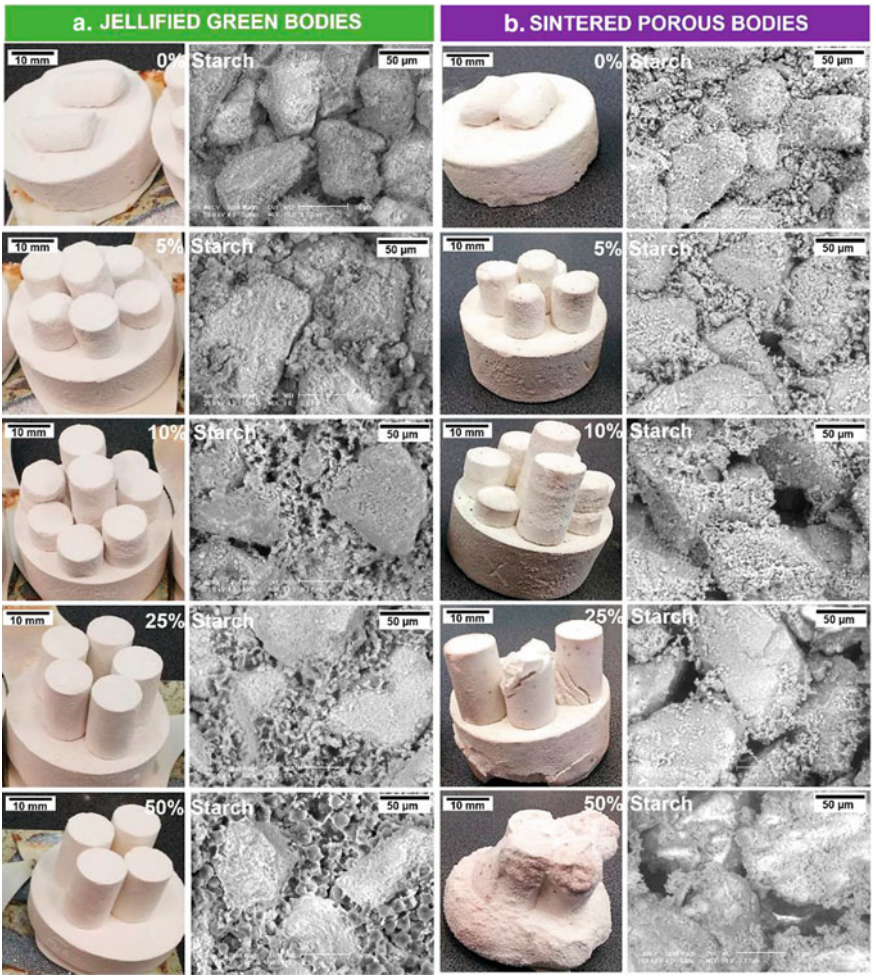

Fig. 6 Hydroxyapatite-starch samples with different starch concentrations: 0, 5, 10, 25, 50wt. %. Visual aspect and morphology of **a** Jellified composites; **b** Sintered bodies

did not preserve their shapes after sintering. Moreover, after storing these samples in normal conditions of temperature and humidity they completely lost their shape.

The firing also induced morphological modifications which can be observed in the SEM results displayed in Fig. 6b. The sintered blank sample morphology evolved as some of the ceramic particles were divided into smaller ones during sintering, thus ensuring a better packing of the material and better densification. Few irregular pores are visible in random locations of the microstructure. As the initial starch concentration increases, larger pores are observed within the materials. Also, starch presence prevented ceramic particle division during sintering, as the size and shape of these particles are similar to the ones in the corresponding green body morphology.

On the large particles of the samples prepared with 10–50%wt. starch, some small particles were observed. These particles almost spread on the larger particles surface as they were subjected to significant diffusion during sintering. These observations argue for the double role of starch as pore former agent: pores were formed mainly due to the complete removal of the starch gel by thermal degradation and also, the starch gel prevented the ceramic particle crushing and division thus maintaining the porosity created by the use of a narrow particle size range (100–200 μm).

Based on the initial evaluation of morphology and mechanical properties of hydroxyapatite composites with 0–50% starch gel, the 10%wt. concentration of starch gel was chosen for preparing the scaffold prototypes. This concentration was preferred because while it allowed easy processing of the material to be shaped in the desired form, it also preserved better mechanical properties after sintering for starch burnout and densification of the green part [86, 153].

In this stage of production, a subtractive manufacturing approach was applied for the preparation of hydroxyapatite scaffolds with a porous structure—the scaffold prototypes were macrochanneled by drilling, while the microporosity was preserved from the bovine bone microstructure (due to organics removal), by use of powders with different particles size which ensured a preferential packing within the green bodies, and by use of starch as pore-forming agent. The scaffold can be further modified for better cell ingrowth and bone regeneration through various surface treatments.

The proposed method is an alternative to the common additive manufacturing methods which are commonly used for producing hydroxyapatite scaffolds [71]. The reason for choosing a conventional approach for producing the prototypes is related to the infrastructure usually available in a clinical laboratory (given that most of the specialized ceramic laboratories which need to work with bone scaffolds are not yet provided with 3D printers adequate for producing hydroxyapatite scaffolds). Until additive manufacturing procedures are suitably implemented in laboratories, the conventional approaches are still time- and cost-effective for producing and processing bioceramic scaffolds [154].

In this conventional processing sequence, the hydroxyapatite-starch paste was molded and pressed at 25 MPa in cylindrical shapes with Ø50 × 50 mm (Fig. 7a). The cylindrical samples were dried in the air, at room temperature, for 120 h. After forming, the cylindrical shapes were cut into square shapes (30 × 20 × 10 mm—Fig. 7b) and machined with a ø = 1–2 mm drill, keeping a d = 2–3 mm between every 2 channels (Fig. 7c, d). The green samples were sintered in an electrical furnace, at 1200 °C, for 6 h.

6.6 Prototype Morphology

The images from Fig. 8a, b are photographs of the parallelepipedal scaffold prototypes. The ceramic body presented in Fig. 8a has 30 × 30 × 10 mm and the

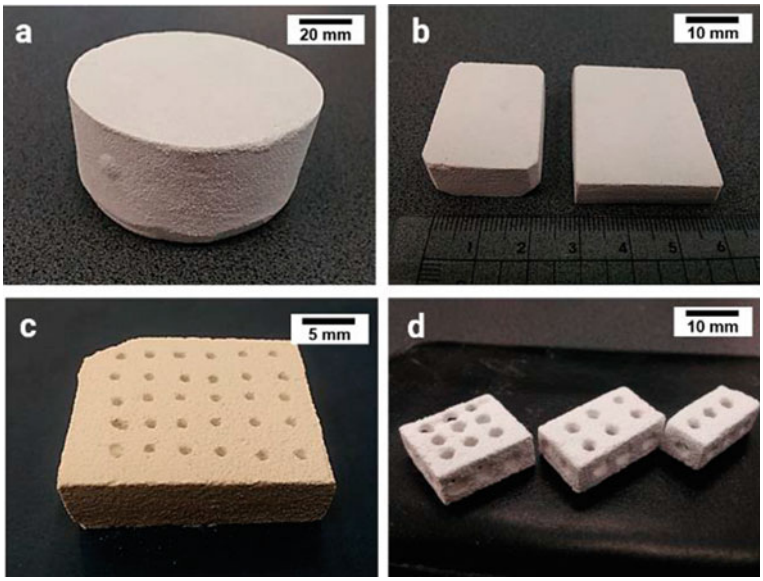

Fig. 7 **a** Cylindrical sample obtained after molding, pressing, and drying; **b** green samples cut from the cylindrical sample; **c**, **d** scaffold prototypes, different dimensions

one presented in Fig. 8b has 20 × 20 × 10 mm. Periodic straight macro channels were formed by drilling, creating 3d-directionally connected macro channels in the ceramic body. The channels from the first ceramic body are smaller (ø = 1 mm) and were drilled at larger distances (distance between two channels d = 3 mm) than the ones drilled in the second ceramic body (ø = 2 mm; distance d = 2 mm).

The SEM results presented in Fig. 8c–f confirm the channel dimensions and the distances between them. Excellent surface finish can be observed near the channels, along with typical morphology for sintered ceramic bodies, with closely consolidated particles and enlarged grains that were subjected to diffusion. The shape, dimension, and particle distribution are best observed in Fig. 8g, h.

At a scale corresponding to the grain size, the similarities between the microstructures of the two prototypes validate the reproducibility of the morphology of the products in different manufacturing conditions (the prototypes differentiate themselves by the particle size of the ceramic powders used in sintering and by the drilled macropores size and distribution with the product). The ratio between the calcium and phosphorus concentration (Ca/P ratio, a popular indicator used for differentiating the various calcium phosphates [155]) was estimated using EDS results. The Ca/P ratio is 1.93 for the first prototype and 1.68 for the second one. These ratios match the Ca/P ratios calculated in the early stages of production (an extensive compositional characterization and Ca/P ratio was performed on the ceramic powders [112]).

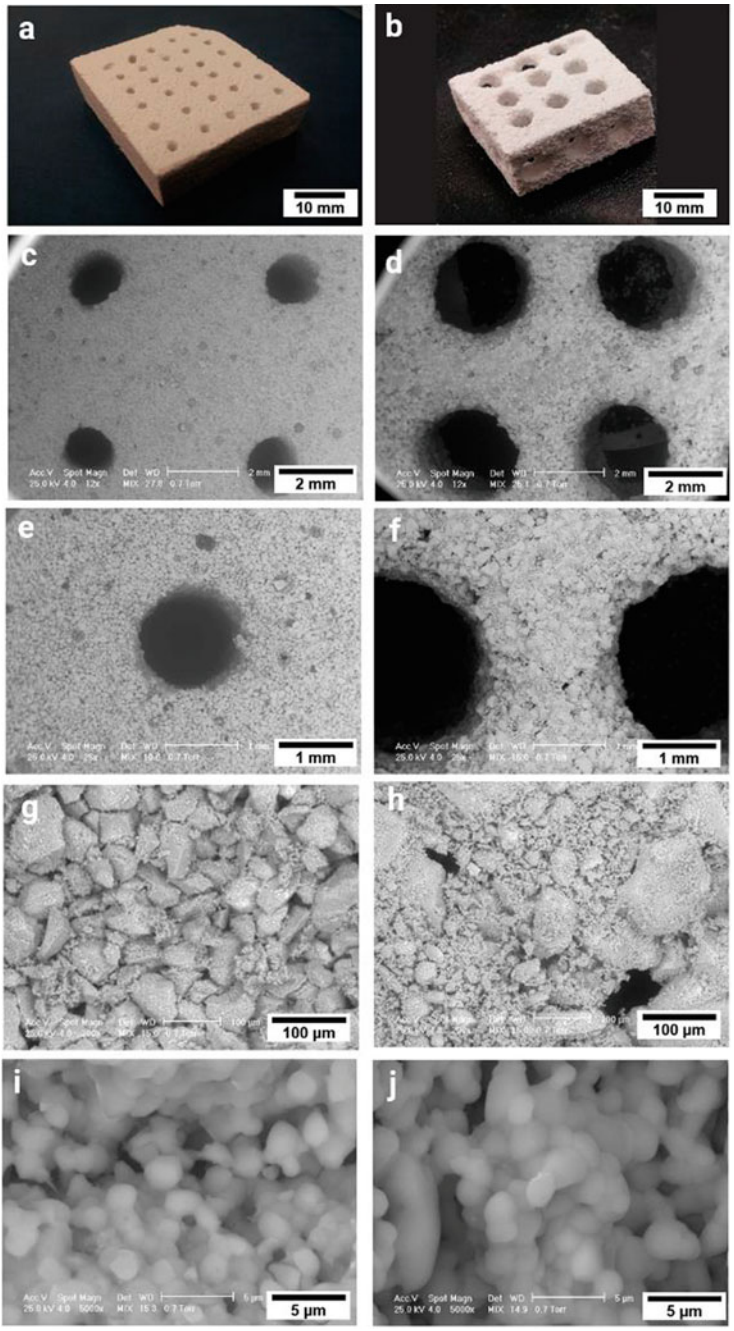

Fig. 8 **a**, **b** Ceramic prototypes fabricated by applying the proposed technology; **c**–**j** morphological aspects of the ceramic products, revealed by SEM

7 Conclusions

Different formulations with bioceramics and biopolymers are used for preparing scaffolds for bone replacement in an attempt to mimic the natural organization of the bone tissue, which is a composite between a ceramic and a polymer. Among the natural polymers, starch was used with all bioceramic categories (ceramic oxides, calcium phosphates, and bioglasses) for preparing bone cement, bone waxes, bone spacers, or bone scaffolds.

Starch was used with bioceramics mainly as a binder and as a pore-forming agent. Its gelling abilities were exploited in a popular fabrication method called starch consolidation. Further technological advancements placed additive manufacturing of bioceramics between researchers' priorities. But although starch was tested for tridimensional printing in the food industry, its gelling abilities were used scarcely for printing bioceramics. So, one current research question emerges: is it convenient to use starch in additive manufacturing of bioceramics?

There are some advantages: starch is a safe natural material, widely available at an affordable price, forms gels in aqueous solutions, and forms pores in bioceramics by complete degradation during high-temperature heat treatments without releasing toxic products or affecting the bioceramic structures. However, there are still some limitations which we need to consider: there is a limited range of additive manufacturing methods that can be used with starch (extrusion-based methods seem to be the most promising) and it is difficult to control the paste temperature during fabrication (because it is necessary to maintain a 60–80 °C paste temperature). Moreover, a relatively large quantity of starch gel is required for producing an optimal porosity for bone scaffolds, but this seems to compromise the mechanical strength of the final products.

Until further refinements of additive manufacturing of bioceramics with starch, conventional methods for scaffold fabrication are a practical alternative, able to provide porous bioceramic structures with tunable properties using affordable materials and equipment. There is a vast amount of literature available on this topic, and all this long acquired knowledge and skillfulness need to be refined and applied for the benefit of ceramic practitioners, physicians, and patients.

References

1. O'Brien FJ (2011) Biomaterials & scaffolds for tissue engineering. Mater Today 14(3):88–95. https://doi.org/10.1016/S1369-7021(11)70058-X
2. Weiner S, Wagner HD (1998) The material bone: structure-mechanical function relations. Annu Rev Mater Sci 28(1):271–298. https://doi.org/10.1146/annurev.matsci.28.1.271
3. Rho J-Y, Kuhn-Spearing L, Zioupos P (1998) Mechanical properties and the hierarchical structure of bone. Med Eng Phys 20(2):92–102. https://doi.org/10.1016/S1350-4533(98)00007-1

4. Damien CJ, Parsons JR (1991) Bone graft and bone graft substitutes: a review of current technology and applications. J Appl Biomater 2(3):187–208. https://doi.org/10.1002/jab.770020307
5. Wang W, Yeung KW (2017) Bone grafts and biomaterials substitutes for bone defect repair: a review. Bioactive Mater 2(4):224–247. https://doi.org/10.1016/j.bioactmat.2017.05.007
6. Dorozhkin SV (2011) Biocomposites and hybrid biomaterials based on calcium orthophosphates. Biomatter 1(1):3–56. https://doi.org/10.4161/biom.1.1.16782
7. Dorozhkin SV (2010) Bioceramics of calcium orthophosphates. Biomaterials 31(7):1465–1485. https://doi.org/10.1016/j.biomaterials.2009.11.050
8. Best SM, Porter AE, Thian ES, Huang J (2008) Bioceramics: Past, present and for the future. J Eur Ceram Soc 28(7):1319–1327. https://doi.org/10.1016/j.jeurceramsoc.2007.12.001
9. Koons GL, Diba M, Mikos AG (2020) Materials design for bone-tissue engineering. Nature Rev Mater1–20. https://doi.org/10.1038/s41578-020-0204-2
10. Hollister SJ (2005) Porous scaffold design for tissue engineering. Nat Mater 4(7):518–524. https://doi.org/10.1038/nmat1421
11. Vallet-Regi M (2014) Bio-ceramics with clinical applications. Wiley
12. Antoniac IV (2016) Handbook of Bioceramics and Biocomposites. Springer, Berlin Heidelberg, New York
13. Hench LL (1991) Bioceramics: from concept to clinic. J Am Ceram Soc 74(7):1487–1510. https://doi.org/10.1111/j.1151-2916.1991.tb07132.x
14. Rahaman MN (2007) Sintering of ceramics. CRC Press
15. Ring TA (1996) Fundamentals of ceramic powder processing and synthesis. Elsevier
16. Bose S, Ke D, Sahasrabudhe H, Bandyopadhyay A (2018) Additive manufacturing of biomaterials. Prog Mater Sci 93:45–111. https://doi.org/10.1016/j.pmatsci.2017.08.003
17. Lc F, Bertrand G, Lenormand P, Grossin D, Ben-Nissan B (2017) A review of the additive manufacturing (3DP) of bioceramics: alumina, zirconia (PSZ) and hydroxyapatite. J Aust Ceram Soc 53(1):11–20. https://doi.org/10.1007/s41779-016-0003-9
18. Gao W, Zhang Y, Ramanujan D, Ramani K, Chen Y, Williams CB, Wang CC, Shin YC, Zhang S, Zavattieri PD (2015) The status, challenges, and future of additive manufacturing in engineering. Comput Aided Des 69:65–89. https://doi.org/10.1016/j.cad.2015.04.001
19. Tempelman E, Shercliff H, van Eyben BN (2014) Chapter 11 - Additive Manufacturing. In: Tempelman E, Shercliff H, Eyben BNv (eds) Manufacturing and Design. Butterworth-Heinemann, Boston, pp 187–200. https://doi.org/10.1016/B978-0-08-099922-7.00011-1
20. Mastalska-Poplawska J, Sikora M, Izak P, Goral Z (2019) Applications of starch and its derivatives in bioceramics. J Biomater Appl 34(1):12–24. https://doi.org/10.1177/0885328219844972
21. Miculescu F, Maidaniuc A, Voicu SI, Thakur VK, Stan GE, Ciocan L (2017) Progress in hydroxyapatite-starch based sustainable biomaterials for biomedical bone substitution applications. ACS Sustain Chem Eng 5(10):8491–8512. https://doi.org/10.1021/acssuschemeng.7b02314
22. Gregorová E, Živcová Z, Pabst W (2009) Porous ceramics made using potato starch as a pore-forming agent. Fruit Veget Cereal Sci Biotechnol 3:115–127
23. Jovic TH, Kungwengwe G, Mills AC, Whitaker IS (2019) Plant-derived biomaterials: A review of 3D bioprinting and biomedical applications. Front Mech Eng 5:19. https://doi.org/10.3389/fmech.2019.00019
24. Wang S, Li C, Copeland L, Niu Q, Wang S (2015) Starch retrogradation: a comprehensive review. Comprehens Rev Food Sci Food Safety 14(5):568–585. https://doi.org/10.1111/1541-4337.12143
25. Roslan MR, Nasir NM, Cheng E, Amin N Tissue engineering scaffold based on starch: a review. In: 2016 International conference on electrical, electronics, and optimization techniques (ICEEOT), 2016. IEEE, pp 1857–1860. https://doi.org/10.1109/ICEEOT.2016.7755010
26. Moad G (2011) Chemical modification of starch by reactive extrusion. Prog Polym Sci 36(2):218–237. https://doi.org/10.1016/j.progpolymsci.2010.11.002

27. Kalambur S, Rizvi SS (2006) An overview of starch-based plastic blends from reactive extrusion. J Plast Film Sheeting 22(1):39–58. https://doi.org/10.1177/8756087906062729
28. Kaseem M, Hamad K, Deri F (2012) Thermoplastic starch blends: a review of recent works. Polym Sci, Ser A 54(2):165–176. https://doi.org/10.1134/S0965545X1202006X
29. Lyckfeldt O, Ferreira J (1998) Processing of porous ceramics by 'starch consolidation.' J Eur Ceram Soc 18(2):131–140. https://doi.org/10.1016/S0955-2219(97)00101-5
30. Mastalska-Popławska J, Sikora M, Izak P, Góral Z (2020) Role of starch in the ceramic powder synthesis: a review. J Sol-Gel Sci Technol, 1–10.https://doi.org/10.1007/s10971-020-05404-x
31. Shekhawat D, Singh A, Banerjee MK, Singh T, Patnaik A (2020) Bioceramic composites for orthopaedic applications: a comprehensive review of mechanical, biological, and microstructural properties. Ceram Int. https://doi.org/10.1016/j.ceramint.2020.09.214
32. Gregorová E, Pabst W (2007) Porous ceramics prepared using poppy seed as a pore-forming agent. Ceram Int 33(7):1385–1388. https://doi.org/10.1016/j.ceramint.2006.05.019
33. Uhlířová T, Gregorová E, Pabst W, Nečina V (2015) Preparation of cellular alumina ceramics via biological foaming with yeast and its microstructural characterization via stereological relations. J Eur Ceram Soc 35(1):187–196. https://doi.org/10.1016/j.jeurceramsoc.2014.08.020
34. Grech J, Antunes E (2019) Zirconia in dental prosthetics: a literature review. J Market Res 8(5):4956–4964. https://doi.org/10.1016/j.jmrt.2019.06.043
35. Zhang X, Wu X, Shi J (2020) Additive manufacturing of zirconia ceramics: a state-of-the-art review. J Market Res 9(4):9029–9048. https://doi.org/10.1016/j.jmrt.2020.05.131
36. Albano MP, Garrido LB, Plucknett K, Genova LA (2009) Processing of porous yttria-stabilized zirconia tapes: influence of starch content and sintering temperature. Ceram Int 35(5):1783–1791. https://doi.org/10.1016/j.ceramint.2008.10.003
37. Kastyl J, Chlup Z, Clemens F, Trunec M (2017) Mechanical properties of zirconia core-shell rods with porous core and dense shell prepared by thermoplastic co-extrusion. J Eur Ceram Soc 37(6):2439–2447. https://doi.org/10.1016/j.jeurceramsoc.2017.02.006
38. Pabst W, Gregorová E, Sedlářová I, Černý M (2011) Preparation and characterization of porous alumina–zirconia composite ceramics. J Eur Ceram Soc 31(14):2721–2731. https://doi.org/10.1016/j.jeurceramsoc.2011.01.011
39. Rezaee S, Ranjbar K, Kiasat AR (2020) Characterization and strengthening of porous alumina-20 wt% zirconia ceramic composites. Ceram Int 46(1):893–902. https://doi.org/10.1016/j.ceramint.2019.09.047
40. Xie H, Cao T, Rodríguez-Lozano FJ, Luong-Van EK, Rosa V (2017) Graphene for the development of the next-generation of biocomposites for dental and medical applications. Dent Mater 33(7):765–774. https://doi.org/10.1016/j.dental.2017.04.008
41. Makvandi P, Ghomi M, Ashrafizadeh M, Tafazoli A, Agarwal T, Delfi M, Akhtari J, Zare EN, Padil VVT, Zarrabi A, Pourreza N, Miltyk W, Maiti TK (2020) A review on advances in graphene-derivative/polysaccharide bionanocomposites: Therapeutics, pharmacogenomics and toxicity. Carbohydrate Polymers 250:116952. https://doi.org/10.1016/j.carbpol.2020.116952
42. Hench LL (1998) Biomaterials: a forecast for the future. Biomaterials 19(16):1419–1423. https://doi.org/10.1016/S0142-9612(98)00133-1
43. Hench LL, Jones JR (2015) bioactive glasses: frontiers and challenges. Front Bioeng Biotechnol 3:194. https://doi.org/10.3389/fbioe.2015.00194
44. Jones JR (2013) Review of bioactive glass: from Hench to hybrids. Acta Biomater 9(1):4457–4486. https://doi.org/10.1016/j.actbio.2012.08.023
45. Fernandes HR, Gaddam A, Rebelo A, Brazete D, Stan GE, Ferreira JM (2018) Bioactive glasses and glass-ceramics for healthcare applications in bone regeneration and tissue engineering. Materials 11(12):2530. https://doi.org/10.3390/ma11122530
46. Miguez-Pacheco V, Hench LL, Boccaccini AR (2015) Bioactive glasses beyond bone and teeth: Emerging applications in contact with soft tissues. Acta Biomater 13:1–15. https://doi.org/10.1016/j.actbio.2014.11.004

47. Baino F, Novajra G, Miguez-Pacheco V, Boccaccini AR, Vitale-Brovarone C (2016) Bioactive glasses: Special applications outside the skeletal system. J Non-Cryst Solids 432:15–30. https://doi.org/10.1016/j.jnoncrysol.2015.02.015
48. Bellucci D, Sola A, Cannillo V (2016) Hydroxyapatite and tricalcium phosphate composites with bioactive glass as second phase: state of the art and current applications. J Biomed Mater Res Part A 104(4):1030–1056. https://doi.org/10.1002/jbm.a.35619
49. Allan I, Newman H, Wilson M (2001) Antibacterial activity of particulate Bioglass® against supra-and subgingival bacteria. Biomaterials 22(12):1683–1687. https://doi.org/10.1016/S0142-9612(00)00330-6
50. Hu S, Chang J, Liu M, Ning C (2009) Study on antibacterial effect of 45S5 Bioglass®. J Mater Sci Mater Med 20(1):281–286. https://doi.org/10.1016/S0142-9612(00)00330-6
51. Gorustovich AA, Roether JA, Boccaccini AR (2010) Effect of bioactive glasses on angiogenesis: a review of in vitro and in vivo evidences. Tissue Eng Part B Rev 16(2):199–207. https://doi.org/10.1089/ten.teb.2009.0416
52. Fu Q, Saiz E, Rahaman MN, Tomsia AP (2011) Bioactive glass scaffolds for bone tissue engineering: state of the art and future perspectives. Mater Sci Eng C 31(7):1245–1256. https://doi.org/10.1016/j.msec.2011.04.022
53. Silva GA, Coutinho OP, Ducheyne P, Shapiro IM, Reis RL (2007) The effect of starch and starch-bioactive glass composite microparticles on the adhesion and expression of the osteoblastic phenotype of a bone cell line. Biomaterials 28(2):326–334. https://doi.org/10.1016/j.biomaterials.2006.07.009
54. Leonor IB, Sousa R, Cunha A, Reis R, Zhong Z, Greenspan D (2002) Novel starch thermoplastic/Bioglass® composites: Mechanical properties, degradation behavior and in-vitro bioactivity. J Mater Sci Mater Med 13(10):939–945. https://doi.org/10.1023/A:1019800411229
55. Vitale-Brovarone C, Verne E, Bosetti M, Appendino P, Cannas M (2005) Microstructural and in vitro characterization of SiO_2–Na_2 O–CaO–MgO glass-ceramic bioactive scaffolds for bone substitutes. J Mater Sci Mater Med 16(10):909–917. https://doi.org/10.1007/s10856-005-4425-0
56. Albee FH (1920) Studies in bone growth: triple calcium phosphate as a stimulus to osteogenesis. Ann Surg 71(1):32. https://doi.org/10.1097/00000658-192001000-00006
57. Klein CP, De Groot K, Drissen A, Van der Lubbe H (1985) Interaction of biodegradable β-whitlockite ceramics with bone tissue: an in vivo study. Biomaterials 6(3):189–192. https://doi.org/10.1016/0142-9612(85)90008-0
58. Habraken W, Habibovic P, Epple M, Bohner M (2016) Calcium phosphates in biomedical applications: materials for the future? Mater Today 19(2):69–87. https://doi.org/10.1016/j.mattod.2015.10.008
59. Omelon SJ, Grynpas MD (2008) Relationships between polyphosphate chemistry, biochemistry and apatite biomineralization. Chem Rev 108(11):4694–4715. https://doi.org/10.1021/cr0782527
60. Dorozhkin S (2009) Calcium orthophosphates in nature, biology and medicine. Materials 2(2):399–498. https://doi.org/10.3390/ma2020399
61. Dorozhkin SV (2017) Calcium orthophosphates (CaPO4): Occurrence and properties. Morphologie 101(334):125–142. https://doi.org/10.1016/j.morpho.2017.03.007
62. Miculescu F, Mocanu A-C, Maidaniuc A, Dascalu C, Miculescu M, Voicu S, Ciocoiu R-C (2018) Biomimetic calcium phosphates derived from marine and land bioresources. Hydroxyapatite—advances in composite nanomaterials, biomedical applications and its technological facets; InTechOpen: London, UK:89–108. https://doi.org/10.5772/intechopen.71489
63. Kokubo T (1991) Bioactive glass ceramics: properties and applications. Biomaterials 12(2):155–163. https://doi.org/10.1016/0142-9612(91)90194-F
64. Dorozhkin SV (2010) Calcium orthophosphates as bioceramics: state of the art. J Funct Biomater 1(1):22–107. https://doi.org/10.3390/jfb1010022
65. Dorozhkin S (2009) Calcium orthophosphate-based biocomposites and hybrid biomaterials. J Mater Sci 44(9):2343–2387. https://doi.org/10.1007/s10853-008-3124-x

66. LeGeros RZ (2008) Calcium phosphate-based osteoinductive materials. Chem Rev 108(11):4742–4753. https://doi.org/10.1021/cr800427g
67. Sheikh Z, Najeeb S, Khurshid Z, Verma V, Rashid H, Glogauer M (2015) Biodegradable materials for bone repair and tissue engineering applications. Materials 8(9):5744–5794. https://doi.org/10.3390/ma8095273
68. Kundu B, Lemos A, Soundrapandian C, Sen P, Datta S, Ferreira J, Basu D (2010) Development of porous HAp and β-TCP scaffolds by starch consolidation with foaming method and drug-chitosan bilayered scaffold based drug delivery system. J Mater Sci Mater Med 21(11):2955–2969. https://doi.org/10.1007/s10856-010-4127-0
69. Studart AR, Gonzenbach UT, Tervoort E, Gauckler LJ (2006) Processing routes to macroporous ceramics: a review. J Am Ceram Soc 89(6):1771–1789. https://doi.org/10.1111/j.1551-2916.2006.01044.x
70. Travitzky N, Bonet A, Dermeik B, Fey T, Filbert-Demut I, Schlier L, Schlordt T, Greil P (2014) Additive manufacturing of ceramic-based materials. Adv Eng Mater 16(6):729–754. https://doi.org/10.1002/adem.201400097
71. Kumar A, Kargozar S, Baino F, Han SS (2019) Additive manufacturing methods for producing hydroxyapatite and hydroxyapatite-based composite scaffolds: a review. Front Mater 6:313. https://doi.org/10.3389/fmats.2019.00313
72. Chua C, Leong K, An J, Narayan R (2014) 1-Introduction to rapid prototyping of biomaterials, vol Rapid. Woodhead Publishing, Prototyping of Biomaterials. https://doi.org/10.1016/B978-0-08-102663-2.00001-0
73. Yang S, Leong K-F, Du Z, Chua C-K (2002) The design of scaffolds for use in tissue engineering. Part II. Rapid prototyping techniques. Tissue engineering 8 (1):1–11. doi:https://doi.org/10.1089/107632702753503009
74. Shirazi SFS, Gharehkhani S, Mehrali M, Yarmand H, Metselaar HSC, Kadri NA, Osman NAA (2015) A review on powder-based additive manufacturing for tissue engineering: selective laser sintering and inkjet 3D printing. Sci Technol Adv Mater 16 (3):033502. https://doi.org/10.1088/1468-6996/16/3/033502
75. Bandyopadhyay A, Bose S, Das S (2015) 3D printing of biomaterials. MRS Bull 40(02):108–115. https://doi.org/10.1557/mrs.2015.3
76. Kietzmann J, Pitt L, Berthon P (2015) Disruptions, decisions, and destinations: Enter the age of 3-D printing and additive manufacturing. Bus Horiz 58(2):209–215. https://doi.org/10.1016/j.bushor.2014.11.005
77. Chia HN, Wu BM (2015) Recent advances in 3D printing of biomaterials. J Biol Eng 9(1):4. https://doi.org/10.1186/s13036-015-0001-4
78. Haleem A, Javaid M, Vaishya R (2018) 4D printing and its applications in orthopaedics. Journal of clinical orthopaedics and trauma 9(3):275. https://doi.org/10.1016/j.jcot.2018.08.016
79. Haleem A, Javaid M, Vaishya R (2019) 5D printing and its expected applications in Orthopaedics. J Clin Orthopaedics Trauma 10(4):809–810. https://doi.org/10.1016/j.jcot.2018.11.014
80. Daguano JKMB, Santos C, Alves MFRP, da Silva JVL, Souza MT, Fernandes MHFV (2019) State of the art in the use of bioceramics to elaborate 3D structures using robocasting. Int J Adv Med Biotechnol-IJAMB 2 (1):55–70. doi:https://doi.org/10.25061/2595-3931/IJAMB/2019.v2i1.28
81. Peng E, Zhang D, Ding J (2018) Ceramic robocasting: recent achievements, potential, and future developments. Adv Mater 30(47):1802404. https://doi.org/10.1002/adma.201802404
82. Jiang T, Duan Q, Zhu J, Liu H, Yu L (2020) Starch-based biodegradable materials: Challenges and opportunities. Adv Industr Eng Polymer Res 3(1):8–18. https://doi.org/10.1016/j.aiepr.2019.11.003
83. Maniglia BC, Castanha N, Rojas ML, Augusto PED (2021) Emerging technologies to enhance starch performance. Curr Opin Food Sci 37:26–36. https://doi.org/10.1016/j.cofs.2020.09.003
84. Le-Bail A, Maniglia BC, Le-Bail P (2020) Recent advances and future perspective in additive manufacturing of foods based on 3D printing. Curr Opin Food Sci 35:54–64. https://doi.org/10.1016/j.cofs.2020.01.009

85. Cesarano III J, King BH, Denham H (1998) Recent developments in robocasting of ceramics and multimaterial deposition. Sandia National Labs., Albuquerque, NM (United States)
86. Miculescu F, Maidaniuc A, Miculescu M, Dan Batalu N, Cătălin Ciocoiu R, Voicu SI, Stan GE, Kumar Thakur V (2018) Synthesis and characterization of jellified composites form bovine bone-derived hydroxyapatite and starch as precursors for robocasting. ACS Omega 3(1):1338–1349. https://doi.org/10.1021/acsomega.7b01855
87. Roleček J, Pejchalová L, Martínez-Vázquez F, González PM, Salamon D (2019) Bioceramic scaffolds fabrication: Indirect 3D printing combined with ice-templating vs. robocasting. J Europ Ceramic Soc 39 (4):1595–1602. doi:https://doi.org/10.1016/j.jeurceramsoc.2018.12.006
88. Faes M, Valkenaers H, Vogeler F, Vleugels J, Ferraris E (2015) Extrusion-based 3D printing of ceramic components. Procedia CIRP 28:76–81. https://doi.org/10.1016/j.procir.2015.04.028
89. Fu Z, Freihart M, Wahl L, Fey T, Greil P, Travitzky N (2017) Micro-and macroscopic design of alumina ceramics by robocasting. J Eur Ceram Soc 37(9):3115–3124. https://doi.org/10.1016/j.jeurceramsoc.2017.03.052
90. Glymond D, Vandeperre LJ (2018) Robocasting of MgO-doped alumina using alginic acid slurries. J Am Ceram Soc 101(8):3309–3316. https://doi.org/10.1111/jace.15509
91. Eqtesadi S, Motealleh A, Pajares A, Guiberteau F, Miranda P (2016) Improving mechanical properties of 13–93 bioactive glass robocast scaffold by poly (lactic acid) and poly (ε-caprolactone) melt infiltration. J Non-Cryst Solids 432:111–119. https://doi.org/10.1016/j.jnoncrysol.2015.02.025
92. Barberi J, Baino F, Fiume E, Orlygsson G, Nommeots-Nomm A, Massera J, Verné E (2019) Robocasting of SiO_2-based bioactive glass scaffolds with porosity gradient for bone regeneration and potential load-bearing applications. Materials 12(17):2691. https://doi.org/10.3390/ma12172691
93. Marques CF, Perera FH, Marote A, Ferreira S, Vieira SI, Olhero S, Miranda P, Ferreira JMF (2017) Biphasic calcium phosphate scaffolds fabricated by direct write assembly: mechanical, anti-microbial and osteoblastic properties. J Eur Ceram Soc 37(1):359–368. https://doi.org/10.1016/j.jeurceramsoc.2016.08.018
94. Miranda P, Saiz E, Gryn K, Tomsia AP (2006) Sintering and robocasting of β-tricalcium phosphate scaffolds for orthopaedic applications. Acta Biomater 2(4):457–466. https://doi.org/10.1016/j.actbio.2006.02.004
95. Franco J, Hunger P, Launey ME, Tomsia AP, Saiz E (2010) Direct write assembly of calcium phosphate scaffolds using a water-based hydrogel. Acta Biomater 6(1):218–228. https://doi.org/10.1016/j.actbio.2009.06.031
96. Simon JL, Michna S, Lewis JA, Rekow ED, Thompson VP, Smay JE, Yampolsky A, Parsons JR, Ricci JL (2007) In vivo bone response to 3D periodic hydroxyapatite scaffolds assembled by direct ink writing. J Biomed Mater Res Part A 83(3):747–758. https://doi.org/10.1002/jbm.a.31329
97. Maazouz Y, Montufar E, Guillem-Marti J, Fleps I, Öhman C, Persson C, Ginebra M (2014) Robocasting of biomimetic hydroxyapatite scaffolds using self-setting inks. J Mat Chem B 2(33):5378–5386. https://doi.org/10.1039/C4TB00438H
98. Martínez-Vázquez F, Pajares A, Guiberteau F, Miranda P (2014) Effect of polymer infiltration on the flexural behavior of β-Tricalcium phosphate robocast scaffolds. Materials 7(5):4001–4018. https://doi.org/10.3390/ma7054001
99. Ahmed YM, Ewais EM, El-Sheikh SM (2014) Effect of dispersion parameters on the consolidation of starch-loaded hydroxyapatite slurry. Process Appl Ceramics 8(3):127–135. https://doi.org/10.2298/PAC1403127A
100. Ahmed Y, Ewais E, El-Sheikh S (2015) Potato starch consolidation of aqueous HA suspension. J Asian Ceramic Societies 3(1):108–115. https://doi.org/10.1016/j.jascer.2014.11.007
101. Gregorova E, Zivcova Z, Pabst W, Stitina J, Keuper M (2008) Rheology of ceramic suspensions with organic or biopolymeric gelling additives part III: suspensions with starch. Ceram-Silik 52:250–259

102. Miculescu F, Antoniac I, Ciocan LT, Miculescu M, Branzei M, Ernuteanu A, Batalu D, Berbecaru A (2011) Complex analysis on heat treated human compact bones. Univ Politehnica Bucharest Scientific Bull Series B Chem Mater Sci 73(4):203–212
103. Miculescu F, Ciocan L, Miculescu M, Ernuteanu A (2011) Effect of heating process on micro structure level of cortical bone prepared for compositional analysis. Dig J Nanomater Biostruct 6(1):225–233
104. Miculescu F, Stan G, Ciocan L, Miculescu M, Berbecaru A, Antoniac I (2012) Cortical bone as resource for producing biomimetic materials for clinical use. Dig J Nanomater Biostruct 7(4):1667–1677
105. Miculescu F, Ciocan LT, Miculescu M, Mocanu A, Maidaniuc A, Purcaru A, Preda O Micro-Analytical Comparison on Elemental Composition of Nonstoichiometric Bovine Bone Derived Hydroxyapatite. In: Key engineering materials, 2015. Trans Tech Publ, pp 3–7. https://doi.org/10.4028/www.scientific.net/kem.638.3
106. Miculescu F, Ciocan LT, Miculescu M, Antoniac I, Purcaru A, Preda O, Maidaniuc A (2015) cooling conditions influence on cortical bovine bones derived hydroxyapatite. In: Key engineering materials, Trans Tech Publ, pp 111–116. https://doi.org/10.4028/www.scientific.net/kem.638.111
107. Miculescu F, Maidaniuc A, Voicu SI, Miculescu M, Berbecaru A, Ciocan LT, Purcaru A, Semenescu A, Preda O (2015) Structural and morphological induced modifications in hydroxyapatite obtained by bone thermal treatments. J Optoelectron Adv Mater 17(7–8):1361–1366
108. Miculescu F, Purcaru A, Miculescu M, Ciocan LT, Voicu SI, Maidaniuc A, Mocanu A, Branzei M (2015) Hydroxyapatite induced microstructure by cooling rate modification of cancellous bone thermal treatment. J Optoelectron Adv Mater 17(9–10):1219–1224
109. COMMISSION REGULATION (EU) No 722/2012 of 8 August 2012 concerning particular requirements as regards the requirements laid down in Council Directives 90/385/EEC and 93/42/EEC with respect to active implantable medical devices and medical devices manufactured utilising tissues of animal origin.
110. ISO/TR 22442 Standard Series—Medical devices utilizing animal tissues and their derivatives
111. Miculescu F, Maidaniuc A, Stan G, Miculescu M, Voicu S, Cîmpean A, Mitran V, Batalu D (2016) Tuning hydroxyapatite particles' characteristics for solid freeform fabrication of bone scaffolds. In: Tiwari A, Alenezi M, Jun S (eds) advanced composite materials. Scrivener Publishing LLC, pp 321–397. doi:https://doi.org/10.1002/9781119242666.ch7
112. Maidaniuc A, Miculescu F, Voicu SI, Andronescu C, Miculescu M, Matei E, Mocanu AC, Pencea I, Csaki I, Machedon-Pisu T (2018) Induced wettability and surface-volume correlation of composition for bovine bone derived hydroxyapatite particles. Appl Surf Sci 438:158–166. https://doi.org/10.1016/j.apsusc.2017.07.074
113. https://ourworldindata.org/meat-production , Accesed in 25.09.2020.
114. Mucalo MR (2015) 14—animal-bone derived hydroxyapatite in biomedical applications. In: Mucalo M (ed) Hydroxyapatite (Hap) for biomedical applications. Woodhead Publishing, pp 307–342. https://doi.org/10.1016/B978-1-78242-033-0.00014-6
115. Maatz R, Bauermeister A (1957) A method of Bone Maceration. Results in animal experiments. J Bone Joint Surg Am 39 (1):153–166
116. McMurray G (1982) The evaluation of Kiel bone in spinal fusions. J Bone Joint Surg Br 64(1):101–104. https://doi.org/10.1302/0301-620X.64B1.7040406
117. Ooi CY, Hamdi M, Ramesh S (2007) Properties of hydroxyapatite produced by annealing of bovine bone. Ceram Int 33(7):1171–1177. https://doi.org/10.1016/j.ceramint.2006.04.001
118. Abdel-Fattah WI, Selim MM (1982) Kinetics of the thermal decomposition of animal bone char. Thermochim Acta 56(3):345–357. https://doi.org/10.1016/0040-6031(82)87042-1
119. Etok S, Valsami-Jones E, Wess T, Hiller J, Maxwell C, Rogers K, Manning DC, White M, Lopez-Capel E, Collins M, Buckley M, Penkman KH, Woodgate S (2007) Structural and chemical changes of thermally treated bone apatite. J Mater Sci 42(23):9807–9816. https://doi.org/10.1007/s10853-007-1993-z
120. Pramanik S, Pingguan-Murphy B, Cho J, Osman NAA (2014) Design and development of potential tissue engineering scaffolds from structurally different longitudinal parts of a bovine-femur. Scientific Reports 4. https://doi.org/10.1038/srep05843

121. Herliansyah MK, Hamdi M, Ide-Ektessabi A, Wildan MW, Toque JA (2009) The influence of sintering temperature on the properties of compacted bovine hydroxyapatite. Mater Sci Eng, C 29(5):1674–1680. https://doi.org/10.1016/j.msec.2009.01.007
122. Mkukuma LD, Skakle JM, Gibson IR, Imrie CT, Aspden RM, Hukins DW (2004) Effect of the proportion of organic material in bone on thermal decomposition of bone mineral: an investigation of a variety of bones from different species using thermogravimetric analysis coupled to mass spectrometry, high-temperature X-ray diffraction, and Fourier transform infrared spectroscopy. Calcif Tissue Int 75(4):321–328. https://doi.org/10.1007/s00223-004-0199-5
123. Nilen RWN, Richter PW (2008) The thermal stability of hydroxyapatite in biphasic calcium phosphate ceramics. J Mater Sci Mater Med 19(4):1693–1702. https://doi.org/10.1007/s10856-007-3252-x
124. Miculescu F, Miculescu M, Ciocan LT, Pencea I, Ernuteanu A, Matei E (2013) Correlation of spectrometric methods in hard tissue heavy elements concentration study. University Politehnica Bucharest Scientific Bull Ser A, Applied Math Phys 75(1):233–242
125. Miculescu F, Mocanu A-C, Dascălu CA, Maidaniuc A, Batalu D, Berbecaru A, Voicu SI, Miculescu M, Thakur VK, Ciocan LT (2017) Facile synthesis and characterization of hydroxyapatite particles for high value nanocomposites and biomaterials. Vacuum 146:614–622. https://doi.org/10.1016/j.vacuum.2017.06.008
126. Tian X, Li D, Heinrich JG (2011) Net-shaping of ceramic components by using rapid prototyping technologies. INTECH Open Access Publisher. https://doi.org/10.5772/19127
127. Motskin M, Wright D, Muller K, Kyle N, Gard T, Porter A, Skepper J (2009) Hydroxyapatite nano and microparticles: correlation of particle properties with cytotoxicity and biostability. Biomaterials 30(19):3307–3317. https://doi.org/10.1016/j.biomaterials.2009.02.044
128. Ding T, Xue Y, Lu H, Huang Z, Sun J (2012) Effect of particle size of hydroxyapatite nanoparticles on its biocompatibility. IEEE Trans Nanobioscience 11(4):336–340. https://doi.org/10.1109/tnb.2012.2190418
129. Wang M, Joseph R, Bonfield W (1998) Hydroxyapatite-polyethylene composites for bone substitution: effects of ceramic particle size and morphology. Biomaterials 19(24):2357–2366. https://doi.org/10.1016/S0142-9612(98)00154-9
130. Thangamani N, Chinnakali K, Gnanam F (2002) The effect of powder processing on densification, microstructure and mechanical properties of hydroxyapatite. Ceram Int 28(4):355–362. https://doi.org/10.1016/S0272-8842(01)00102-X
131. Butscher A, Bohner M, Roth C, Ernstberger A, Heuberger R, Doebelin N, Rudolf von Rohr P, Müller R (2012) Printability of calcium phosphate powders for three-dimensional printing of tissue engineering scaffolds. Acta Biomater 8(1):373–385. https://doi.org/10.1016/j.actbio.2011.08.027
132. Butscher A, Bohner M, Hofmann S, Gauckler L, Müller R (2011) Structural and material approaches to bone tissue engineering in powder-based three-dimensional printing. Acta Biomater 7(3):907–920. https://doi.org/10.1016/j.actbio.2010.09.039
133. Dorozhkin SV (2012) Calcium orthophosphate coatings, films and layers. Prog Biomater 1(1):1. https://doi.org/10.1186/2194-0517-1-1
134. Vorndran E, Moseke C, Gbureck U (2015) 3D printing of ceramic implants. MRS Bull 40(02):127–136. https://doi.org/10.1557/mrs.2015.326
135. Wu J, Ruan C, Ma Y, Wang Y, Luo Y (2017) Vital role of hydroxyapatite particle shape in regulating the porosity and mechanical properties of the sintered scaffolds. J Mater Sci Technol. https://doi.org/10.1016/j.jmst.2017.01.008
136. Dey S, Das M, Balla VK (2014) Effect of hydroxyapatite particle size, morphology and crystallinity on proliferation of colon cancer HCT116 cells. Mater Sci Eng C 39:336–339. https://doi.org/10.1016/j.msec.2014.03.022
137. Lin K, Wu C, Chang J (2014) Advances in synthesis of calcium phosphate crystals with controlled size and shape. Acta Biomater 10(10):4071–4102. https://doi.org/10.1016/j.actbio.2014.06.017

138. Honig F, Vermeulen S, Zadpoor AA, de Boer J, Fratila-Apachitei LE (2020) Natural architectures for tissue engineering and regenerative medicine. J Funct Biomater 11(3):47. https://doi.org/10.3390/jfb11030047
139. Pradhan S, Brooks AK, Yadavalli VK (2020) Nature-derived materials for the fabrication of functional biodevices. Mater Today Bio 7:100065. https://doi.org/10.1016/j.mtbio.2020.100065
140. Hutmacher DW (2001) Scaffold design and fabrication technologies for engineering tissues—state of the art and future perspectives. J Biomater Sci Polym Ed 12(1):107–124. https://doi.org/10.1163/156856201744489
141. Yildirimer L, Seifalian AM (2014) Three-dimensional biomaterial degradation — Material choice, design and extrinsic factor considerations. Biotechnol Adv 32(5):984–999. https://doi.org/10.1016/j.biotechadv.2014.04.014
142. EN ISO 10993–1—Biological evaluation of medical devices—Part 1: Evaluation and testing within a risk management process.
143. Lim J, Lee J, Yun H-S, Shin H-I, Park EK (2013) Comparison of bone regeneration rate in flat and long bone defects: calvarial and tibial bone. Tissue Eng Regener Med 10(6):336–340. https://doi.org/10.1007/s13770-013-1094-9
144. Mitra J, Tripathi G, Sharma A, Basu B (2013) Scaffolds for bone tissue engineering: role of surface patterning on osteoblast response. RSC Adv 3(28):11073–11094. https://doi.org/10.1039/C3RA23315D
145. Silva L, Galdino A, Cardoso G, Zavaglia C (2011) Characterization of hydroxyapatite scaffold using corn starch as porous agent. Paper presented at the 21st Brazilian Congress of Mechanical Engineering Natal, RN, Brazil
146. Prakasam M, Locs J, Salma-Ancane K, Loca D, Largeteau A, Berzina-Cimdina L (2015) Fabrication, properties and applications of dense hydroxyapatite: a review. J Funct Biomater 6(4):1099–1140. https://doi.org/10.3390/jfb6041099
147. Hulbert S, Talbert C, Klawitter J (1971) Investigation Into the Potential of Ceramic Materials as Permanently Implantable Skeletal Prostheses. In: Biomaterials. Bioengineering applied to materials for hard and soft tissue replacement. University of Washington Press, pp 3–77
148. Karageorgiou V, Kaplan D (2005) Porosity of 3D biomaterial scaffolds and osteogenesis. Biomaterials 26(27):5474–5491. https://doi.org/10.1016/j.biomaterials.2005.02.002
149. Cosijns A, Vervaet C, Luyten J, Mullens S, Siepmann F, Van Hoorebeke L, Masschaele B, Cnudde V, Remon JP (2007) Porous hydroxyapatite tablets as carriers for low-dosed drugs. Eur J Pharm Biopharm 67(2):498–506. https://doi.org/10.1016/j.ejpb.2007.02.018
150. Mitran V, Ion R, Miculescu F, Necula MG, Mocanu A-C, Stan GE, Antoniac IV, Cimpean A (2018) Osteoblast Cell Response to Naturally Derived Calcium Phosphate-Based Materials. Materials 11(7):1097. https://doi.org/10.3390/ma11071097
151. Miculescu F, Mocanu AC, Stan GE, Miculescu M, Maidaniuc A, Cîmpean A, Mitran V, Voicu SI, Machedon-Pisu T, Ciocan LT (2018) Influence of the modulated two-step synthesis of biogenic hydroxyapatite on biomimetic products' surface. Appl Surf Sci 438:147–157. https://doi.org/10.1016/j.apsusc.2017.07.144
152. Mocanu A-C, Miculescu M, Machedon-Pisu T, Maidaniuc A, Ciocoiu RC, Ioniță M, Pasuk I, Stan GE, Miculescu F (2019) Internal and external surface features of newly developed porous ceramics with random interconnected 3D channels by a fibrous sacrificial porogen method. Appl Surf Sci 489:226–238. https://doi.org/10.1016/j.apsusc.2019.05.354
153. Maidaniuc A (2018) Contributions regarding the possibilities of obtaining massive tridimensional structures from powdered materials with biomedical applications. PhD Thesis. Politehnica University of Bucharest, Bucharest
154. Trunec M, Chlup Z (2017) Subtractive manufacturing of customized hydroxyapatite scaffolds for bone regeneration. Ceram Int 43(14):11265–11273. https://doi.org/10.1016/j.ceramint.2017.05.177
155. Dorozhkin SV (2017) Calcium Orthophosphate-Based Bioceramics and Its Clinical Applications. In: Clinical Applications of Biomaterials. Springer, pp 123–226. https://doi.org/10.1007/978-3-319-56059-5_5

Chapter 9
Additive Manufacturing of Bioceramic Scaffolds for Bone Tissue Regeneration with Emphasis on Stereolithographic Processing

Francesco Baino, Elisa Fiume, Giulia Magnaterra, and Enrica Verné

Abstract Advanced bone tissue engineering approaches rely on implanting synthetic grafts for the management of mid to large bone defects in order to overcome the common limitations associated with the use of transplant materials. Bioceramics are especially effective due to their versatile functional properties and processing methods. This chapter provides a picture of ceramic scaffolds for bone tissue engineering, focusing on additive manufacturing technologies and, specifically, the emerging method of digital light processing. The functional and structural complexity of natural bone makes the design of scaffolds a complex challenge as their chemical, structural and functional properties have to meet very specific requirements, e.g. adequate support properties, bone-bonding capability and a macro- and microporous structure to promote cell colonization and vascularization. Many fabrication techniques are currently available for the production of porous artificial biomaterials. Among them, the class of additive manufacturing technologies is one of the most promising methods for the development of mechanically competent and structurally highly defined scaffolds with tailored properties for bone tissue engineering applications.

Keywords Bioceramics · Scaffold · Additive manufacturing · Porosity · Digital light processing

1 Scaffolds for Bone Repair: An Overview

The scaffold, also known as tissue template and/or artificial extracellular matrix, is a 3D porous structure that acts as a biocompatible implantable substrate [1] on which cells can attach, proliferate and differentiate in order to synthesize new bone tissue until the complete filling of the original bone defect in achieved [1, 2].

F. Baino (✉) · E. Fiume · G. Magnaterra · E. Verné
Institute of Materials Physics and Engineering, Applied Science and Technology Department, Politecnico di Torino, Corso Duca degli Abruzzi 24, 10129 Torino, Italy
e-mail: francesco.baino@polito.it

A. Kumar et al. (eds.), *3D printable Gel-inks for Tissue Engineering*, Gels Horizons: From Science to Smart Materials, https://doi.org/10.1007/978-981-16-4667-6_9

Table 1 Functions of biomedical scaffolds (adapted from [4])

Primary functions of scaffold
Substrate for cell adhesion
Delivery vehicle for exogenous cell, growth factors and genes
Temporary mechanical support for new tissue growth Barrier to the infiltration of the surrounding tissue that may hinder the process of regeneration
Maintenance of the shape of the defect by avoiding distortion

Andrés Segovia, a Spanish classical guitarist, proposed a fascinating definition of the role of scaffolds using these words [3]: *"When one puts up a building, he makes an elaborate scaffold to get everything into its proper place. But when one takes the scaffold down, the building must stand by itself with no trace of the means by which it was erected. That is how a musician should work"*.

Table 1 summarizes the main functions that should be performed by a scaffold intended for tissue engineering applications.

Given the complex and deeply interlocked nature of a biological system, scaffolds have to satisfy multiple requirements at the same time, as depicted in Fig. 1 [5].

Osteoconductivity, controlled biodegradability and biocompatibility [6] are essential features to be considered in the design of tissue-engineered scaffolds intended for bone defect repair, where new tissue growth and scaffold resorption are concurrent events leading to the replacement of the implanted biomaterials by newly formed bone. Highly biocompatible materials have to be used in order to avoid persistent inflammatory response and cytotoxicity within the body [3]. In addition, scaffolds should have suitable structural properties to provide proper mechanical support over

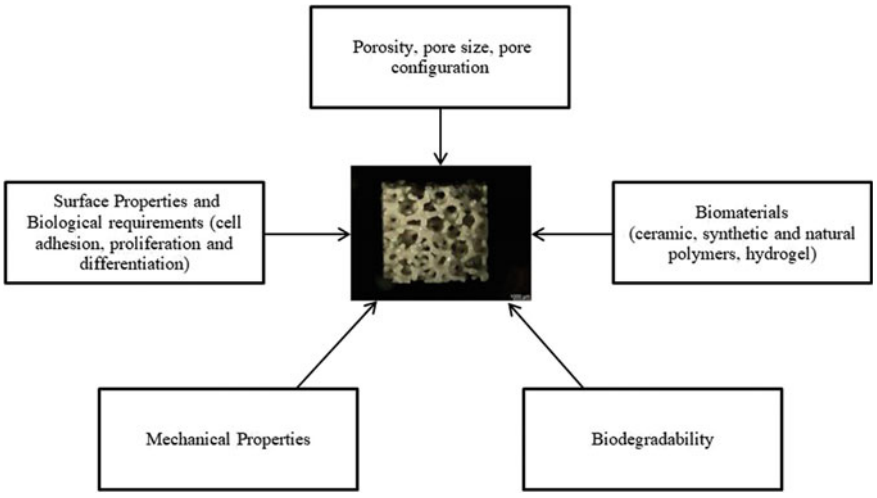

Fig. 1 Key factors involved in the design of scaffolds for bone tissue engineering

the whole healing process [6]. Scaffolds should also exhibit sufficient biological affinities to promote the integration with host tissue, growth of relevant cells [2] and regeneration of healthy tissue [7] as well as have suitable porosity features, which are necessary to allow cell migration, diffusion of nutrients and vascularization [3].

Ideally, the structural parameters of scaffolds (e.g. total porosity, pore size, shape, etc.) should be designed according to the implant site following a similarity criterion; in fact, bone tissue exhibits different structural properties depending on the anatomical position in the skeletal system. Therefore, if surgery on spongy bone is required, highly porous scaffolds are preferable; on the other hand, if the problem concerns the cortical bone, mechanically strong scaffolds with low porosity and oriented strut will be required [7].

2 Scaffold Requirements

Tissue-engineering scaffolds are designed to fulfil a series of requirements that are summarized in Table 2, along with their effects.

Table 2 Characteristics of the scaffold and their desirable effects

Scaffold requirements	Desirable features
Biocompatibility	• Non-toxic degradation products • Non-inflammatory scaffold components, avoiding immune rejection
Biodegradability	• Controlled scaffold degradation which can complement tissue ingrowth while maintaining sufficient mechanical integrity • Degradable by host enzymatic or biological processes • Allows invading host cells to produce their own extracellular matrix
Bioactivity	• Beneficial interaction between scaffold material and host tissue: formation of a stable bond • Osteoconductive and osteoinductive properties • Inclusion of biological cues and growth factors to stimulate cell attachment, proliferation and differentiation
Scaffold architecture	• Interconnected pores allowing diffusion and cell migration • Microporosity, which provides large surface area for improved cell-scaffold interactions • Macroporosity to allow cell migration and invasion of vasculature • Sufficient porosity to facilitate cell ingrowth without weakening mechanical properties • Tailored pore size and distribution to target tissue and cells • Inbuilt vascular channels to enhance angiogenesis in vivo
Mechanical properties	• Compressive, elastic and fatigue strength comparable to host bone, favouring cell mechanoregulation pathways and maintenance of structural integrity in vivo • Scaffold material that can be readily manipulated by clinicians to treat individual patient's bone defects

2.1 Biocompatibility

This is the first criterion that every tissue-engineered scaffold should fulfil [6]. As regards scaffolds, the term biocompatibility was defined as "*the capability of a material to facilitate natural cellular and molecular activity within a scaffold in the absence of systemic toxicity*" [8]. Therefore, biocompatible scaffolds allow cells to adhere, migrate and proliferate on their surface without the risk of triggering any dangerous inflammatory responses [6], and/or potentially toxic effects, both locally and systemically [9]. Good biocompatibility also promotes osteoconductivity, osteoblast proliferation and osteoinductivity [8].

In order for the scaffold to be biocompatible, it is necessary to carefully select the material with which it is manufactured. Suitable materials for bone tissue engineering applications should firmly bond to the natural bone in situ and stimulate new tissue growth and regeneration [9].

It has been shown that calcium phosphate and bioactive glass scaffolds are highly biocompatible and, furthermore, actively improve the tissue repair process through releasing calcium, phosphate and silicate ions that play a role in accelerating osteogenesis [8]. Methods for assessing the biocompatibility of scaffolds can be found in specific international standards [10].

2.2 Porosity

Pore size and porosity percentage of the scaffolds are key parameters to achieve the physiological development of newly formed tissue [11]. An ideal scaffold for cancellous bone repair should have an open-cell porous architecture, with porosity >50–60 vol.% [2], where more than 60% of the pores should have a size between 100 and 400 μm and at least 20% is expected to have a size below 20 μm [3]. Porosity percentage and pore size directly affect the osteoinductive and osteoconductive capabilities of the scaffold [12]. In principle, scaffolds with analogous total pore volume and pore size can also be considered suitable for the repair of cortical bone provided that the mechanical properties are adequate (e.g. compressive strength >100 MPa vs. 2–12 MPa of cancellous bone, see Sect. 2.3).

A suitable porosity range, above 50–60 vol.% of interconnected macropores, confers to the scaffold adequate mass transport properties for cell migration, attachment and interaction with the biological environment [6], as well as the passage of nutrients and bioactive molecules. Moreover, it has been demonstrated that suitable porosity features can improve vascularization and spatial organization between cell growth and extracellular matrix (ECM) production, thus leading to a considerable enhancement of the biomineralization process [8]. Large pores (size around 200–300 μm) lead to direct osteogenic pathways [2, 9]. The prevailing opinion in the literature is that the pore size should be between 200 and 400 μm in order to allow greater cell migration and proliferation, and the consequent formation of new tissue [13].

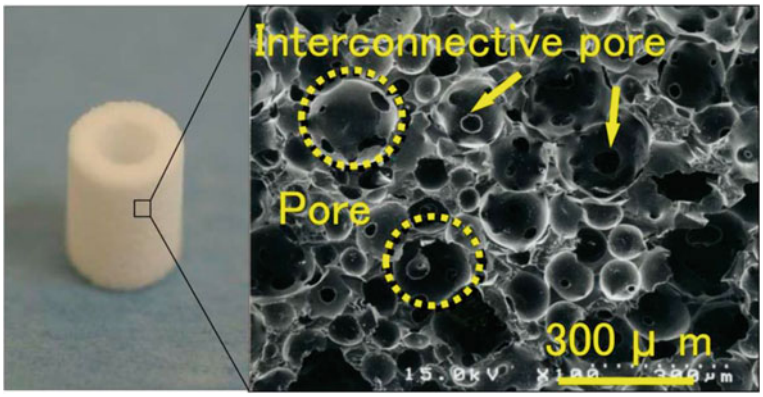

Fig. 2 Pores and interconnectivity of pores showed in hydroxyapatite scaffold. Image reproduced from Doi et al. [16] under the terms of the Creative Commons Attribution Licence

On the contrary, smaller pores (<100 μm) were found to be beneficial for chondrogenesis [14]. Too small pores may lead to poor vascularization [11] and limited cell migration, causing the formation of cell capsules around the edges of the scaffold [9].

In general, it is necessary for the pores not to be too large, as this would excessively decrease the mechanical resistance of the final product [6, 9].

The ideal degree of porosity should be found to allow sufficiently high permeability and interconnectivity for nutrient supply and waste removal as well as adequate stiffness and resistance to the loads transmitted from the healthy bone adjacent to the scaffold [2].

Interconnectivity (Fig. 2) is a key requirement to ensure the transport of nutrients and the elimination of waste products [15]. An in vivo study with hydroxyapatite scaffolds showed that low pore interconnection enables limited tissue penetration and chondral tissue formation but does not guarantee proper bone tissue growth [15].

The shape of the pores can also influence the mechanical of the scaffold [6]. Gong et al. performed fatigue tests (cyclic stress-strain) on scaffolds with triangular and circular pores with a total porosity of about 60 vol.% and found that scaffolds with circular pores are more resistant than those with triangular pores [6].

2.3 Mechanical Properties

In order to be functional, a scaffold should have biomechanical properties comparable to those of the host healthy bone [8, 12]. It has to maintain certain mechanical integrity over the whole duration of the treatment, in order to support the physiological healing process until the newly formed tissue has become able to physically support itself [8]. It should have Young's module similar to that of natural bone in order to avoid stress shielding phenomena and favour early tissue regeneration [17]. Strong scaffolds can

be obtained by building anisotropic structures with oriented pores [9]. For example, in order to replace cortical bone a good scaffold should have a compressive strength ~130–180 MPa and Young's modulus ~12–18 GPa.

Pore size, interconnectivity and architecture directly impact the mechanical properties of porous implants [15]. For example, studies on hydroxyapatite scaffolds have shown that decreasing the pore size yields higher compressive strength [15].

The compressive strength is the most common and easy-to-determine mechanical parameter for brittle ceramic scaffolds [18]. In accordance with ASTM F2883-11, the compressive strength of implantable ceramic scaffolds should be assessed following the ASTM C1424 that is valid for advanced ceramics [18].

In addition, it has been proven that the mechanical properties of the scaffold affect the mechanotransduction properties of the bone cells attached to its surface; in other words, mechanical stimuli from the biomaterial (e.g. stiffness) can be converted in different biochemical responses by cells and, thus, different bone regeneration rates and extent. In fact, there also seems to be a correlation between mechanotransduction and the potential osteoinductive properties of the scaffold [12]. Not all anchorage-dependent cells respond similarly to scaffold stiffness [11]: endothelial cells, for example, migrate and proliferate more easily on more rigid substrates [11].

2.4 Biodegradability

As the tissue regenerates, the scaffold should ideally degrade in a controlled manner over time [8]. This property is not mandatory (for example, hydroxyapatite scaffolds are permanent implants) but is desirable in many cases.

The biodegradability of the scaffold is dependent on the type of material and its clinical application: β-TCP-based scaffolds show a bioresorption rate similar to that of new bone formation, whereas hydroxyapatite scaffolds are generally characterized by better chemical durability [8].

Biomaterials degradation is influenced by the presence of enzymes or macrophages in the physiological fluids [7].

The rate of scaffold degradation may change depending on the different geometry and pore-strut architecture adopted. It is, therefore, necessary to test different production methods to find the optimal one according to the needs [8]. Scaffold degradation can be investigated following the standard ISO 10,993–14 [18].

2.5 Surface Properties and Interaction with Cells

The scaffold needs to be made in complex and even irregular shapes. The scaffold should serve as a model for natural bone growth and should therefore mimic the hierarchical structure of natural bone. With regard to cortical bone, for example, its

internal architecture should be similar to the small vascular channels, Volkmann's channels and the gaps in the osteocytes and Haversian channels [9].

As already mentioned, the scaffold needs to be carefully designed in order to ensure a highly interconnected porous structure [9].

Several studies have shown that the characteristics of the scaffold surface affect the amount, type and conformation of proteins and cells that will adhere to it [9]. A rough surface may improve cell adhesion, but excess roughness must be avoided, otherwise, the cells may fail to develop focal adhesion plaques [4]. This is a general trend but providing an "ideal" range of "optimal" roughness for cell adhesion and proliferation is impossible, as the behaviour of each specific cell type is concurrently influenced by the type of material and shape of nano-/micro-features on the surface (e.g. grooves, pits, islands).

The performance of a scaffold is strongly affected by the interaction between the material surface and the surrounding biological environment and is often mediated by proteins absorption by the biological fluid [19]. Chemistry, roughness and surface topography strongly influence the protein layer on which the formation of surface bonds directly aimed at binding only certain types of cells depends. Proteins create a specific interface through which cells can respond to the scaffold's topographical cues determined by the macrostructure, and the chemical features of the surface are responsible for the cells' attachment to the structure [19]. Surfaces with nanometric topography increase the availability of proteins and amino acids by promoting cell adhesion to a large extent [19].

Some examples in the literature suggest the incorporation of growth factors into scaffolds because they can improve and speed up the growth of new bone [14]. In fact, bone morphogenetic proteins (BMPs) help the development of osseous tissue and can trigger the differentiation and proliferation of osteoprogenitor cells. Vascular endothelial growth factor (VEGF) has often been used because it can improve blood vessel formation [14].

3 Conventional Methods for Ceramic Scaffold Fabrication

Scaffold manufacturing techniques could be divided into two main groups: conventional methods and non-conventional methods, which correspond to additive manufacturing technologies [9].

Scaffolds can be made using conventional techniques such as freeze-drying, gas foaming, sponge replication, solvent casting and particulate leaching, sol–gel-foaming method, phase separation (TIPS, DIPS, RIPS) [13], melt, dry, wet spinning and electrospinning [1]. In general, conventional techniques include all those techniques that are not based on a CAD/CAM design and are relatively easy and cheap to apply [9]. However, these methods have several limitations, including poor reproducibility [1, 13], and the inability to obtain a precise and reliable control on the internal porosity, geometry and interconnectivity of the 3D structure [6]. From the

Table 3 Conventional methods versus non-conventional methods

Conventional methods	Non-conventional methods
– Inability to obtain a scaffold with a precise architecture and controlled porosity – Inadequate to create patient-specific scaffolds – Techniques strongly dependent operators – Usually fast and not too expensive techniques	– Fabrication of complex internal 3D structures and patient-specific geometries – Possibility to use heterogeneous materials – Industrial scalability – Sometimes limited choice of materials – High cost of the process
Methods: Solvent casting and particulate leaching Gas foaming Freeze-drying Sol-gel Melt, dry, wet spinning and electrospinning Phase separation (TIPS, DIPS, RIPS) Sponge replication method	Methods: Select laser sintering (SLS) Stereolithography (SLA) Fused deposition modelling (FDM) Laminated object manufacturing (LOM) Solid ground curing 2-photon polymerization Robocasting Ink-jet printing 3D printing (3DP) 3D fibre deposition

biological point of view, the latter could be a severe drawback as a random and uncontrolled 3D porous network could determine a heterogeneous distribution of cells, causing uneven tissue growth [20]. The most common conventional manufacturing technique are summarized in Table 3 and described in the following sections.

3.1 Foaming Methods

These techniques rely on the use of a foaming agent to produce air bubbles that are responsible for the formation of the porosity at the macroscale. After preparing a colloidal suspension (or slurry), pores are created due to the action of a porogen by either injecting the gas directly or generating gas as a product of a chemical reaction, thermal decomposition or addition of surfactants [9].

Foaming methods include techniques such as gel-cast foaming, H_2O_2 foaming and sol-gel-foaming. However, all these techniques do not assure the high pore interconnectivity required for successful bone implants and do not guarantee a scaffold with good mechanical properties [9]. In this regard, Chen et al. fabricated highly porous 45S5 Bioglass® foams by including a surfactant in the sol that, after vigorous agitation, yielded a bone-like porous structure but the resulting scaffolds were highly brittle [21].

3.2 Phase Separation Methods

These techniques have been originally developed to obtain polymeric scaffolds and are usually divided into three groups depending on the main parameters that cause demixing of the solution [22]; for example, temperature-induced phase separation (TIPS) is based on the change of the temperature causing separation between polymer (optionally embedding ceramic or glass inclusions) and solvent [22]. As regards diffusion-induced phase separation (DIPS), the addition of a vapour or a liquid (i.e. a non-solvent) is necessary; reaction-induced phase separation (RIPS) is based on a chemical reaction leading to the phase separation in the original polymeric solution; precipitation induced by a change in pH is also included in this class [22].

TIPS is used to obtain both polymeric and polymer-matrix composite scaffolds embedding porous ceramic (glass) micro-/nanoparticles to increase bioactivity and mechanical strength/stiffness [9].

TIPS is based on the solubility-temperature dependence existing between two different polymers: two polymers may be soluble in each other at a given temperature but completely insoluble at a lower temperature. Therefore, if a solution of these polymers is made and then the solution is cooled down to the critical temperature of the solution, they will separate, forming two different phases, one less rich in polymer and one richer in polymer. The less polymer-rich phase will be removed and the porous structure will be finally obtained [9].

TIPS is used to obtain porous scaffold with a pore diameter from 1 to 100 μm and porosity over 95 vol.%. For example, Szustakiewicz et al., obtained porous scaffold based on synthetic hydroxyapatite and poly(L-lactide) (PLLA) using TIPS supported by the salt leaching process [23].

Maquet et al. built a scaffold of bioresorbable polymers (poly-(D,L-lactide) (PDLLA) and poly(lactide-co-glycolide) (PLGA)) and 45S5 Bioglass®. They constructed two different sets of samples by varying the amount of glass powder; in both cases, they obtained a porosity greater than 90 vol.% and overall good bioactivity imparted by the glass inclusions [24].

Degli Esposti et al. created bioresorbable and bioactive porous scaffold based on poly(3-hydroxybutyrate) (PHB) and hydroxyapatite particles that were able to sustain the growth and proliferation of MC3T3-E1 cells, had suitable porosity for bone repair and exhibited good bioactivity due to the presence of hydroxyapatite [25].

3.3 Spinning Methods

These techniques allow obtaining nano- or micrometric fibres, which are useful especially for the regeneration of nerves, and are divided into dry, wet, melt spinning methods and electrospinning [22].

Melt spinning technique uses a melted polymer that is extruded through a die with the desired section, while dry spinning and wet spinning use concentrated solutions that are similarly extruded through a die of proper section. For both methods, removal of the solvent is necessary to obtain the fibres.

Electrospinning can use both polymer solutions in a volatile solvent (electrospinning solution) and polymeric melts (melt electrospinning). It is a versatile technique that allows making continuous fibres from submicrometric to nanometric diameters [22].

An interesting study reported the production of 45S5 Bioglass® scaffolds with biodegradable nanofibrous coatings obtained with electrospinning. The composite scaffold obtained by combining bioactive glass and electrospun polymeric nanofibres (PCL-PEO, P(3HB), PHBV) allowed the formation of a layer of bone-like nanostructured hydroxyapatite upon immersion in physiological fluids and the possibility of achieving controlled drug release [26].

Hong et al. fabricated hierarchal nanoporous bioactive glass fibre mats by using the electrospinning technique and P123-PEO as co-templates for the nanopores. As a result, multiscale porosity was obtained with the mesoporous glass fibres arranged into 3D macroporous mats. These hierarchical scaffolds were proposed for potential application in bone tissue engineering combined with drug delivery [27].

3.4 Thermal Consolidation of Particles

The methods that are part of this group are characterized by the use of sacrificial particles added to the green body that will be sintered. These particles will form pores upon thermal degradation and they are typically polymers or of synthetic (e.g. polyethylene) or natural origin (e.g. rice husk or starch) [9]. These techniques are relatively inexpensive but usually they do not allow obtaining highly porous scaffolds with good interconnectivity among pores [9].

3.5 Sponge Replica Method

This method relies on the use of porous templates of natural material (e.g. marine sponge) or synthetic material (e.g. polyurethane sponge) that are immersed in a ceramic (glass) slurry [28] to create sintered positive replicas of the sponges with a high level of porosity and bone-like 3D architecture [9]. The sponge is the organic phase of the scaffolds and only serves as a template for the inorganic phase, since it will be completely removed during the production process [9]. In fact, the ceramic (glass)-coated porous organic template will have to undergo a double heat treatment, the first to eliminate the organic phase and the second to consolidate the ceramic (glass) particle by sintering [9]. As a result, a porous ceramic structure is obtained showing the same architecture of the sacrificial template [28].

This method allows obtaining scaffolds with structures very similar to the trabecular architecture of natural cancellous bone and high levels of porosity (about 90 vol.%), but often these scaffolds have poor mechanical properties [9]. Usually, foam replication is applied to fabricate porous glass, glass–ceramic, biphasic calcium phosphate and hydroxyapatite scaffolds [29]. A limitation of this technique is the poor capability to create a solid network with high density and strong mechanical properties [29].

In 2006, Chen et al. used polyurethane commercial foams as a sacrificial template to be dipped in a slurry of commercial 45S5 Bioglass® containing PVA as a binder. This was one of the first scaffold batches that were successfully obtained by this method: these samples had a very high porosity (85–90 vol.%) and interconnected and open macropores between 510 and 720 μm, which make them very similar to spongy bone but, at the same time, too weak to be used for bone repair (compressive strength between 0.1–0.4 MPa) [30].

Tripathi et al. used this method to build hydroxyapatite scaffolds with interconnected oval pores (diameter 100–300 μm and wall thickness ~ 50 μm). The homogeneous distribution of pores and the pore wall thickness provided a large surface area to promote protein attachment and cell proliferation [31].

Fu et al. fabricated foam-replicated 13–93 glass scaffolds with total porosity of 85 vol.% and pore size of 100–500 μm. In this case, the scaffolds exhibited significantly higher compressive strength (11 MPa) as compared to other examples produced by the same method in the literature due to the good sinterability of the material, yielding well-densified ad strong struts. In addition, 13–93 glass scaffolds successfully supported the proliferation of MC3T3-E1 pre-osteoblastic cells [29].

Wu et al. tried to improve the mechanical properties of mesoporous bioactive glass scaffolds obtained via sponge replica method by depositing a silk coating on their struts; in spite of a certain improvement, the scaffold strength obtained from compressive tests still remained low (< 0.3 MPa).

4 Additive Manufacturing Technologies for Ceramic Scaffold Fabrication

Despite the improvements that have been made over the past years, conventional techniques are still strongly dependent on the process rather than the design and exhibit some inherent limitations that make it impossible to finely control the architecture of the scaffolds [4].

In order to overcome these drawbacks, since the second half of the 1980s [34] many researchers have been developing a number of additive manufacturing technologies as a valid alternative to obtain detailed and extensive control on the fabrication process [4, 35].

Over the past two decades, with the development of rapid prototyping techniques, a great number of tissue-engineered scaffolds have been created for potential use in

clinical practice using new materials and ground-breaking technologies [6]. These methods make it now possible to create customized scaffolds for a targeted tissue regeneration, with good perspectives for quick and reliable commercialization [8].

In literature, the expressions "rapid prototyping techniques" and "additive manufacturing" are often used as synonyms and generally refer to all those fabrication technologies where 3D structures are produced by adding material "layer-by-layer" [4, 32]. Each layer represents the cross-section of the 3D structure at a specific z-position [36]. These techniques offer the possibility of finely controlling the architecture of the scaffold (shape, size, pore interconnectivity, geometry and orientation). Biomimetic structures that vary in material composition and design can be obtained, thus improving the control of mechanical properties, biological response, and degradation rate of the scaffold [36].

Additive manufacturing technologies use different approaches, similar to each other in terms of the main procedures which are usually divided into five phases [37]:

1. Creation of the CAD model.
2. Conversion of the CAD model into STL files.
3. Slicing of the STL file.
4. The additive manufacturing apparatus creates the scaffold layer-by-layer.
5. Post-processing (e.g. sintering, if necessary).

The CAD file can be created by using a proper design software or obtained from magnetic resonance (MR) and computed tomography (CT) investigations, as both these imaging techniques allow obtaining accurate 3D reconstructions at high resolution [17]. If the CT images directly represent the patient's defect, one can create a 3D volumetric reconstruction of the bone defect to be treated in order to print a patient-specific scaffold (Fig. 3) [36].

Another approach to scaffold fabrication is based on the use of hierarchal structures created by repeating a cell unit of known properties and geometry. However, this approach typically creates simple architectures with orthogonal and/or parallel channels, which do not really replicate the morphology of natural bone [38].

In order to overcome this limitation and, at the same time, create marketable shelves, CAD files from natural structures can be used to better imitate the trabecular structure of bone. Synthetic scaffolds inspired by natural structures are having a lot of success because they allow obtaining a much more biomimetic result. For example, the microstructure of cuttlefish bone has inspired the manufacture of bone tissue engineering shelves because its natural architecture is characterized by high porosity and at the same time high compressive strength [39].

In general, once the image is obtained, it is converted into DICOM (Digital Imaging and Communication Medicine) files and subjected to a segmentation process (a key step because the accuracy of the final model will depend on this) [17].

The reconstructed 3D volume is then used to create the 3D CAD model, which is converted into an STL file. The surface of the object is discretized using a polygonal mesh and cut into individual layers [40]. After checking and correcting possible errors in the STL file due to file conversion, all the individual parameters for 3D printing are selected and set. These will vary according to the type of technology adopted and the material chosen [17].

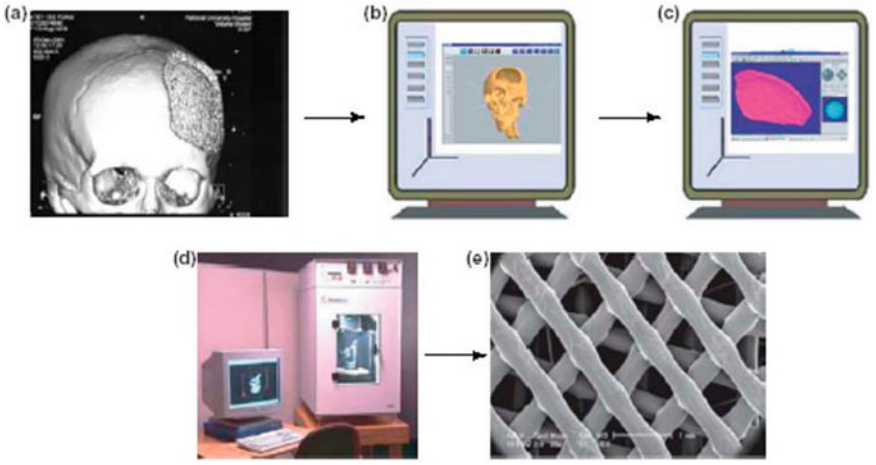

Fig. 3 Steps required for scaffold manufacturing with additive manufacturing techniques that use CAD files. **a** micro-CT imaging is used to generate a patient-specific CAD model of the bone defect. **b** This is sent to the rapid prototyping system software to be "sliced" into thin layers. **c** The "sliced" data are used as input instructions to the printing machine **d** to build a scaffold **e** according to a layer-by-layer deposition mode. Image adapted from Hutmacher et al. [36] with permission

The setting of the layer thickness is a common parameter to all additive manufacturing systems as it will determine the resolution of the object [17].

Some variants of rapid prototyping technologies do not necessarily use the CAD file as an input, but the printing instructions and path may be all provided to the manufacturing apparatus by a text file (script). A relevant example is robocasting, by which a grid-like scaffold is built through the continuous extrusion of a thin filament (until 30 μm) containing ceramic (glass) particles from a nozzle onto a building platform [41].

Over the past two decades, more than 20 different additive manufacturing techniques have been used and marketed for tissue engineering applications [33, 36], and can be divided into three large families (Fig. 4):

(1) **Light/laser-based methods:** light or laser irradiation is used to fabricate cross-linked tissue engineering polymeric scaffolds or ceramic scaffolds in which the inorganic particles are bonded together by an organic binder that polymerizes during the process [33].

A typical setup is usually composed of beam delivery optics, light source and the specific material [42]. The presence of a photoinitiator is required and must be added in small amounts to avoid toxicity [6]. Compared to other strategies, the main disadvantage of these methods is the lower cellular viability due to toxic residues, if not removed [43].

(2) **Nozzle-based methods:** the material is extruded as a filament from a robot-controlled nozzle by applying a controlled pressure [6].

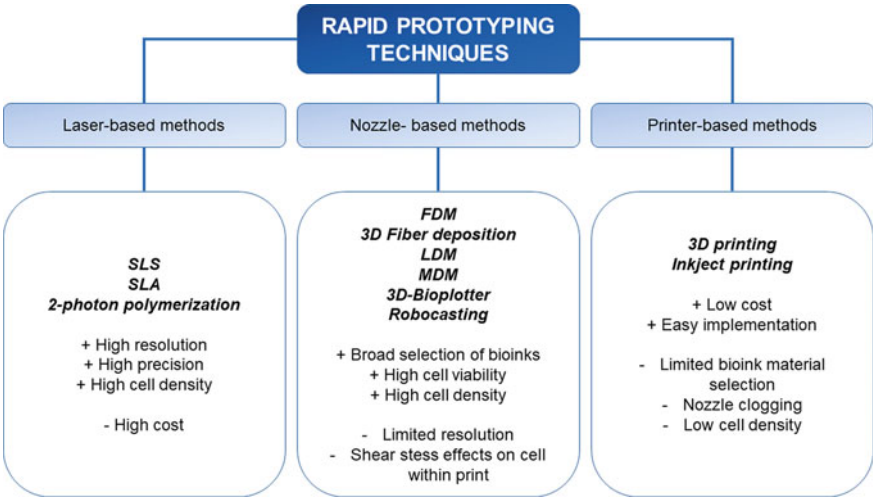

Fig. 4 Rapid prototyping techniques and their advantages (+) and disadvantages (−). Select Laser Sintering, (SLS), Stereolithography (SLA), Fused Deposition Modelling (FDM), Low-Temperature Deposition Manufacturing (LDM), Multi-nozzle deposition manufacturing (MDM)

These methods create continuous and thin streams of material that reproduce the CAD model and are directed by the software connected to the machine. Depending on the material chosen, these methods can also allow incorporating cells into the bioink. They must be subjected to low shear stress, which in turn has a positive effect on their capacity for diffusion and proliferation [6];

(3) **Printer methods:** a head prints a liquid binder onto thin layers of powder, following the design that is generated by the software [33].

Unlike nozzle-based methods, the biomaterial can be extruded as droplets and not as a continuous filament [6]. These methods use a non-contact technology based on the use of piezoelectric, thermal or electromagnetic forces to eject drops of material onto a building platform, thus replicating a CAD design [43]. Printer-based methods are relatively inexpensive and easily applicable to low-viscosity materials [6]. Based on several experiments, it can be stated that such procedures have good potential for bone tissue engineering applications [6]. However, due to frequent nozzle clogging, regular printing is difficult to achieve [6].

Resolution is often the discriminating factor determining the choice of a specific technology rather than another one. Each method has a precise lower limit on the amount of detail that is capable of reproducing [33].

Table 4 provides a comprehensive picture of the additive manufacturing techniques that are commonly used for the production of tissue engineering scaffolds.

Several types of biomaterials can be processed by additive manufacturing technologies to fabricate bone-like scaffolds, including natural and synthetic polymers, ceramics and glasses [13], and even cells (bioinks) [9].

Table 4 Comparison of different additive manufacturing technologies in bone tissue engineering (data from [1, 4, 9, 34])

Technique	Process details	Resolution (μm)	Material for BTE	Advantages	Disadvantages
SLS	Preparing the powder bed Layer-by-Layer addition of powder Sintering each layer	500	Ceramics (HA β-TCP) Polymers (PLLA PCL) Metals	No need for support No post processing	Dependency between feature resolution and laser beam diameter Low surface quality Low mechanical strength
SLA	Immersion of a platform into aphotopolymer liquid Exposure to focused light according to the desired design Layer-by-–layer fabrication	30	Ceramics (HA β-TCP, Bioactive glass) Polymers (PDLLA PPF)	Complex internal features Possible grow factors, proteins and cell patterning	Need for photopolymers High production cost Slow process
FDM	Strands of heated polymer/ceramics extrusion through a nozzle	250	Ceramics (HA TCP, Al_2O_3) Thermoplastic polymers	No need for platform/support Low production costs	Low surface quality Low resolution Low mechanical properties
3D printing	Strands of viscous material (in solution form) extrusion based on the predesigned structure Layer-by-layer deposition strands according to the tear of speed	100- 200	Ceramics (HA Bioactive glass) Polymers (PLA PEG PLGA)	Mild condition Possibility of plotting drugs and biomolecules No need for support material	Low mechanical strength Low accuracy compared to SLA Low surface quality (rough surface)
Robocasting	Direct writing of liquid using a small nozzle while a nozzle is moved across a platform.Consolidation through liquid to gel transition Layer-by-layer fabrication	100–1000	HA/PLA HA/PCL 6P53B glass/PCL	Independent 3D nozzle movement Precise control on thickness No need for platform /support	Material restriction Low accuracy compared to SLA

(continued)

Table 4 (continued)

Technique	Process details	Resolution (μm)	Material for BTE	Advantages	Disadvantages
3D Fibre Deposition	The material is in a granule or pellet form Material flow is regulated by applying pressure to the syringe	250	Polymers (PEGT)	Quick process	Need for high processing temperatures
LDM	The scaffold-building cycle is performed in a low-temperature environment under 0 °C	300–500	Polymers (PLLA)	Possible incorporation of biomolecules	Use of solvents Need for freeze-drying
MDM	It is similar to LDM But in this case a greater range of materials can be used	400	Polymers (PLLA)	Enhanced range of materials Incorporation of biomolecules	Need for solvents Need for freeze-drying
3D Bioplotter	The nozzle system works pneumatically or via volume-driven injection Key difference with other nozzle-based systems is the ability to plot into a liquid medium with matching density	45- 1600	Hydrogel Polymers (PCL PLLA)	Enhanced range of materials Incorporation of biomolecules	Low mechanical strength Low accuracy Slow processing

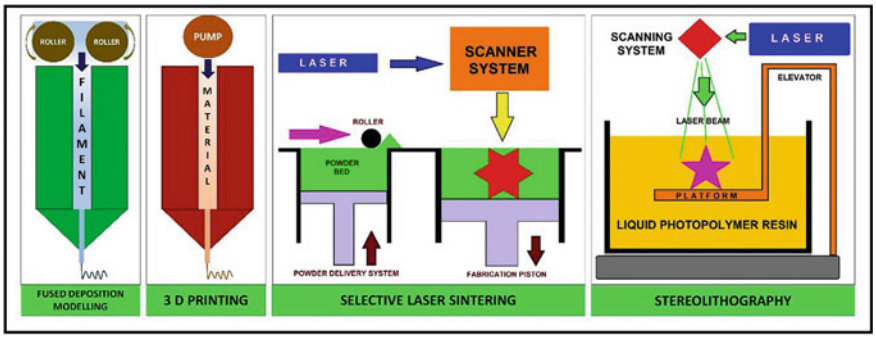

Fig. 5 Schematic representation of the principal techniques used to produce ceramic scaffolds in bone tissue engineering. Image adapted from Mondal and Pal [7] with permission

Among the techniques included in Table 4, the most suitable ones for the production of ceramic scaffolds are FDM, SLS, 3DP, robocasting and SLA, as summarized in Fig. 5.

More specifically, it is possible to divide rapid prototyping techniques for the processing of bioceramic materials into two categories:

(1) **Direct fabrication techniques:**

These techniques allow the production of sintered ceramic components without the need for subsequent thermal post-processing. According to this approach, the ceramic powders are melted using a high-energy laser [32]. However, rough surfaces are often obtained and local thermal stresses may arise. SLS technique or EBM (electron beam melting) are examples of direct techniques [32].

(2) **Indirect fabrication techniques:**

These techniques are based on three fundamental steps: 3D printing, thermal de-binding, and sintering [32]. In these techniques, the printing process does not lead to a finished product but rather to the so-called "green body", which also contains a volatile organic binder in addition to the ceramic powder [40, 44]. Post-processing is, therefore, necessary to obtain the finished object with satisfactory mechanical properties and high relative density [44]. As a result, de-binding and sintering are crucial steps for defining the final properties of the scaffold. De-binding process leads to the thermal decomposition of the binder and then, by the sintering process, a final compact product, free of organic material is obtained [44]. Techniques such as FDM, SLA or 3D printing are part of this family [32].

The accurate internal architecture of the scaffold guaranteed by rapid prototyping techniques and the choice to use ceramic materials can indeed ensure producing structures of high interest for bone tissue engineering applications.

According to the literature studies, among the available additive manufacturing technologies, SLA is one of the most promising due to the high resolution achievable and the possibility of using different kinds of ceramic materials [9]. Following

the development of microstereolithography (MSTL) and digital light process (DLP), the accuracy of the samples can be significantly improved and more complex structures can be successfully produced. Furthermore, SLA is suitable for the processing of methacrylate-based light-curing composites commonly used in clinical practice without any modifications [32].

5 Stereolithographic Methods

Among the various rapid prototyping techniques that can be used with ceramic materials, stereolithography (SLA) ensures maximum control in creating structures with a detailed and precise internal geometry and a high surface finish [1]. Developed in 1986 by Chuck Hull, who is considered the "father of 3D printing", SLA is one of the first techniques to appear on the market [1]. Since then, SLA has been widely used in bone tissue engineering for the production of hydroxyapatite, β-TCP, zirconia, alumina, and bioactive glass scaffolds [1].

5.1 Processing

SLA is an additive manufacturing process using a bath of UV-curable photosensitive liquid, an ultraviolet (UV) laser to build 3D structures layer-by-layer, a movable platform and a dynamic mirror system [1, 33]. When the printing process begins, the laser beam solidifies the photosensitive liquid at the surface of the bath, thus creating the first layer; the irradiated zones are defined in accordance with the previously determined CAD model of the scaffold [36, 45]. If ceramic particles are dispersed in the liquid, it acts as a binder and, once polymerized, glues the particles together. When the irradiation of a layer ends, depending on the configuration of the machine (top-down or bottom-up system, see Fig. 6), the slurry bed is, respectively, raised or lowered by an elevator platform.

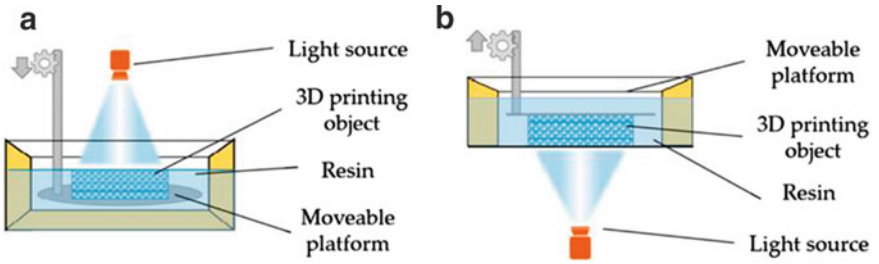

Fig. 6 Stereolithography with **a** bottom-up system; **b** top-down system. Image. Reproduced from Mao et al. [46] under the Creative Common Attribution Licence (CC BY 4.0)

Most SLA apparatuses use the bottom-up system; in this case, the platform moves down so that the new material can cover the newly formed layer, and the laser cures a new layer over the previous one [1]. In the second system, the platform moves upwards and the vat must be completely transparent [9]. The latter has a few more advantages compared to the bottom-up system, first of all, the demand for a smaller amount of raw material [9].

The displacement along the z-axis and the irradiation depth determine the thickness of each single layer, and thus the surface resolution of the final object [1]. Exposure to the UV laser light solidifies the pattern traced on the slurry and allows it to adhere to the layer below [33]. The subsequent deposition of adjacent layers leads to the building of the 3D object characterized by a highly resolved solid structure [47].

5.2 The Slurry: Composition and Characteristics

Long-term stability and suitable rheological behaviour are two of the most relevant characteristics that a ceramic slurry should exhibit to achieve a smooth printing flow [1]. Most of the slurries used are non-aqueous suspensions, because water-based suspensions usually give rise to weak structures; it is, therefore, preferable to use acrylamide resin-based slurries [1].

From a rheological point of view, slurries should exhibit Newtonian flow behaviour [48] and viscosity values should be low enough to facilitate the printing process and to avoid the formation of air bubbles [49]. Slurry viscosity is strictly dependent on the concentration of ceramic particles. In order to obtain high-quality products, the percentage of ceramic powder in green bodies should be at least 50% [49]; as the particle content increases, shrinkage decreases upon sintering, thus significantly improving the quality of the final product [40].

However, if the powder content is too high, viscosity could increase over the optimal value established for the processing of ceramic materials (3 Pa·s) [49]. Moreover, particles should be homogeneously dispersed within the organic liquid and their size should be smaller than the layer height [1].

It is possible to reduce the slurry viscosity by incorporating non-reactive "thinners" (e.g. N-methylpyrolidone) or by increasing the manufacturing temperature [40]. Moreover, the addition of some dispersant agents could be beneficial to the slurry quality, ensuring low-viscosity values and good homogeneity while keeping the solid loading high [50]. Specifically, long-chained fatty acids, phosphine oxides or oligomeric surfactants can reduce particle agglomeration, thereby decreasing viscosity and improving slurry stability and density [40].

Transparency to UV light is another key requirement in order to achieve the desired light penetration depth. In fact, if the slurry is not transparent enough, light penetration will be attenuated, resulting in a considerable cure depth decrease. If required, absorbant agents for visible or UV light could be added in order to limit the cure depth, thus avoiding an excessive polymerisation along the z-axis [40].

5.3 The Photopolymerization Process: Chemical Basis

When the ceramic powder, monomer, and photoinitiator are exposed to UV light, the photoinitiator generates cation species or free radicals attacking the double bonds of the monomer and triggering polymerization [49]. The subsequent reactions between the monomer and the active end of the chain allow the polymeric chains to increase their length until a termination reaction occurs [49].

Two different types of photopolymerization can occur: cationic polymerization or radical polymerization. The latter is generally preferred in SLA processes because it is easier to control [49].

During radical polymerization, the photoinitiator divides and generates radical species. These radicals are extremely reactive and immediately attack the double bonds of the monomer [49]. The main steps of radical polymerization are given below [49]:

$$\text{Initiation } PI \xrightarrow{hv} R \tag{1}$$

$$\text{Propagation } R \cdot + M \rightarrow R(M)_{n\cdot} \tag{2}$$

$$\begin{gathered}\text{Termination } R(M)_{n\cdot} + R(M)_{m\cdot} \rightarrow R(M)_{n+m} \cdot R \\ R(M)_{n\cdot} \rightarrow R)(M)_n\end{gathered} \tag{3}$$

hv.

M = monomer, R = radical, PI = photoinitiator.

For radical photopolymerization, acrylate functionalized monomers (e.g. cured acrylated epoxy, acrylated polyester and acrylated urethane) and telechelic oligomers are usually used due to the rapid rate of their polymerization [49]. Acrylates are often combined with methacrylates to decrease shrinkage during curing. Another method to reduce shrinkage and speed up curing may be a combination of acrylate and epoxy-based resins [40]. The photopolymer acts as a binder between the ceramic powder, making it possible to accurately manufacture the part [44].

The kinetic of reaction and the mechanical properties of the final structure are significantly affected by the quantity of photoinitiator and its selection has to be based on the nature of the monomers used. It has been reported that, as the photoinitiator concentration increases, the polymerization speed and the stiffness of the sample increase as well [40].

However, the quantity of photoinitiator must be limited as their intrinsic cytotoxicity could be harmful to tissue ingrowth and regeneration; for example, photoinitiators for cationic polymerization form strongly acidic protons (H^+) and it is therefore preferable not to use them for biomedical applications. For this reason, radical photoinitiators are usually preferred, although serious DNA damages could occur if not properly dosed [40]. A commonly used low-toxicity photoinitiator is Irgacure 2959 [40].

5.4 Key Parameters for the Photopolymerization Process

Some important parameters need to be set and controlled in order to obtain a good light-curing slurry for printing, as described in the following sections.

5.4.1 Energy of the UV Laser

The energy of the UV source can be calculated as the product between the intensity of the UV light beam and the exposure time [51]. The incident energy dose must be adjusted in order to achieve the correct depth of cure, coinciding with the desired layer thickness [51].

For a single-mode laser beam, the intensity follows a Gaussian distribution [51]. A Gaussian beam of peak intensity I_{max} and width w^2_{Gauss} has an actual distribution of intensity at the surface ($z = 0$) which varies along the y-axis, according to Eq. (4):

$$I_0(y, z = 0) = I_{max} \exp\left(\frac{-2y^2}{w^2_{Gauss}}\right) \tag{4}$$

where z represents the depth from the surface of the suspension and y is the distance from the centre of the beam.

The incident energy dose (E_0) can be calculated as t·I (t illumination time, I intensity) (5):

$$E_0(y, z = 0) = t \cdot I_{max} \exp\left(\frac{-2y^2}{w^2_{Gauss}}\right) \tag{5}$$

At any point, the incident energy dose ($E(z)$) can be estimated by Beer–Lambert's law, which states that the energy dose is attenuated logarithmically as a function of depth (z), according to Eq. (6) [51]:

$$E(Z) = E_0 \exp\left(\frac{-z}{S_d}\right) \tag{6}$$

where E_0 is the dose of incident energy on the surface and S_d is the resin sensitivity in the depth direction.

The energy dose could be estimated by Eq. (7):

$$E(Z) = E_{max} \exp\left(\frac{-2y^2}{w^2_{Gauss}}\right) \exp\left(\frac{-z}{s_d}\right) \tag{7}$$

where E_{max} is the maximum dose of energy.

The polymerization of the slurry will take place at every point in which the energy dose is greater than or equal to the critical energy dose necessary for polymerization to take place (E_d) [51]: polymerization in the cross-section must then take place at points (y*, z*), where $E(y^*, z^*) = E_d$.

We will thus obtain a parabolic curve shape given by Eq. (8) [51]:

$$\ln\left(\frac{E_{\max}}{E_d}\right) = \left(\frac{-2y^2}{w_{Gauss}^2}\right)\exp\left(\frac{z^*}{s_d}\right) \tag{8}$$

5.4.2 Penetration Depth (D_p)

The penetration depth of the laser beam (D_p) is defined as the depth where intensity is reduced by 1/e of the beam intensity measured at the bath surface [45, 47]. D_p depends on the size and quantity of the ceramic particles [49] and the difference in refractive index between the UV curable solution and the ceramic powder [52]. Once E_d and D_p are determined, it is possible to properly choose the laser beam power and the scanning speed [53].

A good slurry for SLA is usually characterized by high D_p values, in order to minimize the layer thickness, and low E_d so that the polymerization reaction can be initiated with a low energy dose [54].

5.4.3 Cure Width (C_w) and Cure Depth (C_d)

The curing width (C_w) is always greater than the diameter of the laser beam due to dispersion phenomena caused by the presence of ceramic particles [55].

Cure depth (C_d) is defined as the maximum depth at which the material receives sufficient light to reach the gel point [49], forming a three-dimensional gel network during light-curing [47]. The gel point indicates the transition of the slurry from visco-plastic (pre-gel) to rigid-elastic (post-gel) behaviour [56]. C_d must be at least equal to the layer thickness [56] and, if the polymerization depth is too large, loss in spatial resolution could be observed.

C_d can be related to the parameters of Beer–Lambert's law according to Eq. (9):

$$C_d = S_d \ln\left(\frac{E_0}{E_d}\right) \tag{9}$$

It is essential to understand how the composition of the slurry influences the relationship between C_d and energy dose in order to obtain photopolymerizable slurries [56]. A compromise between these two parameters must be established so that products with both satisfactory spatial resolution and low manufacturing times can be obtained [51]. High C_d values require high energy density but guarantee an optimization of the working time; on the contrary, a good resolution would require low energy density [55].

It has been confirmed that, by varying the concentration of the ceramic powder, the particle size, and the refractive index, both C_d and C_w could be properly modified, according to the needs [51].

The curing rate increases as the ratio of the refractive index between ceramic particles and polymeric binder decreases. The ceramic powder scatters light, thus decreasing the resolution and cure depth, and increasing printing time [1]. Smaller particles generally have better light scattering properties [1].

Gentry and Halloron have shown that when the refractive index of the precursor monomer corresponds to the refractive index of the ceramic powder, there is an improvement in curing depth [49].

Light scattering effects lead to the polymerization of an area larger than the predetermined area: this effect is called overgrowth [57].

C_d also depends on how much photoinitiator is used for slurry preparation: if the photoinitiator concentration is high, C_d decreases [47].

5.5 Post-processing

Unlike SLS and other direct techniques, where the ceramic material is shaped and sintered in a single step, SLA requires a further step called post-processing once printing is concluded. In fact, the so-called "green body" resulting from the printing process still has to be consolidated by thermal treatments to be transformed into a ceramic part [44, 57].

Besides the ceramic powder (typically ~ 60%), the "green body" still contains a volatile organic matrix which must be eliminated [40, 44]. The post-processing stage involves three fundamental steps: cleaning and drying of pieces from uncured slurry, de-binding and sintering. During de-binding, the binder is thermally decomposed: organic residuals slowly degrade, leaving behind only the loosely compacted ceramic powder [44]. During de-binding, the temperature increase must be slow and constant to avoid the formation of internal stresses which can result in the formation of cracks within the structure [44]. The de-binding temperature and time required depend on several factors, such as quantity of organic components, composition of organic components, size and distribution of ceramic particles, and percentage of solid part contained in the slurry as compared to the organic matrix [58]. Binder removal is a key stage in order to avoid contaminations that could change the properties of the final product [9].

The greens are then densified by sintering to form the final ceramic scaffold [44]. The high-temperature sintering process is usually carried out between 50 and 75% of the melting temperature of the material [9]. Usually, the higher the sintering temperature, the more resistant the final scaffold [7]. However, if the porosity of the sintered scaffold remains too high, the mechanical properties may be affected significantly anyway [9]. During sintering, the scaffold inevitably undergoes volumetric shrinkage [9] that must be carefully considered and preferably estimated before printing at the design stage [32].

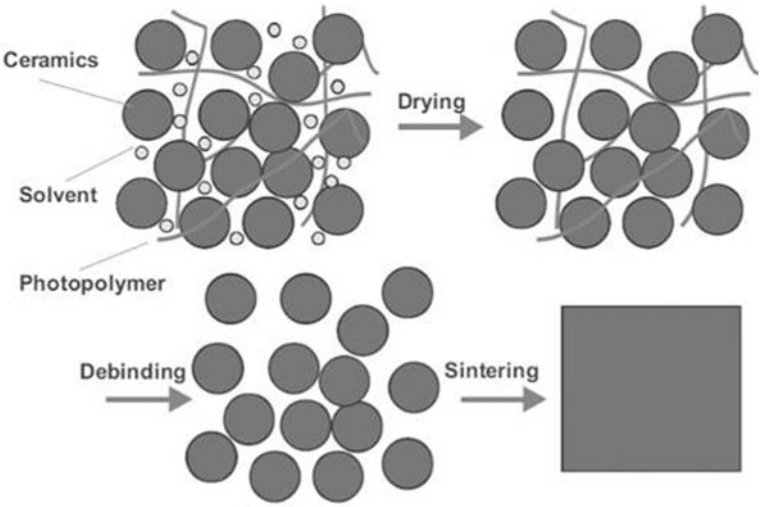

Fig. 7 Main steps of post-processing from the ceramic green body to the sintered dense ceramic. Image reproduced from Lantada et al. [44] under the Creative Commons Attribution Licence (CC BY 3.0)

The main steps of the post-processing are shown in Fig. 7.

In order to minimize shrinkage and increase shape accuracy, the slurry should have a high ceramic particle content (solid loading); however, this can cause the formation of cracks due to gases that are unable to reach the surface of the scaffold, creating a strong internal pressure [1]. The sintering process can be facilitated by applying an external pressure (sintering under pressure). On the contrary, if no external pressure is applied, the sintering is called "sintering without pressure" (or conventional or pressureless sintering) [9].

5.6 SLA: Advantages and Disadvantages

Some more advanced variants, such as microstereolithography (μ-SLA) and two-photon polymerization (TPP), allow an even better quality resolution compared to conventional SLA [9].

With μ-SLA, the thickness of a layer can be decreased up to 10 μm [9], whereas TPP is even capable of achieving a resolution of less than 0.1 μm [40]. The resolution of a standard SLA layer depends on the elevator layer resolution (up to 1.3 mm) and laser spot size (80–250 mm) [36].

Products made by SLA are usually robust and can be used as master patterns for thermoforming, selection moulding, as well as in various metal casting processes [33]. However, this process often has high processing costs: the photo-curable resin can cost from $300 to $800 and an SLA apparatus can cost from $100.000 to more than $500.000 [33].

If the product is very large, point-by-point polymerization of the cross-section of each layer can be very time-consuming, thus making the process computationally long and demanding [40].

In summary, the main parameters that influence the success of SLA printing include type and concentration of monomer, volume ratio between ceramic powder and organic components, chemical interaction between ceramic powder and organic components, viscosity of the slurry, laser beam power, optimization of de-binding and sintering steps, and time of exposure to light [1].

6 The Latest Frontier: Digital Light Processing (DLP)-Based Stereolithography

Recently, a new method based on the SLA technique has been proposed, which allows a considerable reduction in production time. Digital light processing (DLP)-based SLA is an innovative and very efficient rapid prototyping technology particularly appreciated for the production of calcium phosphate scaffolds for bone tissue engineering. Besides its high speed, DLP guarantees an excellent resolution of the final product [59] and reduces the stress to which samples are subjected during processing [60].

The term DLP refers to digital mirror devices that, when properly controlled, selectively expose the photosensitive resin to visible or UV light [61]. The manufacturing process is similar to the classical SLA: the DLP builds complex 3D layer-by-layer structures and the geometry of the various layers is previously determined by cutting the design CAD model on a series of horizontal planes at close range [45]; the operator is also able to set all printing parameters according to the slurry curing characteristics [57]. The major difference compared to classical SLA is the use of a series of computer-programmable arrays of digital micro-mirror devices (DMD) [45], which allow the simultaneous irradiation of the entire desired cross-section [40, 59].

6.1 System Setup

The main components of the DLP system include the digital micro-mirror devices (DMD), a projection lens, a vat containing UV curable resin, a UV light source, and a motorized translation stage. The setup can be implemented in two different ways: a free-surface approach or top-down projection (Fig. 8a) and a constrained surface approach or bottom-up projection (Fig. 8b) [40, 62].

In a free-surface approach, the light exposure is from above and the building platform is immersed in a slurry bath. After the polymerization of a layer, the z-stage is lowered into the resin tank and the new material successively coats the growing part [45].

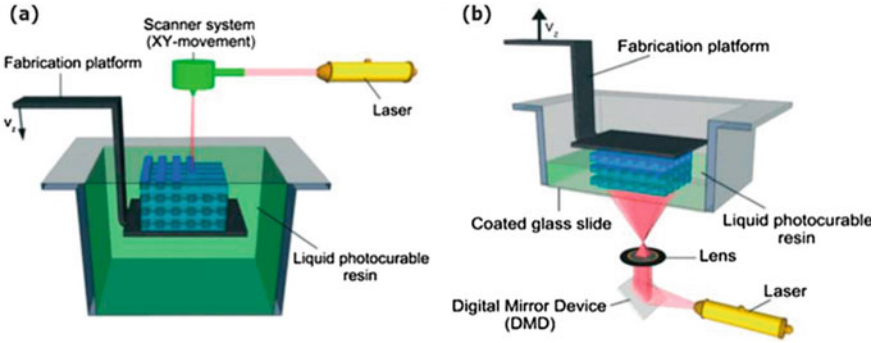

Fig. 8 DLP setup for **a** free-surface approach (top-down) and **b** constrained surface approach (bottom-up). Figure adapted from Ko et al. [62] under the terms of the Creative Commons CC BY license

If a constrained surface approach is adopted, the slurry is illuminated from below through a transparent vat. After the polymerization of each layer, the building platform is raised by a distance equal to the thickness of the individual layer. In this way, the liquid slurry can flow into the cavity and the next layer is created [62].

A constrained surface approach is often preferred as it guarantees certain advantages over the other method, including increased motion accuracy of the z-stage down to precisions of 0.1–1 μm which ensures a smooth surface and precise layer thickness [40], and the possibility of adding new liquid slurry if needed through a pump (fresh material supply is always guaranteed, even for large jobs) [62].

Furthermore, the layer created is not directly exposed to air, allowing faster light-curing [62], and the structure under construction is not completely submerged in the vat, which considerably reduces the amount of material required and, consequently, the cost of production [40].

It is important for the newly created layer not to remain attached to the surface of the vat, but to properly adhere to the previous layer, and for the whole structure to remain firmly attached to the building platform throughout the process. In order to promote the attraction forces between the scaffold and building platform and reduce the attraction forces between scaffold and vat surface, the vat is coated with hydrophobic films, such as polytetrafluoroethylene (PTFE) or polydimethylsiloxane (PDMS) [62].

Furthermore, it is necessary to pay attention to any curved surfaces during printing: the DLP process is particularly suitable for illuminating geometries with 90° angles and may carry the risk of creating saw-tooth roughness when illuminating curved structures [40].

6.2 Digital Micro-mirror Device (DMD)

Digital micro-mirror device (DMD) is the key component of the DLP process. A microelectromechanical system (MEMS) acts as a dynamic mask when connected to the computer [40].

The chip was developed at Texas Instruments in 1987 and consists of an array of reflective aluminium micro-mirrors [45]. Each mirror is fixed on top of a yoke and hinge system on a silicon memory cell, creating a single pixel [40]. If a sufficiently high polarization voltage is applied, the electrostatic attractions bring the mirrors into an unbalanced position of $< 10°$ or $> 10°$ with respect to the position of equilibrium [63]. The address voltage determines in which direction the mirror is tilted [40]. If the micro-mirror is in the condition of $< 10°$ ("tilt on"), the light from the light source is reflected in the projection lens and the image is created [63]. When it is in the condition of $> 10°$ ("tilt off"), the light is not reflected but is collected by a light absorber [63]. Generally, a DMD chip contains more than 442.000 switchable mirrors [63].

The use of the DMD provides many advantages: first, the large number of micro-mirrors allows a better and more uniform intensity of the light [45] and the pixels, being reduced in size, allow a higher resolution of the display [45]. Furthermore, ultra-flat aluminium micro-mirrors permit successful modulation of the UV illumination [45]. There is also greater control over exposure time: this is particularly important so that the modulation of the grayscale intensity can occur at pixel level [45].

In summary, the DLP process exhibit interesting advantages as compared to other rapid prototyping techniques, including high spatial resolution due to the small size/large number of pixels [50], no need for special environmental conditions during processing [61], and high processing speed. As regards the last point, the use of dynamic masks, which allow the polymerization of an entire cross-section at once, drastically reduces the fabrication time regardless of the shape, size and complexity of the structure to be reproduced [61]. The high speed of the process not only carries an economic advantage but is a fundamental requirement when working with partially stable resins that necessarily require fast processing times [40]. By using the constrained surface approach, the amount of material required is much smaller compared to the free-surface approach and this further contributes to lower production costs [61].

Nonetheless, there are also some critical aspects about this technique, including undesirable diffusion of light through the previously formed layers, which might cause uncontrolled polymerization and occlusion of the pore [64], and the need for properly controlling the curing depth of the UV light in order to avoid loss of resolution [64].

7 Current Applications of SLA- and DLP-Derived Ceramic Scaffolds

In recent years, conventional SLA and DLP processes have established themselves as successful techniques for the manufacturing of ceramic scaffolds, owing to the possibility of producing dense, precise and high-strength ceramics [65]. These techniques allow greater flexibility in the realization and modification of designs; samples can be quickly tested and readjusted and parts with precise characteristics can be created [65]. These attractive properties have allowed obtaining good results not only in bone tissue engineering but also in dentistry and craniomaxillofacial procedures [65]. Additive printing based on SLA and high-resolution DLP allow fabricating ceramic products with theoretical densities higher than 99.8%, good mechanical properties, and homogeneous, precise and highly reproducible microstructure [65].

A wide range of ceramic materials can be processed, such as zirconia (ZrO_2), alumina (Al_2O_3), calcium phosphates and hydroxyapatite [65]. Ronca et al. developed a composite shelf applying SLA to nano-hydroxyapatite and poly-(DL-lactide). Due to the presence of hydroxyapatite, the scaffold had a higher structural strength and better biocompatibility with bone cells [37].

Brie et al. created pure hydroxyapatite scaffolds by SLA and implanted them in the skull of 8 human patients. After a 12-month follow-up, these scaffolds did not cause any complications and a perfect continuity between host tissue and the implant was observed [37].

Mangano et al. showed that biphasic calcium phosphate scaffolds made by SLA had better characteristics than scaffolds obtained via foaming and traditional sintering. Porous cylindrical scaffolds were composed of 30% of hydroxyapatite and 70% β-TCP in order to find the right balance for bone regeneration favoured by the rapid resorption of β-TCP and low resorption of hydroxyapatite [66]. The scaffolds obtained by SLA were more effective in mimicking the porous trabecular organization of the maxillary bone characterized by high interconnectivity of void spaces. SLA-moulded specimens had a higher final strength with a smaller plastic region. An average compressive of about 6.4 MPa and a total compressive deformation of about 3.6% were recorded prior to achieving material fracture [66].

Hydroxyapatite cylindrical scaffolds were fabricated through DLP by Tesavibul et al. The samples had a geometry comparable to that of the original CAD model (11.3 mm diameter and 3 mm thickness). The density of the solid skeleton reached 91% of the theoretical one and the scaffold compressive strength was 0.36 MPa; the average pore size was between 500 and 700 μm. Good results were obtained from in vitro biocompatibility tests: after 14 days, pre-osteoblastic MC3T3-E1 cells seeded on the scaffolds began to proliferate and differentiate into an osteoblastic lineage [67].

Several studies for the production of scaffolds using bioresorbable ceramics were recently made by Lithoz GmbH (Austria) using their own CeraFab DLP process system. In 2019, β-TCP-based bone tissue engineering shelves were printed in different geometries (hexagonal Kagome, rectilinear Grid, Schwarz primitive, and

hollow Schwarz architecture) to evaluate the best compromise between porosity and mechanical properties [59]. The rectilinear grid structure showed a compressive strength of 44.7 MPa (Weibull modulus 5.28) with 50 vol.% porosity [59].

Despite the good results that are being obtained towards "ideal" tissue engineering scaffolds, pore microstructure defects, rheological properties of the slurry, correct sintering temperature and satisfactory mechanical properties are still partially open issues that need to be improved [68]. In any case, the various studies have shown that it is almost always possible to obtain scaffolds with high relative density and excellent cell biocompatibility. The main property that should be improved is the compressive strength of the sample, often too low for the requirements of bone scaffolds. For example, 45S5 Bioglass® scaffolds obtained by the DLP process have a lower compressive strength than porous glass foams produced by sponge replication [69].

Table 5 collects a selection of studies found in the literature and the main characteristics of scaffolds printed with classical SLA or DLP techniques.

8 Conclusions

In order to overcome the intrinsic drawbacks of natural grafts (transplant materials), during the past decades bone tissue engineering focused on the development of man-made ceramic scaffolds. These synthetic grafts aim at providing the same function as ECM, thus ensuring cellular activity, adequate mechanical support and proper mechanical and biochemical interactions with cells and proteins. In order to perform these tasks, the scaffold must be carefully designed: in fact, it is not sufficient to choose a biocompatible material, but a minimum degree of porosity (50–60 vol.%), pore interconnectivity and adequate surface characteristics should be achieved to promote effective osteogenesis.

Over the years, many techniques have been developed and improved for this purpose, and additive manufacturing technologies allow obtaining scaffolds with a highly reproducible and customizable structure. These methods rely on the reproduction of CAD files and are able to build 3D porous scaffolds with well-controlled structural properties. Among the various additive manufacturing techniques, SLA is very suitable to be used with ceramic materials, ensuring a very high resolution and ease of processing. At present, this technique has been further improved by replacing UV laser with a new lighting method, called DLP, that is based on a DMD consisting of millions of mirrors and is able to reduce processing time without affecting the spatial resolution. Processing bioceramics with SLA strategies is a winning combination leading to produce high-quality and accurate scaffolds that can be used to manage both small and large bone defects even in load-bearing anatomical sites.

Table 5 Overview of bioceramic scaffolds fabricated by SLA/DLP process

Reference	Material	Scaffold geometry	Technique	Scaffold properties
Mangano et al. [66]	Biphasic calcium phosphate (70% β-TCP/ 30% hydroxyapatite)	Porous cylinders	SLA	– Pore size: 100 μm – Compressive strength: 6.4 MPa – Biocompatible (cell-culturing with MC3T3-E1 pre-osteoblasts)
Tesavibul et al. [67]	Hydroxyapatite	Porous cylinder	DLP	– Relative density: 91% – Pore size: 500–700 μm – Biocompatible (cell-culturing with MC3T3-E1 pre-osteoblasts)
Schimidleithner et al. [59]	TCP	Grid structure	DLP	– Relative density: 99.5% – Pore size: 400 μm – Porosity: 50 vol.% – Compressive strength:44.7 MPa and Weibull modulus: 5.28 – Biocompatible (cell-culturing with MC3T3-E1 pre-osteoblasts)
Yao et al. [68]	Hydroxyapatite	Cubic structure ($10 \times 10 \times 10$ mm^3)	DLP	– Relative density: 95.85% – Shear viscosity < 3.7 Pa·s
Ghayor et al. [70]	TCP	15 scaffolds with different defined pore/bottleneck dimensions and distributions	DLP	– Pore size: 700–1200 μm

(continued)

Table 5 (continued)

Reference	Material	Scaffold geometry	Technique	Scaffold properties
Zeng et al. [60]	Hydroxyapatite	Square pore structure (21 × 21 × 3 mm^3)	DLP	– Compressive strength (z-direction): 11.8 MPa – Compressive strength (x-direction): 5.1 MPa – Biocompatible (cell-culturing with MC3T3-E1 pre-osteoblasts)
Tesavibul et al. [69]	45S5 Bioglass®	Cylindrical cellular structure (d = 9.8 mm; h = 11.6 mm)	DLP	– Pore size: 500 μm – Compressive strength of the cellular structure: 0.33 MPa
Liu et al. [71]	Hydroxyapatite	Porous rectangular scaffold (L = 10 mm; h = 20 mm)	DLP	– Pore size: 300–600 μm – Relative density: 94.9% – Porosity: 49.8 vol.% – Bending strength: 41.3 MPa – Compressive strength: 15.25 MPa – Biocompatible (cell-culturing with MC3T3-E1 pre-osteoblasts)
Feng et al. [72]	Hydroxyapatite (45 vol.%)	Porous cylindrical scaffold (d = 11.8; h = 14.2)	DLP	– Relative density: 66.6% – Flexural strength: 10.0 MPa – Compression strength: 12.0 MPa
Cao et al. [73]	ZrO_2 / hydroxyapatite	Porous rectangular scaffold (L = 7.5 mm; h = 15 mm)	DLP	– Compressive strength (hydroxyapatite 10 wt.%): 52.25 MPa – Biocompatible (cell-culturing with MC3T3-E1 pre-osteoblasts)

References

1. Lin K, Sheikh R, Romanazzo S, Roohani I (2019) 3D printing of bioceramic scaffolds-barriers to the clinical translation: from promise to reality, and future perspectives. Materials (Basel) 12(7):1–20
2. Gerhardt LC, Boccaccini AR (2010) Bioactive glass and glass-ceramic scaffolds for bone tissue engineering. Materials (Basel) 3(7):3867–3910
3. Dorozhkin S (2011) Medical application of calcium orthophosphate Bioceramics. Bio 1(1):1–51
4. Yeong W-Y et al (2004) Rapid prototyping in tissue engineering: challenges and potential. Trends Biotechnol 22(12):643–652
5. Rezwan K, Chen QZ, Blaker JJ, Boccaccini AR (2006) Biodegradable and bioactive porous polymer/inorganic composite scaffolds for bone tissue engineering. Biomaterials 27(18):3413–3431
6. Zhang L, Yang G, Johnson BN, Jia X (2019) Three-dimensional (3D) printed scaffold and material selection for bone repair. Acta Biomater 84:16–33
7. Mondal S, Pal U (2019) 3D hydroxyapatite scaffold for bone regeneration and local drug delivery applications. J. Drug Deliv. Sci. Technol. 53:1–11
8. Jazayeri HE et al (2018) The cross-disciplinary emergence of 3D printed bioceramic scaffolds in orthopedic bioengineering. Ceram Int 44(1):1–9
9. Baino F et al (2019) Processing methods for making porous bioactive glass-based scaffolds—A state-of-the-art review. Int J Appl Ceram Technol 16(5):1762–1796
10. ASTM International Standard Guide for Characterization of Ceramic and Mineral Based Scaffolds used for Tissue-Engineered Medical Products (TEMPs) and as Device for Surgical Implant Applications and ASTM Standard F2883 - 11, "Standard Guide for Characterization of Ceramic and Mineral Based Scaffolds used for Tissue-Engineered Medical Products (TEMPs) and as Device for Surgical Implant Applications," ASTM B. Stand., no. January 2012, pp 1–7, 2011
11. Murphy CM, O'Brien FJ, Little DG, Schindeler A (2013) Cell-scaffold interactions in the bone tissue engineering triad. Eur. Cells Mater. 26:120–132
12. Amini AR, Laurencin CT, Nukavarapu SP (2012) Bone tissue engineering: Recent advances and challenges. Crit Rev Biomed Eng 40(5):363–408
13. Seol YJ, Park DY, Park JY, Kim SW, Park SJ, Cho DW (2013) A new method of fabricating robust freeform 3D ceramic scaffolds for bone tissue regeneration. Biotechnol Bioeng 110(5):1444–1455
14. Turnbull G et al (2018) 3D bioactive composite scaffolds for bone tissue engineering. Bioact. Mater 3(3):278–314
15. Babaie E, Bhaduri SB (2018) Fabrication aspects of porous biomaterials in orthopedic applications: a review. ACS Biomater Sci Eng 4(1):1–39
16. Doi K et al (2012) Development of implant/interconnected porous hydroxyapatite complex as new concept graft material. PLoS One 7(11) 1–10
17. Martinez-Marquez D, Mirnajafizadeh A, Carty CP, Stewart RA (2018) Application of quality by design for 3D printed bone prostheses and scaffolds 13(4)
18. Denry I, Kuhn LT (2016) Design and characterization of calcium phosphate ceramic scaffolds for bone tissue engineering. Dent Mater 32(1):43–53
19. Henkel J et al (2013) Bone Regeneration based on tissue engineering conceptions-A 21st century perspective. Bone Res. 1:216–248
20. Du X, Fu S, Zhu Y (2018) 3D printing of ceramic-based scaffolds for bone tissue engineering: an overview. J Mater Chem B 6(27):4397–4412
21. Chen QZ, Thouas GA (2011) Fabrication and characterization of sol-gel derived 45S5 Bioglass®-ceramic scaffolds. Acta Biomater 7(10):3616–3626
22. Boccaccini AR, Erol M, Stark WJ, Mohn D, Hong Z, Mano JF (2010) Polymer/bioactive glass nanocomposites for biomedical applications: a review. Compos Sci Technol 70:1764–1776

23. Szustakiewicz K et al (2019) The influence of hydroxyapatite content on properties of poly(L-lactide)/hydroxyapatite porous scaffolds obtained using thermal induced phase separation technique. Eur Polym J 113(January):313–320
24. Maquet V, Boccaccini AR, Pravata L, Notingher I, Jérôme R (2004) Porous poly(α-hydroxyacid)-bioglass composite scaffolds for bone tissue engineering. Biomaterials 25(18):4185–4194
25. Degli Esposti M, Chiellini F, Bondioli F, Morselli D, Fabbri P (2019) Highly porous PHB-based bioactive scaffolds for bone tissue engineering by in situ synthesis of hydroxyapatite. Mater Sci Eng C 100:286–296
26. Bretcanu O et al (2009) Electrospun nanofibrous biodegradable polyester coatings on Bioglass®-based glass-ceramics for tissue engineering. Mater Chem Phys 118(2–3):420–426
27. Hong Y et al (2010) Preparation, bioactivity, and drug release of hierarchical nanoporous bioactive glass ultrathin fibers. Adv Mater 22(6):754–758
28. Baino F, Novajra G, Vitale-Brovarone C (2015) Bioceramics and scaffolds: A winning combination for tissue engineering. Front Bioeng Biotechnol 3(December):1–17
29. Fu Q, Rahaman MN, Sonny Bal B, Brown RF, Day DE (2008) Mechanical and in vitro performance of 13–93 bioactive glass scaffolds prepared by a polymer foam replication technique. Acta Biomater 4(6):1854–1864
30. Chen QZ, Thompson ID, Boccaccini AR (2006) 45S5 Bioglass®-derived glass-ceramic scaffolds for bone tissue engineering. Biomaterials 27(11):2414–2425
31. Tripathi G, Basu B (2012) A porous hydroxyapatite scaffold for bone tissue engineering: Physico-mechanical and biological evaluations. Ceram Int 38(1):341–349
32. Gmeiner R et al (2015) Additive manufacturing of bioactive glasses and silicate bioceramics. J Ceram Sci Technol 6(2):75–86
33. Mancuso E, Alharbi N, Bretcanu O, Marshall M, Birch MA, McCaskie AW et al (2017) Three dimensional printing of porous load-bearing bioceramic scaffolds. Proc Inst Mech Eng H 231(6):575–585
34. Bose S, Vahabzadeh S, Bandyopadhyay A (2013) Bone tissue engineering using 3D printing. Mater Today 16(12):496–504
35. Ng AMH et al (2008) Differential osteogenic activity of osteoprogenitor cells on HA and TCP/HA scaffold of tissue engineered bone. J. Biomed Mater Res - Part A 85(2):301–312
36. Hutmacher DW, Sittinger M, Risbud MV (2004) Scaffold-based tissue engineering: Rationale for computer-aided design and solid free-form fabrication systems. Trends Biotechnol 22(7):354–362
37. Hollinger JO, Einhorn TA, Doll BA, Sfeir C (2017) Rapid prototyping technology and its application in bone tissue engineering. J Zhejiang Univ B (Biomedicine Biotechnol 18(4):303–315
38. Fantini M, Curto M, De Crescenzio F (2016) A method to design biomimetic scaffolds for bone tissue engineering based on Voronoi lattices. Virtual Phys. Prototyp. 11(2):77–90
39. Giannitelli SM, Accoto D, Trombetta M, Rainer A (2014) Current trends in the design of scaffolds for computer-aided tissue engineering. Acta Biomater 10(2):580–594
40. Schmidleithner C, Master thesis additive manufacturing of Tricalcium phosphate scaffolds for bone tissue engineering. Vienna University of Technology
41. Baino F, Barberi J, Fiume E, Orlygsson G, Massera J, Vern E (2019) Robocasting of Bioactive SiO_2-$P2O_5$-CaO-MgO-Na_2O-K_2O Glass Scaffolds. J Healthc Eng 2019
42. Moesen M, Craeghs T, Kruth JP, Schrooten J (2011) Robust beam compensation for laser-based additive manufacturing. CAD Comput. Aided Des 43(8):876–888
43. Bishop ES et al (2017) 3-D bioprinting technologies in tissue engineering and regenerative medicine: Current and future trends. Genes Dis. 4(4):185–195
44. Lantada AD, De Blas Romero A, Schwentenwein M, Jellinek C, Homa J (2016) Lithography-based ceramic manufacture (LCM) of auxetic structures: present capabilities and challenges. Smart Mater Struct 25(5)
45. Sun C, Fang N, Wu DM, Zhang X (2005) Projection micro-stereolithography using digital micro-mirror dynamic mask. Sens Actuat A Phys 121(1):113–120

46. Mao Y, Miyazaki T, Sakai K, Gong J, Zhu M, Ito H (2018) A 3D printable thermal energy storage crystalline gel using mask-projection stereolithography. Polymers (Basel) 10(10):1–14
47. Lee JH, Prud'homme RK, Aksay IA (2001) Cure depth in photopolymerization: experiments and theory. J Mater Res 16(12):3536–3544
48. Griffith ML , Halloran JW (1994) Ultraviolet curable ceramic suspensions for stereolithography of ceramics. Am Soc Mech Eng Prod Eng Div PED 68–2:529–534
49. Bae CJ, Ramachandran A, Chung K, Park S (2017) Ceramic stereolithography: additive manufacturing for 3D complex ceramic structures. J Korean Ceram Soc 54(6):470–477
50. de Blas Romero et al A (2017) Lithography-based additive manufacture of ceramic biodevices with design-controlled surface topographies. Int J Adv Manuf Technol 88(5–8):1547–1555
51. Gentry SP, Halloran JW (2013) Depth and width of cured lines in photopolymerizable ceramic suspensions. J Eur Ceram Soc 33(10):1981–1988
52. Hinczewski C, Corbel S, Chartier T (1998) Ceramic suspensions suitable for stereolithography. J Eur Ceram Soc 18(6):583–590
53. Bennett J (2017) Measuring UV curing parameters of commercial photopolymers used in additive manufacturing. Addit Manuf 18:203–212
54. Scalera F, Esposito Corcione C, Montagna F, Sannino A, Maffezzoli A (2014) Development and characterization of UV curable epoxy/hydroxyapatite suspensions for stereolithography applied to bone tissue engineering. Ceram Int 40(10): 15455–15462
55. Chartier T, Chaput C, Doreau F, Loiseau M (2002) Stereolithography of structural complex ceramic parts. J Mater Sci 37(15):3141–3147
56. Halloran JW et al (2011) Photopolymerization of powder suspensions for shaping ceramics. J Eur Ceram Soc 31(14):2613–2619
57. Mitteramskogler G et al (2014) Light curing strategies for lithography-based additive manufacturing of customized ceramics. Addit Manuf 1:110–118
58. Schwarzer E, Götz M, Markova D, Stafford D, Scheithauer U, Moritz T (2017) Lithography-based ceramic manufacturing (LCM)—Viscosity and cleaning as two quality influencing steps in the process chain of printing green parts. J Eur Ceram Soc 37(16):5329–5338
59. Schmidleithner C, Malferarri S, Palgrave R, Bomze D, Schwentenwein M, Kalaskar DM (2019) Application of high resolution DLP stereolithography for fabrication of tricalcium phosphate scaffolds for bone regeneration. Biomed Mater 14(4):1–11
60. Zeng Y et al (2018) 3D printing of hydroxyapatite scaffolds with good mechanical and biocompatible properties by digital light processing. J Mater Sci 53(9):6291–6301
61. Felzmann R et al (2012) Lithography-based additive manufacturing of cellular ceramic structures. Adv Eng Mater 14(12):1052–1058
62. Ko D, Gyak K, Kim D (2017) Emerging microreaction systems based on 3D printing techniques and aeparation technologies. J Flow Chem 7:72–81
63. Lu Y, Mapili G, Suhali G, Chen S, Roy K (2006) A digital micro-mirror device-based system for the microfabrication of complex, spatially patterned tissue engineering scaffolds. J Biomed Mater Res Part A 77(2):396–405
64. Han LH, Mapili G, Chen S, Roy K (2008) Projection microfabrication of three-dimensional scaffolds for tissue engineering. J Manuf Sci Eng Trans ASME 130(2):0210051–0210054
65. Potestio I (2019) Lithoz: How lithography-based ceramic AM is expanding the opportunities for technical ceramics. Powder Inject Mould Int 13(2):2–5
66. Mangano C, Mangano F, Gobbi L, Admakin O, Iketani S, Giuliani A (2019) Comparative study between laser light stereo-lithography 3D-printed and traditionally sintered biphasic calcium phosphate scaffolds by an integrated morphological, morphometric and mechanical analysis. Int J Mol Sci 20(13)
67. Tesavibul P et al (2015) Biocompatibility of hydroxyapatite scaffolds processed by lithography-based additive manufacturing. Biomed Mater Eng 26(1–2):31–38
68. Yao Y, Sha N, Zhao Z (2019) Highly concentrated hydroxyapatite suspension for DLP printing. IOP Conf Ser Mater Sci Eng 678(1):1–8
69. Tesavibul P et al (2012) Processing of 45S5 Bioglass® by lithography-based additive manufacturing. Mater Lett 74:81–84

70. Ghayor C, Weber FE (2018) Osteoconductive microarchitecture of bone substitutes for bone regeneration revisited. Front Physiol 9:1–10
71. Liu Z et al (2019) Additive manufacturing of hydroxyapatite bone scaffolds via digital light processing and in vitro compatibility. Ceram Int 45(8):11079–11086
72. Feng C et al (2020) Additive manufacturing of hydroxyapatite bioceramic scaffolds: Dispersion, digital light processing, sintering, mechanical properties, and biocompatibility. J Adv Ceram 9(3):360–373
73. Cao Y et al (2020) Fabrication and properties of zirconia/hydroxyapatite composite scaffold based on digital light processing. Ceram Int 46(2):2300–2308

Chapter 10
3D Printable Gel-Inks for Microbes and Microbial Structures

Ecem Saygili and Mohamed S. Draz

Abstract Bioprinting and the precise engineering of cells, biological material, and structures into multidimensional tissue models are the most rapidly growing research areas in biology and medicine. 3D bioprinting of tissues holds a great promise for modeling diseases and potential treatment strategies with a far greater resolution than traditional techniques (i.e., cell culture). Notably, 3D modeling of microbes and infections provides an unparalleled opportunity to study, screen, and closely monitor diseases and understanding diseases' progression in a broader sense. The development of model tissues for microbes is, however, challenging and depends on specific parameters such as determination of optimum microenvironment conditions, selection of appropriate scaffold, and cell source. This book chapter provides an overview of state-of-the-art techniques in bioprinting and 3D modeling systems that are developed to study microbes, microbe-host interactions, biofilm formation, antibiotic resistance, and the microbiome.

1 Introduction

Microbes are everywhere, performing essential functions to sustain human life and the entire plant. Microbes can also be harmful to humans, causing various health conditions and diseases, and even death. The best way to study microbes, in both beneficial or harmful forms, is to have a means that enables visualizing and investigating them in their natural habitat, without disruption, and with minimal impact. Such tools do not exist, and the most common technique used for studying microbes is probably the cell culture. Cell culture techniques are widely used to isolate, propagate microbes, and study their interactions, pathogenicity, and mechanism of infection to

E. Saygili
Department of Bioengineering, Faculty of Engineering, Ege University, Bornova 35100 Izmir, Turkey

M. S. Draz (✉)
Department of Medicine, Case Western Reserve University School of Medicine, Cleveland, OH 44106, USA
e-mail: mxd665@case.edu

A. Kumar et al. (eds.), *3D printable Gel-inks for Tissue Engineering*, Gels Horizons: From Science to Smart Materials, https://doi.org/10.1007/978-981-16-4667-6_10

humans. However, cell culture is only useful at the cell level and cannot allow for more details at the tissue level. The ability to study the interaction of microbes as a community and in tissues rather than at the cell level can certainly reveal very useful details about the nature of these communities and how they coordinate their interaction to perform functions and establish infections.

The advances in tissue engineering and the possibility of printing microbes and cells and tissues (i.e., microbial printing) in a way that simulates its actual environment open the door for a future with a better understanding of microbial communities and their interaction with humans and the surrounding habitats. Bioprinting can play a major role in this perspective. It combines living cells and biomaterials through a computer-aided (CAD) additive manufacturing process to generate 2D and 3D engineered living mimics that simulate natural tissues and in vivo conditions and can be used for testing and culturing microbes with high repeatability and accuracy [1, 2]. The challenges are still many, and the applications of bioprinting in microbiology are yet hampered with complexities such as the selection of biomaterials, cell types, growth, and differentiation factors, and technical difficulties related to the handling of microbes and living cells (due to their sensitivity to in vitro environment). Addressing these complexities requires integrating medicine, microbiology, engineering, material chemistry, and physics [1–5]. This book chapter gives an overview of the recent techniques developed for bioprinting and 3D modeling microbes, microbial and host interactions, pathogenesis, stages of infection, the microbiome, and antimicrobial resistance. Also, we discussed the potential use of other cell culture techniques that include scaffold-free and scaffold-based 3D cultures for studying viral and bacterial infections and their impact on infected tissues.

2 Bioprinting

Bioprinting can be defined as the precise positioning and patterning of cells and supporting material to form 3D structures of living tissues. This process includes the controlled mixing of cells with optimized concentrations of biological material and biochemicals (i.e., bioink) needed by cells to grow into 3D structures. There are multiple approaches for bioprinting, including biomimicry, autonomous self-assembly, and mini-tissue building blocks, that are currently used to fabricate 3D tissue constructs with biological and mechanical properties suitable for modeling diseases [3]. It is, therefore, a prerequisite requirement for bioprinting systems to have a controlled dispensing of multiple bioinks with different viscosities while preserving cell viability. Bioprinters are usually comprised of three essential elements: (i) a robotic motor system, (ii) bioink dispensers, and (iii) computer-based software-enabled operational control to print bioink with satisfactory resolution [2, 4–7]. The bioprinting process starts by using CAD software to build a blueprint design of the target tissue or organ that is used to precisely guide the mechanical motion of a robotic system and enables the bioprinter motion in different directions (i.e., x-, y-, and z-axes) with a highly controlled resolution. This dispensing robotic system

can be pneumatic-, mechanical-, or fluidic-driven, loaded with the bioink that is deposited, solidified, and stacked layer-by-layer in the 3D bioprinting process and the post-printing step [1, 7, 8].

3 Bioprinting Techniques

Most of the technologies applied in the bioprinting process require capabilities for manipulating cells with high precision. Currently, there are three major approaches used in bioprinting: (i) layer-by-layer (stereolithographic), (ii) line-by-line (extrusion-based), (ii) droplet-based, and (iii) laser-assisted bioprinting [7].

The stereolithography (SLA) is a solid freeform, nozzle-free bio-printing method that has both high printing quality and speed and utilizes photo polymerization—a process in which a UV light or laser is directed in a pattern over a path of photopolymerizable liquid polymer, crosslinking the light-sensitive polymers into a hardened layer. SLA operates via a layer-by-layer process, where each 2D layer is entirely cured before moving to the next layer of the construct. As each layer is polymerized, the printing platform can be lowered further into the polymer solution, allowing multiple cycles to form a 3D structure [9–13]. SLA is simple and easy to use; however, its wide use is limited by the lack of biocompatible and biodegradable polymers, harmful effects from toxic photocuring reagents, and the inability of complete removal of the supporting structure. In addition, several studies have reported the inability to form horizontal gradients in the constructs using this method [9, 10].

Extrusion-based bioprinting is the most common and affordable method for biological and non-biological 3D printing and the fabrication of complex, multi-layered scaffolds, and tissue constructs. This method relies on using mechanical-, pneumatic- or solenoid micro-extrusion-driven systems to extrude the bioink, in the form of cylindrical filament-formed through a nozzle [10, 14]. It can be used for printing vertically and for high viscosity bioinks, such as complex polymers, cell spheroids, and clay-based substrates, and most importantly, for high cell density printing needed for tissue formation [10, 14]. However, they are only proper for viscous printing material, and the distortion of cellular structures and loss of viability has been reported [10, 14].

Droplet-based bioprinting methods utilize thermal-, piezo-, or acoustic-driven mechanisms to deposit droplets of cell suspension in a high-throughput manner and assembled drop-by-drop [3, 7, 11, 14]. The approaches used in droplet-based bioprinting can be classified into (i) inkjet bioprinting, (ii) acoustic droplet ejection, and (iii) microvalve bioprinting.

(i) Inkjet bioprinting. The first generation of inkjet bioprinters was a modified version of the commercially available 2D ink-based printers [3, 11, 15]. They have been popular due to their wide availability at low cost, and ability to highly precise and fast printing, and the printing of low viscose biomaterials with concentration gradients in 3D constructs [9, 10, 16]. Inkjet bioprinters are, however, have multiple

disadvantages: the inability to provide a continuous flow; improper for slow printing process; thermal, mechanical, and shearing stress on biological structures; and desiccation sedimentation of cells [9, 10, 16, 17]. Furthermore, they have poor efficiency for vertical printing, and they can print limited types of materials with low viscosity and low density of cells [9, 10]. There are different types of inkjet bioprinters: continuous, drop-on-demand (DOD), or electrohydrodynamic. In the continuous inkjet bioprinting, the pressure is applied to force the bioink through a nozzle, which subsequently breaks up into a stream of droplets to minimize its potential energy and surface tension [15, 18]. In contrast, the DOD inkjet bioprinting relies on a non-contact technique that applies thermal, piezoelectric, electrostatic, or electromagnetic forces to expel successive droplets of bioink onto a substrate [8, 18]. Moreover, DOD inkjet bioprinters are preferable to continuous bioprinters for tissue bioprinting purposes because they are cost-effective, easy to control, and accessible to design biological patterns. It is worth mentioning that DOD needs a high pressure to eject droplets through a nozzle with a small orifice diameter, which can deteriorate cells and biological material. On the contrary, electrohydrodynamic inkjet bioprinters utilize an electric field (resulting from the electrical potential difference between the print head and the substrate) to move the bioink droplets through the printhead orifice, and thus limiting the need for substantially high pressure, shearing stress, or cell damage [13, 15, 18].

(ii) Acoustic droplet ejection bioprinting. Acoustic bioprinting relies on applying an acoustic field, carefully controlled by an acoustic actuator, on ejecting droplets that contain the cell-laden bioink solution. It is a quick, easy, and viable method, in which bioink is an open pool rather than in a nozzle and picoliter quantities of the medium or hydrogel encapsulating a single cell in a droplet can be deposited. Therefore, this method preferentially eliminates the exposure of cells to detrimental heat, mechanical stress, pressure, and high voltage [15, 18–20]. However, viscous bioinks are not dispensable, and there is not an intact ready-to-use commercial system available [13, 15].

(iii) Microvalve bioprinting. In microvalve printers, the bioink solution is under constant pneumatic pressure and dispensed from cartridge tips by opening and closing a small valve. Interchangeable electromechanical/solenoid valves are commonly used to generate droplets of cell-laden bioink by applying a voltage pulse to the valve [15, 16, 18, 20], and thus allows for printing bioink with a wide range of printable viscosity through controlling the pressure and gating time [16]. The microvalve bioprinting method is reliable, cheap, and the cell damage because of high shear stress on cells during droplet ejection is limited. But it suffers from cell sedimentation and the formation of large droplets (50–300 μm), leading to a lower printing resolution [15].

Laser-assisted bioprinting utilizes laser energy to selectively print and precisely pattern cells onto a substrate without the need for a nozzle [7, 9, 10, 16]. Laser-assisted printing was initially developed to pattern metals (i.e., computer chip fabrication) with high resolution [14]; it uses laser pulses to heat and deposits bioactive contents

(e.g., growth factors, cells) onto a scaffold with biomaterials and in a wide range of viscosity [10, 16]. However, this method is costly and slow. It can cause thermal damage due to nanosecond/femtosecond laser irritation and toxic effect on the cells because of the needed metal film [9, 10, 16]. Moreover, because of the nonuniform thickness of the transparent layer (ribbon), cell homogeneity is limited, and it is challenging to incorporate multiple types of biological material [16].

4 Bioprinting Materials

Bioprinting with different types of materials, including. Bioinks are a distinct class of biomaterials made up of cellular material, additives (such as growth factors and signaling molecules), and supportive scaffolds, i.e., artificial extracellular matrix (ECM) to provide structural and functional support for the cells and tissue constructs [14, 21]. Bioink material needs to possess certain characteristics such as specific fabrication temperature, gelation (cross-linking) kinetics, swelling, bioactive components, biocompatibility, bioprintability, affordability, scalability, practicality as well as resolution, mechanical/structural integrity, bioprinting/post-bioprinting maturation times, and biodegradability [13].

Hydrogels are generally considered an ideal material that mimics the physiological ECM naturally exists in the body. Hydrogels have high water content, high permeability to oxygen, nutrients, and other water-soluble compounds, the ability to protect cells/drugs, and to be modified with specific ligands to create an environment for cell adhesion/proliferation [14, 21, 22]. In addition, hydrogel-based bioink materials should have specific properties such as shape fidelity, zero-shear viscosity, controlled crosslinking to facilitate bioprinter deposition, suitable swelling characteristics, and short-term stability [21]. These properties are essential to ensure that tissue structures such as pores, channels, and networks do not collapse [3]. During bioprinting, a hydrogel with suspended cells is processed into a precisely defined shape, which is successively fixed by gelation, a physical crosslinking reaction depends on meshes of high molecular polymer chains, ionic interactions, and hydrogen bridges because of compatibility with biological systems, such as growth factors and living cells [2, 13].

Natural-derived hydrogels, such as matrigel, collagen, gelatin, gelatin methacryloyl (GelMA), fibrin, alginate, chitosan/chitin, hyaluronic acid (HA), are among the heavily utilized bioprinting materials due to their biocompatibility. For instance, bioprinted ECM- and collagen-based cardiac tissue construct [23] (Fig. 1a), agarose-based bioink for 3D tubular structure [24] (Fig. 1b), GelMA-based cartilage [25], and osteochondral tissues with supramolecular polymer and hydroxyapatite reinforced GelMA forms [26] (Fig. 1c) has been demonstrated for bioprinting applications. However, there are concerns regarding immunogenicity, characterizing their intrinsic properties, variations in properties between species, tissue, the batch of production, and relatively instability compared to their synthetic counterparts. Therefore, fully

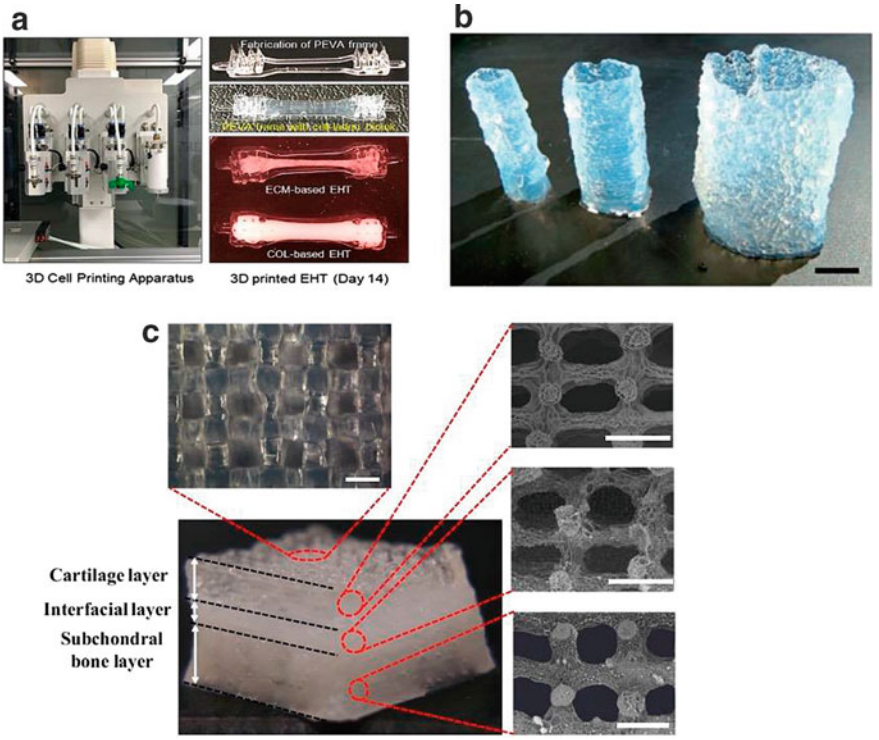

Fig. 1 Bioprinting Material. **a** bioprinting of ECM- and collagen-based engineered heart tissue. **b** bioprinting of 3D tubular constructs with agarose gel. **c** bioprinted GelMa/GelMA-nanohydroxyapatite based trilayered scaffold for osteochondral defects. Reprinted from publications [23–26]

synthetic functionalized hydrogels and their combinations with proteins/natural-derived hydrogels such as protein/poly-D-lysine modified poly (2-hydroxyethyl methacrylate) (PHEMA) [27], alginate- hydroxyapatite- poly (vinyl alcohol) (PVA) mixture [28], and poly (ethylene glycol) (PEG) that are also used as bioinks due to their benefits (e.g., highly tunable and consistent properties, and large- scale production capacity) [29]. Furthermore, hydrogels can be mechanically unstable, and thermoplastic materials such as polycaprolactone (PCL), poly (lactic-co-glycolic acid) (PLGA), and other acellular materials like nanocellulose, hydroxyapatite (HA), and β-tricalcium phosphate (β-TCP) are used for enhancing their mechanical strength and shape fidelity to generate functional, bioprinted tissue constructs made with hybrid bioinks [13, 14, 22, 30, 31].

5 Bioprinting and Microbes

5.1 Viruses

Viruses are noncellular obligate parasites—highly contagious and affect almost every type of human tissue, causing various serious diseases and health conditions. Viral diseases present a counting public health threat to human life, welfare, and the economy [32–34]. It continues to emerge at a rapid pace, causing significant morbidity and mortality worldwide to the extent of entirely changing the way of how people live [35–37]. Animal models are widely used for studying viruses and testing and evaluating potential control strategies to virus infections, including drugs and vaccines [38–41]. The susceptibility of the animal model to virus infection is the most critical parameter that defines its application. For instance, mice have been commonly used as an animal model for different viruses (e.g., influenza), but they are not permissible to other viruses (e.g., HIV), and humanized systems are needed for evaluating the efficiency of drugs and vaccines. However, it remains challenging to translate data from mice into human physiology. Researchers have focused on developing advanced engineering approaches to study the underlying mechanisms of viral infections and increase the knowledge that can constitute future studies [36]. Recent studies have shown that advanced 3D cell culture models have the potential to model the native microenvironments of virus-associated diseases and the corresponding structural and functional changes. It is probably the most promising model that allows for accurate and detailed information about the host response to infections, especially for difficult-to-culture pathogens. Most in vitro infection studies have been performed using cell lines. However, researchers try to develop complex 3D model systems with different cell types, including primary/stem cells, immune cells, e.g., T cells, macrophages under different physical conditions [13, 42–45]. Because of that, the localization of ECM deposition can impact the process of the in vitro infection, reconstituting a protecting barrier and pre- serving host cell integrity against invasion. Moreover, a significant challenge for studying host–pathogen mechanisms in 3D is the use of biomaterials that do not affect very similar cell exposure to pathogens and exclude a non-physiologically manner interaction [46]. Therefore, these difficulties have motivated many groups toward the development of bioprinting and new bioink composition approaches.

Microfluidic platforms that combine the advances in 3D cell culture offer multicompartmental structures that mimic native tissues and provide an opportunity to observe physical and biological changes under dynamic conditions. Although the applications of microfluidics in virology are still very much in their infancy, their potential has been proven in many studies [13]. For instance, Villenave et al. [47] used coxsackievirus B1 (CVB1) to model enteric virus infection using a dynamic gut-on-a-chip microfluidic platform where human villus intestinal epithelium was cultured. It is reported that the platform, running under conditions of physiological peristalsis-like motions (i.e., comprising relaxation of circular smooth muscles while maintaining luminal flow), is suitable to model in vitro enteric virus infection

and investigate mechanisms of pathogenesis [13]. Similarly, the demand for miniaturized cell culture systems, which can serve as a platform for studying hepatitis B virus (HBV) infections on hepatocyte physiology, led researchers to focus on microfluidics to model HCB-associated liver disease using human HepG2 hepatocellular carcinoma cells and rat hepatocytes [48]. Other approaches, including dynamic radial flow [49, 50] and rotating wall vessel [51, 52] cell culture bioreactor systems, have been developed to study viruses such as hepatitis C virus (HCV) and hepatitis E virus (HEV).

The latest studies on using 3D bioprinting to study viruses have mostly focused on modeling liver [53], lung [54], and brain [55, 56] tissues. Bioprinting enables fabricating of cell-laden scaffolds that may contain many different cell types with various biomaterials within the structure. As the combination of material and cells can be well controlled, it is possible to use 3D bioprinting to generate human-cell-based scaffolds to reflect human physiology and like animal models for virus studies [53, 54, 57, 58]. In addition, the bioprinted network that includes arginyl-glycyl-aspartic acid (RGD), the most common tripeptide sequence on ECM, induces cell migration, adhesion, and proliferation [59–61], and that it is essential to prepare well-mixed bioink including suspended cells in growth media and hydrogel solution in bioprinting process [13]. References [53, 92] described the optimization of a bioink mixture composing of alginate, gelatin, and human ECM to print human HepaRG liver cells with a pneumatic extrusion printer for transduction and infection studies through a liver model (Fig. 2). In addition, [54, 53] manipulated the same bioink mixture by using matrigel instead of human ECM to provide a scaffold for human alveolar A549 cells. Reference [62] established easy-to-handle 3D-cell culture platforms based on bioprinted 3D matrices for virus detection and characterization. This work included using different cell types to produce tissue-like growth in which cells developed an in vivo-like morphology. This advantage of the established platforms provided the ability for testing different viruses (in host range, tissue tropism, cytopathogenicity, and genomic organization: e.g., *Cowpox virus*, *Puumala virus*, *Feline calicivirus*, Modified *Vaccinia Ankar,* and *Yellow Fever virus*) (Fig. 3). It allowed for sensitive monitoring and characterization of the interactions of the tested viruses with host cells and their replication under physiologically relevant conditions [62].

In addition to modeling virus infections, virus particles—as a biomaterial component, can be used to expand the potential of 3D bioprinting. References [64, 63] used 3D bioprinting to produce a virus-activated matrix as a porous bone scaffold to promote endothelial cell activation, migration, and adhesion. They used ceramic, b-tricalcium phosphate (b-TCP), and HA to get the ink mixture. It is possible to induce differentiation of mesenchymal stem cells (MSCs) into osteoblasts in 3D printed structures using RGD phages without any additional osteogenic supplements [96, 102]. References [92, 64] focused on glioblastoma gene therapy by using vesicular stomatitis virus (VSV) as plasmid DNA encoding VSVMP, which can eliminate cancer cells and induce an anti-cancer immunity response.

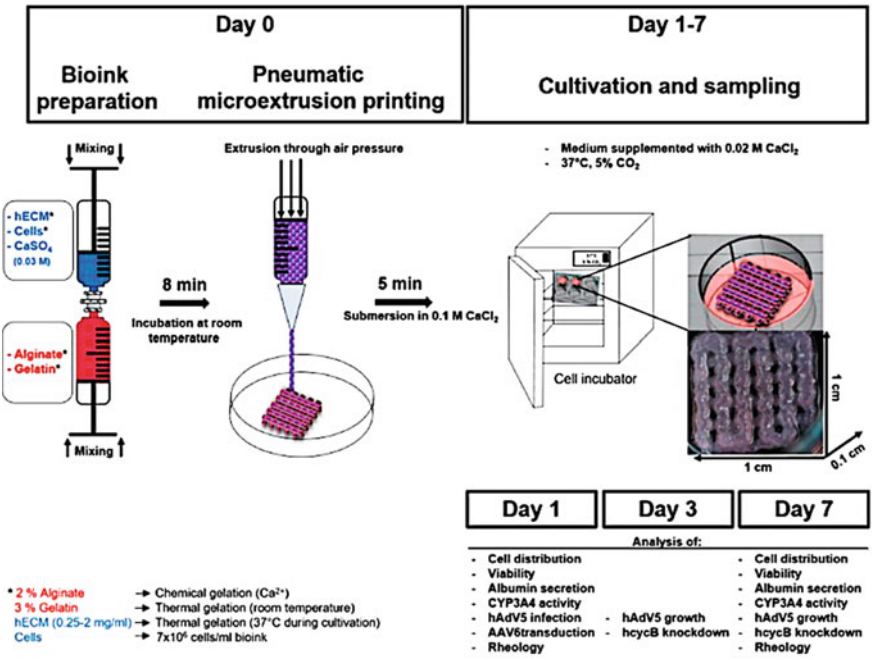

Fig. 2 Bioprinting and viruses. 3D bioprinting of liver model for virus infection using cell-laden hybrid alginate/gelatin/human extracellular matrix (hECM) constructs and living mature HepaRG cells. Reproduced with permission from [53]

3D cell culturing was developed as a pioneering method for a range of applications in biological engineering [32, 65–67], regenerative medicine [14, 20], infection biology [32, 68, 69]. 3D culture techniques provide artificial and yet functional tissue constructs that can serve as model platforms that display many complex characteristics of in vivo systems. They are prepared through two main approaches: (i) a top-down approach in which cells are seeded on top of pre-made biodegradable scaffolds that provide sufficient mechanical support for a uniform monoculture tissue layer, and (ii) a bottom-up approach that relies on the assembly of soluble components together with the cells as building hundred-micrometer-scale cellular constructs under conditions compatible with cell viability [13, 70]. Overall, advances in 3D printing/bioprinting technologies have allowed the creation of complex constructs used in a wide range of medical applications such as dentistry [71–74], drug/pharmaceutical fabrication [75–77], in vitro drug screening [78–80], surgical instruments [81–83], medical training and education [84–86], TE and RM [87–90].

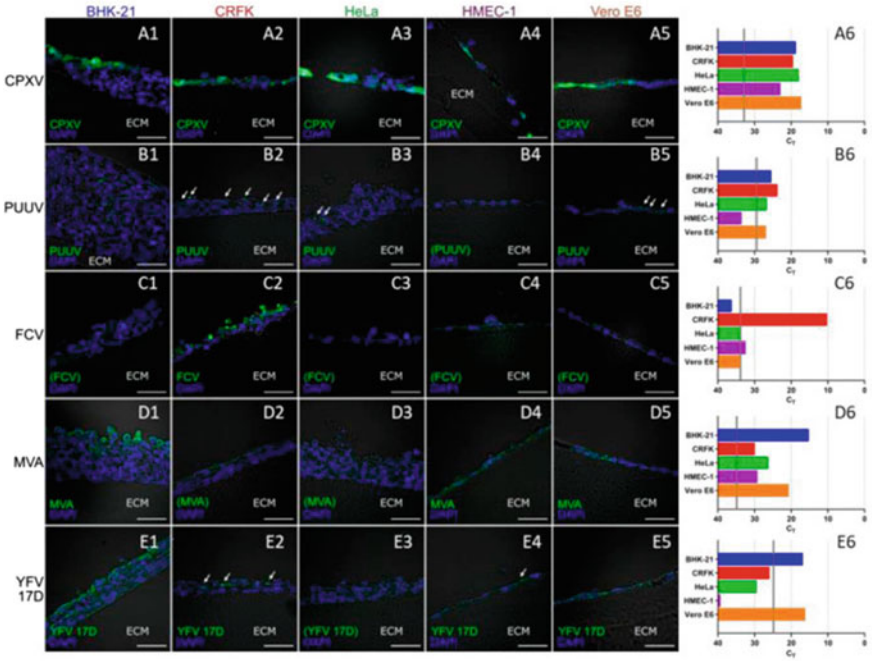

Fig. 3 Bioprinting of viruses. 3D cell culture of different cell lines on Wellbricks (10 wt% gelatine, w/o Collagen A) for infection with different viruses, including *Cowpox virus* (CPXV), *Puumala virus* (PUUV) Kazan, *Feline calicivirus* (FCV), Modified *Vaccinia Ankara* (MVA), and *Yellow Fever virus* (YFV). Reproduced with permission from [62]

5.2 Bacteria and Bacterial Structures

Bacteria are unicellular pathogens that vary in size and shape and are widely associated with various diseases in humans. Bacterial cell cultures formed of a single cell type have given significant insight into understanding the morphology, life cycle, and host–pathogen interactions of bacterial pathogens and the mechanisms by which they cause diseases [91]. However, these limited in vitro cell culture models lack many primary criteria present in the native, 3D dynamic host microenvironments that are associated with host–pathogen interactions; regulating infection, multicellular complexity, bacterial microbiota, gas exchange, and nutrient gradients, and physiologically relevant biomechanical forces [42] (e.g., fluid shear, stretch, compression). 3D cell culture techniques such as spheroid/organoid cultures [92–96], explant/organotypic cultures [97–101], polymeric scaffolds [68, 102, 103], natural [104–120] and synthetic hydrogel [121–129] scaffolds, and microfluidics [129–141], programmable and customizable platforms to engineer cell-laden constructs have been under development to mimic host tissues for studying bacteria and the associate diseases in human [13].

The development of such 3D cell culture systems can be very useful in many ways. It would enable applications such as (i) modeling the microbiome [68, 97–102, 142–146], (ii) testing the antibacterial activity [65, 66, 129, 131, 133, 141, 147–153] and, (iii) studying microbial structures such as biofilm development and formation [154, 155]. Studies of bacterial communities indicated that the ecological niche of bacteria could significantly improve our understanding of how bacteria perform their natural activities such as growth, reproduction, motility, and pathogenic relationships [156–159]. Bacteria form biofilms as complex microbial structures that help survive hostile environments and speed up their activities. In these structures, bacteria communicate via short-range physical and chemical signals, interactions, and other adaptive phenotypes, adapt their mechanical properties under stress to match conditions imposed by the surrounding environment (Fig. 4) [13, 158–161]. In such communities, bacteria communicate via signaling molecules, which allow bacteria to monitor and alter functional behaviors in the microenvironment through producing, release, sense, and respond to chemical inducers in a phenomenon named quorum sensing [162, 163].

Moreover, artificial microenvironments are useful in supporting bacterial cell viability [118, 164, 165]. Recently, bacteria-associated 3D bioprinting applications have been focused on studying and monitoring the intercellular microscale communications through the spatial configuration of populations, observation of quorum sensing mechanisms, and fabrication of suitable biomaterial for bacterial microenvironments [160, 163, 166, 167]. In these studies, biofilms are formed in a non-immobilized state on various surfaces and interfaces by incubating the bacteria suspended in a fluid culture medium and naturally allowing the deposition of a layer of

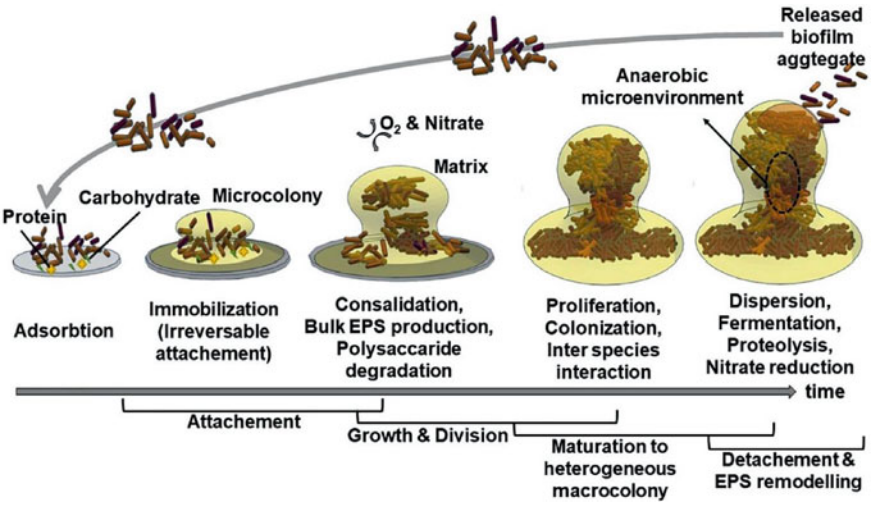

Fig. 4 Bioprinting of bacteria and bacterial biofilm. Schematic presentation of the different stages of bacterial colonization and the formation of biofilm. Reprinted from publication [13]

bacteria on the desired substrate. Several immobilization approaches such as adsorption on surfaces, cross-linking, encapsulation, and entrapment for providing bacteria with a free-formed, defined geometrical microenvironment to enhance the metabolic activity of bacteria [13]. This is increasingly important in various biotechnological applications and industries due to the corresponding increase in the biological yield, biodegradation, and synthesis of chemicals, polymers, enzymes, and proteins. Reference [168] has described an easy and cost-effective method for 3D printing of bacteria and biofilms. They used simple alginate chemistry to print a bacteria-alginate bioink mixture onto calcium-containing agar surfaces to form bacteria-encapsulating hydrogels with varying geometries. In which bacterial cells, i.e., *E. coli*, remained intact, spatially patterned, and viable for several days, and thus allow for biofilm formation of multilayered three-dimensional structures that can tolerate harsh chemical treatments [168].

On the other hand, numerous studies focused on developing bioprinted antibacterial materials or modifying existing biomaterials to become bacterial resistant, mainly by forming gel films- or nanoparticle-coating or loading the structures with antibiotics. For instance, plant-based nanocellulose was printed in a 3D porous structure for modifying film surfaces as a bio-responsive, elastic gel to carry/release antimicrobial components for wound dressing applications [169]. Also, Yang et al. [170] created a 3D chitosan-based polymeric nanocomposite porous scaffold that possesses less risk of antibiotic resistance to enhance repairing and restoring of infected bones. Moreover, Zhang et al. [171] developed a combination of a 3D-printing method and a layer-by-layer coating technique to prepare antibacterial silver-graphene oxide nanocomposite coated-bioceramic scaffolds for bone defect therapy and reconstruction. Similarly, researchers fabricated nano-magnesium oxide modified polymeric scaffolds with 3D interconnected and well-ordered microporous structures with strong antibacterial activity while preserving essential cellular adhesion properties, proliferation, and osteogenic differentiation [172]. In addition, antibiotic loading is used to fabricate modified-functional scaffolds to improve the anti-inflammatory and bactericidal effects. Shim et al. [173] developed a 3D printed antibiotic-loaded biodegradable polymeric scaffold, which is useful for rapid and efficient eradication of chronic osteomyelitis and regeneration of bone tissues. This can be a promising solution as a carrier for the delivery of antibiotics in orthopedics. In another example, Floroian et al. [174] built antibiotic-loaded-bioactive glass-based polymeric composite films to coat stainless steel implants and showed an anti-biofilm/antimicrobial activity. Ning et al. (2019) demonstrated 3D bioprinting of a significantly thick biofilm (>4 mm) of clinically relevant bacterial species, including *E. coli*, *Staphylococcus aureus*, Methicillin-resistant *Staphylococcus aureus,* and *Pseudomonas aeruginosa*, using a double-crosslinked alginate bioink. The bioprinted constructs provided the possibility to follow the complete five-step biofilm life cycle in vitro. Interestingly, the formed 3D biofilm constructs were found to show greater resistance to antimicrobials than corresponding two-dimensional (2D) cultures, confirming the clinical relevance of using 3D printed models versus 2D culture models for antimicrobial testing (Fig. 5) [175].

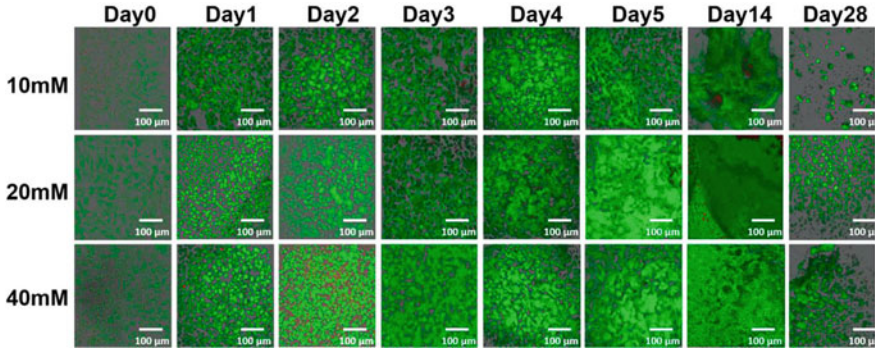

Fig. 5 Bioprinting of bacteria and imaging of bacterial biofilm. 3D reconstructed confocal laser scanning microscopy (CLSM) Z-stacks of 3D bioprinted biofilm images of MRSA in 1 mm, porous scaffolds exposed to increasing concentration of $BaCl_2$ from 10 to 40 mM. Reproduced with permission from [175]

6 Summary and Concluding Remarks

The applications of 3D bioprinting systems in modeling microbial infections have expanded to encompass a wide range of bacteria and viruses. The approaches used in the 3D bioprinting of microbes, such as stereolithographic, extrusion-based, droplet-based, and laser-assisted bioprinting, are widely reported, and procedures for their use in producing tissue models and constructs are well addressed in the literature. 3D culture and bioprinting systems have proven to be powerful tools to model microbial infections, host–pathogen interactions, niches for microbiota, biofilm formation, and determine microbial resistance to antibiotics. They enable the development of host cell-based scaffolds that mimic the in vivo conditions and replace animal models to study challenging virus infections, including HPV, HIV, HSV, VZV, ADV, CVB1 HBV, HCV, and HEV. Interestingly, 3D printed models were successfully used to generate reproducible bacterial biofilms (e.g., *E. coli*, *P. aeruginosa*, and *S. aureus*) and uncover the mystery of the involved quorum sensing. However, bioprinting approaches and 3D systems that support the growth of fungi, yeast, and the modeling of unicellular and multicellular parasitic infections remain missing, and they will likely be developed soon. The applications of 3D bioprinting are rapidly growing, and bioprinted platforms are moving to become the main components in studying infectious diseases and will occupy the interest of scientists from all disciplines in biology and medicine, whether fundamental, environmental, clinical, or industrial, in the future.

References

1. Mironov V et al (2009) Organ printing: tissue spheroids as building blocks. Biomaterials 30(12):2164–2174
2. Dababneh AB, Ozbolat IT (2014) Bioprinting technology: a current state-of-the-art review. J Manuf Sci Eng 136(6)
3. Murphy SV, Atala A (2014) 3D bioprinting of tissues and organs. Nat Biotechnol 32(8):773–785
4. Ozbolat IT (2015) Bioprinting scale-up tissue and organ constructs for transplantation. Trends Biotechnol 33(7):395–400
5. Ozbolat IT (2016) 3D Bioprinting: fundamentals, principles and applications. Academic Press
6. Sachlos E, Czernuszka J (2003) Making tissue engineering scaffolds work. Review: the application of solid freeform fabrication technology to the production of tissue engineering scaffolds. Eur Cell Mater 5(29): p. 39–40
7. Ozbolat IT, Hospodiuk M (2016) Current advances and future perspectives in extrusion-based bioprinting. Biomaterials 76:321–343
8. Ozbolat IT, Moncal KK, Gudapati H (2017) Evaluation of bioprinter technologies. Additive Manuf 13:179–200
9. Li J et al (2016) Recent advances in bioprinting techniques: approaches, applications and future prospects. J Transl Med 14(1):1–15
10. Derakhshanfar S et al (2018) 3D bioprinting for biomedical devices and tissue engineering: A review of recent trends and advances. Bioactive materials 3(2):144–156
11. Bittner SM et al (2018) Three-dimensional printing of multilayered tissue engineering scaffolds. Mater Today 21(8):861–874
12. Dunham S et al (2018) Applications of 3D printing. 3D printing applications in cardiovascular medicine. Elsevier, pp 61–78
13. Saygili E et al (2020) 3D bioprinting: a powerful tool to leverage tissue engineering and microbial systems. Bioprinting 8:e00071.
14. Bishop ES et al (2017) 3-D bioprinting technologies in tissue engineering and regenerative medicine: Current and future trends. Genes Diseases 4(4):185–195
15. Gudapati H, Dey M, Ozbolat I (2016) A comprehensive review on droplet-based bioprinting: past, present and future. Biomaterials 102:20–42
16. Ng WL et al (2017) Microvalve-based bioprinting–process, bio-inks and applications. Biomater Sci 5(4):632–647
17. Li B et al (2019) A bio-inspired 3D micro-structure for graphene-based bacteria sensing. Biosens Bioelectron 123:77–84
18. Leberfinger AN et al (2017) 3D printing for cell therapy applications. Cell Therapy. Springer, pp 227–248
19. Starly, B. and R. Shirwaiker, 3D bioprinting techniques. 3D Bioprinting nanotechnology in tissue engineering regenerative medicine; Zhang, LG, Fisher, JP, Leong, KW, Eds, 2015: pp 57–77
20. Vijayavenkataraman S et al (2018) 3D bioprinting of tissues and organs for regenerative medicine. Adv Drug Deliv Rev 132:296–332
21. Williams D et al (2018) A perspective on the physical, mechanical and biological specifications of bioinks and the development of functional tissues in 3D bioprinting. Bioprinting 9:19–36
22. Hospodiuk M et al (2017) The bioink: a comprehensive review on bioprintable materials. Biotechnol Adv 35(2):217–239
23. Das S et al (2019) Decellularized extracellular matrix bioinks and the external stimuli to enhance cardiac tissue development in vitro. Acta Biomater 95:188–200
24. Fan R et al (2016) Bio-printing cell-laden Matrigel–agarose constructs. J Biomater Appl 31(5):684–692
25. Daly AC et al (2016) A comparison of different bioinks for 3D bioprinting of fibrocartilage and hyaline cartilage. Biofabrication 8(4) 045002

26. Liu J et al (2019) 3D printing of biomimetic multi-layered GelMA/nHA scaffold for osteochondral defect repair. Mater Design 171: 107708
27. Badea A et al (2017) 3D-printed pHEMA materials for topographical and biochemical modulation of dorsal root ganglion cell response. ACS Appl Mater Interfaces 9(36):30318–30328
28. Bendtsen ST, Quinnell SP, Wei M (2017) Development of a novel alginate-polyvinyl alcohol-hydroxyapatite hydrogel for 3D bioprinting bone tissue engineered scaffolds. J Biomed Mater Res Part A 105(5):1457–1468
29. Slaughter BV et al (2009) Hydrogels in regenerative medicine. Adv Mater 21(32–33):3307–3329
30. Min L et al (2015) Biomaterials for bioprinting. 3D Bioprinting and nanotechnology in tissue engineering and regenerative medicine, 129–148
31. Nowicki M et al (2020) 3D printing multiphasic osteochondral tissue constructs with nano to micro features via PCL based bioink. Bioprinting 17:e00066
32. Ramanan V et al (2014) New methods in tissue engineering: improved models for viral infection. Ann Rev Virology 1:475–499
33. Draz MS, Shafiee H (2018) Applications of gold nanoparticles in virus detection. Theranostics 8(7):1985
34. Draz MS et al (2014) Nanoparticle-mediated systemic delivery of siRNA for treatment of cancers and viral infections. Theranostics 4(9):872
35. Guha C et al (2004) Cell culture and animal models of viral hepatitis. Part I: hepatitis B. Lab animal 33(7):37–46
36. Bouvier N, Lowen A (2010) Animal Models for Influenza Virus Pathogenesis and Transmission. Viruses 2(8):1530–63. Epub 2010/01/01. https://doi.org/10.3390/v20801530 PMID: 21442033
37. Draz MS, Tang Y, Zhang P (2020) Bio-Nanoparticles: Nanoscale Probes for Nanoscale pathogens. In: 21st Century Nanoscience–A Handbook. CRC Press, pp 20–1–20–23
38. Mifsud EJ, Tai CM, Hurt AC (2018) Animal models used to assess influenza antivirals. Expert Opin Drug Discov 13(12):1131–1139
39. Bodewes R, Rimmelzwaan GF, Osterhaus AD (2010) Animal models for the preclinical evaluation of candidate influenza vaccines. Expert Rev Vaccines 9(1):59–72
40. Ibeh BO, Ashano E (2018) Experimental animal models of HIV/AIDS for vaccine trials. Experimental animal models of human diseases—an effective therapeutic strategy. IntechOpen, London, pp 159–180
41. Tatara AM et al (2015) Infected animal models for tissue engineering. Methods 84:17–24
42. Barrila J et al (2018) Modeling host-pathogen interactions in the context of the microenvironment: three-dimensional cell culture comes of age. Infection Immunity 86(11)
43. Barrila J et al (2017) Three-dimensional organotypic co-culture model of intestinal epithelial cells and macrophages to study Salmonella enterica colonization patterns. Npj Microgravity 3(1):1–12
44. Perez del Rio E et al (2018) Artificial 3D culture systems for T cell expansion. ACS omega 3(5):5273–5280
45. Crabbé A et al (2011) Alveolar epithelium protects macrophages from quorum sensing-induced cytotoxicity in a three-dimensional co-culture model. Cell Microbiol 13(3):469–481
46. Nickerson CA, Richter EG, Ott CM (2007) Studying host–pathogen interactions in 3-D: organotypic models for infectious disease and drug development. J Neuroimmune Pharmacol 2(1):26–31
47. Villenave R et al (2017) Human gut-on-a-chip supports polarized infection of coxsackie B1 virus in vitro. PloS one 12(2): e0169412
48. Sodunke TR, Bouchard MJ, Noh HM (2008) Microfluidic platform for hepatitis B viral replication study. Biomed Microdevice 10(3):393–402
49. Murakami K et al (2008) Dynamic behavior of hepatitis C virus quasispecies in a long-term culture of the three-dimensional radial-flow bioreactor system. J Virol Methods 148(1–2):174–181

50. Aizaki H et al (2003) Production and release of infectious hepatitis C virus from human liver cell cultures in the three-dimensional radial-flow bioreactor. Virology 314(1):16–25
51. Berto A et al (2013) Replication of hepatitis E virus in three-dimensional cell culture. J Virol Methods 187(2):327–332
52. Sainz B, TenCate V, Uprichard SL (2009) Three-dimensional Huh7 cell culture system for the study of Hepatitis C virus infection. Virology journal 6(1):1–8
53. Hiller T et al (2018) Generation of a 3D liver model comprising human extracellular matrix in an alginate/gelatin-based bioink by extrusion bioprinting for infection and transduction studies. Int J Mol Sci 19(10):3129
54. Berg J et al (2018) Optimization of cell-laden bioinks for 3D bioprinting and efficient infection with influenza A virus. Sci Rep 8(1):1–13
55. Kang K et al (2018) Three-dimensional bioprinting of hepatic structures with directly converted hepatocyte-like cells. Tissue Eng Part A 24(7–8):576–583
56. Johnson BN et al (2016) 3D printed nervous system on a chip. Lab Chip 16(8):1393–1400
57. Miranda P et al (2008) Mechanical properties of calcium phosphate scaffolds fabricated by robocasting. J Biomed Mater Res Part A: Official J Soc Biomater Jpn Soc Biomater Austr Soc Biomater Korean Soc Biomater 85(1):218–227
58. Lee D-Y et al (2016) Phage as versatile nanoink for printing 3-D cell-laden scaffolds. Acta Biomater 29:112–124
59. Roth AD et al (2018) Polymer coating on a micropillar chip for robust attachment of PuraMatrix peptide hydrogel for 3D hepatic cell culture. Mater Sci Eng, C 90:634–644
60. Bellis SL (2011) Advantages of RGD peptides for directing cell association with biomaterials. Biomaterials 32(18):4205–4210
61. Yu C-H et al (2011) Early integrin binding to Arg-Gly-Asp peptide activates actin polymerization and contractile movement that stimulates outward translocation. Proc Natl Acad Sci 108(51):20585–20590
62. Koban R et al (2020) Simplified Bioprinting-based 3D cell culture infection models for virus detection. Viruses 12(11):1298
63. Steward AJ, Wagner DR, Kelly DJ (2014) Exploring the roles of integrin binding and cytoskeletal reorganization during mesenchymal stem cell mechanotransduction in soft and stiff hydrogels subjected to dynamic compression. J Mech Behav Biomed Mater 38:174–182
64. Wang J et al (2014) Phage nanofibers induce vascularized osteogenesis in 3D printed bone scaffolds. Adv Mater 26(29):4961–4966
65. Touri M et al (2019) Optimisation and biological activities of bioceramic robocast scaffolds provided with an oxygen-releasing coating for bone tissue engineering applications. Ceram Int 45(1):805–816
66. Li Q et al (2015) Magnetically guided fabrication of multilayered iron oxide/polycaprolactone/gelatin nanofibrous structures for tissue engineering and theranostic application. Tissue Eng Part C Methods 21(10):1015–1024
67. O'brien FJ (2011) Biomaterials & scaffolds for tissue engineering. Mater Today 14(3):88–95
68. Mohiti-Asli M, Pourdeyhimi B, Loboa EG (2014) Skin tissue engineering for the infected wound site: biodegradable PLA nanofibers and a novel approach for silver ion release evaluated in a 3D coculture system of keratinocytes and Staphylococcus aureus. Tissue Eng Part C Methods 20(10):790–797
69. Andrei G et al (2005) Organotypic epithelial raft cultures as a model for evaluating compounds against alphaherpesviruses. Antimicrob Agents Chemother 49(11):4671–4680
70. Tiruvannamalai-Annamalai R, Armant DR, Matthew HW (2014) A glycosaminoglycan based, modular tissue scaffold system for rapid assembly of perfusable, high cell density, engineered tissues. PloS One 9(1): e84287
71. Nagrath M et al (2018) Functionalized prosthetic interfaces using 3D printing: Generating infection-neutralizing prosthesis in dentistry. Mater Today Commun 15:114–119
72. Athirasala A et al (2018) A dentin-derived hydrogel bioink for 3D bioprinting of cell laden scaffolds for regenerative dentistry. Biofabrication 10(2):024101

73. Ozcan M, Additive manufacturing technologies used for processing polymers: current status and potential application in.
74. Park G-S et al (2017) Emulating host-microbiome ecosystem of human gastrointestinal tract in vitro. Stem Cell Rev Reports 13(3):321–334
75. Solanki NG et al (2018) Formulation of 3D printed tablet for rapid drug release by fused deposition modeling: screening polymers for drug release, drug-polymer miscibility and printability. J Pharm Sci 107(1):390–401
76. Sadia M et al (2018) Channelled tablets: An innovative approach to accelerating drug release from 3D printed tablets. J Control Release 269:355–363
77. Fuenmayor E et al (2019) Comparison of fused-filament fabrication to direct compression and injection molding in the manufacture of oral tablets. Int J Pharm 558:328–340
78. Glatzel S et al (2016) A portable 3D printer system for the diagnosis and treatment of multidrug-resistant bacteria. Chem 1(3):494–504
79. Chen X et al (2018) 3D printed microfluidic chip for multiple anticancer drug combinations. Sens Actuators B Chem 276:507–516
80. Louzao I et al (2018) Identification of novel "Inks" for 3D printing using high-throughput screening: bioresorbable photocurable polymers for controlled drug delivery. ACS Appl Mater Interfaces 10(8):6841–6848
81. Rankin TM et al (2014) Three-dimensional printing surgical instruments: are we there yet? J Surg Res 189(2):193–197
82. Wong JY, Pfahnl AC (2014) 3D printing of surgical instruments for long-duration space missions. Aviat Space Environ Med 85(7):758–763
83. George M et al (2017) 3D printed surgical instruments: the design and fabrication process. World J Surg 41(1):314–319
84. Lim KHA et al (2016) Use of 3D printed models in medical education: a randomized control trial comparing 3D prints versus cadaveric materials for learning external cardiac anatomy. Anat Sci Educ 9(3):213–221
85. Biglino G et al (2017) Use of 3D models of congenital heart disease as an education tool for cardiac nurses. Congenit Heart Dis 12(1):113–118
86. Smith M, Jones J (2017) Dual-extrusion 3D printing of anatomical models for education construction of airway models. Anat Sci Educ
87. Foyt DA et al (2018) Exploiting advanced hydrogel technologies to address key challenges in regenerative medicine. Adv Healthcare Mater 7(8):1700939
88. Faramarzi N et al (2018) Patient-specific bioinks for 3D bioprinting of tissue engineering scaffolds. Adv Healthcare Mater 7(11):1701347
89. Yu HS et al (2018) Feasibility of polycaprolactone scaffolds fabricated by three-dimensional printing for tissue engineering of Tunica Albuginea. World J Men's Health 36(1):66
90. Haring AP et al (2019) Process-and bio-inspired hydrogels for 3D bioprinting of soft free-standing neural and glial tissues. Biofabrication 11(2): 025009
91. Jia H, Draz MS, Ruan Z (2019) Functional Nanomaterials for the Detection and Control of Bacterial Infections. Curr Top Med Chem 19(27):2449–2475
92. Yang Y et al (2017) A 3D-Engineered conformal implant releases DNA nanocomplexs for eradicating the postsurgery residual glioblastoma. Adv Sci 4(8):1600491
93. Mulberry G et al (2017) 3D printing and milling a real-time PCR device for infectious disease diagnostics. PLoS One 12(6):e0179133
94. Song J et al (2016) Instrument-free point-of-care molecular detection of Zika virus. Anal Chem 88(14):7289–7294
95. Shen H et al (2018) A novel fluorescent immunochromatographic strip combined with pocket fluorescence observation instrument for rapid detection of PRV. Anal Bioanal Chem 410(29):7655–7661
96. Singh H et al (2015) Increased sensitivity of 3D-Well enzyme-linked immunosorbent assay (ELISA) for infectious disease detection using 3D-printing fabrication technology. Bio-Med Mater Eng 26(s1):S45–S53

97. Krejcova L et al (2014) 3D printed chip for electrochemical detection of influenza virus labeled with CdS quantum dots. Biosens Bioelectron 54:421–427
98. Tseng H et al (2016) A high-throughput in vitro ring assay for vasoactivity using magnetic 3D bioprinting. Sci Rep 6(1):1–8
99. Schneeberger K et al (2017) Converging biofabrication and organoid technologies: the next frontier in hepatic and intestinal tissue engineering? Biofabrication 9(1): 013001
100. Gutzweiler L et al (2017) Large scale production and controlled deposition of single HUVEC spheroids for bioprinting applications. Biofabrication 9(2):025027
101. Taniguchi D et al (2018) Scaffold-free trachea regeneration by tissue engineering with bio-3D printing. Interact Cardiovasc Thorac Surg 26(5):745–752
102. Türker E, Demirçak N, Arslan-Yildiz A (2018) Scaffold-free three-dimensional cell culturing using magnetic levitation. Biomater Sci 6(7):1745–1753
103. Popov L et al (2014) Three-dimensional human skin models to understand Staphylococcus aureus skin colonization and infection. Front Immunol 5:41
104. Dabija-Wolter G et al (2012) Limited in-depth invasion of Fusobacterium nucleatum into in vitro reconstructed human gingiva. Arch Oral Biol 57(4):344–351
105. Reuter C et al (2018) An adherent mucus layer attenuates the genotoxic effect of colibactin. Cellular microbiology 20(2): e12812
106. Marrazzo P et al (2016) 3D reconstruction of the human airway mucosa in vitro as an experimental model to study NTHi infections. PloS One 11(4):e0153985
107. Maboni G et al (2017) A novel 3D skin explant model to study anaerobic bacterial infection. Front Cell Infect Microbiol 7:404
108. Chen Y et al (2017) In vitro enteroid-derived three-dimensional tissue model of human small intestinal epithelium with innate immune responses. PloS One 12(11): e0187880
109. Lai Y et al (2019) Osteogenic magnesium incorporated into PLGA/TCP porous scaffold by 3D printing for repairing challenging bone defect. Biomaterials 197:207–219
110. Koch L et al (2012) Skin tissue generation by laser cell printing. Biotechnol Bioeng 109(7):1855–1863
111. Lee VK et al (2014) Generation of multi-scale vascular network system within 3D hydrogel using 3D bio-printing technology. Cell Mol Bioeng 7(3):460–472
112. Ding H, Chang RC (2018) Simulating image-guided in situ bioprinting of a skin graft onto a phantom burn wound bed. Addit Manuf 22:708–719
113. Maver T et al (2018) Combining 3D printing and electrospinning for preparation of pain-relieving wound-dressing materials. J Sol-Gel Sci Technol 88(1):33–48
114. Schöneberg J et al (2018) Engineering biofunctional in vitro vessel models using a multilayer bioprinting technique. Sci Rep 8(1):1–13
115. Ma X et al (2018) Rapid 3D bioprinting of decellularized extracellular matrix with regionally varied mechanical properties and biomimetic microarchitecture. Biomaterials 185:310–321
116. Mazzocchi A et al (2018) Optimization of collagen type I-hyaluronan hybrid bioink for 3D bioprinted liver microenvironments. Biofabrication 11(1): 015003
117. Won J-Y et al (2019) A potential dermal substitute using decellularized dermis extracellular matrix derived bio-ink. Artif Cells Nanomed Biotechnol 47(1):644–649
118. Leva V et al (2018) Direct laser printing of liver cells on porous collagen scaffolds. J Laser Micro Nanoengineering 13(3):234–237
119. Loozen LD et al (2013) Porous bioprinted constructs in BMP-2 non-viral gene therapy for bone tissue engineering. J Mater Chem B 1(48):6619–6626
120. Lee V et al (2014) Design and fabrication of human skin by three-dimensional bioprinting. Tissue Eng Part C Methods 20(6):473–484
121. Ng WL, Yeong WY, Naing MW (2016) Polyelectrolyte gelatin-chitosan hydrogel optimized for 3D bioprinting in skin tissue engineering. Int J Bioprinting 2(1)
122. Cubo Mateo N et al (2016) 3D bioprinting of functional human skin: production and in vivo analysis
123. Benning L et al (2018) Assessment of hydrogels for bioprinting of endothelial cells. J Biomed Mater Res Part A 106(4):935–947

124. Aljohani W et al (2018) Three-dimensional printing of alginate-gelatin-agar scaffolds using free-form motor assisted microsyringe extrusion system. J Polym Res 25(3):1–10
125. Min D et al (2018) Bioprinting of biomimetic skin containing melanocytes. Exp Dermatol 27(5):453–459
126. Datta S et al (2018) Alginate-honey bioinks with improved cell responses for applications as bioprinted tissue engineered constructs. J Mater Res 33(14):2029–2039
127. Nguyen DG et al (2016) Bioprinted 3D primary liver tissues allow assessment of organ-level response to clinical drug induced toxicity in vitro. PloS One 11(7): e0158674
128. Norona LM et al (2019) Bioprinted liver provides early insight into the role of Kupffer cells in TGF-β1 and methotrexate-induced fibrogenesis. PLoS One 14(1): e0208958
129. Horváth L et al (2015) Engineering an in vitro air-blood barrier by 3D bioprinting. Sci Rep 5(1):1–8
130. Madden LR et al (2018) Bioprinted 3D primary human intestinal tissues model aspects of native physiology and ADME/Tox functions. IScience 2:156–167
131. Ying GL et al (2018) Aqueous two-phase emulsion bioink-enabled 3D bioprinting of porous hydrogels. Adv Mater 30(50):1805460
132. King SM et al (2017) 3D proximal tubule tissues recapitulate key aspects of renal physiology to enable nephrotoxicity testing. Front Physiol 8:123
133. Ma X et al (2016) Deterministically patterned biomimetic human iPSC-derived hepatic model via rapid 3D bioprinting. Proc Natl Acad Sci 113(8):2206–2211
134. Pereira RF et al (2018) A single-component hydrogel bioink for bioprinting of bioengineered 3D constructs for dermal tissue engineering. Mater Horiz 5(6):1100–1111
135. Zhang Y et al (2016) A bioadhesive nanoparticle–hydrogel hybrid system for localized antimicrobial drug delivery. ACS Appl Mater Interfaces 8(28):18367–18374
136. Chang R et al (2010) Biofabrication of a three-dimensional liver micro-organ as an in vitro drug metabolism model. Biofabrication 2(4): 045004
137. Lee J-H et al (2012) Microfluidic 3D bone tissue model for high-throughput evaluation of wound-healing and infection-preventing biomaterials. Biomaterials 33(4):999–1006
138. Lee J-H et al (2011) Microfluidic approach to create three-dimensional tissue models for biofilm-related infection of orthopaedic implants. Tissue Eng Part C Methods 17(1):39–48
139. Al-Ahmad A et al (2008) Bacterial and Candida albicans adhesion on rapid prototyping-produced 3D-scaffolds manufactured as bone replacement materials. J Biomed Mater Res Part A: Offic J Soc Biomater Jpn Soc Biomater Austr Soc Biomater Korean Soc Biomater 87(4):933–943
140. Snyder J et al (2011) Bioprinting cell-laden matrigel for radioprotection study of liver by pro-drug conversion in a dual-tissue microfluidic chip. Biofabrication 3(3):034112
141. Snyder J et al (2015) Hetero-cellular prototyping by synchronized multi-material bioprinting for rotary cell culture system. Biofabrication 8(1):015002
142. Homan KA et al (2016) Bioprinting of 3D convoluted renal proximal tubules on perfusable chips. Sci Rep 6(1):1–13
143. Gao Q et al (2017) 3D bioprinting of vessel-like structures with multilevel fluidic channels. ACS Biomater Sci Eng 3(3):399–408
144. Grix T et al (2018) Bioprinting perfusion-enabled liver equivalents for advanced organ-on-a-chip applications. Genes 9(4):176
145. Lin NY et al (2019) Renal reabsorption in 3D vascularized proximal tubule models. Proc Natl Acad Sci 116(12):5399–5404
146. Lee VK et al (2014) Creating perfused functional vascular channels using 3D bio-printing technology. Biomaterials 35(28):8092–8102
147. Lee J-H et al (2010) Effects of Staphylococcus epidermidis on osteoblast cell adhesion and viability on a Ti alloy surface in a microfluidic co-culture environment. Acta Biomater 6(11):4422–4429
148. Kavanagh N, O'Brien FJ, Kerrigan SW (2018) Staphylococcus aureus protein A causes osteoblasts to hyper-mineralise in a 3D extra-cellular matrix environment. PLoS One 13(6): e0198837

149. Hind LE et al (2018) Interaction with an endothelial lumen increases neutrophil lifetime and motility in response to P aeruginosa. Blood J Amer Soc Hematol 132(17):1818–1828
150. Shambat SM et al (2015) Modelling staphylococcal pneumonia in a human 3D lung tissue model system delineates toxin-mediated pathology. Dis Model Mech 8(11):1413–1425
151. Flood P, Alvarez L, Reynaud E (2016) Free-floating epithelial micro-tissue arrays: a low cost and versatile technique. Biofabrication 8(4): 045006
152. Olaniyi RO et al (2018) Deciphering the Pathological role of staphylococcal α-Toxin and Panton-Valentine leukocidin Using a novel Ex Vivo human skin Model. Front Immunol 9:951
153. Tian R et al (2018) Fabrication of self-healing hydrogels with on-demand antimicrobial activity and sustained biomolecule release for infected skin regeneration. ACS Appl Mater Interfaces 10(20):17018–17027
154. Zhou Z et al (2018) Antimicrobial activity of 3D-printed poly (ε-caprolactone)(PCL) composite scaffolds presenting vancomycin-loaded polylactic acid-glycolic acid (PLGA) microspheres. Med Sci Monitor: Int Med J Exp Clinical Res 24:6934
155. Yang J et al (2018) Reverse reconstruction and bioprinting of bacterial cellulose-based functional total intervertebral disc for therapeutic implantation. Small 14(7):1702582
156. Tang Y et al (2012) Layer-by-layer assembly of antibacterial coating on interbonded 3D fibrous scaffolds and its cytocompatibility assessment. J Biomed Mater Res, Part A 100(8):2071–2078
157. Xu Z-L et al (2016) Enhanced antibacterial activity and osteoinductivity of Ag-loaded strontium hydroxyapatite/chitosan porous scaffolds for bone tissue engineering. J Mater Chem B 4(48):7919–7928
158. El-Rashidy AA et al (2018) Antibacterial activity and biocompatibility of zein scaffolds containing silver-doped bioactive glass. Biomed Mater 13(6): p. 065006
159. García-Alvarez R, Izquierdo-Barba I, Vallet-Regí M (2017) 3D scaffold with effective multidrug sequential release against bacteria biofilm. Acta Biomater 49:113–126
160. Cheng H et al (2017) Mussel-inspired multifunctional hydrogel coating for prevention of infections and enhanced osteogenesis. ACS Appl Mater Interfaces 9(13):11428–11439
161. Kim HJ et al (2016) Contributions of microbiome and mechanical deformation to intestinal bacterial overgrowth and inflammation in a human gut-on-a-chip. Proc Natl Acad Sci 113(1):E7–E15
162. Ofiţeru ID et al (2010) Combined niche and neutral effects in a microbial wastewater treatment community. Proc Natl Acad Sci 107(35):15345–15350
163. Jeraldo P et al (2012) Quantification of the relative roles of niche and neutral processes in structuring gastrointestinal microbiomes. Proc Natl Acad Sci 109(25):9692–9698
164. Curtis T et al (2013) Microbial community assembly, theory and rare functions. Front Microbiol 4:68
165. Liao J et al (2016) The importance of neutral and niche processes for bacterial community assembly differs between habitat generalists and specialists. FEMS Microbiol Ecol 92(11)
166. Connell JL et al (2013) 3D printing of microscopic bacterial communities. Proc Natl Acad Sci 110(46):18380–18385
167. Schaffner M et al (2017) 3D printing of bacteria into functional complex materials. Sci Adv 3(12):eaao6804
168. Balasubramanian S, Aubin-Tam M-E, Meyer AS (2019) 3D printing for the fabrication of biofilm-based functional living materials. ACS Publications
169. Schmieden DT et al (2018) Printing of patterned, engineered E. coli biofilms with a low-cost 3D printer. ACS Synth Biol 7(5):1328–1337
170. Ulusu Y et al (2017) Thermal stability and rheological properties of the 'non-stick'Caf1 biomaterial. Biomed Mater 12(5):051001
171. Zhang Y et al (2017) 3D-printed bioceramic scaffolds with antibacterial and osteogenic activity. Biofabrication 9(2):025037
172. Blanchette CD et al (2016) Printable enzyme-embedded materials for methane to methanol conversion. Nat Commun 7(1):1–9
173. Xu F et al (2011) Living bacterial sacrificial porogens to engineer decellularized porous scaffolds. PloS One 6(4):e19344

174. Rodríguez-Dévora JI et al (2012) High throughput miniature drug-screening platform using bioprinting technology. Biofabrication 4(3): 035001
175. Ning E et al (2019) 3D bioprinting of mature bacterial biofilms for antimicrobial resistance drug testing. Biofabrication 11(4):045018

Chapter 11
Methods of Polysaccharides Crosslinking: Future-Promising Crosslinking Techniques of Alginate Hydrogels for 3D Printing in Biomedical Applications

Refat M. Hassan (El-Moushy)

This chapter is dedicated to the memory of our First & Last Beloved Instructor AL-MUSTAFA

Abstract Recently, the development in wound dressing materials for wound cares that prevent inflammation and scars for human beings as well as enhancing the performance for controlling the drug delivery release became one of the most essential and urgent demands in the world. This is because the bone problems were recognized as the second transplant tissues by using bone grafts or bone substitute materials for patients. Unfortunately, sometimes, significant defects may arise from the traditional bone graft treatments. Therefore, keen efforts by numerous investigators in the field of tissue engineering research have been directed toward creating alternative materials in order to overcome such observed defects in traditional bone grafts treatments. Unfortunately, one of the most difficult challenges that investigators faced in such goal achieving is how to obtain an ideal material includes biocompatibility, suitable microstructure, and high mechanical stability with degradation rates for supporting the cell residence and allow retention of metabolic functions. Fortunately, it has been found that the bioactive three-dimensional (3D) scaffolds of the biomaterial hydrogels with their amorphous nature are the most suitable for satisfying the requirement of bone treatment challenges. It is well known that polysaccharides and their hydrogel derivatives are mainly amorphous in nature, possess a three-dimensional network (3D), and are of excellent hydrophilic affinity for absorbing a large quantity of water without change in the network structure as well as they having the capability for refractory wounds treatments and filling into the irregular wounds sites with providing sufficient adhesiveness. Therefore, the polysaccharide hydrogels in particularly alginate substrate were recognized to be the more favorable biomaterials and the key to overcome the challenges and solve all problems faced by the scaffold tissue engineering and drug delivery demands.

R. M. Hassan (El-Moushy) (✉)
Faculty of Science, Chemistry Department, Assiut University, Assiut 71516, Egypt

A. Kumar et al. (eds.), *3D printable Gel-inks for Tissue Engineering*, Gels Horizons: From Science to Smart Materials, https://doi.org/10.1007/978-981-16-4667-6_11

1 Introduction

Polysaccharides are well-known biomaterials built of different sugar units and are characterized by their low cost, sustainable, biodegradable, biocompatible, nontoxic, and ecofriendly natural polymers. They are water-soluble macromolecules forming viscous colloidal solutions of hydrophilic nature when dissolved in water. The high tendency of water solubility is owing to the presence of one or more of the functional, –OH, $–COO^{-}$, and $–SO_3H^{-}$ group moieties within the monomers of their macromolecular chains. In aqueous solutions, the swelling and orientation of the spherical or coiled colloids will transfer them into copolymers of linear blocks structure. Therefore, an interface between the macromolecule and the water was formed. The polysaccharides have received worldwide applications in the traditional medical, pharmaceutical, agricultural, and food industry [4, 25, 34, 39, 40, 43, 58, 78, 79, 121, 124, 128, 140, 160, 158, 181, 182, 192].

Alginate and its derivatives were recognized as the most commonly distinguishable biomaterials among the polysaccharide. This fact is attributed to its obvious properties such as holding a large amount of water within the network without dissolving, fast ability for gelling, viscosifying, emulsifying, stability of chemical and mechanical properties, and the temperature independence of the sol–gel transition processes together with the other advantages mentioned before on polysaccharides [9, 26, 35, 38, 112]. Consequently, sodium alginate (Alg–Na) and its derivatives were considered as one of the most important and essential constituents for applications in the biomedical industry, particularly in the tissue engineering area. In the beginning, great attention has been focused to use the polysaccharides in traditional medical and pharmaceutical products such as detergents, emulsifiers, paper textile, paint, latex, and of hydrophilic colloidal nature in ceramic glazed; in cosmetic pharmaceutics as binders, thickeners, toothpaste binders, hand lotion, shampoo, hair treatment components, food industry such as drinks, jellies, relishes, pizza, fish gels, pet foods, and milk products [4, 26, 34, 44, 54, 124, 128, 129, 131, 140, 181].

Today, after the recognition that the polysaccharide hydrogels in particularly the alginates and their derivatives are the key for solving the wound dressing and bone regeneration owing to the distinguishable advantages of its physical properties. This fact was encouraged by both scientists and industrial investigators to exert more efforts for modifying and improving the physical properties of biomaterials since they represent the determining factors. The limitation feature demands for such sector involves the efficiency, performance, degree of substitution (DS), distribution of substituents and the degree of polymerization, homogeneity of substituent distribution, shearing stability, and the rheological behavior of the hydrogels [22, 78, 79, 90, 118]. The keen attempts by the researchers have met with great success to overcome the challenges and difficulties that were faced in such biomedicine industry. They found that crosslinking the polysaccharides have been accompanied by remarkable improvements in the physical properties of polysaccharides such as

biocompatibility, nontoxicity, selectivity, and rheological properties (the mechanical strength and swelling capability), which act as the limitation demands in the biomedical industry. Various crosslinking techniques were used in scaffold tissue engineering, micro-capsulation, and drug delivery applications.

Consequently, crosslinked polysaccharides and their derivatives have been recognized as the more applicable biomaterials in the wound dressing, blood-anticoagulants, stomach ulcer controllers, skin grafting, medical adhesive, adhesive prevention barriers, bone regeneration and substitution, surgical wounds, leg ulcers, pressures ulcers, diabetic ulcer, graft, and donor sites and trauma wounds applications [6, 8, 18, 29,44, 58, 59, 76, 77, 89, 103,123, 130, 131, 141–147, 164, 174].

On the other hand, the polysaccharides were applied not only in the biomedical, pharmaceutical, and food industries but also in the purification of water using cellulose and chitosan-based membranes polysaccharides [168], in per-vaporization dehydration processes ethanol manufacturing, immobilization, chelating agents as biosorbents for removal of toxic heavy metal cations and radionuclides pollutants from wastewater and contaminated matters [7, 50, 62, 159, 175, 176, 184]. Moreover, the pectin [72, 73]; chondroitin-4-sulfate [79], and alginate [73, 127, 166] were found to be good efficient inhibitors for applying in corrosion field for inhibition the dissolution of the metal in either acidic or alkaline media. The progress in crosslinking techniques with the increase of its applications in different industrial purposes altered the polysaccharides and their hydrogel derivatives to the forefront of the biocompatible polymer architecture [25, Alistari 2001; 34, 40, 43, 108, 121, 124, 129, 142, 192].

2 Types of Polysaccharides

Two categories of polysaccharides were commonly recognized. The first one contains the –CHOH; $–CH_2OH$; $–COO^–$; $–COOCH_3$; $–CH_2OCH_3$; $–CH_2OCH_2COO^–$; $–NH_2$ or $–NHCOCH_3$ as moieties functional groups together with the presence of one or more sulfonic groups ($–SO_3H$) one of which on C-2 position on the monomers and this category is termed by sulfated polysaccharides. The unit consists of two monomers. The second category contains the –CHOH; $–COO^–$; $–COOCH_3$; $–CH_2OCH_3$; $–CH_2OCH_2COO^–$, $–NH_2$ or $–NHCOCH_3$ functional groups without the presence of any sulfonic groups ($–SO_3H^–$) and is termed by non-sulfated polysaccharides. In the second category, the unit is consisting of only one monomer.

2.1 Sulfated Polysaccharides

The sulfated polysaccharides are usually containing a lot of sulfur atoms within their macromolecular chains such as in carrageenans and chondroitin substrates. Those two substrates possess both primary and secondary alcoholic groups as

functional groups within monomers of the macromolecular chains. They have the common structural feature of being polysaccharides built, alternative 1,3-linked β -D-galactopyranosyl and 1,4-linked α-D-galactopyranosyl units such as in carrageenans which correspond to the major structural red algae polysaccharides that consist of the(1 → 3) β-D-galactose-4-sulfate and (1 → 4) 3,6-anhydro-α-D-galactose units [34] and are shown in Fig. 1. On the other hand, the chondroitin-4-sulfate is build up of N-acetyl-D-galactosamine 4-sulfate with D-glucuronic acid repeating units [13] as shown in Fig. 2.

2.2 Non-sulfated Polysaccharides

This category involves the alginates (Alg), pectates (PEC), carboxymethyl cellulose (CMC) and methyl cellulose (MC), chitin (CIN), and chitosan (CSAN) as the most well-known non-sulfated polysaccharides. They are water-soluble polysaccharides formed from metabolic and life processes in plants, marine, fruits, and plants [34, 40, 124].

The most known distinguished polysaccharide for application in biomedicine is sodium alginate substrate. The major structural formula of sodium alginate is $(C_6H_7COONa)_n$. It is extracted from brown algae and regarded as a collective term of irregular linear blocks like structure comprises the α-L-guluronic acid and β-D-mannuronic acid unites linked in (1 → 4) positions. Studies of alginates indicated that the two different uronic acid residues exist as blocks of homopolymeric sequences of (M blocks) and (G blocks), separated by long sequences of heteropolymeric sequences (MG blocks), arranged in a nearly alternating fashion. The M and G blocks are distributed within the polymer chain in varying proportions to produce heterogeneous alternating (MG) and homogeneous (MM or GG) sequences in the primary structure of algae [42, 82, 84, 89, 153, 154, 158, 160]. These sequences are illustrated below.

_M_M_M_M_M_M..M_G_M_G_M_G_M_G_.. . G_G_G_G_G_G_

M-block MG-block G-block

The monomers are arranged in a clock-wise manner around the macromolecular chains, but the distribution of arrangements is not random. It demands that the relatively long sequences should contain only one hexauronic acid residue (mainly G block). The presence of multiple hydroxyl functionality enhances the formation of linear linked chains. The biological and physical properties in aqueous solutions depend not only on the G/M ratio but also on the distribution of these blocks along the chain [160]. On the other hand, the G/M ratio is dependent on the source of the alginate reagent. The alginates have widespread in industrial applications due to their high ability for forming hydrogels in different shapes such as pellets, beads, membranes, columns, fibers, and films in the presence of divalent metal ions owing to

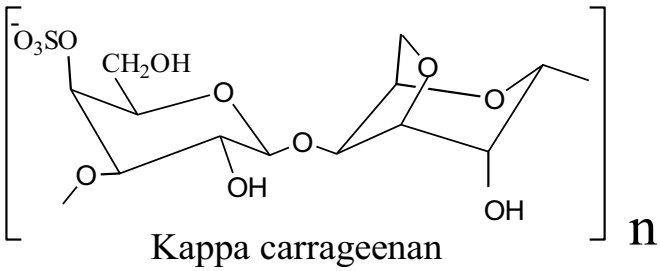

Kappa carrageenan

$$(C_{12}H_{17}O_{12}S)_n$$

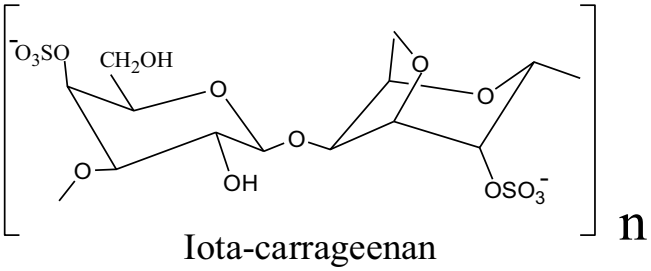

Iota-carrageenan

$$(C_{12}H_{16}O_{15}S_2)_n$$

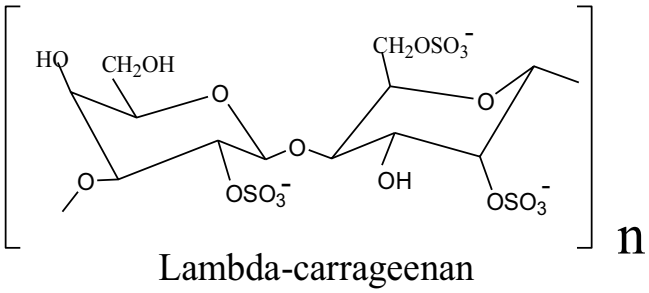

Lambda-carrageenan

$$(C_{12}H_{17}O_{19}S_3)_n$$

Fig. 1 Geometrical configuration for Kappa, Lambda, and Iota carrageenans as sulfated G-block polysaccharides

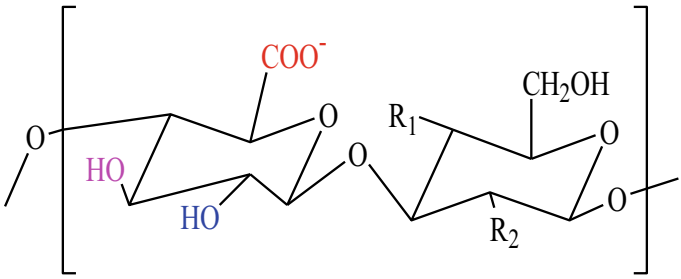

Chondroitin-4-sulfate

$(C_{14}H_{21}NO_{14}S)_n$

$(R_1 = -OSO_3^-$ and $R_2 = -NH\text{-}CO\text{-}CH_3)$

Fig. 2 Geometrical configuration of chondroitin as sulfated polysaccharides

the presence of zones rich in GG blocks [67, 68, 171] The geometrical configuration, of (G) and (M) glycoside units of alginate, are shown in Fig. 3.

The functional groups on the C-6 position are being in equatorial positions and correspond to: $–CH_2OCH_2COOH$ in carboxymethyl cellulose, $–CH_2OCH_3$ in methyl cellulose, –COOH in both alginates and pectates and to $–CH_2OH$ in both chitin and chitosan. On the other hand, the functional groups on the C-2 position are corresponding to $–NH_2$ in chitosan and $–NHCOCH_3$ in chitin, whereas it corresponds to –OH in all other cited non-sulfated polysaccharides. A great similarity of the structures exists between end pectates and alginates. The difference is that the two secondary alcoholic groups (-OH) present on C-2 and C-3 positions, are in cis position in alginates but in the trans position in the pectates (as well as in the methyl cellulose and, carboxymethyl cellulose) [57, 82, 84, 150–152]. It has been found that the presence of COOH and OH moieties as functional groups within the alginate

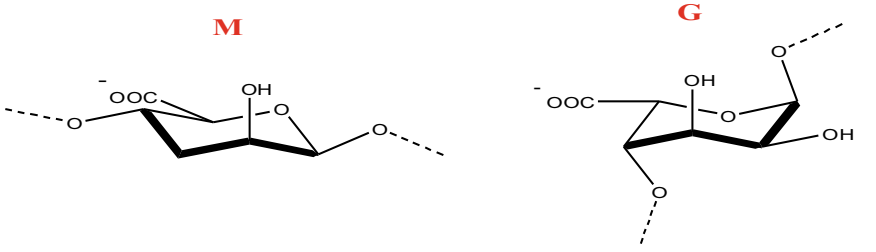

β-(1-4)-D-Mannuronic Acid α –(1-4)-L-Guluronic Acid

Fig. 3 Geometrical configuration of non-sulfated polysaccharides

macromolecular monomer chains render the alginate to be a typical example for crosslinking the polysaccharides.

3 Methods for Crosslinking the Polysaccharides

The term crosslinking in polysaccharides can be defined as the linking of one monomer's chain to another chain at certain junction points via the formation of either temporary or permanent ionic and covalent bonds. These polysaccharides are hydrated in aqueous solutions to give the so-called colloidal sol. On the other hand, the hydrophilic polymers behave the Newtonian behavior at a low moderate concentration where no chain entanglement occurs [131, 137]. Therefore, crosslinking of the chains by using a suitable crosslinker leads to viscoelastic or pure elastic behavior which promotes some improvement of the physical properties of polysaccharide macromolecule such as the biocompatibility and nontoxicity in order to meet the recent developments that occurred in pharmaceutics, drug delivery, scaffold for bone tissue engineering, biomedicine, microencapsulation, and biocatalyst applications [6, 8, 58, 59, 78, 79, 101, 110, 118, 131, 133, 143, 174, 177, 179, 187]. Generally, there are two categories of crosslinking the polysaccharides including alginates, namely the physical and chemical crosslinking, respectively. The crosslinking by either physical or chemical types was based on the presence of reactive functional groups such as OH, COOH, and NH_2 moieties within the monomers of the macromolecular chains of polysaccharides.

3.1 Physical Crosslinking

This category can be applied for reversible hydrogels in which the formed polymeric network involves temporary interaction junctions arising from the polymeric chains entanglements owing to the conformational changes where the chemical hydrogels are permanent. Physical crosslinking becomes of great interest when the use of the chemical crosslinking is not preferred for the possibility of occurrence of some toxicity. This type of crosslinking can be achieved by different methods either ionic interaction (through attraction forces of the opposite charges, hydrogen bonding, hydrophilic, non-covalent, and chain complexation interactions) formation of blends or composites (i.e., by mixing two polymers together), or by the use of multifunctional crosslinking [23, 32, 57, 84, 96, 102, 103, 126, 150–152, 178, 187].

It stated that alginate polysaccharide is a promising biomaterial not only at the present time but also for the future in the sector of biomedical, pharmaceutical, and drug delivery applications [140]. Here, the term biomaterial means a substance that has been engineered to take a form which alone or as part of a complex system is used to interact directly with components of living cell systems such as in therapeutic or diagnostic procedures for regeneration of the tissues lost by degenerative processes

or trauma. Therefore, this chapter is essentially concerned with the crosslinking methods fabricated three-dimensional (3D)-based alginate hydrogels primarily for general application in biomedicine, bioprinting scaffold tissue engineering, pharmaceutics, and drug delivery. This is because alginate was recognized as the typical example for crosslinking polysaccharides since it is readily processable for application as three-dimensional scaffolding biomaterials [53, 164]. This fact may be attributed to its obvious advantages such as sustainability, biodegradability, biocompatibility together with the above-mentioned features for the alginate. This means that alginate hydrogels will have thermal stability and deodorize wound sand absorption pain stimulating compounds. Therefore, the modification of such properties has become of great importance in order to meet the biomedical application requirements such as scaffold tissue engineering including wound healing, cartilage repair, bone regeneration as well as for control the drug delivery releasing. This goal can be easily achieved through the application of the following crosslinking methods.

3.1.1 Ionic Bond Interaction

The high negatively charged anionic polymers such as in alginate and carrageenan polysaccharides render them to possess a high tendency to form hydrogels. This chelation (or binding) takes place by the ionic interaction of the anionic alginate polysaccharide with the cationic polyvalent metal ions. Such interaction between the alginate and the divalent metal cations in particularly with the calcium (II) ion is considered as the simplest, straightforward, and most common method for physical crosslinking forming the corresponding coordination biopolymer ionotropic hydrogels of anisotropic nature [87, 169, 171, 172]. This is because it can be performed at room temperature and the physiological pHs [32, 71, 75]. The anisotropic properties are attributed to the orientation of the solvent molecules and the chains toward the chelated metal ion [10–11, 67, 68, 169, 171]. This interaction can be achieved with solid sodium alginate and the polyvalent metal ions giving gel complexes of granule nature instead of the hydrogel forms. The nature of the formed corresponding coordination biopolymer complexes formed in either hydrogels or granule forms depending on the nature of alginate reagent and the method of preparation. Therefore, the negative carboxylate groups create the largest section of titratable sites along the alginate backbone. Hence, the negative carboxylate groups are considered as the key of the crosslinking processes as well as the affinity of the alginate for binding the polyvalent metal cations. This type of crosslinking has been used to develop the alginate hydrogels for achieving fibers, films, nano- and microparticles as well as it is frequently applied as a matrix of encapsulation of living cells [56, 173] or for releasing of proteins [183]. The release of proteins from alginate microcapsules is achieved by spraying a solution of sodium alginate sol into an aqueous solution of calcium chloride or calcium acetate which can be modulated by coating the particles with cationic polysaccharides such as chitosan [134]. The term hydrogel means that the network of the polymer is the dispersion medium. Hydrogels are often used as cellular scaffolds in tissue engineering. In general, the biodegradable hydrogel systems were found to be typically excellent crosslinkers for such purpose. It has been found that

the calcium (II)-alginate hydrogel is a model example in scaffold tissue engineering purposes since it possesses all the requirements.

It reported that alginate hydrogels are of three-dimensional network hydrophilic polymer chains in which the water content exceeds 95% of the hydrogel weight. These hydrogels are capable of swelling or shrinking in the presence of water or other media [71, 75]. If the water is completely removed, the hydrogel will collapse to form xerogels. The ability for swelling or shrinking are reversible processes, therefore, the xerogels will swell to return to the hydrogels once again in the presence of water. The networks are extremely swollen or shrunk with water without dissolving. In such crosslinking, the divalent metal ion crosslinks both monomer blocks of the same chain or different chains [61] via charge interaction of the positively chelated metal ions and the negative carboxylate group moieties. Therefore, the calcium(II)-alginate can be used for encapsulation of living cells [6] and protein releasing [173, 183]. The classification of hydrogels is depending on their origin, physical properties, resources, degradation rates, crosslinking, ionic charges, rheology behavior [135], and has been reviewed in more detail elsewhere [78, 102, 178].

Among the techniques used for such crosslinking is dripping the alginate sol into an aqueous solution divalent metal ion electrolytes such as calcium (II) (0.5–1.0 mol/L). As the alginate sol gets in contact with the surface of Ca^{2+} metal ion electrolyte, a primary membrane is formed between the alginate and the metal ion electrolyte (or surround the alginate sol pellet in case of using a syringe for obtaining hydrogel spheres) to prevent the scattering or deterioration of the alginate sol. This is followed by a rapid exchange process for replacing the Na^{+} counter ions of alginate sol outward into the electrolyte of Ca(II) metal ion with a simultaneous diffusion of the Ca^{2+} ion inward direction into the alginate sol. The net ion exchange process between the two exchangeable counter ions leads to the formation of the corresponding coordination biopolymer hydrogels. The formation of such hydrogels occurs not only with the divalent metal cations (except magnesium (II)) [36, 37] but also with silver(I) as monovalent cation as well as with the polyvalent metal cations of higher oxidation states such as the trivalent, tetravalent up to hexavalent states of metal ions [61, 78, 79]. There upon binding the divalent metal ions to the α-L-guluronic blocks between two different chain monomers results in the **3D** network. The kinetics of such sol–gel transformation (gelation) as well as the factors which affected the gelation processes in terms of the kinetic parameters have been investigated and discussed [27, 60, 64, 74] as well as the electrical properties under the influence of a wide range of high frequencies [65, 66], and for other metal ions rather than calcium (II) ion were reported earlier [79]. The nature of such formed hydrogel is whether, in the shapes of pellets (spheres or beads), membranes, or columns (tubes) is depending on the apparatus used for the preparation of the metal-alginate hydrogels. Using the syringes, Petri dishes or columns (one side closed with cellophane paper) containing the dripping alginate sols were accompanied by the formation of elastic and transparent metal-alginate of the corresponding hydrogels in the shapes of pellets [71, 75]; membranes [65, 67, 68, 73] and columns hydrogel forms [69, 70], respectively. Sometimes, these coordination biopolymer metal-alginate complexes were prepared in the gel granule form [69, 80, 81, 148] or in the microsphere's nature

[109, 110]. The physical properties of the formed hydrogels such as elasticity, transparency, mechanical, and rheology properties, are depending on the nature of the metal ions such as valence, ionic charge, ionic radii, pH of the media, concentration of alginate sol, ionic strength, and the temperature as reported in more details earlier [67, 71, 75, 78]. On the other hand, the morphological structure depends on the direction of diffusion of the metal ion is whether is upward or downward through its diffusion into the sodium alginate sol network in order to replace the Na^+ counter ions to form its corresponding hydrogel complexes [67, 74]. The morphological structures of calcium (II)-alginate hydrogels are shown in Fig. 4 [62, 74]. The other physicochemical properties such as electrical conductivity (Kharou and Hassan 2002), thermal degradation [193], and heterogeneous chemical equilibrium [46, 81] of Ca(II)-alginate gels of granule nature were investigated and reported in details earlier. The chelation (binding) of the interdiffused metal ions with the carboxylate and hydroxyl functional groups of alginate is not just simple, but partially ionic and partially coordinate bonds are formed between the carboxylate and hydroxyl functional groups and the interdiffused metal ions, respectively, through the formation of bridges of carton-box-like structure [19, 20, 57, 138, 139, 150–152]. Sometimes, the preparation of the hydrogels occurs by hydrophobic modification such as in chitosan and dextran [1–3] structures. The degree of crosslinking is mainly dependent on the number of guluronic acid sequences in the alginate polysaccharide, which in turn depends on the source of reagent, the concentration of alginate, the nature of chelated metal ions such as ionic radius polarizability, strength of chelation, pH of the media, and the nature of the geometrical structure of the formed hydrogel complexes [78]. It is well known that the viscosity of alginate sol increases with increasing the concentration of the dissolved sodium alginate reagent and varies with the pH. Decreasing the pH to a certain limit below (<3.3) may cause precipitation of the alginate biopolymer formed (Tobati et al. 2020). The inherent and reduced viscosities for 4% sodium alginate sol of [Sica Reagent Co. Ltd.] in doubly distilled water (w/w) using Ubbelhode viscometer were found to be 2.78 and 9.87 dl/g at 25 °C, respectively [71, 75]. Whereas, the pK of alginic acid of the same reagent mark was found to be 2.93 whereas the alginic acid takes up 5.4 meqiuv Na^+/g at pH 3.3 [68].

3.1.2 Stoichiometry of Chelation for Ionic Interaction Crosslinking

The sol–gel transformation processes (i.e., gelation process) are inherently stoichiometric ion exchange processes even the two counter ions are different in valences or motilities [85]. The stoichiometry can be expressed by the following equation:

$$\underset{\text{Sol(solid)}}{Z(Alg-Na)_n} + \underset{\text{Electrolyte}}{n\,M^{z+}} = \underset{\text{Hydrogel (Granule)}}{(Alg_z-M)_n} + \underset{\text{Electrolyte}}{Z(Na^+)_n}$$

where the symbol M denotes the interdiffused (binding) metal ion and Z stands for its valence, respectively.

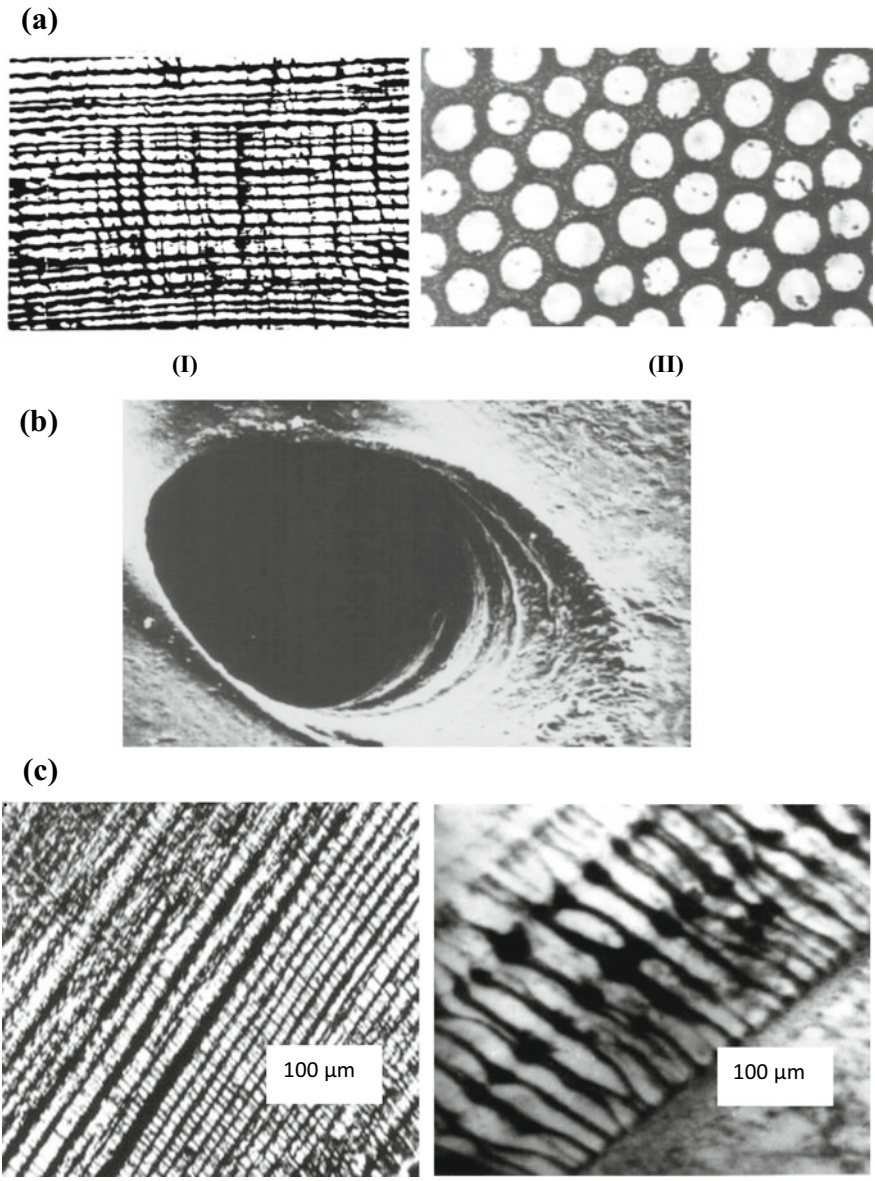

Fig. 4 Optical images: **a** longitudinal (i) and transverse (ii) sections; **b** Polarizing scanning; **c** SEM (I) and TEM (II) Scanning for crosslinked Ca(II)-alginate hydrogel complex

3.1.3 Geometrical Configurations of the Formed Coordination Biopolymer Hydrogel Complexes

Generally, two geometrical models have been postulated for chelation of alginate functional groups with polyvalent metal ions and silver(I) as monovalent ions for giving their corresponding coordination biopolymer of either hydrogel or granule gel forms on using the ionic interaction crosslinking as illustrated by Schemes I, II, III, IV, and V). The first geometry corresponds to an intramolecular association in which the functional groups involved in chelation belong to the same chain (planar geometry) as illustrated by Scheme IA [19, 20, 22, 40, 57, 61, 138, 139, 150–152]. The second type of geometry corresponds to an intermolecular association (Scheme IB) in which the functional groups involved in chelation are related to different chains [61, 78]. However, the divalent metal cations have the choice to chelate by the two geometrical configurations, they tend to coordinate via the intramolecular association type. The tri-, tetra-, and hexavalent metal cations are restricted to chelate via the intermolecular association for attaining the more geometrical stabilities [61] as illustrated by Scheme II. If these polyvalent metal ions are chelated via intramolecular association geometry, bond elongation has become of great necessity. Such elongation is not acceptable from the ground energy may be points of view? On the other hand, the uranyl (VI), silver(I), and alginic acid have the choice for chelating by both two suggested geometries as shown in Schemes III, IV, and V, respectively. However, in view of the measured electrical conductivities of these complexes [61, 66] the intermolecular association was suggested to be the more favorable one for chelation in comparison with the observed electrical conductivity values of the divalent metal ions hydrogel complexes. This means that the nature of the geometrical structure is whether of ether intra- or intermolecular association type is mainly dependent on the valence of the coordinated metal ion and the physical properties of the formed complexes, and plays an important role in determining the physicochemical properties of the hydrogel complexes.

In the presence of divalent metal ions, the G blocks present within the macromolecular chains will lightly associate with the junctions. So, the alginate that is

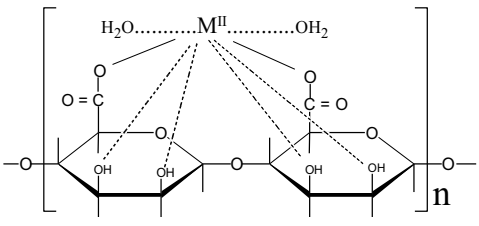

Intramolecular association (A)

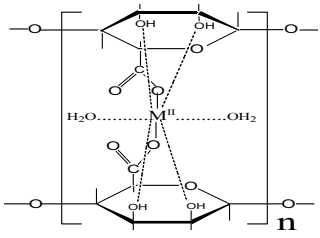

Intermolecular association (B)

Scheme I Chelation in hydrogel complexes of divalent metal ions

Chelation in trivalent metal ion complexes

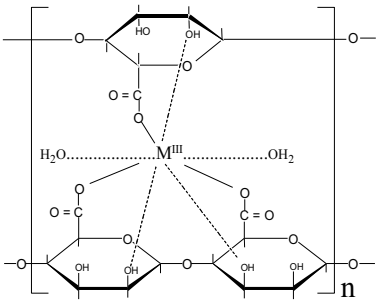

(Intermolecular association)

Chelation in tetravalent metal ion complexes

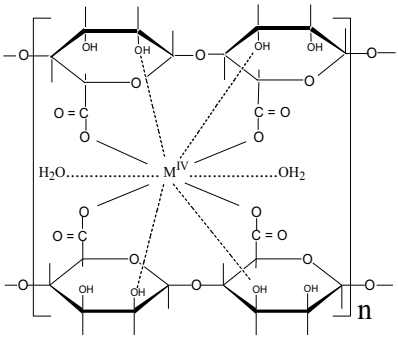

(Intramolecular association)

Scheme II Chelation in hydrogel complexes of trivalent tetravalent metal ions

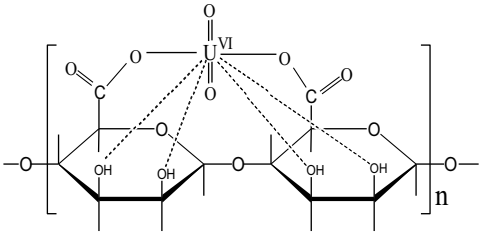

(Intramolecular association)

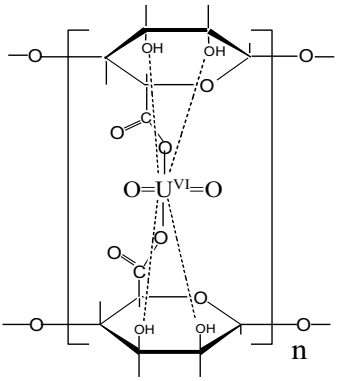

(Intermolecular association)

Scheme III Chelation in hydrogel complexes in uranyl (VI) metal ion

rich in the G blocks promotes stronger hydrogel formation. The affinity of alginate for binding the metal ions also plays a major role in determining the crosslinking efficiency since it affected by the physical properties of the coordination biopolymer hydrogels formed [78, 90, 131, 137]. It reported that the magnitude of the affinity of the rate constant for gelation will give us an overview of the spatial homogeneity of the crosslinking procedure together with univocal information on the mechanical stability [78, 83]. The affinity of alginate toward the divalent metal ions was found

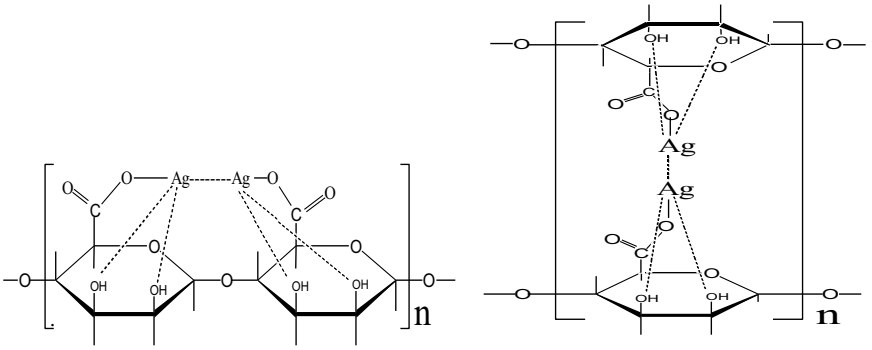

Scheme IV Chelation in hydrogel complexes in silver (I) ion hydrogel complex

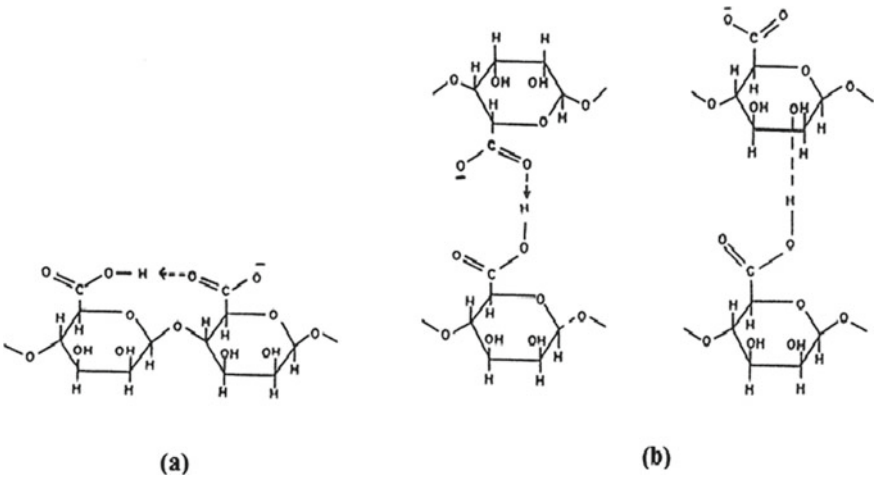

Scheme V Chelation in alginic acid hydrogels

to decrease in the order: Pb > Cu > Cd > Ba > Sr > Ca > Co,Ni, Zn > Mn [83]. However, the calcium(II) ion does not possess the highest affinity; it is the most preferred divalent cation to be used in crosslinking with alginate for applications in biomedicine, tissue engineering, and drug delivery industries. This is because the large pore size and higher water absorbing of Ca^{2+} ion among divalent polysaccharides which has potentially more utilizable in wound dressing and management aids. The hydrophilic sponge produced from the alginate hydrogels of Ca^{2+} ions was found

to have good absorption affinity for both blood and wound [151]. When the Ca(II)-alginate hydrogel contacts with blood, the Ca^{2+} ions are liberated which activates the aggregation and, hence, reduces the coagulation time.

3.1.4 Hydrogen Bonding Interaction

Generally, the crosslinking via hydrogen bonding was physically formed by the interaction between polymeric chains which were comprising active oxygen with other chains containing atoms promoting hydrogen bonding such as H, N, or F atoms. Here, the formation of the hydrogels using such hydrogen bonding is based on the sol–gel viscoelastic transition where the formation of hydrogen bonds can be directly considered as an evocation process**.** Whereas, in the case of alginic acid, the formation of hydrogen bonds occurs between the oxygen of carboxylate groups in the presence of H^+ ions forming hydrogels [66]. It can be achieved by dropping the alginate sol from a syringe into a dilute mineral acid solution such as HCl or $HClO_4$ (0.1 mol/L). However, the formed hydrogels are transparent and elastic, they are of weak mechanical properties. Alginic acid hydrogels of stronger mechanical properties can be obtained by replacing the Ca^{2+} counter ions of the calcium(II)-alginate hydrogels by using H^+ ions using dilute mineral acids [38, 65, 142, 152]. In other polysaccharides like gelatin, hydrogen bonding occurs by the hydrophobic interaction through the gels-like structure in nature. In such a case, the formation of a hydrogen bond may be accompanied by other bonds likes esters or peptides [150].

3.1.5 Blending

This type of crosslinking was applied as an alternative technique in order to overcome the unpredictable and uncontrollable degradation which may occur from the loss of some bounded metal cations or leaking of water from the spongy network of the backbone matrix by aging for a long term in case of ionic crosslinking. Again, however, the alginate has been widely applied in scaffold tissue engineering and drug delivery applications [110] owing to its high biocompatibility, easy and rapid formation of hydrogels under mild conditions even at room temperature and physiological pHs [113], it shows low self-adhesiveness. This was attributed to the poor protein adsorption in the hydrophilic nature [110]. Therefore, the alginates were blended with other polymers to overcome these challenges by enhancing the physical properties in case of blending crosslinking such as adhesion, interaction, and proliferation in order to be suitable and valid for application in biomedicine, drug delivery, and scaffold tissue engineering. Typical examples for polymers used for blending with alginate are the following:

1. Chitosan: Xue et al. [5, 28, 97, 98, 105, 162, 186, 189] for antibabacterial properties.
2. Gelatin [20, 41, 104] with chlopyrifos [100].

3. Poly (vinyl alcohol [93] with poly (acrylic acid) [163] with starch [115].
4. Genipin [51] with lignin [136] or with dry paracetemol [122].

These above mentioned methods for blending were found to be accompanied by distinct modification and improvement of the physical properties of alginate hydrogel such as the capacity, tensile strength, drug diffusion, bioadhesion, and water vapor. Sometimes, the blending of alginate takes place by either mixing with nanoparticles such as Ag NPs [92] or blending the alginate with two other polymers instead of one polymer [16].

3.1.6 Amphiphilic Crosslinking

This type of crosslinking can be synthesized by addition reactions via conjugation of long alkyl chains like dodecyl, octadecyl [132], or 1,6-hexamethylene diisocyante in the organic solvent [33, 63] as crosslinkers to the alginate backbone via ester bonds formation. The latter synthesized crosslinking was preferred to perform in organic since the hexamethylene 1,6-diisocyanate crosslinker has a high tendency to hydrolyze in water. Aqueous solutions of these alginate derivatives exhibited the typical rheological properties of physically crosslinked gel-like networks in the semidilute regime and can be applied in tissue engineering for cartilage repair and regeneration [102] and drug delivery [131].

3.2 Chemical Crosslinking

This type of crosslinking is applied with irreversible hydrogels via creating bonds which can be achieved by using a suitable crosslinker of either bifunctional or multifunctional crosslinkers. In the case of crosslinking, the alginate itself with bifunctional glutaraldehyde, an acetal link was performing with the hydroxyl groups of alginate [165]. Some typical examples for chemical crosslinking the alginate using various crosslinkers are summarized below:

I. Gulutaraldehyde [24, 59, 101, 141, 167].
II. Acrylamide [73, 161] with polyamides [30].
III. Epichlorohydrin [26, 111, 116, 118, 157].
IV. Siloxanic units [120] or with sodium trimetaphosphate [47, 49, 118].
V. Sometimes, the chemical crosslinking occurs by either the generation of free-radicals via either radiation or photolysis processes of polysaccharides [15, 91, 174] or the oxidation of the polysaccharide prior to the crosslinking process for obtaining the keto or aldehyde derivatives that used in the crosslinking processes [17, 48, 76, 77, 99].

The details of physical and chemical crosslinking categories have been reported elsewhere [42, 86, 89, 178, 180]. However, a large number of techniques have been

applied for crosslinking among the polysaccharides including alginate, the most developed research work of such applied crosslinking techniques still remains patent [29].

Another category of crosslinking may be considered, namely dual-network hydrogel crosslinking which can be achieved by the combination between physical and chemical crosslinked hydrogels via electrostatic interaction [88]. This method has been applied to overcome the disadvantages of solely using physical or chemical hydrogels such as in the case of the high liquid uptake capacity over a wide range of pHs or the higher sensitivity of the hydrogel with a variation in the pH of the media compared with the chemical crosslinking method.

4 Some Applications of 3D-Based Cosslinking Alginate Hydrogels in Biomedicine

4.1 Tissue Engineering

The most important factor for the cell culture substrates is the cell adhesion property. It has been found that 3D-based alginate hydrogels based on blending crosslinking have excellent adhesion properties and, hence, they will provide a remarkable jump in the 3D culture in tissue engineering scope. The lack of mammalian cell receptors for alginate hydrogels combined with the low protein adsorption to alginate gels will allow these biomaterials to be served as an ideal blank state. The obvious characterizations of the physical properties of alginate hydrogels such as good cell adhesion and degradation behavior together with the other mentioned properties above render the 3D-based alginate hydrogels to be typical ideal models in the surgical treatments. These hydrogels can be applied in different shapes depending on the nature of the polymer to be blended with alginate in the crosslinking process. Some examples can be summarized as follows:

I. Alginate–chitosan blends: As fibers [98].
II. Alginate–gelatin blends: As hydrogels [41, 104, 125]
III. Alginate (Na)–calcium phosphate blends: As scaffold [45].
IV. Alginate–lignin blends: Aerogel [136].
V. Alginate–Ag blend: As nanoparticles [92].
VI. Alginate–starch blends: As aerogels [115].

4.2 Wound Dressing

The treatment of acute and chronic wounds is the most important aim in wound dressing which needs more care precautions to avoid any bad defects. The traditional wound dressing was to allow the wound to dry and, hence, acquire a hard protective

coating on the scab by using gauze-type materials produced from cotton or lint. This classical treatment acts as a barrier function which simply provided a protective layer that is capable of absorbing the wound fluid while preventing the entry of the pathogen into the wound. Alginate dressing in its dry form can absorb the wound fluid and transform it to hydrogel and the formed hydrogel will provide the wound with water that maintains the physiological moist as well as minimize the bacterial infection of the wound. Therefore, discovering such moist wound dressing treatment for faster healing of wounds was considered as a revolution compared with the traditional dry dressing. The absorption characteristic of alginate was found to have unique gel blocking properties of wound dressings. In addition, alginate wound dressings also have novel hemostatic and antimicrobial properties as well as the ability to promote wound healing. They are now widely used in the management of highly exuding wounds such as leg ulcers, pressure sores, and surgical wound dressing [16, 88, 102]. These hydrogels were utilized in different shapes depending on the nature of polymer blended with alginate for crosslinking process. Some examples for blending used for wound dressing can be summarized as follows:

I. Alginate–chitosan blends: As fibers [98, 165]; membranes [117]; hydrogels [163].
II. Alginate–gelatin: blends: As hydrogels [14].
III. Alginate–poly(vinyl alcohol) blends: As hydrogels [52, 55].

4.3 Drug Delivery

Alginate hydrogels will be more effective when a primary or secondary is formed between the drug and the alginate hydrogel for controlling the drug release behavior. This was achieved by crosslinking the alginate with various polymer substrates via blending methods. Some examples can be summarized as follows:

I. Alginate–chitosan blends: Hydrogels [188] and Beads [5, 155, 185].
II. Alginate–starch blends: As blends [114].
III. Alginate–polyacrylamide blends: As hydrogels [149].
IV. Alginate–polyacrylic acid blends: As hydrogels [163].

Also, blends consisting of three polymers, the alginate with two other polymers were employed for drug delivery [16].

5 Summary

The alginate polysaccharides and their derivatives were extensively utilized in the traditional industries of medical, pharmaceutical, and food industries a long time ago. Nowadays, the modification and improvement of the physical properties of

alginate hydrogels such as the compatibility, toxicity, desired structures, properties, and functions via applying both physical and chemical crosslinking techniques render the alginate to be in the forefront and a competitive biomaterial that can be used widely in most recent developed applications in biomedical industry such as 3D bioprinting tissue engineering, building of blocks for tissues, repair and regeneration of bones as well as enhanced the control of the drug delivery releasing. Alginate-based biomaterials were considered as the promising future treatments in the tissue engineering area with the advantage that both drugs and cells can be readily integrated into the scaffolding matrix. The success of tissue constructs was found to be mainly dependent on the design of the alginate-based scaffolds including physical, chemical, and biological properties. Successful exploitation of alginate-based biomaterials in different tissues and organs such as skin, cartilage, and bone suggests more success in the repair and regeneration in future applications. However, the alginate still faces some challenges to meet all the design parameters simultaneously (e.g., degradation, bioactivities, or mechanical properties). But, we expected that the exerted keen efforts to improve and modify the physical properties of alginate will overcome such challenging problems that have been mentioned before.

Acknowledgements I would like to present my grateful acknowledgment with thanks to Dr. Samia M Ibrahim, Associate Professor, Faculty of Science, New-Valley University, El-Kharja72511, New Valley, Egypt, for her appreciated help during the preparation of this chapter.

References

1. Akiyoshi K, Deguchi S, Moriguchi N, Yamaguchi S, Sunamoto J (1993) Self-aggregates of hydrophobized polysaccharides in water—formation and characterization nanoparticle. Macromol 26:3062–3068
2. Akiyoshi K, Tanuguchi I, Sunamoto J (1999) Self-aggregate nanoparticles of cholesteryl galactoside groups-substituted pullulan and their specific binding to galactose specific lectin, RCA120. Macromol Chem Phys 200:1555–1560
3. Akiyoshi K, Kang EC, Kurumada S, Sunamoto J (2000) Controlled association amphiphilic polymers in water: thermosensitive nanoparticles formed by self of assembly of hydrophobically modified pullulans and poly(N-iso propylacrylamides). Macromol 33:3244–3249
4. Alistair S (2001) Food polysaccharide and their applications. Merckel Dekker Inc.
5. Anal AK, Stevens WF (2005) Chitosan–alginate multilayer beads for controlled release of ampicillin. Int J Pharm 290:45
6. Anozie UC, Ju L-K (2020) Microcapsulation of sulfur by calcium alginate. Appl Polym 137:1–14
7. Asapozhnikov Y, Kalmykov SN, Efimov IP, Remez VP (1996) The sorption of Sr-50 from waters by alginates. Appl Radiat Isot 47(1996):887–888. Symposium series, vol 627. Libarary of Congress Cataloging, Washington, USA
8. Asiyanbi TT, Bio-sawe, Idris MA, Hammed AH (2017) Gelatin polysaccharide–based materials: a review of processing and properties. Int Food Rese J 24:5313–5319
9. Augast AD, Kong HJ, Mooney DJ (2006) Alginate hydrogel as biomaterials. Macromol Biosci 6:623–633
10. Awad A, El-Cheikh F (1980) Electric resistance and anisotropic properties of some metal alginate gels. J Coll Sci 80:107–110

11. Awad A, El-Cheikh F (1981) Electrical resistance and anisotropic properties of some metal alginate gels. J Coll Interf Sci 80:107–110
12. Awad A, El-Cheikh F, Hassan RM (1979) Kinetics of sol-gel transformation especially ionotropic gels. Rev Roum Chim 24:563–568
13. Baeurle SA, Kislev MG, Makarova ES, Nogovitsin EA (2009) Effect of the counterion behavior on the shear of compressive properties of chondroitin sulfate solutions. Polyme 50:1805–1813
14. Balakrishnan B, Mohanty M, Umashankar P, Jayakrishnan A (2005) Evaluation of an in situ forming hydrogel wound dressing based on oxidized alginate and gelatin. Biomater 26:6335–6342
15. Baroli M (2007) Photopolymerization of biomaterials: tissue and potentialities in drug delivery, tissue engineering and cell encapsulation application. J Mater Sci Eng C 57:414–433
16. Batista PSP, Morias AAMB, Pintado MM (2019) Alginate: pharmaceutical and medical applications. Ind J Plant Chem 12:1–35
17. Bertoni FA, Bellu SE, Conzalez JC, Sala LF (2014) Carbohydrate Polym 114:1–11
18. Bose S, Roy M, Bandyopadhyay A (2012) Recent advances in bone tissue engineering scaffolds. Trends Biotechnol 30:546–554
19. Braccini I, Grasso RP, Perez S (1999) Conformational and configurationally features of acidic polysaccharides and their interactions with calcium ions: a molecular modeling investigation. Carbohyd Res 317:119–130
20. Braccini I, Perez S (2001) Molecular basis of induced gelation in alginates and pectins. The egg box model revisited. Biomacromolecules 2:1089–1096
21. Burfield L, David RB, Kim-H L, Roger HS (1977) Desiccant efficiency in solvent drying. a reappraisal by application of a novel method for solvent water. J Org Chem 42:3060–3065
22. Cesaro A, Bellich B, Borgogana M (2012) Biophysical functionality in polysaccharides: from Lego-blocks to nanoparticles. Eur Bipolm J 41:379–395
23. Chan LW, Jin Y, Heng PWS (2002) Crosslinking mechanisms of calcium and zinc production of alginate microspheres. Int J Pharm 212:255–288
24. Chan AW, Whitney RA, Neufeld RJ (2009) Semi-synthesis of a controlled stimuli-responsive alginate hydrogel. Biomacromol 10:609–616
25. Chandra R, Rustgi R (1998) Biodegradable polymers. Prog Polym Sci 23:1273–1335
26. Chatarjee S, Known II, Park K (2007) Smart polymeric sol-gel redefining the limits of biomedical devices. Prog Polym Sci 32:1083–1122
27. Chavez MS, Luna JA, Garrote PL (1994) Crosslinking kinetics of thermally preset alginate gels. J Food Sci 59:1108–1110
28. Chen H, Yang WO, Lawuyl B, Parakash S (2006) Genpin crosslinked alginate-chitosan microcapsules: Membrane optimization of crosslinking reaction. Bio- macromol 7:2091–2098
29. Colo E, Khutorgansiky VB (2011) Biomedical applications of hydrogel: a review of patent and commercial products. Eur Polym J 65:232–262
30. Connor NA, Abughabeigh A, Yasmen F, Buaberg F, Mathe S, Samariaco D, Cherg HP (2015) The crosslinking of polysaccharides with polyamines and dextran-polyallglamine antibacterial hydrogels. Int J Biolg Macromol 72:88–93
31. Correst C, Bugattiv V (2012) Pectin filled with LHD antimicrobial molecules: preparatioon, characterization and physical properties. Carbohydrate Polym 89:132–137
32. Cui J, Wang M, Zhang Y, Muniz GMR, Campo AD (2013) Light-trigged crosslinking of alginate with caged Ca^{2+}. Biomacromol 14:1251–1286
33. Damnik LO, Dijkstra PJ, Vanlyun HTA, Van-Wachem PB, Nieuwenhuis P, Feijen J (1995) Crosslinking of dermal sheep collagen using hexamethylene 1,6-diisocyanate. J Mater Sci Mater Med 6:429–434
34. Davidson RI (1980) Handbook of water-soluble gums and resins. McGraw Hill Book Company, New York, USA
35. Dennis JM (2003) A guide to the Seaweed Industry. FAO, Fisheries Technical Paper Inc. Food and Agriculture Organization of the United Nations

36. Donati I, Asaro F, Paoletti S (2009) Experimental evidence of counterion affinity inalginates: the case of non-gelling ion Mg^{2+}. J Phy Chem B 113:12877–12886
37. Donati I, Ceasaro A, Paoletti S (2006) Specific versus counterion condensation. Nongelling ions/polyuronate systems. Biomacromol 7:281–287
38. Draget KI, Smidsrod O, Skjak–Brack G (2005) Alginate from Algae in Polysaccharides and Polyamides in the "Food Industry, Properties, Production and Patents". Steinbuchel A, Rheesk Edu, Verlag, Wiley, USA, pp1–30
39. Draget KL, Skjak–Brack G, Stokke BT (2006) Similarity and differences between alginic acid and gels and ionically crosslinked alginate gels. Food Hydrocolloids 170–175
40. Draget KI (2009) Handbook of hydrocolloids, Edited by Phillips GO and Williams PA, Norwegien University of Science and Technology, 2nd ed. Wood head Publishing Limited, Chapter 29, pp 807–828
41. Duan B, Hockaday LA, Kang KH, Butcher JT (2013) 3D bioprinting of heterogeneous aortic valve conduits with alginate/gelatin hydrogels. J Biomed Mater Res A 101:1255–1264
42. Dubey S, Sharma R, Mody N, Vyas SP (2018) Polymeric hydrogels: a flexible carrier system for drug delivery. In: Thakur VK, Thakur MA (eds) Polymer gels: synthsis and characterization. Springer, Chapter 6, pp 141–184
43. Dumitriu S (2001) Polysaccharides, structural diversity and functional vitality. Marcel Dekker Inc.
44. Dumitriu S (2006) Polysaccharides in medical applications. Marcel Dekker Inc.
45. Egorov AA, Fedotov AY, Mironov AV, Komlev VS, Popov VK, Zobkov YV (2016) 3D printing of mineral–polymer bone substitutes based on sodium alginate and calcium phosphate. Beilstein J Nanotechnol 21:1794–1799
46. El-Shatoury SA, Hassan RM, Said AA (1992) Alginate polyelectrolyte ionotropic gels. XVI. Kinetics and chemical equilibria studies for heterogeneous ion exchange of polyvalent metal ions in alginate gel complexes. High Perform Polym 4:173–179
47. Fang YY, Wang KJ, Li BZ, Bhandari B, Chen XD, Mao Z-H (2008) Preparation of crosslinking starch microspheres and their drug loading and releasing. Carbohyd Polym 74:379–384
48. Fawzy A (2016) Oxidation of alginate and pectate biopolymers by cerium (IV) in perchlorate acidic solutions: a comparative kinetic and mechanistic study. Carbohyd Polym 138:356–364
49. Fei GD, Li CB, Ahihuai M, Benu A (2014) Preparation and characterization of starch crossinked with sodium trimetaphosphate and hydrolyzed enzymes. Carbohyd Polym 103:310–318
50. Francois F, Francois B, Patricio AR (2008) Review on the removal removal of metal ions from effluents using seaweeds, alginate derivatives and other sorbents. J Water Sci 21:283–308
51. Fujikawa S, Yokata T, Koga K (2004) Immobilization of glucose in calcium alginate gel using penipin as a new type of crosslinking reagent of natural origin. Appl Microbio Biotech 440–441
52. George L, Bavya MC, Rohan KV, Srivastava R (2017) A therapeutic polyelectrolyte–vitamin C nanoparticulate system in polyvinyl alcohol–alginate hydrogel: an approach to treat skin and soft tissue infections caused by *Staphylococcus aureus*. Coll Surf B: Biointerfaces 160:315–324
53. Gillinsky M (2018) Biopolymer hydrogel bioinks. In: Thomas DJ, Jozef ZM, Whitaker LS (eds) 3D bioprinting for reconstructive surgery, 1st edn. Elsevier Publisher, Chapter 6, pp 125–136
54. Giovognoli S, Luca G, Blasi P, Mancuso F, Schoubben A, Arato I, Cavihi M, Faabelle G, Bast G, Bodo M, Calafiore R, Ricci M (2015) Alginates in pharmaceutics and biomed: Is the future so bright. Current Pharm Design 21:4917–4935
55. Golafshan N, Rezahasani R, Tarkesh Esfahani M, Kharaziha M, Khorasani SN (2017) Nanohybrid hydrogels of laponite: PVA-alginate as a potential wound healing material. Carbohydr Polym 176:392–401
56. Goosen MFA, O'Shea GM, Gharapetian HM, Chou S, Sun AM (1985) Optimization of microencapsulation parameters: semipermiable microcapsules as a bioartificial pancrease. Biotechnol Bioeng 27:146–150

57. Grant GT, Morris ER, Rees DA, Smith JC, Thom D (1973) Biological interactions between polysaccharides and divalent cations: the egg-box model. Federation of Eur Biochem Soci (FEBS) Lett 32:195–198
58. Grassauer A, Weinmuellner R, Meier C, Pretsch A, Prieschi A, Prieschl-Grassauer E, Unger H (2008) Iota-carrageenan is a potent inhibitor of rhinovirus infection. Virol J 26:107–111
59. Gribnau TCJ, Vesser J, Nivard RGF (1982) Purification of various petcic enzymes on crosslinked polyuronide. In: Affinity chromatography and related techniques. Elsevier Publishers, Amsterdam, Netherland, p 255
60. Hassan RM (1991) Alginate polyelectrolyte ionotropic gels. III. Kinetics of exchange of chelated divalent transition metal ions especially cobalt(II) and copper(II) by hydrogen ions in capillary ionotropic metal alginate polymembrane gels. J Mater Sci 26:5806–5810
61. Hassan RM (1993) Alginate polyelectrolyte ionotropic gels. XIII. Geometrical aspects for chelation in metal alginate complexes related to their physicochemical properties. Polym Int 31:81–86
62. Hassan RM (2020) Prospective and comparative new technique for evaluation the affinity of alginate for binding the alkaline-earth metal ions during formationthe coordination biopolymer hydrogel complexes. Int J Biol Macromol 165:1002–1028
63. Hassan RM (2021) Novel synthesis of natural cation exchange resin by crosslinking the sodium alginate as a natural polymer with 1,6-hexamethylene diisocyanate in inert solvents: characteristics and applications. Int J Biol Macromol 184:926–935
64. Hassan RM, El-Shatoury SA, Mousa MA, Hassan A (1988) Kinetics and mechanism of sol-gel transformation for polyelectrolytes of capillary cupper alginate ionotropic membranes. Eur Polym J 24:1173–1175
65. Hassan RM (1989a) Influence of frequency on electrical properties of acid and trivalent metal alginate ionotropic gels. A correlation between strength of chelation and stability of polye1ectrolyre gels. High Perform Polym 1:275–284
66. Hassan RM, Makhlouf MT, Summan AM, Awad A (1989b) Influence of frequency on specific conductance of polyelectrolyte gels with special correlation between strength of chelation and stability of divalent metal alginate ionotropic gels. Eur Polym J 25:993–996
67. Hassan RM, Awad AA, Hassan A (1991a) Separation of metal alginate ionotropic gels to polymembranes with special evidence on the position of chelation in copper alginate complex. Jl Polym Sci 29(1):645–1648
68. Hassan RM, Abd-All MA (1991b) Ionotropic gels of alginate polyelectrolyte. I. Potentiometric determination of the ionization constant of alginic acid polyelectrolyte in relation to sol-gel transformation mechanism. Acta Polym 42:447–450
69. Hassan RM, El-Shatoury SA, Makhlouf MT (1992a) Alginate polyelectrolyte ionotropic gels. IX. Diffusion control effects on the relaxation time of sol-gel transformation of divalent metal alginate ionotropic gel complexes. Coll Polym Sci 12:1237–1242
70. Hassan RM, El-Shatoury SA, Makhlouf MT (1992b) Alginate polyelectrolyte ionotropic gels. XII. Chromatographic separation of metal ions in mixture solutions. High Perf Polym 4:49–54
71. Hassan RM, Tirkistani FA, Zaafarany IA, Fawzy A, Khairy M, Iqbal S (2012) Polymeric biomaterial hydrogels. I. Behavior of some ionotropic cross-linked metal-alginate hydrogels especially copper-alginate membranes in some organic solvents and buffer solutions. Adv Biosci Biotechno 3:845–854
72. Hassan RM, Zaafarany IA (2013a) Kinetics of corrosion inhibition in acidic media by water-soluble natural polymeric pectates as anionic polyelectrolyte inhibitors. Materials 6:1–16
73. Hassan RM, Zaafarany IA, Gobouri A, Takagi HD (2013b) A revisit to the corrosion inhibition of aluminum in aqueous alkaline solutions by water-soluble alginates and pectates as anionic polyelectrolyte inhibitors. Int J Corr 1–8
74. Hassan RM, Gobouri A, Zaafarany IA (2013c) Kinetics and mechanism of sol-gel transformation between sodium alginate anionic polyelectrolyte and some alkaline earth metal ions with formation of coordination biopolymer ionotropic polymembrane hydrogels of capillary structures. Advan Biosen Bioelectron 2:47–56

75. Hassan RM, Zaafarany IA, Gobouri AA, Fawzy A, Takagi HD (2014) Polymeric biomaterial hydrogels: II. Behavior of some coordination biopolymeric metal-alginate ionotropic hydrogels in aqueous solutions. J Life Med 1:41–47
76. Hassan RM (2016a) Oxidation of some sulfated macromolecules using various oxidizing agents: focusing on the nature of electron-transfer process and oxidation mechanistics with synthesis of coordination biopolymer oxidation precursors as novel chelating agents. In: Taylor JC (eds) Advances in chemistry research, vol 30. Nova Publishers, New York, Chapter 8, pp 141–211
77. Hassan RM (2016b) Kinetics and mechanistic orientation to the nature of electron-transfer process of oxidation of biodegradable water-soluble polymers by chromic acid in aqueous perchlorate solutions: a linear free- energy correlation. In: Thakur VJ, Thakur MK (eds) Handbook of sustainable polymers: structure and chemistry. Pan Stanford Publishers, USA Chapter 12, pp 413–455
78. Hassan RM, Khairou KS, Awad AM (2018a) New aspects physicochemical properties of polymer-gels in particularly the coordination biopolymeric metal-alginate ionotropic hydrogels. In: Thakur VK, Thakur MK (eds) Polymer gels: synthesis and characterization. Springer Publisher, USA, Chapter 10, pp 275–354
79. Hassan RM, Ibrahim SM, Takagi HD, Sayed SA (2018b) Kinetics of corrosion inhibition of aluminum in acidic media by water-soluble natural polymeric chondroitin-4-sulfate as anionic polyelectrolyte inhibitor, Carbohyd Polym 192:356–363
80. Hassan RM, Takagi HD (2019a) Degradation kinetics of some coordination biopolymers of transition metal complexes of alginates: influence of geometrical structure and strength of chelation on the thermal stability. Mater Sci 1:1–6
81. Hassan RM, Ibrahim SM (2019b) Heterogeneous equilibria: an equilibrium study of ion exchange process between hydrogen ions and divalent metals counter ions in some coordination biopolymer metal-alginate gel complexes. J Membrane Sci Technol 9(198)
82. Haug A, Larsen B (1971) Biosynthesis of alginate: Part III. Polymannuronicacid C-5 epimerase from azotobacter vinelandii (Lipman). Carbohyd Res 17:297–308
83. Haug A, Smidsrod O (1970) Selectivity of some anionic polymers for divalent metal ions. Acta Chem Scand 24:843
84. Haugh A (1964) Composition and properties of alginate. Thesis, Norwegian Institute of Technology, Trondheim, Norway
85. Hellferich (1962) Ion exchange. Mc-Graw Hill, New York
86. Hennik W, Nastrun CV (2012) Novel crosslinking methods to design hydrogels. Drug Deliv Rev 64:223–236
87. Higdon WT (1958) Studies of ionotropy: a special case of gelation. J Phys Chem 62:1277–1281
88. Hu Y, Zhang Z, Li Y, Ding X, Li W, Chen C, Xu F (2018) Dual crosslinking amorphous polysaccharide hydrogel based on chitosan/alginate for wound healing applications. Macromol Rapid Commun 39:1800069(1–5)
89. Ibrahim NA, Nada AA, Eid BM (2018) Polysaccharides: based polymer gels and their potential applications. In: Thakur VJ, Thakur MK (eds) Polymer gels: synthesis and characterizations. Springer, USA, Chapter 4, pp 97–126
90. Idota Y, Kogure Y, Kato T,Yano K, Arakawa H, Chihiro MC, Kasahara F, Ogihara T (2016) The pharmaceutical society of Japan note relationship between physical parameters of various metal ions and binding affinity for alginate. Biol Pharm Bull 39:1893–1896
91. Jeon O, Bauhadir KH, Mansour TM, Alsberg E (2009) Photocrosslinking alginate hydrogel with turntable biodegradation and mechanical properties. Biomatials 30:2724–2734
92. Jovanović Ž, Stojkovska J, Obradović B, Mišković-Stanković V (2012) Alginate hydrogel microbeads incorporated with Ag nanoparticles obtained by electrochemical method. Mater Chem Phys 133:182–189
93. Kamoon EA, Kenawy RS, Tamer TM, El-Meleigy MA, Mohy-Eldin MS (2015) Polyvinyl alcohol-alginate physically crosslinking hydrogel membranes for wound dressing applications: characterization and bioevaluation. J Chem 8:38–47

94. Khairou KS, Hassan RM (2002) Temperature-dependence of electrical conductivity for cross-linked mono- and divalent metal alginate complexes. High Perfor Polyme 14:93–99
95. Khon R (1975) Ion binding of polyuronates-alginate and pectin. Pure Appl Chem 42:371–397
96. Kim M, Lee ST (2002) Characteristics of crosslinked potato starch and starch filled linear density polyethylene. Carbohyd Polym 50:331–337
97. Kim JH, Kim JH, Legal J, Lee KH (2003) Optical resolution of α -amino acids through canttiso selective polymeric membranes based on polysaccharides. J Mem Sci 213:278–283
98. Knill CJ (2004) Alginate fibers modified with unhydrolized and hydrolyzed chitosans for wound dressings. Carbohyd Polym 55:65–76
99. Kristaniansen KA, Patghiasrst A, Christaniansen E (2010) Oxidation of polysaccharides for modification of chemical and physical properties. Carbohyd Polym 45:1264–1271
100. Kullarani AR, Soppimat KS, Aminobavi TH, Dove AM (2002) Polymeric sodium alginate interpenetrating network beads for the controlled release of chlopyrifos. J App Polym Sci 85:911–918
101. Kumar MVA (2000) A review of chitin and chitosan applications. React Funct Polym 46:1–27
102. Lee KY, Boughdir KH, Mooney DJ (2012) Alginate properties and biomedical applications. Prog Polym Sci 37:106–126
103. Lee KY, Buhadir KH, Mooney DJ (2004) Controlled degradation of hydrogel using multifunction crosslinking molecules. Biomater 25:2461–2466
104. Lewandowska-Łańcucka J, Mystek K, Mignon A, Van Vlierberghe S, Łatkiewicz A, Nowakowska M (2017) Alginate- and gelatin-based bioactive photocross-linkable hybrid materials for bone tissue engineering. Carbohyd Polym 157:1714–1722
105. Li P, Dai Y-N, Zhang J-P, Wang A-Q, Wei Q (2008) Chitosan-alginate nano-particles as a novel drug delivery system for nifedipine. Int J Biomed Sci 4:221–228
106. Lin YH, Liang HF, Chung K, Chen MC, Sung HW (2005) Physically crosslinked alginate N.O. CMC/Chtosan hydrogels for drug delivery with calcium for oral delivary of protein drugs. Biomater 26:2105–2113
107. Lioyd LL, Kennedy J, Methacaanon P, Paterson M (1998) Carbohydrate polymers. As wound managements aids. Carbohyd Polym 37:315–322
108. Lioyd LL, Kennedy J, Methacaanon P, Paterson M (1998) Carbohydrate polymers. As wound managements aids. Carbohyd Polym 37:315–332
109. Liu L-S, Liu S-Q, Ng SY, Froix M, Ohno T, Heller J (1997) Controlled release of interleukin-2 for tumor immunotherapy using alginate/chitosan porous microspheres. J Cont Rel 43(1):65–74
110. Liu H, Wang C, Li C, Oin Y, Wang Z, Yang F, Li Z, Wang J (2018) A functional Chitosan-based hydrogel as a wound dressing and drug delivery system in the treatment of woundhealing. RSC Adv 8:7533–7546
111. Luniak L, Marchessault RH (1972) Study of crosslinking reaction between epichlorohydrin starch and starch. Biosynth Nutr Biomed 24:110–116
112. Madav M, Ahmadi Y (2019) Alginates: source, chemistry and properties. In: Hassanin MS, Nayak AK (eds) Alginate verstile polymers in biomedical applications and therapeutics. Taylor and Francis Publishers, Chapter 1, pp 1–24
113. Malafaya PB, Silva GA, Reis RL (2007) Natural–origin polymers as carriers and scaffolds for biomolecules and cell delivery in tissue engineering applications. Adv Drug Deliv Rev 59:207–233
114. Malakar J, Nayak AK, Das A (2013) Modified starch (cationized)–alginate beads containing aceclofenac: formulation optimization using central composite design. Starch-Stärke 65:603–612
115. Martins M, Barros AA, Quraishi S et al (2015) Preparation of macroporous alginate-based aerogels for biomedical applications. J Supercrit Fluids 106:152–159
116. Mazza C, Ferrero MT (1971) Ion exchanger from alginic acid crosslinked with epichlorohudrin. Annali Di Chim 61:348–362
117. Meng X, Tian F, Yang J, He C-N, Xing N, Li F (2010) Chitosan and alginate polyelectrolyte complex membranes and their properties for wound dressing application. J Mater Sci Mater Med 21:1751–1759

118. Merakchi A, Bettayeb S, Douiche N, Adour L, Lounici H (2019) Crosslinking and modifaction of sodium alginate for dye removal in aqueous solution. Polym Bull 76:3535–3554
119. Merakchi A, Bettayeb S, Drouiche N, Adour L, Lounci H (2019) Crosslinking and modification of sodium alginate biopolymer for dye removal in aqueous solutions. Polym Bull 76:3535–3554
120. Mocanu G, Miyahi D, Lecerf D, Pictan L, Dulong V (2007) New polysaccharide based microparticles crosslinked with siloxanic units: synthesis and characterization. Reactt Funct Polym 67:60–66
121. Mohanta R, Mohanta R (2016) Sustainable polymers sand applications. In: Thakur VK, Thakur MA (eds) Handbook of sustainable polymers: processes and applications. Pan Stanford Publishing, USA, Chapter 1, pp 1–58
122. Mukhoadhya Y, Reid H, Savitle D, Tuker IG (2005) Crosslinking of dried paractemol-aginate granules. Part I. The effect of the crosslinking process variables. Int J Pharml 299:134–145
123. Muzzarelli RAA (2009) Chitin and Chitosan for the repair wounded skin, cartilage and bones. Carbohyd Polym 76:167–182
124. Muzzarelli RAA (1973) Natural chelating polymers, 1st edn. Pergamon Press, New York, USA
125. Naghizadeh Z, Karkhaneh A, Khojasteh A (2018) Self-crosslinking effect of chitosan and gelatin on alginate based hydrogels: injectable in situ forming scaffolds. Mater Sci Eng C 89:256–264
126. Nataraj D, Reddy N (2020) Chemical modifications of alginates and its derivatives. Int J Cheml Res 4:1–16
127. Obat IB, Onyeachu IB, Kumar AM (2017) Sodium alginate: a promising biopolymer for corrosion protection of APIX 60high strength carbon steel in saline medium. Carbohyd Polym 178:200–208
128. Okada M (2002) Chemical synthesis of biodegradable polymers. Prog Polym Sci 27:87–133
129. Papa V (1996) Polysaccharides in medicinal and pharmaceutical applications. Smother Publishing, UK
130. Park H, Park K (1996) In: Ottenbrite RM, Huang SJ, Park K (eds) Hydrogels and biodegradable polymers for bioapplications, Chapter 1, ACS
131. Patil S (2008) Crosslinking of polysaccharides: methods and Applications. Pharm Revs 6:1–10
132. Pelletier S, Hubert P, Payan E, Marchal P, Choplin L, Amphiphilic DE (2001) Derivatives of sodium alginate and hyaluronate for cartilage repair: rheological properties. J Biomed Mater Res 54:102–108
133. Peppas NA (1986) Hydrogels in medicine and pharmacy, vol I, II, III. CRC Press, Boca Raton, FL
134. Polk A, Amsden B, DeYa K, Peng T, Goosen MFA (1994) Controlled release of albumin from chitosan-alginate microcapsules. J Pharm Sci 83:178–185
135. Qiu Y, Park K (2001) Environment sensitive hydrogels for biomedical applications. Adv Drug Deliv Rev 33:321–339
136. Quraishi S, Martins M, Barros AA et al (2015) Novel non-cytotoxic Alginate ligninhybrid aerogels as scaffolds for tissue engineering. J Super Fluids 105:112
137. Rees DA (1967) The shape of molecules. Carbohyd Polym 57:630–636
138. Rees DA (1972a) Polysaccharide gels. A molecular view. Chem Indust, London 16
139. Rees DA (1972b) Shapely Polysaccharide the eighth colworth medal lecture. Biochem J 126:257–273
140. Ricci M (2015) Alginates in pharmaceutics and biomedicine: is the future so bright. Curr Pharm Design 21:4917–4935
141. Rimdusti S, Jingiid S, Darmongsakkul S, Tiptipakoru S, Takkeich T (2008) Biodegradability and property characterization of methyl cellulose effect of mono compositing and chemical crosslinking. Carbohyd Polym 46:440–455
142. Rinaudo M (2014) Biomaterials—based on a natural ride natural polysaccharide. Revista Especializada en Ciencias Químico-Biológicas 17:92–96

143. Rosiak JM, Yoshii F (1999) Hydrogels and their medical applications. Nucl Instrum Methods Phy Res B 151:56–64
144. Roy N, Saha N, Kitano T, Saha P (2010a) Development and characterization of novel medicated hydrogel wound dressing. Soft Mater 8:130–148
145. Roy N, Saha N, Humpolicek P, Saha P (2010b) Permeability and biocompatibility of novel medicated hydrogel wound dressing. Soft Mater 8:338–357
146. Saarai A, Saha N, Kitano T, Saha P (2009) Natural resource based medicated hydrogel for health care. In: Proceedings frontiers in polymer science, international symposium celebrating the 50th anniversary of the journal polymer, Mainz, Germany.
147. Saha N, Roy N, Saha P (2008) Allicin containing novel anti- microbial hydrogel. Proceedings Fifth International Conference on Polymer Modification, Degradation and stabilization, Liege, Belgium.
148. Said AA, Hassan RM (1993) Thermal decomposition of some divalent metal alginate gel compounds. J Polym Degrad Stab 39:393–397
149. Samanta HS, Ray SK (2014) Synthesis, characterization, swelling and drug release behavior of semi-interpenetrating network hydrogels of sodium alginate and polyacrylamide. Carbohydr Polym 99:666–678
150. Saxena A, Tahir A, Kaloti M, Ali J, Bohidar HB (2011) Effect of agar-gelatin compositions on the release of salbutamol tablets. Int J Pharm Invest 1(2):93–98
151. Schmidt RJ (1986) Xerogel dressing. In: Tuner TD, Schmidt RJ, Harding KJ (eds.) Advanced in wound management. Wiley Publisher, Chichter, pp 65–71
152. Schweiger RG (1964) Complexing of alginic acid with metal ions. Koll Z Polym 196:47–55
153. Schweiger RG (1962a) Acetylation of alginic acid. I. Preparation and viscosities of align acetate. J Org Chem 27:1786–1789
154. Schweiger RG (1962b) Reaction of align acetates with calcium and other divalent ions. J Orgn Chem 27:1786–1791
155. Shi J, Alves NM, Mano JF (2008) Chitosan coated alginate beads containing poly (N-isopropylacrylamide) for dual-stimuli-responsive drug release. J Biomed Mater Res B Appl Biomater 84:595–603
156. Shiotsuka RN (2014) Hexamethylene diisocyanate. In: Encyclopedia of toxicology, 3rd edn. Elsevier Publisher
157. Siimkovic I, Lazzlo J, Thomson AR (1996) Preparation of weakly basic ion exchanger crosslinking starch with epichlorohydrin in presence of NH_4OH. Carbohydr Polym 30:25–30
158. Smidsrod O (1974) Molecular basis for some physical properties of alginates in the gel State. Farad Discuss Chem Soci 57:263–274
159. Smidsrod O, Skaajak-Barak G (1990) Alginate as immobilization matrix for cells. Trends Biotech 8:71–78
160. Smidsrod O (1973) Some physical properties of alginates in solution and in the gel state. Thesis, Norwegian Institute of Technology, Trondheim
161. Solpan D, Torun H (2005) Investigation of complex formation between (Alginate-acrylamide) semi-interpenetrating polymer network and lead, cadmium, nickel, iron. Coll Surf A 268:12–18
162. Spidhar US, Khan AA (2005) Chitosan-alginate polyion complexes as full membranes. Euro Polym J 41:1859–1866
163. Straccia MC, d'Ayala GG, Romano I, Oliva A, Laurienzo P (2015) Alginate hydrogels coated with chitosan for wound dressing. Mar Drugs 13:2890–2908
164. Sun J, Tan H (2013) Alginate-based biomaterials for regenerative medicine applications. Mater 6:1285–1309
165. Sweeney I, Miraftab M, Collyer G (2014) Absorbent alginate fibres modified with hydrolysed chitosan for wound care dressings–II. Pilot scale development. Carbohydr Polym 102:920–927
166. Tawfik SM (2015) Alginate surfactant derivatives as an ecofriendly corrosion inhibitor for carbon steel in acidic environments. RSC Adv 126(10):4535–4550

167. Thacharodi D, Rao P (1993) Propanol hydrochloride release behavior of crosslinked chitosan membranes. Jl Chem Technol Biotechnol 58:177–181
168. Thakur VK, Voicu S (2016) Recent advances in cellulose and chitosan based membranes for water purification: a concise review. Carbohyd Polym 146:148–165
169. Thiele H, Hallich K (1957) Capillary structure in ionotropic gels. Kolloid Z 151:1–12
170. Thiele H, Hallich K (1959) Application of capillary structure of ionotropic alginate gels as filters. Coll Polym Sci 163:115–122
171. Thiele H, Anderson G (1955) Iontropic gels. Part II. Orders. Colloid and Polymer
172. Thiele H, Awad A (1966) Ions and their biological effects. Investigation on ionotropic gels. Biotechnol 3:63–75
173. Thu B, Bruheim T, Espauvik O, Smidsrod O, Shiony P, Skajak-Barak G (1996) Alginate Polyanion microcapsules: 1: Interaction between alginate polyanion. Biomater 177:1031–1040
174. Tillet G, Boutevin B, Ameduri R (2011) Chemical reactions of polymer crosslinking and post-crosslinking at room and medium temperatures. Progr Polym Sci 36:191–217
175. Torres LG, Velasquez A, Mrito-Arias MA (2011) Ca-alginate spheres behavior in presence of some solvents and water-solvent mixturs. Adv Biosci Biotech 2:8–12
176. Torres LG, de Sanchez LV, Beltran NA, Jimenez BE (1998) Production and characterization of Ca-akginate biocatalyst for removal of phenol and chlorophenol from water. Process Biochem 33:625–634
177. Turnbull G, Clarke J, Picard F, Riches P, Jia L, Han,F, Li B, Shu W (2018) 3D bioactive composite scaffolds for bone tissue engineering. Bioact Mater 3:278–314
178. Ullah F, Othma MBH, Jeved F, Ahmed Z, Akil HMD (2015) Clssification, processing and applications of hydrogels: a review. Mater Sci Eng C 57:414–433
179. Vanvlierberg SV, Duburei P, Schact E (2011) Biopolymer based hydrogel scaffold for tissue engineering applications. A review, Biomacromol 12:1387–1408
180. Verga MD, Caro RR, Illana AM, Perez N, Lona RC (2018) Polymer gels in vaginal drug deliver. In: Thakur VK, Thakur MA (eds) Polymer gels: synthesis and characterizations. Springer, Chapter 8, pp 197–246
181. Viroman L, Tighzert L (2009) Biodeg polym: Mater 3:307–344
182. Virorman A, Tiwae A, Panda B, Jain A (2019) Alginate based composites in drug delivery application. In: Hasanin MDS, Nayak AK (eds) Alginate: versatile polymers in biomedical applications and therapeutics. Taylor and Francis Group, pp 1–23
183. Wee SF, Gombotz WR (1998) Protein release from alginate matrices. Adv Drug Deliv Rev 31:267–2857
184. Wu V, Mimura H, Nibori Y (2009) Selective uptake of plutonium(IV) on calcium alginate gel polymer and TBP microcapsule. J Radioanal Nucl Chem 281:513–520
185. Xie H, Chen X, Shen X et al (2018) Preparation of chitosan-collagen-alginate composite dressing and its promoting effects on wound healing. Int J Biol Macromol 107:93–104
186. Xu W, Shen R, Yan Y, Gao J (2017) Preparation and characterization of elctrospun alginate/PLA nanofibers as tissue engineering material by emulsion eletrospinning. J Mech Behav Biomed Mater 65:428–438
187. Yalpani M (2013) Polysaccharides: synthesis, modifications and structure of Ca^{2+} ion property relations. Series of Studies in organic chemistry, vol 36. Elsevier, New York
188. Yang J, Chen J, Pan D, Wan Y, Wang Z (2013) pH-sensitive interpenetrating network hydrogels based on chitosan derivatives and alginate for oral drug delivery. Carbohydr Polym 92:719–725
189. Yang JS, Xie JY, Weu He (2011) Research progress on chemical modification of alginate: a review. Carbohydrate Polym 84:33–39
190. Yang Hu, Zhenyan Zhang, Yang Li, Xiaokang Ding, Dawei Li, Chuanan Shen and Fu Jian Xu (2018) Dual-Crosslinked morphous polysaccharide hydrogels based on Chitosan/Alginate for wound healing applications. Macromol Rapid Commun 1800069:1–5
191. Yao R, Zhang R, Luan J, Lin F (2012) Alginate and alginate/gelatin microspheres for human adipose-derived stem cell encapsulation and differentiation. Biofabr 4:025007

192. Yasshihito FO, Gong JP (1998) Soft and wet materials polymer gels. Adv Mater 10:827–835
193. Zaafarany IAK, Khairou KS, Tirkistani FA., Iqbal SM, Khairy M, Hassan RM (2012) Kinetics and mechanism of non-isothermal decomposition of Ca(II), Sr(II), and Ba(II) cross-linked divalent metal alginate complexes, Int J Chem 4:7–14

Chapter 12
Future Perspectives for Gel-Inks for 3D Printing in Tissue Engineering

Anuj Kumar, Vijay Kumar Thakur, and Stefan Ioan Voicu

Abstract Medicine has evolved over time from diagnostic methods, has gone through the development of treatments (initially natural, then based on synthesis substances) and reached at the beginning of the twentieth century to the development of biomaterials. Towards the end of the twentieth century, a new field slowly made its way between medical sciences and that of tissue engineering. Ideally, tissue engineering is that inter and multidisciplinary science that aims to design and obtain parts of tissues or even organs in their entirety. This book presented in previous chapters the current level of research in the field of hydrogels as precursors for 3D printing with obtaining constructions for tissue engineering. This chapter aims to present some of the challenges that 3D bioprinting will have to face in order to solve some of the challenges of current regenerative medicine. The main directions are presented both from the point of view of the precursors used, as well as from the point of view of the organs or specific challenges that will have to be solved.

Keywords 3D bioprinting · Tissue engineering · Future perspectives

1 Introduction

The human, as he is today, is about a million years old. Since the beginning of its existence, it has realized that it needs food and shelter. These primary needs led him to look for solutions to hunt, grow plants and process food. As these needs began to be met, the following concern arose—the well-being of the body, prevention and

A. Kumar
School of Chemical Engineering, Yeungnam University, 280 Daehak-ro, Gyeongsan 38541, Korea

V. K. Thakur (✉)
Biorefining and Advanced Materials Research Center, Scotland's Rural College (SRUC), Kings Buildings, West Mains Road, Edinburgh E9 3JG, UK
e-mail: Vijay.Thakur@sruc.ac.uk

S. I. Voicu (✉)
Advanced Polyemrs Materials Group, Faculty of Applied Chemistry and Materials Science, Politehnica University of Bucharest, Bucharest, Romania

A. Kumar et al. (eds.), *3D printable Gel-inks for Tissue Engineering*, Gels Horizons: From Science to Smart Materials, https://doi.org/10.1007/978-981-16-4667-6_12

resolution of health problems. The first step in the evolution of 'medicine' was the awareness of health problems and their determination or evaluation—medical analysis. This medical analysis has evolved throughout the history from Hippocrates, with the determination of the medical condition based on the colour of urine, to this day to modern methods of analysis, such as computed tomography, nuclear magnetic resonance or flow analyses for quantitative and qualitative determination of the components and constituents of the body, from hormones and proteins to tumour markers. Once the problem of diagnosis has been solved, the man has moved on to the next step—establishing a treatment. From herbal cures, products of animal origin, to today's pharmaceuticals, thousands of therapeutic solutions have been investigated, tried and used, administered orally, injectable or surgically, to restore 'well-being or health'. And yet, administering a treatment works biochemically, this mechanism has been understood for a long time. Since a long time ago, besides the need for substances to treat health problems or diseases, there has been an additional problem. What would be the solution if a member was amputated? What would be the solution if an organ lost its function? What would be the solution if an organ or part of an organ is lost—ear, bone, eye, lung, intestine, etc.? For a very long time, any of the situations described represented a fatality without a solution even on a theoretical level. Taking a pill or treatment that causes the growth of an amputated organ is an impossibility even from a theoretical point of view. Same for removing a kidney, part of a lung, bone ear or eye. As science evolved, solutions gradually emerged—a piece of a cariated tooth was replaced with a filling of mercury amalgam (because it has the same thermal dilation coefficient as dentin). A tooth has been replaced with one of gold (because it does not corrode in the presence of saliva). An infection in a large bone in the leg led to amputation of the leg (either due to lack of treatment or with the discovery of antibiotics from the inability to cover a major bone effect and the impossibility of supporting the limb). An amputated leg has been replaced with a wooden prosthesis initially, reaching carbon fibre prostheses nowadays, which also allows partitioning to sports competitions. With the advancement of knowledge about medicine, the problem of the organs that were lost has been partially solved for transplantable organs. What if there's no donor? Slowly, came a new science, perhaps the most complex of those that exist, inter- and multidisciplinary, involving biology, medicine, physics, chemistry, materials science, computer science and mathematics—tissue engineering. From the initial development of prostheses this science has evolved to the replacement of parts of organs (breast implants, bone implants, etc.) and has reached to this day the search for solutions to generate organs in their entirety. But how did it go from assessing the medical condition based on the colour of urine to 3D tissue printing? This chapter of the book aims to exemplify some of the therapeutic challenges that will be solved by tissue engineering, underlining that the same precursors used so far in terms of polymers that we have at hand will be used in the future, 3D bioprinting however makes possible two things that until now were impossible—the improvement of the desired shapes and the possibility to add the living element—the cells (with all the functions and properties they offer).

2 From Biomaterials to Tissue Engineering

The first health problems solved otherwise than surgically or with drugs were solved with the help of biomaterials. From cavities, prostheses, titanium rods used to weld large bones to surgical support nets, the synthesis of new polymers, the discovery of new methods of processing and sterilization has made it possible to improve the quality of life. Around the same time, the increasingly clear understanding of anatomical and physiological processes allowed the advance of therapeutic methods one step ahead. The transition between biomaterials and the early results of tissue engineering was represented by some technical solutions, which combining materials science and physics, chemistry and biology that allowed the replacement of organs in their entirety through the extracorporeal circulation of blood. A first example is the increase in life expectancy for patients with chronic kidney dysfunction. In the case of these patients, the kidneys no longer function at all, the body no longer having the ability to eliminate excess water, salts, urea, uric acid and creatinine. The problem was solved by the development of hemodialysis—circulating blood outside the body and filtering it with the help of a membrane for four hours, every two days. In those four hours, the membrane does exactly what the kidneys do in two days. In contrast to biomaterials (where chemically inert materials are used and therefore the problem of biocompatibility is solved), in this case, the blood being circulated outside the body appears an additional challenge—coagulation. It is no longer sufficient that the material used does not interact with a biological fluid, must not affect and alter [1–5]. Once the problem of hemodialysis has been achieved, another technical problem was solved—breathing during heart or the lungs surgery. With the help of oxygenators, blood is removed from the body and recirculated over a membrane that has the ability to remove carbon dioxide and improve blood with oxygen. Emergency solution and for those who are on the waiting lists for lung transplantation [6–9]. Also based on extracorporeal blood circulation, an artificial liver was developed. A composite membrane with hepatocytes from porcine origin ensures liver function until a viable donor is found. But the membranes are manufactured to order, custom-made, because the cells do not have good enough viability inside the material, not living more than 2–3 weeks [10–13]. But all three procedures, although they increase life expectancy, affect the quality of life (patients are directly related to the hospital environment in order to be able to access treatment and therapeutic procedures). A patient with chronic renal dysfunction cannot schedule an out-of-town trip longer than a day if he does not ensure access to the hemodialysis process. A patient who needs assisted lung or liver function cannot leave the hospital because they risk decompensation of the entire body. A much more elegant solution, from a scientific point of view, ideally, would be to have the ability to produce a new kidney or a new lung. These things are becoming more and more possible with the help of tissue engineering. This extremely complex branch of science aims to practically ‘manufacture tissues’. What kind of tissue? Any tissue that would be needed. How much? Whatever it takes. But ever since the targets that this science has a problem arises—a tissue is a living ‘something’ that we want to manufacture through techniques that are not

related to the living world. The most elegant solution is we use the tissue-specific morphological and functional units that we want to manufacture—cells, in a matrix who about the shape, size and properties we can control.

Basically, tissue engineering aims to regenerate tissue using biomimetic scaffolds. This achievement is based on the synthesis of materials capable of promoting cellular adhesion, proliferation and differentiation for the replacement of affected tissue [14]. 3D printing opens up the possibility of obtaining these forms, but many problems and challenges remain valid and are far from solved, the most important being in close correlation with the vascularization of the scaffolds obtained [15–18]. The main 3D printing techniques are exemplified in Fig. 1 and consist of stereolithography (SLA), selective laser sintering (SLS), binder jetting (BJ), melt extrusion—additive manufacturing (ME-AD), solution extrusion—additive manufacturing (SE-AM) and bioprinting [19].

Of all the techniques available for 3D printing techniques, bioprinting is the most suitable for tissue engineering, being able to add the 'living element'—the cells, during the printing process. Following, will be presented succinctly, some future perspectives related to 3D bioprinting with the possibility of obtaining tissues, both from the perspective of challenges, and from the perspective of the polymers that we have at our disposal for the synthesis of the supporting matrices for cells.

3 Future Perspectives for 3D Bioprinting

3D printing has emerged as a 'wonderful' solution for many branches of engineering. There are entire domains at present that are based and depend on this technique. The leading domains of engineering (e.g., aeronautics and aerospace) generate a large part of the components 'custom-made in-house' by 3D printing, no longer depending on other suppliers and, most importantly, eliminating potential manufacturing defects. The probability of having a defect for a spare part in a complex manufacturing line is much higher than in the case of using a single production step with a very well-developed model and process (simultaneously eliminating matrix errors, processing stages, deviations on the production line, etc.). In leading areas such as engineering used in sports like Formula 1, 85% of components are produced in-house, more than 50% being obtained by 3D printing. It was a matter of time before this technique attracted the attention of researchers in the field of biomaterials. But the technique offering much more possibilities regarding the shape and function of the product, 3D printing paved the way for the 'next generation of therapeutic solutions'.

The first problem that 3D bioprinting raised was the type of precursor used. The first candidates were, of course, polymers of natural origin, as such or modified like cellulose, chitosan [20], gelatin [21], keratin [22], collagen [19, 23]. Synthetic polymers include poly-etherether-ketone (PEEK) [24, 25], aliphatic polyesters [26, 27], polyurethanes [28] or poly (vinyl alcohol) [29].

Metamaterials have been investigated because of the niche properties they possess (at least one characteristic/property other than specific ones), which would have

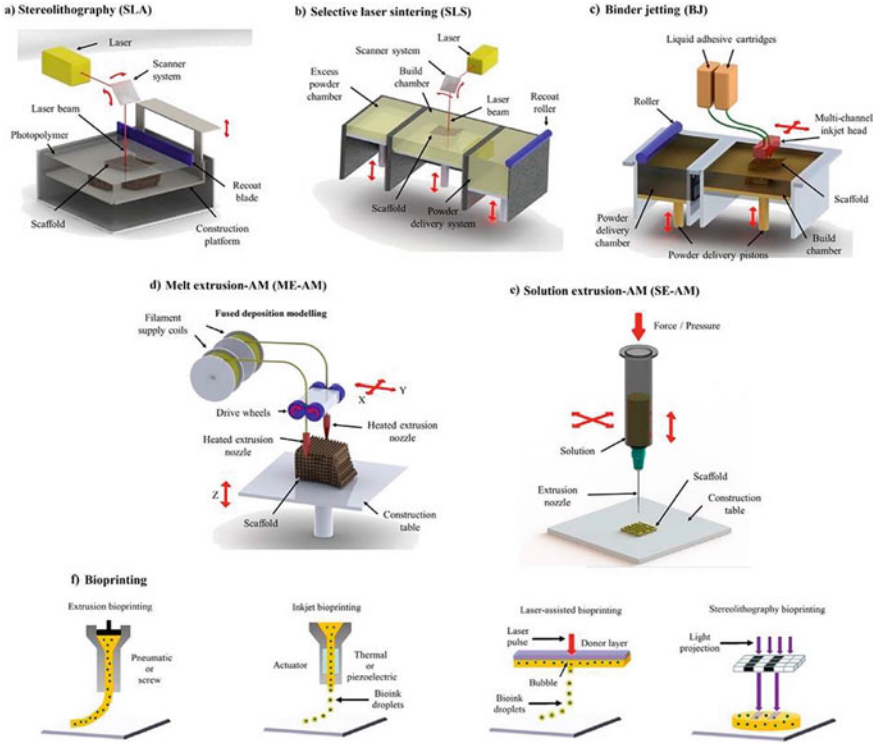

Fig. 1 AM commonly employed for biodegradable polymers processing. **a** Stereolithography (SLA): a light [19] source is irradiated over the surface of a vat filled with a photosensitive resin. **b** Selective laser sintering (SLS): based on selective sintering of a powder bed made of polymer, ceramic or hybrid particles by means of a computer-controlled laser beam. **c** Binder jetting (BJ): a liquid binder is selectively posted on a bed of polymer, ceramic, metallic or composite powder by means of an inkjet head. **d** Melt extrusion-AM (ME-AM): e.g., fused depository modelling (FDM), based on the extrusion of a polymeric filament through a nozzle kept at a temperature higher than the polymer T**g**. **e** Solution extrusion-AM (SE-AM): a polymer, ceramic or composite solution is extruded through a translation nozzle by means of a pneumatic or mechanical-driven dispensing system. **f** Extrusion bioprinting: based on pneumatics or mechanical force to continuously extruded cells suspended in a hydrogel solution; inkjet bioprinting: based on a piezoelectric or thermal actuator to sequentially eject small droplets made of cells and a hydrogel; laser-assisted bioprinting: based on a laser pulse to vaporize a region in the donor layer (top) forming a bubble that propels a suspended bioink to fall onto the substrate; stereolithography bioprinting: based on projected light to selectively crosslink bioinks layer-by-layer

advantages as precursors to tissue engineering, but precisely these properties 'outside the rules', make these materials difficult to process and manipulate. In Fig. 2 are presented some applications of metamaterials in tissue engineering—skin, bone, liver and cartilage [30].

Following, some perspectives related directly with biology will be presented. One of the main organs that will benefit from tissue engineering will be lung. According

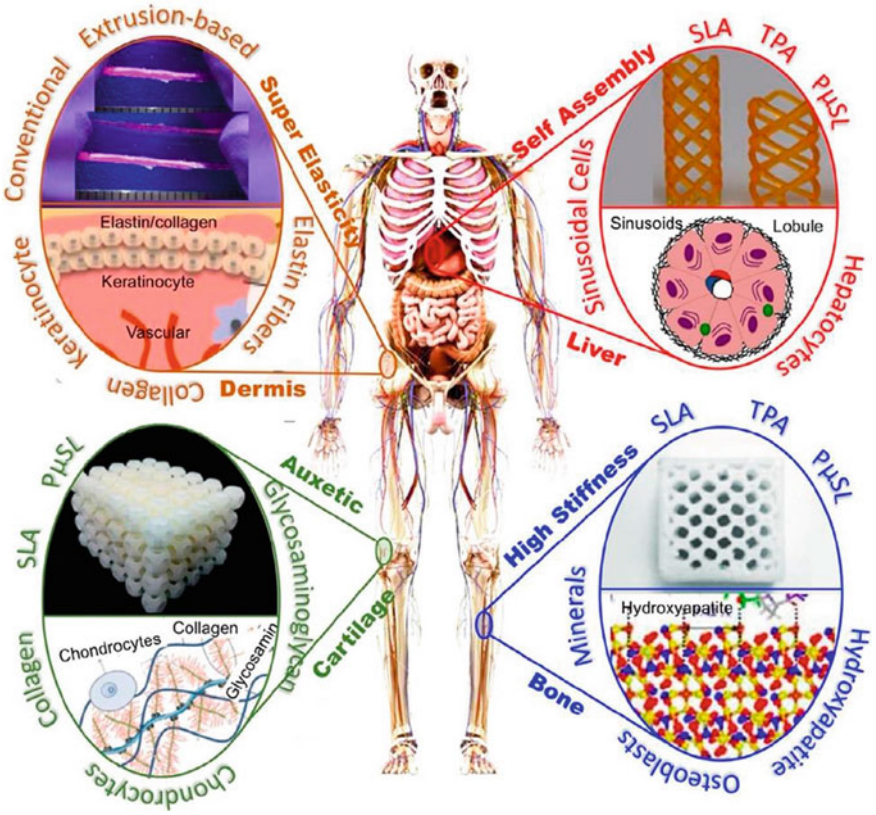

Fig. 2 Proposed meta-biomaterials: An overview of proposed mechanical meta-biomaterials for four different organs in fabric engineering and regenerative medicine: super-elastic models for dermis/skin fabric, auxetic models for articular cartilage, self-assembly models for liver, and high-stiff models for cortical bone. Reproduced with permission after Ref. [30]

to the World Health Organization (WHO) approximately 65 million people worldwide suffer from moderate or severe forms of chronic obstructive pulmonary disease (COPD), with the SARS-CoV-2 pandemic increasing several times their number [31]. For this reason, tissue engineering research applicable in the field of lung tissue has seen an explosion in 2020. The steps for obtaining lung tissue by bioprinting are illustrated in Fig. 3 and are represented by the determination of polymers for the underlying matrix (natural or synthetic), the cells used, printing technique (by inkjet, laser-assisted, extrusion or stereolithography) and the conditioning of the tissue obtained for transplantation. The tissue complexity of the trachea and lungs leads to the search for a universal bioink, based on pulmonary stem cells. The best matrix for this bioink could be hydrogels based on fibrillated proteins with high molecular mass, a challenge to solve being represented by the mechanical properties

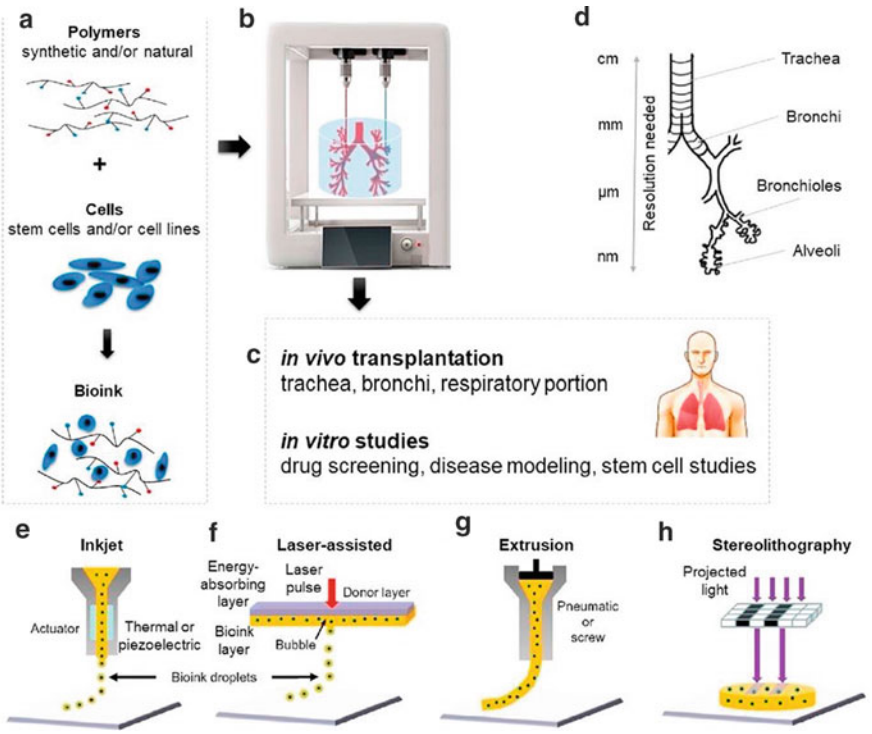

Fig. 3 Schematic of 3D bioprinting of lungs and trachea using bioinks in a bioprinter. (**a**–**c**) Bioprinting process and applications. **a** Bioinks are created by combining various synthetic and/or natural polymers and stem cells and/or cell lines. **b** Bioprinters use bioinks to produce functional 3D-printed (3DP) constructs. **c** 3DP constructs can be transplanted into patients and also can be used for drug screening, disease modeling, and in vitro stem cell studies. **d** Schematic of the long showing the required solutions for bioprinting different parts of a long work. **e**–**h** Simplified illustrated of 3D bioprinting types. **e** Inkjet printers eject small droplets of the bioink sequentially to construct tissues. **f** Laser-assisted prints use a laser to vaporize a region in the donor layer forming a bubble that drives the suspended bioink to fall onto the substrate. **g** Extrusion prints use pneumatics or mechanical pressure to continuously extrude a highly viscos bioink. **h** Stereolithographic prints use a digital light projector to selectively crosslink bioinks plane-by-plane. Reproduced with permission from Ref. [32]

of these hydrogels that raise problems in printing especially through the technique of stereolithography [32].

The problem of mechanical properties of matrix precursors could be solved by the use of synthetic and natural modified polymers such as modified type-I collagen to collagen methacrylamide [33] or gelatin methacrylate (GelMA), a photopolymerizable hydrogel that has proven good properties both mechanically and in terms of the matrix's abilities to favour cell proliferation and differentiation [21, 32]. GelMA was also used to obtain bioink in 10% concentration in a matrix of polyethylene glycol diacrylate (PEGDA) that can be used both for printing lung tissue by cell addition

and as such, for cartilage tissue [32, 34]. Bioprinting of lung or tracheal tissue will not only involve obtaining bioink with solving problems related to the nature of precursors, their mechanical properties or printing technique, or the viability and differentiation of cells within the matrix, but also related to bringing the printed tissue to the biological parameters of natural lung tissue, in terms of hydration and capacity to exchange gases, vascularize and nourish tissue, as well as to eliminate the products of the cells. Conditioning the tissue in order to bring it into parameters will be possible with the help of bioreactors that will be able to provide maturation factors and physiological stimuli such as ventilation and infusion, leading to the maturation of the entire printed construct. Monitoring of the structure, as well as parameters such as pH, oxygen level or dairy are ways to facilitate the control of cell cultures in the printed matrix and implicitly the possibility of obtaining mature and viable lung tissue [32].

Special attention is paid to the tubular tissues obtained by bioprinting, such as those related to the circulatory system (veins, arteries, capillaries), respiratory (trachea), urinary (urethra or bladder), or gastrointestinal [35]. In this case, the natural polymers used as precursors of hydrogels are collagen for the manufacture of blood vessels [36], or agarose, fibrin, gelatin, and hyaluronic acid, amongst others [35], and of the synthetic plurionic F-127 (triblock copolymers consisting of two hydrophilic polyethylene glycol (PEG) blocks at each end of a hydrophobic polypropylene glycol (PPG) block) [35, 37]. In addition, recent research has used DNA-based hydrogels for the bioprinting of tubular tissues, in such cases functional cells reaching a viability of up to 98.8% [38]. The prospects and challenges of the future in this field relate to the development of DNA-based hydrogels that have proven best as precursors for the biofabrication of tubular tissues.

The intestine is one of the most complex organs, having both membrane and membrane reactor role (enzymatic absorption and degradation), as well as complex functions such as peristalsis, variable volume, and capacity for maintenance of bacterial flora [39]. Obtaining intestines by tissue engineering (not necessarily in its entirety, even only parts of it that can be integrated into the intestines) will be one of the biggest challenges. Because of the complexity of this organ, initial research began from obtaining 2D components (the intestinal wall), in order to try to resolve both the presence of bacterial flora components and functional cells [40, 41]. Apart from the problem of vascularization, valid for any construction obtained by 3D bioprinting, in the case of obtaining the intestine there are two additional challenges—bioreactor function [42] and microfluidic function. From the point of view of the hydrogel precursors used, a key factor is the improvement of their mechanical properties to ensure the necessary resistance of the synthesized construct. To this day, an optimal solution has not been found from this point of view (which also provides elasticity, and sufficient mechanical resistance), the most investigated precursor being polyethylene glycol with different molecular weight and degrees of reticulation. Also, the type of cell line used, and its choice is still a problem to study, the main candidates being cell lines or intestinal crypts (derived from rats or mouse) [39].

The construction of aligned structures for guided cells orientation will lead to the possibility of obtaining constructs for muscles, tendons, dentin or even nerves [43].

Printing 3D high-resolution microstructures capable of enabling targeted cell proliferation will be a challenge both from a technical point of view (micron resolutions) and from the point of view of the precursors used. Various mixtures have so far been used to obtain microchannel-printed structures for nerve regeneration and nerve cell proliferation, such as cellulose-collagen [44] or structure aligned based on graphene and graphene oxide (GO) [45] or GO-modified poly (D, L-lactide-co-caprolactone) [46]. One of the challenges that will require a large volume of work and creativity is getting muscle builds. In this case, the importance is not only the printing of a structure and cell proliferation but also the maintenance of the motor function of the cellular constructs. Early research was carried out on aligned collagen fibres [47, 48]. 3D-printed nanofibers from poly (lactic-co-glycolic acid) (PLGA) interspersed with actin fibres were closest to the natural structure of the human muscle [49, 50].

When gaining muscle tissue will no longer be a challenge, the most important organ that keeps us alive will be able to be 'repaired' easily, or perhaps in the not-too-distant future, replaced—the heart. The initial challenge that will be solved will probably be to obtain biomimetic valves, followed by the synthesis of muscle tissues to replace parts of the myocardium affected by the infarction. It is well known that, for the time being, after a stroke in the heart, part of the muscle will be affected by necrosis, the pump activity being irretrievably diminished. Replacing necrotic tissue with near-complete restoration of heart function may become possible in the near future. From solving this problem to obtaining a heart in its entirety will take a few more steps, but probably with a reissue of this book in 10 years, either the problem will be solved, or it will be very close to solving it. The replacement of current solutions for pacemakers is not only a necessity for quality of life but also to eliminate a long set of restrictions that these patients have in their daily lives (restrictions on being in the presence of medium-intensity magnetic fields). or high or the inability to affect a number of medical investigations such as NMR). Also obtaining muscle constructs that can be integrated into the natural muscle will solve many problems in regenerative medicine in the case of patients who have suffered accidents, the recovery being much faster and easier. Some of the problems caused by serious accidents are no longer a challenge in the case of bone tissue, although 15–20 years ago they could lead to the loss of a limb or irreversible conditions. Another challenge, which will probably be solved soon by 3D bioprinting, is the regeneration of nerve tissue. If in the case of other tissues, such as muscle, polymeric precursors can be used to generate support matrices, in the case of nerve tissue, obtaining hydrogels for printing support structures, it will be possible to rely, probably exclusively on modified proteins or DNA-based polymers. With all the current perspectives or problems already solved, there are still limitations of the knowledge we have and problems for which there are not even theoretical solutions. If crystalline 3D can be printed, including diopters, 3D printing of an eye's entirety remains a problem that will not be solved in the near future. Certainly, many problems cannot be solved at this moment, but the road we are on gives hope for solving a large number of problems. Despite the large volume of scientific literature published in the last 5 years, there is still an engineering problem—moving from the laboratory to the hospital all these solutions, the ability to produce them on a large scale or even the possibility of obtaining custom-made

constructions in the hospital, for a specific patient. Unlike industrial landmarks, no two organisms are identical, which is why the biggest challenge will be their production and transposition from laboratory research into practice.

4 Conclusions

3D bioprinting is used to obtain printed structure with the ability to adapt its shape and behaviour in response to various stimuli. This technique represents the initiation of another technique—4D printing—the ability of printed constructs to have biomimicry towards natural tissue, integration capacity and complete morphogenetic function [51]. Most recently, a so-called '5D printing' approach has also been reported for printing complex architectures in multiple directions [52, 53]. This book presents enough information to give the reader a comprehensive look about the field of hydrogels used as precursors to 3D bioprinting with applications in tissue engineering. Instead of conclusions. The challenge that editors launch to readers is to compare at the end of this decade, in 2030, how many of the methods and materials presented in this book are already a common solution used in everyday life.

References

1. Stamatialis DF, Papenburg BJ, Girones M, Saiful S, Bettahalli SNM, Schmitmeier S, Wessling M (2008) Medical applications of membranes: drug delivery, artificial organs and tissue engineering. J Membr Sci 308:1–34
2. Oprea M, Voicu SI (2020) Recent advances in composites based on cellulose derivatives for biomedical applications. Carbohydr Polym, 116683
3. Pandele AM, Iovu H, Orbeci C, Tuncel C, Nicolescu A, Deleanu C, Miculescu F, Voicu SI (2020) Surface modified cellulose acetate membranes for the reactive retention of tetracycline. Sep Purif Technol 249:117145
4. Ionita M, Crica LE, Voicu SI, Pandele AM, Iovu H (2016) Fabrication of cellulose triacetate/graphene oxide porous membrane. Polym Adv Technol 27(3):350–357. https://doi.org/10.1002/pat.3646
5. Raicopol MD, Andronescu C, Voicu SI, Vasile E, Pandele AM (2019) Cellulose acetate/layered double hydroxide adsorptive membranes for efficient removal of pharmaceutical environmental contaminants. Carbohydr Polym 214:204–212
6. Oprea M, Voicu SI (2020) Cellulose composites with graphene for tissue engineering applications. Materials 13(23):5347
7. Muhulet A, Tuncel C, Miculescu F, Pandele AM, Bobirica C, Orbeci C, Bobirica L, Palla Papavlu A, Voicu SI (2020) Synthesis and characterization of polysulfone-TiO_2 doped MWCNT composite membranes by sonochemical method. Appl Phys A 126(3):233
8. Pandele AM, Constantinescu A, Radu IC, Miculescu F, Voicu SI, Ciocan LT (2020) Synthesis and characterization of PLA—microstructured hydroxyapatite composite films. Materials 13(2):274
9. Voicu SI, Pandele MA, Vasile E, Rughinis R, Crica L, Pilan L, Ionita M (2013) The impact of sonication time through polysulfonegraphene oxide composite films properties. Dig J Nanomater Biostruct 8(4):1389–1394

10. Voicu SI, Thakur VK (2021) Aminopropyltriethoxysilane as a linker for cellulose-based functional materials: new horizons and future challenges. Curr Opin Green Sust Chem, 100480
11. Oprea M, Voicu SI (2020) Recent advances in applications of cellulose derivatives-based composite membranes with hydroxyapatite. Materials 13:2481
12. Pandele AM, Serbanescu OS, Voicu SI (2020) Polysulfone composite membranes with carbonaceous structure. Synthesis and Applications. Coatings 10(7):609
13. Satulu V, Mitu B, Pandele AM, Voicu SI, Kravets L, Dinescu G (2019) Composite polyethylene terephthalate track membranes with thin teflon-like layers: preparation and surface properties. Appl Surf Sci 476:452–459
14. Sahranavard M, Zamanian A, Ghorbani F, Shahrezaee MH (2020) A critical review on three dimensional-printed chitosan hydrogels for development of tissue engineering. Bioprinting 17:e00063
15. Joshi S, Rawat K, Karunakaran C, Rajamohan V, Mathew AT, Koziol K, Thakur VK, Balan ASS (2020) 4D printing of materials for the future: opportunities and challenges. Appl Mater Today 18:100490
16. He F, Thakur VK, Khan M (2021) Evolution and new horizons in modeling crack mechanics of 3D printing polymeric structures. Mater Today Chem 20:100393
17. Chen S, Skordos A, Thakur VK (2020) Functional nanocomposites for energy storage: chemistry and new horizons. Mater Today Chem 17:100304
18. Daminabo SC, Goel S, Grammatikos SA, Nezhad HY, Thakur VK (2020) Fused deposition modeling-based additive manufacturing (3D printing): techniques for polymer material systems. Mater Today Chem 16:100248
19. Puppi D, Chiellini F (2020) Biodegradable polymers for biomedical additive manufacturing. Appl Mater Today 20:100700
20. Morris VB, Nimbalkar S, Younesi M, McClellan P, Akkus O (2017) Mechanical properties, cytocompatibility and manufacturability of chitosan: PEGDA hybrid-gel scaffolds by stereolithography. Ann Biomed Eng 45:286–296
21. Nichol JW, Koshy ST, Bae H, Hwang CM, Yamanlar S, Khademhosseini A (2010) Cell-laden microengineered gelatin methacrylate hydrogels. Biomaterials 31:5536–5544
22. Placone JK, Navarro J, Laslo GW, Lerman MJ, Gabard AR, Herendeen GJ, Falco EE, Tomblyn S, Burnett L, Fisher JP (2017) Development and characterization of a 3D printed, keratin-based hydrogel. Ann Biomed Eng 45:237–248
23. Zhang W, Li D, Wang K, Bian W, Li X, Lian Q, Zhongmin J (2012) Fabrication of a bio-inspired beta-Tricalcium phosphate/collagen scaffold based on ceramic stereolithography and gel casting for osteochondral tissue engineering. Rapid Prototyp J 18:68–80
24. Adamzyk C, Kachel P, Hoss M, Gremse F, Modabber A, Hölzle F, Tolba R, Neuss S, Lethaus B (2016) Bone tissue engineering using polyetherketoneketone scaffolds combined with autologous mesenchymal stem cells in a sheep calvarial defect model. J Craniomaxillofac Surg 44:985–994
25. Morrison RJ, Hollister SJ, Niedner MF, Mahani MG, Park AH, Mehta DK, Ohye RG, Green GE (2015) Mitigation of tracheobronchomalacia with 3D-printed personalized medical devices in pediatric patients. Sci Transl Med 7(285):285ra64
26. Antonov EN, Bagratashvili VN, Whitaker MJ, Barry JJA, Shakesheff KM, Konovalov AN, Popov VK, Howdle SM (2004) Three-dimensional bioactive and biodegradable scaffolds fabricated by surface-selective laser sintering. Adv Mater 17:327–330
27. Lee PH, Chang E, Yu S, Lee SW, Kim IW, Park S, Chung H (2013) Modification and characteristics of biodegradable polymer suitable for selective laser sintering. Int J Precis Eng Manuf 14:1079–1086
28. Thompson DG, Osborn JC, Kober EM, Schoonover JR (2006) Effects of hydrolysis-induced molecular weight changes on the phase separation of a polyester polyurethane. Polym Degrad Stab 91:3360–3370
29. Chiellini E, Corti A, D'Antone S, Solaro R (2003) Biodegradation of poly (vinyl alcohol) based materials. Prog Polym Sci 28:963–1014

30. Dogan E, Bhusal A, Cecen B, Miri AK (2020) 3D Printing metamaterials towards tissue engineering. Appl Mater Today 20:100752
31. World Health Organization (2020) Burden of COPD. https://www.who.int/respiratory/copd/burden/en/. Accessed 25 May 2020
32. Mahfouzi SH, Tali SHS, Amoabediny G (2021) 3D bioprinting for lung and tracheal tissue engineering: criteria, advances, challenges, and future directions. Bioprinting 21:e00124
33. Drzewiecki KE, Malavade JN, Ahmed I, Lowe CJ, Shreiber DI (2017) A thermoreversible, photocrosslinkable collagen bio-ink for free-form fabrication of scaffolds for regenerative medicine. Technology 5(4):185–195
34. Nichol JW, Koshy ST, Bae H, Hwang CM, Yamanlar S, Khademhosseini A (2010) Cell-laden microengineered gelatin methacrylate hydrogels. Biomaterials 31:5536–5544ss
35. Zhu W, Cui H, Boualam B, Masood F, Flynn E, Rao RD, Zhang ZY, Zhang LG (2018) 3D bioprinting mesenchymal stem cell-laden construct with core-shell nanospheres for cartilage tissue engineering. Nanotechnology 29:185101
36. Holland I, Logan J, Shi J, McCormick C, Liu D, Shu W (2018) 3D biofabrication for tubular tissue engineering. Bio-Des Manuf 1:89–100
37. Patel A, Fine B, Sandig M, Mequanint K (2006) Elastin biosynthesis: the missing link in tissue-engineered blood vessels. Cardiovasc Res 71:40–49
38. Diniz IMA, Chen C, Xu X, Ansari S, Zadeh HH, Marques MM, Shi S, Moshaverinia A (2015) Pluronic F-127 hydrogel as a promising scaffold for encapsulation of dental-derived mesenchymal stem cells. J Mater Sci Mater Med 26:1–10
39. Li C, Faulkner-Jones A, Dun AR, Jin J, Chen P, Xing Y, Yang Z, Li Z, Shu W, Liu D, Duncan RR (2015) Rapid formation of a supramolecular polypeptide-DNA Hydrogel for in situ three-dimensional multilayer bioprinting. Angew Chemie Int Ed 54:3957–3961
40. Agarwal T, Onesto V, Lamboni L, Ansari A,·Maiti TK, Vosough M, Makvandi P, Yang G (2021) Engineering biomimetic intestinal topological features in 3D tissue models: retrospects and prospects. Bio-Des Manufhttps://doi.org/10.1007/s42242-020-00120-5
41. Matai I, Kaur G, Seyedsalehi A, McClinton A, Laurencin CT (2020) Progress in 3D bioprinting technology for tissue/organ regenerative engineering. Biomaterials 226:119536
42. Mandrycky C, Wang Z, Kim K, Kim D-H (2016) 3D bioprinting for engineering complex tissues. Biotechnol Adv 34:422–434
43. Shim K-Y, Lee D, Han J, Nguyen N-T, Park S, Sung JH (2017) Microfluidic gut-on-a-chip with three-dimensional villi structure. Biomed Microdevices 19:37
44. Lu K, Qian Y, Gong J, Zhu Z, Yin J, Ma L, Yu M, Wang H (2021) Biofabrication of aligned structures that guide cell orientation and applications in tissue engineering. Bio-Des Manuf 4:258–277
45. Zhang YG, Sheng QS, Qi FY, Hu XY, Zhao W, Wang YQ, Lan LF, Huang JH, Luo ZJ (2013) Schwann cell-seeded scaffold with longitudinally oriented micro-channels for reconstruction of sciatic nerve in rats. J Mater Sci Mater Med 24(7):1767–1780
46. Huang C, Ouyang Y, Niu H, He N, Ke Q, Jin X, Li D, Fang J, Liu W, Fan C, Lin T (2015) Nerve guidance conduits from aligned nanofibers: improvement of nerve regeneration through longitudinal nanogrooves on a fiber surface. ACS Appl Mater Interfaces 7(13):7189–7196
47. Zhang D, Yao Y, Duan Y, Yu X, Shi H, Nakkala JR, Zuo X, Hong L, Mao Z, Gao C (2020) Surface-anchored graphene oxide nanosheets on cell-scale micropatterned poly(d, l-lactide-co-caprolactone) conduits promote peripheral nerve regeneration. ACS Appl Mater Interfaces 12(7):7915–7930
48. Wang W, He J, Feng B, Zhang Z, Zhang W, Zhou G, Cao Y, Fu W, Liu W (2016) Aligned nanofibers direct human dermal fibroblasts to tenogenic phenotype in vitro and enhance tendon regeneration in vivo. Nanomedicine (London) 11(9):1055–1072
49. Yin Z, Chen X, Song HX, Hu JJ, Tang QM, Zhu T, Shen WL, Chen JL, Liu H, Heng BC, Ouyang HW (2015) Electrospun scaffolds for multiple tissues regeneration in vivo through topography dependent induction of lineage specific differentiation. Biomaterials 44:173–185
50. Wang L, Wu YB, Guo BL, Ma PX (2015) Nanofiber yarn/hydrogel core–shell scaffolds mimicking native skeletal muscle tissue for guiding 3D myoblast alignment, elongation, and differentiation. ACS Nano 9(9):9167–9179

51. Yeo M, Lee H, Kim GH (2016) Combining a micro/nano-hierarchical scaffold with cell-printing of myoblasts induces cell alignment and differentiation favorable to skeletal muscle tissue regeneration. Biofabrication 8(3):035021
52. Gladman AS, Matsumoto EA, Nuzzo RG, Mahadevan L et al (2016) Biomimetic 4D printing. Nat Mater 15:413–418
53. Haleem A, Javaid M, Vaishya R (2019) 5D printing and its expected applications in Orthopaedics. J Clin Orthop Trauma 10:809–810
54. Costello CM, Phillipsen MB, Hartmanis LM, Kwasnica MA, Chen V, Hackam D, Chang MW, Bentley WE, March JC (2017) Microscale Bioreactors for in situ characterization of GI epithelial cell physiology. Sci Rep 7:12515
55. Kumar A, Kargozar S, Baino F, Han SS (2019) Additive manufacturing methods for producing hydroxyapatite and hydroxyapatite-based composite scaffolds: a review. Front Mater 6:313